

University of Groningen

## On the total synthesis of terpenes containing quaternary stereocenters

Buter, Jeffrey

**IMPORTANT NOTE: You are advised to consult the publisher's version (publisher's PDF) if you wish to cite from it. Please check the document version below.**

*Document Version*

Publisher's PDF, also known as Version of record

*Publication date:*

2016

[Link to publication in University of Groningen/UMCG research database](#)

*Citation for published version (APA):*

Buter, J. (2016). *On the total synthesis of terpenes containing quaternary stereocenters: Stereoselective synthesis of the taiwaniaquinoids, mastigophorene A, and tuberculosinyl adenosine*. Rijksuniversiteit Groningen.

### Copyright

Other than for strictly personal use, it is not permitted to download or to forward/distribute the text or part of it without the consent of the author(s) and/or copyright holder(s), unless the work is under an open content license (like Creative Commons).

The publication may also be distributed here under the terms of Article 25fa of the Dutch Copyright Act, indicated by the "Taverne" license. More information can be found on the University of Groningen website: <https://www.rug.nl/library/open-access/self-archiving-pure/taverne-amendment>.

### Take-down policy

If you believe that this document breaches copyright please contact us providing details, and we will remove access to the work immediately and investigate your claim.

Downloaded from the University of Groningen/UMCG research database (Pure): <http://www.rug.nl/research/portal>. For technical reasons the number of authors shown on this cover page is limited to 10 maximum.

# **On the Total Synthesis of Terpenes containing Quaternary Stereocenters**

Stereoselective Synthesis of the Taiwaniaquinoids, Mastigophorene A, and  
Tuberculosinyl adenosine

**Jeffrey Buter**

The work described in this thesis was executed at the Stratingh Institute for Chemistry, University of Groningen, The Netherlands.



The authors of this thesis wish to thank the Netherlands Organization for Scientific Research for funding.



Netherlands Organisation for Scientific Research

Cover design by Jeffrey Buter and Nittert Marinus. The front cover photo "*the four elements*" was taken and kindly provided by Mrs. Franziska Ehrlich.

Printed by Ipskamp Drukkers BV, Enschede, The Netherlands



rijksuniversiteit  
groningen

# **On the Total Synthesis of Terpenes containing Quaternary Stereocenters**

Stereoselective Synthesis of the Taiwaniaquinoids, Mastigophorene A, and  
Tuberculosinyl adenosine

## **Proefschrift**

ter verkrijging van de graad van doctor aan de  
Rijksuniversiteit Groningen  
op gezag van de  
rector magnificus prof. dr. E. Sterken  
en volgens besluit van het College voor Promoties.

De openbare verdediging zal plaatsvinden op

vrijdag 10 juni 2016 om 16.15 uur

door

**Jeffrey Buter**

geboren op 12 november 1985  
te Heerenveen

**Promotor**

Prof. dr. ir. A.J. Minnaard

**Beoordelingscommissie**

Prof. dr. J.H. van Maarseveen

Prof. dr. N. Maulide

Prof. dr. J.G. de Vries

ISBN: 978-90-367-8896-0 (Printed version)

ISBN: 978-90-367-8895-3 (Electronic version)

***“What I cannot create, I do not understand.”***

*Richard P. Feynman*

***“Even if I can create it, I still do not understand it.”***

*Adriaan J. Minnaard*



*Aan mijn ouders*





## Table of Contents

<i>Chapter 1 - The Asymmetric Total Synthesis of Lipids from Mycobacterium tuberculosis</i> .....	1
1.1 Introduction.....	2
1.2 $\beta$ -Mannosyl phosphomycoketide.....	6
1.3 Asymmetric catalytic deoxypropionate synthesis.....	8
1.4 Phthiocerol dimycocerosate A.....	9
1.5 Phenolic glycolipid (PGL-tb1).....	11
1.6 Diacylated sulfoglycolipid (Ac <sub>2</sub> SGL) .....	13
1.7 Sulfolipid-1.....	17
1.8 A tuberculostearic acid containing glycerophospholipid.....	19
1.9 Outline of this thesis.....	21
1.10 References.....	23
 <i>Chapter 2 - Synthesis and Analysis of Mycoketide: A Test of NMR Predictions for Saturated Oligoisoprenoid Stereoisomers</i> .....	27
2.1 Introduction.....	28
2.2 Synthesis of the $\beta$ -mannosyl phosphomycoketide side chain.....	29
2.3 NMR analysis of $\beta$ -mannosyl phosphomycoketide side chain 3c .....	32
2.4 NMR analysis of $\beta$ -mannosyl phosphomycoketide side chain.....	36
2.5 Conclusions .....	39
2.6 Discussion.....	39
2.7 Studies on the stereochemistry of crenarchaeol ( <i>ongoing studies</i> ) .....	40

<b>2.8 Experimentals .....</b>	<b>41</b>
<b>2.9 References.....</b>	<b>42</b>
 <b>Chapter 3 - The discovery of novel terpene nucleosides from <i>Mycobacterium tuberculosis</i> .....</b>	 <b>45</b>
<b>3.1 Introduction .....</b>	<b>46</b>
<b>3.2 Tuberculosinyl adenosines; novel terpene nucleosides from <i>Mycobacterium tuberculosis</i> .....</b>	<b>48</b>
3.2.1 The isolation and structure elucidation of an unknown terpene nucleoside .....	48
3.2.2 A total synthesis of racemic 1-TbAd .....	50
3.2.3 The biosynthetic pathway of 1-TbAd.....	51
<b>3.3 The development of 1-TbAd as a chemical marker for tuberculosis disease....</b>	<b>53</b>
3.3.1 1-TbAd is a major and specific lipid in <i>Mycobacterium tuberculosis</i> .....	53
3.3.2 <i>In vivo</i> detection of 1-TbAd in infected mice .....	55
3.3.3 Identification of another unknown terpene nucleoside .....	56
3.3.4 The biological origin of N <sup>6</sup> -TbAd .....	61
<b>3.4 Conclusions.....</b>	<b>61</b>
<b>3.5 Discussion: a hypothesis for the working mechanism of 1-TbAd.....</b>	<b>62</b>
<b>3.6 Experimental section .....</b>	<b>65</b>
<b>3.7 References.....</b>	<b>82</b>
 <b>Chapter 4 - Asymmetric Total Synthesis of 1-Tuberculosinyl Adenosine .....</b>	 <b>85</b>
<b>4.1 Introduction .....</b>	<b>86</b>
<b>4.2 Retrosynthetic analysis.....</b>	<b>87</b>
<b>4.3 Investigations of the asymmetric synthesis of 1-TbAd .....</b>	<b>89</b>
4.3.1 An attempted chiral pool approach to 1-TbAd .....	89
4.3.2 Towards an asymmetric catalytic Diels-Alder reaction for the construction of 1- TbAd; DNA catalysis .....	92
4.3.3 Development of an asymmetric catalytic Diels-Alder reaction for the construction of 1-TbAd; Organocatalysis.....	94

4.3.4 Development of an asymmetric catalytic Diels-Alder reaction for the construction of 1-TbAd; Copper-catalyzed approach.....	96
4.3.5 A chiral auxiliary based Diels-Alder approach towards 1-TbAd.....	100
4.3.6 Removal of the chiral auxiliary and the battle against steric hindrance.....	101
4.3.7 Determination of asymmetric induction in the chiral auxiliary aided Diels-Alder cycloaddition .....	104
4.3.8 The stereoselective synthesis of 1-TbAd and <i>N</i> <sup>6</sup> -TbAd.....	105
4.3.9 Completion of the stereoselective synthesis of 1-TbAd and <i>N</i> <sup>6</sup> -TbAd .....	106
<b>4.4 On the mechanism and enantioselectivity of the asymmetric Diels-Alder reaction .....</b>	<b>108</b>
<b>4.5 Conclusion .....</b>	<b>113</b>
<b>4.6 Discussion and outlook .....</b>	<b>113</b>
<b>4.7 Experimental section.....</b>	<b>115</b>
<b>4.8 References.....</b>	<b>144</b>
 <b><i>Chapter 5 - Pd-catalyzed Asymmetric Conjugate Addition of Ortho-substituted Arylboronic Acids to Cyclic β-substituted Enones .....</i></b>	
<b>5.1 Introduction.....</b>	<b>150</b>
<b>5.2 Development of the asymmetric Pd-catalyzed conjugate addition of <i>ortho</i>-substituted arylboronic acids to β,β-Disubstituted cyclic enones.....</b>	<b>152</b>
<b>5.3 The shortest asymmetric total syntheses of herbertenediol and enokipodin A and B .....</b>	<b>157</b>
<b>5.4 Conclusion .....</b>	<b>160</b>
<b>5.5 Discussion and outlook .....</b>	<b>160</b>
<b>5.6 Experimental section.....</b>	<b>161</b>
<b>5.7 References.....</b>	<b>188</b>
 <b><i>Chapter 6 - Pd-Catalyzed, <i>t</i>BuLi-mediated dimerization of Aryl Halides and its Application in the Atropselective Total Synthesis of Mastigophorene A .....</i></b>	
	<b>193</b>

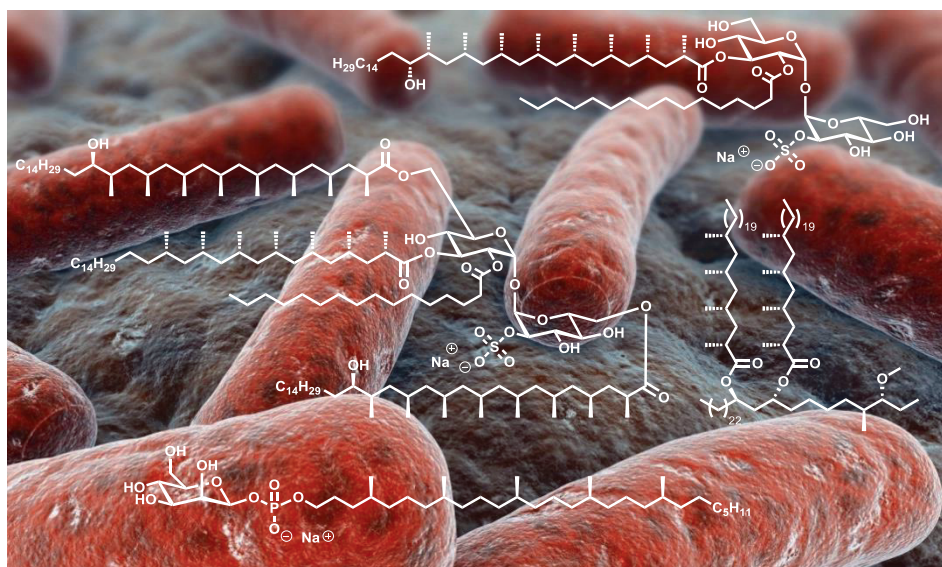
<b>6.1 Introduction .....</b>	<b>194</b>
<b>6.2 Development of a Pd-catalyzed homo-coupling employing aryllithium reagents .....</b>	<b>196</b>
<b>6.3 Application in the asymmetric total synthesis of mastigophorene A.....</b>	<b>199</b>
<b>6.4 Conclusion .....</b>	<b>208</b>
<b>6.5 Discussion and future prospects .....</b>	<b>208</b>
6.5.1 Reflection on the Pd-catalyzed homo-coupling.....	208
6.5.2 Other natural product targets for the point-to-axial chirality transfer using the Pd-catalyzed homo-coupling of aryllithium reagents.....	210
<b>6.6 Experimental section .....</b>	<b>213</b>
<b>6.7 References.....</b>	<b>233</b>
<b><i>Chapter 7 - Towards an Asymmetric Total Synthesis of the Taiwaniaquinoids .....</i></b>	<b><i>237</i></b>
<b>7.1 Introduction .....</b>	<b>238</b>
<b>7.2 Previous total syntheses of the taiwaniaquinoids based on asymmetric conjugate additions.....</b>	<b>240</b>
<b>7.3 Retrosynthetic, strategic and mechanistic analysis.....</b>	<b>243</b>
<b>7.4 Ventures into the asymmetric conjugate addition to cycloheptenone 24 .....</b>	<b>246</b>
<b>7.5 Investigation into the ring contraction of the cycloheptanone adduct .....</b>	<b>249</b>
<b>7.6 Conclusions.....</b>	<b>252</b>
<b>7.7 Future prospects and discussion.....</b>	<b>253</b>
<b>7.8 Experimental section .....</b>	<b>254</b>
<b>7.9 References.....</b>	<b>272</b>
<b><i>English Summary .....</i></b>	<b><i>275</i></b>
<b><i>Nederlandse Samenvatting .....</i></b>	<b><i>283</i></b>
<b><i>Acknowledgements/Dankwoord .....</i></b>	<b><i>291</i></b>





## \*\*\* CHAPTER 1 \*\*\*

### ‡ *The Asymmetric Total Synthesis of Lipids from Mycobacterium tuberculosis* ‡



**ABSTRACT:** *Mycobacterium tuberculosis* is a disease causing bacterium which infects several million people and leads to over 1.5 million deaths on an annual basis. The success of *Mycobacterium tuberculosis* as world's most important bacterial pathogen can be attributed to two key factors. First, an intricate intracellular survival mechanism protects it from immune responses during a decades long infection process. Secondly, its unusually hydrophobic, multi-layered, cell wall protects it even further from penetration by drugs. Despite of over a century of active research into *Mycobacterium tuberculosis*, the function of the lipid components which make up for its cell wall, remain largely unknown. Additionally, no definite, tuberculosis specific chemical marker based diagnostic test for this disease exists. Discovery of new lipids can help to understand *Mycobacterium tuberculosis*' survival and virulence mechanism, and when the lipids are specific to pathogenic *Mycobacterium tuberculosis*, these can be used as chemical markers for the disease. This chapter gives an overview of our previous efforts regarding the asymmetric total synthesis of *Mycobacterium tuberculosis* lipids. In the final paragraph an outline of this dissertation is presented.

*This chapter will be published in part in the form of a review article:  
J. Buter, A. J. Minnaard, manuscript in preparation*



## 1.1 Introduction

Tuberculosis is an infectious disease caused by the bacterium *Mycobacterium tuberculosis* (*Mtb*).<sup>[1]</sup> It is a disease which primarily attacks the pulmonary tract (e.g. lungs and throat), hence the “typical” tuberculosis cough, but can also attack the kidney, spine, and/or brain.<sup>[2a]</sup> Tuberculosis is a fatal human disease and is contagious as the bacterium can easily be transmitted from individual to individual simply by coughing and sneezing. It is therefore not surprising that tuberculosis manifests itself as one of world’s leading pathogens causing over five million infections and over one and a half million deaths annually.<sup>[1]</sup> The majority of casualties from this disease are inhabitants of the developing countries, and more specifically from regions with high HIV (human immunodeficiency virus) infection rates. It is the decrease in immune response in HIV patients which make these individuals more vulnerable for tuberculosis infection.<sup>[2b]</sup> Luckily not everybody infected with tuberculosis becomes sick and as a result there are basically two tuberculosis-related conditions. One can either have latent tuberculosis infection or have the active tuberculosis disease (Figure 1).<sup>[2c]</sup> Treatment<sup>[2d,e,3]</sup> of both forms is possible but, as the high number of fatalities indicates, is far from trivial. Patients diagnosed with latent tuberculosis infection do have tuberculosis bacilli in their body but these are not active. Such individuals are therefore not contagious and do not exhibit the tuberculosis symptoms. However, the danger of developing active tuberculosis is associated with having latent tuberculosis infection, and it is for this reason that treatment of the latter is initiated. Typical treatment involves the use of either isoniazid, rifampicin/rifampin or rifapentine for several months (first-line drugs).<sup>[2d,3]</sup>

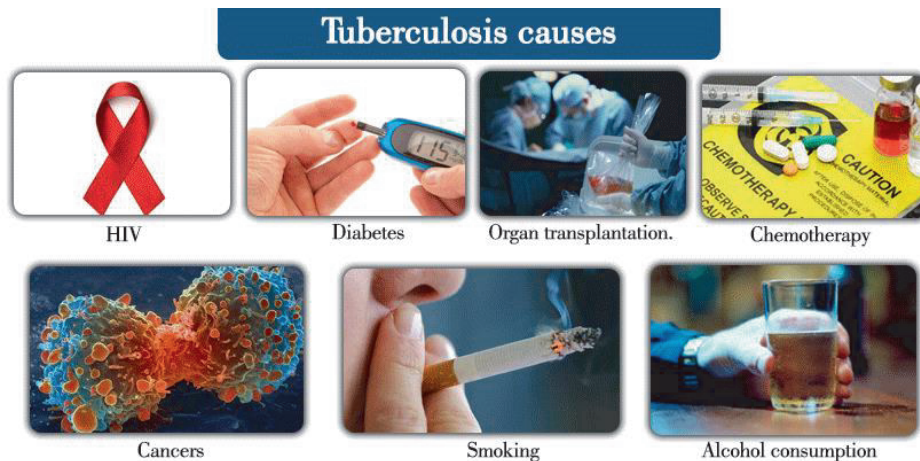


**Figure 1.** Tuberculosis risk factors, causing active Tb disease from latent Tb infection.

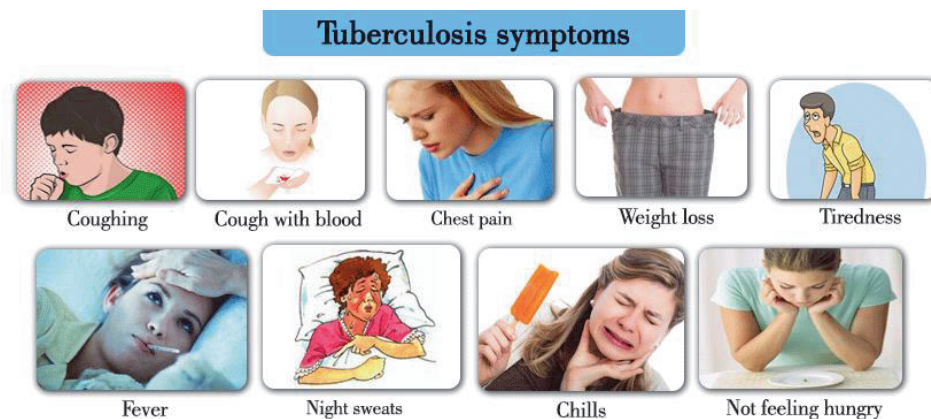
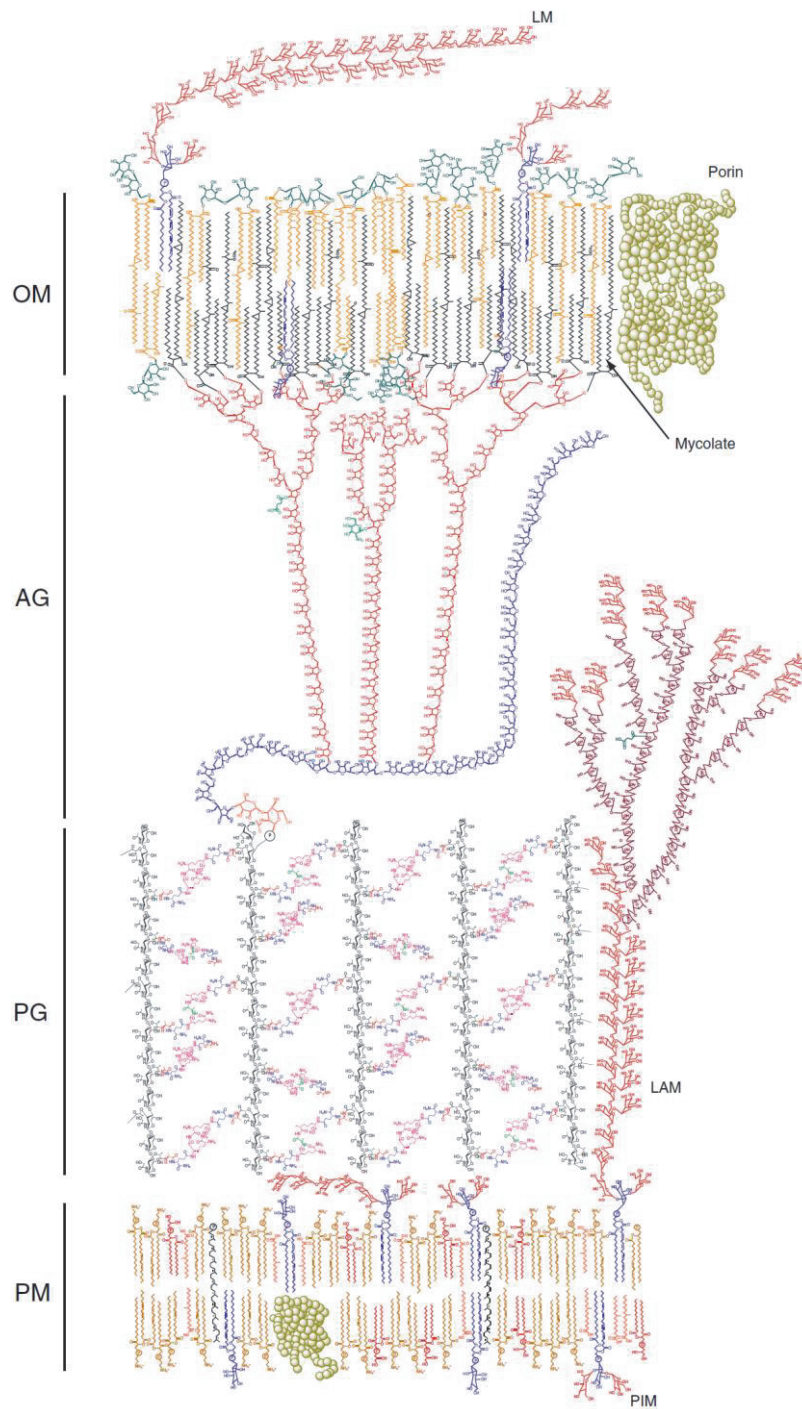


Figure 1 (continued). Tuberculosis symptoms.

When the immune system in a latent TB infected patient is unable to stop the tuberculosis bacteria from growing, it multiplies and causes the active Tb disease. The patient becomes sick, showing typical tuberculosis symptoms and more importantly becomes contagious. Due to multiplication of the bacterium inside the human host there are more bacteria compared to those having latent tuberculosis infection, making treatment harder. Drug-susceptible tuberculosis involves a treatment with the previously mentioned first-line drugs, pyrazinamide and ethambutol (also first-line drugs), generally in a combinatorial fashion, for several months.<sup>[2e,3]</sup>

Since tuberculosis is caused by a living organism it is subjected to evolutionary principles causing, inevitably, drug resistance.<sup>[4]</sup> It goes without saying that the regimen for treatment of (multi- or extensively-) drug resistant tuberculosis<sup>[5]</sup> complicates the situation, necessitating, dependent on the pattern of drug resistance, a regimen of up to two years.<sup>[2e,3]</sup> This involves the use of a combination of first-line drugs, fluoroquinolone based drugs, injectable agents (e.g. streptomycin, amikacin, kanamycin, or capreomycin) and alternative agents (e.g. cycloserine, *p*-aminosalicylic acid, clarithromycin, amoxicillin-clavulanate). As medicines are not exonerated from adverse effects the extensive use of tuberculosis drugs will take its toll on the patient, in the worst case forcing discontinuation of treatment.<sup>[6]</sup>

It is evident from the preceding paragraphs that treatment of tuberculosis is apparently very demanding. The origin of hampered treatment of tuberculosis lies for a large part within its cell envelope (cell wall). Consisting of a complex array of (glyco)lipids, polysaccharides and peptidoglycans, the cell wall exhibits low permeability of drugs into the mycobacterial cell.<sup>[7]</sup> In figure 2, based on our current understanding, one sees a molecular representation of the cell envelope of *Mycobacterium tuberculosis*, showing an exquisite architecture build-up of many different layers.



**Figure 2.** A schematic molecular representation of the cell envelope of *Mycobacterium tuberculosis* (© and reproduced with permission from Elsevier, reference 7c).

### *The Asymmetric Total Synthesis of Lipids from Mycobacterium tuberculosis*

On the inside of the cell envelope lays the so-called plasmic membrane (PM). This bilayer consists primarily of glycerol based lipids and phosphatidylethanolamines (cephalins), a class of glycerophospholipids. Here one also finds the well-known phosphatidylinositol mannosides (PIMs). Connected in a non-covalent manner to the plasma membrane is the lipoarabinomannan (LAM), a complex oligosaccharide which is a known virulence factor of tuberculosis. LAM consists of a phosphatidylinositol moiety linked to mannopyranan core to which is attached an arabinan, spanning the peptidoglycan (PG) into the arabinogalactan (AG) region of the membrane.

The peptidoglycan determines the cellular shape and plays an important role in surviving osmotic pressure. The amino saccharide backbone of the peptidogalactan is cross-linked with peptide bonds which enhances rigidity of the cell wall. Covalently connected to PG sugar moieties is the arabinogalactan, with as the backbone a 30-mer galactofuran linker. This functionality is linked at the 8, 10 and 12 position, with arabinofurans. These polymeric saccharides span a large part of the overall cell wall and eventually branch out connecting with mycolic acids. The mycolate based glycolipid structures form the outer membrane (OM), an interwoven network of the long aliphatic (C60-C90) mycolic acid chains. The cell-wall is topped by an outermost compartment, a loosely bound structure called a capsule (*not shown in Figure 2*), primarily consisting mainly of polysaccharides and peptides.

Due to the high lipid content the cell envelope is very hydrophobic. This therefore forms an almost unsurpassable barrier for drugs, making the treatment of the tuberculosis disease difficult. To complicate the situation even further, intracellular survival of the bacterium is granted by successful infection of endosomal phagocytes. Residing in phagosomes, and actively inhibiting pH dependent killing mechanisms, it is protected from both drugs and immune responses.<sup>[8]</sup>

Because of over a century of active research on *Mycobacterium tuberculosis*, many of the lipid components which make up for its cell membrane are largely known.<sup>[7]</sup> It is however surprising how little is known about the function and antigenic properties of these lipids.<sup>[7c]</sup> As the mycobacterial cell envelope is at the interface with the human host, it plays a key role in *Mycobacterium tuberculosis*' virulence but also in the immune response. The identification of new lipids is therefore instrumental to understand *Mycobacterium tuberculosis*' survival and virulence, and provides an opportunity to develop anti-mycobacterial drugs. Moreover, when specific to *Mycobacterium tuberculosis*, these lipids can serve a potential source of chemical markers for the tuberculosis disease, making them useful for developing diagnostic tests.<sup>[9]</sup>

The discovery of biologically active "small molecules" (secondary metabolites) and in particular the studies thereof are counteracted by small isolated quantities. In order to facilitate investigation, more specifically the structure elucidation and assessment of their biological activity, the need for significant quantities of material is undeniable and for *Mycobacterium tuberculosis* total synthesis is the technology to serve these needs.

In this chapter an overview of our in-house executed total syntheses, of *Mycobacterium tuberculosis* produced lipids, is presented. The emphasis lies on the synthetic strategies employed, with a brief description of the molecule's biological activity.

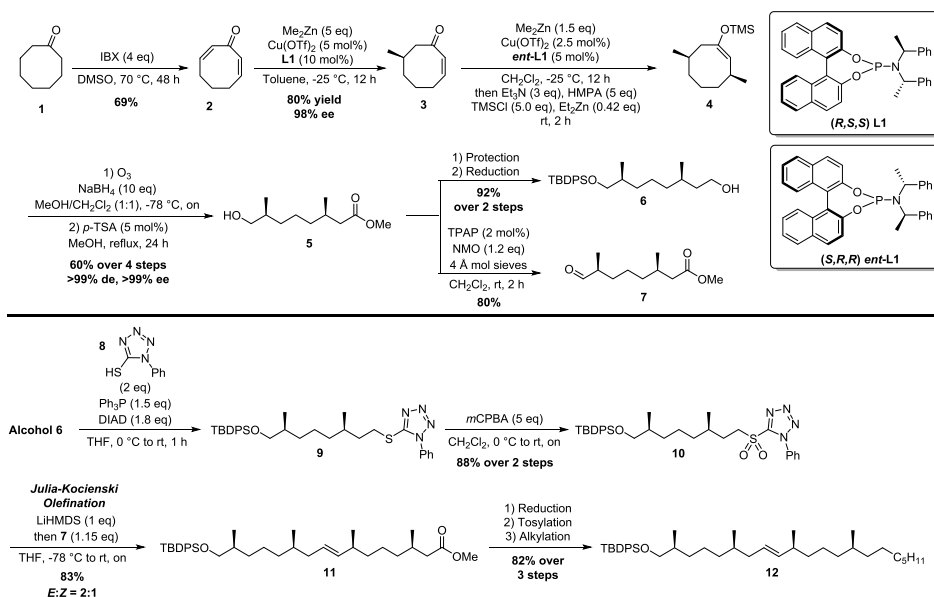
## 1.2 $\beta$ -Mannosyl phosphomycoketide

In 2000 Moody and co-workers, isolated a new compound from *Mycobacterium tuberculosis* and *Mycobacterium avium*, named mannosyl phosphomycoketide (MPM).<sup>[10]</sup> This polyketide (not terpenoid!) was found to be a potent mycobacterial antigen for a CD1c-restricted mycobacterial T-cell line. Antigen presentation of MPM by CD1c was postulated to arise from binding of the chain within a hydrophobic groove of the CD1c protein. The hydrophilic mannosyl phosphate functionality is recognized by the T-cell receptor. The importance of the hydrophobic tail in T-cell response was assessed, showing T-cell response to be dependent on the length of the chain, with an optimum around C35.<sup>[10]</sup> Also the hydrophilic head group was shown to be crucial for T-cell response as a glucose, instead of mannose, was not recognized.

The structure elucidation did not include the assignment of the stereochemical elements present in the MPM chain, due to its limited availability. In 2002, Crich and Dudkin confirmed the overall chemical structure of MPM by means of a stereorandom total synthesis.<sup>[11]</sup> It was confirmed that MPM has a  $\beta$ -glycosidic bond but the stereochemistry in the chain remained unresolved. In 2005, the Minnaard/Feringa laboratory set out to perform this task (Scheme 1 and 2).<sup>[12]</sup> However, before the synthesis was started, a hypothesis had to be made about the stereochemistry (out of the 32 possibilities!). For this the biosynthesis of the mycoketides was considered leading to the conclusion that the methyl groups are introduced through the iterative action of polyketide synthase pks12, providing the all-*syn* compound.<sup>[13]</sup> Subsequently, all-(*S*)-MPM was arbitrarily chosen as the target.

Starting from cyclooctanone (Scheme 1), a double oxidation employing IBX gave dienone **2** in 69% yield. This compound was then subjected to the first of two conjugate additions, in which 5 mol% of Cu(OTf)<sub>2</sub> and 10 mol% Feringa ligand **L1** were utilized.<sup>[14]</sup> The conjugate addition proceeded smoothly giving enone **3** in an excellent *ee* of 98%. The second conjugate addition was performed using half the catalyst loading, and using *ent*-**L1**. Trapping of the *in situ* formed enolate as its TMS enol ether gave, after ozonolysis and esterification, alcohol **5** in 60% over the four steps with an excellent *de* and *ee* of >99%. **5** was then converted into alcohol **6** and aldehyde **7** employing standard chemistry. These building blocks were united with a Julia-Kocienski olefination. To achieve this, alcohol **6** was subjected to a Mitsunobu reaction in the presence of thiol **8**. Oxidation of **9** with *m*CPBA delivered sulfone **10** which was used in the Julia-Kocienski reaction with aldehyde **7** to obtain alkene **11** as an, inconsequential, mixture of isomers (*E:Z* = 2:1). Complete reduction of the ester with DIBAL-H followed by tosylation and subsequent alkylation, using CuBr•SMe<sub>2</sub> and C<sub>5</sub>H<sub>11</sub>MgBr, gave tetramethyl alkane **12** in 82% yield over the three steps.

## The Asymmetric Total Synthesis of Lipids from *Mycobacterium tuberculosis*

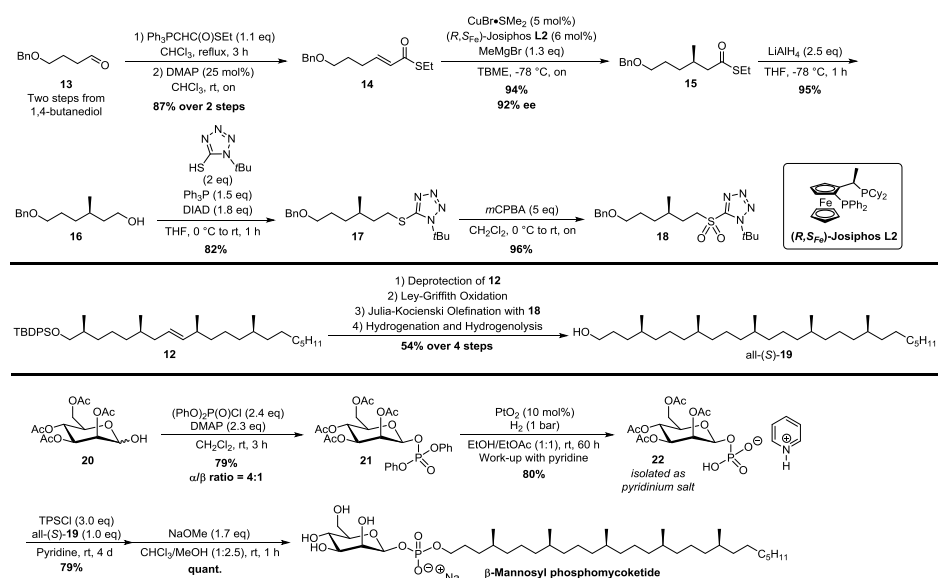


**Scheme 1:**  $\beta$ -mannosyl phosphomycoketide building block synthesis and unification.

Completion of the MPM side chain only required the installation of an additional methyl functionality (Scheme 2). This was achieved by constructing sulfone building block **18** from 1,4-butanediol derived aldehyde **13**. A Wittig olefination and subsequent DMAP-catalyzed isomerization afforded thioester **14**. At this stage the final stereocenter of the MPM side chain was introduced via the asymmetric copper-catalyzed conjugate addition of methylmagnesium bromide. Employing 5 mol% of  $\text{CuBr}\cdot\text{SMe}_2$  in combination with josiphos ligand **L2** provided the methyl-substituted stereocenter in **15** in 94% yield with 92% *ee*.<sup>[15]</sup> Reduction of the thioester, Mitsunobu functionalization and sulfone formation afforded enantiopure building block **18**. Unification of this molecule with tetramethyl substrate **12** was again achieved via a Julia-Kocienski olefination, after TBDPS deprotection and Ley-Griffith oxidation of **11**. The alkene functionalities and benzyl group were then removed by a Pd/C-catalyzed hydrogenolysis/hydrogenation to give the MPM side chain **19**.

Completion of  $\beta$ -mannosyl phosphomycoketide was effected by connecting the MPM-side chain with mannose (Scheme 2). For this, hemiacetal **20** was reacted with diphenyl chlorophosphate to give predominantly the  $\beta$ -anomer of mannosyl phosphate **21**. Removal of the phenyl groups using Adams' catalyst and quenching with pyridine afforded pyridinium mannosyl phosphate **22**. Linking this fragment with MPM side chain **19**, with the assistance of 2,4,6-triisopropylbenzenesulfonyl chloride (TPSCI), provided, after removal of the acetyl protecting groups, all-(*S*)- $\beta$ -mannosyl phosphomycoketide, its first asymmetric total synthesis.

## CHAPTER 1



**Scheme 2.** Completion of  $\beta$ -mannosyl phosphomycoketide.

The completion of the total synthesis allowed the elucidation of the relative and absolute stereochemistry by proving sufficient material for biological evaluation. Gratifyingly, the hunch to make the all-(*S*) MPM paid off since immunological essays, performed by the Moody laboratory, showed that the synthetic material exhibited a similar antigenic T-cell response compared to the natural isolate.<sup>[16]</sup> Interestingly, the stereorandom mixture of MPMs was significantly less potent, indicating a strong, somewhat unexpected, influence of lipid moiety on T-cell response. Additionally it was reported that T-cell response was even dependent on the stereochemistry of the C4-methyl (the first methyl-branched stereocenter from the left), where (*S*)-stereochemistry proved to be significantly more active than the (*R*)-isomer. The study therefore indicates a strong, influence of the lipid stereochemistry, more specifically the chiral methyl ramification, on T-cell response.

The total synthesis of all-(*S*)- $\beta$ -mannosyl phosphomycoketide was recently also reported by the Piccirilli group.<sup>[17]</sup> Whereas in our synthesis asymmetric catalysis stood central, the Piccirilli synthesis mined from the chiral pool, synthesizing the natural product with >96% stereopurity.

### 1.3 Asymmetric catalytic deoxypropionate synthesis

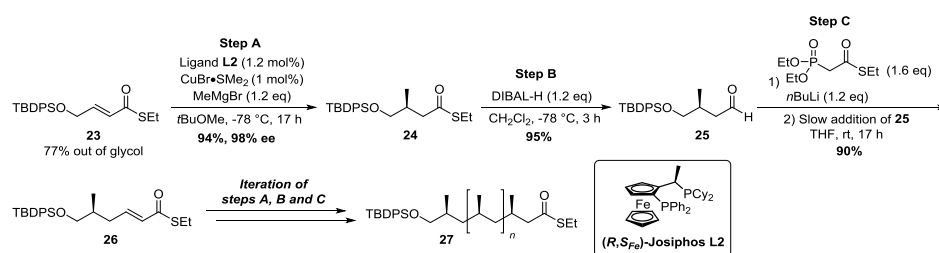
After our synthesis of  $\beta$ -mannosyl phosphomycoketide, bearing the chiral 1,5-methyl array, the focus shifted towards other *Mycobacterium tuberculosis* lipids comprising asymmetric methyl branches. Our attention was drawn in particular by the complex glycolipids Ac<sub>2</sub>SGL and its “big brother” sulfolipid-1. Of special interest was the so-called deoxypropionate unit (1,3-methyl ramification) on the lipid side chains. Both

## The Asymmetric Total Synthesis of Lipids from *Mycobacterium tuberculosis*

glycolipids contain lipid chains with up to eight repeating 1,3-methyl groups making it a challenging moiety for the asymmetric synthesis community. Also the somewhat smaller molecules PDIM-A, PGL-tb1 and mycoside B isolated from *Mycobacterium tuberculosis* bear this structural feature, though shorter in length, and therefore also became part of our synthesis program.

Deoxypropionates are polyketides and are an abundant moiety in a wide variety of natural products.<sup>[18]</sup> It is therefore not surprising that many synthetic strategies towards the 1,3-methyl array have been reported.<sup>[19]</sup> In order to construct deoxypropionates, an iterative synthetic sequence is an especially appealing strategy. In such way the 1,3-methyl ramification can be introduced relatively fast, reliable and efficient, albeit at the cost of the route's convergence. Since the discussion of the different iterative methodologies to construct deoxypropionates falls outside the scope of this chapter we like to refer to our review on this specific topic.<sup>[19]</sup>

One of the methodologies which does need to be mentioned in light of this overview is the copper-catalyzed asymmetric Michael addition of methylmagnesium bromide to  $\alpha,\beta$ -unsaturated thioesters, by Feringa and Minnaard in 2005.<sup>[15]</sup> For the iterative construction of the deoxypropionate units in the *Mycobacterium tuberculosis* lipids,  $\alpha,\beta$ -unsaturated thioester **23** was used as the starting material (Scheme 3). The asymmetric conjugate addition of MeMgBr to this substrate proceeded in 94% yield and an excellent 98% *ee*. The thioester was converted into the corresponding aldehyde by the aid of DIBAL-H. A Horner-Wadsworth-Emmons olefination then provided  $\alpha,\beta$ -unsaturated thioester **26** in 86% over the two steps. Repetition of this sequence also proved to be highly stereoselective as each consecutive methyl introduction led to increased diastereoselectivity. This feature, the high yield and ease of execution of the steps made this methodology ideal to synthesize long deoxypropionates (*vide infra*).



**Scheme 3.** General iterative deoxypropionate synthesis strategy used in the construction of *Mtb* lipids.

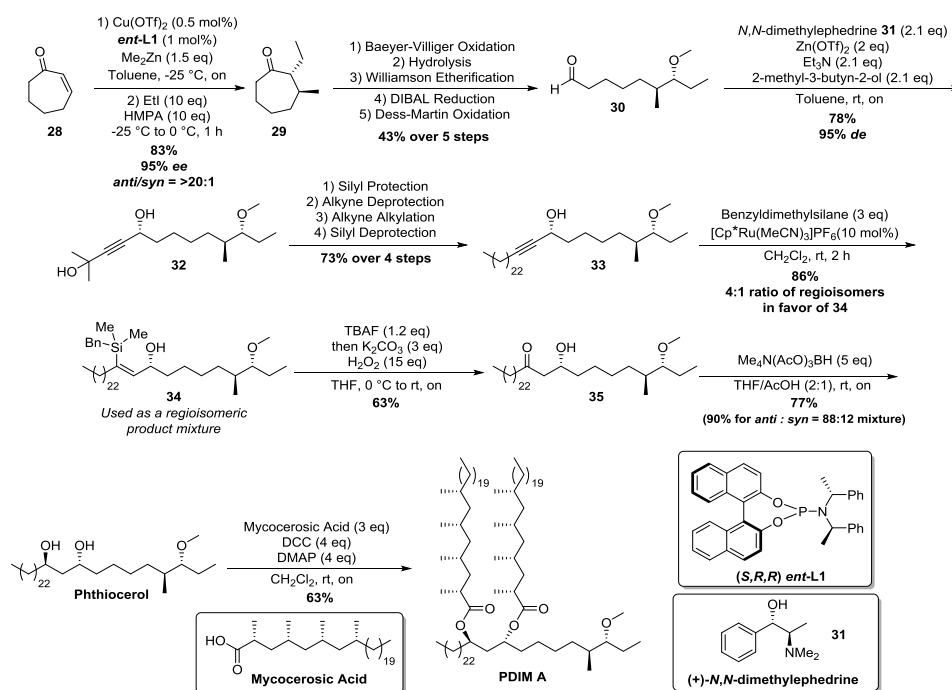
### 1.4 Phthiocerol dimycocerosate A

The first *Mtb*-borne lipid successfully crafted in our laboratory applying the described iterative asymmetric conjugate addition sequence was phthiocerol dimycocerosate A (PDIM A).<sup>[20]</sup> In 1999 two independent studies found that *Mycobacterium tuberculosis*



## CHAPTER 1

mutant strains, deficient in PDIM A, showed attenuated virulence.<sup>[21]</sup> This finding strongly suggested an important role for the PDIM A lipid as a virulent determinant. The structure and absolute configuration of the phthiocerol and mycocerosic acid chains were proposed as early as in 1963 and 1973 respectively.<sup>[22]</sup> Confirmation of the structure, by means of rigorous <sup>1</sup>H-NMR analysis, was provided by Daffé and co-workers.<sup>[23]</sup> However, absolute proof of the structure by means of total synthesis was not provided until our group embarked upon an asymmetric total synthesis of PDIM A (Scheme 4).



**Scheme 4.** Asymmetric total synthesis of PDIM A.

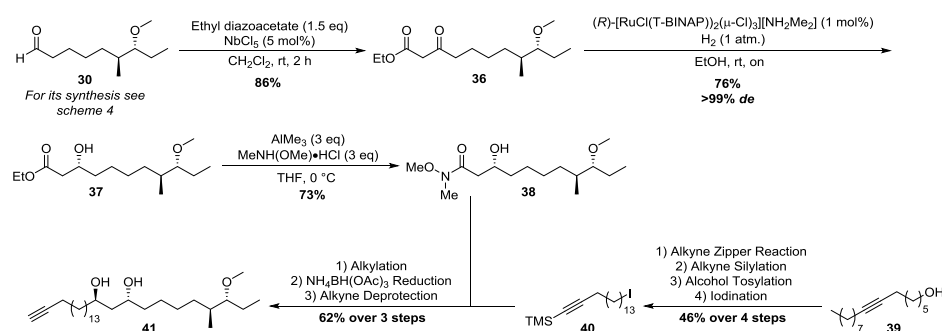
PDIM A initially attracted our attention mainly due to the mycocerosic acid side chains, but the molecule contains an additional four stereocenters in the phthiocerol backbone. The stereogenic methyl-branch with a vicinal asymmetric methoxy stereocenter prompted us to employ another asymmetric conjugate addition strategy. Treatment of cycloheptenone with  $\text{Me}_2\text{Zn}$ , in the presence of  $\text{Cu}(\text{OTf})_2$  (0.5 mol%) and Feringa ligand **L1** (1 mol%),<sup>[14]</sup> followed by trapping of the *in situ* formed enolate with ethyl iodide provided **29** with 95% *ee* and >20:1 *de*. Opening of the ring via a Baeyer-Villiger oxidation/hydrolysis sequence gave after further transformations aldehyde **30**. An asymmetric 1,2-addition of 2-methyl-3-butyn-2-ol to aldehyde **30** following Carreira's procedure gave propargylic alcohol **32** with an excellent selectivity of 95% *de*.<sup>[24]</sup> Multiple steps led to alkyne **33** which was hydrosilylated to furnish vinyl silane **34** in 86% yield. A Tamao-Fleming oxidation and subsequent directed reduction of the ketone

with tetramethylammonium triacetoxyborohydride selectively produced phthiocerol. Esterification with mycocerosic acid, constructed using the iterative asymmetric conjugate addition sequence,<sup>[25,15]</sup> produced PDIM A thereby confirming its proposed chemical structure. The produced material also aided in the development of an analytical procedure to detect PDIM A in *Mtb* samples.<sup>[26]</sup> Moreover, the synthetic material helped to establish the role of PDIM A as virulence factors of *Mycobacterium tuberculosis*.<sup>[27]</sup> It was shown that *Mtb* strains lacking PDIM A are susceptible to killing in early stages of infection indicating that PDIM A protects *M. tuberculosis* from an early innate host response.

### 1.5 Phenolic glycolipid (PGL-tb1)

A compound closely related to PDIM A, is the phenolic glycolipid PGL-tb1. This compound was first isolated and characterized by Daffé *et al.*, and was found in the outer layer of the cell envelope in several strains of *Mtb*.<sup>[28]</sup> Where the closely related DIM/PDIMs are required for the multiplication and persistence of *Mtb in vivo*,<sup>[29]</sup> PGL-tb1 has also been suspected to be involved in hypervirulence of specific *Mtb* strains.<sup>[30]</sup> Given its presence in specific *Mtb* strains, PGL-tb1 is one of the most unusual virulence factors modulating its defense systems and causing disease. This feature can be exploited since there is a great need for *Mtb*-specific compounds that permit to distinguish between prior BCG vaccination and infection. Steps towards such a distinction have been made with the recent development of an enzyme-linked immunosorbent assay (ELISA) based on PGL-tb1, a potential method for the diagnosis of TB in HIV-infected patients.<sup>[31]</sup> To facilitate further studies, there is a need for pure synthetic material since the natural isolate comes only in minute quantities.

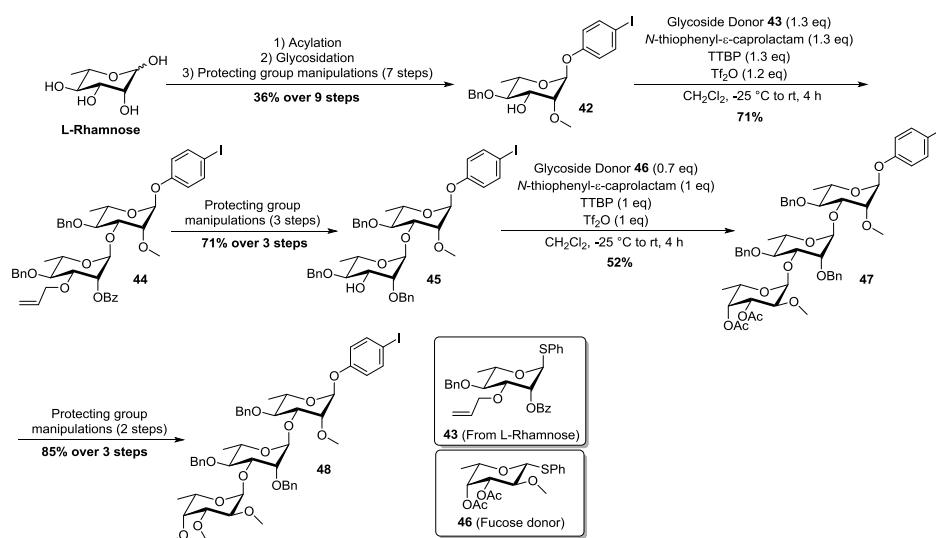
Our synthetic endeavor on the synthesis of PGL-tb1 (Scheme 5) involved the preparation of the previously mentioned aldehyde **30** (Scheme 4).<sup>[20]</sup> Conversion into keto-ester **36** was followed by a Noyori asymmetric hydrogenation, installing the third stereocenter in >99% *de*. Ester **37** was transformed into Weinreb amide **38** which was alkylated with alkyl iodide **40**. The intermediate ketone was reduced and the alkyne was liberated from its protecting group to give phthiocerol analogue **41**.



Scheme 5. Asymmetric synthesis of the phthiocerol backbone in PGL-tb1.

## CHAPTER 1

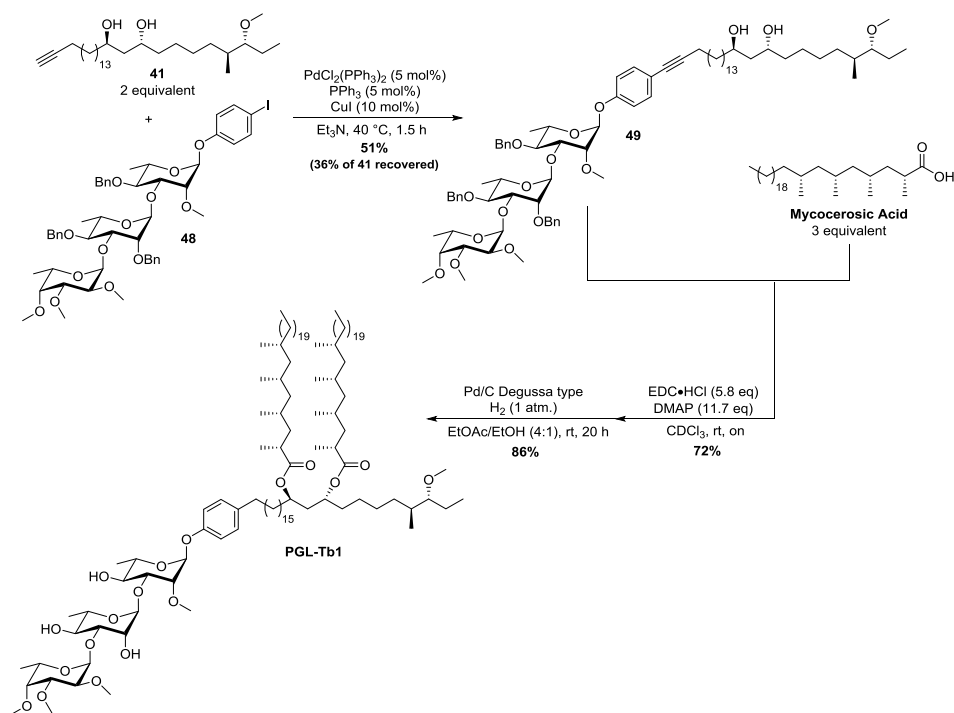
The trisaccharide building block was synthesized starting from *L*-rhamnose, which in multiple steps was converted into glycoside acceptor **42** (Scheme 6). Glycosylation of this compound with rhamnoside **43**, by the aid of *N*-thiophenyl- $\epsilon$ -caprolactam,  $\text{TiF}_2\text{O}$  in a tri-*t*-butyl-pyrimidine (TTBP) buffered solution, provided the  $\alpha$ -linked di-rhamnoside **44** with full stereocontrol in 71% yield. The third sugar functionality was introduced in 52% yield, following a similar procedure, this time with **46**, to give after two more steps trisaccharide **48**.



**Scheme 6.** Construction of trisaccharide **48** for the PGL-tb1 synthesis.

The unification of the two aforementioned building blocks, **41** and **48** came about in the form of a Sonogashira coupling (Scheme 7). Careful optimization led to the isolation of 51% of the desired cross-coupled product **49**, with the recovery of 36% of **41**. After introduction of the mycocerosic side chains, deprotection concluded the first asymmetric total synthesis of PGL-tb1. The synthetic material is currently under investigation for the development of diagnostic tools for the detection of hypervirulent strains of *Mtb*. Also its role in virulence is being studied.

The Asymmetric Total Synthesis of Lipids from *Mycobacterium tuberculosis*



Scheme 7. Completion of the PGL-tb1 total synthesis.

### 1.6 Diacylated sulfoglycolipid ( $\text{Ac}_2\text{SGL}$ )

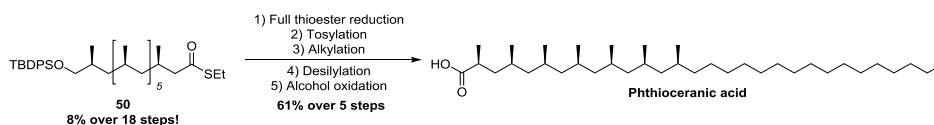
In 2004, Gilleron *et al.* communicated the isolation and characterization of the *Mycobacterium tuberculosis* specific lipid  $\text{Ac}_2\text{SGL}$ , which is present in the outer cell membrane.<sup>[32]</sup> This molecule was found to be a potent antigen, stimulating populations of CD1b-restricted human T lymphocytes during infection with *Mtb*.<sup>[33]</sup> That  $\text{Ac}_2\text{SGL}$  is a promising candidate for the development of new tuberculosis vaccine was quickly recognized due to its antigenic properties. It was shown that T-cells activated by  $\text{Ac}_2\text{SGL}$  release interferon- $\gamma$ , recognize *M. tuberculosis* infected antigen-presenting cells, and kill intracellular mycobacteria *in vitro*.<sup>[34]</sup>

In 2008, Prandi and co-workers constructed and biologically evaluated a set of  $\text{Ac}_2\text{SGL}$  analogues containing the trehalose-sulfate functionality, but varying in the acyl side chain.<sup>[35]</sup> T-cell receptor recognition and T-lymphocyte activation was shown to be dependent on the number and stereochemistry of the methyl substituents, and the respective location of the acyl chains on the trehalose core. Despite the finding that  $\text{Ac}_2\text{SGL}$ -specific T-cell activation occurred at low concentration ( $<100\text{ nM}$ ,  $\sim 0.1\ \mu\text{g mL}^{-1}$ ) for the analogues, their antigenicity was significantly attenuated compared to the naturally occurring  $\text{Ac}_2\text{SGL}$ .

Due to the limited access of  $\text{Ac}_2\text{SGL}$  from the pathogenic *Mycobacterium tuberculosis* ( $\sim 1\text{ mg/L}$ ) culture, and the painstaking isolation procedure, the development of a

## CHAPTER 1

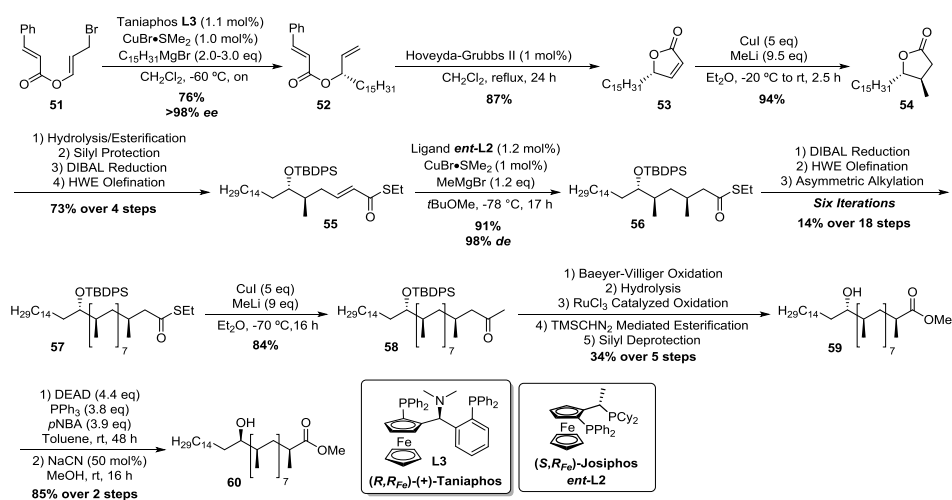
vaccine program is depending on total synthesis efforts. Our group embarked on the first total synthesis of naturally occurring  $\text{Ac}_2\text{SGL}$ ,<sup>[36]</sup> which started with the construction of the long deoxypropionate lipids phthioceranic acid<sup>[37]</sup> and hydroxyphthioceranic acid. The former was constructed in a straightforward manner using the iterative conjugate addition sequence to install the seven methyl groups in a linear fashion in 8% yield over 18 steps (Scheme 3). Thioester **50** was subsequently reduced to the alcohol, tosylated, substituted by the long alkyl chain followed by desilylation and oxidation to give phthioceranic acid (Scheme 8).



**Scheme 8.** Asymmetric synthesis of phthioceranic acid.

For the synthesis of hydroxyphthioceranic acid we adopted a slightly different strategy since a chiral hydroxy group is present in this molecule. In our first generation synthesis (Scheme 9) we decided to install this hydroxyl group by means of a copper/taniaphos-catalyzed allylic alkylation of ester **51** with  $\text{C}_{15}\text{H}_{31}\text{MgBr}$ .<sup>[38]</sup> The desired terminal olefin **52** was obtained in 76% yield and an excellent *ee* of >98%. Ring-closing metathesis afforded lactone **53** which was diastereoselectively methylated using a cuprate addition, preparing **54**. A straightforward four step protocol afforded  $\alpha,\beta$ -unsaturated thioester **55**, which set the stage for the iterative introduction of the remaining seven methyl groups.<sup>[15]</sup> The first methyl group to be installed using the iterative sequence gave thioester **56** in 91% yield and a 98% *de*. Six iterations (18 steps!) on this molecule provided deoxypropionate **57** in 14% yield over these 18 steps. With **57** in hand the thioester was converted into the corresponding methyl ketone **58**. Baeyer-Villiger oxidation followed by hydrolysis of the formed ester provided the desired chain length of hydroxyphthioceranic acid. The obtained alcohol was oxidized and esterified where after the hydroxyl group was deprotected, giving **59**. At this stage, comparison with natural hydroxyphthioceranic acid showed the stereochemistry of the hydroxyl function to be incorrect and therefore the alcohol functionality in **59** was inverted by a Mitsunobu reaction using *p*-nitrobenzoic acid. The obtained ester was transesterified using MeOH and catalytic NaCN, affording hydroxyphthioceranic acid methyl ester **60** in 85% over the two steps.

### The Asymmetric Total Synthesis of Lipids from *Mycobacterium tuberculosis*

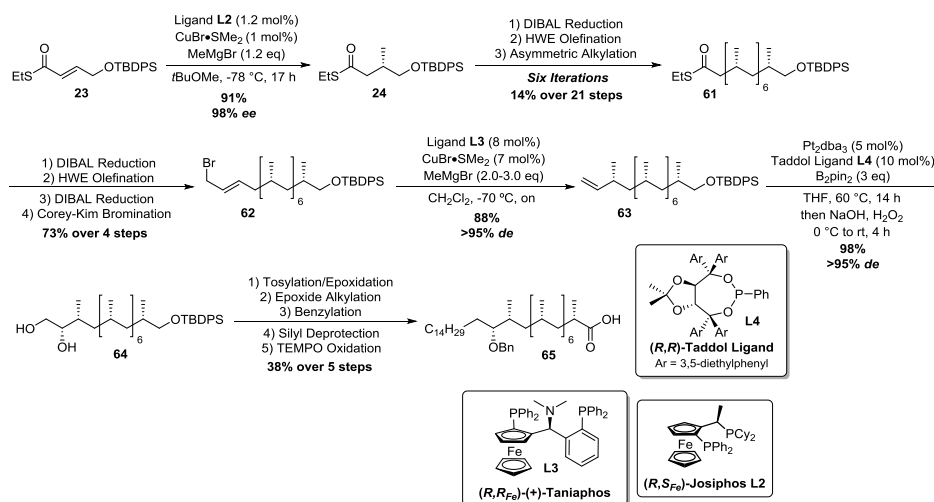


**Scheme 9.** First generation asymmetric catalytic synthesis of hydroxyphthioceranic acid.

A critical view at our first generation hydroxyphthioceranic acid synthesis, reveals that it lacks the flexibility to also obtain phthioceranic acid from this route. This is a consequence of the early introduction of the latent chiral hydroxyl moiety in **52** (Scheme 9). This downside was addressed in a second generation synthesis in which the chiral hydroxyl moiety was installed *after* the iterative conjugate addition sequence, thereby allowing the preparation of phthioceranic acid as well (Scheme 10).<sup>[36]</sup>

After the iterative conjugate addition sequence, installing seven of the desired methyl groups, **61** was converted into allylic bromide **62** using standard chemistry. This compound was treated with 7 mol% of CuBr•SMe<sub>2</sub> and 8 mol% of (*R,R*)<sub>Fe</sub>-taniaphos **L3** in presence of MeMgBr.<sup>[39]</sup> The allylic alkylation provided octamethyl alkene **63** in 88% yield with an excellent diastereomeric excess of >95%. The alkene functionality served as an excellent scaffold for the introduction of the hydroxyl stereogenic center. Initial attempts with the Sharpless asymmetric dihydroxylation led to the desired product, albeit with an unsatisfying diastereomeric excess of 70%.<sup>[40]</sup> We therefore set out to install the dihydroxy functionality via asymmetric diborylation, which after oxidation gives the desired product. Such methodology has been developed by the Morken laboratory in which bis(pinacolato)diboron (B<sub>2</sub>pin<sub>2</sub>) is added across the double bond catalyzed by Pt<sub>2</sub>dba<sub>3</sub> and taddol-based ligand **L4**.<sup>[41]</sup> The diborylation/oxidation smoothly furnished desired diol **64** in 98% yield with an diastereomeric excess exceeding 95%. With all the stereocenters set, a straightforward five step sequence was employed to install the aliphatic side chain, benzyl protecting group and carboxylic acid moiety to furnish protected hydroxyphthioceranic acid **65** in 38% over the steps.

CHAPTER 1

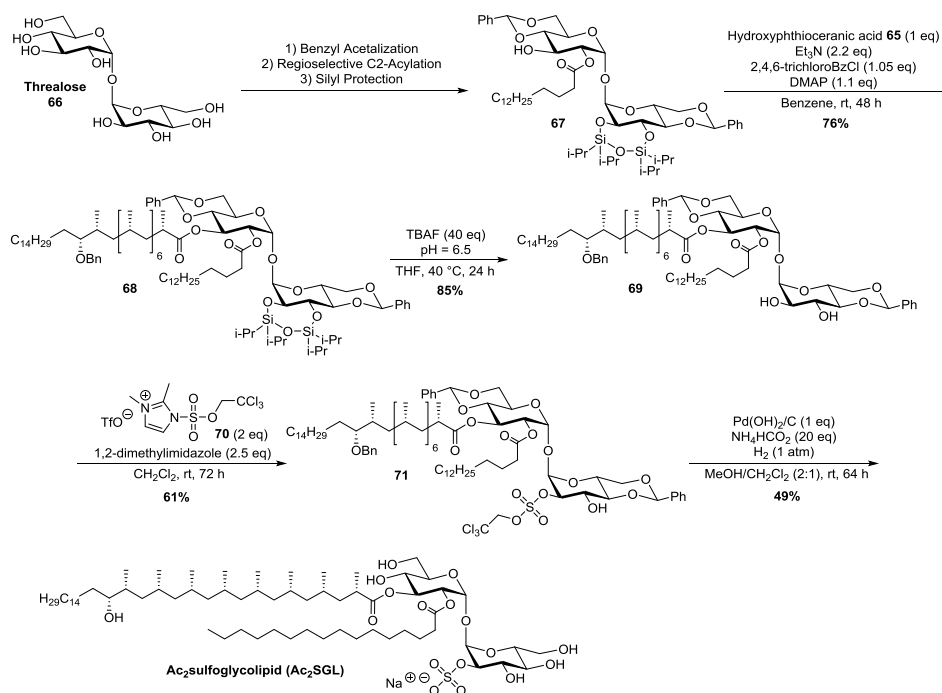


**Scheme 10.** Second generation asymmetric catalytic synthesis of hydroxyphthioceranic acid.

With hydroxyphthioceranic acid successfully crafted, unification with the trehalose core was left to complete the total synthesis of Ac<sub>2</sub>SGL (Scheme 11). Trehalose **66** was first protected and acylated in such a way that only the C3-position remained available. **67** was then used in a Yamaguchi esterification with hydroxyphthioceranic acid **65** to give **75** in 76% yield. Removal of the bis(diisopropylsilyl)ether under standard conditions smoothly provided diol **69** which was regioselectively sulfated using 2,2,2-trichloroethyl sulfuryl imidazolium salt **70** as reported by Taylor and co-workers.<sup>[42]</sup> The approach reported by Taylor was preferred because the 2,2,2-trichloroethyl group can be removed under hydrogenolysis conditions, identical to those planned for the removal of the benzylidene acetals. Introduction of the protected sulfate group furnished **71** in 61% yield which after hydrogenolysis with Pd(OH)<sub>2</sub>/C and ammonium formate under an hydrogen atmosphere provided us, after 39 steps, with Ac<sub>2</sub>SGL. All analytic data were in agreement with those of the natural material and additional biological studies confirmed the successful synthesis of Ac<sub>2</sub>SGL.

To date our laboratory reported the only complete total synthesis of Ac<sub>2</sub>SGL. The hydroxyphthioceranic acid side chain on the other hand has been synthesized several times.<sup>[43]</sup> In 2012, Pfaltz and Schneider communicated a total synthesis in which chiral methyl groups were largely installed via iridium-catalyzed substrate controlled asymmetric hydrogenation reactions.<sup>[43a]</sup> The Aggarwal laboratory reported their hydroxyphthioceranic acid total synthesis in 2014, based on their in-house developed stereoselective lithiation–borylation–protodeboronation sequence.<sup>[43b]</sup> More recently the same group showed elegant use of this methodology in an iterative fashion by an “assembly-line synthesis” of hydroxyphthioceranic acid.<sup>[43c]</sup> The most recent synthesis came from the hands of Negishi and co-workers who employed their developed Zr-catalyzed asymmetric carboalumination of alkenes to install the chiral methyl groups.<sup>[43d]</sup>

The Asymmetric Total Synthesis of Lipids from *Mycobacterium tuberculosis*



Scheme 11. Completion of naturally occurring Ac<sub>2</sub>SGL.

### 1.7 Sulfolipid-1

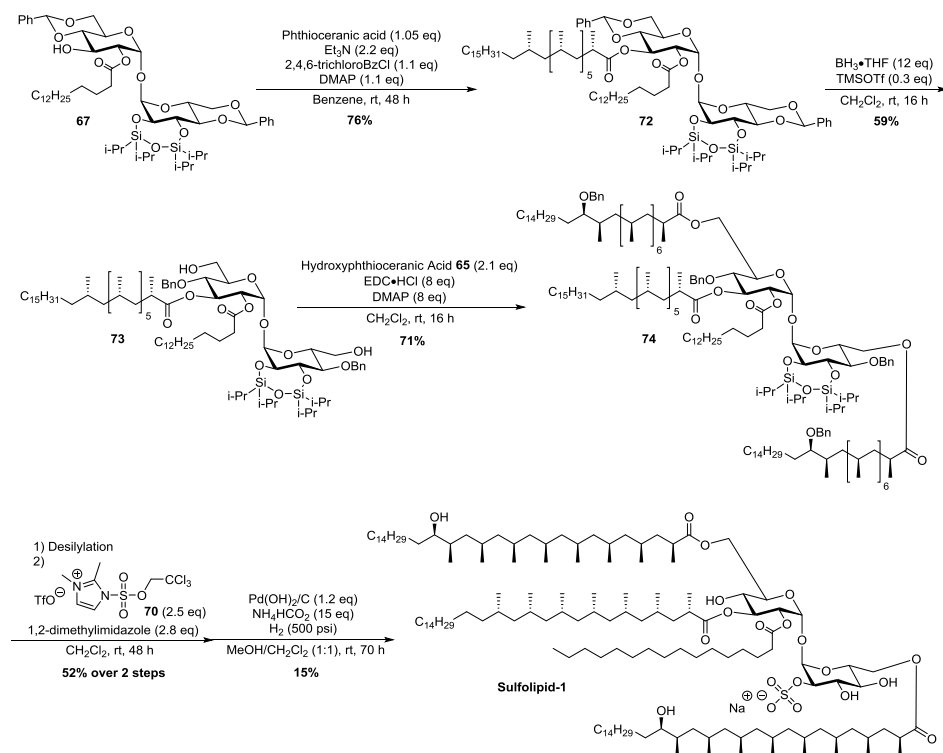
Shortly after our synthesis of Ac<sub>2</sub>SGL we set out to construct the even more complex molecule sulfolipid-1.<sup>[44]</sup> Whereas Ac<sub>2</sub>SGL was isolated in 2004, sulfolipid-1 is known for over 40 years since its isolation and structure elucidation, by meticulous degradation studies in 1970 by Goren.<sup>[45]</sup> Sulfolipid-1 is a prominent cell wall constituent of *Mycobacterium tuberculosis* and was postulated to be a virulence factor. Studies with knockout mutants unable to produce sulfolipid-1 supported this hypothesis, indicating a role in host-pathogen interactions by mediating between a cationic human antimicrobial peptide and the bacterium.<sup>[46]</sup>

For the synthesis of sulfolipid-1 we used our previously gained knowledge in the Ac<sub>2</sub>SGL total synthesis.<sup>[36]</sup> Yamaguchi esterification of protected trehalose **67** with phthioceranic acid gave **72** with a satisfying yield of 76% (Scheme 12). Installation of the two hydroxyphthioceranic side chains required the regioselective ring-opening of the benzylidene acetals to liberate the free 6-OH and 6'-OH groups while maintaining benzyl protecting groups on the C4 and C4' hydroxyl moieties. Several reductive ring-opening strategies were studied, among them CoCl<sub>2</sub>, Cu(OTf)<sub>2</sub>, and TMSOTf in combination with BH<sub>3</sub>•THF.<sup>[40]</sup> With cobalt the reaction did not give any conversion, whereas Cu(OTf)<sub>2</sub> and TMSOTf afforded **73**, albeit with low yields. However, when TMSOTf was used in combination with 12 equivalents of BH<sub>3</sub>•THF, **73** was obtained in



## CHAPTER 1

a satisfactory 59% yield. Whether this result can be attributed to the kinetics of the desired reaction, or to the quenching of adventitious water, is still not clear.



**Scheme 12.** The Geerdink and Minnaard synthesis of sulfolipid-1.

The free alcohol moieties were successfully doubly acylated with hydroxyphthioceranic acid **65** using EDC as the coupling agent (71% yield), since the Yamaguchi esterification only gave rise to monoacylated product. Desilylation then set the stage for the sulfation à la Taylor.<sup>[42]</sup> This time, however, sulfation did not merely affected the C2'-OH position, as in the Ac<sub>2</sub>SGL synthesis, but also gave rise to sulfation at the 3'-OH position. This observation was attributed to the reduced rigidity of desilylated **74** (compared to **68**, Scheme 11) due to opening of the benzylidene acetal. However, with sulfated product in hand the final hydrogenolysis was initially performed under conditions described for the Ac<sub>2</sub>SGL synthesis. Since atmospheric H<sub>2</sub> pressure did not lead to any conversion the pressure was increased to 250 psi, which again, did not lead to full conversion. Further enhancement of the pressure to 500 psi did lead to sulfolipid-1, however, in a low yield of 15%. To account for the high pressure needed it was hypothesized that the long-tailed lipids induced significant steric hindrance, making it difficult for the heterogeneous palladium catalyst to reach the reaction center. As a result of these drastic hydrogenolysis conditions, desulfation of the quite labile sulfate group occurred in part, as confirmed by isolation of the desulfated product next to the

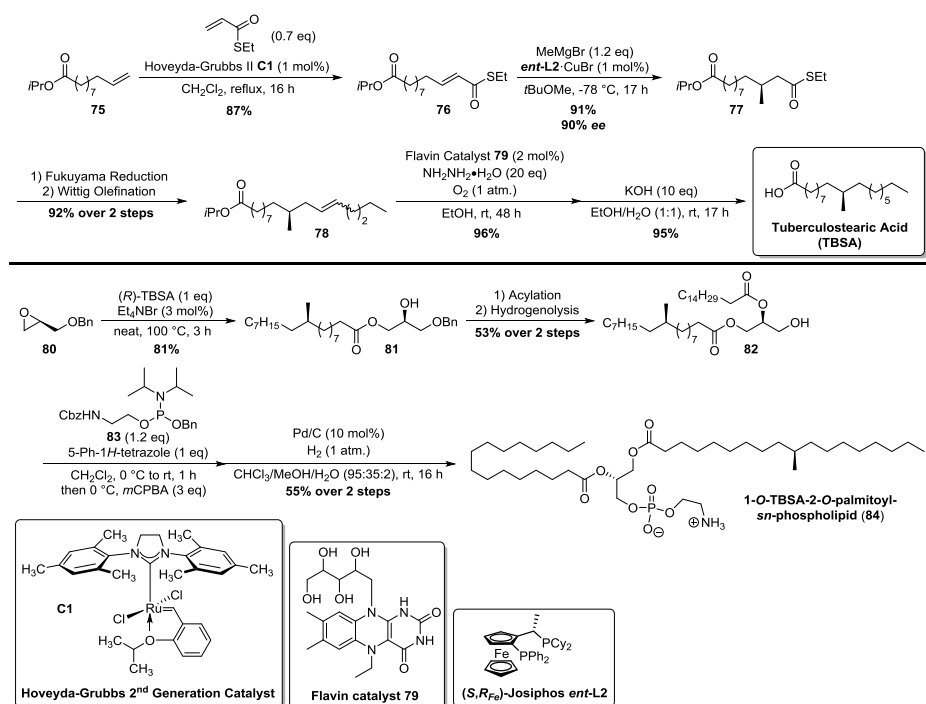
desired product. All in all, 40 years after its isolation we managed to describe the full total synthesis of sulfolipid-1 in 46 steps, thereby confirming the structure of this impressive molecule.

### **1.8 A tuberculostearic acid containing glycerophospholipid**

Phosphatidylethanolamines (cephalins) form a class of glycerophospholipids which play an important role in the structure and function of cellular membranes.<sup>[47]</sup> In collaboration with the Moody laboratory, a new and abundant glycerophospholipid was isolated from the virulent *M. tuberculosis* strain, H37Rv.<sup>[48]</sup> Such natural products can be used for identification of specific mycobacterial species and are therefore potentially useful as chemical markers in diagnostic tests for tuberculosis infection. Identification of such products is therefore of utmost importance.

Initial efforts to elucidate the chemical composition of the natural isolate led to the identification of cephalin, palmitoyl, and tuberculostearoyl fragments.<sup>[48]</sup> Decisive insight into the connectivity of the fatty acids to the cephalin core could not be obtained from mass-spectrometry data, and since the isolated quantities were too low for NMR studies, this hampered full characterization of the natural product. To find out whether the palmitoyl, and tuberculostearoyl fragments were connected to the primary and secondary alcohol in the glycerol core, or *vice versa*, a total synthesis of both isomers was embarked upon to answer this question (Scheme 13, *only one product shown*).<sup>[48]</sup>

The total synthesis started with a cross-metathesis reaction between thioacrylate and terminal alkene **75** to provide  $\alpha,\beta$ -unsaturated thioester **76**. As a novel substrate for the well-developed asymmetric conjugate addition reaction,<sup>[15]</sup> a yield of 91% with an enantiomeric excess of 90% could be achieved in the construction of methyl branched **77**. Reduction of the thioester via a Fukuyama reduction followed by a Wittig olefination then provided alkene **78** in 92% over the two steps. The alkene was then reduced by an in-house developed Flavin-catalyzed reduction<sup>[49]</sup> to, after hydrolysis of the isopropyl ester, afford tuberculostearic acid. Coupling of the latter with commercially available (*R*)-benzyl glycidyl ether **79**, using Et<sub>4</sub>NBr as the catalyst, gave a smooth opening of the epoxide to yield alcohol **81**. Acylation with palmitic acid and debenzoylation gave then furnished alcohol **82**, without significant acyl migration of the palmitic acid. Installation of the phosphatidylethanolamine was achieved by reaction of **82** with phosphoramidite reagent **83**. Oxidation of the intermediate product gave, after hydrogenolysis of the Bn and Cbz protecting groups, the desired product **84**.



**Scheme 13.** Total synthesis of a newly isolated *Mycobacterium tuberculosis* specific diacyl glycerol based phospholipid.

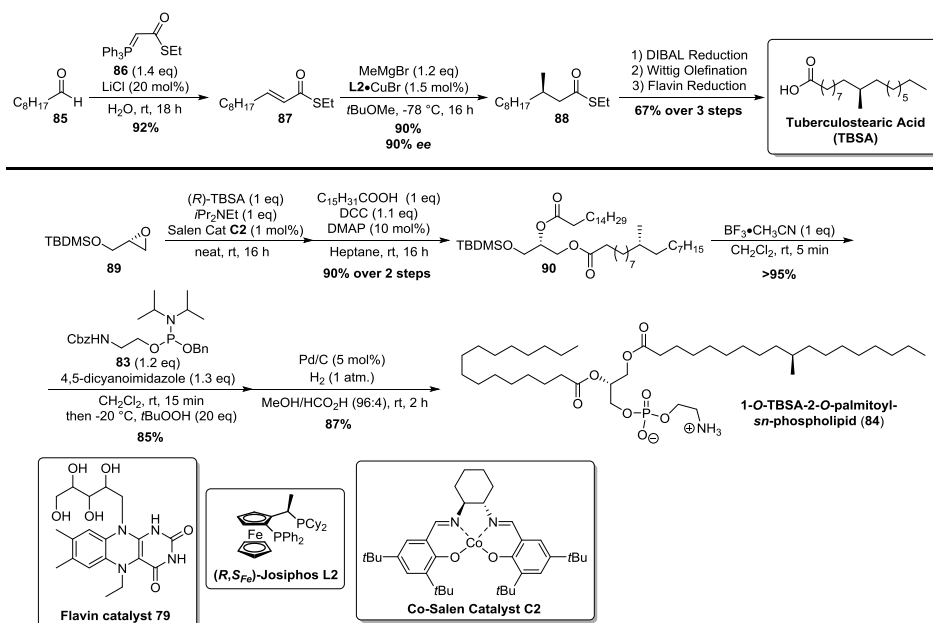
Comparison of the mass spectral data of the natural isolate with 1-*O*-TBSA-2-*O*-palmitoyl-*sn*-phospholipid **84** and its regioisomeric counterpart, that is 1-*O*-palmitoyl-2-*O*-TBSA-*sn*-phospholipid (*structure not shown*), established the natural product to be **84**. The synthesis of the phospholipid not only proved to be helpful in elucidation of the structure, but also provided material to function as an LC-MS standard for the development as a chemical marker.

A revised synthesis of phospholipid **84** was reported in 2013 during our studies into the stereoselective synthesis of glycerol-based lipids (Scheme 14).<sup>[50]</sup> The previous synthesis of tuberculostearic acid was re-evaluated, providing a two-step shorter route. To achieve this, nonanal **85** was olefinated by means of a Wittig reaction with ylide **86** in the presence of LiCl using “on water” conditions, constructing unsaturated thioester **87** in 92% yield with an excellent *E:Z* ratio exceeding 95:5. Introduction of the methyl group was achieved in 90% *ee* and 90% yield. Reduction of the thioester, olefination with the free acid(!) and reduction of the formed double bond using the flavin catalyst, provided tuberculostearic acid in the shortest synthesis to date.

Construction of the glycidyl part was this time accomplished starting from silyl protected glycidol **89** by treatment with Co-salen catalyst **C2**, Hünig’s base and tuberculostearic acid. The reaction cleanly provided the acylated product and could be acylated in the same pot with palmitic acid under Steglich esterification conditions. The

## The Asymmetric Total Synthesis of Lipids from *Mycobacterium tuberculosis*

diacyl TBDMS protected glycerol **90** was then deprotected using  $\text{BF}_3 \cdot \text{CH}_2\text{CN}$  to the free alcohol without migration of the palmitoyl functionality. Further elaboration to install the phosphate group, as previously described, then afforded phospholipid **84**.



**Scheme 14.** A revised total synthesis of diacyl glycerol based phospholipid **84**.

### 1.9 Outline of this thesis

As evident from this chapter, the Minnaard lab has a longstanding interest in the asymmetric total synthesis of (glyco)lipids, and preferably those exhibiting some sort of biological activity. This already led to fruitful collaborations over the past years in which the biological relevance of several *Mycobacterium tuberculosis* produced lipids have been investigated. These synthetic efforts not only helped to assess bioactivity, but also led to structure–function analysis and assistance in structural assignment of natural isolates. In addition to natural product synthesis, the laboratory also develops new synthetic methodology with an emphasis on asymmetric catalysis.

This dissertation describes my efforts within natural product synthesis and the development of new asymmetric synthesis methodology. Application of the latter in total synthesis, biological studies of synthesized natural products, and the use of synthetic material in structure elucidation are all presented in this thesis.

In chapter 2, research on the stereochemical assignment of saturated oligoisoprenoids is described. Using the  $\beta$ -mannosyl phosphomycoketide side chain as a model, we have demonstrated that the relative stereochemistry of the 1,5-methyl array can be elucidated

## CHAPTER 1

---

by comparison of a Traficante processed high field  $^{13}\text{C}$  (175 MHz) or  $^1\text{H}$ -NMR (700 MHz) spectrum, with that of a predicted set of spectra of all possible stereoisomers. The results in this chapter show that the developed method is capable of assessing diastereopurity, and is potentially useful for the structural assignment of saturated oligoisoprenoid bearing natural products, a feature previously absent in the literature.

The content of chapter 3 involves the investigation into a, previously unknown, “lipid” of *Mycobacterium tuberculosis*. Now known as 1-tuberculosinyl adenosine (1-TbAd), the molecule was not only found to be specific for pathogenic *Mtb*, but also a highly abundant lipid of which its production is encoded by the virulent associate Rv3377c-Rv3378c locus. In addition, its development into a chemical marker, for a diagnostic test for tuberculosis infection, is reported. This investigation also led to the discovery of a rearranged version of 1-TbAd, called  $N^6$ -TbAd.

Chapter 4 describes the first enantioselective and diastereoselective total synthesis of 1-TbAd and  $N^6$ -TbAd. Containing a cyclohexene motive, an asymmetric Diels-Alder cycloaddition is at the heart of the synthesis. Besides successful completion of the synthesis on a multi-gram scale, an extensive overview of the development of a highly stereoselective Diels-Alder reaction is outlined. Furthermore, the synthetic material allows further studies of TbAd as virulence factors.

In chapter 5, the development of the asymmetric palladium-catalyzed conjugate addition of *ortho*-substituted arylboronic acids to 3-methyl cyclic enones, creating benzylic all carbon quaternary stereocenters, is communicated. Despite previous reports of the conjugate addition of arylboronic acids to 3-substituted cyclic enones, *ortho*-substituted arylboronic acids were not tolerated in these studies, proving only trace amounts of products, or as one case showed, modest enantioselectivity. The developed methodology was applied in the shortest synthesis of herbertenediol, enokipodin A and enokipodin B to date.

With the asymmetric total synthesis of herbertenediol reported (chapter 5), the synthesis of its dehydrodimer mastigophorene A serves the central theme of chapter 6. Mastigophorene A, containing a benzylic quaternary stereocenter, also bears axial chirality in the form of a tetra-*ortho*-substituted biaryl axis. With the advent of lithium cross-coupling methodology, developed by the Feringa laboratory, the biaryl axis was introduced with a newly discovered palladium-catalyzed homo-coupling of aryl bromides using lithium reagents. The chiral biaryl axis was constructed with high diastereoselectivity arising from an unexpected point-to-axial chirality transfer.

Chapter 7, provides an overview of our synthetic efforts on the asymmetric total synthesis of taiwaniaquinoid family members. This class of natural products contains a benzylic all-carbon quaternary stereocenter, which is planned to be introduced on a highly unusual substituted 3-methyl cycloheptenone derivative. The conjugate addition

is planned to be followed by a rearrangement cascade, of which preliminary data is provided, to build the tricyclic [6,5,6]-*abeo*-abietane core-structure.

### 1.10 References

- [1] World Health Organization. (2015). Global Tuberculosis Report. [http://apps.who.int/iris/bitstream/10665/191102/1/9789241565059\\_eng.pdf?ua=1](http://apps.who.int/iris/bitstream/10665/191102/1/9789241565059_eng.pdf?ua=1) (retrieved: 24/11/2015).
- [2] The center for disease control and prevention dedicated a large part of their website to the tuberculosis disease. a) For basic facts about tuberculosis see: <http://www.cdc.gov/tb/topic/basics/default.htm> b) For information on Tb and HIV infection see: <http://www.cdc.gov/tb/topic/tbhivcoinfection/default.htm> c) For the differences between latent Tb infection and the Tb disease see: <http://www.cdc.gov/tb/topic/basics/difference.htm> d) for treatment of latent Tb disease see: <http://www.cdc.gov/tb/topic/treatment/default.htm> e) for treatment of drug resistant Tb disease see: <http://www.cdc.gov/tb/topic/treatment/tbdisease.htm>
- [3] Treatment of tuberculosis, Morbidity and mortality weekly report **2003**, 52, RR-11.
- [4] S. H. Gillespie, *Antimicrob. Agents Chemoter.* **2002**, 46, 267.
- [5] G. Günther, *Clin. Med.* **2014**, 14, 279.
- [6] Lawrence Flick memorial tuberculosis clinic Philadelphia tuberculosis control program, Guidelines for the management of adverse drug effects of antimycobacterial agents, **1998**.
- [7] a) *The mycobacterial cell envelope* (Eds. M. Daffé, J-M. Reyrat), ASM Press, Washington DC, **2008**. b) D. E. Minnikin, L. Kremer, L. G. Dover, G. S. Besra, *Chem. Biol.* **2002**, 9, 545. c) D. Kaur, M. E. Guerin, H. Škovierová, P. J. Brennan, M. Jackson, *Adv. Appl. Microbiol.* **2009**, 69, 23. d) P. J. Brennan, *Annu. Rev. Biochem.* **1995**, 64, 29. e) D. E. Minnikin, L. Kremer, L. G. Dover, G. S. Besra, *Chem. Biol.* **2002**, 9, 545.
- [8] S. Sturgill-Koszycki, P. H. Schlesinger, P. Chakraborty, P. L. Haddix, H. L. Collins, A. K. Fok, R. D. Allen, S. L. Gluck, J. Heuser, D. G. Russell, *Science*, **1994**, 263, 678.
- [9] R. S. Wallis, P. Kim, S. Cole, D. Hanna, B. B. Andrade, M. Maeurer, M. Schito, A. Zumla, *Lancet Infect. Dis.* **2013**, 13, 362.
- [10] D. B. Moody, T. Ulrichs, W. Mühlecker, D. C. Young, S. S. Gurucha, E. Grant, J-P. Rosat, M. B. Brenner, C. E. Costello, G. S. Besra, S. A. Porcelli, *Nature* **2000**, 404, 884.
- [11] D. Crich, V. Dudkin, *J. Am. Chem. Soc.* **2002**, 124, 2263.
- [12] a) R. P. van Summeren, D. B. Moody, B. L. Feringa, A. J. Minnaard, *J. Am. Chem. Soc.* **2006**, 128, 4546. b) R. P. van Summeren, S. J. W. Reijmer, B. L. Feringa, A. J. Minnaard, *Chem. Commun.* **2005**, 1387.

## CHAPTER 1

---

- [13] I. Matsunaga, A. Bhatt, D. C. Young, T. Y. Cheng, S. J. Eyles, G. S. Besra, V. Briken, S. A. Porcelli, C. E. Costello, W. R. Jr. Jacobs, D. B. Moody, *J. Exp. Med.* **2004**, *200*, 1559.
- [14] B. L. Feringa, M. Pineschi, L. A. Arnold, R. Imbos, A. H. M. de Vries, *Angew. Chem. Int. Ed.* **1997**, *36*, 2620.
- [15] R. Des Mazery, M. Pullez, F. López, S. R. Harutyunyan, A. J. Minnaard, B. L. Feringa, *J. Am. Chem. Soc.* **2005**, *127*, 9966.
- [16] A. de Jong, E. Casas-Arce, T-Y. Cheng, R. P. van Summeren, B. L. Feringa, V. Dudkin, D. Crich, I. Matsunaga, A. J. Minnaard, D. B. Moody, *Chem. Biol.* **2007**, *14*, 1232.
- [17] a) N-S. Li, L. Scharf, E. J. Adams, J. A. Piccirilli, *J. Org. Chem.* **2013**, *78*, 5970. b) N-S. Li, J. A. Piccirilli, *Tetrahedron* **2013**, *69*, 9633.
- [18] C. Khosla, R. S. Gokhale, J. R. Jacobsen and D. E. Cane, *Annu. Rev. Biochem.* **1999**, *68*, 219.
- [19] B. ter Horst, B. L. Feringa, A. J. Minnaard, *Chem. Commun.* **2010**, *46*, 2535.
- [20] E. Casas-Arce, B. ter Horst, B. L. Feringa, A. J. Minnaard, *Chem. Eur. J.* **2008**, *14*, 4157.
- [21] a) J. S. Cox, B. Chen, M. McNeil, W. R. Jacobs, Jr. *Nature* **1999**, *402*, 79. b) L. R. Camacho, D. Ensergueix, E. Pérez, B. Gicquel, C. Guilhot, *Mol. Microbiol.* **1999**, *34*, 257.
- [22] a) N. Polgar, W. Smith, *J. Chem. Soc.* **1963**, 3081. b) K. Maskens, N. Polgar, *J. Chem. Soc. Perkin Trans. 1* **1973**, 1909.
- [23] L. R. Camacho, P. Constant, C. Raynaoud, M-A. Lanéelle, J. A. Triccas, B. Gicquel, M. Daffé, C. Guilhot, *J. Biol. Chem.* **2001**, *276*, 19845.
- [24] D. Boyall, F. López, H. Sasaki, D. Frantz, E. M. Carreira, *Org. Lett.* **2000**, *2*, 4233.
- [25] B. ter Horst, B. L. Feringa, A. J. Minnaard, *Chem. Commun.* **2007**, 489.
- [26] K. N. Flentie, C. L. Stallings, J. Turk, A. J. Minnaard, F-F. Hsu, *J. Lipid Res.* **2016**, *57*, 142.
- [27] T. A. Day, J. E. Mittler, M. R. Nixon, C. Thompson, M. D. Miner, M. J. Hickey, R. P. Liao, J. M. Pang, D. M. Shayakhmetov, D. R. Sherman, *Inf. Immun.* **2014**, *82*, 5214.
- [28] a) M. Daffé, C. Lacave, M-A. Lanéelle, G. Lanéelle, *Eur. J. Biochem.* **1987**, *167*, 155. b) M. Daffé, P. Servin, *Eur. J. Biochem.* **1989**, *185*, 157.
- [29] C. Rousseau, N. Winter, E. Pivert, Y. Bordat, O. Neyrolles, P. Avé, M. Huerre, B. Gicquel, M. Jackson, *Cell. Microbiol.* **2004**, *6*, 277.
- [30] a) M. B. Reed, P. Domenech, C. Manca, H. Su, A. K. Barczak, B. N. Kreiswirth, G. Kaplan, C. E. Barry III, *Nature* **2004**, *431*, 84. b) D. Sinsimer, G. Huet, C. Manca, L. Tsenova, M-S. Kool, N. Kurepina, B. Kana, B. Mathema, S. A. E. Marras, B. N. Kreiswirth, C. Guilhot, G. Kaplan, *Infect. Immun.* **2008**, *76*, 3027.
- [31] N. Simonney, P. Chavanet, C. Perronne, M. Leportier, F. Revol, J-L. Herrmann, P. H. Lagrange, *Tuberculosis* **2007**, *87*, 109.

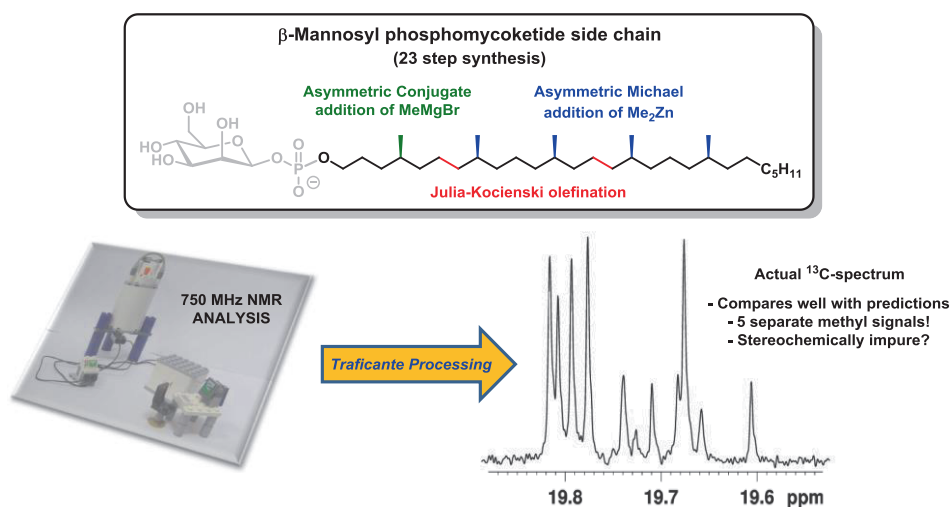
- [32] M. Gilleron, S. Stenger, Z. Mazorra, F. Wittke, S. Mariotti, G. Bohmer, J. Prandi, L. Mori, G. Puzo, G. De Libero, *J. Exp. Med.* **2004**, *199*, 649.
- [33] D. C. Barral, M. B. Brenner, *Nat. Rev. Immunol.* **2007**, *7*, 929.
- [34] J. Guiard, A. Collmann, L. F. Garcia-Alles, L. Mourey, T. Brando, L. Mori, M. Gilleron, J. Prandi, G. De Libero, G. Puzo, *J. Immunol.* **2009**, *182*, 7030.
- [35] J. Guiard, A. Collmann, M. Gilleron, L. Mori, G. De Libero, J. Prandi, G. Puzo, *Angew. Chem. Int. Ed.* **2008**, *47*, 9734.
- [36] D. Geerdink, B. J. ter Horst, M. Lepore, L. Mori, G. Puzo, A. K. H. Hirsch, M. Gilleron, G. de Libero, A. J. Minnaard, *Chem. Sci.* **2013**, *4*, 709.
- [37] B. ter Horst, B. L. Feringa, A. J. Minnaard, *Org. Lett.* **2007**, *9*, 3013.
- [38] K. Geurts, S. P. Fletcher, B. L. Feringa, *J. Am. Chem. Soc.* **2006**, *128*, 15572.
- [39] F. Lopez, A. W. van Zijl, A. J. Minnaard, B. L. Feringa, *Chem. Commun.* **2006**, 409.
- [40] D. Geerdink, *Total synthesis of enantiopure lipids; on mycobacterial glycolipids and a putative sex pheromone of Trichogramma turkestanica*, PhD dissertation, University of Groningen, **2013**.
- [41] L. T. Kliman, S. N. Mlynarski, J. P. Morken, *J. Am. Chem. Soc.* **2009**, *131*, 13210.
- [42] a) L. J. Ingram, A. Desoky, A. M. Ali, S. D. Taylor, *J. Org. Chem.* **2009**, *74*, 6479. b) A. Y. Desoky, S. D. Taylor, *J. Org. Chem.* **2009**, *74*, 9406.
- [43] a) M. C. Pischl, C. F. Weise, M-A. Müller, A. Pfaltz, C. Schneider, *Angew. Chem. Int. Ed.* **2013**, *52*, 8968. b) R. Rasappan, V. K. Aggarwal, *Nat. Chem.* **2014**, *6*, 810. c) S. Balieu, G. E. Hallett, M. Burns, T. Bootwicha, J. Studley, V. K. Aggarwal, *J. Am. Chem. Soc.* **2015**, *137*, 4398. d) S. Xu, A. Oda, T. Bobinski, H. Li, Y. Matsueda, E-I. Negishi, *Angew. Chem. Int. Ed.* **2015**, *54*, 9319.
- [44] D. Geerdink, A. J. Minnaard, *Chem. Commun.* **2013**, *50*, 2286.
- [45] a) M. B. Goren, *Biochim. Biophys. Acta* **1970**, *210*, 116. b) M. B. Goren, *Biochim. Biophys. Acta* **1970**, *210*, 127. c) M. B. Goren, O. Brokl, B. C. Das, E. Lederer, *Biochemistry* **1971**, *10*, 72.
- [46] S. A. Gilmore, M. W. Schelle, C. M. Holsclaw, C. D. Leigh, M. Jain, J. S. Cox, J. A. Leary, C. R. Bertozzi, *ACS Chem. Biol.* **2012**, *7*, 863.
- [47] J. E. Vance, *J. Lipid Res.* **2008**, *49*, 1377.
- [48] B. ter Horst, C. Seshadri, L. Sweet, D. C. Young, B. L. Feringa, D. B. Moody, A. J. Minnaard, *J. Lipid Res.* **2010**, *51*, 1017.
- [49] C. Smit, M. W. Fraaije, A. J. Minnaard, *J. Org. Chem.* **2008**, *73*, 9482.
- [50] P. Fodran, A. J. Minnaard, *Org. Biomol. Chem.* **2013**, *11*, 6919.





## \*\*\* CHAPTER 2 \*\*\*

### ‡ *Synthesis and Analysis of Mycoketide: A Test of NMR Predictions for Saturated Oligoisoprenoid Stereoisomers* ‡



**ABSTRACT:** This chapter describes the asymmetric synthesis and NMR analysis of the side chain of  $\beta$ -mannosyl phosphomycoketide, a natural product from *Mycobacterium tuberculosis*. Mycoketide, containing a 1,5-methyl ramification with the five stereocenters exhibiting an all-syn relationship, was subjected to NMR analysis and compared to predicted spectra of all possible diastereoisomers. The resolution of empirical NMR data was enhanced by Traficante processing which allowed detailed analysis of the 1,5-methyl array. Comparison of the predicted and actual NMR spectra of mycoketide allowed us to unambiguously assess the relative stereochemistry and isomeric purity.

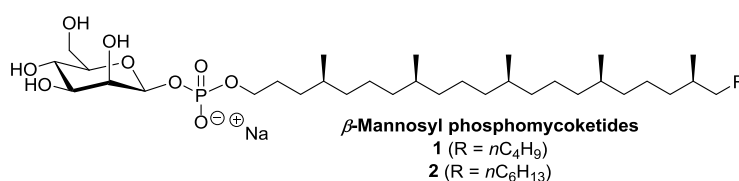
Part of this chapter has been published:

J. Buter, E. A-H. Yeh, O. W. Budavich, K. Damodaran, A. J. Minnaard, D. P. Curran, *J. Org. Chem.* **2013**, 78, 4913.

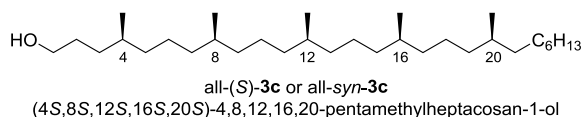
The work in this chapter is the result of a collaboration with the Curran laboratory (Pittsburgh University) who performed the NMR-studies of the provided synthetic material.

## 2.1 Introduction

$\beta$ -Mannosyl phosphomycoketides (MPMs) **1** and **2** (Figure 1a) are potent T-cell antigens produced by *Mycobacterium avium* and *Mycobacterium tuberculosis*.<sup>[1]</sup> The MPMs are composed of  $\beta$ -D-mannose and a long, aliphatic chain linked together as a phosphate diester. In the MPM biosynthesis, the polyketide side chain is formed from a fatty acid precursor by repetitive incorporation of malonyl and methyl malonyl CoA followed by full reduction. Although MPM's side chains have a polyketide origin, a large part of the chain **3c** (C2–C21) bears methyl groups on every fourth carbon and therefore resembles a saturated oligoisoprene. In polymer terminology, such repeat units are also called alternating propylene/ethylene co-oligomers or 1-methyltetramethylene oligomers.<sup>[2]</sup> Rigorously assigning the configuration of the five stereocenters of such oligomers is difficult.

(a) Naturally occurring  $\beta$ -Mannosyl phosphomycoketides:

## (b) The mycoketide side chain, in its natural configuration:



## (c) Homologous series of saturated polyisoprenoids

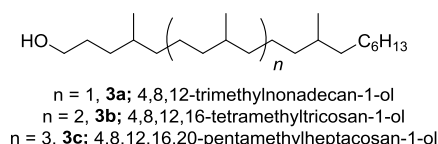


**Figure 1.** Structures of  $\beta$ -mannosyl phosphomycoketide and its side chains.

Crich *et al.* intentionally synthesized a mixture of MPMs **1** (R =  $n\text{C}_4\text{H}_9$ ) with complete stereocontrol of the mannosyl anomeric center but with all possible configurations of the methyl-branched stereocenters.<sup>[3]</sup> Analysis of this mixture of 32 stereoisomers confirmed the constitution of **1**. Our laboratory more recently synthesized a pentamethylheptacosan-1-ol side chain with all five methyl-branched stereocenters in the (*S*)-configuration (all-(*S*)-**3c**, Figure 1b) and coupled this to  $\beta$ -mannose phosphate to make MPM **2** (R =  $n\text{-C}_6\text{H}_{13}$ ).<sup>[4]</sup> This sample was assayed against Crich's mixture and a

natural product sample and exhibited activity similar to that of the natural isolate.<sup>[5]</sup> The stereorandom mixture was found to be considerably less active.

The five stereocenters in the side chains of **1** and **2** are biosynthesized in an iterative way by the polyketide synthase pks12 and therefore presumably have the same configuration.<sup>[1,6]</sup> This means that the 1,5-relative configurations of the methyl-branched stereocenters are *syn*. Of the two remaining configurations, all stereocenters (*R*) or all (*S*), the results of the bioassays support the all-(*S*) assignment of **2**.<sup>[4a,5]</sup> In addition, the crystal structure of all-(*S*)-MPM **2** bound to CD1c has been reported recently.<sup>[7]</sup> However, assignment of the absolute configuration as all-(*S*) contradicts a predictive model by Leadlay and co-workers, who investigated the biochemical introduction of chiral methyl groups by polyketide synthases.<sup>[8]</sup> Therefore, spectroscopic or chemical means to assess the side chain configurations is needed both to confirm the structure of the natural product and to assay structures and purities of synthetic samples.<sup>[9]</sup> Recently the Curran laboratory synthesized all four diastereomers of the truncated MPM side chain model 4,8,12-trimethylnonadecanol **3a** (Figure 1c).<sup>[10]</sup> The methyl regions of both the <sup>1</sup>H- and <sup>13</sup>C-NMR spectra of the four isomers exhibited small but reliable differences depending on whether the nearest neighbor methyl groups were *syn* or *anti*. We used the data to predict the <sup>1</sup>H- and <sup>13</sup>C-NMR spectra of all stereoisomers of higher saturated oligoisoprenoids including **3b** (8 isomers) and **3c** (16 isomers). Unfortunately, it is not possible to test these predictions retrospectively with published spectra because special conditions for processing are required to enhance resolution.

In this chapter we report the synthesis of a new sample of all-(*S*)-**3c**. Analysis of resolution-enhanced NMR spectra show that the sample is predominately all-(*S*) but also that the isomer ratio is lower than expected. Further analysis of a lower homologue prepared from synthetic intermediates suggests that the impurities arose not because an asymmetric synthesis step was compromised, but instead because of a late-stage partial epimerization. Just as the predicted spectra help to analyze the experimental spectra, the reverse is also true. The new chemical shift values obtained from the experimental spectra help to refine and expand the NMR model.

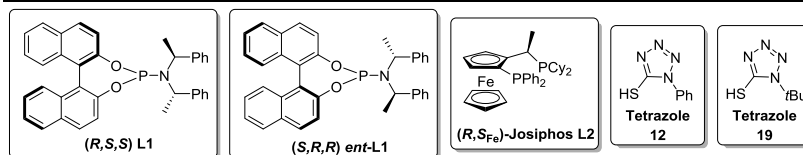
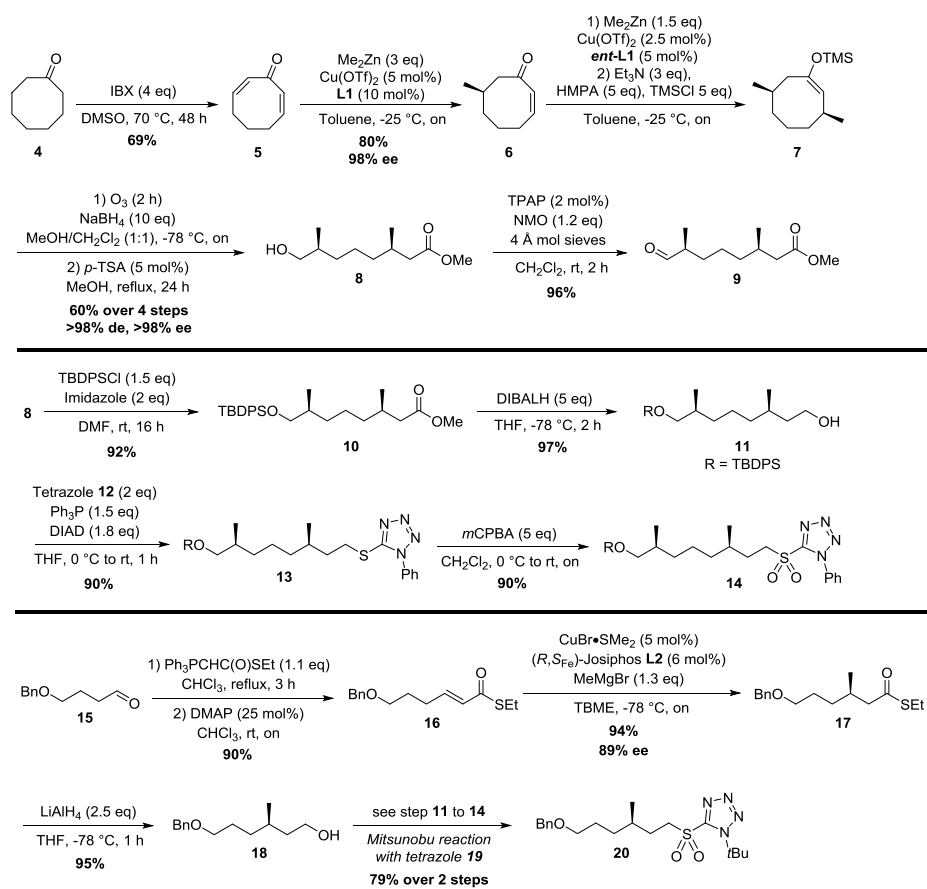
## 2.2 Synthesis of the $\beta$ -mannosyl phosphomycoketide side chain

To facilitate the NMR studies envisioned, we needed to synthesize a new sample of **3c** as no synthetic material from the previous endeavor was available.<sup>[4a]</sup> The synthesis started with the construction of three key intermediates, chiral building blocks **9**, **14**, and **20** (Scheme 1) and relied heavily on the asymmetric conjugate addition strategy developed by the Feringa laboratory. Consecutive, asymmetric Cu-catalyzed Michael addition of Me<sub>2</sub>Zn to dienone **5** using phosphoramidite **L1** and its enantiomer *ent*-**L1** respectively, provided after quenching with TMSCl silyl enol ether **7**. An ozonolysis with oxidative work-up was performed and subjected to a Fischer esterification to provide acyclic methyl ester **8** (64% yield over the 4 steps).<sup>[11a]</sup> At this stage the asymmetric induction was analyzed to exceed a diastereomeric and enantiomeric excess

## CHAPTER 2

of 98%.<sup>[11b]</sup> Oxidation of **8** with TPAP afforded our first asymmetric building block **9** in 96% yield.

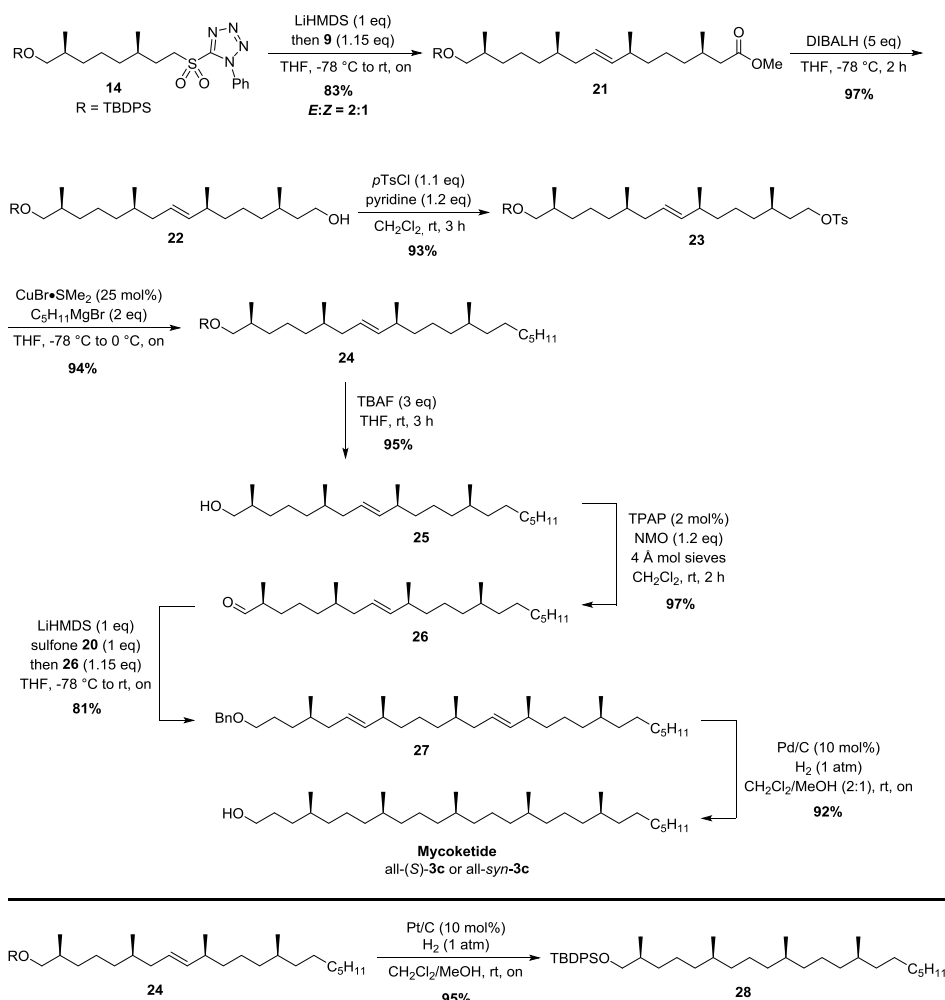
Compound **8** was also used in the synthesis of sulfone **14**, our second asymmetric building block. Its construction started with silyl protection of the free alcohol in **8**. Reduction of the methyl ester was followed by a Mitsunobu reaction with thiotetrazole **12** to afford sulfide **13**. The sulfur atom was then oxidized affording **14** in 72% yield over the four steps.



**Scheme 1.** Asymmetric synthesis of the mycoketide side chain building blocks **9**, **14**, and **20**.

The final building block to be crafted before unification was sulfone **20** bearing one stereocenter. After synthesis of  $\alpha,\beta$ -unsaturated **16** the methyl group was introduced

using an asymmetric conjugate addition of MeMgBr, catalyzed by copper/Josiphos **L2**. Compound **17** was obtained with 89% *ee* in 94% yield. Full reduction of the thioester with LiAlH<sub>4</sub> and subsequently the Mitsunobu/oxidation sequence furnished asymmetric building block **20**.



**Scheme 2.** Unification of the building blocks in the synthesis of mycoketide all-(S)-3c.

With the desired building blocks in hand the unification was performed to construct the mycoketide side chain all-*syn*-3c (Scheme 2). A Julia-Kocienski<sup>[12]</sup> coupling between aldehyde **9** and sulfone **14** was performed to construct alkene **21**. The ester was reduced to the alcohol (**22**), which was converted into a good leaving group, by means of a tosylation, to then introduce the *n*-pentyl group. Compound **24** was liberated from its protecting group to give after a Ley-Griffith oxidation aldehyde **26**. Another Julia-

Kocienski olefination, this time with chiral building block **20**, was used to install the final stereogenic methyl unit. Dialkene **27** was thus obtained which after global hydrogenation and hydrogenolysis gave the desired all-*syn* mycoketide **3c**.

Additionally we also constructed late-stage derivative **28**, which is a phytanyl-type oligoisoprenoid with a silyl-protected hydroxy group on the left end and four repeating stereocenters. Compound **28** was isomerically pure (*vide infra*) so by implication all the reactions leading to **27** occurred with high stereoselectivity, and the so-formed stereocenters were retained with fidelity.

### 2.3 NMR analysis of $\beta$ -mannosyl phosphomycoketide side chain **3c**

To assess the structure and isomeric purity of **3c**, the observed resonances in the methyl regions of both its  $^1\text{H}$ - and  $^{13}\text{C}$ -NMR spectra were compared with recent predictions.<sup>[10]</sup> The basis for predicting the resonances of any isomer of **3c** ( $n = 3$ ) from the observed resonances of **3a** ( $n = 1$ ) is shown in figure 2. Briefly, we divide the spectrum into three parts, the left-end, the middle, and the right-end, and then add in resonances of the methyl branches from the model set (all isomers of **3a**) that have the appropriate stereochemical relationship to match those in **3c**. End Me groups can be *syn* or *anti*, while middle ones can be *syn/syn*, *anti/anti*, or *anti/syn* (or *syn/anti*).

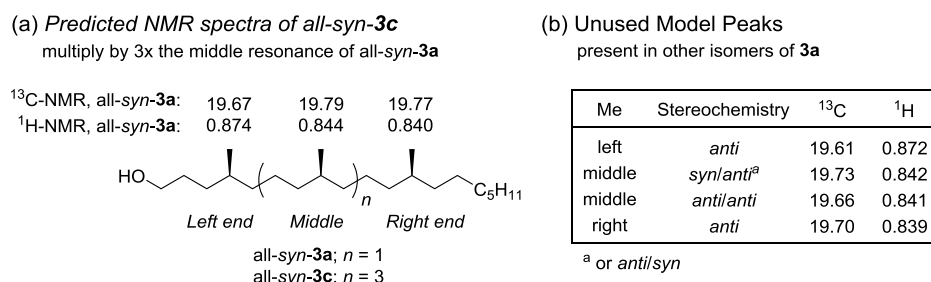


**Figure 2.** Basis for predictions of NMR spectra of all-*syn*-**3c** and its stereoisomers.

To predict a spectrum of the all-*syn* isomer of **3c** (all-*(S)*-**3c** or all-*(R)*-**3c**), we simply take the spectrum of all-*syn* **3a** and multiply the middle resonances by three (because all three middle Me groups have *syn/syn* relationships), as shown in figure 2a. Figure 2b lists the remaining resonances from the complete model set. These are not used for all-*syn*-**3c** but are needed to predict spectra of its stereoisomers.

Standard spectra of all-*syn*-**3c** were first recorded in the usual way at 400 MHz. These compared favorably to the spectra of the prior sample<sup>[4a]</sup> but as expected did not provide information about isomer identity or purity. New sets of spectra were then recorded at 700 MHz for  $^1\text{H}$  and 175 MHz for  $^{13}\text{C}$ , and the data sets were processed by the Traficante algorithm<sup>[13]</sup> for resolution enhancement.

In its essence the Traficante algorithm is an apodization (“*changing the shape of a mathematical function*”) which deemphasizes the tail of the free induction decay (FID). The use of the “transform of reverse added FIDs” (TRAF) algorithm allows the

enhancement of resolution of the recorded NMR spectrum with little to no decrease in signal-to-noise ratio. As exemplified in figure 3, a dramatic increase of spectral detail can be obtained for the Traficante algorithm treated FID (black spectrum) compared to a regular processed FID (red spectrum). As we will also show for all-*syn*-**3c** (*vide infra*) the increased resolution allowed the assessment of stereochemical purity for synthetic all-*syn*-**3a**.<sup>[10]</sup>

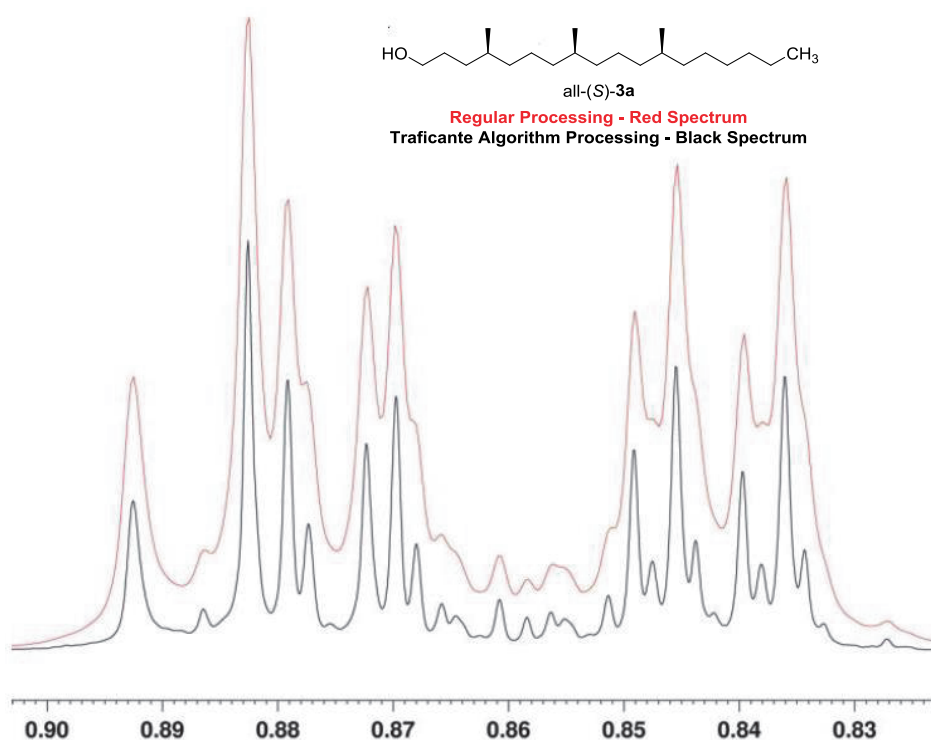


**Figure 3.** A direct comparison of the methyl region in the  $^1\text{H-NMR}$  spectrum of synthetic **3a**<sup>[10]</sup> showing the regular (**red**) vs. Traficante algorithm (**black**) processed spectrum. Notice the dramatic increase in spectral resolution allowing detailed analysis (Reproduced from reference 10b).

Figure 4a,b shows the methyl regions of the  $^{13}\text{C}$ - and  $^1\text{H-NMR}$  spectra of all-*syn*-**3c**, both predicted (bottom spectrum) and actual (top spectrum). Importantly, the use of Traficante processing renders the spectra of such samples interpretable for the first time! The predicted  $^{13}\text{C-NMR}$  spectrum of all-*syn*-**3c** (Figure 4a, bottom) shows three resonances: the left-end Me resonates at 19.67 ppm, while the right-end Me resonates at 19.77 ppm. The predicted chemical shift of the three middle methyl groups (on C8, C12, C16) is 19.79 ppm, with a relative intensity of three.



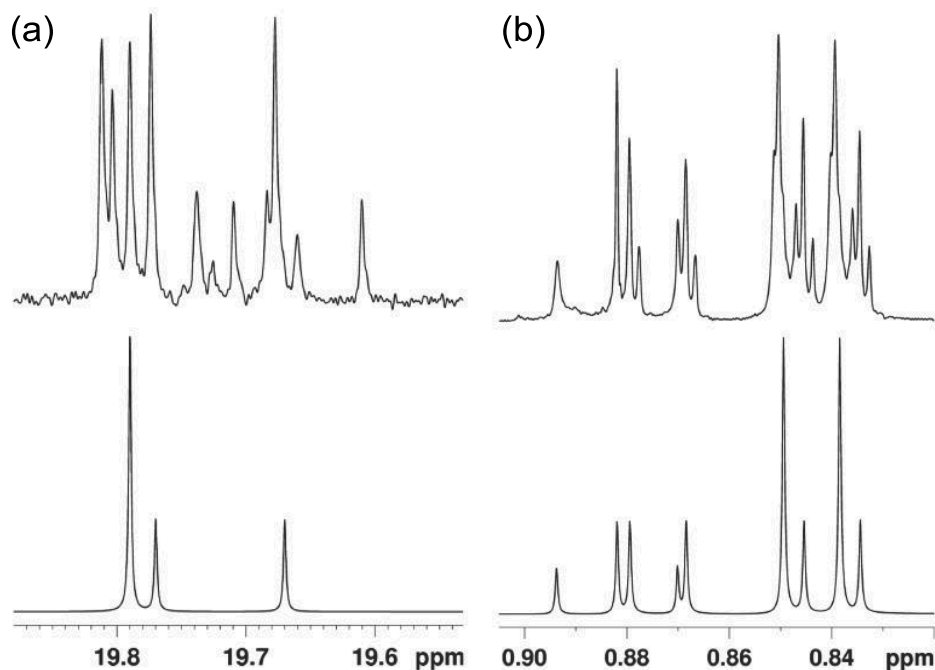


**Figure 4.** Comparison of the predicted and the experimental NMR spectra of the branched methyl group region for all-*syn*-**3c**. (a) actual (top) and predicted (bottom)  $^{13}\text{C}$ -NMR spectra of **3c**. (b) actual (top) and predicted (bottom)  $^1\text{H}$ -NMR spectra of **3c**.

The experimentally obtained  $^{13}\text{C}$ -NMR spectrum (Figure 4a, top) is at first glance much more complex. There are 10 resonances grouped in two sets of five with a ratio of about 70/30. Thus, the sample is not isomerically pure. Three of the five resonances of the major set (19.79, 19.77, and 19.67 ppm) match perfectly (<10 ppb difference) to the predicted resonances. The two most downfield major resonances at 19.80 and 19.81 ppm are slightly downfield from their predicted location at 19.79 ppm. We compared the major set of resonances in the experimental spectrum of all-*syn*-**3c** to the predicted spectra of all 16 isomers of **3c**,<sup>[10]</sup> and none matches as well as the spectrum of the all-*syn*-isomer. Thus, we conclude that the five major resonances in the actual spectrum in figure 4a belong to all-*syn*-**3c**. This means that the predicted spectrum in figure 4a is only partially correct. Because the model **3a** is too simple (it has only one middle unit), it cannot anticipate the very small differences in chemical shifts of the three “repeating” methyl groups in the middle of all-*syn*-**3c**. Indeed, given their chemical and stereochemical similarity, it is remarkable that separate resonances for these methyl groups are observed. The methyl regions of the predicted and experimental  $^1\text{H}$ -NMR spectra of all-*syn*-**3c** are shown in figure 4b. The predicted spectrum is again simpler than the actual one. Now there is an additional resonance; the triplet at 0.882 ppm is the terminal methyl group (C29 on the far right end). This triplet has the same predicted chemical shift in all of the isomers, so its value is not diagnostic. This leaves three

major doublets in a ratio of 1:3:1 for the five branched Me groups of the major isomers. The smaller ones at 0.874 and 0.840 ppm are the left and right-end methyl groups. As in the predicted  $^{13}\text{C}$ -NMR spectrum, the three middle methyl groups overlap, now at 0.844 ppm. The major resonances of the spectrum match the predictions of the all-*syn* isomer closely. Again, the match is clearly the best among all 16 predicted spectra.<sup>[10]</sup> The experimental  $^1\text{H}$ -NMR spectrum again has a minor set of resonances; at least three minor doublets can be seen in the 1D spectrum. To find the other two minor resonances and to correlate all the resonances, we conducted a  $^1\text{H}$ - $^{13}\text{C}$  COSY experiment. Figure 5 shows two slices of the resulting spectrum: plot (a) is a higher slice that shows only the cross resonances of the five major resonances, while plot (b) is a lower slice that shows both sets, but only the five minor cross resonances are highlighted.

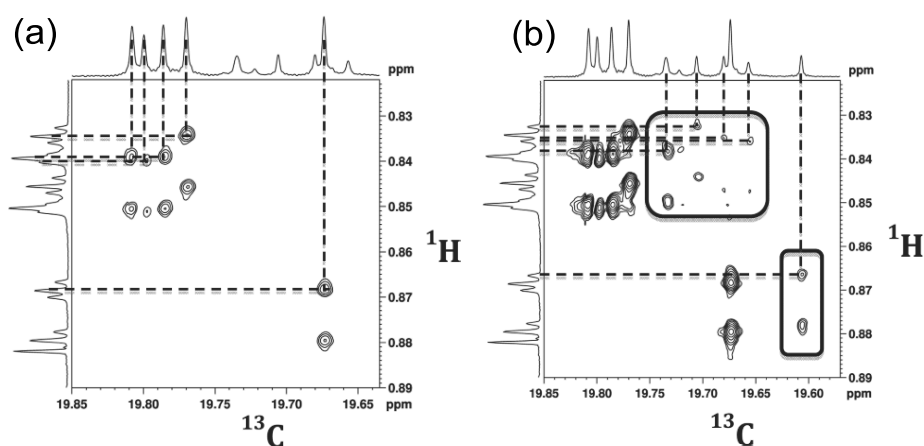


**Figure 5.** The branched methyl region of the  $^1\text{H}$ - $^{13}\text{C}$  COSY of all-*syn* **3c**. (a) a higher slice that shows only major cross resonances. (b) a lower slice with minor cross resonances highlighted.

All of the major resonances correlate as predicted by the model in figure 2a, thus reinforcing the assignment of the major component of **3c** as all-*syn*. The reason that the largest doublet at 0.844 ppm in the  $^1\text{H}$ -NMR spectrum also appears to be further resolved into three resonances is revealed. The right shoulder comes from a minor isomer, correlated at 19.73 ppm in the  $^{13}\text{C}$  spectrum, while the left shoulder comes from one of the middle carbons of the major isomer correlated at 19.81 ppm. The large center part correlates to the other two middle methyl groups in the major isomer at 19.80 and 19.79 ppm. So in the  $^1\text{H}$ -NMR spectrum, the prediction that three middle methyl groups of all-*syn*-**3c** would coincide is again wrong, but only just. This time, two resonances coincide, while the third is a smidge downfield ( $\sim 1$  ppb), appearing as a shoulder on the other two.

In contrast to the clear situation with the major set of five resonances, assignment of the minor set of five resonances is not straightforward. Four of the  $^{13}\text{C}$  and  $^1\text{H}$  resonances correspond well to other resonances predicted by the model (see unused resonances in

Figure 2b): 19.73/0.842 ppm is a middle methyl group with a *syn/anti* (or *anti/syn* relationship) to its neighbors; 19.70/0.839 ppm is the right methyl group with an *anti* neighbor; 19.66/0.841 ppm is a middle methyl group with an *anti/anti* relationship; and 19.61/0.872 ppm is left methyl group with an *anti* neighbor. There is also a minor signal at 19.68 ppm in the  $^{13}\text{C}$ -NMR that is not in the model set. This signal is only 10 ppb downfield from model signal 19.67, a left methyl group with a *syn* neighbor. However, if this assignment were correct, then that  $^{13}\text{C}$  signal should correlate to a  $^1\text{H}$  resonance at 0.874 ppm. Instead, it correlates to a resonance at 0.842 ppm.

In short, the major isomer in the new sample of **3c** is clearly the all-*syn* isomer. However, because of the simplicity of the model (it provides only seven resonances for all resonances in all possible isomers), we cannot yet assign the minor resonances. If they come from a single isomer, then one of the resonances (19.68 ppm) is poorly predicted in the  $^{13}\text{C}$ -NMR spectrum. If they come from a mixture of isomers, then there must be other minor resonances under the major resonances in varying ratios, so direct interpretation is not easy.

## 2.4 NMR analysis of $\beta$ -mannosyl phosphomycoketide side chain

We next conducted a series of experiments trying to localize the stage of the synthesis where the minor isomer(s) originated. Small samples of key intermediates saved during the synthesis, especially the sample of **24** (Scheme 1), proved very helpful. This alkene could not be analyzed directly for stereochemical integrity because it already contains *E:Z* isomers from the Julia–Kocienski reaction. So about 2 mg of **24** was carefully hydrogenated (Pt,  $\text{H}_2$ ,  $\text{CH}_2\text{Cl}_2/\text{MeOH}$ ) to make a sample of **28** whose spectra were recorded as above.

The predicted spectrum of all-*syn*-**3b** was used for comparison, and the structures of **3b** and **28** are compared in figure 6. Notice that while the right-end and middle fragments of **28** and all-*syn*-**3b** are the same, the left-end fragment is different. Sample **28** has two carbon atoms less than model **3b** at the left end, and its hydroxy group is protected with a TBDPS (*tert*-butyldiphenylsilyl) ether. Clearly the predicted left-end resonances for all-*syn*-**3b** cannot be applied to the left end of **28**.

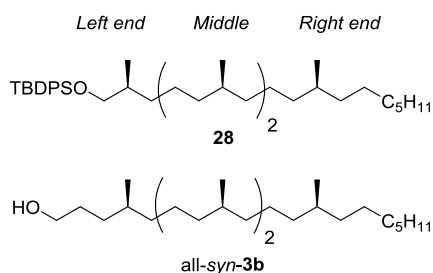


**Figure 6.** Predicted spectra of all-*syn*-**3b** are used to interpret the actual spectra of **28**. Only the middle and right-end predictions can be used because the left ends are different.

The methyl region of the experimental  $^1\text{H}$ -NMR spectrum of **28** is shown in figure 7 (left spectrum). There is only one set of resonances: four doublets and one triplet (the terminal methyl group on the end of the chain, C21). The resonances were assigned by 2D-NMR experiments, and these assignments are collected in table 1. Likewise, the  $^{13}\text{C}$ -NMR spectrum showed one set of resonances (right spectrum in Figure 7 and Table 1). Clearly this sample is a single isomer. To assign the configuration of **28**, we compared the predicted methyl resonances of all-*syn* **28** with the actual resonances, as summarized in table 1. The observed resonances for the left-end methyl group ( $\text{Me}^{22}$ ) appear at 0.917 ppm in the  $^1\text{H}$ -NMR spectrum and 16.99 ppm in the  $^{13}\text{C}$ -NMR spectrum. This pair of resonances has no equivalent in the model, but the values are not crucial to the stereochemical assignment because the chemical shifts of the next methyl group ( $\text{Me}^{23}$ ) also contain the information about whether the relationship of the two is *syn* or *anti*.

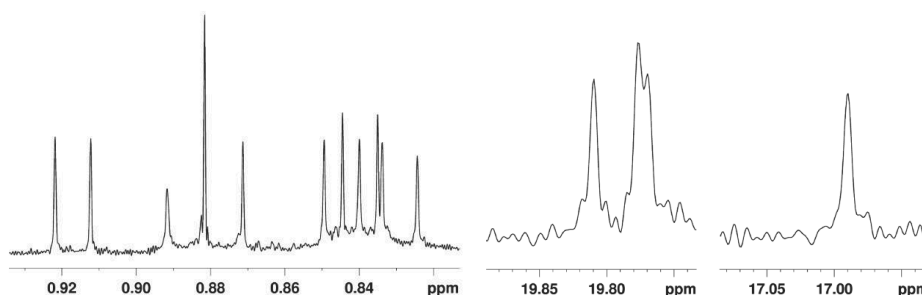
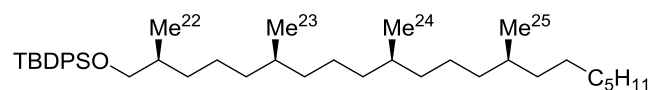


**Figure 7.** Expansions of the methyl regions of the  $^1\text{H}$ - (left) and  $^{13}\text{C}$ -NMR spectra (right) of **28**. The  $^1\text{H}$ -NMR expansion contains the terminal methyl group ( $\text{C}^{21}$ ) resonance, the  $^{13}\text{C}$ -NMR spectrum does not.

Now compare (see table 1) the predicted and actual resonances for the remaining Me groups ( $\text{Me}^{23}$ ,  $\text{Me}^{24}$ , and  $\text{Me}^{25}$ ) in structure **28**, starting at the right end of the molecule. In both the  $^1\text{H}$ - and the  $^{13}\text{C}$ -NMR spectra, the actual and predicted resonances for the right-end methyl group ( $\text{Me}^{25}$ ) and its neighbor ( $\text{Me}^{24}$ ) are spot on or almost spot on. At 0.830 ppm ( $^1\text{H}$ ) and 19.76 ( $^{13}\text{C}$ ) ppm, the actual resonances of the next methyl group in ( $\text{Me}^{23}$ ) are slightly different from both  $\text{Me}^{24}$  and the prediction. As above, this is again a deficiency of the model, which provides only a single middle resonance that is used to model both  $\text{Me}^{23}$  and  $\text{Me}^{24}$ . It is sensible that the model is spot on for  $\text{Me}^{24}$ , which is further away from the left end (the part that differs between the model and the actual sample), and slightly off for  $\text{Me}^{23}$ , which is closer to the left end.

The values of the experimental  $^1\text{H}$ -NMR spectra of **28** in table 1 are much closer to the predicted values for the all-*syn* isomer of **3b** than to any of the other seven isomers.<sup>[10]</sup> Thus, both the relative configuration of the sample (all-*syn*) and the high level of purity ( $\geq 95\%$ ) are confirmed.



Resonance	$^1\text{H}$		$^{13}\text{C}$	
	obs.	pred.	obs.	pred.
Me <sup>22</sup>	0.917	<i>a</i>	16.99	<i>a</i>
Me <sup>23</sup>	0.830	0.844 <sup><i>b</i></sup>	19.76	19.79 <sup><i>b</i></sup>
Me <sup>24</sup>	0.845	0.844 <sup><i>b</i></sup>	19.80	19.79 <sup><i>b</i></sup>
Me <sup>25</sup>	0.840	0.840 <sup><i>c</i></sup>	19.76	19.77 <sup><i>c</i></sup>

<sup>a</sup> The model does not predict the left-end resonance

<sup>b</sup> Middle resonance, see figure 2. <sup>c</sup> Right-end resonance, see figure 2

**Table 1.** Comparison of methyl resonances of the actual spectra of **28** with predicted resonances for the all-*syn* isomer of **28** derived from the predicted spectra of all-*syn* **3b**; Data in ppm.

These experiments show that the four stereocenters of key synthetic intermediate **24** are intact and have the configurations predicted by the various asymmetric reactions used to introduce them (Scheme 1). Thus, the minor stereoisomer(s) in sample **3c** must have formed in a late stage of the synthesis, during or after the coupling of the last two fragments **20** and **26** (Scheme 2). Primary candidate steps for the epimerization are the Julia–Kocienski reaction (the aldehyde reactant has an adjacent stereocenter) and the final hydrogenation reaction (alkene migration to form a trisubstituted double bond, prior to hydrogenation, results in loss of stereointegrity).<sup>[14]</sup>

Finally, this exercise establishes a new left-end model compound with a CH<sub>2</sub>OTBDPS group from which spectra of saturated isoprenoids and related reduced polyketides can be predicted. Compounds such as **28** terminating in CH<sub>2</sub>OTBDPS on the left end will have a chemical shift of 0.830 and 19.76 ppm for the left-end methyl group (Me<sup>22</sup>) if it is *syn* to the next methyl group (Me<sup>23</sup>). On the basis of the established trends with **3a**, we predict that Me<sup>22</sup> will resonate a little further upfield in both the  $^1\text{H}$ - and  $^{13}\text{C}$ -NMR spectra if it is *anti* to Me<sup>23</sup> (about 2 and 60 ppb, respectively, see Figure 2). From the chemical shifts in table 1, small upfield adjustments also need to be made for the resonances of Me<sup>23</sup> in the *syn/syn* isomer to predict the spectra of isomers with this group *syn/anti* (or *anti/syn*) and *anti/anti* to Me<sup>22</sup>/Me<sup>24</sup>. The magnitudes of the adjustments can again be estimated from the values for the analogous middle methyl groups in figure 2.

These new resonances can be added to the existing middle (used for Me<sup>24</sup>) and right (used for Me<sup>25</sup>) resonances in figure 2 to fill out predicted spectra for any isomer of **28** or a higher oligomer. Because the model **28** has four resonances, every isomer of **28** (or a higher oligomer) will also have four predicted resonances. This is an improvement over the use of **3a** to model **3b** and **3c**, where two or three middle Me groups have the same predicted chemical shift in some isomers, even though in reality there are small differences.

## 2.5 Conclusions

In summary, for the first time it has been possible through NMR spectroscopy both to assess isomer purity and to assign relative configurations of saturated oligoisoprenoids such as **3c**. Predictions of the methyl regions of the  $^1\text{H}$ - and  $^{13}\text{C}$ -NMR spectra of all 16 stereoisomers of **3c** enabled this analysis.<sup>[10]</sup> The predicted  $^1\text{H}$ -NMR spectrum of all-*syn*-**3c** is very close to the actual spectrum, but the predicted  $^{13}\text{C}$ -NMR spectrum proved to be too simple in one aspect: the three resonances from the middle methyl groups were predicted to coincide because they all have the *syn/syn* relationship, but they did not. However, the observed differences between predicted and actual spectra were small compared to the differences expected for other stereoisomers, so the value of the  $^{13}\text{C}$ -NMR predictions was not compromised.

The analysis of the synthetic sample of **3c** showed that the all-*(S)* (all-*syn*) isomer was indeed the major component, present to the extent of about 70%. Unexpectedly, a minor stereoisomer component (or components) was present to the extent of about 30%. We cannot yet identify the minor component or pinpoint where it was introduced. However, by similar comparison of actual and predicted spectra, we could show that **28** (derived from a key synthetic intermediate **24** bearing four of the five stereocenters) is both pure (>90%) and has the expected all-*(S)* configuration. This narrows the source of the problem to the last few steps of the synthesis.

Perhaps most importantly, the values from the predicted spectra of compounds like **3c** can now be leveraged to related compounds bearing different right or left ends. As an example, intermediate **28** with four stereocenters has a left end different from that of **3a-c**. Even though we only made one of the eight possible stereoisomers of **28**, we can now combine the new data obtained for **28** with the data for **3a** to assemble predicted spectra of the other seven isomers of **28** and its higher oligomers. This ability to directly analyze complex, saturated oligoisoprenoids is a powerful tool to clarify a heretofore cloudy situation with respect to stereoisomer structure and purity of synthetic and natural samples.

## 2.6 Discussion

The unfortunate loss of stereochemical purity during the course of the synthesis was an initial setback. This result however allowed us to show application of the method in assessment of stereochemical purity of synthetic MPM side chain **3c**. Shortly after our publication of the content within this chapter, Piccirilli and co-workers reported an alternative asymmetric synthesis of  $\beta$ -mannosyl phosphomycoketide.<sup>[15]</sup> Aware of our NMR analysis method the authors confirmed the stereochemical purity of their synthesized  $\text{C}_{32}$ -mycoketide, showing the ease of use, and direct application of the methodology.

The stereopurity issues in our synthesis potentially raises questions about our previous synthesis of  $\beta$ -mannosyl phosphomycoketide in 2006.<sup>[4]</sup> Despite the loss of stereochemical purity in the present case, we do not have doubts about our claims

regarding the overall stereochemical purity of  $\beta$ -mannosyl phosphomycoketide produced in 2006. The latter synthetic product was subjected to biological studies in which the material exhibited equal antigenic T-cell response to that of the natural isolate. In the same study a stereorandom mixture of MPMs was shown to be significantly less potent ( $\sim 30$  times less). Additionally it was reported that T-cell response was even dependent on the stereochemistry of the C4-methyl, where (*S*)-stereochemistry proved to be dramatically more active than the (*R*)-isomer. The study therefore indicates a strong influence of the lipid stereochemistry, more specifically the methyl ramification, on T-cell response. The biological evaluation of the 2006 produced natural product therefore indicates a high stereochemical purity of the synthetic material.

### 2.7 Studies on the stereochemistry of crenarchaeol (*ongoing studies*)

The use of Traficante-processed high-field NMR data, together with the produced set of predictions of chemical shifts was useful in the stereochemical assessment of the 1,5-methyl ramification of synthetic material. However, the potential of this method is far from fully exploited and we reasoned that this method might be helpful, that is without synthetic reference material, in the structural assignment of complex natural saturated oligoisoprenoids. We therefore set out to find a molecule of sufficient complexity, arriving at crenarchaeol (Figure 8).<sup>[16]</sup>

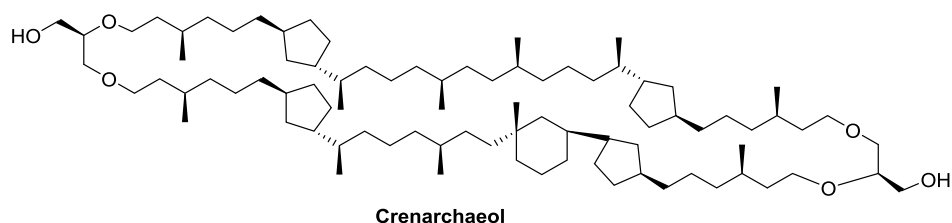


**Figure 8.** *The molecular architecture of crenarchaeol.*

Crenarchaeol is a complex membrane-spanning lipid found in *Archaea*, although in very low concentrations. The molecule exhibits an exquisite chemical architecture with an intriguing set of stereochemical features. Besides the obvious 1,5-methyl array, crenarchaeol also contains a 1,4-methyl relation, four cyclopentyl rings, a cyclohexyl ring, and two glycerol moieties, with a grand total of 22 stereocenters!

The excitement we experienced observing its chemical structure provided us with the idea to investigate the stereochemical elements (relative stereochemistry) in crenarchaeol using Traficante processed high field NMR spectra in combination with predicted spectra of all possible stereoisomers. Although there is no substantiated doubt about the proposed structure of crenarchaeol (Figure 8),<sup>[16]</sup> there are several reasons to, with the current state of equipment and techniques, repeat this structure elucidation. 1) Some assumptions about the stereochemistry had to be made at that time as the

spectrum was largely but not fully resolved. 2) at several points, stereochemistry was inferred in analogy with other, related, compounds but not independently established. We therefore believe that crenarchaeol is a beautiful test case of the methodology.

In this investigation we hope to gain more insight into several key questions. 1) Are we able to successfully assign the relative stereochemistry of crenarchaeol beyond reasonable doubt using this method? 2) Do the predictions match with data empirically obtained? 3) Is the Traficante processing in combination with high field NMR (750 MHz to 900 MHz) able to successfully resolve all stereochemical elements, even those of stereochemically similar methyl groups? 4) Will the data invoke revision of the previous assigned stereochemistry?

Concurrent with writing this dissertation we managed to obtain 5 mg of >95% pure crenarchaeol. This was the result of a three months isolation procedure performed in the Schouten laboratory at the NIOZ institute (Royal Netherlands Institute for Sea Research). The natural isolate was analyzed with 600 MHz and 900 MHz NMR providing us with  $^1\text{H}$ ,  $^{13}\text{C}$ , COSY, NOESY, TOCSY, HMQC, HMBC, and DEPT spectra. Momentarily the extensive data set is carefully scrutinized in collaboration with the Curran laboratory (Pittsburgh University) to independently assign the relative stereochemistry of crenarchaeol.

## 2.8 Experimentals

### General information on NMR experiments:

NMR spectra were recorded on a 700 MHz spectrometer using deuterated chloroform spiked with 1% tetramethylsilane (TMS), unless otherwise indicated. The signals are given as in parts per million ( $\delta$ , ppm) and were determined relative to the proton and carbon resonance of TMS. For the resolution-enhanced spectra of **3c** and **28**, data were collected and processed as described in D. D. Traficante, G. A. Nemeth, *J. Magn. Reson.* **1987**, *71*, 237.

Copies of predicted  $^1\text{H}$  and  $^{13}\text{C}$ -NMR spectra of all stereoisomers of both **3b** and **3c** (48 spectra total) are found in the Supporting Information associated with E. A. Yeh, E. Kumli, K. Damodaran, D. P. Curran, *J. Am. Chem. Soc.* **2013**, *135*, 1577.

All the obtained and detailed NMR spectra of **3c** and **28** are available free of charge in the supporting information of: J. Buter, E. A. Yeh, O. W. Budavich, K. Damodaran, A. J. Minnaard, D. P. Curran, *J. Org. Chem.* **2013**, *78*, 4913.

### General information on the synthesis efforts:

For a detailed discussion and experimental procedure for the asymmetric total synthesis of the mycoketide side chain **3c** we like to refer to the 2005 PhD dissertation of Ruben P. van Summeren, *Total synthesis of enantiopure biomolecules: on mycolactones*,



saturated isoprenoid building blocks and  $\beta$ -mannosyl phosphomycoketides. As an alternative source references [4a], [11a] and [11b] can be consulted.

## 2.9 References

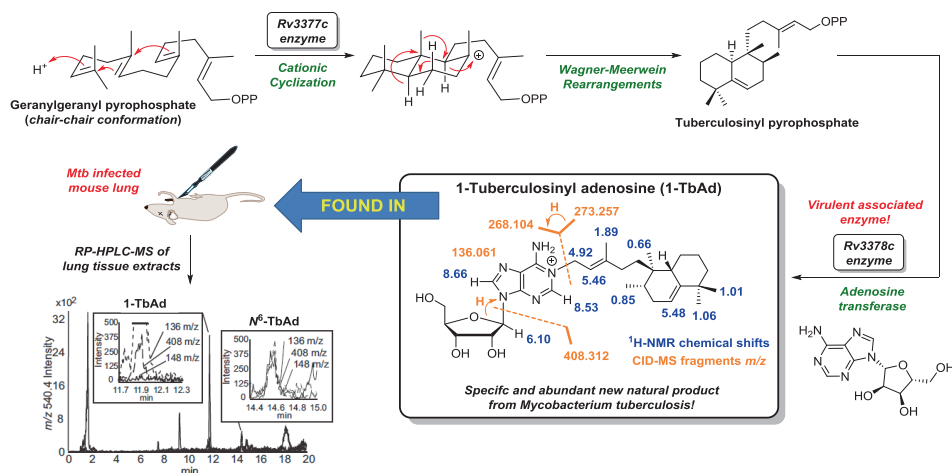
- [1] D. B. Moody, T. Ulrichs, W. Mühlecker, D. C. Young, S. S. Gurcha, E. Grant, J-P. Rosat, M. B. Brenner, C. E. Costello, G. S. Besra, S. A. Porcelli, *Nature* **2000**, *404*, 884.
- [2] L. Zetta, G. Gatti, G. Audisio, *Macromolecules* **1978**, *11*, 763.
- [3] D. Crich, V. Dudkin, *J. Am. Chem. Soc.* **2002**, *124*, 2263.
- [4] a) R. P. van Summeren, D. B. Moody, B.L. Feringa, A. J. Minnaard, *J. Am. Chem. Soc.* **2006**, *128*, 4546. b) C. Ferrer, P. Fodran, S. Barroso, R. Gibson, E. C. Hopmans, J. Sinninghe Damsté, S. Schouten, A. J. Minnaard, *Org. Biomol. Chem.* **2013**, *15*, 2482.
- [5] A. de Jong, E. C. Arce, T-Y. Cheng, R. P. van Summeren, B. L. Feringa, V. Dudkin, D. Crich, I. Matsunaga, A. J. Minnaard, D. B. Moody, *Chem. Biol.* **2007**, *14*, 1232.
- [6] I. Matsunaga, A. Bhatt, D. C. Young, T-Y. Cheng, S. J. Eyles, G. S. Besra, V. Briken, S. A. Porcelli, C. E. Costello, W. R. Jacobs, D. B. Moody, *J. Exp. Med.* **2004**, *200*, 1559.
- [7] L. Scharf, N-S. Li, A. J. Hawk, D. Garzón, T. Zhang, L. M. Fox, A. R. Kazen, S. Shah, E. J. Haddadian, J. E. Gumperz, A. Saghatelian, J. D. Faraldo-Gómez, S. C. Meredith, J. A. Piccirilli, E. J. Adams, *Immunity* **2010**, *33*, 853.
- [8] D. H. Kwan, Y. Sun, F. Schulz, H. Hong, B. Popovic, J. C. C. Sim- Stark, S. F. Haydock, P. F. Leadlay, *Chem. Biol.* **2008**, *15*, 1231.
- [9] H. Ohru, *Proc. Jpn. Acad. Ser. B* **2007**, *83*, 127.
- [10] a) E. A. Yeh, E. Kumli, K. Damodaran, D. P. Curran, *J. Am. Chem. Soc.* **2013**, *135*, 1577. b) The predicted spectra for **3b** and **3c**, and synthesis and detailed analysis of **3a** can be found in: E. A. Yeh, *Fluorous mixture synthesis (FMS) of four isomers of 4,8,12-trimethylnonadecanol and the development of an NMR-based method for determining the configurations of polyisoprenoid Structures*, PhD dissertation, **2011**.
- [11] a) R. P. van Summeren, S. J. W. Reijmer, B. L. Feringa, A. J. Minnaard, *Chem. Commun.* **2005**, 1387. b) J. Naito, S. Kuwahara, M. Watanabe, J. Decatur, P. H. Bos, R. P. Van Summeren, B. ter Horst, B. L. Feringa, A. J. Minnaard, N. Harada, *Chirality* **2008**, *20*, 1053.
- [12] P. R. Blakemore, *J. Chem. Soc., Perkin Trans. 1* **2002**, 2563.
- [13] a) D. D. Traficante, *J. Magn. Reson.* **1986**, *182*, 186. b) D. D. Traficante, G. A. Nemeth, *J. Magn. Reson.* **1987**, *71*, 237.
- [14] a) S. Dandapani, M. Jeske, D. P. Curran, *J. Org. Chem.* **2005**, *70*, 9447. b) J. F. Teichert, T. den Hartog, M. Hanstein, C. Smit, B. ter Horst, V. Hernandez-Olmos, B. L. Feringa, A. J. Minnaard, *ACS Catal.* **2011**, *1*, 309.

- [15] a) N-S. Li, L. Scharf, E. J. Adams, J. A. Piccirilli, *J. Org. Chem.* **2013**, *78*, 5970. b) N-S. Li, J. A. Piccirilli, *Tetrahedron* **2013**, *69*, 9633.
- [16] J. S. Sinninghe Damsté, S. Schouten, E. C. Hopmans, A. C. T. van Duin, J. A. J. Geenevasen, *J. Lipid Res.* **2002**, *43*, 1641.



## \*\*\* CHAPTER 3 \*\*\*

### ‡ The discovery of novel terpene nucleosides from *Mycobacterium tuberculosis* ‡



**ABSTRACT:** The discovery of new natural products from *Mycobacterium tuberculosis* is an important field of research as the natural isolates can shine light on the bacterium's survival and virulence mechanism, and are potentially applicable as chemical markers for the tuberculosis disease. This chapter describes the isolation and structure elucidation of an abundant and *Mycobacterium tuberculosis* specific lipid. In addition, the elucidation of the biosynthetic pathway of the natural isolate and its development into a chemical marker are presented. The studies were supported by a racemic chemical synthesis of the natural product, allowing unambiguous assignment of the molecular structure and its biosynthesis.

This chapter has been published in part:

E. Layre, H. J. Lee, D. C. Young, A. Jezek Martinot, J. Buter, A. J. Minnaard, J. W. Annand, S. M. Fortune, B. B. Snider, I. Matsunaga, E. J. Rubin, T. Alber, D. B. Moody, *Proc. Nat. Acad. Sci. USA*, **2014**, *111*, 2978.

D.C. Young, E. Layre, S. J. Pan, A. Tapley, J. Adamson, C. Seshadri, Z. Wu, J. Buter, A. J. Minnaard, M. Coscalla, M. Gagneux, R. Copin, J. D. Ernst, W. R. Bishai, B.B. Snider, D. B. Moody, *Chem. Biol.* **2015**, *22*, 516.

The content of this chapter resulted from a large collaboration involving several research groups, led by the Moody laboratory (Harvard medical school). All biochemical/biological work was performed by either Moody and co-workers or collaborating groups.

### 3.1 Introduction

Tuberculosis (TB) remains a leading cause of death worldwide, resulting in over 1.5 million deaths annually.<sup>[1]</sup> Surprisingly, yet no rapid, sensitive, and specific diagnostic test exists. Diagnosis based on detection of *Mycobacterium tuberculosis* (*Mtb*) in patient samples mainly relies on sputum microscopy, which is insensitive and inaccurate, or on *in vitro* culture, which is slow, insensitive and infeasible in many clinics. T-cell antigen recall tests, such as intradermal injection of purified protein derivative (the PPD-skin test, also known as the Mantoux test) or interferon- $\gamma$  release assays (IGRA) are in widespread use but give delayed results or are expensive and have suboptimal test characteristics related to sensitivity and specificity.<sup>[2]</sup> Vaccination with live Bacille Calmette–Guérin (BCG) in most parts of the world leads to antigen-specific T-cell responses, which create false-positive results, rendering the PPD test unusable in many populations. Accordingly, there is now strong consensus that developing better diagnostic tests for *M. tuberculosis* infection is the key issue for improved disease control through rapid initiation of antibiotics and categorization of patients for vaccine trials.<sup>[3]</sup>

Detection of pathogen-specific shed molecules or antigens provides rapid and specific diagnosis of many infectious diseases. Such antigen tests have long been a mainstay of diagnosis for infection by *Cryptococci*, *Legionella*, and other pathogens.<sup>[4]</sup> The strengths of antigen test technology are high diagnostic specificity and rapid detection of molecules using a simple ELISA of urine or serum.<sup>[5]</sup> Therefore, the key criterion for discovery of chemical targets for antigen tests is specific expression of the target by the disease-causing pathogen, combined with lack of expression among other microbes, especially those that are abundant in the environment or cause diseases that mimic the disease of interest. Other desirable criteria related to test sensitivity involve identifying targets with broad expression among most infecting strains in clinical settings, expression of the antigen at high concentrations, expression *in vivo* under conditions of infection, and lack of host degradation or metabolism to unrecognizable chemical forms.

In addition to antigen capture, pathogen-specific molecules can be coated onto plastic and used to detect target-specific host antibodies, functioning as a serological test. Such tests have not yet moved into widespread clinical use for TB due in part to specificity concerns that may be related to immune responses to environmental mycobacteria, mildly pathogenic mycobacteria, or live vaccine strains<sup>[6]</sup> against TB.<sup>[7]</sup>

Despite the widespread use of antigen and serological tests in other infectious diseases, neither type of test is widely used for TB. Although the urine lipoarabinomannan (LAM) enzyme-linked immunosorbent assay (ELISA) has usefulness for TB-HIV coinfection,<sup>[6]</sup> no antigen or serological test has emerged as having widespread clinical usefulness for tuberculosis. The current chemical targets for testing were chosen based on their ready availability and represent only a small fraction of the candidate small molecules that could be developed. For example, among 169 subclasses of mycobacterial lipids in the MycoMass and Lipid DB databases, more than 90% are

expressed only by mycobacteria.<sup>[8,9]</sup> Thus, the potential range of specific mycobacterial targets for diagnostics development is vast and largely unexplored.

To broadly compare the lipid profiles of virulent and avirulent mycobacteria, we took advantage of a recently validated metabolomics platform.<sup>[8]</sup> This high performance liquid chromatography–mass spectrometry (HPLC-MS) system uses methods of extraction, chromatography, and databases that are specialized for mycobacteria. After extraction of total bacterial lipids into organic solvents, HPLC-MS enables massively parallel detection of thousands of ions corresponding to diverse lipids that range from apolar polyketides to polar phosphoglycolipids. Software-based (XCMS) ion finding algorithms report reproducibly detected ions as molecular features. Each feature is a 3D data point with linked mass, retention time, and intensity values from one detected molecule or isotope. All features with equivalent mass and retention time from two bacterial lipid extracts are aligned, allowing pairwise comparisons of MS signal intensity to enumerate molecules that are overproduced in one strain with a false-positive rate below 1%.<sup>[8]</sup>

This comparative lipidomics system allowed an unbiased, organism-wide analysis of lipids from *M. tuberculosis* and the attenuated vaccine strain, *Mycobacterium bovis* Bacillus Calmette–Guérin (BCG). BCG was chosen because of its worldwide use as a vaccine and its genetic similarity to *M. tuberculosis*.<sup>[10]</sup> These two species are evolutionarily related and share more than 99% sequence identity but only *M. tuberculosis* causes widespread disease. We reasoned that any features that are specifically detected in *M. tuberculosis* might be clinically useful as markers to distinguish tuberculosis-causing bacteria from vaccines. Furthermore, given the differing potential for productive infection by the two strains, any *M. tuberculosis*-specific compounds would be candidate virulence factors. Comparative genomics of *M. tuberculosis* and BCG successfully identified “regions of deletion” (RD) that encode genes that were subsequently proven to promote productive *M. tuberculosis* infection,<sup>[11]</sup> including the 6-kDa early secreted antigenic target (ESAT-6) secretion system-1 (ESX-1).<sup>[12,13]</sup> We reasoned that a metabolite-based screen might identify new virulence factors because not all functions of RD genes are known. Also, biologically important metabolites could emerge from complex biosynthetic pathways that cannot be predicted from single-gene analysis.

In this chapter we describe our collaborative efforts with the Moody laboratory on the isolation and structure elucidation of two novel terpene nucleosides from *M. tuberculosis*. The investigation led to a biosynthetic proposal which revised the function of the virulence associated enzyme Rv3378c. One of the natural isolates was found to be an abundant and specific tuberculosis produced compound which has considerable potential as a chemical marker in a diagnostic test for tuberculosis disease. The research was facilitated by chemical synthesis of the natural products. The synthetic material was used in cross-confirmation of the molecular structure of the terpene nucleosides and the biosynthesis thereof.

## 3.2 Tuberculosinyl adenosines; novel terpene nucleosides from *Mycobacterium tuberculosis*

### 3.2.1 The isolation and structure elucidation of an unknown terpene nucleoside

Using HPLC-MS for comparative analysis of lipid extracts of *M. tuberculosis* H37Rv and BCG (Pasteur strain), 7852 molecular features were detected. By aligning datasets and seeking features that significantly differed in intensity, we identified 1845 features that were only detected in one bacterium or the other. Among these features, we focused on molecules selectively detected in *M. tuberculosis* that showed the highest fold-change ratios and intensity. We identified four molecular features corresponding to a singly charged molecular ion at  $m/z$  540.357 ( $C_{30}H_{45}N_5O_4$ ) and its isotopes, but this chemical formula did not match entries in the MycoMass<sup>[8,9]</sup> or other public databases. We named the unknown molecule substance A.

The molecular ion of substance A was one of the most intense ions in the *M. tuberculosis* lipidome, suggesting that it was produced in abundance. Identification of an apparently abundant molecule in a widely studied pathogen was unexpected, leading to questions about whether substance A was truly a natural product. However, this compound was absent in media, solvent blanks, and BCG lipid extracts but was reproducibly detected in three reference strains of *M. tuberculosis* (H37Ra, Erdman and H37Rv). As observed with cell associated compounds, culture filtrate yielded a conspicuous ion at  $m/z$  540.357 whose intensity was higher than that of the abundantly secreted siderophore, carboxymycobactin. Its release into the extracellular space likely results from transmembrane transport, rather than budding of intact cell wall fragments, because cell wall-embedded lipids, trehalose monomycolate and mycobactin, were not detected in filtered supernatants. We detected substance A in *M. tuberculosis* during exponential or stationary phase and several types of media or when subject to acid stress. Thus, substance A is a natural product that is constitutively produced under many conditions and accumulates within and outside *M. tuberculosis*.

*M. tuberculosis* often compartmentalizes lipid biosynthesis so that lipids are assembled after transport across the plasma membrane. Sulfoglycolipids and phthiocerol dimycocerosates become undetectable when MmpL transporters are interrupted, even when biosynthetic genes are intact.<sup>[14-16]</sup> Because ESX-1 is a transport system lacking in BCG, lack of export of an ESX-1-dependent lipid synthase might account for the loss of substance A. However, ESX-1-deficient *M. tuberculosis* lacking either the *espA* gene (Rv3616c) or the entire RD1 locus,<sup>[17]</sup> which are both necessary for ESX-1 function, produces substance A at normal levels. After ruling out a major known species-specific difference in transport, we devised a screen to detect genes responsible for substance A biosynthesis.

Collision-induced mass spectrometry (CID-MS) identified the structural components of substance A as adenine ( $[M+H]^+$ ,  $C_5H_6N_5$ ,  $m/z$  136.0618), adenosine ( $[M+H]^+$ ,  $C_{10}H_{14}N_5O_4$ ,  $m/z$  268.1040), and a polyunsaturated C20 hydrocarbon ( $[M+H]^+$ ,  $C_{20}H_{33}$ ,  $m/z$  273.2576). A common C20 diterpene is geranylgeraniol, and *M. tuberculosis*

produces two C<sub>20</sub> lipids containing bicyclic halimane skeletons: tuberculosinol and isotuberculosinol.<sup>[18,19]</sup> Initially, CID-MS spectra could not distinguish among these three candidate diterpenes (Figure 1), and multistage CID-MS studies isolated the diterpene unit of substance A (*m/z* 273.3) and yielded collision patterns that matched both tuberculosinol and geranylgeraniol (Figure 1).

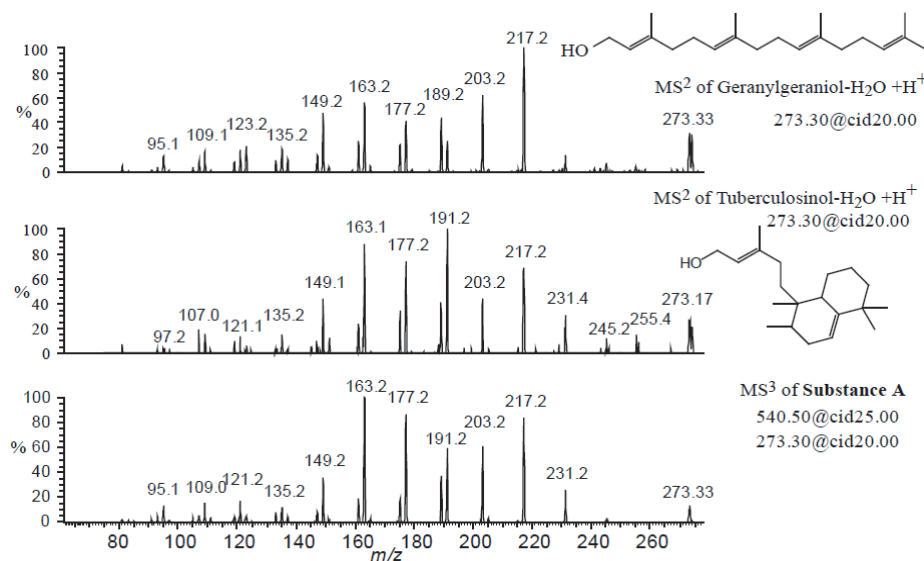


**Figure 1.** Mass fragmentations of the C<sub>20</sub>H<sub>33</sub> chain and MS + <sup>1</sup>H-NMR assignments for 1-TbAd.

The lack of sufficient data impeded our structural assignment efforts, and NMR analysis of the unknown terpene nucleoside was preferential. After tedious purification of the natural product, we carried out NMR analyses using <sup>1</sup>H-NMR, <sup>13</sup>C-NMR, COSY, HMQC, and NOESY spectra, which unequivocally established the structure of substance A as 1-tuberculosinyl adenosine (1-TbAd, see Figure 1). The NMR signals of the diterpene moiety matched those of tuberculosinol<sup>[18b,c,19,20]</sup> except for the expected difference in the side chain protons and carbons. The spectral data of the adenosine and adjacent atoms correspond closely to those of 1-prenyladenosine analogs.<sup>[21]</sup> The allylic methylene group absorbs downfield as a doublet at  $\delta$  4.92 ( $J = 6.6$  Hz). A NOESY cross

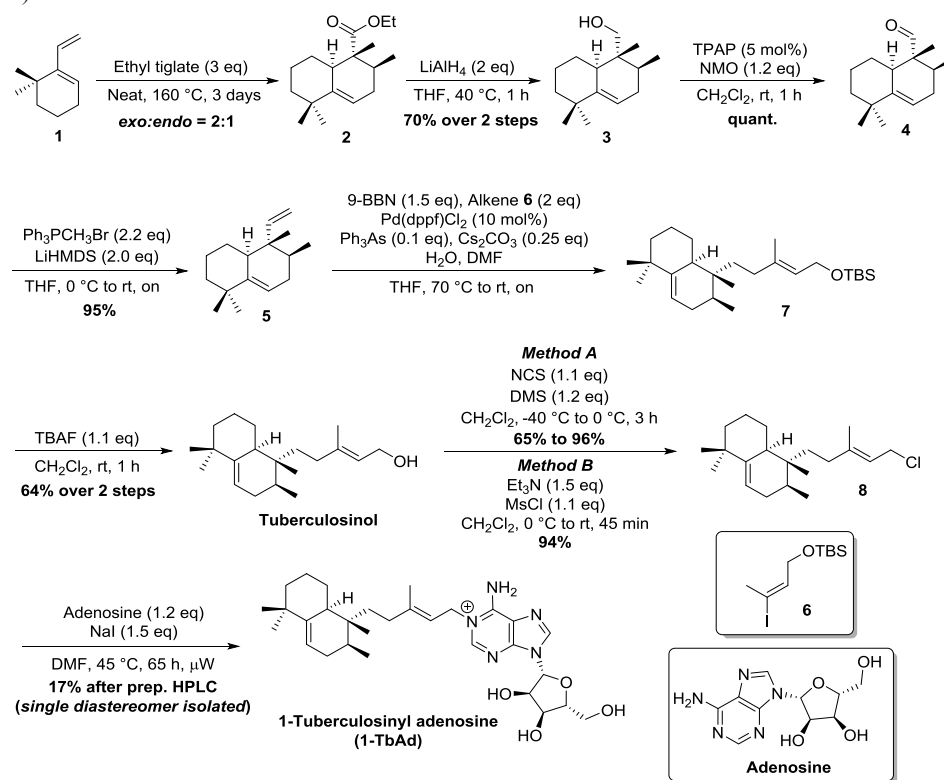


## CHAPTER 3

peak between the adenine H-2 at  $\delta$  8.53 and the alkene hydrogen and allylic methylene and methyl groups at  $\delta$  5.46, 4.92, and 1.89, respectively, confirm that the tuberculosinyl group is attached to the adenine at the 1-position. Thus, *M. tuberculosis* produces a previously unknown type of diterpene nucleoside.

### 3.2.2 A total synthesis of racemic 1-TbAd

Concurrent with the elucidation of the chemical structure of the isolated terpene nucleoside, we initialized a racemic synthesis to cross confirm the obtained data. As our synthesis was racemic in nature we decided to reproduce in a large part the recently reported racemic total synthesis of tuberculosinol by Sorensen and co-workers (Scheme 1).<sup>[22a]</sup>



**Scheme 1.** The racemic total synthesis of 1-TbAd.

The synthesis started with a Diels-Alder reaction between diene **1**<sup>[23]</sup> (for its synthesis see supporting information and chapter 4) and ethyl tiglate. The reaction provided a diastereomeric mixture of (2:1) of *exo* and *endo* Diels-Alder adducts **2** respectively. Reduction of the ester with LiAlH<sub>4</sub> then provided alcohol **3** in 70% yield over the two steps. Oxidation was then followed by a Wittig olefination providing us with terminal alkene **5** in 95% over the two steps. At this stage a Suzuki-Miyaura coupling was

performed,<sup>[24]</sup> however this reaction was somewhat troublesome in our hands as we were unable to perfectly reproduce the literature procedure. Whereas in the literature unprotected vinyl iodide (**6** – TBS group) was used to directly construct tuberculosinol, we only managed to achieve coupling with the protected vinyl iodide **6**. After careful experimentation we managed to obtain TBS protected tuberculosinol **7**, which was deprotected by the aid of TBAF, yielding tuberculosinol in 67% over the two steps.

The spectral data of the obtained tuberculosinol were in agreement with the literature and the compound was subsequently used in the total synthesis of 1-TbAd. For that we first had to convert the tuberculosinol into its electrophilic counterpart for coupling with the nucleophilic adenosine. At first we performed a Corey-Kim chlorination as reported by the Poulter laboratory.<sup>[25]</sup> The chlorination could be performed rather smoothly, but we found the method showed some inconsistencies regarding the reproducibility. The chloride could be obtained but the yields were varying from 65% to 96% yield. As an alternative the chlorination was performed with mesyl chloride providing tuberculosinyl chloride **8**, consistently, averaging to 94% yield. The chloride was then coupled with adenosine<sup>[26]</sup> under Finkelstein conditions, heated by microwave. Preparative HPLC-MS analysis (performed at Harvard medical school) of the reaction mixture afforded 1-TbAd in only 17% yield as a single diastereoisomer. To our surprise, a significant contaminant was found in the reaction mixture which corresponded to the tuberculosinyl triethylammonium ion. This side product was apparently formed in the chlorination reaction (method B) in which triethylamine substituted the chloride in **8**. Because of inattentiveness during analysis of the <sup>1</sup>H-NMR, the characteristic ethyl resonances were mistaken for residual diethyl ether. The low yield in the adenosine coupling and the aforementioned contamination problems were addressed and solved in later synthetic efforts (*see chapter 4*). The synthetic 1-TbAd cross-confirmed the chemical structure and provided the first quantities of 1-TbAd for further investigations.

### 3.2.3 The biosynthetic pathway of 1-TbAd

To identify the genes necessary for 1-TbAd production, an existing library of random transposon insertional mutants<sup>[27]</sup> was screened in high throughput (4196 mutants) for 1-TbAd production using a simplified 3-min HPLC-MS method. Thirty mutants showing low or absent signals were rescreened using the original, high-resolution lipidomic separation method. Reporting only mutants with complete signal loss of 1-TbAd signal in both assays, we identified two 1-TbAd–null mutants carrying transposons in Rv1796 (mutant 1) and Rv2867c (mutant 2). The concurrently performed structure elucidation described above identified the highly characteristic tuberculosinyl moiety as the terpene component of 1-TbAd, and the Rv3377c-Rv3378c locus was known to encode enzymes needed for tuberculosinol and isotuberculosinol production.<sup>[18,19,20,28]</sup> Sequencing identified spontaneous mutations in Rv3378c in both mutants.<sup>[18,19,20]</sup> Mutant 1 encoded a predicted Asp→Gly substitution at residue 34, and mutant 2 encoded a Pro→Ser substitution at residue 231. We generated complementation constructs to separately test whether the point mutations in Rv3378c or the transposon insertions were responsible

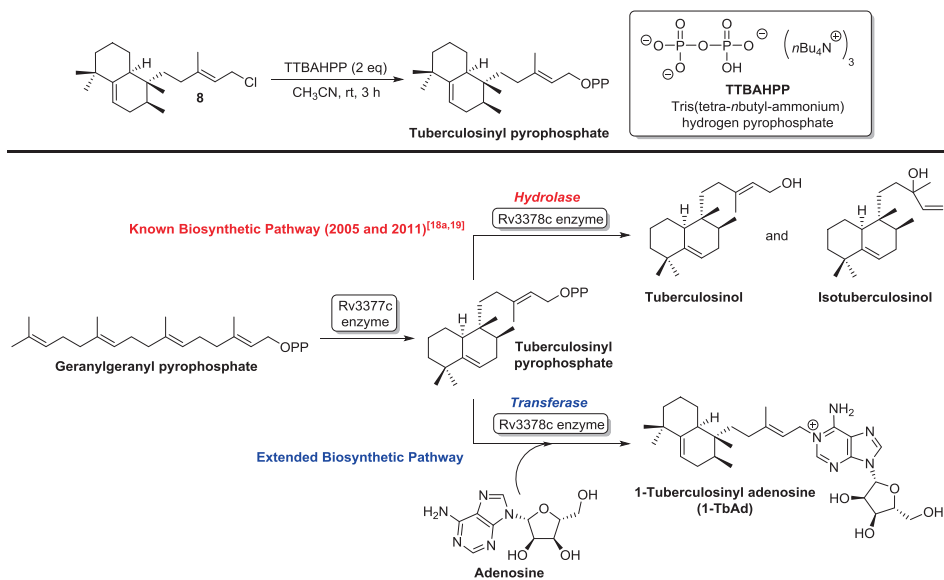
for 1-TbAd loss. Transfer of Rv1796 and Rv2867c failed to restore 1-TbAd production, but transfer of Rv3377c-Rv3378c reconstituted 1-TbAd production in both mutants. Thus, Rv3377c-Rv3378c genes are necessary for 1-TbAd biosynthesis in *M. tuberculosis*.

Furthermore, the known role of Rv3377c and Rv3378c enzymes in tuberculosinol production potentially provided a mechanism to connect Rv3377c and Rv3378c genes with the production of a nucleoside-modified tuberculosinol. Rv3377c is a terpene cyclase, which acts on geranylgeranyl pyrophosphate (GGPP) to generate tuberculosinyl pyrophosphate (TbPP).<sup>[18]</sup> Rv3378c was thought to be a phosphatase, which converts TbPP to free tuberculosinol.<sup>[19,20]</sup> Extending current models, 1-TbAd might result from downstream action of an unknown enzyme on free tuberculosinol to transfer it to adenosine. Polyprenol synthase genes and the Rv3377c-Rv3378c locus are coordinately regulated and encoded at adjacent sites on the chromosome.<sup>[29]</sup>

Therefore, we searched *M. tuberculosis* databases for genes located near this locus that might plausibly function as adenosine transferases. We failed to find candidates and noted that no transposon insertion that blocked 1-TbAd production mapped to genes adjacent to this locus. Therefore, we considered a revised biosynthetic model in which Rv3378c protein is not a simple phosphatase, as currently believed, but instead acts with combined phosphatase and tuberculosinyl transferase functions, using adenosine as the nucleophilic substrate (Scheme 2). This model is mechanistically simple and might explain the lack of an apparent stand-alone transferase gene. Also, whereas current models predict that tuberculosinol is the end product of this pathway, we did not detect tuberculosinol in lipidomics experiments. The revised model posits that 1-TbAd is the end product of Rv3378c pathway, explaining why it accumulates to high levels as one of the brightest ions in the lipidome. After chemical synthesis of TbPP, by reaction of tuberculosinyl chloride with tris(tetra-*n*-butylammonium) hydrogen pyrophosphate, we tested TbPP and GGPP as substrates for the recombinant Rv3378c protein.<sup>[18]</sup> Rv3378c catalyzed the condensation of adenosine and TbPP to generate 1-TbAd but produced no detectable product from GGPP. Free tuberculosinol was not detected in these assays. Thus, Rv3378c shows tuberculosinyl transferase activity, which rules in the revised biosynthetic pathway.

To test the sufficiency of this locus for 1-TbAd production in cells, we transferred the Rv3377c-Rv3378c locus to *Mycobacterium smegmatis*. In all three clones tested, expression of Rv3377c-Rv3378c transferred production of a molecule with the mass, retention time, and CID-MS spectrum of 1-TbAd. Thus, no other *M. tuberculosis*-specific co-factor or transporter is needed for 1-TbAd production. Rv3377c-Rv3378c is sufficient to synthesize 1-TbAd from ubiquitous cellular precursors present in most bacteria, likely GGPP and adenosine. This finding is particularly interesting and important as the gene cluster Rv3377c-Rv3378c have been shown to be crucial in the virulence and survival mechanism of *Mycobacterium tuberculosis*. Genetic deletion of the enzyme necessary for 1-TbAd biosynthesis (Rv3378c) rendered *M. tuberculosis* unable to grow in macrophages *in vivo*, suggesting a non-redundant role of this biosynthetic pathway in virulence.<sup>[30]</sup>

## The discovery of novel terpene nucleosides from *Mycobacterium tuberculosis*



**Scheme 2.** Extension of the biosynthetic function of the Rv3378c protein.

### 3.3 The development of 1-TbAd as a chemical marker for tuberculosis disease

#### 3.3.1 1-TbAd is a major and specific lipid in *Mycobacterium tuberculosis*

Our described isolation efforts of 1-TbAd prompted us with the idea to develop 1-TbAd into a chemical marker for tuberculosis disease. In order to function as a successful marker a series of requirements have to be met, starting with abundance and specificity. The molecule used as a marker has to be abundant and easily detectable to exclude false negative results. Additionally the molecule has been specific to the pathogen so that the chances of false positive results are minimized. To see whether 1-TbAd fulfills these initial requirements we set out to investigate these criteria.

As shown, 1-TbAd was identified in *M. tuberculosis* using an (ESI)-MS-based lipidomics platform. Among 7852 ions, 1-TbAd ( $C_{30}H_{46}N_5O_4^+$ ;  $m/z$  540.3545) was the second most intense ion in the lipidome. The high intensity might have resulted from 1-TbAd's accumulation to high concentration. Yet it was difficult to imagine that any abundant class of molecule would have escaped detection over decades of study of a pathogen of worldwide importance. Alternatively, 1-TbAd might have been present only in trace amounts, yet its intrinsically charged nature and amphipathic character might have promoted particularly efficient ionization in ESI-MS. To measure the mass of 1-TbAd as a percentage of all lipids, we analyzed extracts from *M. tuberculosis* strain H37Rv using the method of standard additions. We compared the area under the curve of retention time versus intensity measured at the mass ( $m/z$  540) of 1-TbAd ( $A_{540}$ ) and

phosphatidylethanolamine (A<sub>720</sub>), which controls for the efficiency of ESI-MS detection. As with other polar lipids,<sup>[8]</sup> we observed a nearly linear relationship between mass input and 1-TbAd signal intensity. In three experiments, we determined that 1-TbAd comprises 1.1%, 1.4%, and 1.5% of the mycobacterial lipids. Thus, contrary to expectations that terpene nucleosides previously escaped detection due to scarcity, 1-TbAd is a highly abundant molecule that comprises a major class of lipid in *M. tuberculosis*. The basis for lack of prior detection remains unknown, but the near co-elution of 1-TbAd and abundant membrane phospholipids in normal-phase thin-layer chromatography and HPLC methods might have obscured 1-TbAd detection in the past.

To function as a sensitive marker of infection, molecules must be expressed in most strains of *M. tuberculosis* that infect patients and among the seven recognized *M. tuberculosis* lineages that exist worldwide.<sup>[31]</sup> 1-TbAd derives from geranylgeranyl pyrophosphate (GGPP) and adenosine, which are present in nearly all organisms. Lipid cyclization and coupling to adenosine are performed by specialized enzymes, Rv3377c (prenyl cyclase) and Rv3378c (tuberculosinyl transferase), which together with polyprenyl synthases comprise a functional gene island<sup>[32]</sup> that is necessary and sufficient for 1-TbAd biosynthesis.<sup>[33]</sup> Knowledge of the essential TbAd biosynthetic genes allowed a survey of the genomes of 432 phylogeographically diverse clinical isolates of the *M. tuberculosis* complex (*Mtb* complex) for an intact biosynthetic locus. We found that TbAd genes were detected among all clinical strains examined and most clinical isolates have an intact Rv3377c-3378c locus and no clear evidence for selection driving the mutations identified.

To determine whether 1-TbAd biosynthesis exists in species other than *M. tuberculosis*, we sought genetic orthologues of Rv3377c and Rv3378c across the biological kingdoms. Considering all non-mycobacterial species, we did not identify candidate orthologues organized into a locus with both essential genes present. Among mycobacteria, orthologues of Rv3377c and Rv3378c could not be identified in most species, including disease-causing members of the *M. avium* complex, *M. kansasii*, and *M. marinum*. Instead, orthologues were present only within the *Mtb* complex: in *M. bovis*, *M. bovis* BCG (Pasteur strain), *M. cannetti*, and *M. africanum*.

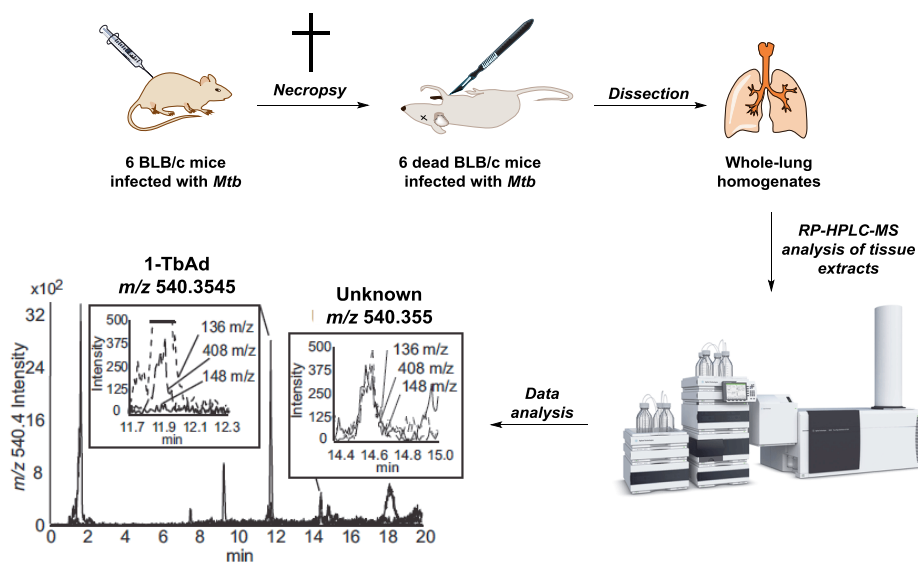
Despite our intensive investigation, gaps in the analysis remained. Some but not all of the Rv3378c mutations, including those present in *M. africanum*, have been proven to inactivate lipid biosynthesis.<sup>[33,34]</sup> Second, BCG vaccine strains are of particular interest because they cause false-positive immunological tests. Although the locus in BCG strain Pasteur was inactivated through frameshift, other BCG or *M. bovis* strains might never have acquired these mutations, or they might have done so and then reverted to wild-type sequences. The 12 widely used BCG vaccine strains show variations in efficacy,<sup>[35]</sup> so differential expression of TbAd might account for this.<sup>[30]</sup> However, further analysis of all common vaccine strains used worldwide (Pasteur, Copenhagen, Japan, Mexican, Australian, Russia, Glaxo, Prague, Phipps, Connaught, Denmark, Tice) confirmed the presence of the frameshift mutation in all cases, so 1-TbAd is likely absent from all major vaccines used worldwide.

A general limitation of genetic analysis is that genes might exist that are functionally equivalent to Rv3377c and Rv3378c but lack the sequence identity needed for identification as orthologues. Therefore, we undertook biochemical analysis, using the HPLC lipidomics platform, for 1-TbAd production, focusing on non-tuberculous mycobacteria and microbes, whose infection can mimic tuberculosis disease.

In agreement with the genetic results, we did not detect 1-TbAd among disease-causing bacteria that are related to *M. tuberculosis* but lack identifiable orthologues of Rv3377c-3378c (*M. avium*, *M. marinum*) or those with orthologous loci containing a known frameshift mutation (*M. bovis*). Among all organisms tested to date, only *M. tuberculosis* produces 1-TbAd.

### **3.3.2 *In vivo* detection of 1-TbAd in infected mice**

With the biosynthetic and genetic evidence gathered, confirming that 1-TbAd is *M. tuberculosis* specific and also abundant, an initial platform for 1-TbAd detection in context of a chemical marker could be developed. To determine if 1-TbAd is detectable *in vivo*, we infected BALB/c mice via inhalation for 21 days followed by collection of whole lung homogenates. Target validation *in vivo* does not require scanning of the complete lipidome, but instead focuses on sensitive and specific detection of predetermined targets, which are likely to be highly diluted within host tissues. We developed a reversed-phase method to increase chromatographic resolution, while taking advantage of the specificity and accuracy of triple quadrupole mass detection. This method detected a 1-TbAd standard at 11.8 min based on its known transition for 1-TbAd ( $m/z$  540/408/136). Direct analysis of unfractionated lipids from whole-lung homogenates did not detect signal corresponding to 1-TbAd in uninfected lung but did detect a signal corresponding to 1-TbAd that was well above background signals in six of six infected mice tested, with representative data shown in scheme 3. Thus, 1-TbAd is produced *in vivo* and is readily detected *ex vivo* in a one-step HPLC-MS method.



**Scheme 3.** Schematic overview of initial investigations of a diagnostic test using 1-TbAd.

### 3.3.3 Identification of another unknown terpene nucleoside

Ion chromatograms of the ion 540→408 also showed a second, later-eluting peak (~14.6 min) with transitions that were distinct from 1-TbAd in all six mice tested (Scheme 3). Unlike 1-TbAd, the unknown lipid contained a 540→148 ion and a relatively bright 540→408 transition that was equivalent in intensity to the 540→136 ion. Returning to normal-phase HPLC-quadrupole time-of-flight (Q-TOF)-MS experiments using *in vitro* grown *M. tuberculosis*, ion chromatograms measured at  $m/z$  540.4 also showed two peaks at ~25 and ~7 min, which corresponded to late-eluting 1-TbAd and an early-eluting unknown lipid detected in mice. Collision-induced dissociation (CID)-MS analysis of the unknown showed fragment ions of  $m/z$  148.062 and 408.313, matching the pattern of the late-eluting unknown from reversed-phase chromatography, suggesting that they were the same molecule. Thus, the unknown later-eluting compound detected in mice was likely derived from *M. tuberculosis* rather than the host. Also, separate tracking of the unknown and 1-TbAd in the bacterial pellet and conditioned supernatant demonstrated a much higher ratio of signal for the unknown in supernatants. Thus, the early-eluting unknown was likely generated during or after transit from the cytosol to the extracellular space.

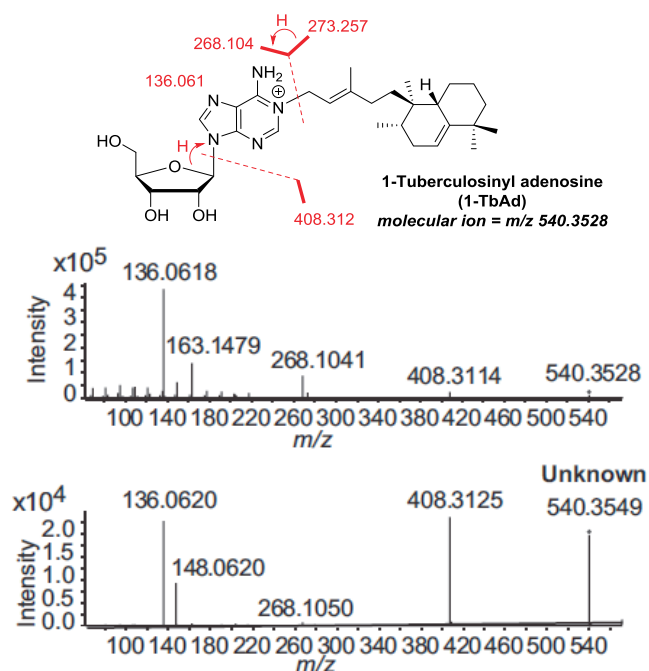


Figure 2. Differences in 1-TbAd and its unknown isomer.

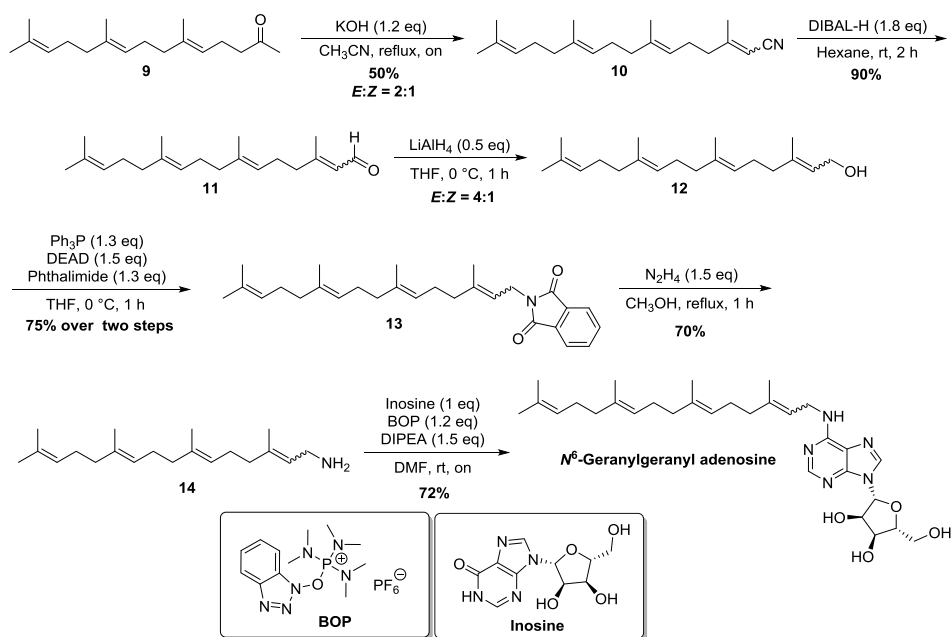
The unknown ( $m/z$  540.3549, measured) and 1-TbAd ( $m/z$  540.3545, calculated) had identical molecular ion masses ( $\pm 2$  ppm) and similar fragmentation patterns (Figure 2). The unknown had a much lower retention time in normal-phase chromatography. Therefore, the unknown was likely a much less polar isomer of 1-TbAd. CID-MS ions were assigned unequivocally as  $C_5H_6N_5^+$  ( $m/z$  136.0618) and  $C_{10}H_{14}N_5O_4^+$  ( $m/z$  268.1040), matching the mass of adenine and adenosine, respectively. The neutral loss leading to  $m/z$  268.1040 suggested the loss of  $C_{20}H_{32}$ , likely a diterpene moiety. A fragment ion with the formula  $C_{25}H_{38}N_5$  (calculated  $m/z$  408.3122) matches the loss of a pentose-derived fragment ( $C_5H_8O_4$ , calculated 132.0423 Da). Therefore, the unknown was a diterpene-substituted adenosine ( $C_{30}H_{45}N_5O_4$ ). Experiments were guided by two hypotheses. The unknown isomer and 1-TbAd might differ in the type of diterpene carried, or a tuberculosinyl group could have an alternate linkage to adenine. *M. tuberculosis* produces geranylgeranyl pyrophosphate and tuberculosinyl pyrophosphate is hydrolyzed, besides tuberculosinol, to isotuberculosinol *in vitro*.<sup>[19]</sup> Therefore, 1-geranylgeranyl adenosine and 1-isoTbAd were candidate structures. However, they would be expected to have largely the same ionic properties as 1-TbAd. Alternatively, a tuberculosinyl linkage at the  $N^6$ -adenosine position would mimic common  $N^6$ -linked adenine compounds like zeatin<sup>[36]</sup> and would be expected to alter the ionic properties observed in the unknown. Therefore, we considered  $N^6$ -tuberculosinyl adenosine as a candidate structure. Although during the structure elucidation of 1-TbAd we ruled out



### CHAPTER 3

the geranylgeranyl side chain as the C<sub>20</sub>H<sub>32</sub> unit, primarily on the basis of NMR data, we now were in search for more definite evidence. As the unknown 1-TbAd isomer could not be isolated in sufficient quantities for NMR analysis we were dependent on MS-analysis alone to solve the structure. We therefore set out to synthesize *N*<sup>6</sup>-geranylgeranyl adenosine (Scheme 4).

Commercially available farnesyl acetone **9** was reacted with acetonitrile under alkaline conditions to produce an isomeric mixture of  $\alpha,\beta$ -unsaturated nitrile **10** in 50% yield. The nitrile was reduced to geranylgeraniol **12** in two steps. A Mitsunobu reaction was performed to construct phthalimide **13** which in a Gabriel reaction was converted into geranylgeranyl amine **14**. To complete the synthesis, geranylgeranyl amine **14** was coupled with inosine, with BOP as the coupling reagent, to provide *N*<sup>6</sup>-geranylgeranyl adenosine in 72% yield.<sup>[37]</sup> HPLC-MS analysis of *N*<sup>6</sup>-geranylgeranyl adenosine showed divergent data compared to that of the natural isolate. The significant differences in the fragmentation pattern and signal intensities, together with an inconsonant retention time led us to conclude that the isomeric terpene nucleoside did not correspond to *N*<sup>6</sup>-geranylgeranyl adenosine.

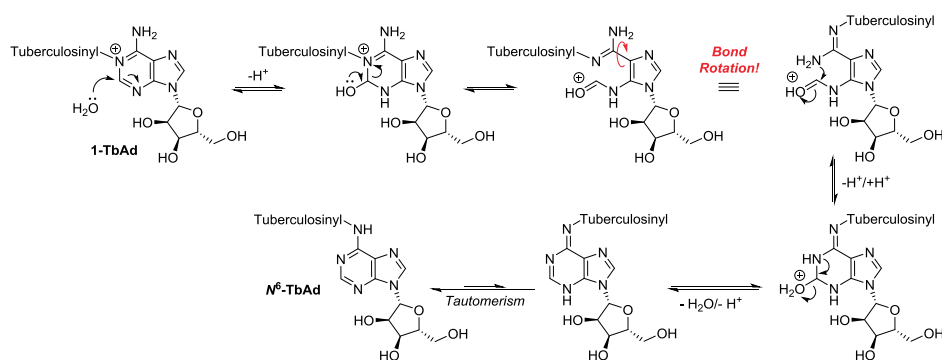


**Scheme 4.** Synthesis of *N*<sup>6</sup>-geranylgeranyl adenosine.

We also proposed *N*<sup>6</sup>-tuberculosinyl adenosine to be the structure of the unknown *N*<sup>6</sup>-terpene nucleoside. *N*<sup>6</sup>-TbAd was assumed easily accessible via a Dimroth rearrangement of 1-TbAd. That process is facilitated under nucleophilic conditions with as a driving force the formation of neutral *N*<sup>6</sup>-TbAd from positively charged 1-TbAd (Scheme 5).<sup>[38]</sup> Subjecting 1-TbAd to a nucleophile like water, as is likely for *in vivo*

*The discovery of novel terpene nucleosides from Mycobacterium tuberculosis*

conversion of 1-TbAd to  $N^6$ -TbAd, induces ring-opening of the aminopyrimidine. Bond rotation places the amine functionality in proximity to the electrophilic carbon inducing a ring-closure. Water is then eliminated to give after tautomerization  $N^6$ -TbAd. It should be pointed out that, as 1-TbAd has a considerably higher pKa than  $N^6$ -TbAd, the Dimroth rearrangement is accompanied by proton loss and therefore formally not an isomerization.

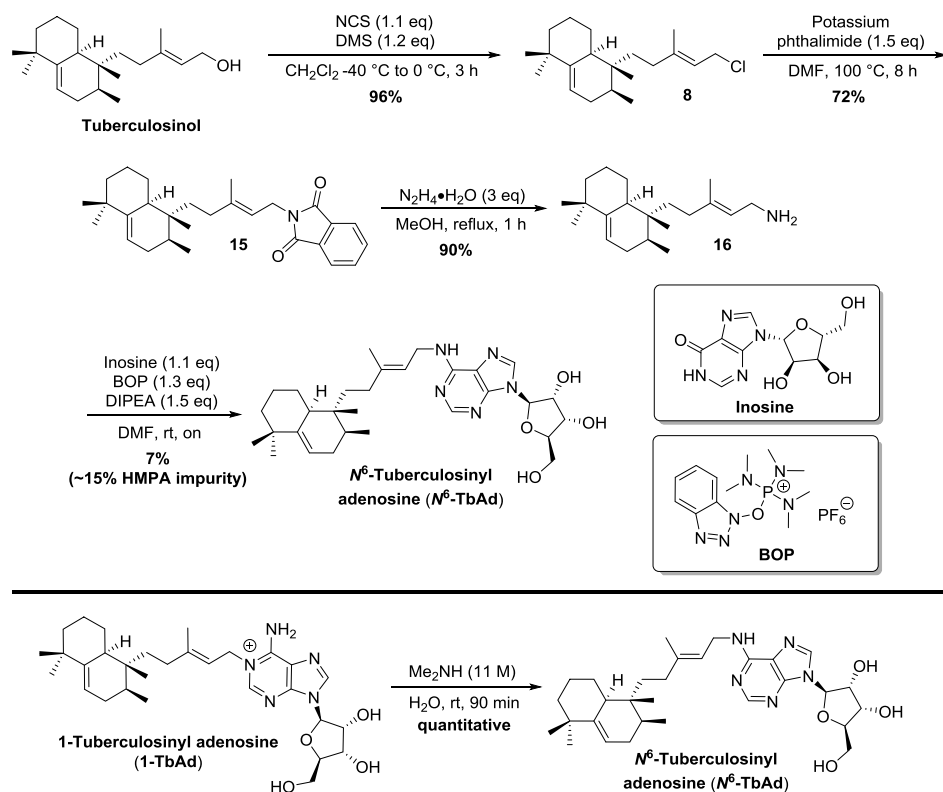


**Scheme 5.** The Dimroth rearrangement mechanism in the synthesis of  $N^6$ -TbAd from 1-TbAd.

With the unknown structure now postulated to correspond to  $N^6$ -tuberculosinyl adenosine we decided to synthesize this compound to provide clarification (Scheme 6). In our first approach,  $N^6$ -TbAd was accessed via the inosine coupling reaction. Since at this stage of the research we only had tuberculosinyl chloride, the phthalimide was accessed by a substitution reaction with potassium phthalimide. Cleavage of the phthalimide with hydrazine provided tuberculosinyl amine **16** in 65% yield over the two steps. Coupling of **16** with BOP provided the product with good conversion however we failed to separate HMPA from the product. HMPA is formed from BOP as the coupling agent to activate the inosine. Repetitive flash chromatography produced a meager 7% yield of  $N^6$ -TbAd containing ~15% HMPA as an impurity.

With little 1-TbAd left from the racemic synthesis (Scheme 6) the Dimroth rearrangement was performed. Treatment of 1-TbAd with diethylamine in MeOH at room temperature smoothly provided  $N^6$ -TbAd in quantitative yield. Mass analysis and the retention time of the synthetic material matched perfectly with the natural isolate, thereby providing overwhelming evidence that the structure of the terpene nucleoside corresponds to  $N^6$ -TbAd.

CHAPTER 3



**Scheme 6.** Total synthesis of *N*<sup>6</sup>-TbAd via an inosine coupling and Dimroth rearrangement.

A definite confirmation of the *N*<sup>6</sup>-TbAd structure came about by isolation from the natural source. After growing *M. tuberculosis* cultures in roller bottles, ~50 mg of lipid was fractionated by normal-phase column chromatography followed by reversed-phase HPLC. Adding 0.2% trifluoroacetic acid (TFA) to the mobile phase increased the retention of 1-TbAd in reversed-phase chromatography but did not affect the unknown isomer, confirming that the two compounds differed in their ionic properties. This purification sequence produced ~300 μg of each isomer so that the combined yield (~1.2%) confirmed ESI-MS studies.

Analysis of the <sup>1</sup>H-NMR, <sup>13</sup>C-NMR, COSY, NOESY and HMQC spectra (800 MHz) established the structure of the unknown as *N*<sup>6</sup>-TbAd. A geranylgeranyl side chain could not produce signals as low as the observed signals at 1 ppm. The single vinylic proton would be replaced by the two protons in the isotuberculosinyl group, also ruling out this possibility. The spectral data, especially the methyl resonances, for *N*<sup>6</sup>-TbAd corresponded near perfectly to that of its isomer 1-TbAd. Additionally, the side chain protons correspond closely to those of *N*<sup>6</sup>-(3-methyl-2-butenyl)adenosine.<sup>[21]</sup> The adenine protons at δ 8.24 and 8.26 are characteristic of an *N*<sup>6</sup>-substituted adenosine and are different from those of 1-TbAd at δ 8.53 and 8.66. The absorption of the allylic

methylene group is a broad peak at 4.22–4.16 ppm due to slow rotation at room temperature around the C- $N^6$  bond.<sup>[39]</sup> All COSY and NOESY correlations are consistent with the assignment of the unknown as  $N^6$ -TbAd.

### 3.3.4 The biological origin of $N^6$ -TbAd

A plausible mechanism to account for the biological origin of  $N^6$ -TbAd is that 1-TbAd converts to  $N^6$ -TbAd by a Dimroth rearrangement,<sup>[38]</sup> as explained in scheme 5. Products from recombinant Rv3378c enzyme showed a strong signal for 1-TbAd and no signal for  $N^6$ -TbAd, demonstrating that the latter is not a primary product of this enzyme. Furthermore, we observed that treating 1-TbAd under conditions known to favor the Dimroth reaction ( $\text{Me}_2\text{NH}$  in water) led to clean conversion into  $N^6$ -TbAd (Scheme 6). This data suggest a two-step model of biosynthesis whereby Rv3378c mediates conjugation of tuberculosinyl pyrophosphate and adenosine to produce 1-TbAd in the cytosol and 1-TbAd could later rearrange to  $N^6$ -TbAd in other compartments. However, *in vivo* transformation of 1-TbAd to  $N^6$ -TbAd in mice could not be unequivocally established because mouse lung analysis required harvest, homogenization, and HPLC-MS analysis at the bench. The *ex vivo* workup of lung might have inadvertently induced Dimroth rearrangement but this possibility was ruled out by workup of lung spiked with 1-TbAd, which detected only 1-TbAd. We therefore postulate, Rv3378c produces 1-TbAd, which is transformed to  $N^6$ -TbAd by the Dimroth rearrangement, and both compounds occur *in vivo* and represent specific markers of *M. tuberculosis* infection.

## 3.4 Conclusions

In summary we reported the identification of two novel terpene nucleosides from *Mycobacterium tuberculosis*, namely 1-TbAd and  $N^6$ -TbAd. The former compound was shown to be an abundant and *M. tuberculosis* specific lipid which rendered it suitable for the development of a diagnostic test. It was shown that 1-TbAd is produced *in vivo* in tuberculosis infected mice and can be readily detected *ex vivo* using a RP-HPLC-MS method. Concurrent with the detection of 1-TbAd, its pseudo-isomer  $N^6$ -TbAd was discovered which was postulated to arise from an *in vivo*, non-enzymatic, Dimroth rearrangement of 1-TbAd. This novel *in vivo* produced product was present in all infected mice and therefore can function, next to 1-TbAd, as a specific marker for the tuberculosis disease.

Another very interesting, and potentially groundbreaking, discovery was the fact that 1-TbAd, an abundant and specific *M. tuberculosis* natural product, is produced by the virulence associated enzyme Rv3378c. Although the function of 1-TbAd has not been shown, we do however suspect 1-TbAd to be pivotal in the virulence and survival mechanism of tuberculosis (*vide infra* for a postulated mechanism of action).

We also communicated the first chemical, racemic, total synthesis of 1-TbAd and  $N^6$ -TbAd. It was shown that synthetic chemistry and biology perfectly complemented each

other, leading to a successful research project on tuberculosinyl adenosines, research which is still ongoing (*see also chapter 4*). The total synthesis of the TbAd compounds and tuberculosinyl pyrophosphate proved to be important as the chemical structures and biosynthesis could be unequivocally assigned.

### 3.5 Discussion: a hypothesis for the working mechanism of 1-TbAd

In this chapter we showed the identification of 1-TbAd and its potential application as an abundant and specific chemical marker for tuberculosis disease. Also its biosynthesis, which requires the virulent associated enzyme Rv3378c,<sup>[30]</sup> was elucidated. The abundance, specificity and production by Rv3378c makes 1-TbAd highly likely to be involved in virulence<sup>[40]</sup> and survival<sup>[41]</sup> of *Mycobacterium tuberculosis*. The key question however is, what role does 1-TbAd play and what is the mechanism of action?

As discussed in the first chapter of this dissertation, *Mycobacterium tuberculosis* is difficult to treat with antibiotics. One of the factors that contributes to this is the thick hydrophobic cell envelope (cell wall). Consisting of a complex array of (glyco)lipids, polysaccharides and peptidoglycans, the cell wall exhibits low permeability by drugs, forming an almost impenetrable fortress.<sup>[42]</sup> Another major contributor to virulence<sup>[40]</sup> and survival<sup>[41]</sup> of *Mtb* is its ability to successfully infect endosomal phagocytes. Residing in phagosomes, *M. tuberculosis* actively inhibits pH dependent killing mechanisms, protecting itself from both drugs and immune responses.<sup>[43]</sup> In order to understand the importance of this mechanism a simplistic and partial introduction into human immunology is given (Figure 3).

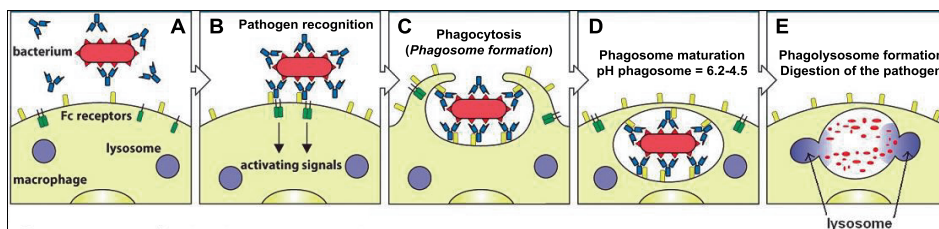


**Figure 3.** A schematic representation of phagocytosis. © 2009 from of *The Immune System, Third Edition* by Parham. Reproduced and modified by permission of Garland Science/Taylor & Francis Group LLC.

When a bacterial pathogen enters the human host, an immune response is set in motion which recognizes the invader as foreign (step A in Figure 3). The recognized pathogen activates a macrophage (a type of white blood cell, step B) which starts to encapsulate the pathogen in a process called phagocytosis (step C). The compartmentalized pathogen now resides in a vesicle called an early phagosome (step D). In order to devour the pathogen, the phagosome has to mature from an early to a late phagosome which is governed by a complex cascade of events.<sup>[44]</sup> One crucial step however is

acidification of the phagosomal space to set up the phagosome for fusion with the lysosome. The pH in an early stage phagosome is ~6.2 which gradually decrease to pH <5.0 in late stage phagosomes. The late stage phagosome then fuses with the lysosome, in which the lysosomal contents (acid lipases and esterases) are released (step E). The lipases and esterases are capable of breaking down the pathogen, thereby stopping infection of the human host.

Despite the intricacies of the human immune system, *Mycobacterium tuberculosis* evolved an ingenious mechanism to evade the immune response guaranteeing its survival in the human host. Upon encapsulation of the bacterium, the phagosome has to mature, and it is exactly this process which is blocked by *M. tuberculosis* leading to phagosome maturation arrest. In particular, the gradual acidification of the phagosomal space is inhibited, a process which involves the Rv3377c-Rv3378c locus.<sup>[30]</sup> The early phagosome therefore does not mature to form an acidified late stage phagosome which can fuse with the lysosome. The fact that phagolysosome formation does not take place results in survival of the bacterium inside the human host. Although the bacteria are isolated, from the perspective of the pathogen it is more protected from drug penetration than only by its thick cell envelope. Additionally, the bacteria are shielded from further immune responses allowing it to await a weakening of the human immune system whereupon it will start multiplying. The involvement of the 1-TbAd producing Rv3377c-Rv-3378c locus in phagosome maturation arrest raised our interest in the role 1-TbAd plays in this process. An obvious starting point to answer this question is the molecular structure of 1-TbAd, which was therefore examined.

Our immediate attention went out to the positively charged exocyclic NH<sub>2</sub> and the implication it has on 1-TbAd's acidic properties. The pKa of 1-TbAd's exocyclic NH<sub>2</sub> has not been established experimentally but from the literature it was known that the measured pKa of 1-dimethyl allyl adenosine in water is 8.47.<sup>[45]</sup> Although we are well aware that 1-dimethyl allyl adenosine is structurally different than 1-TbAd and that the pKa was measured under non-physiological conditions, we assume the pKa of 1-TbAd is close to this value.

From this analysis we could conclude 1-TbAd is a weak acid and is therefore subjected to an acid-base equilibrium. Together with the knowledge that phagosome maturation requires phagosome acidification,<sup>[44]</sup> and that *Mycobacterium tuberculosis* is effectively blocking this process,<sup>[43]</sup> we could come up with testable hypothesis on the mode of action of 1-TbAd. The acidic properties of 1-TbAd led us to propose a mechanism in which the conjugate base of 1-TbAd blocks phagosome acidification (Figure 4).

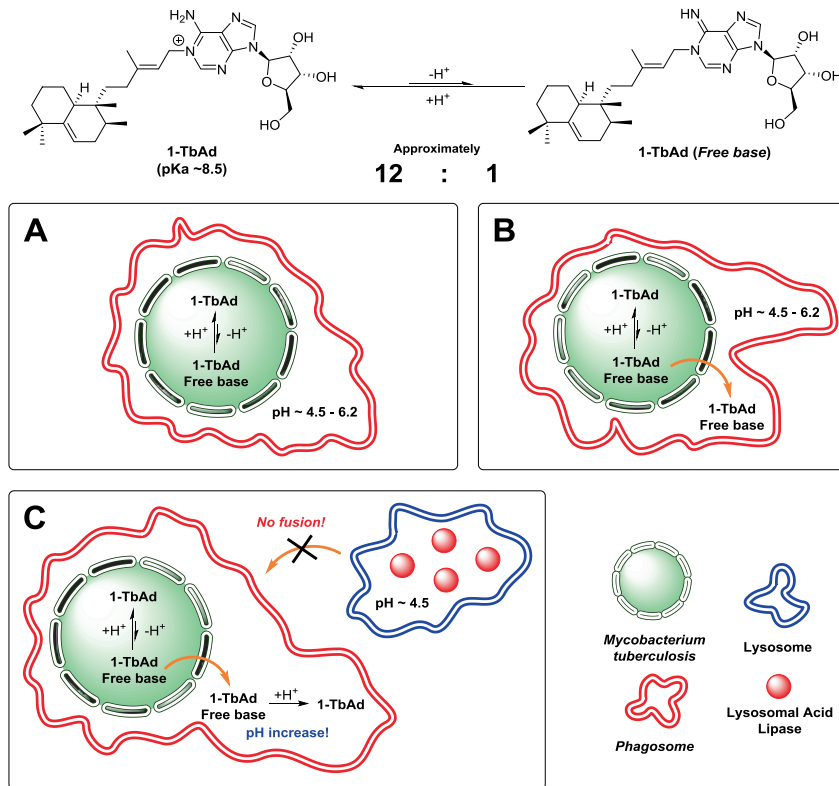


**Figure 4.** A schematic representation of the 1-TbAd buffering hypothesis. a) *Mtb* in the phagosome. b) “Basic 1-TbAd” is passing the *Mtb* membrane, into the acidic phagosome. c) Buffering of the acidic phagosome by 1-TbAd’s free base. Maturation arrest follows, and no fusion with lysosomes (= pathogen survival).

Assuming that the pKa of 1-TbAd under physiological conditions is  $\sim 8.5$  the Henderson-Hasselbalch equation ( $\text{pH} = \text{pKa} + \log_{10}[\text{A}^-]/[\text{HA}]$ ) is used to calculate the ratio of 1-TbAd/1-TbAd free base. The pH of the *M. tuberculosis* cytosol, where 1-TbAd is produced, is 7.4 which gives an acid/base ratio of  $\sim 12:1$  (step A in Figure 4). We hypothesize that 1-TbAd is too polar to cross the bacterial cell wall and that only the free base will do so (step B). Upon release in the phagosome 1-TbAd accepts a proton, raising the pH (step C) and thereby avoiding fusion between the phagosome and lysosome.

As discussed previously, phagolysosome formation is a crucial step in the immune response as it is responsible for breaking down the pathogen, stopping the infection of the host. The postulated hypothesis of 1-TbAd’s involvement in phagosome maturation arrest can therefore be an important step in unraveling this moderately understood mechanism.

It goes without saying that the hypothesis itself raises some interesting questions. How is 1-TbAd free base passing the thick, hydrophobic, mycobacterial cell wall, is this by transport or passively? And what is the fate of the 1-TbAd formed in the phagosome?

The second question is whether, and at which rate, 1-TbAd will undergo Dimroth rearrangement to produce *N*<sup>6</sup>-TbAd. We have shown the *in vivo* production of this compound in mice and as discussed in scheme 3 the Dimroth rearrangement produces a proton. Since the rearrangement is thermodynamically down-hill one can argue that over time 1-TbAd acts as an acid (the pKa of *N*<sup>6</sup>-TbAd is estimated to be 3.8).<sup>[45]</sup> In other words, the buffering of the phagosome by 1-TbAd is probably only temporarily. Although this is potentially a weakness of the hypothesis we like to remind the reader that the virulence and survival mechanism of *Mycobacterium tuberculosis* is complex and does not only constitute one mechanism. It might therefore be that 1-TbAd buffers the phagosome, delaying phagolysosome formation, which is then by other factors prohibited indefinitely, making the Dimroth rearrangement not a concern.

### 3.6 Experimental section

#### General remarks:

All reactions were performed using oven-dried glassware under an atmosphere of nitrogen (unless otherwise specified) by standard Schlenk techniques, using dry solvents. Reaction temperature refers to the temperature of the oil bath/cooling bath. Solvents were taken from an MBraun solvent purification system (SPS-800). All other reagents were purchased from Sigma-Aldrich, Acros, TCI Europe or Fluorochem and used without further purification unless noted otherwise.

TLC analysis was performed on Merck silica gel 60/Kieselguhr F254, 0.25 mm. Compounds were visualized using either Seebach's stain (a mixture of phosphomolybdic acid (25 g), cerium (IV) sulfate (7.5 g), H<sub>2</sub>O (500 mL) and H<sub>2</sub>SO<sub>4</sub> (25 mL)), a KMnO<sub>4</sub> stain (K<sub>2</sub>CO<sub>3</sub> (40 g), KMnO<sub>4</sub> (6 g), H<sub>2</sub>O (600 mL) and 10% NaOH (5 mL)), or elemental iodine.

Flash chromatography was performed using SiliCycle silica gel type SiliaFlash P60 (230 – 400 mesh) as obtained from Screening Devices.

<sup>1</sup>H- and <sup>13</sup>C-NMR spectra were recorded on a Varian AMX400 or a Varian 400-MR (400 and 100.59 MHz, respectively) using CDCl<sub>3</sub> or DMSO-*d*<sub>6</sub> as solvent, unless stated otherwise. Chemical shift values are reported in ppm with the solvent resonance as the internal standard (CDCl<sub>3</sub>: δ 7.26 for <sup>1</sup>H, δ 77.16 for <sup>13</sup>C, MeOH-*d*<sub>4</sub> δ 3.31 for <sup>1</sup>H, δ 49.0 for <sup>13</sup>C). Data are reported as follows: chemical shifts (δ), multiplicity (s = singlet, d = doublet, dd = double doublet, ddd = double double doublet, ddp = double double pentet, td = triple doublet, t = triplet, q = quartet, b = broad, m = multiplet), coupling constants *J* (Hz), and integration.

GC-MS measurements were performed with an HP 6890 series gas chromatography system equipped with a HP 5973 mass sensitive detector. GC measurements were made



### *CHAPTER 3*

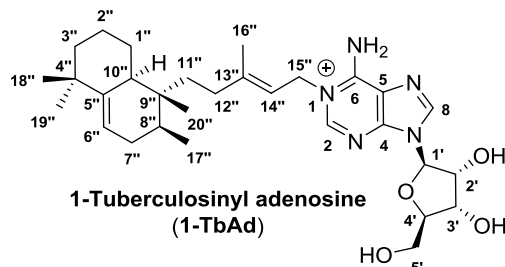
---

using a Shimadzu GC 2014 gas chromatograph system bearing an AT5 column (Grace Alltech) and FID detection.

Enantiomeric excesses were determined by chiral HPLC analysis using a Shimadzu LC-10ADVP HPLC instrument equipped with a Shimadzu SPD-M10AVP diode-array detector. Integration at three different wavelengths (254, 225, 190 nm) was performed and the reported enantiomeric excess is an average of the three integrations. Retention times (t<sub>R</sub>) are given in min.

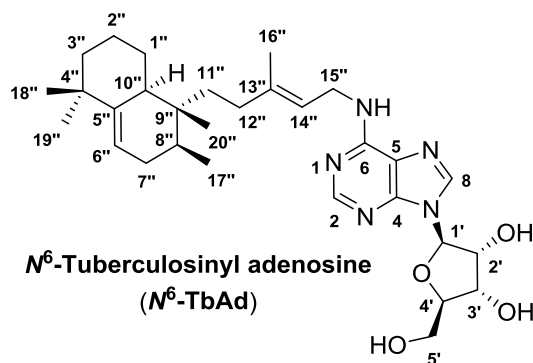
High resolution mass spectra (HRMS) were recorded on a Thermo Scientific LTQ Orbitrap XL.

NMR Analysis of 1-TbAd isolated from *Mycobacterium tuberculosis*



Atom	Carbon	Hydrogen	COSY	NOESY
2	147.2	8.53		1'', 15'', 16'' <sup>a</sup>
8	144.2	8.66		1', 2', 3'' <sup>a</sup>
1'	90.2	6.10 (d, 5.2)	2'	8, 2'
2'	76.4	4.61 (dd, 5.2, 5.1)	1', 3'	8, 1', 3'
3'	71.8	4.34 (dd, 5.1, 4.1)	2', 4'	8, 2', 5'
4'	87.3	4.14 (ddd, 4.1, 3.4, 3.1)	3', 5', 5'	5', 5'
5'	62.4	3.87 (dd, 12.6, 3.1) 3.78 (dd, 12.6, 3.4)	4', 5' 4', 5'	4' 3', 4'
1 $\alpha$ ''	28.4	1.77	1'', 2'', 2''	1'', 2'', 10''
1 $\beta$ ''		1.04	1'', 2'', 2''	1'', 2 $\beta$ '', 20''
2 $\alpha$ ''	23.0	1.62	1'', 1'', 3'', 3''	1'', 3'', 19''
2 $\beta$ ''		1.62	1'', 1'', 3'', 3''	1'', 3''
3 $\alpha$ ''	41.9	1.41	3'', 2'', 2''	2'', 18'', 19''
3 $\beta$ ''		1.21 (ddd, 13.1, 13.1, 4.8)	3'', 2'', 2''	2'', 18''
4''	--	--		
5''	--	--		
6''	117.2	5.48	7'', 7'', 10''	7'', 7'', 18''
7 $\alpha$ ''	32.5	1.87	6'', 7'', 8''	6'', 7'', 8'', 17''
7 $\beta$ ''		1.77	6'', 7'', 8''	6'', 7'', 16'', 17'', 20''
8''	34.5	1.54	7'', 7'', 17''	7'', 7'', 10'', 17''
9''	--	--		
10''	41.1	2.22 (br d, 12.9)	1'', 1'', 6''	2'', 7'', 10'', 12'', 19''
11''	35.5	1.58 1.42	11'', 12'', 12'' 11'', 12'', 12''	8'', 10'', 12'', 16'', 17'', 20'' 8'', 10'', 12'', 16'', 17'', 20''
12''	33.7	2.05 2.05	11'', 11'', 12'' 11'', 11'', 12''	10'', 11'', 11'', 14'', 16'' 10'', 11'', 11'', 14'', 16''
13''	--	--		
14''	115.2	5.46	12'', 15'', 16''	2, 12'', 12''
15''	49.5	4.92 <sup>b</sup> 4.92 <sup>b</sup>	14'' 14''	2, 14'', 16'' 2, 14'', 16''
16''	16.9	1.89		2, 12'', 15''
17''	15.3	0.85 (d, 6.7)	8''	7'', 7'', 8'', 11'', 11'', 20''
18''	30.1	1.06		3'', 3'', 6'', 19''
19''	29.3	1.01		2'', 3'', 10'', 18''
20''	16.5	0.66		1'', 7'', 11'', 17''

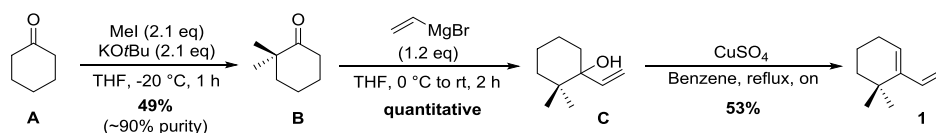
<sup>a</sup>) The expected COSY and NOESY cross peaks are seen within the terpene, base and sugar fragments. NOESY cross peaks between the three fragments are seen between H<sub>8</sub> and the three sugar protons H<sub>1'</sub>, H<sub>2'</sub> and H<sub>3'</sub>, and between H<sub>2</sub> and the terpene protons H<sub>14''</sub>, H<sub>15''</sub>, and H<sub>16''</sub>. <sup>b</sup>) The allylic methylene peak is the expected doublet.

NMR Analysis of  $N^6$ -TbAd isolated from *Mycobacterium tuberculosis*

Atom	Carbon	Hydrogen	COSY	NOESY
2	not observed	8.24		
8	141.3	8.26		1 <sup>a</sup>
1'	90.8	5.95 (d, 6.6)	2'	8, 3' 2'
2'	75.3	4.74 (dd, 6.6, 5.0)	1', 3'	1', 3',
3'	72.4	4.32 (dd, 5.0, 2.6)	2', 4'	2', 5'
4'	88.0	4.17 (ddd, 2.6, 2.4, 2.4)	3', 5', 5'	5', 5'
5'	63.3	3.89 (dd, 12.6, 2.4)	4', 5'	4'
		3.75 (dd, 12.6, 2.4)	4', 5'	3', 4'
1 $\alpha$ ''	28.4	1.77	1'', 2'', 2''	1'', 2'', 10''
1 $\beta$ ''		1.04	1'', 2'', 2''	1'', 2 $\beta$ '', 20''
2 $\alpha$ ''	23.0	1.62	1'', 1'', 3'', 3''	1'', 3'', 19''
2 $\beta$ ''		1.62	1'', 1'', 3'', 3''	1'', 3'',
3 $\alpha$ ''	41.8	1.41	3'', 2'', 2''	2'', 18'', 19''
3 $\beta$ ''		1.21 (ddd, 13.1, 13.1, 4.8)	3'', 2'', 2''	2'', 18''
4''	--	--		
5''	--	--		
6''	117.2	5.48	7'', 7'', 10''	7'', 7'', 18''
7 $\alpha$ ''	32.5	1.86 (br d, 17.3)	6'', 7'', 8''	6'', 7'', 8'', 17''
7 $\beta$ ''		1.77	6'', 7'', 8''	6'', 7'', 16'', 17'', 20''
8''	34.3	1.54	7'', 7'', 17''	7'', 7'', 10'', 17''
9''	--	--		
10''	40.9	2.25 (br d, 12.9)	1'', 1'', 6''	2'', 7'', 10'', 12'', 19''
11''	35.8	1.58	11'', 12'', 12''	8'', 10'', 12'', 16'', 17'', 20''
		1.42	11'', 12'', 12''	8'', 10'', 12'', 16'', 17'', 20
12''	33.7	2.00	11'', 11'', 12''	10'', 11'', 11'', 14'', 16''
		2.00	11'', 11'', 12''	10'', 11'', 11'', 14'', 16''
13''	--	--		
14''	120.5	5.42	12'', 15'', 16''	12'', 12'',
15''	39.3	4.22-4.16 <sup>b</sup>	14''	14'', 16''
		4.22-4.16 <sup>b</sup>	14''	14'', 16''
16''	16.8	1.80		12'', 15''
17''	15.2	0.85 (d, 6.7)	8''	7'', 7'', 8'', 11'', 11'', 20''
18''	30.0	1.06		3'', 3'', 6'', 19''
19''	29.3	1.02		2'', 3'', 10'', 18''
20''	16.4	0.65		1'', 7'', 11'', 17''

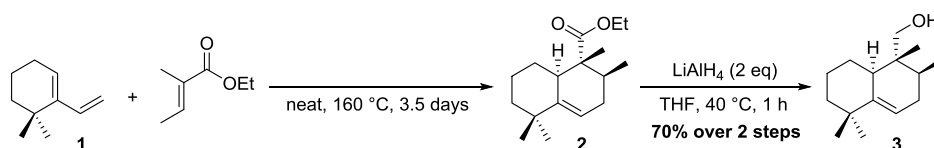
<sup>a</sup>) The expected COSY and NOESY cross peaks are seen within the terpene, base and sugar fragments. The only NOESY cross peak between the three fragments is between H<sub>1'</sub> and H<sub>8</sub>. <sup>b</sup>) The allylic methylene peak is broad rather than the expected doublet due to slow rotation about the C<sub>6</sub>-N bond.

**Experimental procedures and data:**



**6,6-dimethyl-1-vinylcyclohex-1-ene (1):**

For the synthesis of diene **1** see chapter 4.



**(1,2,5,5-tetramethyl-1,2,3,5,6,7,8,8a-octahydronaphthalen-1-yl)methanol (3):**

6,6-dimethyl-1-vinylcyclohex-1-ene **1** (1.5 g, 11.0 mmol) was dissolved in (*E*)-ethyl 2-methylbut-2-enoate (4.55 ml, 33.0 mmol 3 eq) in a pressure vessel and heated at 160 °C for 3.5 d. After the reaction mixture was cooled to rt, the excess of ethyl tiglate was removed under reduced pressure. GC-MS indicated near pure ethyl 1,2,5,5-tetramethyl-1,2,3,5,6,7,8,8a-octahydronaphthalene-1-carboxylate **2** as an *exo:endo* mixture of 2:1. The near pure mixture was used in the next step without further purification.

To a solution of crude Diels-Alder adduct **2** (2.91 g, 11.0 mmol) in dry THF (55 mL) was added portion wise lithium aluminum hydride (835 mg, 22.0 mmol). After addition the reaction was warmed up to 40 °C and stirred for 1 h. GC-MS indicated complete conversion of the starting material. The reaction mixture was cooled to -10 °C using an ice/salt bath, and quenched using water. After phase separation the etherial layer was washed with an aqueous 1 M HCl solution, water, and brine, where after it was dried over MgSO<sub>4</sub>, filtered and concentrated under reduced pressure to afford 2.7 g of a yellow oil. Flash column chromatography using pentane : ether (4:1) gave (1,2,5,5-tetramethyl-1,2,3,5,6,7,8,8a-octahydronaphthalen-1-yl)methanol **3** (1.7 g, 7.7 mmol, 70% yield over the two steps).

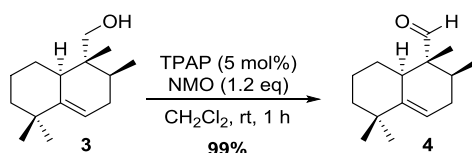
<sup>1</sup>H-NMR (400 MHz, CDCl<sub>3</sub>) δ 5.43 (d, *J* = 5.2 Hz, 1H), 3.48 (d, *J* = 11.4 Hz, 1H), 3.39 (d, *J* = 11.3 Hz, 1H), 2.36 (d, *J* = 12.9 Hz, 1H), 1.91 – 1.81 (m, 1H), 1.81 – 1.71 (m, 2H), 1.70 – 1.63 (m, 2H), 1.61 – 1.51 (m, 2H), 1.38 (s, 1H), 1.28 – 1.14 (m, 2H), 1.05 (s, 3H), 1.00 (s, 3H), 0.86 (d, *J* = 6.5 Hz, 3H), 0.51 (s, 3H).

<sup>13</sup>C-NMR (101 MHz, CDCl<sub>3</sub>) δ 146.12, 116.11, 65.78, 41.07, 39.33, 38.05, 36.27, 31.93, 31.33, 29.86, 28.86, 27.74, 22.26, 15.09, 11.63.

HRMS (ESI<sup>+</sup>): Calculated mass [M+H]<sup>+</sup> C<sub>15</sub>H<sub>27</sub>O<sup>+</sup> = 223.2056; found: 223.2059

### CHAPTER 3

The analytical data are in agreement with: a) J. E. Spangler, C. A. Carson, E. J. Sorensen, *Chem. Sci.* **2010**, *1*, 202. and b) N. Mangel, F. M. Mann, M. L. Hillwig, R. J. Peters, B. B. Snider, *Org. Lett.* **2010**, *12*, 2626.



#### 1,2,5,5-tetramethyl-1,2,3,5,6,7,8,8a-octahydronaphthalene-1-carbaldehyde (**4**):

Alcohol **3** (1.60 g, 7.2 mmol) was dissolved in CH<sub>2</sub>Cl<sub>2</sub> (30 mL) where after TPAP (126 mg, 0.36 mmol, 5 mol%) and NMO (1.01 g, 8.64 mmol, 1.2 eq) were added, and the reaction mixture was stirred for 1 h. When TLC analysis confirmed completion of the reaction, the solvent was evaporated, and the crude was filtered through a short silica column, flushing with a 1:1 pentane : ether mixture, giving aldehyde **4** (1.58 g, 99% yield).

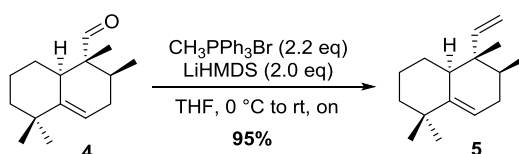
<sup>1</sup>H-NMR (400 MHz, CDCl<sub>3</sub>) δ 9.38 (s, 1H), 5.52 – 5.47 (m, 1H), 2.50 (d, *J* = 13.1 Hz, 1H), 2.00 – 1.91 (m, 1H), 1.90 – 1.80 (m, 1H), 1.80 – 1.69 (m, 1H), 1.57 – 1.49 (m, 2H), 1.45 – 1.37 (m, 1H), 1.36 – 1.28 (m, 1H), 1.27 – 1.14 (m, 2H), 1.08 (s, 3H), 1.04 (s, 3H), 0.80 (s, 3H), 0.78 (d, *J* = 6.5 Hz, 3H).

<sup>13</sup>C-NMR (101 MHz, CDCl<sub>3</sub>) δ 207.16, 143.92, 116.56, 52.26, 40.61, 38.15, 36.28, 32.65, 30.47, 29.66, 29.13, 28.68, 21.77, 16.14, 7.49.

Some of the characteristic signals of the *endo* product are:

<sup>1</sup>H-NMR (400 MHz, CDCl<sub>3</sub>) δ 9.65 (s, 1H), 1.06 (s, 3H), 1.04 (s, 3H), 1.02 (s, 3H), 0.99 (s, 3H), 0.92 (s, 3H), 0.82 (d, *J* = 6.7, 3H), 0.79 (s, 3H).

The analytical data are in agreement with: a) J. E. Spangler, C. A. Carson, E. J. Sorensen, *Chem. Sci.* **2010**, *1*, 202. and b) N. Mangel, F. M. Mann, M. L. Hillwig, R. J. Peters, B. B. Snider, *Org. Lett.* **2010**, *12*, 2626.



#### 1,1,5,6-tetramethyl-5-vinyl-1,2,3,4,4a,5,6,7-octahydronaphthalene (**5**):

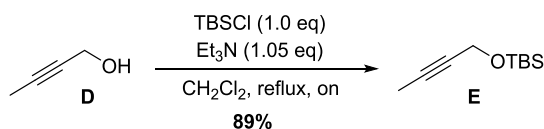
A stirred suspension of methyltriphenylphosphonium bromide (585 mg, 1.64 mmol, 2.2 eq) in dry THF (9 mL) was treated with a solution of LiHMDS (1.5 mL, 1.5 mmol, 1 M in THF, 2.0 eq) at 0 °C. The initial suspension was stirred for 30 min after which a clear bright yellow solution was obtained. To the solution, still at 0 °C, was added dropwise

*The discovery of novel terpene nucleosides from Mycobacterium tuberculosis*

1,2,5,5-tetramethyl-1,2,3,5,6,7,8,8a-octahydronaphthalene-1-carbaldehyde **4** (164 mg, 0.744 mmol) in dry THF (9 mL). The resulting reaction mixture was allowed to warm up to rt and was stirred overnight. The reaction was quenched with a saturated solution of NaHCO<sub>3</sub> and diluted with ether. The phases were separated and the organic layer was washed with distilled water, brine and dried over Na<sub>2</sub>SO<sub>4</sub>. Flash chromatography employing pentane furnished 1,1,5,6-tetramethyl-5-vinyl-1,2,3,4,4a,5,6,7-octahydronaphthalene **5** (155 mg, 0.710 mmol, 95% yield) as a colorless oil.

<sup>1</sup>H-NMR (400 MHz, CDCl<sub>3</sub>) δ 5.55 (dd, *J* = 17.5, 10.8 Hz, 1H), 5.49 – 5.45 (m, 1H), 5.06 (dd, *J* = 10.8, 1.6 Hz, 1H), 4.92 (dd, *J* = 17.5, 1.6 Hz, 1H), 2.03 – 1.96 (m, 1H), 1.95 – 1.84 (m, 1H), 1.78 – 1.69 (m, 1H), 1.67 – 1.59 (m, 1H), 1.57 – 1.36 (m, 4H), 1.35 – 1.15 (m, 1H), 1.07 (s, 3H), 1.01 (s, 3H), 0.97 – 0.91 (m, 1H), 0.75 (d, *J* = 6.8 Hz, 3H), 0.71 (s, 3H).

The analytical data are in agreement with: a) J. E. Spangler, C. A. Carson, E. J. Sorensen, *Chem. Sci.* **2010**, *1*, 202.

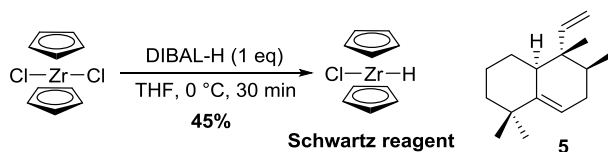


**(but-2-yn-1-yloxy)(tert-butyl)dimethylsilane (E):**

To a solution of but-2-yn-1-ol **D** (1.0 ml, 13.4 mmol) and triethylamine (2.0 mL, 14.0 mmol, 1.05 eq) in CH<sub>2</sub>Cl<sub>2</sub> (60 ml) at rt was added TBSCl (2.0 g, 13.4 mmol, 1.0 eq). The reaction mixture was refluxed overnight, cooled to rt, and quenched with a saturated NaHCO<sub>3</sub> solution (10 mL). The two phases were separated and the organic layer was washed with water (3x20 mL). The organic layer was dried over Na<sub>2</sub>SO<sub>4</sub>, filtered and concentrated under reduced pressure. Flash column chromatography employing pentane as an eluent furnished (but-2-yn-1-yloxy)(*tert*-butyl)dimethylsilane **E** (2.2 g, 11.9 mmol, 89% yield) as a colorless oil.

<sup>1</sup>H-NMR (400 MHz, CDCl<sub>3</sub>) δ 4.28 (s, 2H), 1.83 (t, *J* = 2.4 Hz, 3H), 0.91 (s, 9H), 0.86 (s, 6H).

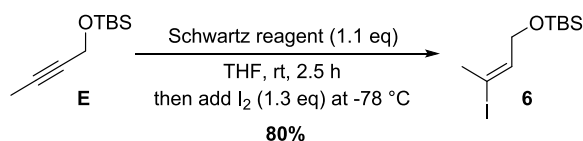
The analytical data are in agreement with: D. F. Harvey, D. A. Neil, *Tetrahedron* **1993**, *49*, 2145.

**Schwartz reagent:**

To a suspension of  $\text{ZrCp}_2\text{Cl}_2$  (2.0 gr, 6.84 mmol) in dry THF (15.6 mL) was added dropwise neat DIBAL-H (1.21 mL, 6.84 mmol, 1 eq). The reaction was stirred for 45 min where after the suspension was decanted. The white solid (the Schwartz reagent) was washed 3 times with THF (3x8 mL) and vacuum was applied to evaporate the residual solvent. The remaining white solid (0.8 g, 45% yield) was transferred into a fridge in a glovebox.

*The low yield can be attributed to the solubility of Schwartz reagent in THF. Next experiments should be performed using cold THF and with a double Schlenk flask with a glass filter in between to make the washing and decantation more effective.*

The analytical data are in agreement with: Z. Huang, E-I. Negishi, *Org. Lett.* **2006**, 8, 3675.

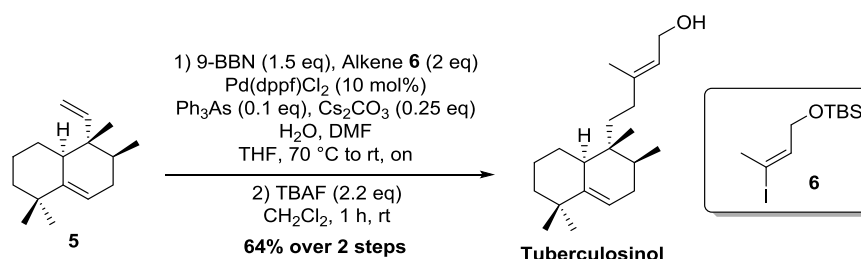
**(E)-tert-butyl((3-iodobut-2-en-1-yl)oxy)dimethylsilane (6):**

To a suspension of Schwartz reagent (462 mg, 1.8 mmol, 1.1 eq) in dry THF (4 mL) was added (but-2-yn-1-yloxy)(*tert*-butyl)dimethylsilane **E** (300 mg, 1.62 mmol) in dry THF (2 mL). The reaction was stirred for 2.5 h. The resulting suspension was cooled to  $-78^\circ\text{C}$  where after  $\text{I}_2$  (537 mg, 2.1 mmol, 1.3 eq) was added. The reaction was stirred for 90 min after which the reaction was quenched with an aqueous 1 M HCl solution (3 mL). The two phases were separated and the combined organic layers were washed thoroughly with an aqueous saturated  $\text{Na}_2\text{S}_2\text{O}_3$  solution (3x5 mL) and brine (5 mL). The organic layer was dried using  $\text{Na}_2\text{SO}_4$ , filtered and concentrated under reduced pressure. Flash column chromatography employing pentane : ether (97:3) as the eluent afforded pure vinyl iodide **6** (405 mg, 1.2 mmol, 80% yield).

$^1\text{H-NMR}$  (400 MHz,  $\text{CDCl}_3$ )  $\delta$  5.75 (t,  $J = 4.7$  Hz, 1 H), 4.25 (d,  $J = 4.7$  Hz, 2 H), 2.57 (s, 3 H), 0.98 (s, 9 H) 0.16 (s, 6 H).

$^{13}\text{C-NMR}$  (101 MHz,  $\text{CDCl}_3$ )  $\delta$  135.66, 99.30, 68.73, 33.84, 26.31 (3xC), 18.49, -4.96 (2xC).

The analytical data are in agreement with: Z. Huang, E-I. Negishi, *Org. Lett.* **2006**, *8*, 3675.



**(E)-3-methyl-5-(-1,2,5,5-tetramethyl-1,2,3,5,6,7,8,8a-octahydronaphthalen-1-yl)pent-2-en-1-ol (tuberculosinol):**

To alkene **5** (300 mg, 1.37 mmol) was added a solution of 9-BBN (4.2 mL, 0.5 M in THF, 1.5 eq). The resulting mixture was heated to 70 °C for 3 h, and cooled to rt, after TLC analysis indicated full consumption of the starting material. Iodo-alkene **6** (1.14 g, 2.74 mmol, 2 eq) was dissolved in degassed DMF (10 mL). Pd(dppf)Cl<sub>2</sub> (100 mg, 0.137 mmol, 0.1 eq), triphenyl arsine (42 mg, 0.137 mmol, 0.1 eq), cesium carbonate (110 mg, 0.34 mmol, 0.25 eq) and degassed distilled water (0.95 mL, 54 mmol, 40 eq) were added, yielding a dark solution with Cs<sub>2</sub>CO<sub>3</sub> being suspended.

The hydroboration reaction was added to the DMF mixture mentioned above, using syringe. The combined reaction was immediately degassed after mixing, utilizing three freeze-pump-thaw cycles. After vigorously stirring the reaction overnight at rt, the reaction was checked by TLC and GC-MS. As the conversion was complete, the mixture was diluted with water, and extracted three times with diethyl ether. The combined organic layers were dried with magnesium sulfate, concentrated *in vacuo* and purified using column chromatography, using pentane : ether (95:5) as an eluent.

The obtained product was stirred with TBAF (3 mL, 1 M in THF, 3.0 mmol, 2.2 eq) in CH<sub>2</sub>Cl<sub>2</sub> (10 mL). After 1 h, the reaction was complete, as indicated by TLC. The reaction mixture was concentrated *in vacuo*, and purified by flash chromatography (pentane : ether 7:3) yielding *rac*-tuberculosinol as a colorless oil (64% yield over two steps).

<sup>1</sup>H-NMR (400 MHz, CDCl<sub>3</sub>) δ 5.43 – 5.33 (m, 2H), 4.08 (d, *J* = 6.8 Hz, 2H), 2.57 (s, 1H), 2.13 (d, *J* = 12.6 Hz, 1H), 1.92 – 1.85 (m, 2H), 1.81 – 1.67 (m, 3H), 1.65 (s, 3H), 1.59 – 1.28 (m, 6H), 1.28 – 1.10 (m, 1H), 1.02 (s, 3H), 0.97 (s, 3H), 0.78 (d, *J* = 6.8 Hz, 3H), 0.59 (s, 3H).

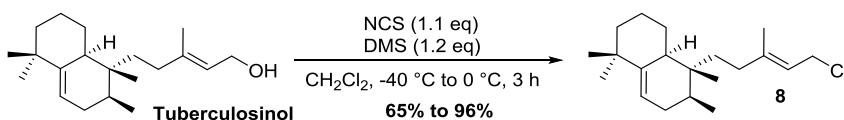
<sup>13</sup>C-NMR (101 MHz, CDCl<sub>3</sub>) δ 145.99, 140.10, 123.11, 116.13, 59.09, 40.94, 39.81, 36.92, 36.05, 34.97, 33.38, 32.76, 31.65, 29.78, 29.00, 27.44, 22.27, 16.46, 16.18, 15.10.



### CHAPTER 3

Some of the characteristic signals of the *endo* product are  $^1\text{H-NMR}$  (400 MHz,  $\text{CDCl}_3$ )  $\delta$  5.29 – 5.15 (m, 2H), 4.02 (d,  $J = 6.8$ , 2H), 2.4 – 0.7 (m, 13H), 1.56 (s, 3H), 0.93 (s, 3H), 0.87 (s, 3H), 0.68 (d,  $J = 6.7$ , 3H), 0.49 (s, 3H).

The analytical data are in agreement with: a) J. E. Spangler, C. A. Carson, E. J. Sorensen, *Chem. Sci.* **2010**, *1*, 202. and b) N. Mangel, F. M. Mann, M. L. Hillwig, R. J. Peters, B. B. Snider, *Org. Lett.* **2010**, *12*, 2626.



#### 5-((*E*)-5-chloro-3-methylpent-3-en-1-yl)-1,1,5,6-tetramethyl-1,2,3,4,4a,5,6,7-octahydronaphthalene (Tuberculosinyl chloride) – Method A

NCS (20 mg, 0.15 mmol, 1.1 eq) was dissolved in  $\text{CH}_2\text{Cl}_2$  (5 mL), and cooled to  $-30\text{ }^\circ\text{C}$ . DMS (10 mg, 0.16 mmol, 1.16 eq) was added, and the mixture was allowed to warm to  $0\text{ }^\circ\text{C}$  for 5 min. Subsequently, the mixture was cooled to  $-40\text{ }^\circ\text{C}$ , and tuberculosinol (40 mg, 0.14 mmol, 1 eq) in  $\text{CH}_2\text{Cl}_2$  (2 mL) was added over 3 min. The reaction mixture was removed from the cooling bath, and stirred at  $0\text{ }^\circ\text{C}$  for 15 min, before being stirred at rt for 1 h. TLC analysis showed complete conversion, and after evaporating the solvent, the crude mixture was purified by filtration on silica with pentane. Tuberculosinyl chloride **10** was obtained as a colorless oil (41 mg, 96% yield)\*

\* Typical yields obtained employing method A varied from 65% to 96%.

#### (4a*S*,5*R*,6*S*)-5-((*E*)-5-chloro-3-methylpent-3-en-1-yl)-1,1,5,6-tetramethyl-1,2,3,4,4a,5,6,7-octahydronaphthalene (Tuberculosinyl chloride) – Method B

To a solution (0.2 M) of tuberculosinol (32 mg, 0.103 mmol) in dry  $\text{CH}_2\text{Cl}_2$  was added triethylamine (15.6 mg, 21.6  $\mu\text{L}$ , 0.154 mmol, 1.5 eq). The obtained solution was cooled with an ice/salt bath and mesyl chloride (13.0 mg, 8.8  $\mu\text{L}$ , 0.114 mmol, 1.1 eq) was added. The ice/salt bath was removed and the reaction was allowed to stir at rt for 45 min whereupon NMR analysis indicated that the reaction was complete. The reaction mixture was diluted with  $\text{Et}_2\text{O}$ , transferred to a separatory funnel and washed with water (2 mL), HCl solution (2 mL, 2 M), saturated aqueous  $\text{NaHCO}_3$  solution (2 mL) and brine (2 mL). The organic layer was dried using  $\text{Na}_2\text{SO}_4$ , filtered and concentrated under reduced pressure. Tuberculosinyl chloride **10** was isolated as a yellowish oil (32 mg, 94% yield).

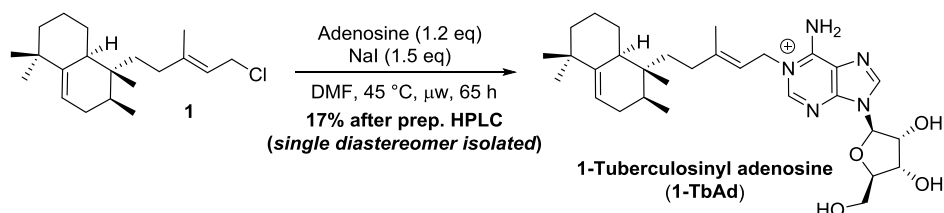
$^1\text{H-NMR}$  (400 MHz,  $\text{CDCl}_3$ )  $\delta$  5.51 – 5.41 (m, 2H), 4.09 (d,  $J = 7.9$  Hz, 2H), 2.16 (d,  $J = 12.8$  Hz, 1H), 1.96 (dt,  $J = 10.4$ , 4.6 Hz, 2H), 1.83 (ddd,  $J = 17.7$ , 14.5, 3.5 Hz, 2H), 1.75 (s, 3H), 1.72 (s, 1H), 1.63 – 1.25 (m, 7H), 1.20 (td,  $J = 12.9$ , 4.8 Hz, 1H), 1.06 (s, 3H), 1.01 (s, 3H), 0.82 (d,  $J = 6.8$  Hz, 3H), 0.63 (s, 3H).

*The discovery of novel terpene nucleosides from Mycobacterium tuberculosis*

$^{13}\text{C}$ -NMR (101 MHz,  $\text{CDCl}_3$ )  $\delta$  146.11, 144.03, 119.92, 116.27, 41.34, 41.05, 39.93, 37.11, 36.20, 34.82, 33.51, 32.88, 31.75, 29.90, 29.13, 27.56, 22.37, 16.46, 16.28, 15.22.

HRMS (APCI): Calculated mass  $[\text{M}-\text{Cl}]^+ \text{C}_{20}\text{H}_{30}^+ = 273.2582$ ; found: 273.2576.

**Important note:** *The tuberculosinyl chloride 8 was purified using column chromatography. Later work showed purification by these means led to degradation of the product on the column. Therefore an alternative purification strategy was developed which is presented in the experimental section of chapter 4. This procedure is recommended as the stability of the tuberculosinyl chloride on silica is suspected to be batch dependent.*



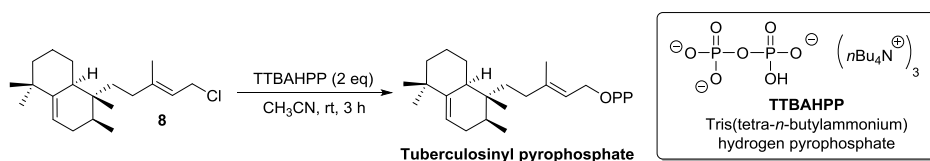
**6-amino-9-((2R,3R,4S,5R)-3,4-dihydroxy-5-(hydroxymethyl)tetrahydrofuran-2-yl)-1-((E)-3-methyl-5-(1,2,5,5-tetramethyl-1,2,3,5,6,7,8,8a-octahydronaphthalen-1-yl)pent-2-en-1-yl)-9H-purin-1-ium (1-TbAd):**

To a solution of **10** (11 mg, 35.6  $\mu\text{mol}$ ) in peptide grade DMF (0.7 mL) was added adenosine (11.4 mg, 42.7  $\mu\text{mol}$ , 1.2 eq) and sodium iodide (8 mg, 53.4  $\mu\text{mol}$ , 1.5 eq). The resulting reaction mixture was exposed to microwave heating (45 °C with an initial overshoot to 48 °C) for 65 h where after it was concentrated under reduced pressure. The resulting oil was purified employing preparative HPLC. 1-TbAd was obtained a colorless oil (3 mg, 17% yield).

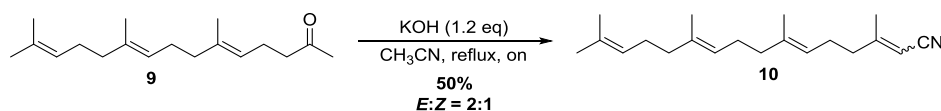
$^1\text{H}$ -NMR (400 MHz,  $\text{CD}_3\text{OD}$ )  $\delta$  8.62 (s, 1H), 8.49 (s, 1H), 6.08 (d,  $J = 5.2$  Hz, 1H), 5.51 – 5.42 (m, 2H), 4.91 (d,  $J = 6.6$  Hz, 2H), 4.62 (t,  $J = 5.1$  Hz, 2H), 4.58 (s, 1H), 4.38 – 4.31 (m, 2H), 4.15 (q,  $J = 3.3$  Hz, 1H), 3.87 (dd,  $J = 12.3, 2.9$  Hz, 1H), 3.77 (dd,  $J = 12.2, 3.4$  Hz, 1H), 2.23 (d,  $J = 12.1$  Hz, 2H), 2.12 – 2.04 (m, 2H), 1.89 (s, 3H), 1.87 – 1.82 (m, 1H), 1.84 – 1.71 (m, 2H), 1.65 – 1.47 (m, 5H), 1.47 – 1.36 (m, 3H), 1.21 (ddd,  $J = 12.7, 5.7$  Hz, 1H), 1.06 (s, 3H), 1.01 (s, 3H), 0.85 (d,  $J = 6.7$  Hz, 3H), 0.66 (s, 3H).

$^{13}\text{C}$ -NMR (101 MHz,  $\text{CD}_3\text{OD}$ )  $\delta$  152.52, 147.78, 147.58, 147.31, 147.08, 143.74, 121.49, 117.34, 115.89, 90.43, 87.41, 76.35, 71.79, 62.62, 49.39, 42.00, 41.06, 38.05, 36.94, 35.87, 34.52, 33.88, 32.62, 30.29, 29.49, 28.53, 23.18, 17.35, 16.58, 15.54.

HRMS (ESI+): Calculated mass  $[\text{M}+\text{H}]^+ \text{C}_{30}\text{H}_{46}\text{N}_5\text{O}_4^+ = 540.3544$ ; found: 540.3542.

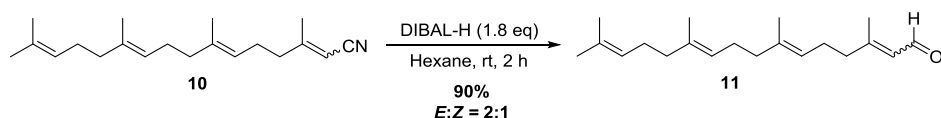
**Tuberculosinyl pyrophosphate:**

To a solution of TTBAHPP (58 mg, 64.3  $\mu\text{mol}$ , 2 eq.) in  $\text{CH}_3\text{CN}$  (1 mL), in an oven-dried Schlenk flask under nitrogen atmosphere, was added a solution of tuberculosinyl chloride **8** (10 mg, 32.2  $\mu\text{mol}$ ) in dry  $\text{CH}_3\text{CN}$  (0.5 mL). The solution was stirred for 3 h after which TLC analysis, using *pentane* as an eluent, indicated complete conversion of the starting material. The solvent was removed under reduced pressure where after the residue was dissolved in dry methanol and passed through a pre-washed column DOWEX<sup>®</sup> 50WX2  $\text{Na}^+$ -form (50-100 mesh). This process was repeated twice after which the methanol was evaporated. The compound was used without further purification.

**(2*E*,6*E*,10*E*)- and (2*Z*,6*E*,10*E*)-3,7,11,15-tetramethyl-2,6,10,14-hexadecatetraenitrile (10):**

A solution of farnesylacetone **9** (5.0 g, 19.1 mmol) in MeCN (20 mL) was added to a stirred solution of powdered KOH (1.3 g, 23.2 mmol, 1.2 eq) in MeCN (30 mL) at reflux. The mixture was subsequently stirred overnight at reflux. The mixture was cooled down to rt, 30 mL of water was added, and the mixture was extracted with ether. The combined organic layers were washed with brine, dried over  $\text{Na}_2\text{SO}_4$ , filtered, and concentrated under reduced pressure. The residue was purified by column chromatography on silica gel (50:1) pentane : EtOAc to afford **10** (2.7 g, 50%, *E:Z* = 2:1) as a pale yellow oil.

<sup>1</sup>H-NMR (400 MHz,  $\text{CDCl}_3$ )  $\delta$  5.12 – 5.03 (m, 4H), 2.46 – 2.41 (m, 1H), 2.24-2.15 (m, 3H), 2.11 – 1.96 (m, 10H), 1.91 – 1.90 (m, 1H), 1.68 (s, 6H), 1.60 (s, 6H).

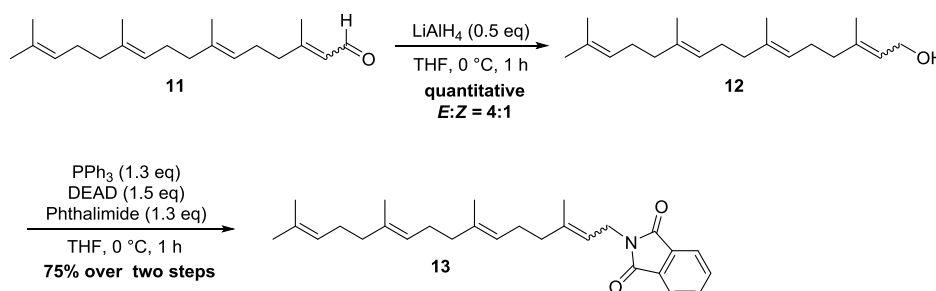
**(2*E*,6*E*,10*E*)- and (2*Z*,6*E*,10*E*)-3,7,11,15-tetramethyl-2,6,10,14-hexadecatetraenal (11):**

To a solution of **10** (1.6 g, 5.6 mmol) in dry hexane (10 mL) at rt was slowly added DIBAL-H (10 mL, 1M in hexane, 10 mmol, 1.8 eq). The reaction mixture was stirred

*The discovery of novel terpene nucleosides from Mycobacterium tuberculosis*

for 2 h at rt and carefully hydrolyzed by addition of 10% aq. HCl. The solid material was filtered off and washed with ether. The combined organic layers were washed with brine, dried over Na<sub>2</sub>SO<sub>4</sub>, filtered off and concentrated under reduced pressure. The residue was purified by column chromatography on silica gel (pentane : EtOAc, 20:1) to afford **11** (1.5 g, 90%, 2:1 *E:Z* = 2:1) as a pale yellow oil.

<sup>1</sup>H-NMR (400 MHz, CDCl<sub>3</sub>) δ 10.00 – 9.89 (m, 1H), 5.88 (d, *J* = 8.0 Hz, 1H), 5.12 – 5.07 (m, 3H), 2.27 – 2.16 (m, 5H) 2.07 – 1.97 (m, 10H), 1.68 (s, 6H), 1.60 (s, 6H).



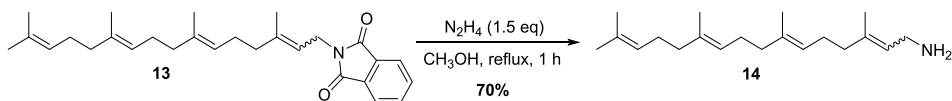
**(2*E*,6*E*,10*E*)- and (2*Z*,6*E*,10*E*)-3,7,11,15-Tetramethyl-2,6,10,14-hexadecatetraenyl-1*H*-isoindole-1,3(2*H*)-dione (**13**):**

To a solution of **11** (129 mg, 0.45 mmol) in dry THF (2 mL) was added dropwise LiAlH<sub>4</sub> (0.23 mL, 1M in THF, 0.23 mmol, 0.5 eq) at 0 °C under nitrogen atmosphere. The mixture was stirred at this temperature for 1 h and ether (3 mL) was added, followed by 1 M NaOH (1 mL). The solid material was filtered off and washed with ether. The filtrate was concentrated to give crude geranylgeraniol (**12**) as a pale yellow oil, which was used for the next step with further purification.

<sup>1</sup>H-NMR (400 MHz, CDCl<sub>3</sub>) δ 5.43-5.40 (m, 1H), 5.13-5.09 (m, 3H), 4.16-4.08 (m, 2H, *E:Z* = 4:1), 2.14-1.95 (m, 13H), 1.68 (s, 8H), 1.60 (2s, 6H).

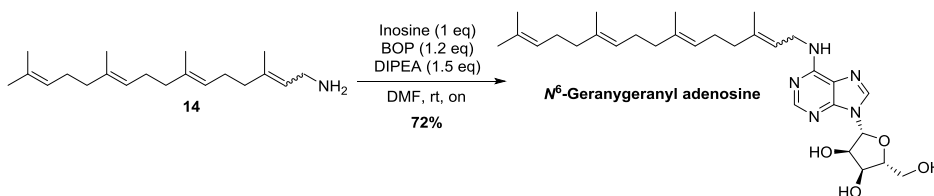
To a solution of crude **12** in THF (3 mL) was added triphenylphosphine (154 mg, 0.59 mmol, 1.3 eq), diethyl azodicarboxylate (DEAD, 0.27 mL, 40% in toluene, 0.69 mmol, 1.5 eq) and phthalimide (87 mg, 0.59 mmol, 1.3 eq) at 0 °C. The mixture was stirred at this temperature for 1 h and subsequently concentrated under reduced pressure. The residue was dissolved in CH<sub>2</sub>Cl<sub>2</sub> (10 mL) and the solution was washed with 1 M aq. NaOH and brine, dried over Na<sub>2</sub>SO<sub>4</sub>, filtered, and concentrated under reduced pressure. Crude **13** was purified by column chromatography on silica gel (40:1 pentane : EtOAc) to afford **13** (140 mg, 75% over two steps) as a pale yellow oil.

<sup>1</sup>H-NMR (400 MHz, CDCl<sub>3</sub>) δ 7.83 – 7.81 (m, 2H), 7.71 – 7.68 (m, 2H), 5.29 – 5.25 (m, 1H), 5.10 – 5.04 (m, 3H), 4.27 (d, *J* = 7.2, 2H), 2.10 – 1.92 (m, 12H), 1.83 – 1.71 (m, 3H), 1.66 – 1.63 (m, 6H), 1.60 – 1.56 (m, 6H) The spectral data are identical to those previously reported.



**(2*E*,6*E*,10*E*)- and (2*Z*,6*E*,10*E*)-3,7,11,15-tetramethyl-2,6,10,14-hexadecatetraenyl-1-amine (14):**

To a solution of **13** (140 mg, 0.33 mmol) in methanol (3 mL) was added hydrazine hydrate (24  $\mu$ L, 0.50 mmol, 1.5 eq). The resulting mixture was heated at reflux for 1 h and then concentrated under reduced pressure. The residue was dissolved in 1 M aq. HCl and solid material was removed by filtration. The filtrate was made basic with 5 M aq. NaOH, filtered and concentrated under reduced pressure to afford **14** (68 mg, 70%), which was used for the next step without further purification.

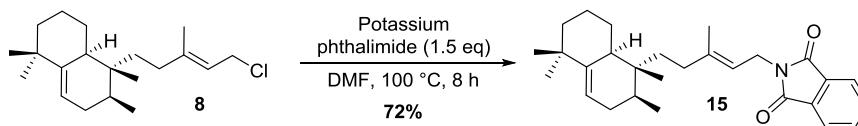


***N*<sup>6</sup>-geranylgeranyladenosine:**

To a solution of **14** (30 mg, 0.104 mmol) in DMF (1.5 mL) was added inosine (28 mg, 0.104 mmol, 1 eq), BOP (benzotriazole-1-yl-oxy-tris-(dimethylamino)-phosphonium hexafluorophosphate, 55 mg, 0.12 mmol, 1.2 eq) and DIPEA (27  $\mu$ L, 0.16 mmol, 1.5 eq) at rt under nitrogen atmosphere. The reaction was stirred overnight at this temperature. The solvent was removed under reduced pressure and the crude product was purified by column chromatography on silica gel using CH<sub>2</sub>Cl<sub>2</sub> : CH<sub>3</sub>OH (20:1) to afford *N*<sup>6</sup>-geranylgeranyl adenosine (45 mg, 72%, mixture of *E* and *Z* isomers) as a dark yellow oil.

<sup>1</sup>H-NMR (400 MHz, CDCl<sub>3</sub>)  $\delta$  8.11 (br s, 1H), 7.75 (s, 1H), 5.92 (br s, 1H), 5.78 (d, *J* = 7.2 Hz, 1H), 5.3.6 – 5.32 (m, 1H), 5.09 (s, 3H), 5.00 – 4.97 (m, 1H), 4.42 (d, *J* = 4.8 Hz, 1H), 4.30 (s, 1H), 4.25 – 4.05 (2x br s, 2H, rotamers due to slow rotation about the C-*N*<sup>6</sup> bond), 3.91 (d, *J* = 12.4 Hz, 1H), 3.71 (d, *J* = 12.0 Hz, 1H), 2.13-1.94 (m, 12H), 1.75 – 1.72 (m, 3H), 1.66 (s, 6H), 1.59 (s, 6H), 1.48 – 1.41 (m, 3H, OH); (the peak at  $\delta$  2.55 (d, *J* = 9.6 Hz) is due to residual HMPA).

HRMS (ESI<sup>+</sup>): calculated for [M+H<sup>+</sup>] C<sub>30</sub>H<sub>46</sub>N<sub>5</sub>O<sub>4</sub><sup>+</sup> = 540.3544; found: 540.3525.



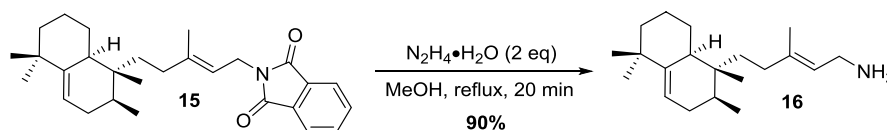
**2-((*E*)-3-methyl-5-(1,2,5,5-tetramethyl-1,2,3,5,6,7,8,8a-octahydronaphthalen-1-yl)pent-2-en-1-yl)isoindoline-1,3-dione (**15**):**

Chloride **8** (35 mg, 0.114 mmol) was dissolved in peptide grade DMF (10 mL) and potassium phthalimide (31.6 mg, 0.171 mmol, 1.5 eq) was added. The solution was stirred for 8 h at 100 °C. The resulting mixture was concentrated, and purified by flash chromatography with pentane : ether (4:1), yielding phthalimide **15** (34 mg, 72%).

<sup>1</sup>H-NMR (400 MHz, CDCl<sub>3</sub>) δ 7.83 (dd, *J* = 5.4, 3.0, 2H), 7.70 (dd, *J* = 5.3, 3.1, 2H) δ 5.42 – 5.26 (m, 2H), 4.27 (d, *J* = 8.0, 2H), 2.19 – 1.86 (m, 5H), 1.85 (s, 3H) 1.84 – 1.10 (m, 9H), 1.03 (s, 3H), 0.97 (s, 3H), 0.78 (d, *J* = 6.7, 3H), 0.59 (s, 3H).

<sup>13</sup>C-NMR (101 MHz, CDCl<sub>3</sub>) δ 168.15, 146.07, 141.71, 133.77, 132.33, 123.13, 117.40, 116.10, 40.91, 39.74, 36.93, 36.06, 35.87, 34.66, 33.35, 32.69, 31.62, 29.75, 28.99, 27.38, 22.21, 16.63, 16.10, 15.07.

HRMS (ESI+): calculated for [M+H]<sup>+</sup> C<sub>28</sub>H<sub>37</sub>NO<sub>2</sub><sup>+</sup> = 420.2903 found 420.2891.



**(*E*)-3-methyl-5-(1,2,5,5-tetramethyl-1,2,3,5,6,7,8,8a-octahydronaphthalen-1-yl)pent-2-en-1-amine (**16**):**

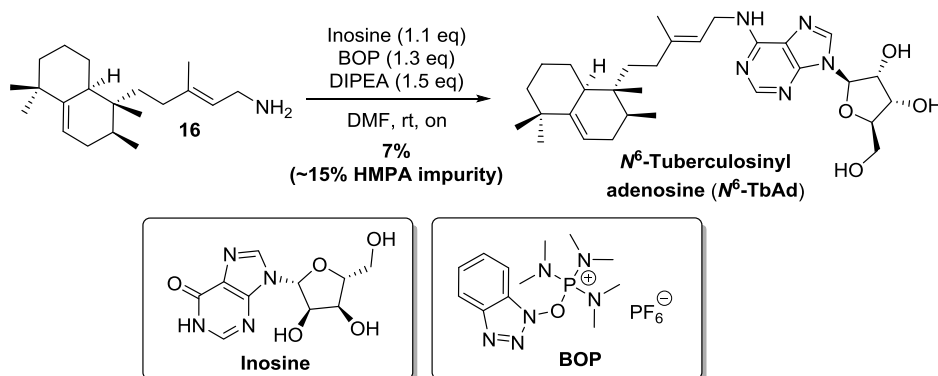
Phthalimide **15** (13 mg, 0.032 mmol) was dissolved in methanol (2 mL), and treated with hydrazine hydrate (3.3 μL, 0.62 mmol, 2 eq). The reaction was heated to reflux for 20 min, after which TLC indicated the reaction was complete. The methanol was completely evaporated under reduced pressure, and the resulting oil was diluted with water, and extracted twice with pentane. The combined pentane layers were dried using magnesium sulfate, and concentrated under reduced pressure to yield amine **16** as slightly yellow oil (8 mg, 90%).

<sup>1</sup>H-NMR (400 MHz, CDCl<sub>3</sub>) δ 5.50 – 5.26 (m, 2H), 3.27 (d, *J* = 6.7, 2H), 2.20 – 1.68 (m, 5H), 1.65 (s, 3H), 1.60 – 1.15 (m, 11H), 1.06 (s, 3H), 1.00 (s, 3H), 0.81 (d, *J* = 6.7, 3H), 0.61 (s, 3H).

<sup>13</sup>C-NMR (101 MHz, CDCl<sub>3</sub>) δ 146.10, 137.48, 125.28, 116.11, 40.94, 39.79, 39.68, 36.93, 36.07, 35.08, 33.37, 32.69, 31.65, 29.77, 29.69, 29.01, 27.42, 22.26, 16.33, 16.17, 15.08.

CHAPTER 3

HRMS (ESI+): calculated for  $[M+H]^+ C_{20}H_{35}N^+ = 290.2848$  found 290.2843.



**(2R,3S,4R,5R)-2-(hydroxymethyl)-5-(6-(((E)-3-methyl-5-(1,2,5,5-tetramethyl-1,2,3,5,6,7,8,8a-octahydronaphthalen-1-yl)pent-2-en-1-yl)amino)-9H-purin-9-yl)tetrahydrofuran-3,4-diol ( $N^6$ -TbAd):**

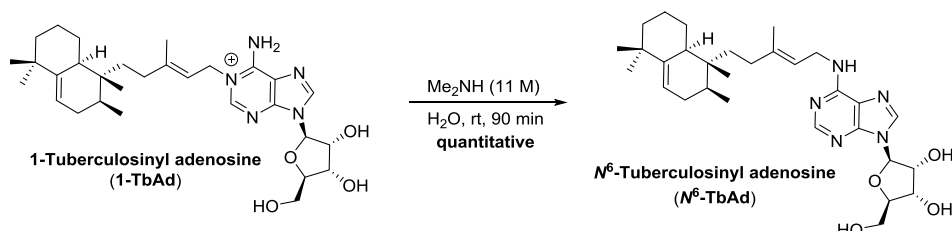
Amine **16** (7 mg, 0.024 mmol), inosine (7 mg, 0.026 mmol, 1.1 eq), benzotriazol-1-yloxytris(dimethylamino)-phosphonium hexafluorophosphate (Castro's reagent, BOP) (13.7 mg, 0.0312 mmol, 1.3 eq.) and DIPEA (7  $\mu$ l, 0.038 mmol, 1.5 eq) were dissolved in peptide grade DMF (3 mL).<sup>\*</sup> The reaction mixture was stirred overnight at rt, after which the solvent was removed under reduced pressure. The product was purified by repeated (3 times) flash chromatography using  $CH_2Cl_2$  : methanol (9:1).<sup>\*\*</sup>  $N^6$ -TbAd was isolated as a white waxy solid (1 mg, 7%,  $\pm 15\%$  HMPA impurity<sup>\*\*\*</sup>). The NMR spectra of synthetic material matched those obtained from the natural source.

<sup>\*</sup> It was observed that the use peptide grade DMF significantly improved the reaction. Small quantities of dimethyl amine in standard DMF might interfere with the reaction.

<sup>\*\*</sup> Due to the very similar  $R_f$  of HMPA (0.22) and  $N^6$ -TbAd (0.21), repetitive column chromatography was required to separate the majority of the HMPA.

<sup>\*\*\*</sup> Appears as a doublet at 2.64 ppm in  $^1H$ -NMR.

The discovery of novel terpene nucleosides from *Mycobacterium tuberculosis*



**(2*R*,3*S*,4*R*,5*R*)-2-(hydroxymethyl)-5-(6-(((*E*)-3-methyl-5-(1,2,5,5-tetramethyl-1,2,3,5,6,7,8,8a-octahydronaphthalen-1-yl)pent-2-en-1-yl)amino)-9H-purin-9-yl)tetrahydrofuran-3,4-diol ( $\text{N}^6$ -TbAd):**

A solution of 1-TbAd (5 mg, 0.01 mmol) in 60% Me<sub>2</sub>NH in water (5.5 mL) was stirred for 90 min. NMR analysis indicated complete conversion of the 1-TbAd. The reaction mixture was concentrated under reduced pressure and subsequently subjected to flash column chromatography, with 15% MeOH in CH<sub>2</sub>Cl<sub>2</sub>, to afford  $\text{N}^6$ -TbAd as a white solid (5 mg, 0.01 mmol, quantitative yield) as yellowish oil.

*Note: The rearrangement could be performed with similar results using Et<sub>2</sub>NH or iPr<sub>2</sub>NEt (2*M*) in MeOH.*

<sup>1</sup>H-NMR (400 MHz, CD<sub>3</sub>OD)  $\delta$  8.25 (s, 1H), 8.23 (s, 1H), 5.95 (d,  $J$  = 6.4 Hz, 1H), 5.51 – 5.44 (m, 1H), 5.41 (t,  $J$  = 6.5 Hz, 1H), 4.74 (t,  $J$  = 5.6 Hz, 1H), 4.35 – 4.29 (m, 1H), 4.20 (s, 1H), 4.17 (s, 1H), 3.89 (dd,  $J$  = 12.6, 2.1 Hz, 1H), 3.74 (dd,  $J$  = 12.9, 2.3 Hz, 1H), 2.24 (d,  $J$  = 15.9 Hz, 1H), 2.07 – 1.93 (m, 3H), 1.91 – 1.82 (m, 2H), 1.80 (s, 3H), 1.65 – 1.49 (m, 4H), 1.49 – 1.36 (m, 3H), 1.21 (td,  $J$  = 11.9, 7.3 Hz, 2H), 1.06 (s, 3H), 1.02 (s, 3H), 0.85 (d,  $J$  = 6.6 Hz, 3H), 0.65 (s, 3H).

<sup>1</sup>H-NMR (400 MHz, CDCl<sub>3</sub>)  $\delta$  8.19 (s, 1H), 7.81 (s, 1H), 5.86 (bs, 1H), 5.82 (d,  $J$  = 7.2 Hz, 1H), 5.44 (d,  $J$  = 4.7 Hz, 1H), 5.36 (d,  $J$  = 7.3 Hz, 1H), 5.00 (s, 1H), 4.47 (d,  $J$  = 4.9 Hz, 1H), 4.33 (s, 1H), 4.19 (bs, 2H), 3.94 (d,  $J$  = 12.9 Hz, 1H), 3.76 (d,  $J$  = 12.9 Hz, 1H), 3.23 (s, 2H), 2.49 (bs, 2H), 2.16 (d,  $J$  = 10.4 Hz, 1H), 2.01 – 1.90 (m, 2H), 1.85 (d,  $J$  = 23.8 Hz, 2H), 1.76 (s, 3H), 1.72 (s, 1H), 1.64 – 1.28 (m, 6H), 1.21 (tt,  $J$  = 13.0, 6.2 Hz, 2H), 1.06 (s, 3H), 1.01 (s, 3H), 0.82 (d,  $J$  = 6.6 Hz, 3H), 0.63 (s, 3H).

<sup>13</sup>C-NMR (101 MHz, CDCl<sub>3</sub>)  $\delta$  154.59, 152.44, 147.00, 146.09, 141.73, 140.05, 120.70, 118.96, 116.23, 91.08, 87.56, 73.89, 72.46, 63.15, 41.00, 39.89, 38.87, 37.04, 36.17, 35.00, 33.47, 32.80, 31.71, 29.87, 29.12, 27.51, 22.33, 16.83, 16.26, 15.22.

HRMS (ESI<sup>+</sup>): Calculated mass [M+H]<sup>+</sup> C<sub>30</sub>H<sub>46</sub>N<sub>5</sub>O<sub>4</sub><sup>+</sup> = 540.3544; found: 540.3542.

The spectral data are consistent with that of the natural isolate.



## 3.7 References

- [1] World Health Organization, Global Tuberculosis Report (2015) [http://apps.who.int/iris/bitstream/10665/191102/1/9789241565059\\_eng.pdf?ua=1](http://apps.who.int/iris/bitstream/10665/191102/1/9789241565059_eng.pdf?ua=1) (retrieved: 24/11/2015).
- [2] A. Lalvani, M. Pareek, *Br. Med. Bull.* **2010**, *93*, 69.
- [3] a) W. A. Hanekom, H. M. Dockrell, T. H. Ottenhoff, T. M. Doherty, H. Fletcher, H. McShane, F. F. Weichold, D. F. Hoft, S. K. Parida, U. J. Fruth, *PLoS Med.* **2008**, *5*, e145. b) R. S. Wallis, P. Kim, S. Cole, D. Hanna, B. B. Andrade, M. Maeurer, M. Schito, A. Zumla, *Lancet Infect. Dis.* **2013**, *13*, 362.
- [4] J. H. Shelhamer, V. J. Gill, T. C. Quinn, S. W. Crawford, J. A. Kovacs, H. Masur, F. P. Ognibene, *Ann. Intern. Med.* **1996**, *124*, 585.
- [5] M. R. Couturier, E. H. Graf, A. T. Griffin, *Clin. Lab. Med.* **2014**, *34*, 219.
- [6] S. D. Lawn, A. D. Kerkhoff, M. Vogt, R. Wood, *Lancet Infect. Dis.* **2012**, *12*, 201.
- [7] R. Baumann, S. Kaempfer, N. N. Chegou, W. Oehlmann, A. G. Loxton, S. H. Kaufmann, P. D. van Helden, G. F. Balck, M. Singh, G. Walzl, *J. Infect.* **2014**, *69*, 581.
- [8] E. Layre, L. Sweet, S. Hong, C. A. Madigan, D. Desjardins, D. C. Young, T-Y. Cheng, J. W. Annand, K. Kim, I. C. Shamputa, M. J. McConnell, C. A. Debona, S. M. Behar, A. J. Minnaard, M. Murray, C. E. Barry III, I. Matsunaga, D. B. Moody, *Chem. Biol.* **2011**, *18*, 1537.
- [9] M. J. Sartain, D. L. Dick, C. D. Rithner, D. C. Crick, J. T. Belisle, *J. Lipid Res.* **2011**, *52*, 861.
- [10] M. A. Behr, M. A. Wilson, W. P. Gill, H. Salamon, G. K. Schoolnik, S. Rane, P. M. Small, *Science*, **1999**, *284*, 1520.
- [11] G. G. Mahairas, P. J. Sabo, M. J. Hickey, D. C. Singh, C. K. Stover, *J. Bacteriol.* **1996**, *178*, 1274.
- [12] P. Drodin, I. Rosenkrands, P. Andersen, S. T. Cole, R. Brosch, *Trends Microbiol.* **2004**, *12*, 500.
- [13] S. M. Fortune, A. Jaeger, D. A. Sarracino, M. R. Chase, C. M. Sasseti, D. R. Sherman, B. R. Bloom, E. J. Rubin, *Proc. Nat. Acad. Sci. USA* **2005**, *102*, 10676.
- [14] P. Domenech, M. B. Reed, C. S. Dowd, C. Manca, G. Kaplan, C. E. Barry III, *J. Biol. Chem.* **2004**, *279*, 21257.
- [15] M. Jain, J. S. Cox, *PLoS Pathog.* **2005**, *1*, e2.
- [16] S. E. Converse, J. D. Mougous, M. D. Leavell, J. A. Leary, C. R. Bertozzi, J. S. Cox, *Proc. Nat. Acad. Sci. USA* **2003**, *100*, 6121.
- [17] A. Garces, K. Atmakuri, M. R. Chase, J. S. Woodworth, B. Krastins, A. C. Rothchild, T. L. Ramsdell, M. F. Lopez, S. M. Behar, D. A. Sarracino, S. M. Fortune, *PLoS Pathog.* **2010**, *6*, e1000957.

- [18] a) C. Nakano, T. Okamura, T. Sato, T. Dairi, T. Hoshino, *Chem. Commun.* **2005**, 1016. b) C. Nakano, T. Hoshino, *ChemBioChem* **2009**, *10*, 2060. c) L. Prach, J. Kirby, J. D. Keasling, T. Alber, *FEBS J.* **2010**, *277*, 3588.
- [19] C. Nakano, T. Ootsuka, K. Takayama, T. Mitsui, T. Sato, T. Hoshino, *Biosci. Biotechnol. Biochem.* **2011**, *75*, 75.
- [20] T. Hoshino, C. Nakano, T. Ootsuka, Y. Shinohara, T. Hara, *Org. Biomol. Chem.* **2011**, *9*, 2156.
- [21] a) R. Ottria, S. Casati, E. Daldoli, J. A. Maier, P. Ciuffreda, *Bioorg. Med. Chem.* **2010**, *18*, 8396. b) S. Casati, A. Manzcocchi, R. Ottria, P. Ciuffreda, *Magn. Reson. Chem.* **2010**, *48*, 745. c) S. Casati, A. Manzcocchi, R. Ottria, P. Ciuffreda, *Magn. Reson. Chem.* **2011**, *49*, 279.
- [22] a) J. E. Spangler, C. A. Carson, E. J. Sorensen, *Chem. Sci.* **2010**, *1*, 202. b) N. Mangel, F. M. Mann, M. L. Hillwig, R. J. Peters, B. B. Snider, *Org. Lett.* **2010**, *12*, 2626.
- [23] a) S. Knapp, S. Sharma, *J. Org. Chem.* **1985**, *50*, 4996. b) S. P. Tanis, Y. M. Abdallah, *Synth. Commun.* **1986**, *16*, 251.
- [24] a) A. Kojima, S. Honzawa, C. D. J. Boden, M. Shibasaki, *Tetrahedron Lett.* **1997**, *38*, 3455. b) D. Meng, P. Bertinato, A. Balog, D-S. Su, T. Kamencka, E. J. Sorensen, S. J. Danishefsky, *J. Am. Chem. Soc.* **1997**, *119*, 10073. c) S. R. Chemler, D. Trauner, S. J. Danishefsky, *Angew. Chem. Int. Ed.* **2001**, *40*, 4544.
- [25] a) V. J. Davisson, A. B. Woodside, T. R. Neal, K. E. Stremmer, M. Muehlbacher, C. D. Poulter, *J. Org. Chem.* **1986**, *51*, 4768. b) A. B. Woodside, Z. Huang, C. D. Poulter, *Org. Syn.* **1988**, *66*, 211.
- [26] J. W. Jones, R. K. Robins, *J. Am. Chem. Soc.* **1963**, *85*, 193.
- [27] C. M. Sassett, D. H. Boyd, E. J. Rubin, *Proc. Nat. Acad. Sci. USA* **2001**, *98*, 12712.
- [28] F. M. Mann, S. Pristic, H. Hu, M. Xu, R. M. Coates, R. J. Peters, *J. Biol. Chem.* **2009**, *284*, 23574.
- [29] F. M. Mann, M. Xu, E. K. Davenport, R. J. Peters, *Front. Microbiol.* **2012**, *3*, 368.
- [30] K. Pethe, D. L. Swenson, S. Alonso, J. Anderson, C. Wang, D. G. Russell, *Proc. Nat. Acad. Sci. USA* **2004**, *101*, 13642.
- [31] I. Comas, M. Coscolla, T. Luo, S. Borrell, K. E. Holt, M. Kato-Maeda, J. Parkhill, B. Malla, S. Berg, G. Thwaites, D. Yeboah-Manu, G. Bothamley, J. Mei, L. Wei, S. Bentley, S. R. Harris, S. Niemann, R. Diel, A. Aseffa, Q. Gao, D. Young, S. Gagneux, *Nat. Genet.* **2013**, *45*, 1176.
- [32] F. M. Mann, R. J. Peters, *MedChemComm* **2012**, *3*, 899.
- [33] E. Layre, H. L. Lee, D. C. Young, A. J. Martinot, J. Buter, A. J. Minnaard, J. W. Annand, S. M. Fortune, B. B. Snider, I. Matsunaga, E. J. Rubin, T. Alber, D. B. Moody, *Proc. Nat. Acad. Sci. USA* **2014**, *111*, 2978.

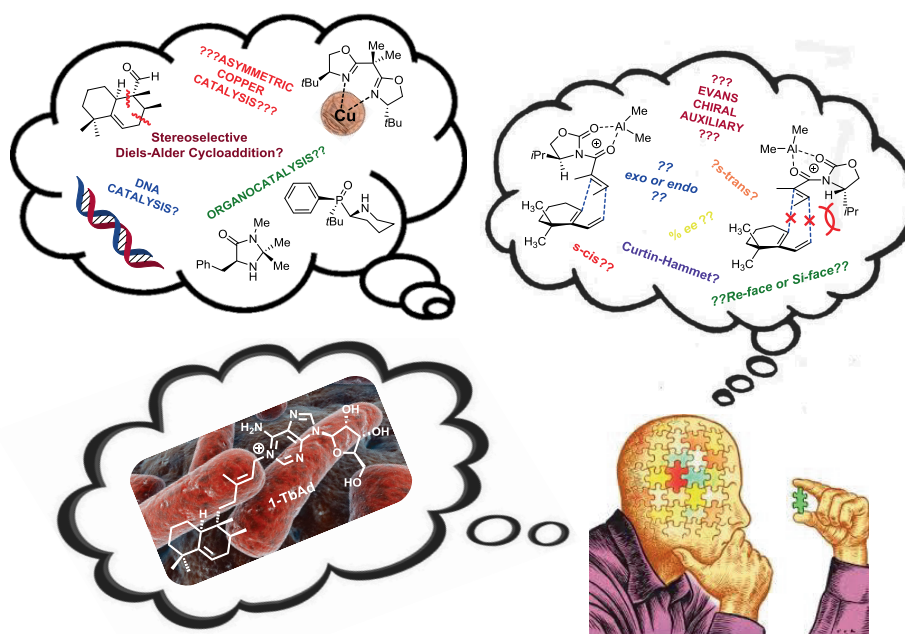
### CHAPTER 3

---

- [34] H-C. Chan, X. Feng, T-P. Ko, C-H. Huang, Y. Hu, Y. Zheng, S. Bogue, C. Nakano, T. Hoshino, L. Zhang, P. Lv, W. Liu, D. C. Crick, P-H. Liang, A. H-J. Oldfield, R-T. Guo, *J. Am. Chem. Soc.* **2014**, *136*, 2892.
- [35] N. Ritz, W. A. Hanekom, R. Robins-Browne, W. J. Britton, N. Curtis, *FEMS Microbiol. Rev.* **2008**, *32*, 821.
- [36] A. Heyl, M. Riefler, G. A. Romanov, T. Schmulling, *Eur. J. Cell. Biol.* **2012**, *91*, 246.
- [37] Z-K. Wan, E. Binnun, D. P. Wilson, J. Lee, *Org. Lett.* **2005**, *7*, 5877.
- [38] For representative reviews on the Dimroth rearrangement see: a) T. Fujii, T. Itaya, *Heterocycles*, **1998**, *48*, 359. b) E. S. H. El Ashry, S. Nadeem, M. R. Sha, Y. El Kilany, *Adv. Heterocycl. Chem.* **2010**, *101*, 161. c) E. S. H. El Ashry, Y. El Kilany, N. Rashed, H. Assafir, *Adv. Heterocycl. Chem.* **1999**, *75*, 80.
- [39] J. Uzawa, K. Anzai, *Liebigs Ann. Chem.* **1988**, 1195.
- [40] M. A. Forrellad, L. I. Klepp, A. Gioffré, J. S. y García, H. R. Morbidoni, M. de la Paz Santangelo, A. A. Cataldi, F. Bigi, *Virulence* **2013**, *4*, 3.
- [41] S. Laxman, R. Meena, *FEBS J.* **2010**, *277*, 2416.
- [42] a) *The mycobacterial cell envelope* (Eds. M. Daffé, J-M. Reyrat), ASM Press, Washington DC, **2008**. b) D. E. Minnikin, L. Kremer, L. G. Dover, G. S. Besra, *Chem. Biol.* **2002**, *9*, 545. c) D. Kaur, M. E. Guerin, H. Škovierová, P. J. Brennan, M. Jackson, *Adv. Appl. Microbiol.* **2009**, *69*, 23. d) P. J. Brennan, *Annu. Rev. Biochem.* **1995**, *64*, 29. e) D. E. Minnikin, L. Kremer, L. G. Dover, G. S. Besra, *Chem. Biol.* **2002**, *9*, 545.
- [43] a) S. Sturgill-Koszycki, P. H. Schlesinger, P. Chakraborty, P. L. Haddix, H. L. Collins, A. K. Fok, R. D. Allen, S. L. Gluck, J. Heuser, D. G. Russell, *Science*, **1994**, *263*, 678. b) For a review on the topic of acid resistance of *M. tuberculosis* see: O. H. Vandal, C. F. Nathan, S. Ehrh, *J. Bacteriol.* **2009**, *191*, 4714.
- [44] N. Lu, Z. Zhou, *Int. Rev. Cell Mol. Biol.* **2008**, *293*, 269.
- [45] D. M. G. Martin, C. B. Reese, *J. Chem. Soc. C* **1968**, 1731.

## \*\*\* CHAPTER 4 \*\*\*

### ‡ Asymmetric Total Synthesis of 1-Tuberculosinyl Adenosine ‡



**ABSTRACT:** Shortly after the discovery of the *Mycobacterium tuberculosis* specific and abundant lipid 1-tuberculosinyl adenosine (1-TbAd), which is associated with the virulent enzyme Rv3378c, enantiopure synthetic material was desired to facilitate further research. This chapter highlights our efforts focusing on the first asymmetric total synthesis of 1-TbAd. Two routes were explored: a chiral pool synthesis starting from the commercially available natural product sclareolide, and a strategy based on an asymmetric Diels-Alder cycloaddition. The total synthesis was accompanied by computational mechanistic studies into the course of the Diels-Alder reaction, understanding its mechanism of stereinduction.

This chapter will be published in part:

J. Buter, D. Heijnen, I. C. Wan, F. M. Bickelhaupt, D. C. Young, E. Otten, D. B. Moody, A. J. Minnaard, *Manuscript submitted*.

The DFT studies were performed by I. C. Wan and Prof. Dr. F. M. Bickelhaupt.

## 4.1 Introduction

Tuberculosis is an infectious disease caused by the bacterium *Mycobacterium tuberculosis* (*Mtb*). Although not prevalent in First World countries, it is responsible for a mortality rate exceeding 1.5 million deaths annually, mainly in developing countries.<sup>[1]</sup> The persistence of *Mtb* as the world's most important bacterial pathogen can be attributed to two key factors. First, intracellular survival of the bacterium is granted by successful infection of the endosomal network of phagocytes. In these phagosomes *Mtb* is able to arrest phagosome maturation by actively inhibiting pH-dependent killing mechanisms and is protected from immune responses during a decades long infection process.<sup>[2]</sup>

Secondly, its unusually hydrophobic, multi-layered cell wall functions as an additional source of protection.<sup>[3]</sup> Despite of over a century of active research on *Mtb*, the precise lipid composition, which makes up for its cell wall, remains unknown. Discovery of new lipids in *Mtb* can assist understanding *Mtb*'s survival and virulence. In addition, providing that these lipids are specific for pathogenic *Mtb*, these compounds could act as *bona fide* chemical markers for infection, as no such tests exists currently.<sup>[4]</sup>

An analytical chemistry approach allowing rapid profiling of lipid components in *Mycobacteria* is the recently developed comparative lipidomics platform.<sup>[5]</sup> The lipidomics platform allows detailed chemotaxonomic analysis of *Mtb* and already proved to be useful in the revision of the biosynthetic pathway of mycobactin.<sup>[6]</sup> Recently, we communicated the isolation of a novel halimane-type diterpene nucleoside produced by *Mtb* using this lipidomics platform.<sup>[7]</sup> The compound, characterized as 1-tuberculosinyl adenosine (1-TbAd, Figure 1) was found to be an abundant, pathogenic *Mtb*-specific lipid.<sup>[8]</sup> The biosynthesis of 1-TbAd requires the virulence-associated enzyme Rv3378c, of which its locus (Rv3377c–Rv3378c) has shown to be essential in phagosome maturation arrest.<sup>[9]</sup> 1-TbAd is therefore expected to be involved in phagosomal survival of *Mtb*. Very recently, two closely related compounds, tuberculosinyl-2'-deoxyadenosine ("2'-deoxy 1-TbAd") and tuberculosinyl 2'-*O*-acetyladenosine (2'-acetyl TbAd, Figure 1), were discovered.<sup>[10]</sup> The structures of these analogues were tentatively assigned based on mass spectrometry.

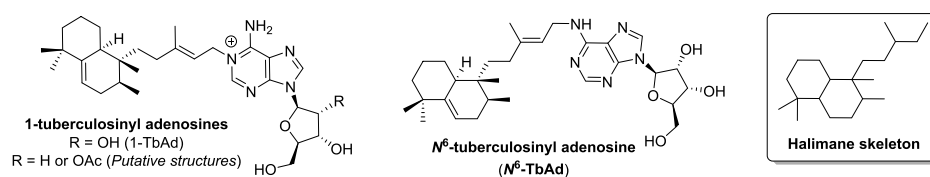


**Figure 1.** Tuberculosinyl adenosines from *Mycobacterium tuberculosis*.

The specificity of 1-TbAd in the pathogenic *Mtb* makes it a promising chemical marker for tuberculosis infection. It was shown that 1-TbAd is produced *in vivo* in infected BLB/c mice and could be readily detected *ex vivo* in whole-lung homogenates using a

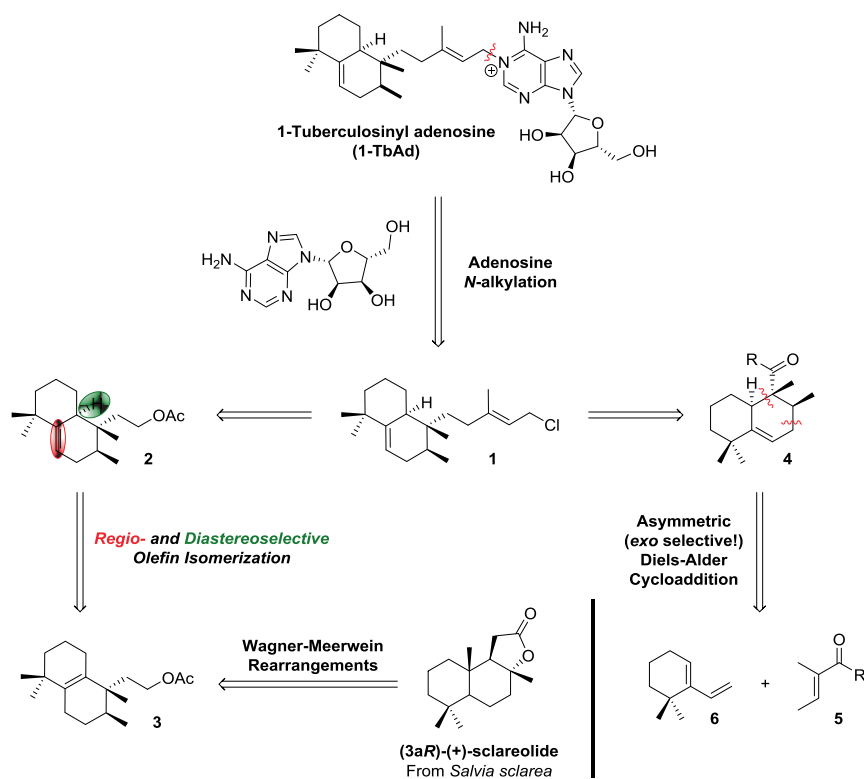
one-step RP-HPLC-MS method.<sup>[8]</sup> Next to the detection of 1-TbAd, an unknown isomer with a nearly identical fragmentation pattern was observed which, was shown to be the *pseudo*-isomer *N*<sup>6</sup>-tuberculosinyl adenosine (*N*<sup>6</sup>-TbAd, Figure 1). This compound is also a specific chemical marker and was postulated to arise from an *in vivo* Dimroth rearrangement of 1-TbAd.<sup>[8]</sup> Notably, it was recently shown that 1-TbAd and *N*<sup>6</sup>-TbAd can also be detected in human patient sputum samples.<sup>[11]</sup>

In this chapter, we report our extensive efforts regarding the enantio- and diastereoselective total synthesis of 1-TbAd and *N*<sup>6</sup>-TbAd. Throughout the course of the investigation several synthetic strategies towards the optically active halimane-skeleton were scrutinized. We mainly focused on the installation of the bicyclic core by means of an asymmetric Diels-Alder cycloaddition. Although many reactions were met with failure, we eventually managed to successfully complete the total synthesis of 1-TbAd (and its congeners, (*Z*)-1-TbAd, 2'-deoxy 1-TbAd, and <sup>13</sup>C-labelled 1-TbAd) and *N*<sup>6</sup>-TbAd in a stereoselective manner.

## 4.2 Retrosynthetic analysis

As outlined in the previous chapter, 1-TbAd can be accessed by *N*-alkylation of adenosine with tuberculosinyl chloride **1**, our first retrosynthetic disconnection (Scheme 1). The interesting part of the molecule from a synthetic perspective is the bicyclic core structure of the halimane (*tuberculosinyl*) skeleton. Containing three contiguous stereogenic centers, one being all-carbon quaternary, two synthetic routes were explored to stereoselectively construct this structure.

At first we envisioned acetate **2** as a suitable precursor to tuberculosinyl chloride **1**. We knew from the literature that isomeric acetate **3** could be easily constructed starting from naturally occurring and commercially available (+)-sclareolide (~105 \$ / 25 gr), as reported by the George laboratory in 2012.<sup>[12]</sup> Rearrangement of the sclareolide core by consecutive, stereospecific, Wagner-Meerwein shifts produces acetate **3**, having the all-carbon quaternary stereocenter constructed. One intriguing and daunting problem arises however, as a challenging olefin isomerization in **3** has to be performed to access **4**. Due to the intrinsic (near) symmetry of **3**, regioselective isomerization is regarded provocative. Aside from regioselectivity in the isomerization, another difficult task, namely diastereoselectivity has to be addressed,. Despite these foreseen challenges, we were eager to investigate this synthetic route, as rapid access to the halimane core structure was guaranteed, when successful.



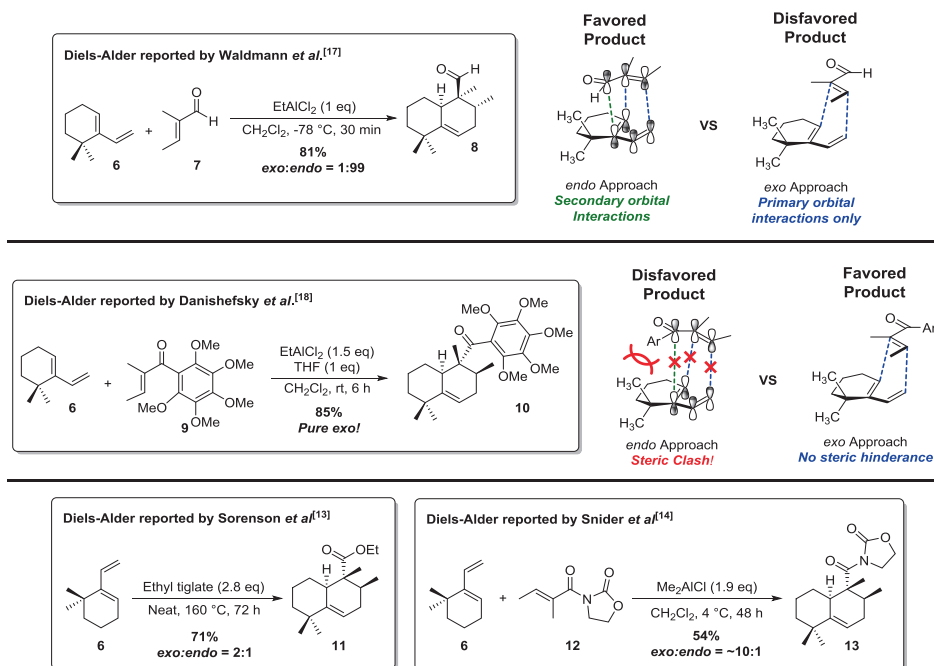
**Scheme 1.** Retrosynthesis of 1-tuberculosinyl adenosine (1-TbAd).

In 2010, the groups of Sorensen<sup>[13]</sup> and Snider<sup>[14]</sup> independently reported a synthesis of tuberculosinol (see chapter 3).<sup>[15]</sup> Both routes relied on a Diels-Alder reaction between 6,6-dimethyl-1-vinylcyclohexene **6**<sup>[16]</sup> and a tigloyl based dienophile **5** leading to the racemic core (Scheme 2). This Diels-Alder reaction is as such very productive, as it forms the three stereocenters, one which is quaternary. The reaction, however, is also highly demanding, as neither the diene nor the dienophile is very reactive and the cycloaddition has to occur with *exo* selectivity.

Regarding the diastereoselectivity of the Diels-Alder cyclization, some empirical data was gathered which allowed us to theorize on *exo* selectivity in the [4+2] cycloaddition with 6,6-dimethyl-1-vinylcyclohexene **6** (Scheme 2). Whereas tiglic aldehyde **7** gives a high *endo* selectivity (99:1),<sup>[17]</sup> it is known from work by Danishefsky and co-workers that a bulky tiglic acid derivative **9** leads to an increased *exo* selectivity.<sup>[18]</sup> The process can be visualized as depicted in scheme 2 (Danishefsky's model) and it is the bulkiness of the dienophile which governs diastereoselectivity since steric hindrance, exerted by the geminal dimethyl in diene **6**, directs towards an *exo* approach.

In the total synthesis of tuberculosinol by the Sorensen group, the Diels-Alder reaction was performed with the relatively small ethyl tiglate, providing a modest diastereoselectivity of 2:1 in favor of the *exo* diastereoisomer.<sup>[13]</sup> Increase of the steric

bulk by using *N*-tigloyloxazolidinone **12** in the Snider synthesis led to an *exo:endo* selectivity of ~10:1.<sup>[14]</sup>



**Scheme 2.** *Exo* selectivity explained in the diastereoselective Diels-Alder reaction (Danishefsky's model).

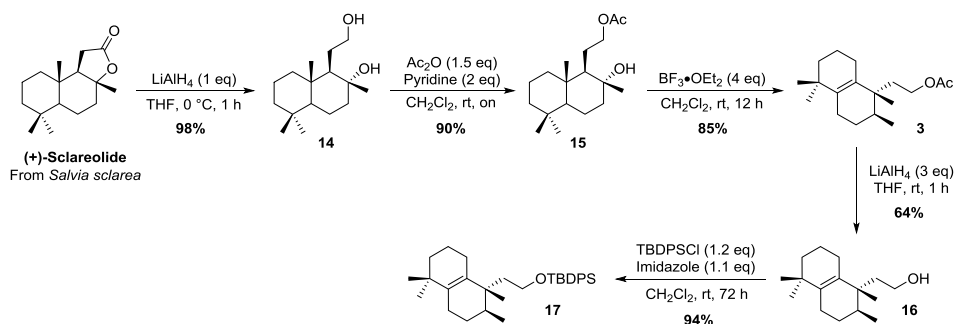
Although the use of 6,6-dimethyl-1-vinylcyclohexene **6** in diastereoselective Diels-Alder cycloadditions has been reported several times, it has not been used in an enantioselective version.<sup>[19]</sup> We realized that meeting this challenge would provide a direct entry to the halimane family of diterpenes, and in particular to the members of the TbAd-cluster as discussed above.

### 4.3 Investigations of the asymmetric synthesis of 1-TbAd

#### 4.3.1 An attempted chiral pool approach to 1-TbAd

The chiral pool approach to 1-TbAd started from commercially available and naturally occurring sclareolide. This molecule is a sesquiterpene isolated from either *salvia sclarea*<sup>[20]</sup> or *salvia yosgadensis*.<sup>[21]</sup> Sclareolide contains four contiguous stereogenic centers and also the desired amount of carbon atoms required for the chiral bicyclic core of the halimane skeleton. It was recently shown by George and co-workers in their total synthesis of aureol, that the stereocenters in sclareolide could readily be rearranged to set two of the three stereogenic centers present in 1-TbAd's bicyclic core structure (Scheme 3).<sup>[12]</sup>



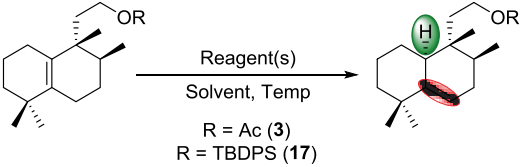


**Scheme 3.** Stereospecific synthesis of alkenes **3** and **17** from naturally occurring sclareolide.

Treatment of sclareolide with  $\text{LiAlH}_4$  opens the lactone to provide diol **14**. After acetylation of the primary alcohol, compound **15** was rearranged via two simultaneous Wagner-Meerwein rearrangements to furnish acetate **3**. Since the 1,2-shifts (Wagner-Meerwein shifts) are stereospecific, two of the three desired stereogenic centers were set with known stereochemistry. Acetate **3** was also converted into the silyl protected analogue **17**, and both compounds were subjected to a variety of conditions to achieve alkene isomerization (Table 1).<sup>[22]</sup>

The isomerization of the unsaturated decalin in both **3** and **17** is intrinsically difficult as a tetra-substituted double bond has to be isomerized to a theoretically less stable tri-substituted double bond. An additional feature which complicates the situation is the close proximity of the geminal dimethyl and quaternary stereocenter to the double bond. If this is not challenging enough, the isomerization has to proceed regioselective and diastereoselective to furnish the desired bicyclic core structure present in 1-TbAd). As evident from Table 1, a wide variety of different conditions to achieve alkene isomerization were studied. Despite extensive efforts not even a trace of isomerization was observed. We assume that the steric crowding around the double bond impeded any reaction from happening.

**Regio- and Diastereoselective Isomerization**

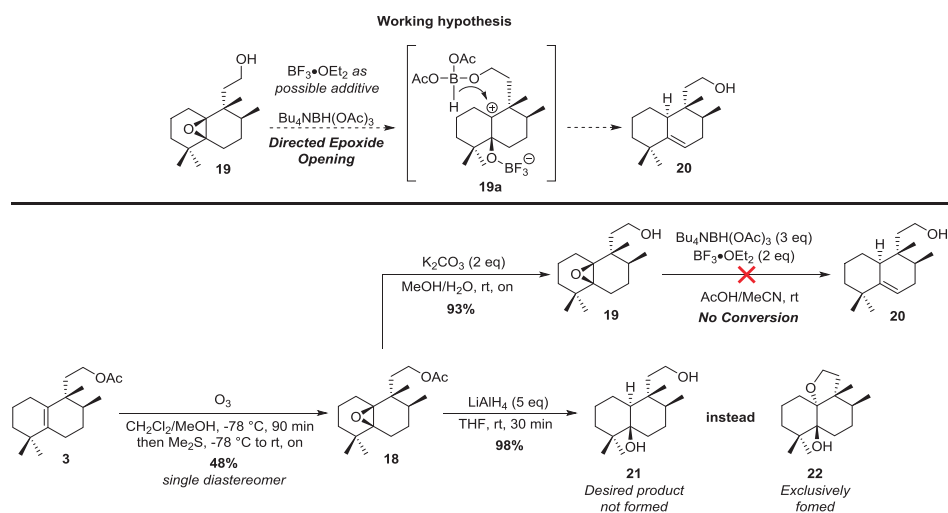


Entry	Starting material	Reagent(s)	Solvent	Temp (°C)
1	3 or 17	RhCl <sub>3</sub> •3H <sub>2</sub> O (10 mol%)	EtOH	reflux
2	3 or 17	Grubbs II (10 mol%)	MeOH	60
3	3 or 17	Cp <sub>2</sub> ZrHCl (2 eq)	THF	reflux
4	3 or 17	Hoveyda-Grubbs II (10 mol%)	MeOH	reflux
5	3 or 17	RuCl(PPh <sub>3</sub> ) <sub>3</sub> + Et <sub>3</sub> SiH (10 mol%)	Toluene	reflux
6	3 or 17	RuH(PPh <sub>3</sub> ) <sub>3</sub> (10 mol%)	THF	reflux
7	3 or 17	Raney nickel ( <i>excess</i> )	EtOH	reflux
8	3 or 17	PdCl <sub>2</sub> (MeCN) <sub>2</sub> (10 mol%)	CHCl <sub>3</sub>	reflux
9	17	KOtBu (2 eq)	DMSO	100 (μW)
10	17	KOtBu + <i>n</i> BuLi (2 eq)	THF	-78 to rt
11	17	KOtBu + <i>n</i> BuLi + TMEDA (2 eq)	THF	-78 to rt
12	17	BH <sub>3</sub> •THF	THF	reflux

**Table 1.** Failed attempts in the regio- and diastereoselective alkene isomerization of **3** and **17**.

As isomerization could not be realized in one step, we focused our attention on a multi-step sequence to achieve this objective. It was known from the work of Baldwin and Adlington that the double bond in **3** lacking the OAc group could be diastereoselectively epoxidized with ozone.<sup>[23]</sup> In 1988 Evans communicated the directed reduction of aldol products using tetrabutylammonium triacetoxo borohydride.<sup>[24]</sup> These reports led us to design a directed epoxide opening with this borohydride reagent (Scheme 4). We also postulated that the addition of BF<sub>3</sub>•OEt<sub>2</sub> to the reaction mixture would facilitate the epoxide opening, and hopefully occur with concurrent dehydration to produce alcohol **20**.

We thus epoxidized acetate **3** under ozonolysis condition to give epoxide **18** in 48% yield as a single diastereomer. Although the relative stereochemistry in **18** was not determined, the facial selectivity of epoxidation by ozone was assumed to correspond to that observed by Baldwin and Adlington.<sup>[23]</sup> The acetate on **15** was removed by treatment with K<sub>2</sub>CO<sub>3</sub> providing alcohol **19**. We tested our hypothesis for the directed epoxide opening in several attempts, varying stoichiometry, concentration, and temperature, all leading to the conclusion that no conversion could be achieved. Treatment of acetate **18** with LiAlH<sub>4</sub> did lead to epoxide opening, but the desired product **21** was not obtained. Instead **22** was formed, which was considered a dead-end in the synthesis.

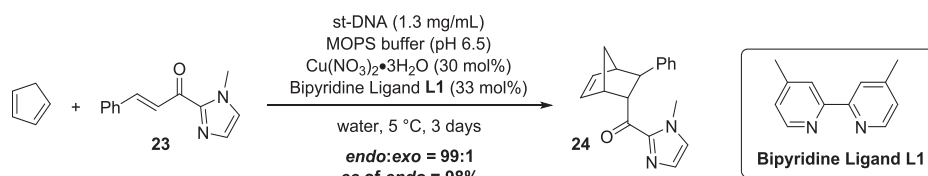


**Scheme 4.** Alternative strategy to achieve alkene isomerization.

Although the chiral pool strategy seemed attractive at first, the failure of the direct alkene isomerization forced us to come up with a more elaborate isomerization sequence. With these efforts also being futile we decided to abandon the chiral pool approach, as we felt the initial benefits of this route were overruled by step count. We therefore focused our efforts on the development of an asymmetric Diels-Alder cyclization to produce the bicyclic core structure.

#### 4.3.2 Towards an asymmetric catalytic Diels-Alder reaction for the construction of 1-TbAd; DNA catalysis

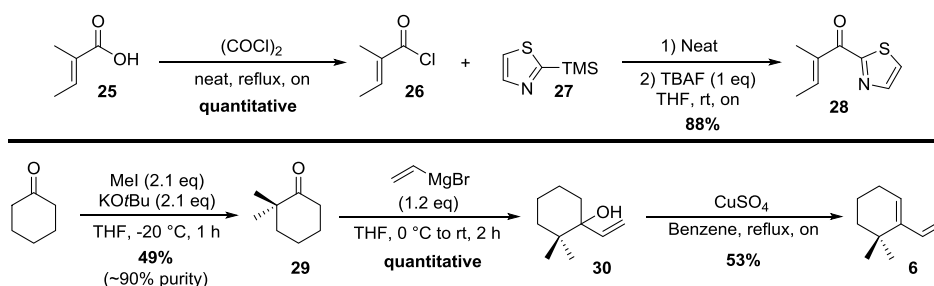
At the start of the investigation into the development of a stereoselective Diels-Alder reaction, we were intrigued by the possibility to perform the cycloaddition using DNA-based catalysis, developed in our institute by the Roelfes laboratory.<sup>[25]</sup> In 2007 the group communicated an asymmetric Diels-Alder reaction with DNA as the chiral ligand.<sup>[26]</sup> Although the scope of the reaction was limited to the use of cyclopentadiene and  $\alpha,\beta$ -unsaturated 2-acyl methyl-imidazoles (Scheme 5), we did not like to waste this opportunity and in-house expertise.



**Scheme 5.** The first asymmetric DNA-based catalytic Diels-Alder reaction by the Roelfes laboratory.

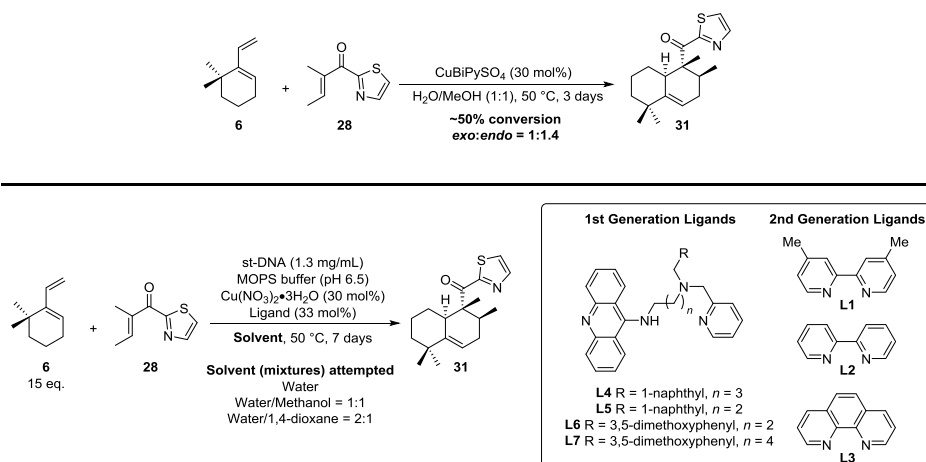
On the outset of the DNA-catalyzed reactions it was decided to use thiazole tiglitate as the dienophile rather than the corresponding methyl-imidazole. From unpublished results by Roelfes laboratory, it was known that  $\alpha$ -substitution in the dienophile was not tolerated, as it probably interfered with the methyl substituent on the imidazole.<sup>[27]</sup>

The starting materials for the Diels-Alder reaction had to be synthesized, as none of them was commercially available (Scheme 6). Thiazole tiglitate **28** was readily available by reaction of tigloyl chloride **26** with TMS-thiazole **27** (Dondoni's reagent), according to a procedure by Dondoni and co-workers.<sup>[28]</sup> The synthesis of diene **6** however was more laborious. At first, 2,2-dimethylcyclohexanone **29** had to be prepared, as the commercial source was expensive (€260 / 1 gr, 92% purity). The most economical way was to alkylate cyclohexanone at -20 °C using KO<sup>t</sup>Bu (2.1 eq) and MeI (2.1 eq). Although a mixture of all homologues was obtained, these were to a large extent separable using flash column chromatography. The reaction was found to be selective for the formation of 2,2-dimethylcyclohexanone **29** which we managed to obtain in 49% yield and 90% purity. Reaction with vinyl Grignard furnished alcohol **30** which was subsequently dehydrated to provide the desired ketone. Dehydration with KHSO<sub>4</sub> at 150 °C could be achieved but gave significant polymerization in our hands.<sup>[29a,b]</sup> The reaction with anhydrous CuSO<sub>4</sub><sup>[29a,c]</sup> proved to be more reliable, providing diene **6** in 53% yield, although reproducibility could only be assured by using freshly prepared anhydrous CuSO<sub>4</sub>.



**Scheme 6.** Synthesis of diene **6** and dienophile **28**.

With the diene and dienophile in hand we first investigated the possibility to achieve a copper-catalyzed Diels-Alder reaction (Scheme 7). To our delight, we found that the [4+2] cycloaddition was possible, as our test reaction using CuBiPySO<sub>4</sub> (30 mol%) in H<sub>2</sub>O/MeOH (1:1) provided 50% conversion over three days. In addition we made the surprising observation that the reaction provided the product with a low *endo* selectivity. This result was somewhat mysterious, but the conversion did indicate that the DNA-based catalytic Diels-Alder reaction might be feasible.



**Scheme 7.** Attempts of a catalytic DNA-based asymmetric Diels-Alder reaction.

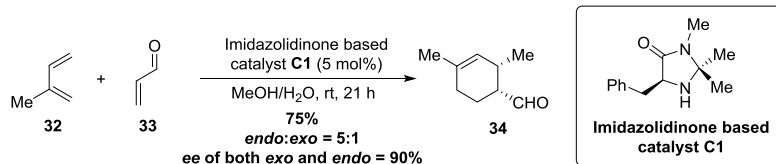
In collaboration with Dr. Almudena García Fernández (Roelfes laboratory) we initiated our attempts by subjecting diene **6** and dienophile **28** to standard DNA-based catalysis conditions.<sup>[26]</sup> The reactions were carried out with salmon testes DNA as the chiral ligand, a DNA-chelating ligand (**L1-L7**) and  $\text{Cu}(\text{NO}_3)_2 \cdot 3\text{H}_2\text{O}$ . As for the reaction medium, a MOPS buffer (pH 6.5) and water, or a mixture with either methanol or 1,4-dioxane, was used. Unfortunately, despite all the efforts, we did not observe any product formation. It is likely that a combination of low solubility of the substrates, the inherent poor reactivity of diene **6**, and the relatively high dilution, causes reaction failure. The problem of solubility cannot be solved as we could not maneuver within the confinements of the solvent mixtures allowed within DNA-based catalysis. This inevitably caused us to shift our attention to more conventional asymmetric catalytic Diels-Alder reactions.

### 4.3.3 Development of an asymmetric catalytic Diels-Alder reaction for the construction of 1-TbAd; Organocatalysis

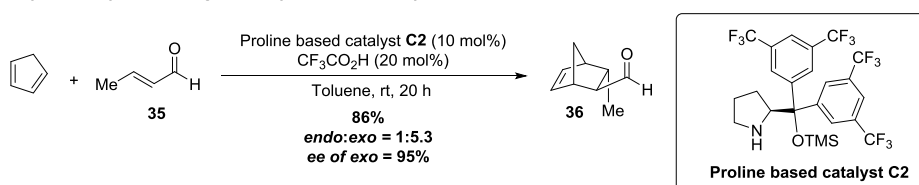
Our venture into the asymmetric Diels-Alder reaction was continued by investigation of organocatalytic methods. In a pioneering study, the MacMillan laboratory reported the first asymmetric organocatalytic Diels-Alder reaction (Scheme 8) using imidazolidinone based catalyst **C1**.<sup>[30]</sup> It was shown that even unreactive dienes such as **32** could successfully be used. Hayashi and co-workers reported an *exo* selective asymmetric organocatalytic Diels-Alder based on proline based catalyst **C2**.<sup>[31]</sup> These two reports caught our attention and led us to investigate the possibility of an organocatalytic entry to the halimane scaffold.

## Asymmetric Total Synthesis of 1-Tuberculosinyl Adenosine

**MacMillan's asymmetric organocatalytic Diels-Alder cycloaddition:**



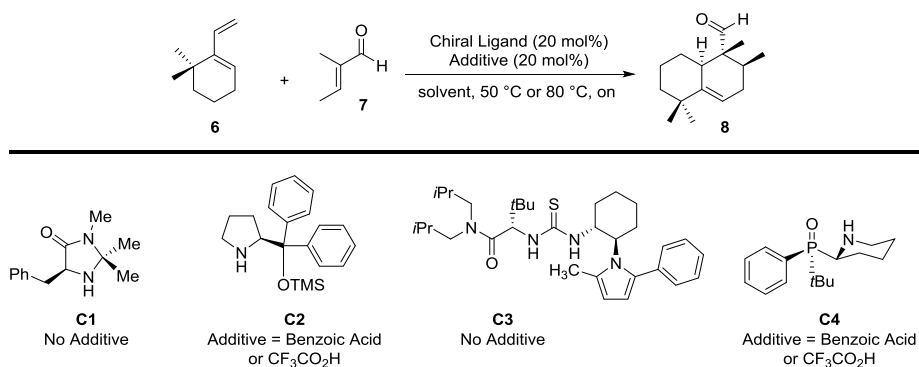
**Hayashi's asymmetric organocatalytic Diels-Alder cycloaddition:**



**Scheme 8.** Organocatalytic Diels-Alder reactions by MacMillan and Hayashi.

For our organocatalytic experiments we decided to use Hayashi's catalyst **C2**,<sup>[31]</sup> thiourea based catalyst **C3**,<sup>[32]</sup> MacMillan's catalyst **C1**,<sup>[30]</sup> and chiral aminophosphine oxide **C4** (Scheme 9). The latter structure (**C4**)<sup>[33]</sup> has not been reported in the literature but was synthesized in our laboratory during investigations on chiral phosphine oxides.<sup>[34]</sup> Although this compound has never been used as an organocatalyst, we regarded it worthy of trying in our asymmetric Diels-Alder reaction.

We performed the organocatalytic reactions with the aforementioned catalysts to activate tiglic aldehyde **7**. The reactions were initially executed at elevated temperatures, but unfortunately to no avail, as no Diels-Alder adduct could be detected. The origin of reaction impediment is likely due to the  $\alpha$ -substituent in the dienophile which exerts steric hindrance on the catalyst, prohibiting proper activation of the tiglic aldehyde **7**. With no result in hand at this stage we also cut short our organocatalysis investigation and shifted our attention to organometallic asymmetric catalysis.

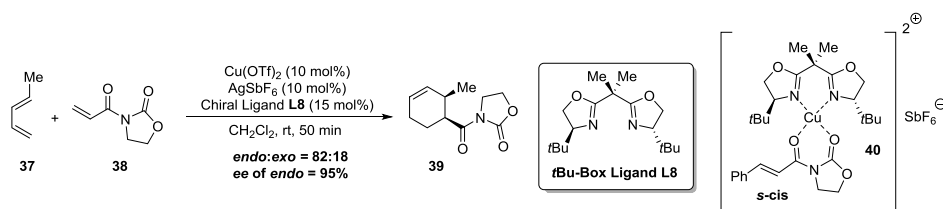


**Scheme 9.** Short investigation into organocatalytic Diels-Alder reactions.

## CHAPTER 4

### 4.3.4 Development of an asymmetric catalytic Diels-Alder reaction for the construction of 1-TbAd; Copper-catalyzed approach

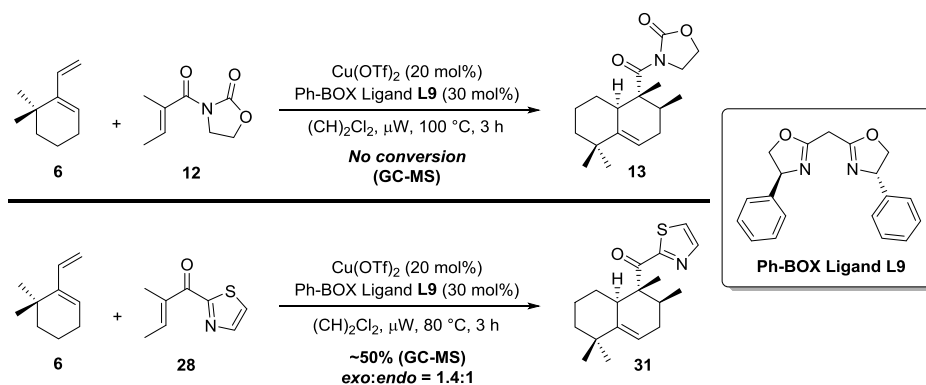
In 1999 the Evans laboratory communicated pioneering studies in the field of asymmetric copper-catalyzed Diels-Alder reactions.<sup>[35]</sup> In their manuscript, they outlined the use of the now famous BOX ligands to achieve asymmetric induction in copper-catalyzed [4+2] cycloaddition reactions (Scheme 10). Interestingly, oxazolidinone based dienophile **38**, activated by the Cu-*t*Bu-BOX catalyst, could be successfully coupled even with the unreactive piperylene **37**. This report and our in-house expertise regarding copper catalysis prompted us to investigate the asymmetric Diels-Alder under copper-catalyzed conditions.



**Scheme 10.** Asymmetric copper-catalyzed Diels-Alder reactions reported by Evans and co-workers.

Based on Evans' report, we synthesized *N*-tigloyloxazolidinone **12** according to the procedure of Snider.<sup>[35]</sup> This dienophile, and the tigloylthiazole based dieneophile **28** used in the DNA-based catalysis studies (*vide supra*), were both screened for their usefulness in the copper-catalyzed Diels-Alder reaction with diene **6** (Scheme 11). The dienophiles were subjected to Cu(OTf)<sub>2</sub> (20 mol%) in combination with chiral Ph-BOX-ligand **L9** (30 mol%). Initial reaction at room temperature proved to be fruitless, and the reaction temperature was therefore elevated. In case of dienophile **12**, no conversion was detected even at 100 °C for three hours under microwave conditions. This initial setback however was nullified, as it was found that the thiazole based dienophile **28** did give conversion with copper-catalysis. With this promising result in hand, we decided to set up a ligand screening and evaluate stereoselective induction.

Asymmetric Total Synthesis of 1-Tuberculosinyl Adenosine



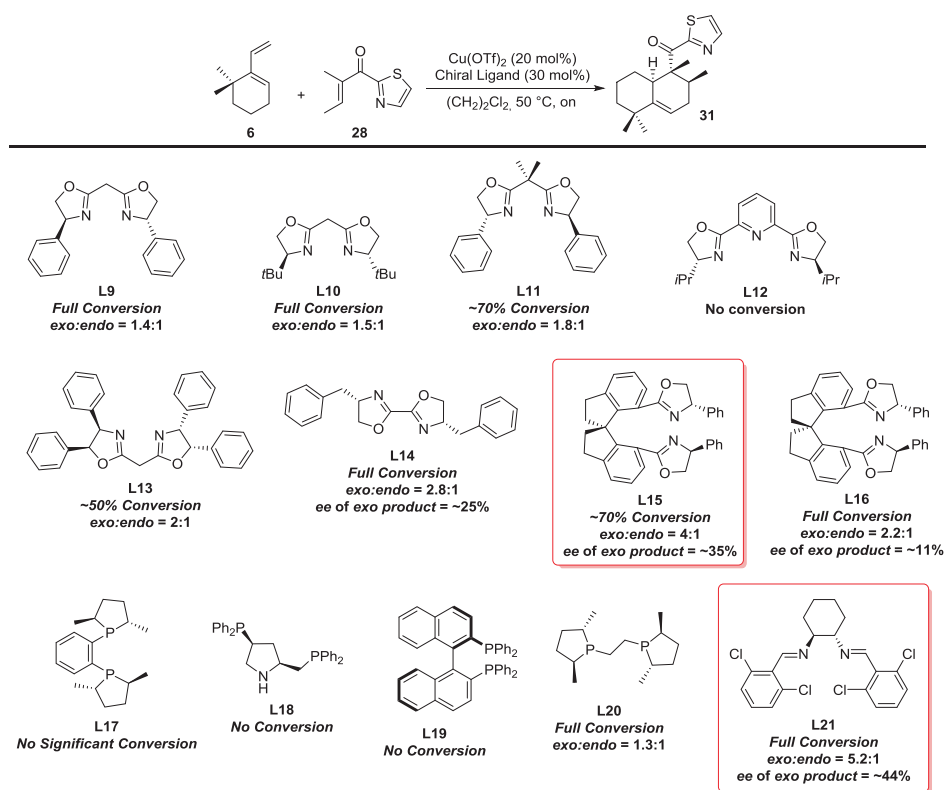
**Scheme 11.** Aiming for conversion in the asymmetric copper-catalyzed Diels-Alder reaction.

In our ligand screening, eight BOX-ligands (**L9** to **L16**), four phosphine ligands (**L17** to **L20**) and bis-imine ligand **L21** were investigated (Scheme 12). The BOX and phosphine ligands were purchased from commercial sources, whereas the bis-imine ligand **L21**<sup>[36]</sup> was prepared in-house<sup>[37]</sup> and apparently had survived storage over more than 17 years. 20 mol% of *in situ* formed chiral catalyst was used with dichloroethane as the solvent, at 50 °C overnight. The reaction outcomes were analyzed by chiral HPLC analysis which proved to be troublesome and not always reproducible. It was found that separation of the enantiomers for both the *exo* and the *endo* diastereomer was difficult. Separation could only be achieved with pure heptane as the eluent and placing two chiral columns after each other. The reproducibility problems arose probably from polar impurities present in the crude samples. Since pure heptane, was used these polar impurities can significantly disturb reproducibility in the HPLC analysis. Despite these difficulties we did manage to acquire data indicating the stereochemical induction exerted by the chiral ligands.

At first the BOX ligands were studied. Although full conversion was achieved in most of the cases, ligand **L12** proved to be useless. Unfortunately, the diastereoselectivity in most cases was rather poor (see **L9-L13**). In those cases where the *exo:endo* ratio exceeded 2:1, as for ligands **L14-L16**, the enantioselectivities for the desired *exo* product were determined. Ligand **L14** and **L16** gave ~25% and ~11% *ee* respectively, but the most interesting result was obtained with spiro-BOX ligand **L15**. An acceptable diastereomeric ratio of 4:1 in favor of the desired *exo* isomer was found, together with ~35% *ee*.

Next we investigated the four phosphine ligands. To our surprise no conversion was obtained except for **L20**, but the diastereoselectivity was low. As a final entry we used bis-imine ligand **L21**, for which we found a diastereoselectivity in favor of the *exo* isomer of 5.2:1. Together with this result we found that the *exo* isomer exhibited an enantiomeric excess ~44%. These results matched with that obtained for spiro-BOX ligand **L15**, so we had two potential lead ligands to follow up the initial screening process.

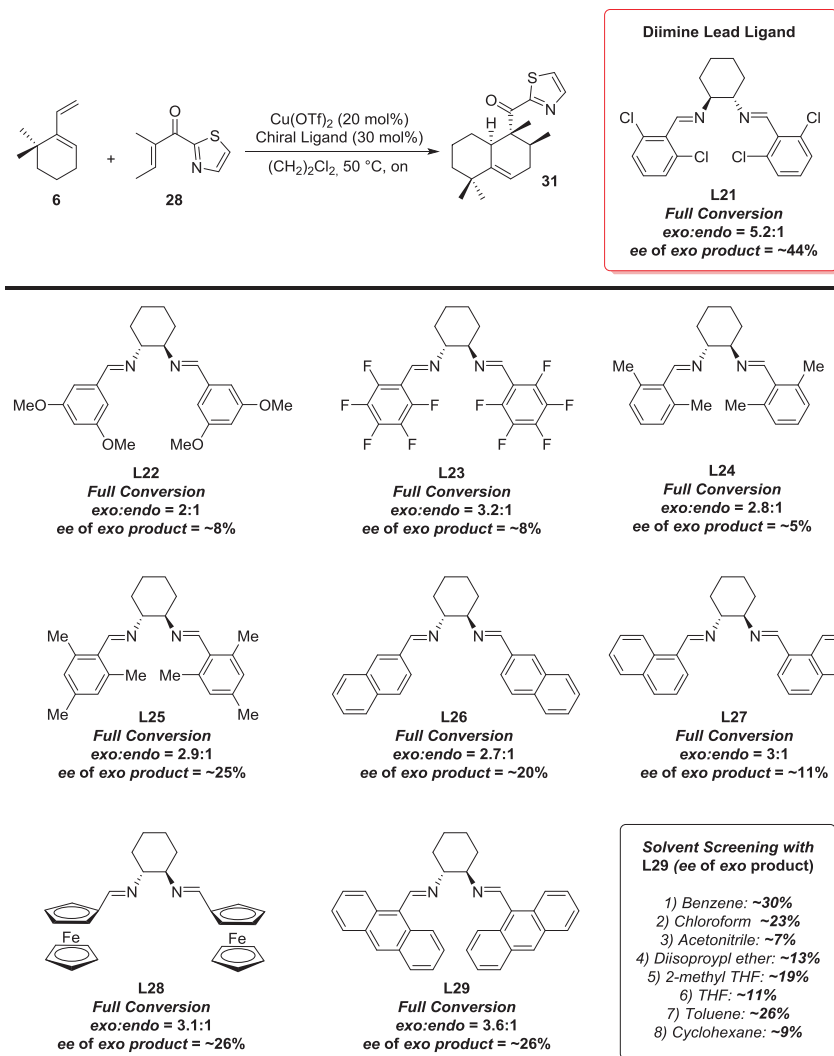




**Scheme 12.** Ligand screening in the asymmetric Diels-Alder reaction.

To function as a promising lead ligand, easy access to related structures is important. Spiro-BOX ligands do not fit this requirement as the synthesis requires multiple steps with a relatively small window for structural diversity. On the other hand, the bis-imine ligands are readily accessible by reaction of a chiral 1,2-diamine and a functionalized benzaldehyde.<sup>[36]</sup> As many of such reagents are commercially available, a broad scope of chiral bis-imines can be accessed. We therefore set out to construct a variety of bis-imine ligands (**L21-L29**) and employed those in the asymmetric Diels-Alder reaction (Scheme 13).

## Asymmetric Total Synthesis of 1-Tuberculosinyl Adenosine



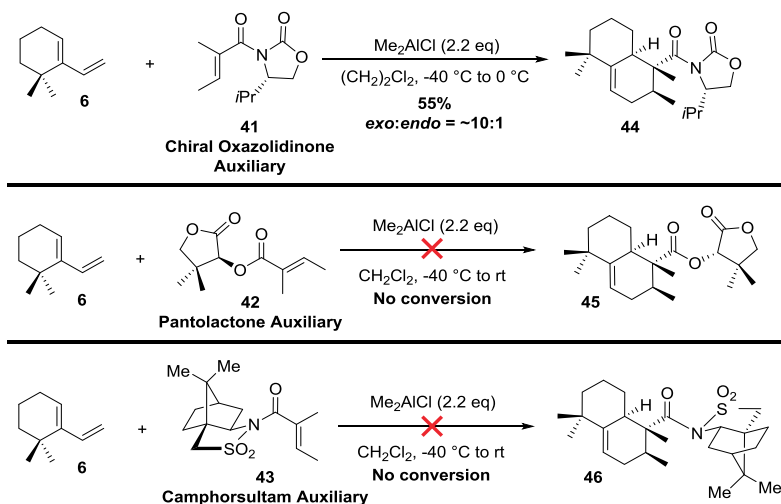
**Scheme 13.** Ligand screening in the asymmetric Diels-Alder reaction.

Encouraged by the results using bis-amine ligand **L21** we investigated seven other bis-imine ligands (**L22-L29**)<sup>[36]</sup> which span a wide range of structural variety, both electronically as sterically. None of the ligands showed an improvement in diastereoselectivity or the enantioselectivity (5-26% *ee*). A solvent screening was performed for reactions involving ligand **L29**, but also these reactions were to no avail. The results significantly narrowed down our window of opportunities to achieve an asymmetric Diels-Alder using (copper) catalysis, and we therefore had to reconsider our approach.

## 4.3.5 A chiral auxiliary based Diels-Alder approach towards 1-TbAd

Concurrent with our work on the copper-catalyzed Diels-Alder reactions we explored chiral auxiliaries to achieve stereinduction. We chose our auxiliaries on the basis of reports by Helmchen, Oppolzer and Evans, who successfully employed pantolactone,<sup>[38]</sup> camphorsultam,<sup>[39]</sup> and oxazolidinone<sup>[40]</sup> auxiliaries in Diels-Alder reactions, respectively. We were particularly interested in how the Evans auxiliary would perform since in their tuberculosinol total synthesis publication Snider and co-workers stated the following:

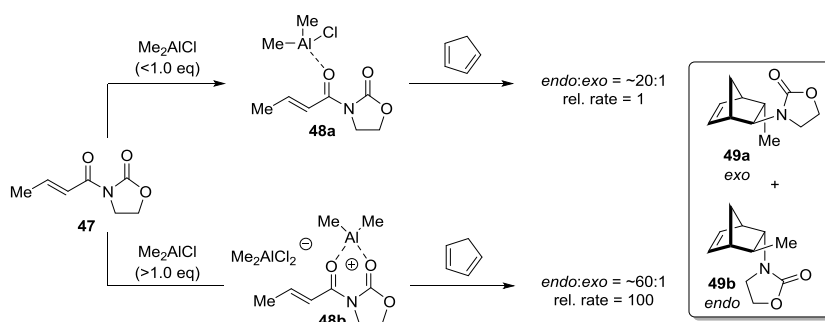
*“The unsubstituted oxazolidinone 12 (number in this chapter) was chosen to minimize steric interactions between the  $\alpha$ -methyl group and the oxazolidinone and because asymmetric induction seemed unlikely in an *exo* Diels-Alder reaction in which a chiral oxazolidinone would be far away from the diene.”<sup>[13]</sup>*



**Scheme 14.** Chiral auxiliary containing tiglate dieneophiles tested.

We thus synthesized tigloyl based dienophiles **41-43** that were reacted with diene **6** in the presence of  $\text{Me}_2\text{AlCl}$  (Scheme 14). The choice for this Lewis acid was based on previous work regarding Lewis Acid activation in Diels-Alder cycloadditions with diene **6**. Danishefsky and co-workers reported in their work that  $\text{TiCl}_4$ , and  $\text{BF}_3 \cdot \text{OEt}_2$  were not compatible with diene **6**, which decomposed under the reaction conditions.<sup>[18]</sup> In unpublished results from the Snider laboratory it was reported that Lewis activation with  $\text{Et}_2\text{AlCl}$  or  $\text{EtAlCl}_2$ , in reaction between an isomer of diene **6** and oxazolidinone **12** (Scheme 2), led to poor and no conversion, respectively.<sup>[41]</sup> In their published synthesis,  $\text{Me}_2\text{AlCl}$  was shown to be a suitable Lewis acid,<sup>[14]</sup> which we therefore used in our chiral auxiliary based reactions. The stoichiometry of the Lewis acid was based on work by the Evans group which showed that the use two equivalents of Lewis acid provides a

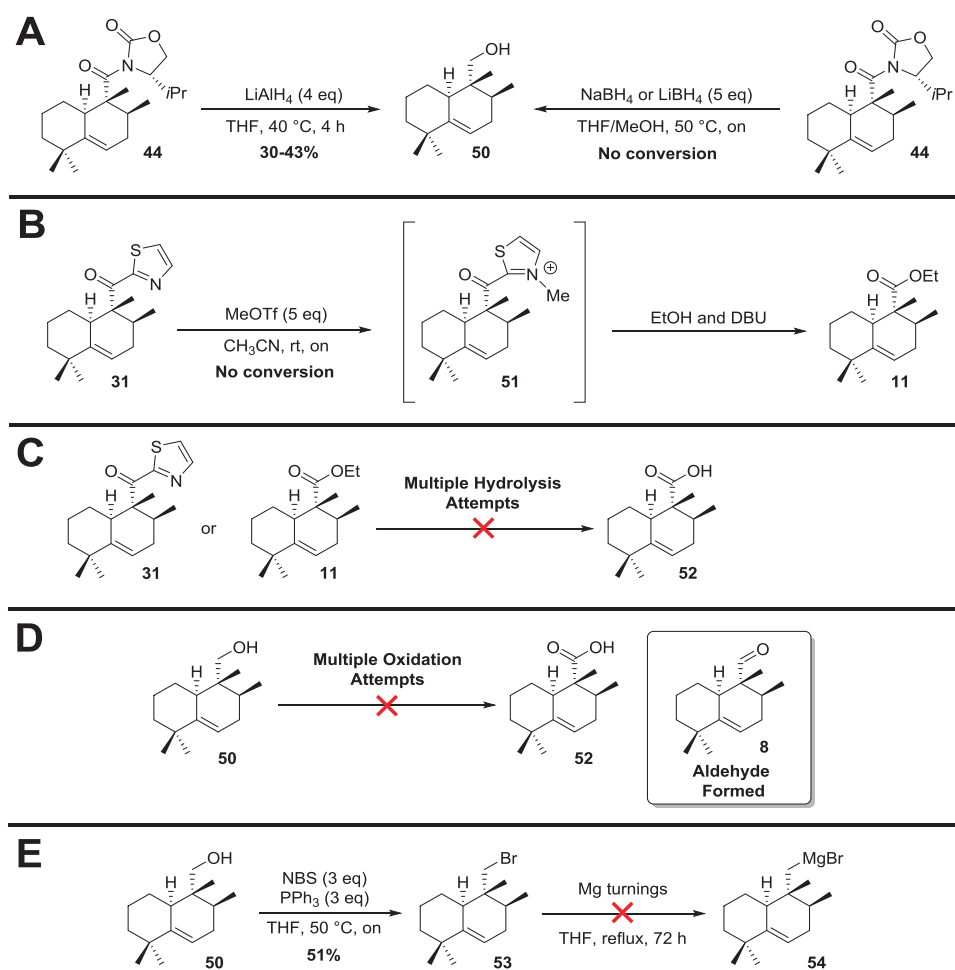
bidentate coordination with the dienophile via chloride abstraction, considerably enhancing both diastereoselectivity and reactivity in the reaction (Scheme 15).<sup>[42]</sup> The Diels-Alder reactions with pantoyltiglate **42** and camphorsultam **43** were unproductive, as no conversion of the starting materials was observed. On the other hand, as expected, the reaction with (*S*)-isopropyl-*N*-tigloyloxazolidinone **41**<sup>[43]</sup> gave the desired cycloaddition, providing **44** in 55% yield with a diastereomeric ratio of ~10:1. These results matched with that reported for the achiral variant (Scheme 2).<sup>[14]</sup>



**Scheme 15.** Enhanced reactivity by the used of an excess of Lewis acid.

#### 4.3.6 Removal of the chiral auxiliary and the battle against steric hindrance

With the desired cycloadduct **44** in hand, we had to determine whether asymmetric induction had taken place. We decided to first remove the chiral auxiliary by converting Diels-Alder adduct **44** to the corresponding alcohol, since this compound had been shown by Sorenson and co-workers to be easily separable using liquid chromatography. Snider and co-workers had shown the removal of the oxazolidinone auxiliary was trivial for their racemic adduct **13** (Scheme 2), as the oxazolidinone was cleaved with  $\text{LiBH}_4$  in 82% yield. In our case however, both  $\text{LiBH}_4$  and  $\text{NaBH}_4$  failed to cleave the chiral auxiliary even at elevated temperatures for prolonged reaction times (Scheme 16a). The use of  $\text{LiAlH}_4$  did produce **50** but in only a moderate yield of 30-43%.



**Scheme 16.** Steric hindrance hampers reactivity at the neopentyl-type position.

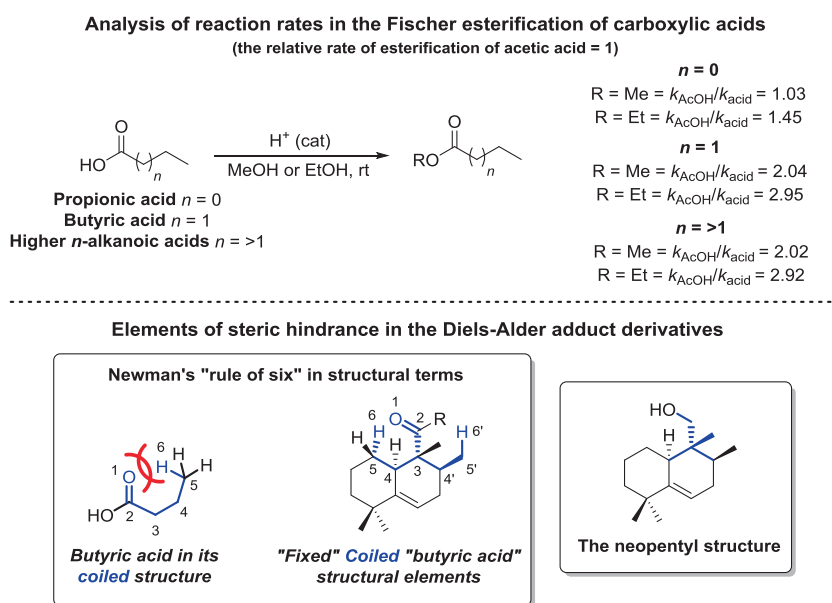
The difficulties encountered in the removal of the chiral auxiliary were not surprising. Prior to these reactions, we performed a plethora of experiments on functionalities proximal to the quaternary stereocenter (see Scheme 16 for a selection). In early studies on the cleavage of the thiazole in Diels-Alder adduct **31**, *N*-methylation with MeOTf did not take place (Scheme 16b). Instead *O*-methylation was observed, causing the esterification with ethanol to fail. An apparently simple hydrolysis of ethyl ester **11** (or thiazole **31**) also proved cumbersome as even after reaction under harsh conditions (10 eq KOH, EtOH/H<sub>2</sub>O, reflux, 72 h), starting material was retrieved (Scheme 16c). Ethyl ester **11** however is reduced with LiAlH<sub>4</sub> to **50** in near quantitative yield (see chapter 3).<sup>[13]</sup> Accessing the carboxylic acid via oxidation of **50** was also troublesome. For example; RuCl<sub>3</sub>/NaIO<sub>4</sub>,<sup>[44]</sup> CrO<sub>3</sub>/H<sub>5</sub>IO<sub>6</sub>,<sup>[45]</sup> and CrO<sub>3</sub>/H<sub>2</sub>SO<sub>4</sub> (Jones oxidation)<sup>[46]</sup> failed to produce the carboxylic acid as the reaction stopped in the aldehyde stage (Scheme

16d). Even Grignard formation of bromide **53** using freshly activated magnesium turnings, and a pinch of iodine, in refluxing THF over the weekend failed and the starting material was quantitatively retrieved!

It was evident from the examples given that the carbonyl functionality is considerably shielded. In particular, reactions involving a tetrahedral intermediate are problematic. An obvious candidate which imposes steric hindrance is the neighboring quaternary stereocenter (= neopentyl type structure). However, we reason another less known contributing factor is present, which can be explained by Newman's "rule of six".<sup>[47a]</sup>

In 1950 Newman analyzed the reaction rates in the Fischer esterification of carboxylic acids. It was found that the rate of reaction for acetic acid and propionic acid with MeOH are equal (Scheme 17). However, a significant rate decrease was observed for butyric acid which does not further decrease for higher homologues. This low reactivity of butyric acid has been observed before, and it was postulated by Smith and McReynolds that a "coiled" conformation of butyric acid might be responsible for the impediment of reaction (Scheme 17).<sup>[47b]</sup> This proposition together with the empirical data for other carboxylic acids led Newman to postulate the "rule of six" stating: "In reactions involving additions to an unsaturated function, the greater number of atoms in the six position, the greater will be the steric effect".

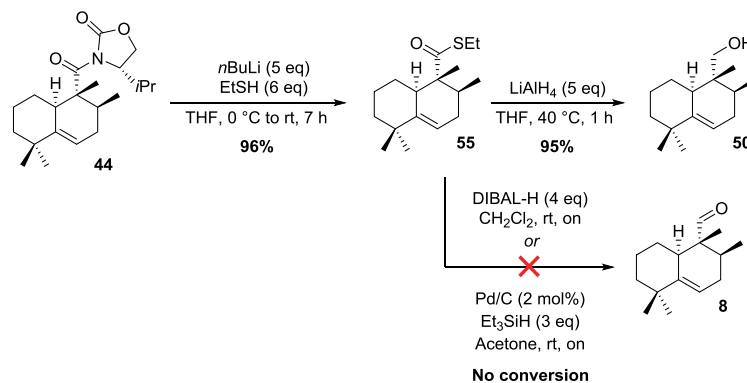
Interestingly, in the Diels-Alder adduct, there are actually two "coiled butyric acids" present (in blue and numbered). Moreover, in contrary to butyric acid itself, the coiled structural element is fixed in the decalin structure and might therefore be a significant contributing factor of steric hindrance.



Scheme 17. Newman's "rule of six" to explain steric hindrance in the Diels-Alder adducts.

## CHAPTER 4

Despite the inherent steric hindrance, we did manage to remove the chiral auxiliary with  $\text{LiAlH}_4$ , however alcohol **50** was obtained in only a moderate yield up to 43% (Scheme 16a). This outcome was attributed to irreversible attack of the reducing agent onto the more accessible carbonyl group of the chiral auxiliary. It was therefore concluded that auxiliary cleavage had to be performed with a powerful, small nucleophile allowing reversibility in the attack on the auxiliary's carbonyl group. Lithium ethyl thiolate was therefore considered suitable (Scheme 18). We were delighted to see the reaction worked to great satisfaction as thioester **55** was cleanly produced in 96% yield. Reduction of **55** with  $\text{LiAlH}_4$  then produced alcohol **50**, this time in 95% yield. Somewhat naively, we also tried to convert thioester **55** directly into aldehyde **8**, an intermediate used in the eventual total synthesis (*vide infra*). Treatment with DIBAL-H and using Fukuyama reduction<sup>[48]</sup> conditions gave no reaction as we already expected. In spite of the introduction of an additional step to our total synthesis, the drastic increase in overall yield of alcohol **50** outweighed this disadvantage.



**Scheme 18.** Successful cleavage of the chiral oxazolidinone in Diels-Alder adduct **44**.

### 4.3.7 Determination of asymmetric induction in the chiral auxiliary aided Diels-Alder cycloaddition

Alcohol **50** allowed to assess the enantioselectivity of the Diels-Alder reaction. Chiral HPLC analysis of racemic alcohol **50** obtained in our racemic 1-TbAd synthesis (see chapter 2) provided the HPLC trace depicted in figure 2, top. The *exo* and *endo* isomer are completely separated, as are the enantiomers (17.55 min and 21.15 min) of the *exo* diastereoisomer. We were excited to see the HPLC trace of our enantioenriched alcohol **50** as we found complete disappearance of the peak at 21.15 min (figure 2, bottom). So **50** had been prepared with an enantiomeric excess exceeding 98% for the *exo* isomer. The previously discussed assertion from Snider and co-workers, regarding the notion that asymmetric induction with a chiral oxazolidinone being unlikely, had therefore to be reconsidered.

Further confirmation of the excellent stereoselectivity was obtained by comparison of the optical rotation with that reported in the literature. The optical rotation of **50** ( $[\alpha]_D^{23}$

### Asymmetric Total Synthesis of 1-Tuberculosinyl Adenosine

= +27.0 ( $c = 0.2$ ,  $\text{CHCl}_3$ ) matched with that of the Sorensen laboratory ( $[\alpha]_D^{23} = +28.3$  ( $c = 0.2$ ,  $\text{CHCl}_3$ )),<sup>[13]</sup> who obtained enantiopure alcohol **50** by chiral SFC (supercritical fluid chromatography) of the racemic diastereomeric mixture. The enantiomeric excess of the minor *endo* isomer (15.6 min and 15.9 min) was measured to be ~60% *ee*.

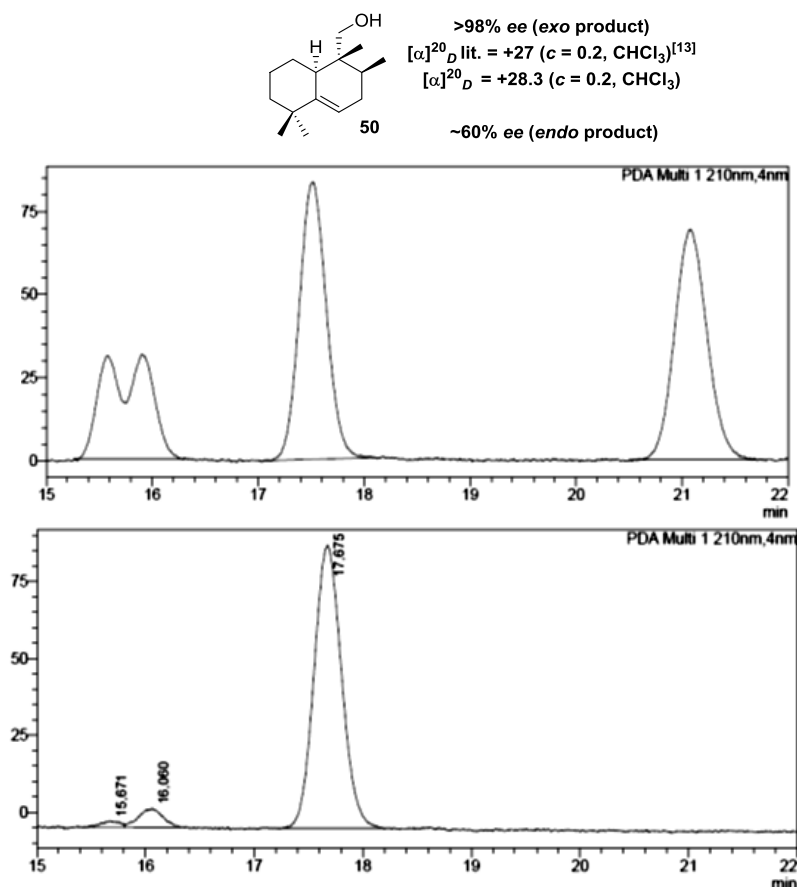


Figure 2. Chiral HPLC analysis of alcohol **50**; racemic (top), asymmetric (bottom).

#### 4.3.8 The stereoselective synthesis of 1-TbAd and $N^6$ -TbAd

With this exquisite result in hand we were now eager to elucidate the absolute stereochemical outcome of the Diels-Alder reaction. Up to this point we had performed the asymmetric Diels-Alder reactions on a small scale (0.4 mmol = ~50 mg of diene **6**). Scaling up of the reaction proved to be facile as we ultimately managed to perform the reaction starting from 40 mmol (~5.4 g) of diene **6**. No complications in the scale-up were met as equal results in terms of yield and stereoselectivity were obtained compared to the small scale reactions.



A welcoming feature which arose from the scale-up was that we managed to obtain multi-grams of crystalline material. This provided us with a crystal suitable for X-ray crystallography, revealing the absolute stereochemistry of Diels-Alder adduct **44** and consequently that of tuberculosinol. Remarkably, despite the interest in tuberculosinol and related compounds, the absolute stereochemistry of tuberculosinol had not been unequivocally established. It had been tentatively assigned<sup>[49]</sup> by comparing the sign of the optical rotation of tuberculosinol with that of neopolypodatetraene A, which has the same bicyclic core structure with known absolute configuration.<sup>[50]</sup> This is not fully convincing, since small differences in structure can lead to a different sign of rotation. In addition, tuberculosinol is formed by the GGPP cyclase Rv3377c,<sup>[15]</sup> whereas neopolypodatetraene A is formed by a squalene cyclase.<sup>[50]</sup> The X-crystal structure of **44** closed the debate as the absolute stereochemistry was found to correspond to that in figure 3.

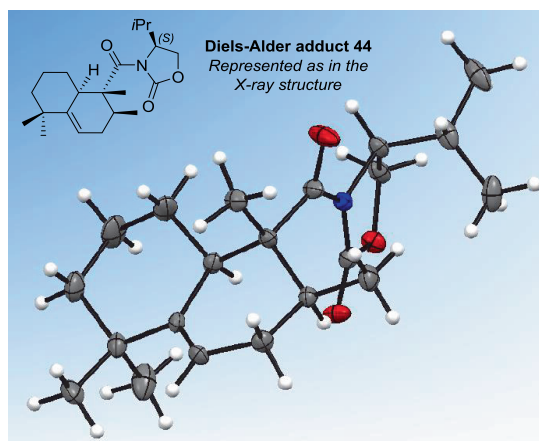


**Figure 3.** X-ray crystal structure (ORTEP) of Diels-Alder adduct **44**. Atom color code: Carbon = grey; Hydrogen = white; Oxygen = red; Nitrogen = blue.

#### 4.3.9 Completion of the stereoselective synthesis of 1-TbAd and $N^6$ -TbAd

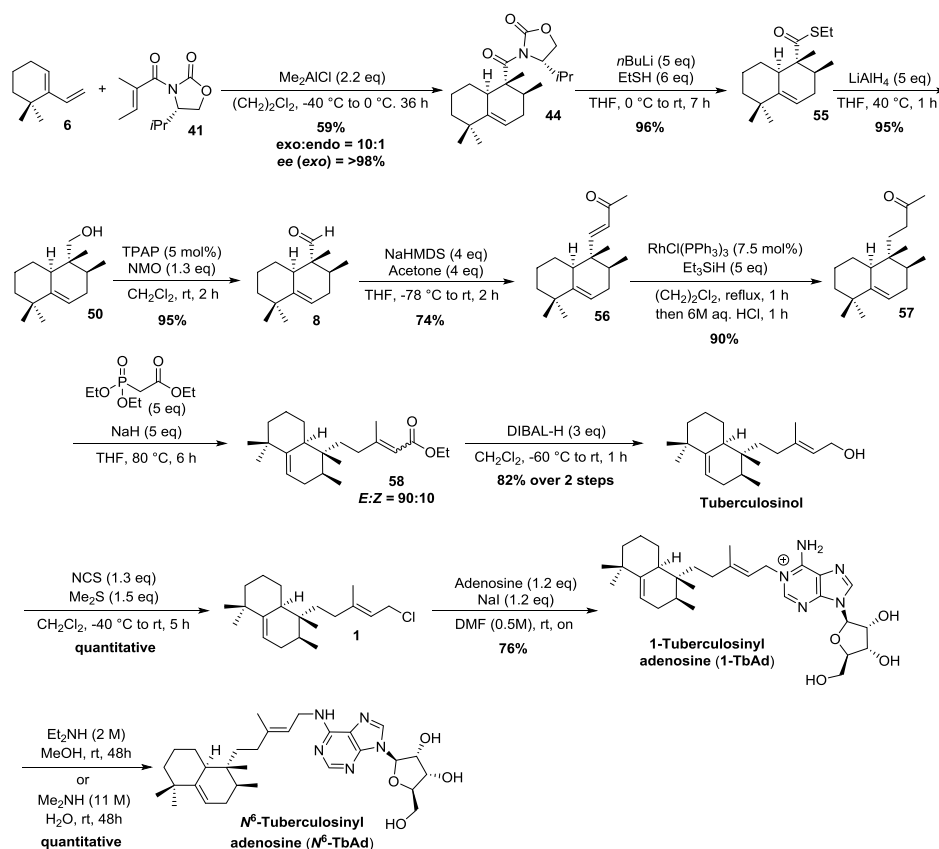
Finally, we could complete our total synthesis of the tuberculosinyl adenosines. As shortly discussed within the introduction of this chapter (see for details chapter 3), both 1-TbAd and  $N^6$ -TbAd were shown to be potential chemical markers for tuberculosis.<sup>[8,11]</sup> Additionally, 1-TbAd is produced by the virulence-associated enzyme Rv3378c, of which its locus (Rv3377c–Rv3378c) has shown to be essential in phagosome maturation arrest.<sup>[9]</sup> 1-TbAd is therefore expected to be involved in phagosomal survival of *Mtb*, although the exact role it plays remains to be investigated. To facilitate further studies of the TbAd molecules, reference material is essential, and we therefore set out to produce multi-grams of the natural product.

At this stage of our synthesis, we had several grams of Diels-Alder adduct **44** in hand which was subjected to removal of the chiral auxiliary and reduction of the

*Asymmetric Total Synthesis of 1-Tuberculosinyl Adenosine*

corresponding thioester **55**, providing alcohol **50** in 91% yield over the two steps (Scheme 19). In earlier efforts to racemic TbAd, we found the Sorensen<sup>[13]</sup> and Snider<sup>[14]</sup> routes reproducible and high yielding. We therefore decided to pursue the route along these lines.

A Ley-Griffith oxidation of alcohol **50** provided aldehyde **8** which subsequently was condensed with acetone to furnish enone **56**, in 70% yield over the two steps. The enone was then efficiently reduced by Wilkinson's catalyst in combination with triethylsilane in 90% yield. Installation of the double bond was achieved by a Horner-Wadsworth-Emmons olefination with triethyl phosphonoacetate to produce the desired enoate **58** in a 90:10 *E:Z* mixture. This mixture was reduced with DIBAL-H, which after purification afforded pure, naturally occurring, tuberculosinol in 82% yield over the two steps.



**Scheme 19.** Asymmetric total synthesis of the tuberculosinyl adenosines, 1-TbAd and *N*<sup>6</sup>-TbAd.

To complete the synthesis of the tuberculosinyl adenosines, tuberculosinol was converted into tuberculosinyl chloride **1**, using a Corey-Kim chlorination, in near quantitative yield.<sup>[51]</sup> **1** proved to be unstable on silica, but purification was efficiently achieved by straightforward precipitation of the residual NCS and succinimide.

Addition of pentane to the reaction mixture and subsequent filtration afforded, after removal of the volatiles, near pure **1**. We were now only one step removed from finalizing our total synthesis of 1-TbAd, which required alkylation of adenosine with tuberculosinyl chloride **1**. In our racemic total synthesis this step was performed in a poor 17% yield (Chapter 3). After a thorough study of the alkylation of adenosine with **1**, we eventually managed to produce 1-TbAd in 76% yield with a procedure involving NaI (Finkelstein conditions) in DMF (0.5 M in **1**).<sup>[52]</sup>

In addition to the synthesis of naturally occurring 1-TbAd, we also used this alkylation procedure to construct the derivatives (*Z*)-1-TbAd, 2'-deoxy 1-TbAd<sup>[10]</sup> and <sup>13</sup>C-labelled 1-TbAd (see the experimental section). The latter compound, made from adenosine which was fully <sup>13</sup>C-labelled in the ribose, was prepared to facilitate the development of 1-TbAd as a chemical marker for tuberculosis. Isotope-labelled chemical markers are important as internal standards for quantification with HPLC-MS.<sup>[53]</sup>

In order to verify its chemical structure, as proposed by Lau *et al.*,<sup>[10]</sup> 2'-deoxy 1-TbAd was produced, by reacting tuberculosinyl chloride with 2'-deoxy adenosine. CID/MS-analysis of synthetic 2'-deoxy 1-TbAd produced MS spectra closely matching that of the proposed natural product. This, and the fact that 2'-deoxy adenosine is an abundant nucleoside, provides strong evidence that 2'-deoxy 1-TbAd is a *Mycobacterium tuberculosis* produced natural product.

The finishing touch of our synthesis was the construction of *N*<sup>6</sup>-TbAd. It is known that 1-alkyl adenosines rearrange to *N*<sup>6</sup>-alkyl adenosines under nucleophilic conditions via a so-called Dimroth rearrangement.<sup>[54]</sup> Treatment of 1-TbAd with 60% aqueous Me<sub>2</sub>NH brought about this rearrangement to *N*<sup>6</sup>-TbAd quantitatively, concluding our total synthesis of the naturally occurring tuberculosinyl adenosines.

#### 4.4 On the mechanism and enantioselectivity of the asymmetric Diels-Alder reaction

This Diels-Alder cycloaddition is the first of its kind to produce the halimane core structure with both high diastereo- and enantioselectivity. As previously mentioned, in 2010 the Snider laboratory discarded the use of a tigloyl based chiral oxazolidinone to achieve such stereoselection.<sup>[14]</sup> Intrigued by this discrepancy, we decided to systematically investigate the stereoselective nature of the reaction.

The aforementioned statement from the Snider laboratory was based on the mechanistic model proposed by Danishefsky (Figure 4a), explaining *exo*-selectivity in the Diels-Alder reaction with diene **6**.<sup>[18]</sup> A steric clash between the diene's geminal dimethyl group and the bulky dienophile disfavors the *endo* approach, hence providing the *exo*-Diels-Alder adduct selectively. This model, however, only addresses the dienophile in its *s-trans* conformation. Although this model predicts the observed *exo*-selectivity, it ignores a possible contribution of the *s-cis* conformation of the dienophile.<sup>[55]</sup> In a combined experimental and computational study by Houk, Gouverneur *et al.*, it was shown that Evans chiral auxiliary-based dienophiles provide efficient chiral induction and *endo* or *exo*-selectivity depending on the substitution at the β-position of the

dienophile and the diene.<sup>[56]</sup> The reaction takes place from the *s-cis* conformation of the dienophile as expected as the diene is not substituted at the  $\alpha$ -position, like in the current tigloyl-based dienophile.

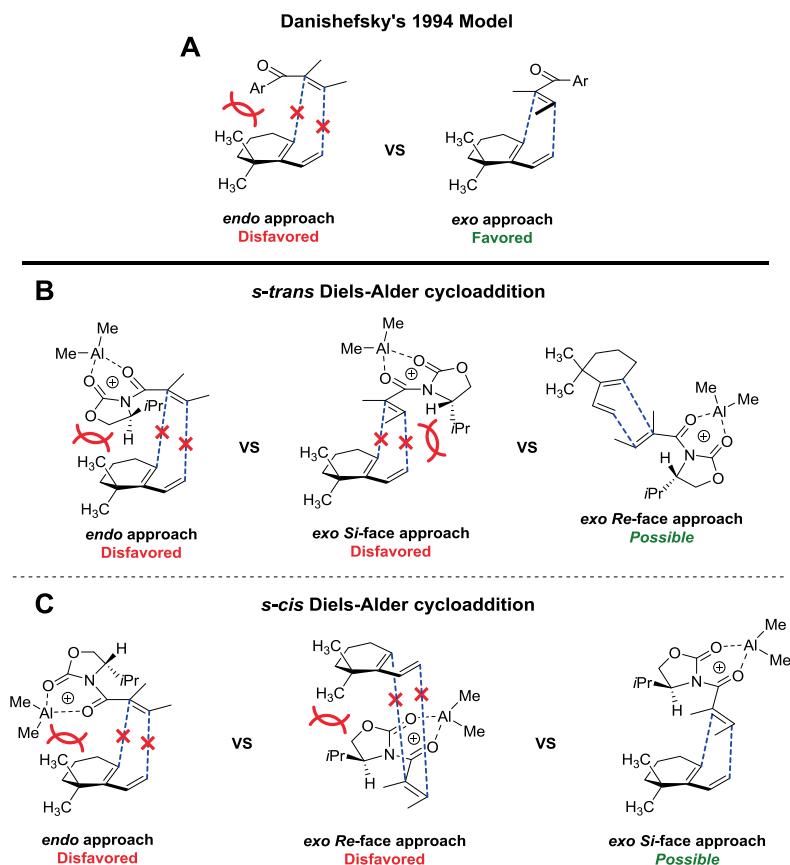


**Figure 4.** Models for asymmetric induction in the Diels-Alder cycloaddition between diene **6** and dienophile **41**.

In figure 4b, a model for the [4+2] cycloaddition between diene **6** and dienophile **41**, in its *s-trans* conformation, is presented. As in Danishefsky's model,<sup>[18]</sup> the *endo* approach is disfavored for reasons previously mentioned. The *exo* approach on the *Si*-face of the dienophile seems disfavored, as the isopropyl group on the chiral oxazolidinone clashes with the vinyl substituent of the diene. The *Re*-face approach on the other hand seems plausible, as no obvious steric interactions shield this face from reaction. However, this facial approach would provide the Diels-Alder adduct **44** with a stereochemistry opposite to that observed experimentally.

Considering the *s-cis* conformer of dienophile **41** (Figure 4c), the *endo* approach is again disfavored, this time because of a clash between the dimethylaluminum chelate

and the geminal dimethyl functionality. The *Re*-face appears unapproachable due to a steric interaction between the isopropyl group and the geminal dimethyl group in diene **6**. A *Si*-face approach does not result in such steric clash *and* provides Diels-Alder adduct **44** with the experimentally obtained stereochemistry. This model therefore seems to be a better picture of the course of the reaction, despite the expectation that the *s-cis* conformation of the dienophile is unfavorable compared to the *s-trans* conformation. To get a complete picture of the reaction we studied the reaction through *in silico* studies.

Calculations were carried out using the ADF program suite<sup>[57]</sup> at the BP86<sup>[58]</sup>/TZ2P level of theory. The geometries of all stationary points were optimized in the gas phase and verified to be proper local minima or transition states through vibrational analyses. The gas-phase harmonic frequencies were used for the enthalpic and entropic corrections to the free energies at 233.15 K (-40 °C).

First, it was determined whether the *s-cis* conformer is energetically feasible by calculating the *s-trans*/*s-cis* equilibrium for Me<sub>2</sub>Al-complexed dienophile **41** (Figure 5). We found the *s-trans* **41b** conformer is favored over the *s-cis* **41a** conformer by 0.2 kcal/mol on the Gibbs free energy surface at 233.15 K, providing a ratio of 6 : 4 respectively at -40 °C. With a rotational barrier of  $\Delta G^\ddagger = 3.2$  kcal/mol, however, the conformers are readily interconvertible and, due to the Curtin-Hammett principle,<sup>[59]</sup> the observed product can be reached via the *s-cis* conformer.<sup>[55]</sup>

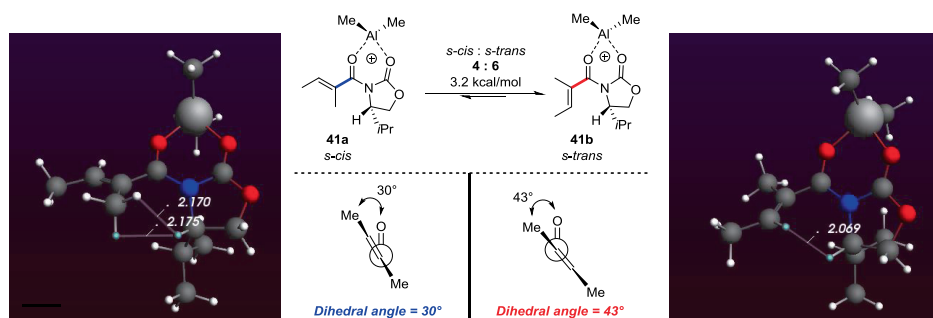


**Figure 5.** Intramolecular distances (between the chiral oxazolidinone hydrogen atom and the  $\beta$ -hydrogen atoms) and dihedral angle of *s-cis* conformer **41a** and *s-trans* conformer **41b** obtained from the optimized geometries.

The energy profile for the entire reaction pathway was calculated next (Figure 6). On the basis of our calculations, and according to the models in figure 4, the *endo* approach for both the *s-trans* and *s-cis* conformers can be ruled out. Attack of the *s-trans* conformer from the *exo* *Si*-face, and attack of the *s-cis* conformer from the *exo* *Re*-face are prohibited as well as the computations showed significant steric clash for initial bond formation (*see experimental section*). The two models in which calculations were carried out were the *Re*-face approach and the *Si*-face approach for the *s-trans* and *s-cis* conformers respectively (both *exo* attack).

The reaction of the *s-trans* conformer (Figure 6, **red pathway**) has a considerably higher activation energy ( $\Delta G^\ddagger = 19.4$  kcal/mol) for the initial and enantio-determining step, than the reaction of the *s-cis* conformer (**blue path**,  $\Delta G^\ddagger = 15.5$  kcal/mol). This convincingly explains the reaction outcome.

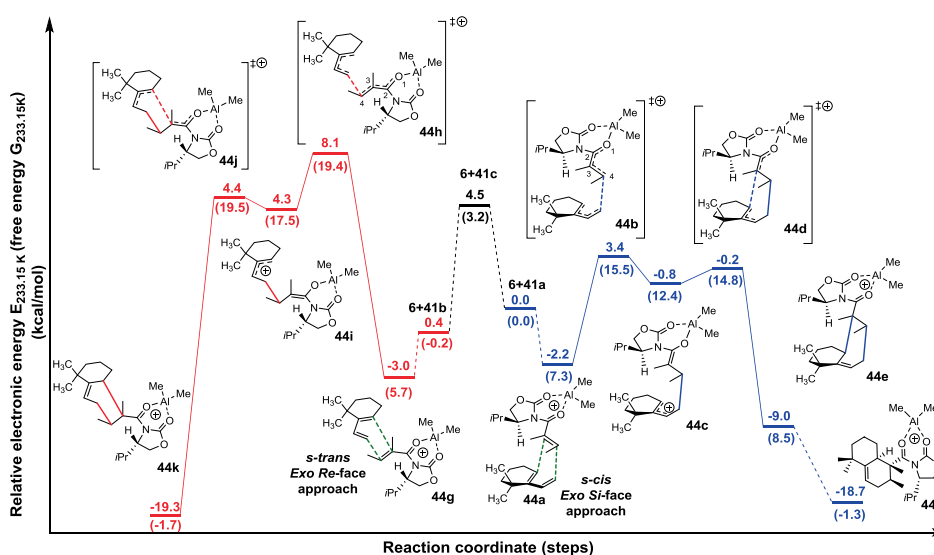


**Figure 6.** DFT BP86/TZ2P calculated reaction coordinate for the Diels-Alder cycloaddition between diene **6** and dienophile **41**. For these studies, the *s-cis* *exo* *Si*-face approach was chosen as the reference point. IRC analysis were performed on both transition states on the *s-cis* pathway (blue lines) and are connected with solid lines. The dashed lines connect the structures in which IRC was not performed, but was found to exist on the potential energy surface. (Relative electronic energies are given in kcal/mol, and relative Gibbs free energies are given in kcal/mol in parentheses). The geometry of diene **6**, aluminum-complexed *s-cis* conformer of the dienophile (**41a**) aluminum-complexed *s-cis* conformer of the dienophile (**41b**), and the transition state between **41a** and **41b** corresponding to the rotation along the C(2)-C(3) bond (**41c**) were optimized separately. The energies of the three states **6+41a**, **6+41b** and **6+41c** are the sum of the corresponding diene and aluminum-complexed dienophile fragments (See Supporting Information).

The Diels-Alder reaction was found to proceed stepwise rather than concerted. After the first bond formation, the cationic intermediate is in an energy well with a relative energy of 12.4 kcal/mol, before proceeding to form the second bond through a saddle point at 14.8 kcal/mol. From this point, the reaction is thermodynamically downhill to form the Me<sub>2</sub>Al complexed Diels-Alder adduct **44f** with a relative  $\Delta G = -1.3$  kcal/mol. The differences in activation energies between the two pathways can be rationalized by using the activation strain model.<sup>[60]</sup> In this model, the electronic activation energy ( $\Delta E^\ddagger$ ) is the sum of strain energy ( $\Delta E^\ddagger_{\text{strain}}$ ), which is associated with the deformation of the starting materials to the geometry they acquire in the TS, and the interaction energy

( $\Delta E_{\text{int}}^{\ddagger}$ ), which is associated with the favorable electronic interactions between the deformed starting materials, *i.e.*,

$$\Delta E^{\ddagger} = \Delta E_{\text{strain}}^{\ddagger} + \Delta E_{\text{int}}^{\ddagger}$$

As outlined in Table 2, the difference in  $\Delta E^{\ddagger}$  between TS **44b** and TS **44h** is mainly due to strain, not due to orbital interaction. Upon inspection on the geometry of the dienophile at the transition state, the dihedral angle O(1)-C(2)-C(3)-C(4) is deviating 17.2° and 18.2° from planarity for TS **44b** and TS **44h** respectively, while the corresponding dihedral angle of the *s-cis* and *s-trans* conformers are deviating 29.8° and 43.0° from planarity respectively (Figure 5).

Transition states	$\Delta E^{\ddagger}$	$\Delta E_{\text{strain}}^{\ddagger}$	$\Delta E_{\text{int}}^{\ddagger}$	$\Delta H^{\ddagger}$	T $\Delta S^{\ddagger}$	$\Delta G^{\ddagger}$
<b>44b</b>	3.4	16.5	-13.1	4.2	-11.4	15.6
<b>44h</b>	7.7	23.4	-15.7	8.4	-11.3	19.7
<b>44d</b>	-0.2	79.1	-79.3	2.2	-12.6	14.8
<b>44j</b>	3.9	75.6	-71.6	5.8	-13.9	19.7

**Table 2.** Activation strain analysis (in kcal/mol) for the four transition states shown in figure 5.

The larger deviation from planarity, of the dihedral angle O(1)-C(2)-C(3)-C(4), in the *s-trans* conformer might be attributed to a steric interaction between the hydrogen atom at the stereocenter of the oxazolidinone scaffold, and that of the hydrogen atom at C(4) (Figure 5). The distance between these two hydrogen atoms is 2.07 Å for the *s-trans* conformer, while the closest distance between the hydrogen atom at the oxazolidinone and the hydrogens on the  $\alpha$ -methyl group in the *s-cis* conformer is 2.17 Å. Since both distances are less than the sum of the van der Waals radii of two hydrogen atoms (2.4 Å), the steric interactions between the hydrogen atoms in both cases are non-negligible, and the steric interaction in the *s-cis* conformer is indeed less severe than that in the *s-trans* conformer. The *s-cis* conformer can thus retain a relatively planar geometry without experiencing severe steric interactions. The larger difference of the dihedral angle between the ground state and the transition state of the *s-trans* conformer (**44h**) compared to that of the *s-cis* conformer (**44b**) could explain the difference in activation strain.

While  $\Delta E_{\text{int}}^{\ddagger}$  plays a larger role in determining the  $\Delta E^{\ddagger}$  of the second transition state, this difference is argued to be less important due to the fact that enantioselectivity is determined at the first transition state.

To the best of our knowledge, this computational study is the first to shine light on the mechanism of Diels-Alder reactions with tigloyl (that means,  $\alpha,\beta$ -disubstituted) chiral oxazolidinones. Although the Curtin-Hammet principle in Diels-Alder reactions has been described before,<sup>[55]</sup> for the use of tigloyl based dienophiles this concept is novel.

#### 4.5 Conclusion

In summary, 1-TbAd and *N*<sup>6</sup>-TbAd have been prepared as pure stereoisomers in 10 and 11 steps respectively, starting from diene **6**. Installation of the three chiral centers in tuberculosinol was efficiently achieved (*exo:endo* = 10:1, >98% *ee* for the *exo* isomer) employing a chiral oxazolidinone auxiliary aided Diels-Alder reaction. The synthesis has been scaled to produce 2.4 g of 1-TbAd in 21% overall yield. In addition, the family members *N*<sup>6</sup>-TbAd and 2'-deoxy 1-TbAd have been prepared, confirming the structure of the latter. The synthetic material was shared with the Moody laboratory who is currently investigating the virulence-promoting effects of 1-TbAd, and its use as a chemical marker for tuberculosis.

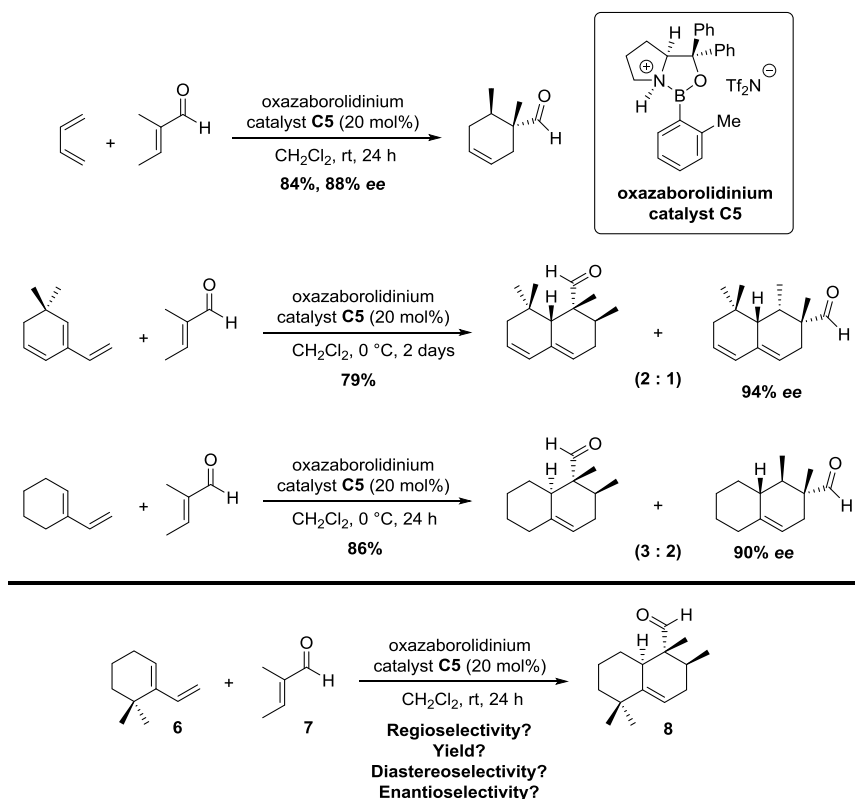
The enantioselective nature of the Diels-Alder reaction was also investigated. *In-silico* studies showed the Diels-Alder cycloaddition proceeds according to the Curtin-Hammet principle in which the thermodynamically less stable *s-cis* conformer of the dienophile reacts to form Diels-Alder adduct **44**, because this conformer needs less deformation in the transition state which results in a lower reaction barrier. Additionally, the reaction was also found to follow a step-wise mechanism rather than concerted.

#### 4.6 Discussion and outlook

As evident from this chapter, a thorough investigation into the asymmetric total synthesis of 1-TbAd was performed, focusing mainly on the development of an asymmetric catalytic Diels-Alder reaction. Unfortunately, we did not accomplish this objective, as we cut short our investigation, since we found excellent stereoselectivities with the chiral auxiliary approach. We realized that our sources for achieving asymmetric induction using dienophile **28** slowly dried up, so we started to browse the literature for other methods to achieve our goal.

In 2006 the Corey laboratory applied oxazaborolidinium catalyst **C5** in asymmetric Diels-Alder reactions between tiglic aldehyde **7** and several unreactive dienes (Scheme 20).<sup>[61]</sup> If further research is aspired, regarding the development of an asymmetric catalytic Diels-Alder reaction with diene **6**, the Corey procedure is definitely worth a study. An especially attractive feature is that tiglic aldehyde can be used as a substrate which would allow the presented synthetic route (Scheme 19) to be cut short by three steps, as the cycloaddition directly produces aldehyde **8**. Although the three steps to form aldehyde **8** out of Diels-Alder adduct **44** are all high yielding, the sequence can be regarded inefficient from both a step-count as a redox-economy point of view.<sup>[62]</sup>





**Scheme 20.** A promising asymmetric Diels-Alder approach using Corey's oxazaborolidinium catalyst.

The key-step of the TbAd total synthesis is clearly the asymmetric Diels-Alder reaction, which resembles a first asymmetric [4+2] cycloaddition based entry to the halimane bicyclic core structure. This has opened the opportunity for the stereoselective total synthesis of other natural products bearing such scaffold (Figure 7). Relatively straightforward asymmetric syntheses of neopolypodatetraene **A**,<sup>[50]</sup> mamanuthaquinone,<sup>[63]</sup> and a halimane diterpenoid from *Plectranthus ornatus*<sup>[64]</sup> are now within reach. This also holds for natural products with an oxidized halimane structure as present in the agelasimines **A** and **B**<sup>[65]</sup> and in purino-diterpene.<sup>[66]</sup> From a synthetic perspective however, cacospongionolide **F**<sup>[67]</sup> and akaterpin are of significant interest.<sup>[68]</sup> Both compounds possess the halimane skeleton but also additional stereochemical intricacies that are synthetically challenging. Interestingly, akaterpin contains another halimane type moiety within its overall structure which is envisioned to be accessible using a Diels-Alder reaction based on the investigations described within this chapter.

## Asymmetric Total Synthesis of 1-Tuberculosinyl Adenosine

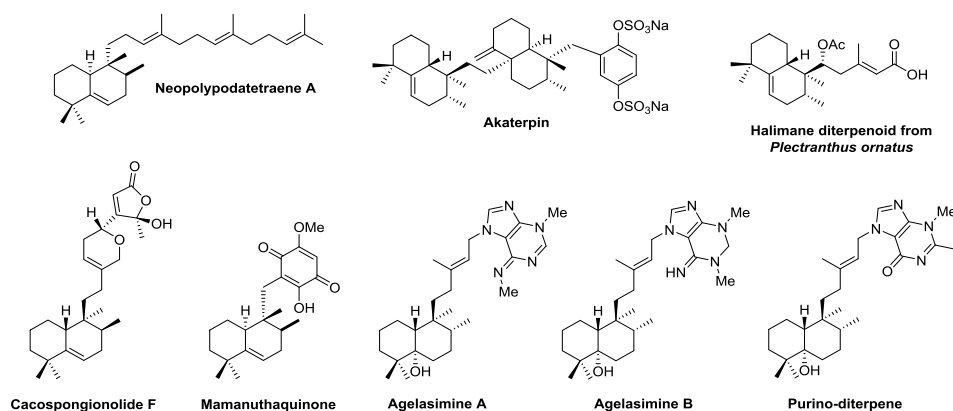


**Figure 7.** Natural products envisioned to be accessible using the developed asymmetric Diels-Alder cycloaddition.

### 4.7 Experimental section

#### General remarks:

All reactions were performed using oven-dried glassware under an atmosphere of nitrogen (unless otherwise specified) by standard Schlenk techniques, using dry solvents. Reaction temperature refers to the temperature of the oil bath/cooling bath. Solvents were taken from an MBraun solvent purification system (SPS-800). All other reagents were purchased from Sigma-Aldrich, Acros, TCI Europe or Fluorochem and used without further purification unless noted otherwise.

TLC analysis was performed on Merck silica gel 60/Kieselguhr F254, 0.25 mm. Compounds were visualized using either Seebach's stain (a mixture of phosphomolybdic acid (25 g), cerium (IV) sulfate (7.5 g), H<sub>2</sub>O (500 mL) and H<sub>2</sub>SO<sub>4</sub> (25 mL)), a KMnO<sub>4</sub> stain (K<sub>2</sub>CO<sub>3</sub> (40 g), KMnO<sub>4</sub> (6 g), H<sub>2</sub>O (600 mL) and 10% NaOH (5 mL)), or elemental iodine.

Flash chromatography was performed using SiliCycle silica gel type SiliaFlash P60 (230 – 400 mesh) as obtained from Screening Devices or with automated column chromatography using a Reveleris flash purification system purchased from Grace Davison Discovery Sciences.

<sup>1</sup>H- and <sup>13</sup>C-NMR spectra were recorded on a Varian AMX400 or a Varian 400-MR (400 and 100.59 MHz, respectively) using CDCl<sub>3</sub> or DMSO-*d*<sub>6</sub> as solvent, unless stated otherwise. Chemical shift values are reported in ppm with the solvent resonance as the internal standard (CDCl<sub>3</sub>: δ 7.26 for <sup>1</sup>H, δ 77.16 for <sup>13</sup>C, MeOH-*d*<sub>4</sub> δ 3.31 for <sup>1</sup>H, δ 49.0 for <sup>13</sup>C). Data are reported as follows: chemical shifts (δ), multiplicity (s = singlet, d = doublet, dd = double doublet, ddd = double double doublet, ddp = double double pentet, td = triple doublet, t = triplet, q = quartet, b = broad, m = multiplet), coupling constants *J* (Hz), and integration.

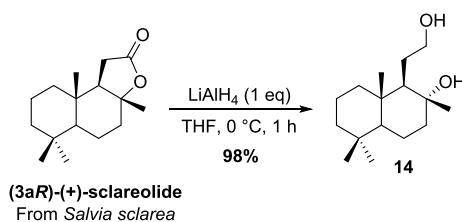
## CHAPTER 4

GC-MS measurements were performed with an HP 6890 series gas chromatography system equipped with a HP 5973 mass sensitive detector. GC measurements were made using a Shimadzu GC 2014 gas chromatograph system bearing an AT5 column (Grace Alltech) and FID detection

Enantiomeric excesses were determined by chiral HPLC analysis using a Shimadzu LC-10ADVP HPLC instrument equipped with a Shimadzu SPD-M10AVP diode-array detector. Integration at three different wavelengths (254, 225, 190 nm) was performed and the reported enantiomeric excess is an average of the three integrations. Retention times (tR) are given in min.

High resolution mass spectra (HRMS) were recorded on a Thermo Scientific LTQ Orbitrap XL. Optical rotations were measured on a Schmidt+Haensch polarimeter (Polartronic MH8) with a 10 cm cell (c given in g/mL) at ambient temperature ( $\pm 23$  °C). Melting points were recorded on a Stuart SMP 11 apparatus.

### Experimental procedures and data:



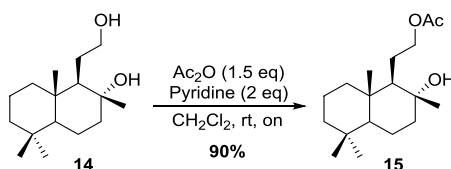
### (1R,2R,8aS)-1-(2-hydroxyethyl)-2,5,5,8a-tetramethyldecahydronaphthalen-2-ol (14):

To a suspension of lithium aluminium hydride (4.55 g, 120 mmol, 1 eq) in dry THF (48 mL) was slowly added a solution of sclareolide (20 g, 80 mmol) in dry THF (200 mL) at 0 °C. After addition the reaction was stirred at rt for 1 h after which TLC analysis (pentane : ether = 1:1) indicated complete conversion of the starting material. The reaction was quenched at 0 °C using EtOAc (40 mL) where after a saturated aqueous solution of Rochelle salt (480 mL) was added. The mixture was stirred for 1 h at rt after which the phases were separated. The aqueous phase was extracted with CH<sub>2</sub>Cl<sub>2</sub> (3x200 mL) and the combined organic phases were washed with 1 M HCl (120 mL), water and brine. The organic phase was dried over MgSO<sub>4</sub>, filtered and concentrated under reduced pressure affording (1R,2R,8aS)-1-(2-hydroxyethyl)-2,5,5,8a-tetramethyldecahydronaphthalen-2-ol **14** (19.9 g, 78 mmol, 98 % yield) as a white solid.

<sup>1</sup>H-NMR (400 MHz, CDCl<sub>3</sub>)  $\delta$  3.74 (br s, 2H), 3.69 (dt,  $J = 10.0, 4.5$  Hz, 1H), 3.39 – 3.33 (m, 1H), 1.83 (dt,  $J = 12.5, 3.0$  Hz, 1H), 1.61 – 1.03 (m, 11H), 1.11 (s, 3H), 0.87 (m, 2H), 0.80 (s, 3H), 0.72 (s, 6H).

$^{13}\text{C}$ -NMR (101 MHz,  $\text{CDCl}_3$ )  $\delta$  72.8, 63.9, 59.3, 56.0, 44.0, 41.9, 39.3, 38.9, 33.4, 33.2, 27.8, 24.5, 21.5, 20.4, 18.4, 15.3.

The analytical data are in agreement with: K. K. W. Kuan, H. P. Pepper, W. M. Bloch, J. H. George, *Org. Lett.* **2012**, *14*, 4710.



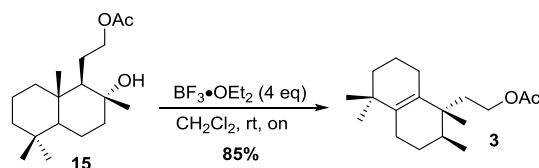
**2-((1*R*,2*R*,8*aS*)-2-hydroxy-2,5,5,8*a*-tetramethyldecahydronaphthalen-1-yl)ethyl acetate (**15**):**

To a solution of **14** (9.0 g, 35.4 mmol) in dry  $\text{CH}_2\text{Cl}_2$  (80 mL) were added acetic anhydride (5.0 mL, 53 mmol, 1.5 eq) and pyridine (5.7 mL, 71 mmol, 2 eq). The reaction mixture was stirred overnight where after it was quenched using an saturated aqueous  $\text{NH}_4\text{Cl}$  solution (100 mL). The phases were separated and the aqueous phase was extracted with  $\text{CH}_2\text{Cl}_2$  (2x100 mL). The combined organic phases were washed with a saturated aqueous  $\text{NH}_4\text{Cl}$  solution, water and brine. The organic phase was dried over  $\text{MgSO}_4$ , filtered and concentrated under reduced pressure. Flash column chromatography employing pentane : ether (1:1) resulted in the isolation of 2-((1*R*,2*R*,8*aS*)-2-hydroxy-2,5,5,8*a*-tetramethyldecahydronaphthalen-1-yl)ethyl acetate. Pyridine impurities were still visible in the  $^1\text{H}$ -NMR spectrum. The oil was therefore dissolved in  $\text{Et}_2\text{O}$  (200 mL) and washed with a saturated aqueous  $\text{CuSO}_4$  solution (3x100 mL) and once with brine (100 mL). The organic phase was dried over  $\text{MgSO}_4$ , filtered and concentrated under reduced pressure affording pure 2-((1*R*,2*R*,8*aS*)-2-hydroxy-2,5,5,8*a*-tetramethyldecahydronaphthalen-1-yl)ethyl acetate **15** (9.4 g, 31.7 mmol, 90% yield) as a slightly yellow, viscous oil.

$^1\text{H}$ -NMR (400 MHz,  $\text{CDCl}_3$ )  $\delta$  4.16 – 4.08 (m, 2H), 2.05 (s, 3H), 1.89 (dt,  $J = 12.0, 3.0$  Hz, 1H), 1.76 – 1.09 (m, 12H), 1.16 (s, 3H) 0.92 (d,  $J = 12.0$  Hz, 2H), 0.87 (s, 3H), 0.79 (s, 6H).

$^{13}\text{C}$ -NMR (101 MHz,  $\text{CDCl}_3$ )  $\delta$  171.1, 73.5, 66.6, 58.0, 56.0, 44.4, 41.9, 39.6, 38.7, 33.4, 33.3, 24.5, 23.9, 21.5, 21.1, 20.5, 18.4, 15.3.

The analytical data are in agreement with: K. K. W. Kuan, H. P. Pepper, W. M. Bloch, J. H. George, *Org. Lett.* **2012**, *14*, 4710



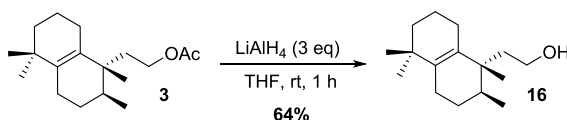
**((1*R*,2*S*)-1,2,5,5-tetramethyl-1,2,3,4,5,6,7,8-octahydronaphthalen-1-yl)ethyl acetate (3):**

To a solution of **15** (9.4 g, 32 mmol) in dry CH<sub>2</sub>Cl<sub>2</sub> (150 mL) was added at rt trifluoroborate ether complex (15.7 ml, 127 mmol, 4 eq). Shortly after addition the solution turned bright yellow. The reaction was stirred overnight where after the reaction was diluted with H<sub>2</sub>O (100 mL) and CH<sub>2</sub>Cl<sub>2</sub> (100 mL). The phases were separated and the aqueous layer was extracted with CH<sub>2</sub>Cl<sub>2</sub> (3x100 mL). The combined organic phases were dried over MgSO<sub>4</sub>, filtered and concentrated under reduced pressure. Flash column chromatography employing pentane : ether (95:5) afforded 2-((1*R*,2*S*)-1,2,5,5-tetramethyl-1,2,3,4,5,6,7,8-octahydronaphthalen-1-yl)ethyl acetate **3** (7.5 g, 27 mmol, 85% yield) as a yellowish oil.

<sup>1</sup>H-NMR (400 MHz, CDCl<sub>3</sub>) δ 4.06 – 4.01 (m, 1H), 3.87 – 3.83 (m, 1H), 2.06 – 1.27 (m, 13H), 2.02 (s, 3H), 0.97 (s, 3H), 0.95 (s, 3H), 0.88 (d, *J* = 7.0 Hz, 3H), 0.84 (s, 3H).

<sup>13</sup>C-NMR (101 MHz, CDCl<sub>3</sub>) δ 171.4, 137.5, 131.9, 62.3, 40.0, 39.9, 34.6, 34.6, 34.5, 29.2, 27.8, 27.3, 26.0, 25.2, 21.3, 21.2, 20.1, 16.3.

The analytical data are in agreement with: K. K. W. Kuan, H. P. Pepper, W. M. Bloch, J. H. George, *Org. Lett.* **2012**, *14*, 4710.



**2-((1*R*,2*S*)-1,2,5,5-tetramethyl-1,2,3,4,5,6,7,8-octahydronaphthalen-1-yl)ethanol (16):**

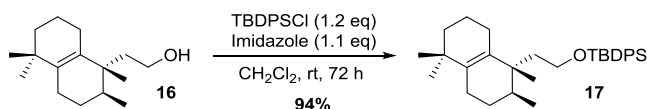
To a suspension of lithium aluminum hydride (1.8 g, 47.4 mmol, 3 eq) in dry THF (15 mL) was slowly added a solution of **3** (4.4 g, 16 mmol) in dry THF (30 mL) at 0 °C. After addition, the reaction was stirred at rt for 1 h after which TLC analysis (pentane : ether = 7:3) indicated complete conversion of the starting material. The reaction was quenched carefully with a saturated aqueous solution of Rochelle salt (100 mL). The mixture was stirred for 1 h at rt after which the phases were separated. The aqueous phase was extracted with Et<sub>2</sub>O (3x75 mL) and the combined organic phases were washed with 1 M HCl (100 mL), water and brine. The organic phase was dried over MgSO<sub>4</sub>, filtered and concentrated under reduced pressure affording 2-((1*R*,2*S*)-1,2,5,5-

tetramethyl-1,2,3,4,5,6,7,8-octahydronaphthalen-1-yl)ethanol **16** (2.4 g, 10 mmol, 64% yield) as a yellowish oil.

<sup>1</sup>H-NMR (400 MHz, CDCl<sub>3</sub>) δ 3.63 – 3.59 (m, 1H), 3.51 – 3.47 (m, 1H), 2.04 – 1.30 (m, 14H), 0.98 (s, 3H), 0.95 (s, 3H), 0.88 (d, *J* = 7.0 Hz, 3H), 0.84 (s, 3H).

<sup>13</sup>C-NMR (150 MHz, CDCl<sub>3</sub>) δ 137.1, 132.6, 60.1, 39.9, 38.9, 34.6, 34.5, 29.1, 27.7, 27.2, 26.1, 25.1, 21.2, 19.9, 16.3.

The analytical data are in agreement with: K. K. W. Kuan, H. P. Pepper, W. M. Bloch, J. H. George, *Org. Lett.* **2012**, *14*, 4710.

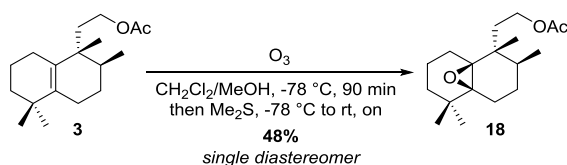


**(1*R*,2*R*,8*aS*)-1-(2-((*tert*-butyldiphenylsilyl)oxy)ethyl)-2,5,5,8*a* tetramethyldecahydronaphthalen-2-ol (**17**):**

To a solution of imidazole (0.25 g, 3.7 mmol, 1.1 eq) in dry CH<sub>2</sub>Cl<sub>2</sub> (10 mL) was added *tert*-butylchlorodiphenylsilane (1.06 mL, 4.06 mmol, 1.2 eq). During addition the mixture became cloudy. The mixture was stirred for 10 min after which **16** (0.8 g, 3.4 mmol) in dry CH<sub>2</sub>Cl<sub>2</sub> (10 mL) was added. The reaction was stirred overnight where after water (20 mL) was added to the reaction mixture. The phases were separated and the aqueous phase was extracted two times with CH<sub>2</sub>Cl<sub>2</sub> (2x30 mL). The organic phases were combined, dried over MgSO<sub>4</sub>, filtered and concentrated under reduced pressure. Flash column chromatography employing pentane : ether (9:1) afforded (1*R*,2*R*,8*aS*)-1-(2-((*tert*-butyldiphenylsilyl)oxy)ethyl)-2,5,5,8*a*-tetramethyldecahydronaphthalen-2-ol **17** (1.5 g, 3.2 mmol, 94% yield) as a very viscous transparent oil.

<sup>1</sup>H-NMR (400 MHz, CDCl<sub>3</sub>) δ 7.71 – 7.65 (m, 4H), 7.45 – 7.34 (m, 6H), 3.68 – 3.57 (m, 1H), 3.45 (tt, *J* = 9.2, 4.3 Hz, 1H), 1.98 – 1.79 (m, 3H), 1.72 (tt, *J* = 9.5, 5.1 Hz, 2H), 1.64 – 1.12 (m, 10H), 1.05 (s, 9H), 0.94 (s, 3H), 0.87 (s, 3H), 0.79 (s, 3H).

<sup>13</sup>C-NMR (150 MHz, CDCl<sub>3</sub>) δ 135.63, 135.60, 129.47, 127.57, 61.11, 39.89, 39.80, 38.76, 34.51, 34.37, 29.10, 27.71, 27.20, 26.92, 26.52, 25.78, 25.03, 21.06, 19.92, 19.15, 16.33, 7.12.

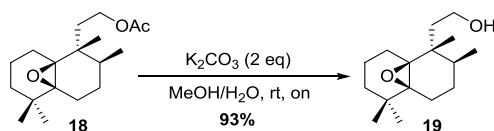


**((1*R*,2*S*,4*aS*,8*aS*)-1,2,5,5-tetramethyloctahydro-4*a*,8*a*-epoxynaphthalen-1-yl)ethyl acetate (**18**):**

To a solution of **3** (1.0 g, 3.6 mmol) in dry CH<sub>2</sub>Cl<sub>2</sub> (40 mL) and MeOH (4 mL), O<sub>3</sub> was bubbled through for 1 h at -78 °C. The reaction mixture turned bright blue. After this time, O<sub>2</sub> was passed through the reaction vessel for 5 min to remove residual O<sub>3</sub>. To the solution was added Me<sub>2</sub>S (2 mL, 27 mmol) at -78 °C where after the reaction was allowed to warm to rt over 3 h. The reaction mixture was concentrated under reduced pressure and purified using flash chromatography (pentane : ether = 9:1). Pure 2-((1*R*,2*S*,4*aS*,8*aS*)-1,2,5,5-tetramethyloctahydro-4*a*,8*a*-epoxynaphthalen-1-yl)ethyl acetate **18** (514 mg, 1.75 mmol, 48% yield) was obtained as a slightly yellow oil.

<sup>1</sup>H-NMR (400 MHz, CDCl<sub>3</sub>) δ 4.23 – 4.13 (m, 1H), 4.13 – 4.02 (m, 1H), 2.05 (d, *J* = 0.9 Hz, 3H), 1.95 – 1.82 (m, 2H), 1.82 – 1.61 (m, 4H), 1.52 – 1.39 (m, 1H), 1.39 – 1.25 (m, 4H), 1.15 – 1.02 (m, 2H), 1.00 (d, *J* = 0.9 Hz, 3H), 0.97 (s, 3H), 0.87 (d, *J* = 0.9 Hz, 3H), 0.84 – 0.79 (m, 3H).

<sup>13</sup>C-NMR (150 MHz, CDCl<sub>3</sub>) δ 170.84, 69.90, 68.35, 61.52, 38.65, 37.99, 35.85, 35.03, 32.82, 27.14, 26.62, 26.27, 24.72, 24.18, 20.98, 17.47, 17.31, 16.29.



**2-((1*R*,2*S*,4*aS*,8*aS*)-1,2,5,5-tetramethyloctahydro-4*a*,8*a*-epoxynaphthalen-1-yl)ethanol (**19**):**

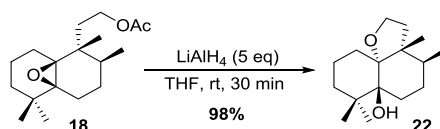
To a solution of **18** (308 mg, 1.05 mmol) in MeOH/H<sub>2</sub>O (2:1, 2 mL) was added potassium carbonate (289 mg, 2.1 mmol, 2 eq). The reaction was stirred for 5 h after which TLC analysis (pentane : ether = 9:1) indicated complete conversion. The reaction mixture was diluted with Et<sub>2</sub>O and the phases were separated. The aqueous phase was extracted three times with Et<sub>2</sub>O after which the combined organic layers were washed with brine. The organic phase was dried over Na<sub>2</sub>SO<sub>4</sub>, filtered and concentrated under reduced pressure to afford 2-((1*R*,2*S*,4*aS*,8*aS*)-1,2,5,5-tetramethyloctahydro-4*a*,8*a*-epoxynaphthalen-1-yl)ethanol **19** (246 mg, 0.98 mmol, 93% yield) as a colorless oil.

<sup>1</sup>H-NMR (400 MHz, CDCl<sub>3</sub>) δ 3.72 (ddd, *J* = 10.4, 9.5, 6.1 Hz, 1H), 3.63 (td, *J* = 10.1, 4.9 Hz, 1H), 1.92 – 1.80 (m, 3H), 1.80 – 1.54 (m, 4H), 1.47 – 1.35 (m, 1H), 1.35 – 1.21

### Asymmetric Total Synthesis of 1-Tuberculosinyl Adenosine

(m, 4H), 1.09 – 0.98 (m, 2H), 0.95 (s, 3H), 0.94 (s, 3H), 0.83 (s, 3H), 0.78 (d,  $J = 6.4$  Hz, 3H).

$^{13}\text{C}$ -NMR (150 MHz,  $\text{CDCl}_3$ )  $\delta$  77.29, 70.16, 68.96, 59.69, 40.39, 38.71, 38.10, 35.17, 32.93, 27.22, 26.76, 26.41, 24.90, 24.30, 17.68, 17.46, 16.50.

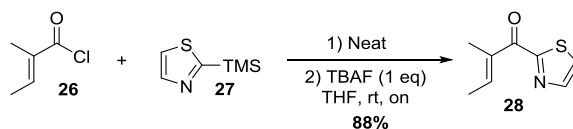


#### (3*aR*,4*S*,6*aS*,10*aR*)-3*a*,4,7,7-tetramethyldecahydro-2*H*-naphtho[8*a*,1-*b*]furan-6*a*-ol (22):

To a suspension of lithium aluminum hydride (32 mg, 0.85 mmol) in dry THF (2 mL) was added a solution of **18** (50 mg, 0.17 mmol) in dry THF (3 mL). The reaction was stirred at rt for 30 min after which TLC (pentane : ether = 8:2) indicated complete conversion. The reaction was carefully quenched with a saturated aqueous  $\text{NH}_4\text{Cl}$  solution. The phases were separated and the aqueous layer was extracted with  $\text{CH}_2\text{Cl}_2$  (2x5 mL). The combined organic phases were dried over  $\text{MgSO}_4$ , filtered and concentrated under reduced pressure affording exclusively (3*aR*,4*S*,6*aS*,10*aR*)-3*a*,4,7,7-tetramethyldecahydro-2*H*-naphtho[8*a*,1-*b*]furan-6*a*-ol **22** (42 mg, 0.17 mmol, 98% yield).

$^1\text{H}$ -NMR (400 MHz,  $\text{CDCl}_3$ )  $\delta$  3.79 (q,  $J = 8.5$  Hz, 1H), 3.68 (ddd,  $J = 10.3, 8.7, 3.3$  Hz, 1H), 1.91 – 1.81 (m, 1H), 1.79 – 1.68 (m, 2H), 1.68 – 1.57 (m, 2H), 1.57 – 1.49 (m, 2H), 1.49 – 1.39 (m, 2H), 1.39 – 1.24 (m, 3H), 1.10 (s, 3H), 0.94 (s, 3H), 0.86 – 0.81 (m, 6H).

$^{13}\text{C}$ -NMR (150 MHz,  $\text{CDCl}_3$ )  $\delta$  70.15, 68.95, 59.75, 40.42, 38.74, 38.12, 35.20, 32.95, 27.25, 26.79, 26.43, 24.91, 24.31, 17.69, 17.48, 16.52.



#### (*E*)-2-methyl-1-(thiazol-2-yl)but-2-en-1-one (28):

To magnetically stirred 2-(trimethylsilyl)thiazole **27** (1.85 mL, 12.7 mmol) was slowly\* (dropwise over 5 min!) added (*E*)-2-methylbut-2-enoyl chloride **26** (1.54 mL, 12.7 mmol). The reaction was stirred overnight after which it was diluted with dry THF (175 mL). To the resulting light yellow solution was added tetrabutylammonium fluoride (TBAF, 12.7 mL, 12.7 mmol, 1 M in THF) which resulted in a color change to bright orange. The reaction was stirred overnight where after it was concentrated under reduced pressure. Flash column chromatography using pentane : ether (96:4) furnished



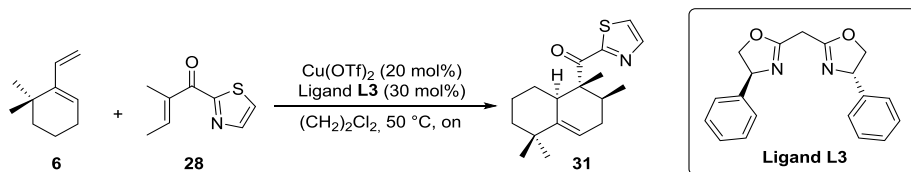
## CHAPTER 4

(*E*)-2-methyl-1-(thiazol-2-yl)but-2-en-1-one **28** (1.86 g, 11.0 mmol, 88% yield) as a light yellow oil.\*\*

\* Approximately one minute after addition of the tigloyl chloride **26** the reaction is exothermic! When performing this reaction on multi-gram scale, cooling with an ice-bath might be necessary!

\*\* Thiazolium tiglate **28** is unstable at room temperature and decomposes over time. Even at 4 °C the product is not entirely stable (the oil darkens significantly over time). Therefore **28** can best be stored at -20 °C at which thiazolium tiglate **28** is a crystalline solid.

<sup>1</sup>H-NMR (400 MHz, CDCl<sub>3</sub>) 7.96 (d, *J* = 3.1 Hz, 1H), 7.77 – 7.69 (m, 1H), 7.60 (d, *J* = 3.1 Hz, 1H), 2.00 – 1.98 (m, 6H).

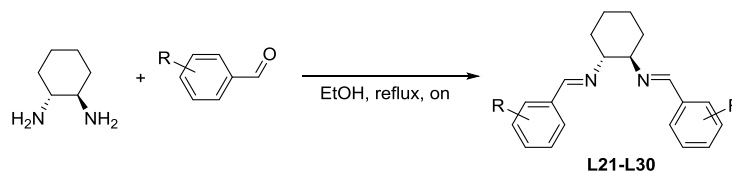


### ((1*R*,2*S*,8*aR*)-1,2,5,5-tetramethyl-1,2,3,5,6,7,8,8*a*-octahydronaphthalen-1-yl)(thiazol-2-yl)methanone (**31**):

To a solution of **L3** (30 mol%) in dry dichloroethane (1 mL) was added Cu(OTf)<sub>2</sub> (20 mol%). The copper complex was allowed to form over 3 h. To the *in situ* generated copper catalyst were added 6,6-dimethyl-1-vinylcyclohex-1-ene **6** (10 mg, 0.073 mmol) and (*E*)-2-methyl-1-(thiazol-2-yl)but-2-en-1-one (18.4 mg, 0.11 mmol) in a total volume of 1 mL dry dichloroethane. The reaction was stirred at 50 °C overnight where after the reaction mixture was concentrated and purified by flash column chromatography to afford ((1*R*,2*S*,8*aR*)-1,2,5,5-tetramethyl-1,2,3,5,6,7,8,8*a*-octahydronaphthalen-1-yl)(thiazol-2-yl)methanone **31** as a diastereomeric mixture of 2:1. The absolute stereochemistry remained unknown.

<sup>1</sup>H-NMR (400 MHz, CDCl<sub>3</sub>) δ 7.95 (d, *J* = 3.1 Hz, 1H), 7.56 (d, *J* = 3.3 Hz, 1H), 5.56 (dt, *J* = 5.8, 2.2 Hz, 1H), 3.86 – 3.72 (m, 1H), 3.15 – 2.94 (m, 2H), 2.11 (dt, *J* = 18.1, 5.6 Hz, 1H), 1.96 (td, *J* = 5.5, 2.1 Hz, 1H), 1.82 – 1.76 (m, 1H), 1.46 – 1.35 (m, 2H), 1.32 – 1.13 (m, 2H), 1.11 (s, 3H), 1.08 (s, 3H), 1.02 (s, 3H), 0.68 (d, *J* = 6.7 Hz, 3H).

<sup>13</sup>C-NMR (150 MHz, CDCl<sub>3</sub>) δ 199.27, 167.74, 145.00, 144.38, 125.41, 116.50, 55.60, 40.76, 36.25, 34.36, 31.47, 29.77, 29.40, 28.65, 21.78, 16.39, 9.72.

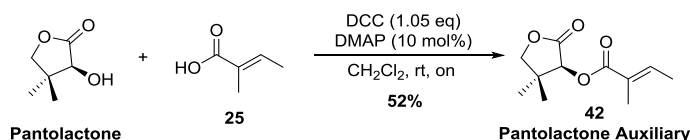


**General procedure for the synthesis of the diimine chiral ligands L21-L30:**

To a solution of (1*S*,2*S*)-cyclohexane-1,2-diamine (75 mg, 0.66 mmol) in EtOH (2 mL) was added a solution/suspension of aromatic aldehyde (2 eq) in EtOH (2-3 mL). The reactions were refluxed overnight. The resulting diimines were crystallized from various mixtures of ethylacetate:pentane, ethanol, or methanol.

The bisimine ligands **L21-L30** prepared and obtained in accordance to:

- a) Z. Li, K. R. Cosner, E. N. Jacobsen, *J. Am. Chem. Soc.* **1993**, *115*, 5326. b) Z. Li, R. W. Quan, E. N. Jacobsen, *J. Am. Chem. Soc.* **1995**, *117*, 5889.

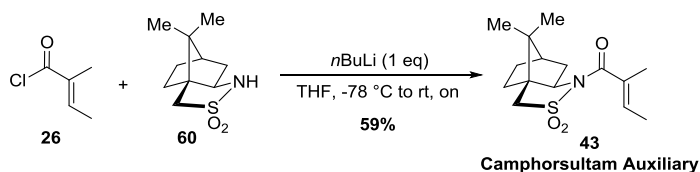


**(*S*)-4,4-dimethyl-2-oxotetrahydrofuran-3-yl (*E*)-2-methylbut-2-enoate (42):**

To a cooled solution (-10 °C) of (*E*)-2-methylbut-2-enoic acid **25** (10 g, 100 mmol), pantolactone (14.3 g, 110 mmol, 1.1 eq), and DCC (21.7 g, 105 mmol, 1.05 eq) in dry CH<sub>2</sub>Cl<sub>2</sub> (250 mL), *N,N*-dimethylpyridin-4-amine (1.22 g, 10 mmol, 10 mol%) in dry CH<sub>2</sub>Cl<sub>2</sub> (40 mL), was added portionwise. The solution was allowed to warm to rt and was stirred overnight. The resulting suspension was filtered through a path of Celite and the residue was washed with DCM. The filtrate was washed with two portions of a saturated aqueous solution of NaHCO<sub>3</sub> (500 mL) and once with brine (200 mL). The organic phase was dried over Na<sub>2</sub>SO<sub>4</sub>, concentrated under reduced pressure and purified performing flash chromatography (eluent 35% ether in pentane) to isolate (*R,E*)-4,4-dimethyl-2-oxotetrahydrofuran-3-yl 2-methylbut-2-enoate **42** (11 g, 52 mmol, 52% yield) as a slightly yellow oil.

<sup>1</sup>H-NMR (400 MHz, CDCl<sub>3</sub>) δ 7.01 – 6.91 (m, 1H), 5.40 (s, 1H), 4.02 (s, 2H), 1.84 (s, 3H), 1.79 (d, *J* = 7.0 Hz, 3H), 1.18 (s, 3H), 1.10 (s, 3H).

<sup>13</sup>C-NMR (150 MHz, CDCl<sub>3</sub>) δ 172.75, 166.55, 139.66, 127.50, 76.22, 74.99, 40.41, 23.05, 19.99, 14.58, 12.09.

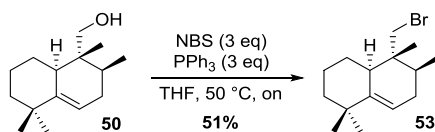


**(*E*)-1-((3*aS*,6*R*,7*aR*)-8,8-dimethyl-2,2-dioxido-tetrahydro-3*H*-3*a*,6-methanobenzo[*c*]isothiazol-1(4*H*)-yl)-2-methylbut-2-en-1-one (43):**

To a  $-78\text{ }^{\circ}\text{C}$  cooled solution of (3*aS*,6*R*,7*aR*)-8,8-dimethylhexahydro-1*H*-3*a*,6-methanobenzo[*c*]isothiazole 2,2-dioxide **60** (490 mg, 2.28 mmol) in dry THF (10 mL) was added *n*BuLi (1.1 mL, 2.5 M solution in hexane, 2.75 mmol, 1.2 eq). The reaction was allowed to warm-up to  $0\text{ }^{\circ}\text{C}$  and was stirred at this temperature for 30 min where after the mixture was re-cooled to  $-78\text{ }^{\circ}\text{C}$  and (*E*)-2-methylbut-2-enoyl chloride **26** (1.51 mL, 13.8 mmol, 6 eq) was added. The reaction was allowed to warm up to room temperature and was stirred overnight where after it was carefully quenched using aqueous HCl (30 mL, 1 M). After phase separation, the aqueous layer was extracted with ether. The combined organic layers were washed with a saturated aqueous solution of NaHCO<sub>3</sub>, dried using Na<sub>2</sub>SO<sub>4</sub>, filtered and concentrated under reduced pressure. The resulting yellow oil was cooled down to  $4\text{ }^{\circ}\text{C}$  which resulted in crystallization of the product. The residual oil was removed where after the crystals were washed with cold ( $-20\text{ }^{\circ}\text{C}$ ) ether until the ether layer stayed clear and transparent. (*E*)-1-((3*aS*,6*R*,7*aR*)-8,8-dimethyl-2,2-dioxido-hexahydro-1*H*-3*a*,6-methanobenzo[*c*]isothiazol-1-yl)-2-methylbut-2-en-1-one **43** (400 mg, 1.35 mmol, 59% yield) was obtained as a white solid.

<sup>1</sup>H-NMR (400 MHz, CDCl<sub>3</sub>)  $\delta$  6.37 (dq,  $J = 8.4, 6.9, 5.5, 1.5$  Hz, 1H), 4.05 (dd,  $J = 7.7, 4.5$  Hz, 1H), 3.45 (q,  $J = 27.7, 13.4$  Hz, 2H), 2.03 (dd,  $J = 13.4, 7.7$  Hz, 1H), 1.97 – 1.87 (m, 4H), 1.87 (s, 3H), 1.82 (d,  $J = 6.9$  Hz, 3H), 1.47 – 1.32 (m, 2H), 1.23 (s, 3H), 0.99 (s, 3H).

<sup>13</sup>C-NMR (150 MHz, CDCl<sub>3</sub>)  $\delta$  139.99, 137.70, 65.53, 53.69, 48.00, 45.36, 38.37, 33.35, 26.68, 21.45, 20.05, 14.74, 14.23, 12.81, 11.82.



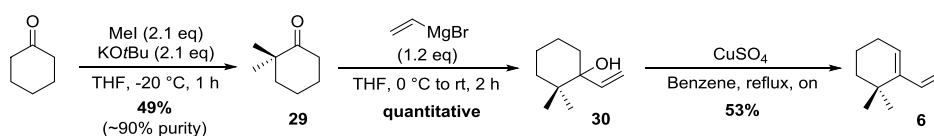
**(4*aR*,5*R*,6*S*)-5-(bromomethyl)-1,1,5,6-tetramethyl-1,2,3,4,4*a*,5,6,7-octahydronaphthalene (53):**

To a solution of 1-bromopyrrolidine-2,5-dione (592 mg, 3.33 mmol) in dry THF (15 mL) was added slowly a solution of triphenylphosphine (873 mg, 3.33 mmol) in dry THF (15 mL). The reaction is exothermic, and upon addition of the PPh<sub>3</sub> a bright yellow solution formed which quickly turned into a suspension by precipitation of a white

solid. This mixture was allowed to stir for 15 min resulting in an orange color. To the suspension was added a solution of ((1*R*,2*S*,8*aR*)-1,2,5,5-tetramethyl-1,2,3,5,6,7,8,8a-octahydronaphthalen-1-yl)methanol (247 mg, 1.11 mmol) in dry THF (7.5 mL). The reaction was stirred over the weekend at 50 °C. GC-MS indicated complete conversion. The reaction mixture was diluted with pentane which resulted in the precipitation of PPh<sub>3</sub>. After gravitational filtration, more PPh<sub>3</sub> crystallized so another filtration was performed. The elute was concentrated under reduced pressure which resulted in an oil. The oil was diluted with pentane which resulted, again, in the precipitation of PPh<sub>3</sub>. The suspension was flushed over a SiO<sub>2</sub> column resulting in a slightly yellow oil. Flash column chromatography employing pentane as the eluent afforded (4*aR*,5*R*,6*S*)-5-(bromomethyl)-1,1,5,6-tetramethyl-1,2,3,4,4*a*,5,6,7-octahydronaphthalene **53** (280 mg, 0.98 mmol, 59% yield) as a colorless oil.

<sup>1</sup>H-NMR (400 MHz, CDCl<sub>3</sub>) δ 5.45 (dt, *J* = 5.7, 2.0 Hz, 1H), 3.53 (d, *J* = 10.5 Hz, 1H), 3.35 (d, *J* = 10.5 Hz, 1H), 2.50 – 2.44 (m, 1H), 2.16 – 2.02 (m, 1H), 1.96 – 1.83 (m, 1H), 1.79 – 1.66 (m, 2H), 1.66 – 1.55 (m, 2H), 1.41 (dtd, *J* = 13.0, 3.3, 1.8 Hz, 1H), 1.32 – 1.12 (m, 2H), 1.07 (s, 3H), 1.03 (s, 3H), 0.84 (d, *J* = 6.3 Hz, 3H), 0.73 (s, 3H).

<sup>13</sup>C-NMR (150 MHz, CDCl<sub>3</sub>) δ 145.67, 116.11, 77.33, 42.75, 40.92, 39.47, 38.72, 36.28, 33.24, 31.29, 29.86, 29.08, 27.32, 22.07, 14.69, 13.52.



#### 6,6-dimethyl-1-vinylcyclohex-1-ene (**6**):

To a solution of cyclohexanone (9.91 ml, 96 mmol) and iodomethane (12.5 ml, 201 mmol) in dry THF (500 mL), cooled to -20 °C, was added dropwise, using a dropping funnel, a solution of KOtBu (22.6 g, 201 mmol) in dry THF (125 mL). Upon addition, a white precipitate, formed and the reaction turned yellow. After addition, the mixture was stirred for 60 min at this temperature after which GC-MS indicated complete conversion of the cyclohexanone. The reaction mixture was quenched with an aqueous saturated NH<sub>4</sub>Cl solution (200 mL). Quenching resulted in significant, but not complete, disappearance of the white precipitate, which was completely removed by filtration of the quenched mixture over a glass filter. The phases were separated and the aqueous phase was extracted twice with Et<sub>2</sub>O. The combined organic layers were dried over Na<sub>2</sub>SO<sub>4</sub>, filtered, and concentrated under reduced pressure. Flash column chromatography of the resulting oil using pentane : ether (4:1) afforded 2,2-dimethylcyclohexanone **29** (18.3 g, 145 mmol, 49% yield) ~90% pure. In order to obtain the desired 90% purity, the individual column fractions were analyzed with GC-MS.

## CHAPTER 4

*Note: The reaction was performed 3x on this scale. The extractions were performed on the combined reaction mixtures. The yield represents that of the combined reactions.*

To a stirred solution of vinylmagnesium bromide (174 mL, 174 mmol) at 0 °C was added dropwise a solution of 2,2-dimethylcyclohexanone **29** (18.3 g, 145 mmol) in dry THF (50 mL) over 30 min. The reaction was allowed to warm up to room temperature and stirred for 2 h. The reaction mixture was carefully quenched with an aqueous saturated NH<sub>4</sub>Cl solution (75 mL). After phase separation the aqueous layer was extracted with Et<sub>2</sub>O (3x25 mL). The organic layers were combined and dried with sodium sulfate, filtered and concentrated under reduced pressure. The resulting yellowish oil (27.3 g, >100% yield) was used in the subsequent dehydration reaction.

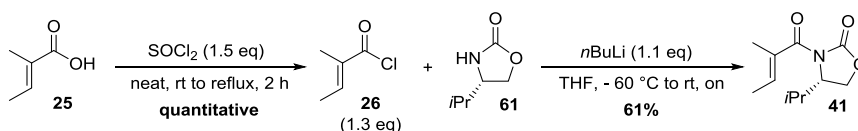
Crude alcohol **30** was dissolved in benzene (300 mL). To the stirred solution, anhydrous CuSO<sub>4</sub> (50 g, 313 mmol, 2.2 eq) was added. The suspension was refluxed under Dean-Stark conditions overnight. The reaction mixture was cooled to rt and thereafter filtered over Celite and flushed with pentane. The filtrate was concentrated under reduced pressure and the residual oil was subjected to flash column chromatography employing pentane as the eluent. Pure 6,6-dimethyl-1-vinylcyclohex-1-ene **6** (10.5 g, 77 mmol, 53% yield) was obtained as a colorless oil.

<sup>1</sup>H-NMR (400 MHz, CDCl<sub>3</sub>) δ 6.32 (dd, *J* = 17.2, 10.9 Hz, 1H), 5.78 (t, *J* = 3.9 Hz, 1H), 5.28 (d, *J* = 17.2 Hz, 1H), 4.92 (d, *J* = 10.9 Hz, 1H), 2.05 (q, *J* = 5.7 Hz, 2H), 1.61 (dt, *J* = 12.0, 5.9 Hz, 2H), 1.53 – 1.46 (m, 2H), 1.07 (s, 6H).

<sup>13</sup>C-NMR (101 MHz, CDCl<sub>3</sub>) δ 144.74, 137.20, 123.20, 112.82, 39.55, 33.33, 28.50, 26.33, 19.30.

*Note: Diene 6 is rather volatile and therefore concentration, after column chromatography, was performed very carefully. As a result the NMR spectra of diene 6 contain benzene and traces of pentane.*

The analytical data are in agreement with: a) S. Knapp, S. Sharma, *J. Org. Chem.* **1985**, 50, 4996–4998. b) S. P. Tanis, Y. M. Abdallah, *Synth. Commun.* **1986**, 16, 251–259.



### (*E*)-2-methylbut-2-enoyl chloride (**26**):

To vigorously stirred thionyl chloride (27.2 ml, 375 mmol) in a 250 mL 3-neck round bottom flask (**open flask!**) was added portion wise (*E*)-2-methylbut-2-enoic acid **25** (25 g, 250 mmol). Each portion was added after significant gas evolution (HCl, SO<sub>2</sub>)

ceased. After addition of all the acid, the reaction mixture (open flask!) was heated to 40 °C until no gas evolution was observed. The 3-neck round bottom flask was equipped with a reflux condenser, and the reaction was refluxed for 1 h. After this time no gas evolution was observed. The excess of thionyl chloride was removed by concentration under reduced pressure. The product was subsequently distilled in the rotavapor to afford (*E*)-2-methylbut-2-enoyl chloride **26** (29.6 g, 250 mmol, quantitative) as a clear liquid.

*Note: The reaction is exothermic with vigorous evolution of HCl/SO<sub>2</sub> gas.*

**(*S,E*)-4-isopropyl-3-(2-methylbut-2-enoyl)oxazolidin-2-one (41):**

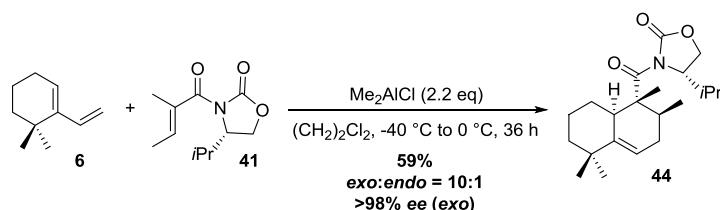
To a cooled solution (-60 °C), of (*S*)-4-isopropylloxazolidin-2-one **61** (25.0 g, 194 mmol) in dry THF (500 mL) was added dropwise *n*-butyllithium (133 ml, 213 mmol) by the aid of a dropping funnel. Upon addition, the reaction mixture became turbid. After addition, the reaction was allowed to warm-up to 0 °C and was stirred at this temperature for 30 min where after the mixture was re-cooled to -60 °C and (*E*)-2-methylbut-2-enoyl chloride **26** (29.6 g, 250 mmol) was added dropwise by the aid of a syringe pump over 20 min. Upon addition the reaction mixture turned yellow/orange. After addition of acid chloride **26** the reaction was allowed to warm up to rt, and the reaction became transparent. The reaction was stirred overnight where after it was carefully quenched using aqueous HCl (1 M). After phase separation, the aqueous layer was extracted with ether. The combined organic layers were washed with a saturated aqueous solution of NaHCO<sub>3</sub> and dried using Na<sub>2</sub>SO<sub>4</sub>, filtered and concentrated under reduced pressure. A solid formed which was dissolved in CH<sub>2</sub>Cl<sub>2</sub> (15 mL) and subjected to flash column chromatography employing pentane : ether (3:2) as the eluent to afford pure (*S,E*)-4-isopropyl-3-(2-methylbut-2-enoyl)oxazolidin-2-one **41** (25 g, 118 mmol, 61% yield) as a waxy solid.

<sup>1</sup>H-NMR (400 MHz, CDCl<sub>3</sub>) δ 6.20 (q, *J* = 7.0 Hz, 1H), 4.51 (dt, *J* = 9.0, 4.9 Hz, 1H), 4.31 (t, *J* = 8.9 Hz, 1H), 4.17 (dd, *J* = 8.9, 5.5 Hz, 1H), 2.36 (dq, *J* = 13.8, 6.9 Hz, 1H), 1.90 (s, 3H), 1.80 (d, *J* = 7.0 Hz, 3H), 0.91 (t, *J* = 6.8 Hz, 6H).

<sup>13</sup>C-NMR (101 MHz, CDCl<sub>3</sub>) δ 171.92, 153.80, 134.69, 131.92, 63.52, 58.39, 28.36, 17.97, 15.14, 14.20, 13.48.

HRMS (ESI+): Calculated mass [M+Na]<sup>+</sup> C<sub>11</sub>H<sub>17</sub>NO<sub>3</sub>Na<sup>+</sup> = 234.1101; found: 234.1101.

The analytical data are in agreement with: O. Miyata, T. Shinada, I. Ninomiya, T. Naito, *Tetrahedron*, **1997**, *53*, 2421-2438.



**(S)-4-isopropyl-3-((1R,2S,8aR)-1,2,5,5-tetramethyl-1,2,3,5,6,7,8,8a-octahydronaphthalene-1-carbonyl)oxazolidin-2-one (**44**):**

To a stirred solution of dienophile **41** (9.13 g, 43.2 mmol, 1.1 eq) in dry  $(\text{CH}_2)_2\text{Cl}_2$  (250 mL) at  $-40\text{ }^\circ\text{C}$  under  $\text{N}_2$  was added  $\text{Me}_2\text{AlCl}$  (86.5 mL, 1 M in hexanes, 86.5 mmol, 2.2 eq) over 15 min, by the aid of a dropping funnel. The yellow reaction mixture was stirred for 20 min, and diene **6** (5.35 g, 39.3 mmol) in dry  $(\text{CH}_2)_2\text{Cl}_2$  (90 mL) was added dropwise over 15 min by the aid of a dropping funnel. The reaction was then allowed to warm to rt and was stirred for 36 h at this temperature. GC-MS indicated complete conversion of the diene.

The reaction mixture was cooled to  $0\text{ }^\circ\text{C}$  and carefully quenched by dropwise addition of aqueous 1 M HCl (50 mL). After phase separation, the aqueous layer was extracted with  $\text{CH}_2\text{Cl}_2$  (3x20 mL). The combined organic layers were dried over  $\text{Na}_2\text{SO}_4$ , filtered and concentrated under reduced pressure. Flash column chromatography with pentane : ether (6:1) provided (S)-4-isopropyl-3-((1R,2S,8aR)-1,2,5,5-tetramethyl-1,2,3,5,6,7,8,8a-octahydronaphthalene-1-carbonyl)oxazolidin-2-one **44** as a white appearing crystalline solid (8.0 g, 19.6 mmol, 59% yield,  $\text{exo:endo} = 10:1$ ).

*Note: the reaction temperature was monitored inside the flask. Excessively low temperatures lead to crystallization of the dienophile.*

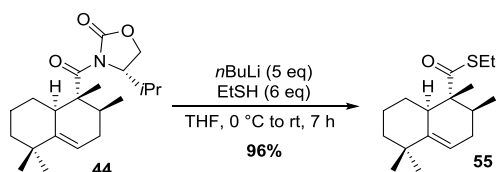
$^1\text{H-NMR}$  (400 MHz,  $\text{CDCl}_3$ )  $\delta$  5.47 (d,  $J = 5.7$  Hz, 1H), 4.54 (d,  $J = 8.2$  Hz, 1H), 4.33 – 4.13 (m, 2H), 3.34 (d,  $J = 12.8$  Hz, 1H), 3.15 (tt,  $J = 12.5, 6.5$  Hz, 1H), 2.39 – 2.30 (m, 1H), 1.95 (dt,  $J = 17.5, 5.5$  Hz, 1H), 1.79 – 1.63 (m, 2H), 1.54 (tt,  $J = 7.0, 3.1$  Hz, 1H), 1.43 – 1.29 (m, 2H), 1.28 – 1.13 (m, 2H), 1.06 (s, 3H), 1.03 (s, 3H), 1.01 (s, 3H), 0.90 (t,  $J = 6.3$  Hz, 6H), 0.78 (d,  $J = 6.8$  Hz, 3H).

$^{13}\text{C-NMR}$  (101 MHz,  $\text{CDCl}_3$ )  $\delta$  178.00, 153.03, 144.80, 116.12, 62.88, 61.16, 53.54, 40.94, 37.57, 36.39, 31.25, 29.71, 29.53, 28.93, 28.31, 22.21, 18.54, 16.48, 14.53, 12.43.

HRMS (ESI+): Calculated mass  $[\text{M}+\text{H}]^+$   $\text{C}_{21}\text{H}_{34}\text{NO}_3^+$  = 348.2533; found: 348.2536. Calculated mass  $[\text{M}+\text{Na}]^+$   $\text{C}_{21}\text{H}_{33}\text{NO}_3\text{Na}^+$  = 370.2353; found: 370.2355.

Melting point:  $96\text{ }^\circ\text{C}$

Optical rotation:  $[\alpha]_D^{23} = +57.4$  ( $c = 0.0135$ ,  $\text{CHCl}_3$ ).



**(1*R*,2*S*,8*aR*)-S-ethyl-1,2,5,5-tetramethyl-1,2,3,5,6,7,8,8*a*-octahydronaphthalene-1-carbothioate (**55**):**

To a solution of ethanethiol (8.3 mL, 115 mmol, 5.9 eq) in dry THF (200 mL), cooled to  $0\text{ }^\circ\text{C}$ , was added dropwise *n*-butyllithium (57.6 mL, 92 mmol, 4.7 eq). Upon addition, a white precipitate formed. After addition, the milk white, now viscous, suspension was allowed to warm to rt. Diels-Alder adduct **44** (8.0 g, 19.6 mmol) in dry THF (50 mL) was added and the reaction was stirred for 7 h. Full conversion was observed by TLC and GC-MS analysis. The reaction was diluted with  $\text{Et}_2\text{O}$  and quenched by addition of a saturated aqueous  $\text{NH}_4\text{Cl}$ . The white precipitate dissolved. The phases were separated, and the aqueous phase was extracted with  $\text{Et}_2\text{O}$ . The combined organic phases were dried over  $\text{MgSO}_4$ , filtered and concentrated under reduced pressure to afford a yellow oil. Upon standing, the oxazolidinone chiral auxiliary crystallized. Pentane was added to wash the crystals, which became transparent in color, and the organic layer turned yellowish. The suspension was cooled to  $-20\text{ }^\circ\text{C}$  where after the cold suspension was filtered over a sintered glass filter (pore size 3). The residue was rinsed with cold pentane ( $-20\text{ }^\circ\text{C}$ ) to provide the chiral auxiliary as needle shaped transparent crystals (2.2 g). The filtrate was concentrated under reduced pressure to afford crude (1*R*,2*S*,8*aR*)-S-ethyl 1,2,5,5-tetramethyl-1,2,3,5,6,7,8,8*a*-octahydronaphthalene-1-carbothioate **55** (7.2 g, 25.7 mmol >100% yield) as a yellowish oil. The product was considered sufficiently pure to be used in the next step.

Alternatively flash column chromatography can be performed: The oil/crystal mixture was dissolved in a minimum amount of ether and loaded on the column. Elution using pentane : ether (98:2) as the eluent afforded pure (1*R*,2*S*,8*aR*)-S-ethyl 1,2,5,5-tetramethyl-1,2,3,5,6,7,8,8*a*-octahydronaphthalene-1-carbothioate **55** (5.06 g, 18.0 mmol, 96% yield) as a yellowish oil. (*The 96% yield was obtained for a reaction starting from 6.5 g of Diels-Alder adduct 3*).

$^1\text{H-NMR}$  (400 MHz,  $\text{CDCl}_3$ )  $\delta$  5.46 (d,  $J = 5.3$  Hz, 1H), 2.88 (q,  $J = 7.4$  Hz, 2H), 2.79 (d,  $J = 12.9$  Hz, 1H), 2.02 – 1.86 (m, 2H), 1.75 (ddt,  $J = 13.4, 11.5, 3.6$  Hz, 1H), 1.53 – 1.46 (m, 3H), 1.44 – 1.36 (m, 1H), 1.25 (t,  $J = 7.4$  Hz, 3H), 1.21 – 1.10 (m, 2H), 1.08 (s, 3H), 1.05 (s, 3H), 0.98 (s, 3H), 0.79 (d,  $J = 6.5$  Hz, 3H).

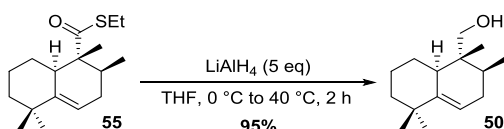


## CHAPTER 4

$^{13}\text{C}$ -NMR (101 MHz,  $\text{CDCl}_3$ )  $\delta$  207.85, 144.94, 116.00, 56.71, 43.49, 40.58, 36.77, 36.04, 31.41, 29.68, 29.44, 28.22, 23.14, 21.68, 15.87, 14.83, 9.61.

HRMS (ESI+): Calculated mass  $[\text{M}+\text{H}]^+$   $\text{C}_{17}\text{H}_{29}\text{OS}^+$  = 281.1934; found: 281.1932.

Optical rotation:  $[\alpha]_{\text{D}}^{23} = +8.7$  ( $c = 0.0184$ ,  $\text{CHCl}_3$ ).



### **((1*R*,2*S*,8*aR*)-1,2,5,5-tetramethyl-1,2,3,5,6,7,8,8a-octahydronaphthalen-1-yl)methanol (50):**

To a cooled (0 °C) solution of crude thioester **55** (7.2 g, 25.7 mmol) in dry THF (150 mL) was added portionwise lithium aluminum hydride (4.9 g, 128 mmol, 5 eq). After addition, the reaction was allowed to warm-up to rt where after the reaction was heated to 40 °C and stirred for 2 h. GC-MS and TLC analysis indicated complete conversion of the starting material. The reaction mixture was cooled to 0 °C, diluted with ether and carefully quenched using a saturated aqueous Rochelle salt. After addition, the quenched reaction mixture was stirred for 30 min. After phase separation, the aqueous layer was extracted three times with ether where after the combined organic layers were washed brine. The organic phase was then dried over  $\text{MgSO}_4$ , filtered and concentrated under reduced pressure to yield ((1*R*,2*S*,8*aR*)-1,2,5,5-tetramethyl-1,2,3,5,6,7,8,8a-octahydronaphthalen-1-yl)methanol **50** (6.2 g, 30 mmol, quantitative yield) as yellow oil. The material was deemed pure enough to be used in the next step without purification.

Alternatively flash column chromatography can be performed: purification of the obtained yellow oil, using pentane : ether (9:1) as the eluent, afforded pure ((1*R*,2*S*,8*aR*)-1,2,5,5-tetramethyl-1,2,3,5,6,7,8,8a-octahydronaphthalen-1-yl)methanol **50** (4.7 g, 21.1 mmol, 91% yield) as a yellowish oil. (*The 91% yield reflects that obtained over the past 2 steps, starting from Diels-Alder adduct 44. With 96% isolated yield for the oxazolidinone cleavage this corresponds to 95% isolated yield for the reduction of thioester 55 to alcohol 50.*)

Chiral HPLC analysis of alcohol **50** showed an enantiomeric excess exceeding 98% for the *exo* isomer. Also the *endo* isomer proved to be enantiomerically enriched, possessing an enantiomeric excess of ~60%.

$^1\text{H}$ -NMR (400 MHz,  $\text{CDCl}_3$ )  $\delta$  5.43 (d,  $J = 5.2$  Hz, 1H), 3.48 (d,  $J = 11.4$  Hz, 1H), 3.39 (d,  $J = 11.3$  Hz, 1H), 2.36 (d,  $J = 12.9$  Hz, 1H), 1.91 – 1.81 (m, 1H), 1.81 – 1.71 (m,

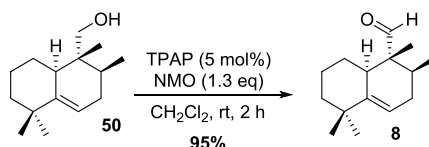
2H), 1.70 – 1.63 (m, 2H), 1.61 – 1.51 (m, 2H), 1.38 (s, 1H), 1.28 – 1.14 (m, 2H), 1.05 (s, 3H), 1.00 (s, 3H), 0.86 (d,  $J = 6.5$  Hz, 3H), 0.51 (s, 3H).

$^{13}\text{C}$ -NMR (101 MHz,  $\text{CDCl}_3$ )  $\delta$  146.12, 116.11, 65.78, 41.07, 39.33, 38.05, 36.27, 31.93, 31.33, 29.86, 28.86, 27.74, 22.26, 15.09, 11.63.

HRMS (ESI+): Calculated mass  $[\text{M}+\text{H}]^+ \text{C}_{15}\text{H}_{27}\text{O}^+ = 223.2056$ ; found: 223.2059.

Chiral HPLC analysis on a Chiracel AD-H column, *n*-Heptane : *i*-PrOH = 98 : 2, 40 °C, flow = 0.5 mL/min, UV detection at 190 nm, 210 nm and 254 nm, retention times (min): 15.7 (*endo* minor), 15.1 (*endo* major), 17.7 (*exo* major), and 21.1 (*exo* minor, not detected for chiral alcohol **50**).

The analytical data are in agreement with: a) J. E. Spangler, C. A. Carson, E. J. Sorenson, *Chem. Sci.* **2010**, *1*, 202-205. b) N. Mangel, F. M. Mann, M. L. Hillwig, R. J. Peters, B. B. Snider, *Org. Lett.* **2010**, *12*, 2626-2629.



**(1*R*,2*S*,8*aR*)-1,2,5,5-tetramethyl-1,2,3,5,6,7,8,8*a*-octahydronaphthalene-1-carbaldehyde (**8**):**

To a solution of alcohol **50** (4.7 g, 21.1 mmol) in dry  $\text{CH}_2\text{Cl}_2$  (80 mL) were added TPAP (371 mg, 1.06 mmol, 5 mol%), 4-methylmorpholine-*N*-4-oxide (or its monohydrate) (3.22 g, 27.5 mmol, 1.3 eq) and 3 Å molecular sieves. The reaction was stirred at rt for 2 h after which TLC and GC-MS analysis indicated complete conversion of the starting material. The reaction mixture was diluted using pentane which resulted in precipitation of the TPAP. The mixture was filtered over Celite to remove the TPAP. Removal of NMO and reduced analogue were removed by flash column chromatography using pentane : ether (95:5) as the eluent to afford pure (1*R*,2*S*,8*aR*)-1,2,5,5-tetramethyl-1,2,3,5,6,7,8,8*a*-octahydronaphthalene-1-carbaldehyde **8** (4.43 g, 20.1 mmol, 95% yield) as a yellowish oil which crystallized upon standing.

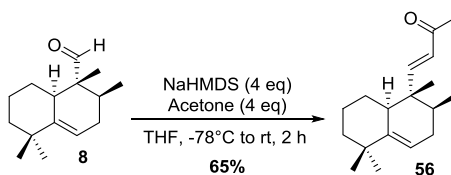
$^1\text{H}$ -NMR (400 MHz,  $\text{CDCl}_3$ )  $\delta$  9.38 (s, 1H), 5.52 – 5.47 (m, 1H), 2.50 (d,  $J = 13.1$  Hz, 1H), 2.00 – 1.91 (m, 1H), 1.90 – 1.80 (m, 1H), 1.80 – 1.69 (m, 1H), 1.57 – 1.49 (m, 2H), 1.45 – 1.37 (m, 1H), 1.36 – 1.28 (m, 1H), 1.27 – 1.14 (m, 2H), 1.08 (s, 3H), 1.04 (s, 3H), 0.80 (s, 3H), 0.78 (d,  $J = 6.5$  Hz, 3H).

$^{13}\text{C}$ -NMR (101 MHz,  $\text{CDCl}_3$ )  $\delta$  207.16, 143.92, 116.56, 52.26, 40.61, 38.15, 36.28, 32.65, 30.47, 29.66, 29.13, 28.68, 21.77, 16.14, 7.49.

HRMS (ESI+): Calculated mass  $[M+H]^+$   $C_{17}H_{25}O^+$  = 221.1900; found: 221.1901.

Melting point: 53 °C

The analytical data was in agreement with: a) J. E. Spangler, C. A. Carson, E. J. Sorenson, *Chem. Sci.* **2010**, *1*, 202-205. b) N. Mangel, F. M. Mann, M. L. Hillwig, R. J. Peters, B. B. Snider, *Org. Lett.* **2010**, *12*, 2626-2629.



**(*E*)-4-((1*S*,2*S*,8*aS*)-1,2,5,5-tetramethyl-1,2,3,5,6,7,8,8*a*-octahydronaphthalen-1-yl)but-3-en-2-one (56):**

A solution of NaHMDS (30 mL, 2 M in THF, 30 mmol, 3 eq) diluted to a 1 M solution with dry THF (30 mL) was cooled to -78 °C. The orange solution became slightly turbid and viscous, however stirring was assured. Acetone (4.4 mL, 60.3 mmol, 3 eq) was added dropwise to the turbid solution which became clear upon addition. The mixture was stirred at this temperature for 20 min after which a solution of aldehyde **8** (4.43 g, 20.1 mmol) in dry THF (125 mL) was added dropwise over 20 min by the aid of a dropping funnel. After addition the reaction was taken out of the cooling bath and allowed to warm-up to rt (by the aid of a water bath at rt). The reaction was stirred for 2 h after which TLC and GC-MS indicated complete consumption of the aldehyde **8**.

The reaction was diluted with ether and quenched with a saturated  $\text{NaHCO}_3$ . The phases were separated, and the organic phase was washed with distilled water and brine. The combined aqueous layers were back-extracted once with  $\text{Et}_2\text{O}$  and the combined organic layers were dried over  $\text{MgSO}_4$ , filtered and concentrated under reduced pressure. Flash column chromatography employing pentane : ether (95:5) afforded (*E*)-4-((1*S*,2*S*,8*aS*)-1,2,5,5-tetramethyl-1,2,3,5,6,7,8,8*a*-octahydronaphthalen-1-yl)but-3-en-2-one **56** as an amorphous solid (3.4 g, 13.1 mmol, 65% yield)

*Note: The aldol condensation was also performed on a 3.5 g scale which resulted in a slightly higher isolated yield of 74%. It is very important to monitor the reaction and not let it run overnight. This gives over-condensation and therefore lower isolated yield.*

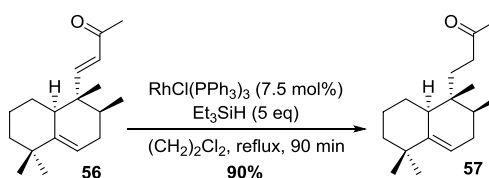
$^1\text{H-NMR}$  (400 MHz,  $\text{CDCl}_3$ )  $\delta$  6.60 (d,  $J = 16.2$  Hz, 1H), 6.02 (d,  $J = 16.3$  Hz, 1H), 5.49 (d,  $J = 5.8$  Hz, 1H), 2.26 (s, 3H), 2.13 (d,  $J = 13.1$  Hz, 1H), 1.93 (dt,  $J = 17.8, 4.7$  Hz, 1H), 1.80 – 1.68 (m, 1H), 1.62 – 1.34 (m, 5H), 1.17 (dd,  $J = 12.6, 5.1$  Hz, 1H), 1.07 (s, 3H), 1.00 (s, 3H), 0.96 – 0.89 (m, 1H), 0.78 (s, 3H), 0.72 (d,  $J = 6.8$  Hz, 3H).

$^{13}\text{C}$ -NMR (101 MHz,  $\text{CDCl}_3$ )  $\delta$  198.72, 158.19, 144.73, 129.58, 116.47, 43.67, 43.00, 40.77, 36.65, 36.22, 31.12, 29.67, 29.28, 28.27, 27.43, 21.96, 16.38, 10.28.

HRMS (ESI+): Calculated mass  $[\text{M}+\text{H}]^+$   $\text{C}_{18}\text{H}_{29}\text{O}^+$  = 261.2213; found: 261.2215.  
Calculated mass  $[\text{M}+\text{Na}]^+$   $\text{C}_{21}\text{H}_{33}\text{NO}_3\text{Na}^+$  = 283.2032; found: 283.2034.

Melting point: 72 °C

The analytical data are in agreement with: a) J. E. Spangler, C. A. Carson, E. J. Sorenson, *Chem. Sci.* **2010**, *1*, 202-205. b) N. Mangel, F. M. Mann, M. L. Hillwig, R. J. Peters, B. B. Snider, *Org. Lett.* **2010**, *12*, 2626-2629.



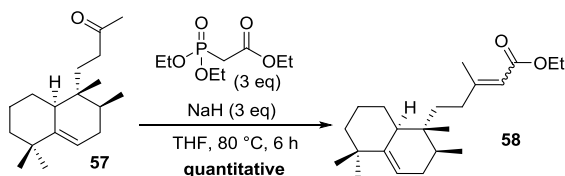
**4-((1*R*,2*S*,8*aS*)-1,2,5,5-tetramethyl-1,2,3,5,6,7,8,8*a*-octahydronaphthalen-1-yl)butan-2-one (57):**

To a solution of  $\alpha,\beta$ -unsaturated ketone **56** (3.4 g, 13.1 mmol) in dry  $(\text{CH}_2)_2\text{Cl}_2$  (150 mL) were added Wilkinson's catalyst (909 mg, 0.98 mmol, 7.5 mol%) and triethylsilane (10.4 mL, 65.5 mmol, 5 eq). The reaction mixture was heated to reflux and stirred for 90 minutes after which TLC indicated complete conversion of the starting material. The reaction was cooled to rt where after it was quenched with an aqueous solution of HCl (6 M, 100 mL). The mixture was stirred for 30 minutes after which the phases were separated, and the organic layer was washed with water, followed by a saturated aqueous solution of  $\text{NaHCO}_3$  and brine. The organic layer was dried over  $\text{MgSO}_4$ , filtered and concentrated under reduced pressure. Flash column chromatography employing pentane : ether (95:5) afforded pure 4-((1*R*,2*S*,8*aS*)-1,2,5,5-tetramethyl-1,2,3,5,6,7,8,8*a*-octahydronaphthalen-1-yl)butan-2-one **57** (3.1 g, 11.7 mmol, 90% yield) as a slightly yellow oil.

$^1\text{H}$ -NMR (400 MHz,  $\text{CDCl}_3$ )  $\delta$  5.41 (s, 1H), 2.37 – 2.28 (m, 2H), 2.14 (s, 3H), 1.99 (d,  $J$  = 12.5 Hz, 1H), 1.88 – 1.60 (m, 4H), 1.60 – 1.32 (m, 6H), 1.17 (td,  $J$  = 13.0, 4.4 Hz, 1H), 1.04 (s, 3H), 0.98 (s, 3H), 0.78 (d,  $J$  = 6.8 Hz, 3H), 0.63 (s, 3H).

$^{13}\text{C}$ -NMR (101 MHz,  $\text{CDCl}_3$ )  $\delta$  209.58, 145.91, 116.30, 40.95, 40.12, 37.77, 36.71, 36.18, 33.59, 31.61, 30.15, 30.07, 29.84, 29.04, 27.57, 22.26, 16.04, 15.11.

The analytical data are in agreement with: a) J. E. Spangler, C. A. Carson, E. J. Sorenson, *Chem. Sci.* **2010**, *1*, 202-205. b) N. Mangel, F. M. Mann, M. L. Hillwig, R. J. Peters, B. B. Snider, *Org. Lett.* **2010**, *12*, 2626-2629.



**Ethyl-3-methyl-5-((1*R*,2*S*,8*aS*)-1,2,5,5-tetramethyl-1,2,3,5,6,7,8,8*a*-octahydronaphthalen-1-yl)pent-2-enoate (**58**):**

ethyl 2-(diethoxyphosphoryl)acetate (6.96 mL, 35.1 mmol, 3 eq) in dry THF (50 mL) was added dropwise to a suspension of sodium hydride (1.4 g, 60% in oil, 35.1 mmol, 3 eq) in dry THF (50 mL) at 0 °C by the aid of a dropping funnel. The suspension turned into a clear solution and was stirred for 20 min after which ketone **57** (3.1 g, 11.7 mmol) in dry THF (100 mL) was added dropwise over 10 minutes by the aid of a dropping funnel. The cooling bath was removed and the mixture was allowed to warm to rt. The reaction vessel was then sealed under N<sub>2</sub> and placed in an oil bath at 80 °C and was allowed to stir for 6 h. TLC and GC-MS indicated full conversion of the starting material.

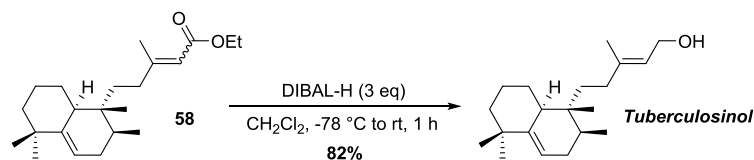
The reaction was cooled to rt and quenched with saturated aqueous NH<sub>4</sub>Cl. The reaction mixture was diluted with ether, and the phases were separated. The aqueous phase was extracted with ether, were after the combined organic layers were dried over MgSO<sub>4</sub>, filtered and concentrated under reduced pressure to afford a yellow oil. Flash column chromatography employing pentane : ether (95:5) afforded crude ethyl 3-methyl-5-((1*R*,2*S*,8*aS*)-1,2,5,5-tetramethyl-1,2,3,5,6,7,8,8*a*-octahydronaphthalen-1-yl)pent-2-enoate **58** (4.0 gr, 12.0 mmol, 103%) as an *E:Z* mixture of ~9:1.

*Note: The sodium hydride was pre-washed three times with pentane to remove the oil.*

<sup>1</sup>H-NMR (400 MHz, CDCl<sub>3</sub>) δ 5.67 (s, 1H), 5.45 – 5.40 (m, 1H), 4.13 (q, *J* = 7.1 Hz, 2H), 2.17 (s, 3H), 2.13 (d, *J* = 13.1 Hz, 1H), 2.03 (dt, *J* = 10.1, 4.4 Hz, 2H), 1.90 – 1.67 (m, 4H), 1.65 – 1.44 (m, 5H), 1.44 – 1.34 (m, 2H), 1.26 (d, *J* = 6.9 Hz, 2H), 1.22 – 1.14 (m, 1H), 1.05 (s, 3H), 0.99 (s, 3H), 0.81 (d, *J* = 6.7 Hz, 3H), 0.63 (s, 3H).

<sup>13</sup>C-NMR (101 MHz, CDCl<sub>3</sub>) δ 166.93, 161.30, 145.98, 116.29, 115.33, 59.52, 40.99, 39.97, 37.19, 36.19, 34.73, 34.60, 33.50, 31.70, 29.87, 29.10, 27.55, 22.33, 19.21, 16.25, 15.18, 14.47.

The analytical data are in agreement with: N. Mangel, F. M. Mann, M. L. Hillwig, R. J. Peters, B. B. Snider, *Org. Lett.* **2010**, *12*, 2626-2629.



**(*E*)-3-methyl-5-((1*R*,2*S*,8*aS*)-1,2,5,5-tetramethyl-1,2,3,5,6,7,8,8*a*-octahydronaphthalen-1-yl)pent-2-en-1-ol (Tuberculosinol):**

To a solution of crude enoate **58** (4.0 g, 12.0 mmol) in dry CH<sub>2</sub>Cl<sub>2</sub> (75 mL) cooled to -78 °C was added dropwise DIBAL-H (36.0 mL, 1.0 M in CH<sub>2</sub>Cl<sub>2</sub>, 36.0 mmol) over 15 min by the aid of a dropping funnel. The cooling bath was removed and the reaction mixture was allowed to slowly warm up to rt. TLC and GC-MS indicated complete conversion of the starting material after 1 h of reaction time.

The reaction mixture was carefully quenched using MeOH (10 mL) where after saturated aqueous Rochelle salt (75 mL) was added at 0 °C. The mixture was stirred for 30 min while warming up to rt where after the phases were separated. The aqueous phase was extracted three times with CH<sub>2</sub>Cl<sub>2</sub> and the combined organic layers were dried over MgSO<sub>4</sub>, filtered and concentrated under reduced pressure to afford a yellowish oil. Flash column chromatography was executed using pentane : ether (4:1) as the eluent, affording pure tuberculosinol (2.33 g, 8.0 mmol, 68% yield) as a colorless oil.

A mixture of (*E*)-tuberculosinol and (*Z*)-tuberculosinol was also obtained (0.9 g). This was subjected to an additional chromatographic purification, affording 460 mg of (*E*)-tuberculosinol, giving a combined yield of 82%.

Also (*Z*)-tuberculosinol (0.4 g, 1.4 mmol, 11%) was isolated as a colorless oil.

*Analytical data for (E)-tuberculosinol:*

<sup>1</sup>H-NMR (400 MHz, CDCl<sub>3</sub>) δ 5.43 – 5.33 (m, 2H), 4.08 (d, *J* = 6.8 Hz, 2H), 2.57 (s, 1H), 2.13 (d, *J* = 12.6 Hz, 1H), 1.92 – 1.85 (m, 2H), 1.81 – 1.67 (m, 3H), 1.65 (s, 3H), 1.59 – 1.28 (m, 6H), 1.28 – 1.10 (m, 1H), 1.02 (s, 3H), 0.97 (s, 3H), 0.78 (d, *J* = 6.8 Hz, 3H), 0.59 (s, 3H).

<sup>13</sup>C-NMR (101 MHz, CDCl<sub>3</sub>) δ 145.99, 140.10, 123.11, 116.13, 59.09, 40.94, 39.81, 36.92, 36.05, 34.97, 33.38, 32.76, 31.65, 29.78, 29.00, 27.44, 22.27, 16.46, 16.18, 15.10.

HRMS (ESI<sup>+</sup>): Calculated mass [M+Na<sup>+</sup>]<sup>+</sup> C<sub>17</sub>H<sub>29</sub>OSNa<sup>+</sup> = 313.2502; found: 313.2500.

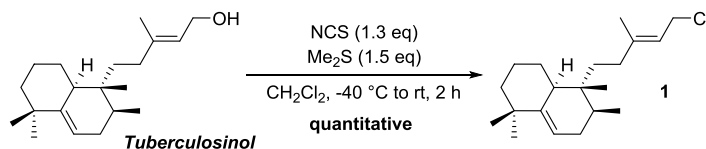
Optical rotation: [α]<sub>D</sub><sup>23</sup> = +40.1 (*c* = 0.024, EtOH) and [α]<sub>D</sub><sup>23</sup> = +39.5 (*c* = 0.013, CHCl<sub>3</sub>).

Analytical data for (*Z*)-tuberculosinol:

<sup>1</sup>H-NMR (400 MHz, CDCl<sub>3</sub>) δ 5.46 – 5.42 (m, 1H), 5.39 (t, *J* = 6.9 Hz, 1H), 4.13 (d, *J* = 7.0 Hz, 2H), 2.21 (d, *J* = 13.2 Hz, 1H), 1.99 (ddp, *J* = 17.4, 12.6, 5.3 Hz, 3H), 1.91 – 1.79 (m, 1H), 1.76 (s, 3H), 1.67 – 1.47 (m, 4H), 1.47 – 1.15 (m, 6H), 1.07 (s, 3H), 1.02 (s, 3H), 0.85 (d, *J* = 6.7 Hz, 3H), 0.62 (s, 3H).

<sup>13</sup>C-NMR (101 MHz, CDCl<sub>3</sub>) δ 145.82, 139.86, 123.89, 116.02, 58.67, 40.86, 39.69, 37.05, 35.97, 35.25, 33.24, 31.56, 29.70, 28.95, 27.48, 25.36, 23.59, 22.23, 16.03, 15.12.

The analytical data are in agreement with: a) J. E. Spangler, C. A. Carson, E. J. Sorenson, *Chem. Sci.* **2010**, *1*, 202-205. b) N. Mangel, F. M. Mann, M. L. Hillwig, R. J. Peters, B. B. Snider, *Org. Lett.* **2010**, *12*, 2626-2629.



**(4a*S*,5*R*,6*S*)-5-((*E*)-5-chloro-3-methylpent-3-en-1-yl)-1,1,5,6-tetramethyl-1,2,3,4,4a,5,6,7-octahydronaphthalene (1):**

To a suspension of 1-chloropyrrolidine-2,5-dione (1.0 g, 7.61 mmol, 1.3 eq) in dry CH<sub>2</sub>Cl<sub>2</sub> (15 mL), cooled to -20 °C, was added dropwise dimethyl sulfide (0.65 mL, 8.78 mmol, 1.5 eq) in dry CH<sub>2</sub>Cl<sub>2</sub> (5.0 mL). The milk white suspension was allowed to warm to 0 °C for 15 min after which the temperature was lowered to -40 °C. Tuberculosinol (1.7 g, 5.85 mmol) in dry CH<sub>2</sub>Cl<sub>2</sub> (20 mL) was added slowly by the aid of a syringe pump over 15 min. After addition, the cooling bath was removed, and the reaction was allowed to warm-up to rt. The reaction was allowed to stir at this temperature for 2 h after which TLC and GC-MS analysis indicated complete conversion of the tuberculosinol. The reaction mixture was concentrated under reduced pressure and treated with pentane upon which succinimide oiled out. The mixture was decanted and filtered and the elute was concentrated under reduced pressure affording nearly pure (4a*S*,5*R*,6*S*)-5-((*E*)-5-chloro-3-methylpent-3-en-1-yl)-1,1,5,6-tetramethyl-1,2,3,4,4a,5,6,7-octahydronaphthalene **1** (1.85 gr, 6.0 mmol, 103% yield) as a yellow oil contaminated only with DMSO formed during the reaction.

Analytical data for (*E*)-tuberculosinyl chloride **1**:

<sup>1</sup>H-NMR (400 MHz, CDCl<sub>3</sub>) δ 5.51 – 5.41 (m, 2H), 4.09 (d, *J* = 7.9 Hz, 2H), 2.16 (d, *J* = 12.8 Hz, 1H), 1.96 (dt, *J* = 10.4, 4.6 Hz, 2H), 1.83 (ddd, *J* = 17.7, 14.5, 3.5 Hz, 2H), 1.75 (s, 3H), 1.72 (s, 1H), 1.63 – 1.25 (m, 7H), 1.20 (td, *J* = 12.9, 4.8 Hz, 1H), 1.06 (s, 3H), 1.01 (s, 3H), 0.82 (d, *J* = 6.8 Hz, 3H), 0.63 (s, 3H).

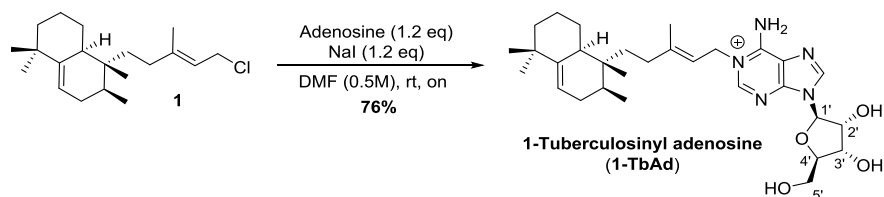
$^{13}\text{C}$ -NMR (101 MHz,  $\text{CDCl}_3$ )  $\delta$  146.11, 144.03, 119.92, 116.27, 41.34, 41.05, 39.93, 37.11, 36.20, 34.82, 33.51, 32.88, 31.75, 29.90, 29.13, 27.56, 22.37, 16.46, 16.28, 15.22.

HRMS (APCI): Calculated mass  $[\text{M}-\text{Cl}]^+ \text{C}_{20}\text{H}_{30}^+ = 273.2582$ ; found: 273.2576.

Analytical data for (*Z*)-tuberculosinyl chloride:

$^1\text{H}$ -NMR (400 MHz,  $\text{CDCl}_3$ )  $\delta$  5.46 – 5.42 (m, 1H), 5.39 (t,  $J = 6.9$  Hz, 1H), 4.13 (d,  $J = 7.0$  Hz, 2H), 2.21 (d,  $J = 13.2$  Hz, 1H), 1.99 (ddp,  $J = 17.4, 12.6, 5.3$  Hz, 3H), 1.91 – 1.79 (m, 1H), 1.76 (s, 3H), 1.67 – 1.47 (m, 4H), 1.47 – 1.15 (m, 6H), 1.07 (s, 3H), 1.02 (s, 3H), 0.85 (d,  $J = 6.7$  Hz, 3H), 0.62 (s, 3H).

$^{13}\text{C}$ -NMR (101 MHz,  $\text{CDCl}_3$ )  $\delta$  145.82, 139.86, 123.89, 116.02, 58.67, 40.86, 39.69, 37.05, 35.97, 35.25, 33.24, 31.56, 29.70, 28.95, 27.48, 25.36, 23.59, 22.23, 16.03, 15.12.



**6-amino-9-((2*R*,3*R*,4*S*,5*R*)-3,4-dihydroxy-5-(hydroxymethyl)tetrahydrofuran-2-yl)-1-((*E*)-3-methyl-5-((1*R*,2*S*,8*aS*)-1,2,5,5-tetramethyl-1,2,3,5,6,7,8,8a-octahydronaphthalen-1-yl)pent-2-en-1-yl)-9H-purin-1-ium (1-TbAd):**

To a solution (0.5 M) of nearly pure tuberculosinyl chloride **1** (1.8 g, 5.8 mmol) in peptide grade DMF (11.6 mL) was added sodium iodide (1.05 g, 7.0 mmol) and adenosine (1.87 g, 7.0 mmol). The suspension was stirred in the dark at rt overnight, forming a dark turbid solution. The reaction mixture was concentrated under reduced pressure and subsequently purified using flash column chromatography (15% MeOH in  $\text{CH}_2\text{Cl}_2$ ) affording 1-TbAd (2.4 g, 4.43 mmol, 76% yield)

The reaction can also be performed in dimethylacetamide as the solvent. Starting from tuberculosinyl chloride **1** (0.4 gr, 1.29 mmol), 1-TbAd (560 mg, 1.04 mmol, 79% yield) was obtained.

*Note: 1-TbAd proved to be difficult to separate from unreacted adenosine due to tailing of the 1-TbAd. It is recommended to use a long column (30 cm) and analyze individual fractions by  $^1\text{H}$ -NMR analysis to determine the presence of free adenosine. Visualization of the adenosine on a TLC plate proved to be difficult.*



## CHAPTER 4

*Analytical data for naturally occurring 1-TbAd:*

<sup>1</sup>H-NMR (400 MHz, CD<sub>3</sub>OD) δ 8.62 (s, 1H), 8.49 (s, 1H), 6.08 (d, *J* = 5.2 Hz, 1H), 5.51 – 5.42 (m, 2H), 4.91 (d, *J* = 6.6 Hz, 2H), 4.62 (t, *J* = 5.1 Hz, 2H), 4.58 (s, 1H), 4.38 – 4.31 (m, 2H), 4.15 (q, *J* = 3.3 Hz, 1H), 3.87 (dd, *J* = 12.3, 2.9 Hz, 1H), 3.77 (dd, *J* = 12.2, 3.4 Hz, 1H), 2.23 (d, *J* = 12.1 Hz, 2H), 2.12 – 2.04 (m, 2H), 1.89 (s, 3H), 1.87 – 1.82 (m, 1H), 1.84 – 1.71 (m, 2H), 1.65 – 1.47 (m, 5H), 1.47 – 1.36 (m, 3H), 1.21 (ddd, *J* = 12.7, 5.7 Hz, 1H), 1.06 (s, 3H), 1.01 (s, 3H), 0.85 (d, *J* = 6.7 Hz, 3H), 0.66 (s, 3H).

<sup>13</sup>C-NMR (101 MHz, CD<sub>3</sub>OD) δ 152.52, 147.78, 147.58, 147.31, 147.08, 143.74, 121.49, 117.34, 115.89, 90.43, 87.41, 76.35, 71.79, 62.62, 49.39, 42.00, 41.06, 38.05, 36.94, 35.87, 34.52, 33.88, 32.62, 30.29, 29.49, 28.53, 23.18, 17.35, 16.58, 15.54.

HRMS (ESI+): Calculated mass [M]<sup>+</sup> C<sub>30</sub>H<sub>46</sub>N<sub>5</sub>O<sub>4</sub><sup>+</sup> = 540.3544; found: 540.3542.

*Analytical data for non-natural (Z)-1-TbAd constructed from (Z)-tuberculosinyl chloride:*

<sup>1</sup>H-NMR (400 MHz, CD<sub>3</sub>OD) δ 8.56 (2x s, 2H), 8.41 (2x s, 1H), 6.09 – 6.02 (m, 1H), 5.44 (dt, *J* = 23.8, 6.5 Hz, 2H), 4.88 (d, *J* = 6.6 Hz, 2H), 4.61 (t, *J* = 4.6 Hz, 1H), 4.33 (t, *J* = 4.3 Hz, 1H), 4.14 (d, *J* = 3.1 Hz, 1H), 3.91 – 3.82 (m, 1H), 3.76 (dd, *J* = 12.8, 2.5 Hz, 1H), 2.32 – 2.14 (m, 2H), 2.07 (t, *J* = 8.2 Hz, 1H), 1.88 (s, 3H), 1.85 – 1.71 (m, 3H), 1.65 – 1.47 (m, 5H), 1.43 (dd, *J* = 14.6, 8.6 Hz, 2H), 1.22 (dd, *J* = 12.4, 6.2 Hz, 1H), 1.06 (s, 3H), 1.02 (2x s, 3H), 0.86 (2x d, *J* = 6.8 Hz, 3H), 0.66 (2x s, *J* = 10.9 Hz, 3H).

<sup>13</sup>C-NMR (101 MHz, CD<sub>3</sub>OD) δ 152.74, 152.49, 147.80, 147.56, 147.30, 147.05, 146.99, 143.57, 143.41, 121.58, 121.49, 117.24, 117.15, 116.46, 115.98, 90.36, 87.36, 76.22, 71.73, 62.60, 42.00, 41.94, 40.96, 38.17, 37.97, 36.93, 36.88, 35.79, 34.44, 34.33, 33.83, 32.56, 30.29, 29.49, 28.70, 28.46, 26.81, 23.94, 23.19, 23.12, 17.46, 16.64, 16.58, 15.84, 15.56.

HRMS (ESI+): Calculated mass [M]<sup>+</sup> C<sub>30</sub>H<sub>46</sub>N<sub>5</sub>O<sub>4</sub><sup>+</sup> = 540.3544; found: 540.3542.

*Note: The appearance of additional signals in the NMR spectra of (Z)-1-TbAd, compared to that of naturally occurring (E)-1-TbAd, is attributed to rotamers.*

### <sup>13</sup>C-labelled 1-TbAd:

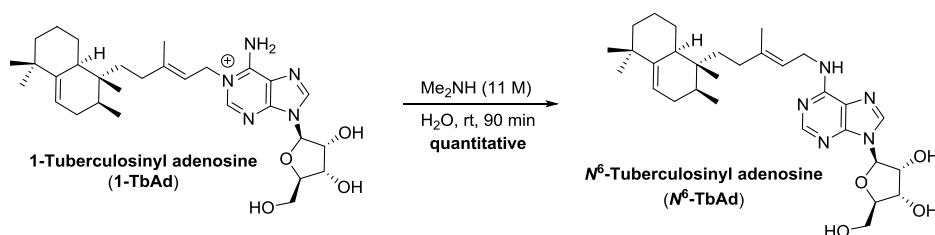
To a solution (0.5 M) of nearly pure tuberculosinyl chloride **1** (142 mg, 0.459 mmol, 1.25 eq) in peptide grade DMF (0.92 mL) was added sodium iodide (69 mg, 0.459 mmol, 1.25 eq) and [1',2',3',4',5'-<sup>13</sup>C<sub>5</sub>] adenosine (100 mg, 0.367 mmol). The suspension was stirred in the dark at rt overnight, forming a dark turbid solution. The reaction mixture was concentrated under reduced pressure where after purified using flash column chromatography (15% MeOH in CH<sub>2</sub>Cl<sub>2</sub>) affording [1',2',3',4',5'-<sup>13</sup>C<sub>5</sub>] 1-TbAd (100 mg, 0.18 mmol, 57% yield) as an off-white solid.

Asymmetric Total Synthesis of 1-Tuberculosinyl Adenosine

$^1\text{H-NMR}$  (400 MHz,  $\text{CD}_3\text{OD}$ )  $\delta$  8.56 (s, 1H), 8.42 (s, 1H), 6.26 (s, 1H), 5.84 (s, 1H), 5.52 – 5.40 (m, 2H), 4.58 (s, 1H), 4.51 (s, 1H), 4.42 (s, 1H), 4.33 (s, 1H), 4.14 (s, 1H), 4.04 (d,  $J = 11.4$  Hz, 1H), 3.94 (d,  $J = 9.7$  Hz, 1H), 3.77 – 3.63 (m, 1H), 3.59 (d,  $J = 12.0$  Hz, 1H), 2.22 (d,  $J = 13.3$  Hz, 2H), 2.07 (t,  $J = 8.3$  Hz, 2H), 1.88 (s, 3H), 1.86 – 1.70 (m, 3H), 1.65 – 1.47 (m, 4H), 1.47 – 1.35 (m, 2H), 1.21 (td,  $J = 12.4, 5.5$  Hz, 1H), 1.06 (s, 3H), 1.01 (s, 3H), 0.84 (d,  $J = 6.7$  Hz, 3H), 0.65 (s, 3H).

$^{13}\text{C-NMR}$  (101 MHz,  $\text{CD}_3\text{OD}$ )  $\delta$  152.56, 147.83, 147.32, 147.09, 147.03, 143.56, 121.55, 117.27, 116.00, 90.40 (dd,  $J = 42.0, 3.7$  Hz), 87.37 (t,  $J = 41.7, 38.5$  Hz), 76.21 (dd,  $J = 42.0, 37.8$  Hz), 71.72 (td,  $J = 38.1, 3.8$  Hz), 62.60 (d,  $J = 41.7$  Hz), 49.85, 41.96, 40.99, 38.00, 36.90, 35.82, 34.47, 33.84, 32.58, 30.27, 29.48, 28.48, 23.14, 17.42, 16.57, 15.54.

HRMS (ESI+): Calculated mass  $[\text{M}+\text{H}]^+$   $\text{C}_{25}({}^{13}\text{C})_5\text{H}_{46}\text{N}_5\text{O}_4^+$  = 545.3712; found: 545.3702



**(2R,3S,4R,5R)-2-(hydroxymethyl)-5-(6-(((E)-3-methyl-5-((1R,2S,8aS)-1,2,5,5-tetramethyl-1,2,3,5,6,7,8,8a-octahydronaphthalen-1-yl)pent-2-en-1-yl)amino)-9H-purin-9-yl)tetrahydrofuran-3,4-diol ( $N^6$ -TbAd):**

A solution of 1-TbAd (550 mg, 1.02 mmol) in 60%  $\text{Me}_2\text{NH}$  in water (5.5 mL) was stirred for 90 min. NMR analysis indicated complete conversion of the 1-TbAd. The reaction mixture was concentrated under reduced pressure and subsequently subjected to flash column chromatography, with 15% MeOH in  $\text{CH}_2\text{Cl}_2$ , to afford  $N^6$ -TbAd as a white solid (550 mg, 1.02 mmol, quantitative yield).

*Note: The rearrangement could be performed with similar results using  $\text{Et}_2\text{NH}$  or  $i\text{Pr}_2\text{NEt}$  (2M) in MeOH.*

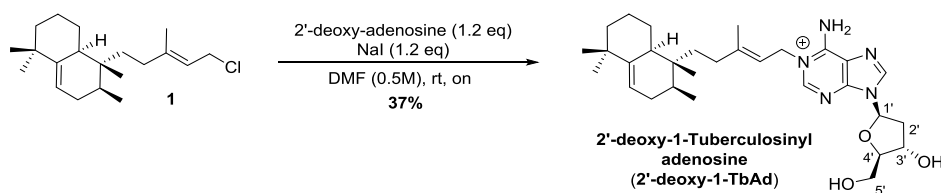
$^1\text{H-NMR}$  (400 MHz,  $\text{CD}_3\text{OD}$ )  $\delta$  8.25 (s, 1H), 8.23 (s, 1H), 5.95 (d,  $J = 6.4$  Hz, 1H), 5.51 – 5.44 (m, 1H), 5.41 (t,  $J = 6.5$  Hz, 1H), 4.74 (t,  $J = 5.6$  Hz, 1H), 4.35 – 4.29 (m, 1H), 4.20 (s, 1H), 4.17 (s, 1H), 3.89 (dd,  $J = 12.6, 2.1$  Hz, 1H), 3.74 (dd,  $J = 12.9, 2.3$  Hz, 1H), 2.24 (d,  $J = 15.9$  Hz, 1H), 2.07 – 1.93 (m, 3H), 1.91 – 1.82 (m, 2H), 1.80 (s, 3H), 1.65 – 1.49 (m, 4H), 1.49 – 1.36 (m, 3H), 1.21 (td,  $J = 11.9, 7.3$  Hz, 2H), 1.06 (s, 3H), 1.02 (s, 3H), 0.85 (d,  $J = 6.6$  Hz, 3H), 0.65 (s, 3H).

$^1\text{H-NMR}$  (400 MHz,  $\text{CDCl}_3$ )  $\delta$  8.19 (s, 1H), 7.81 (s, 1H), 5.86 (bs, 1H), 5.82 (d,  $J = 7.2$  Hz, 1H), 5.44 (d,  $J = 4.7$  Hz, 1H), 5.36 (d,  $J = 7.3$  Hz, 1H), 5.00 (s, 1H), 4.47 (d,  $J = 4.9$  Hz, 1H), 4.33 (s, 1H), 4.19 (bs, 2H), 3.94 (d,  $J = 12.9$  Hz, 1H), 3.76 (d,  $J = 12.9$  Hz, 1H), 3.23 (s, 2H), 2.49 (bs, 2H), 2.16 (d,  $J = 10.4$  Hz, 1H), 2.01 – 1.90 (m, 2H), 1.85 (d,  $J = 23.8$  Hz, 2H), 1.76 (s, 3H), 1.72 (s, 1H), 1.64 – 1.28 (m, 6H), 1.21 (tt,  $J = 13.0, 6.2$  Hz, 2H), 1.06 (s, 3H), 1.01 (s, 3H), 0.82 (d,  $J = 6.6$  Hz, 3H), 0.63 (s, 3H).

$^{13}\text{C-NMR}$  (101 MHz,  $\text{CDCl}_3$ )  $\delta$  154.59, 152.44, 147.00, 146.09, 141.73, 140.05, 120.70, 118.96, 116.23, 91.08, 87.56, 73.89, 72.46, 63.15, 41.00, 39.89, 38.87, 37.04, 36.17, 35.00, 33.47, 32.80, 31.71, 29.87, 29.12, 27.51, 22.33, 16.83, 16.26, 15.22.

HRMS (ESI<sup>+</sup>): Calculated mass  $[\text{M}+\text{H}]^+ \text{C}_{30}\text{H}_{46}\text{N}_5\text{O}_4^+ = 540.3544$ ; found: 540.3542

The spectral data are consistent with that of the natural isolate: D. C. Young, E. Layre, S-J. Pan, A. Tapley, J. Adamson, C. Seshadri, Z. Wu, J. Buter, A. J. Minnaard, M. Coscolla, S. Gagneux, R. Copin, J. D. Ernst, W. R. Bishai, B. B. Snider, D. B. Moody, *Chem. Biol.* **2015**, *22*, 516-526.



**6-amino-9-((2R,4S,5R)-4-hydroxy-5-(hydroxymethyl)tetrahydrofuran-2-yl)-1-((E)-3-methyl-5-((1R,2S,8aS)-1,2,5,5-tetramethyl-1,2,3,5,6,7,8,8a-octahydronaphthalen-1-yl)pent-2-en-1-yl)-9H-purin-1-ium (2'-deoxy-1-TbAd):**

To a solution (0.5 M) of nearly pure tuberculosinyl chloride **1** (300 mg, 0.97 mmol) in peptide grade DMA (2 mL) was added sodium iodide (175 mg, 1.17 mmol, 1.2 eq) and 2'-deoxy-adenosine monohydrate (314 mg, 1.17 mmol, 1.2 eq). The suspension was stirred in the dark at rt overnight, forming a dark turbid solution. The reaction mixture was concentrated under reduced pressure where after purified using flash column chromatography (15% MeOH in  $\text{CH}_2\text{Cl}_2$ ) affording 2'-deoxy-1-TbAd (190 mg, 0.36 mmol, 37% yield) as a white solid.

Also a slightly impure fraction of 2'-deoxy-1-TbAd (150 mg, 0.29 mmol, 31%) was obtained. The impurity, based on NMR analysis, remained unresolved.

$^1\text{H-NMR}$  (400 MHz,  $\text{CDCl}_3$ )  $\delta$  8.54 (s, 1H), 8.44 (s, 1H), 6.46 (t,  $J = 6.5$  Hz, 1H), 5.46 (s, 2H), 4.90 (d,  $J = 6.5$  Hz, 2H), 4.57 (s, 1H), 4.09 – 4.01 (m, 1H), 3.77 (qd,  $J = 12.1, 3.5$  Hz, 2H), 2.76 (dt,  $J = 13.0, 6.3$  Hz, 1H), 2.56 – 2.44 (m, 1H), 2.21 (d,  $J = 12.5$  Hz, 2H), 2.11 – 1.99 (m, 2H), 1.89 (s, 3H), 1.86 – 1.70 (m, 3H), 1.54 (d,  $J = 12.3$  Hz, 4H),

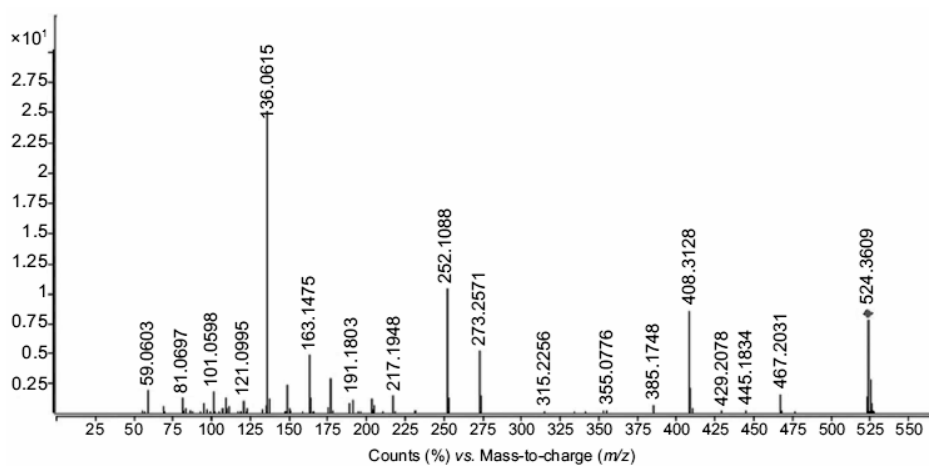
### Asymmetric Total Synthesis of 1-Tuberculosinyl Adenosine

1.42 (dd,  $J = 17.1, 8.8$  Hz, 2H), 1.19 (td,  $J = 12.3, 5.8$  Hz, 1H), 1.05 (s, 3H), 1.00 (s, 3H), 0.83 (d,  $J = 6.6$  Hz, 3H), 0.64 (s, 3H).

$^{13}\text{C}$ -NMR (101 MHz,  $\text{CDCl}_3$ )  $\delta$  152.47, 147.65, 147.05, 146.99, 146.95, 143.45, 121.40, 117.24, 116.06, 89.53, 86.33, 72.30, 62.96, 49.85, 41.95, 41.76, 40.96, 37.98, 36.89, 35.79, 34.45, 33.86, 32.59, 30.32, 29.50, 28.47, 23.14, 17.46, 16.62, 15.59.

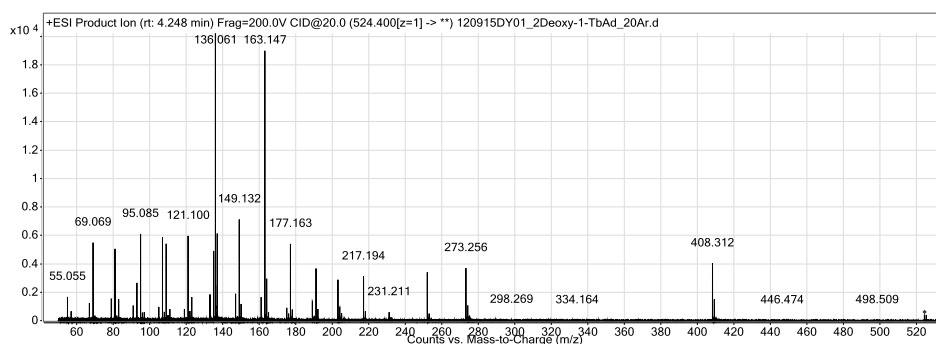
HRMS (ESI+): Calculated mass  $[\text{M}]^+ \text{C}_{30}\text{H}_{46}\text{N}_5\text{O}_3^+ = 524.3595$ ; found: 524.3588.

#### Reported MS spectrum of 2'-deoxy 1-TbAd:



Taken from: *Emerg. Microbes Infect.* **2015**, *4*, e6 (doi: 10.1038/emi.2015.6)

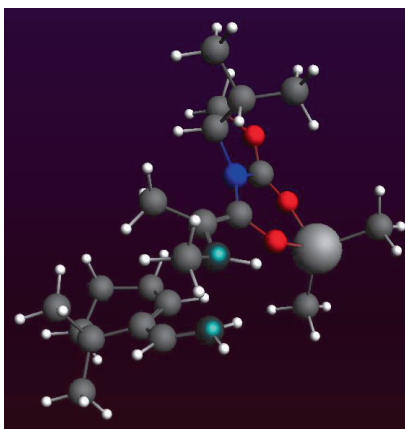
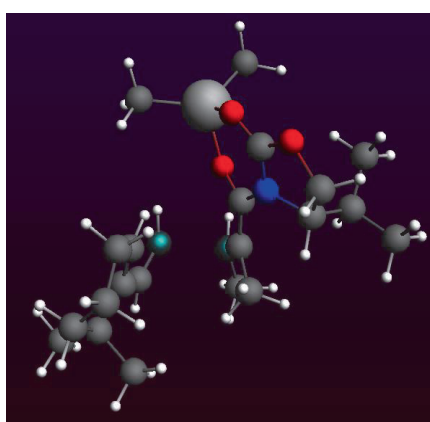
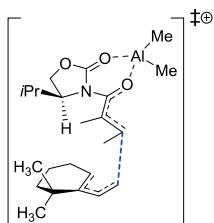
#### Complete CID-MS spectrum of synthetic 2'-deoxy 1-TbAd:



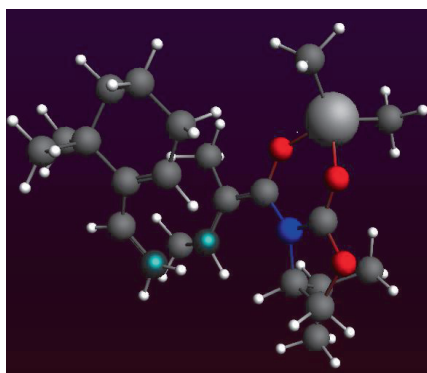
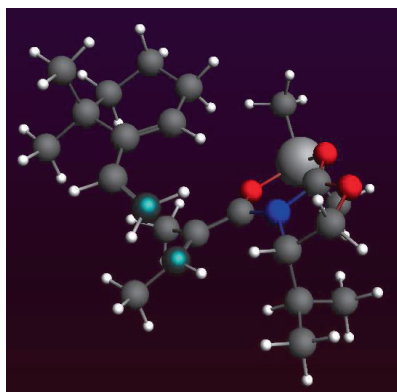
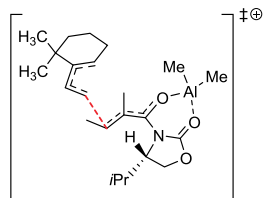
CHAPTER 4

Computational models :

*Aluminum complexed s-cis pathway, first transition state (44b)*

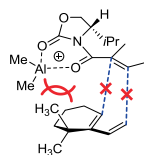


*Aluminum complexed s-trans pathway, first transition state (44h)*

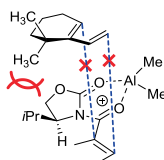
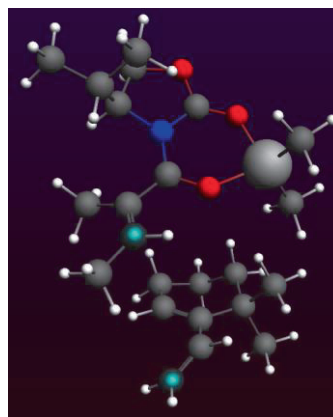
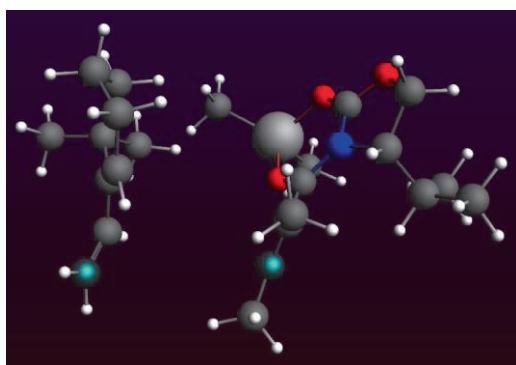


**The disfavored approaches for the Diels-Alder reaction**

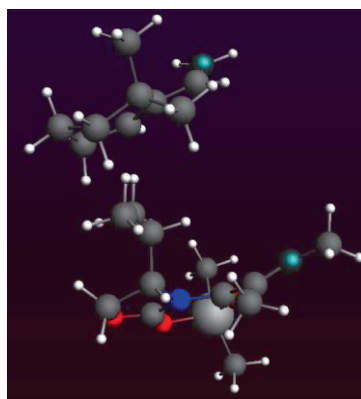
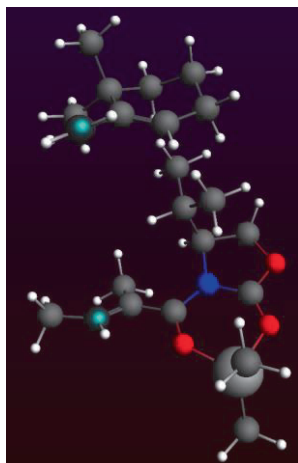
The reaction partners were brought together but not optimized. From the different approaches the steric interactions are clearly visible. The carbons in the diene and dienophile involved in initial bond formation are highlighted.

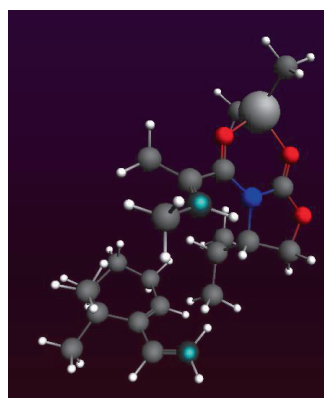
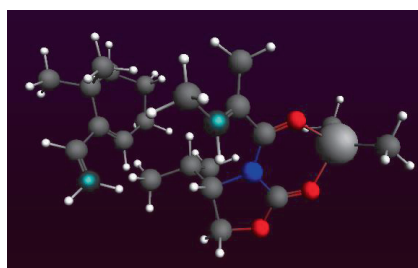
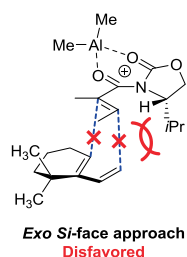


**Endo approach**  
**Disfavored**



**Exo Re-face approach**  
**Disfavored**





#### 4.8 References

- [1] World Health Organization. (2015) Global Tuberculosis Report. [http://apps.who.int/iris/bitstream/10665/191102/1/9789241565059\\_eng.pdf?ua=1](http://apps.who.int/iris/bitstream/10665/191102/1/9789241565059_eng.pdf?ua=1) (retrieved: 24/11/2015).
- [2] S. Sturgill-Koszycki, P. H. Schlesinger, P. Chakraborty, P. L. Haddix, H. L. Collins, A. K. Fok, R. D. Allen, S. L. Gluck, J. Heuser, D. G. Russell, *Science*, **1994**, 263, 678.
- [3] *The mycobacterial cell envelope* (Ed.: M. Daffé, J-M. Reyrat), ASM Press, Washington DC, **2008**.
- [4] R. S. Wallis, P. Kim, S. Cole, D. Hanna, B. B. Andrade, M. Maeurer, M. Schito, A. Zumla, *Lancet Infect. Dis.* **2013**, 13, 362.
- [5] E. Layre, L. Sweet, S. Hong, C. A. Madigan, D. Desjardins, D. C. Young, T-Y. Cheng, J. W. Annand, K. Kim, I. C. Shamputa, M. J. McConnell, C. A. Debona, S. M. Behar, A. J. Minnaard, M. Murray, C. E. Barry III, I. Matsunaga, D. B. Moody, *Chem. Biol.* **2011**, 18, 1537.
- [6] C. A. Madigan, T-Y Cheng, E. Layre, D. C. Young, M. J. McConnell, C. A. Debono, J. P. Murry, J-R. Wei, C. E. Barry III, G. M. Rodriguez, I. Matsunaga, E. J. Rubin, D. B. Moody, *Proc. Nat. Acad. Sci. USA* **2012**, 109, 1257.
- [7] E. Layre, H. L. Lee, D. C. Young, A. J. Martinot, J. Buter, A. J. Minnaard, J. W. Annand, S. M. Fortune, B. B. Snider, I. Matsunaga, E. J. Rubin, T. Alber, D. B. Moody, *Proc. Nat. Acad. Sci. USA* **2014**, 111, 2978.

- [8] D. C. Young, E. Layre, S-J. Pan, A. Tapley, J. Adamson, C. Seshadri, Z. Wu, J. Buter, A. J. Minnaard, M. Coscolla, S. Gagneux, R. Copin, J. D. Ernst, W. R. Bishai, B. B. Snider, D. B. Moody, *Chem. Biol.* **2015**, *22*, 516.
- [9] K. Pethe, D. L. Swenson, S. Alonso, J. Anderson, C. Wang, D. G. Russell, *Proc. Nat. Acad. Sci. USA* **2004**, *101*, 13642.
- [10] S. K. P. Lau, C-W. Lam, S. O. T. Curreem, K-C. Lee, C. C. Y. Lau, W-N. Chow, A. H. Y. Ngan, K. K. W. To, J. F. W. Chan, I. F. N. Hung, W-C. Yam, K-Y. Yuen, P. C. Y. Woo. *Emerg. Microbes Infect.* **2015**, *4*, e6 (doi: 10.1038/emi.2015.6)
- [11] S-J. Pan, A. Tapley, J. Adamson, T. Little, M. Urbanowski, K. Cohen, A. Pym, D. Almeida, A. Dorasamy, E. Layre, D. C. Young, R. Singh, V. B. Patel, K. Wallegren, T. Ndung'u, D. Wilson, D. B. Moody, W. Bishai, *J. Infect. Dis.* **2015**, *212*, 1827.
- [12] K. K. W. Kuan, H. P. Pepper, W. M. Bloch, J. H. George, *Org. Lett.* **2012**, *14*, 4710.
- [13] J. E. Spangler, C. A. Carson, E. J. Sorensen, *Chem. Sci.* **2010**, *1*, 202.
- [14] N. Mangel, F. M. Mann, M. L. Hillwig, R. J. Peters, B. B. Snider, *Org. Lett.* **2010**, *12*, 2626.
- [15] C. Nakano, T. Okamura, T. Sato, T. Dairi, T. Hoshino, *Chem. Commun.* **2005**, 1016. b) F. M. Mann, M. Xu, X. Chen, D. B. Fulton, D. G. Russell, R. J. Peters, *J. Am. Chem. Soc.* **2009**, *131*, 17526. c) a correction regarding reference 14b was published by the same authors: *J. Am. Chem. Soc.* **2010**, *132*, 10953.
- [16] a) S. Knapp, S. Sharma, *J. Org. Chem.* **1985**, *50*, 4996. b) S. P. Tanis, Y. M. Abdallah, *Synth. Commun.* **1986**, *16*, 251.
- [17] (a) D. Brohm, H. Waldmann, *Tetrahedron Lett.* **1998**, *39*, 3995. (b) D. Brohm, N. Philippe, S. Metzger, A. Bhargava, O. Müller, F. Lieb, H. Waldmann, *J. Am. Chem. Soc.* **2002**, *124*, 13171.
- [18] T. Yoon, S. J. Danishefsky, S. de Gala, *Angew. Chem. Int. Ed.* **1994**, *33*, 853.
- [19] For 6,6-dimethyl-1-vinylcyclohexene **6** as the diene, see ref 14, 15, 16b, 17, 18 and: a) H. Hosoi, N. Kawai, T. Suzuki, A. Nakazaki, K. Takao, K. Umezawa, S. Kobayashi, *Tetrahedron Lett.* **2011**, *52*, 4961. b) D. S. de Miranda, G. J. A. da Conceição, J. Zukerman-Schpector, M. A. Guerrero, U. Schuchardt, A. C. Pinto, C. M. Rezende, A. J. J. Marsaioli, *J. Braz. Chem. Soc.* **2001**, *12*, 391.
- [20] L. M. T. Frija, R. F. M. Frade, C. A. M. Afonso, *Chem. Rev.* **2011**, *111*, 4418.
- [21] G. Topcu, A. Ulubelen, T. C-M. Tam, C-T. Che, *J. Nat. Prod.* **1996**, *59*, 113.
- [22] For olefin isomerization using a)  $\text{RuCl}_3 \cdot \text{H}_2\text{O}$  see: K-S. Masters, B. L. Flynn *Org. Biomol. Chem.* **2010**, *8*, 1290. b) Grubbs II see: S. Hanessian, S. Giroux, A. Larsson, *Org. Lett.* **2006**, *8*, 5481. c) Schwartz reagent see: P. Wipf, H. Jahn, *Tetrahedron*, **1996**, *52*, 12853. d) Hoveyda-Grubbs II see: reference 22b. e) Wilkinson catalyst +  $\text{Et}_3\text{SiH}$  see: M. Tanaka, H. Mitsuhashi, M. Maruno, T. Wakamatsu, *Chem. Lett.* **1994**, *23*, 1455. f)  $\text{RuH}$  species see: G-J. Boons, A. Burton, S. Isles, *Chem. Commun.* **1996**, 141. g) Raney nickel see: T. Ohshima,



- R. Takita, S. Shimizu, D. Zhong, M. Shibasaki, *J. Am. Chem. Soc.* **2002**, *124*, 14546. h) PdCl<sub>2</sub>(MeCN)<sub>2</sub> see: C. B. de Koning, R. G. F. Giles, I. R. Green, N. M. Jahed, *Tetrahedron Lett.* **2002**, *43*, 4199. i) KOtBu see: PhD dissertation of Aditya L. N. R. Gottumukkala, *Palladium-catalyzed carbon-carbon bond formation under reductive, oxidative and neutral conditions*, University of Groningen, **2013**. j) Schlosser's base see: H. Turksma, H. Steinberg, T. H. J. de Boer, *Rec. Trav. Chim.* **1963**, *82*, 1057. k) Schlosser's base + TMEDA see: reference j. k) Borane see: H. C. Brown, M. V. Bhatt, *J. Am. Chem. Soc.* **1966**, *88*, 1440.
- [23] J. George, M. McArdle, J. E. Baldwin, R. M. Adlington, *Tetrahedron* **2010**, *66*, 6321.
- [24] D. A. Evans, K. T. Chapman, E. M. Carreira, *J. Am. Chem. Soc.* **1988**, *110*, 3560.
- [25] A. J. Boersma, R. P. Megens, B. L. Feringa, G. Roelfes, *Chem. Soc. Rev.* **2010**, *39*, 2083.
- [26] A. J. Boersma, B. L. Feringa, G. Roelfes, *Org. Lett.* **2007**, *9*, 3647.
- [27] PhD dissertation of Rik Megens, *DNA-Based Asymmetric Catalysis as a Synthetic Tool*, University of Groningen, **2012**, see page 87.
- [28] A. Dondoni, G. Fantin, M. Fogagnolo, A. Medici, P. Pedrini, *J. Org. Chem.* **1988**, *53*, 1748.
- [29] a) see reference 16. b) H. Kakisawa, M. Ikeda, *Nippon Kagaku Zasshi* **1967**, *88*, 476. c) D. M. Hollinshead, S. C. Howell, S. V. Ley, M. Mahon, N. M. Ratcliffe, P. A. Wothington, *J. Chem. Soc. Perkins I* **1983**, 1579.
- [30] K. A. Ahrendt, C. J. Borths, D. C. W. MacMillan, *J. Am. Chem. Soc.* **2002**, *122*, 4243.
- [31] H. Gotoh, Y. Hayashi, *Org. Lett.* **2007**, *9*, 2859.
- [32] M. S. Taylor, E. N. Jacobsen, *J. Am. Chem. Soc.* **2004**, *126*, 10558.
- [33] F. A. Kortman, M-C. Chang, E. Otten, E. P. A. Couzijn, M. Lutz, A. J. Minnaard, *Chem. Sci.* **2014**, *5*, 1322.
- [34] PhD dissertation of Felix A. Kortmann, *Dynamic Crystallization Processes of P-chiral Phosphine Oxides*, University of Groningen, **2014**.
- [35] a) D. A. Evans, S. J. Miller, T. Lectka, *J. Am. Chem. Soc.* **1993**, *115*, 6460. b) D. A. Evans, S. J. Miller, T. Lectka, P. von Matt, *J. Am. Chem. Soc.* **1999**, *121*, 7559.
- [36] a) Z. Li, K. R. Cosner, E. N. Jacobsen, *J. Am. Chem. Soc.* **1993**, *115*, 5326. b) Z. Li, R. W. Quan, E. N. Jacobsen, *J. Am. Chem. Soc.* **1995**, *117*, 5889.
- [37] J. Knol, A. Meetsma, B. L. Feringa, *Tetrahedron Asym.* **1995**, *6*, 1069.
- [38] a) T. Poll, G. Helmchen, *Tetrahedron Lett.* **1984**, *25*, 2191. b) T. Poll, J. O. Metter, G. Helmchen, *Angew. Chem. Int. Ed.* **1985**, *24*, 112. c) T. Poll, A. Sobczak, H. Hartmann, G. Helmchen, *Tetrahedron Lett.* **1985**, *26*, 3095.
- [39] a) W. Oppolzer, C. Chapuis, G. Bernardinelli, *Helv. Chim. Acta* **1980**, *67*, 1397. b) W. Oppolzer, *Tetrahedron* **1987**, *43*, 1969. c) W. Oppolzer, *Pure Appl. Chem.* **1988**, *60*, 39. d) W. Oppolzer, *Pure Appl. Chem.* **1990**, *62*, 1241.

- [40] a) D. A. Evans, K. T. Chapman, J. Bisaha, *J. Am. Chem. Soc.* **1984**, *106*, 4261. b) D. A. Evans, K. T. Chapman, J. Bisaha, *Tetrahedron Lett.* **1984**, *25*, 4071. c) D. A. Evans, K. T. Chapman, D. T. Hung, A. T. Kawaguchi, *Angew. Chem. Int. Ed.* **1987**, *26*, 1184.
- [41] PhD dissertation of N. Maugel, *Palladium-Catalyzed Alkylation, Arylation and Dehydrogenation of Unactivated C-H bonds. Syntheses of the Tetracyclic Aminoquinone Moiety of Marmycin A, (+/-)-Nosyberkol (Isotuberculosinol, Revised Structure of Edaxadiene), and (+/-)-Tuberculosinol*, Brandeis University, **2011**.
- [42] a) D. A. Evans, K. T. Chapman, J. Bisaha, *J. Am. Chem. Soc.* **1988**, *110*, 1238. For detailed studies into bidentate chelation of Lewis acids to *N*-acyloxazolidinones see: b) S. Castellino, W. J. Dwight, *J. Am. Chem. Soc.* **1993**, *115*, 2986. c) S. Castellino, *J. Org. Chem.* **1990**, *55*, 5197.
- [43] O. Miyata, T. Shinada, I. Ninomiya, T. Naito, *Tetrahedron*, **1997**, *53*, 2421.
- [44] L. Halab, L. Bélec, W. D. Lubell, *Tetrahedron*, **2001**, *57*, 6439.
- [45] M. Zhao, J. Li, Z. Song, R. Desmond, D. M. Tschaen, E. J. J. Grabowski, P. J. Reider, *Tetrahedron Lett.* **1998**, *39*, 5323.
- [46] E. J. Eisenbraun, *Org. Synth.* **1965**, *45*, 28.
- [47] a) M. S. Newman, *J. Am. Chem. Soc.* **1950**, *72*, 4783. b) H. A. Smith, J. P. McReynolds, *J. Am. Chem. Soc.* **1939**, *61*, 1963.
- [48] H. Tokuyama, S. Yokoshima, T. Yamashita, S-C. Lin, L. Li, T. Fukuyama, *J. Braz. Chem. Soc.* **1998**, *9*, 381.
- [49] C. Nakano, T. Hoshino, *ChemBioChem* **2009**, *10*, 2060.
- [50] a) T. Sato, T. Hoshino, *Biosci. Biotechnol. Biochem.* **2001**, *65*, 2233. b) T. Hoshino, T. Sato, *Chem. Commun.* **1999**, 2005.
- [51] a) V. J. Davisson, A. B. Woodside, T. R. Neal, K. E. Stremmer, M. Muehlbacher, C. D. Poulter, *J. Org. Chem.* **1986**, *51*, 4768. b) A. B. Woodside, Z. Huang, C. D. Poulter, *Org. Syn.* **1988**, *66*, 211.
- [52] J. W. Jones, R. K. Robins, *J. Am. Chem. Soc.* **1963**, *85*, 193.
- [53] V. C. Wasinger, M. Zeng, Y. Yau, *Int. J. Proteomics* **2013**, Article ID 180605.
- [54] For representative reviews on the Dimroth rearrangement see: a) T. Fujii, T. Itaya, *Heterocycles*, **1998**, *48*, 359. b) E. S. H. El Ashry, S. Nadeem, M. R. Sha, Y. El Kilany, *Adv. Heterocycl. Chem.* **2010**, *101*, 161. c) E. S. H. El Ashry, Y. El Kilany, N. Rashed, H. Assafir, *Adv. Heterocycl. Chem.* **1999**, *75*, 80.
- [55] a) D. A. Evans, J. S. Johnson, Chapter 33: Diels-Alder Reactions, in *Comprehensive Asymmetric Catalysis* (Ed.: E. N. Jacobsen, A. Pfaltz, H. Yamamoto), Springer-Verlag Berlin, Heidelberg, **1999**. b) L. C. Dias, *J. Braz. Chem. Soc.* **1997**, *8*, 289.
- [56] Y-H. Lam, P. H-Y. Cheong, J. M. Blasco Mata, S. J. Stanway, V. Gouverneur, K. N. Houk, *J. Am. Chem. Soc.* **2009**, *131*, 1947.

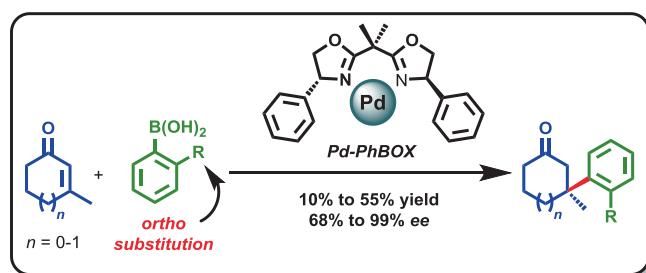
#### CHAPTER 4

---

- [57] G. te Velde, F. M. Bickelhaupt, E. J. Baerends, C. Fonseca Guerra, S. J. A van Gisbergen, J. G. Snijders, T. Ziegler, *J. Comput. Chem.* **2001**, *22*, 931.
- [58] a) A. D. Becke, *Phys. Rev. A* **1988**, *38*, 3098. b) J. P. Perdew, *Phys. Rev. B* **1986**, *33*, 8822.
- [59] a) D. Y. Curtin, *Rec. Chem. Prog.* **1954**, *15*, 111. b) J. I. Seeman, *Chem. Rev.* **1983**, *83*, 83. c) J. I. Seeman, *J. Chem. Ed.* **1986**, *63*, 42. d) J. F. Hartwig, *Organotransition metal chemistry: from bonding to catalysis*, University Science Books, Mill Valley, **2010**.
- [60] a) L. P. Wolters, F. M. Bickelhaupt, *WIREs Comput. Mol. Sci.* **2015**, *5*, 324. b) F. M. Bickelhaupt, *J. Comput. Chem.* **1999**, *20*, 114.
- [61] S. Hong, E. J. Corey, *J. Am. Chem. Soc.* **2006**, *128*, 1347.
- [62] T. Newhouse, P. S. Baran, R. W. Hoffmann, *Chem. Soc. Rev.* **2009**, *38*, 3010.
- [63] J. C. Swersey, L. R. Barrows, C. M. Ireland, *Tetrahedron Lett.* **1991**, *46*, 6687.
- [64] P. Rijo, C. Gaspar-Marques, M. F. Simões, M. L. Jimeno, B. Rodríguez, *Biochem. Syst. Ecol.* **2007**, *35*, 215.
- [65] R. Fathi-Afshar, T. M. Allen, *Can. J. Chem.* **1975**, *53*, 1690.
- [66] T. Nakatsu, D. J. Faulkner, G. K. Matsumoto, J. Clardy, *Tetrahedron Lett.* **1984**, *25*, 935.
- [67] S. De Rosa, A. Crispina, A. De Giulio, C. Iodice, P. Amodeo, T. Tancredi, *J. Nat. Prod.* **1999**, *62*, 1316.
- [68] A. Fukami, Y. Ikeda, S. Kondo, H. Naganawa, T. Takeuchi, S. Furuya, Y. Hirabayashi, K. Shimoike, S. Hosaka, Y. Watanabe, K. Umezawa, *Tetrahedron Lett.* **1997**, *38*, 1201.

## \*\*\* CHAPTER 5 \*\*\*

### ‡ Pd-catalyzed Asymmetric Conjugate Addition of Ortho-substituted Arylboronic Acids to Cyclic $\beta$ -substituted Enones ‡



**ABSTRACT:** In 2012 our laboratory developed the Pd-catalyzed asymmetric conjugate addition of arylboronic acids to cyclic  $\beta$ -substituted enones. Despite the success of the methodology ortho-substituted arylboronic acids were not tolerated in the reaction, limiting its scope. Our recent efforts, highlighted in this chapter, focused on the optimization of the catalytic system to allow reaction with ortho-substituted arylboronic acids, creating a sterically congested quaternary stereocenter. The methodology can potentially be applied in the total synthesis of several natural products, of which herbertenediol and enokipodin A and B were chosen as synthetic targets. This research also set the stage for a short asymmetric total synthesis of the symmetrical biaryl natural product mastigophorene A.

This chapter has been published in part:

J. Buter, R. Moezelaar, A. J. Minnaard, *Org. Biomol. Chem.* **2014**, *12*, 5883.

## 5.1 Introduction

The catalytic asymmetric construction of quaternary stereocenters is widely regarded as one of the major challenges in synthetic organic chemistry.<sup>[1]</sup> One efficient strategy to achieve this goal is the conjugate addition of carbon nucleophiles to  $\beta,\beta$ -disubstituted unsaturated carbonyl compounds.<sup>[2]</sup>

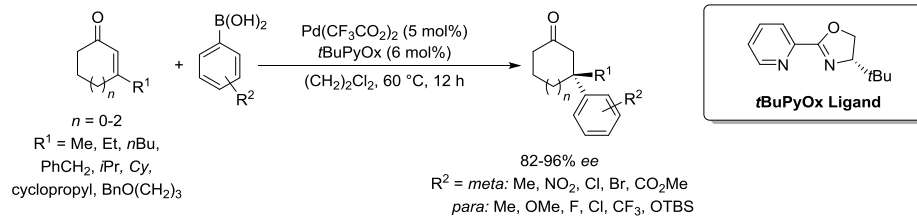
Employing asymmetric copper catalysis, the groups of Alexakis, Fillion and Hoveyda successfully added trialkylaluminum, dialkylzinc and alkyl Grignard reagents to a variety of  $\beta,\beta$ -disubstituted unsaturated electrophiles.<sup>[3]</sup> Though addition of the corresponding arylaluminum and arylzinc reagents was feasible, the general use of aryl Grignard reagents is still problematic due to their high reactivity. Moreover, the use of *ortho*-substituted aryl groups (either in the  $\beta,\beta$ -disubstituted unsaturated electrophile or in the organometallic reagent) is precarious, generally leading either to failure of the reaction, or low to moderate *ee*.<sup>[3q,r,v,y]</sup> A notable exception has been reported by Hoveyda and co-workers who obtained excellent enantioselectivities (>95%) with anisole and *o*-tolyl aluminum reagents.<sup>[3s]</sup> Alternatively, rhodium-catalyzed conjugate addition of organoboron reagents, developed by Hayashi and co-workers, has been employed, but also in these systems the use of *ortho*-substituted arylboronic acids is very limited.<sup>[4,5]</sup>

In 2011, the Stoltz laboratory reported the first asymmetric palladium-catalyzed conjugate addition of arylboronic acids to cyclic  $\beta,\beta$ -disubstituted enones using *t*BuPyOx as the ligand.<sup>[6]</sup> Shortly thereafter we reported the asymmetric Michael addition of arylboronic acids to cyclic  $\beta,\beta$ -disubstituted enones and lactones, catalyzed by PdCl<sub>2</sub>-PhBOX (Scheme 1).<sup>[7]</sup> Both systems showed high enantioselectivities, high yields, broad functional group tolerance, mild reaction conditions and a considerable scope in both the cyclic Michael acceptor and the arylboronic acid. In addition, in both systems the reactions can be carried out in air. However, to date, the successful application of a broad range of *ortho*-substituted arylboronic acids has not been reported,<sup>[8]</sup> although the Stoltz laboratory managed the asymmetric conjugate addition of *o*-fluoro arylboronic acid to 3-methyl cyclohex-2-enone in an enantiomeric excess of 77%. A quaternary center vicinal to an *ortho*-substituted phenyl ring is a very congested situation indeed.

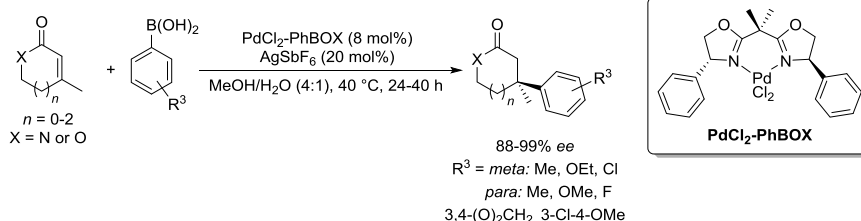
Very recently, Sigman and co-workers reported the asymmetric Pd-catalyzed remote benzylic quaternary stereocenter formation using arylboronic acids.<sup>[9]</sup> A broad substrate scope, consisting exclusively of linear substrates, was reported with very good to excellent enantioselectivities (86-98% *ee*), and yields generally ranging from 50 to 80%. However, when using the *ortho*-substituted *o*-tolylboronic acid and dibenzofuran-4-boronic acid the yields dropped significantly to 35% and 25% respectively, showing the problems associated with *ortho*-substitution.

**Pd-catalyzed Asymmetric Conjugate Addition of *Ortho*-substituted Arylboronic Acids**

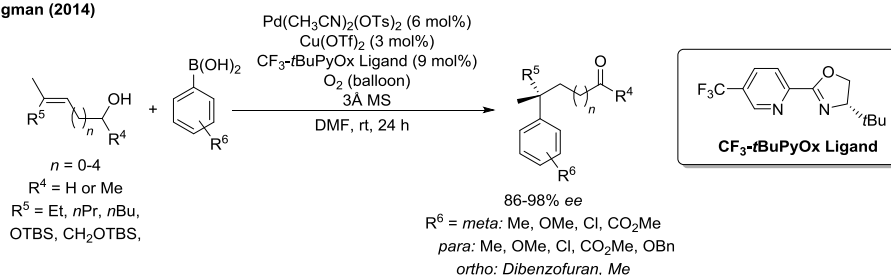
**Stoltz (2011)**



**Our Work (2012)**



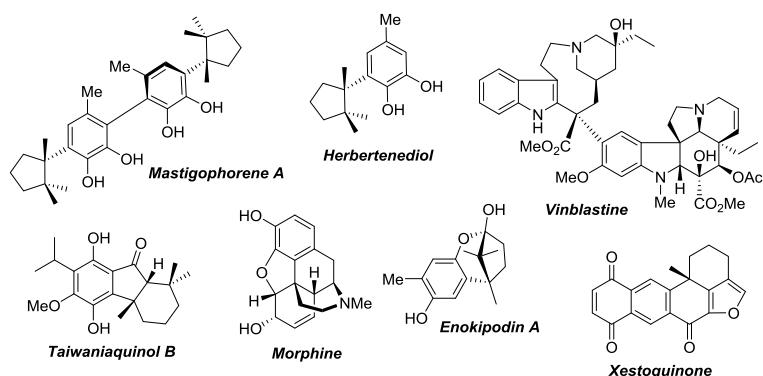
**Sigman (2014)**



**Scheme 1.** The current state of the art (up to April 2014) in Pd-catalyzed asymmetric Michael additions to create benzylic quaternary stereocenters.

Asymmetric synthesis of benzylic quaternary centers with *ortho*-substitution is desired, since many natural products bear such a moiety, several of which are presented in Scheme 2. We also envision this transformation beneficial in the sense that direct installation of the *ortho*-substituted benzylic stereocenter can significantly shorten synthetic endeavors to such natural products.

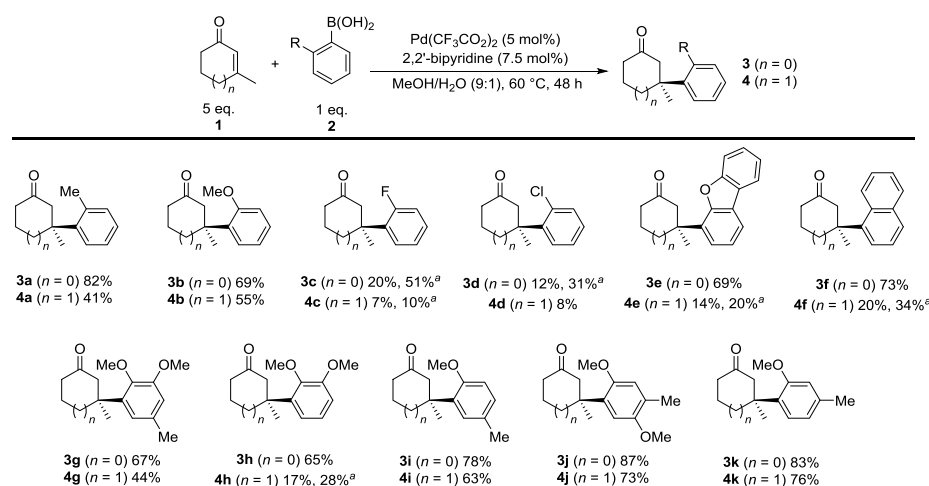
Here, we present the palladium-catalyzed conjugate addition of *ortho*-substituted arylboronic acids to  $\beta$ -methyl substituted cyclic enones, both in an asymmetric and a racemic fashion. The developed methodology is applied in the total synthesis of the sterically congested, biologically active, sesquiterpenes herbertenediol and enokipodin A and B.



**Scheme 2.** Selected natural products bearing *ortho*-substituted benzylic quaternary stereocenters.

## 5.2 Development of the asymmetric Pd-catalyzed conjugate addition of *ortho*-substituted arylboronic acids to $\beta,\beta$ -Disubstituted cyclic enones

In a recent report,<sup>[10]</sup> we showed efficient conjugate addition to cyclic  $\beta$ -substituted enones employing 1 mol% of a  $\text{Pd}(\text{CF}_3\text{CO}_2)_2/2,2$ -bipyridine catalyst, two equivalents of boronic acid, at 60 °C for 18 h. Under these conditions the use of *ortho*-substituted arylboronic acids was fruitless, leading only to trace amounts of product. It was reasoned, however, that increasing the catalyst loading from 1 mol% to 5 mol%, extending the reaction time and changing the stoichiometry of the reaction (7 equivalents of enone instead of 2 equivalents of boronic acid)<sup>[11]</sup> could change this situation. This indeed proved to be the case, and a wide range of *ortho*-substituted arylboronic acids could be employed in the conjugate addition (Scheme 3).



**Scheme 3.** Racemic Pd-catalyzed conjugate addition of *ortho*-substituted arylboronic acids to  $\beta$ -methyl cyclic enones. <sup>a</sup> Double catalyst loading.

### *Pd-catalyzed Asymmetric Conjugate Addition of Ortho-substituted Arylboronic Acids*

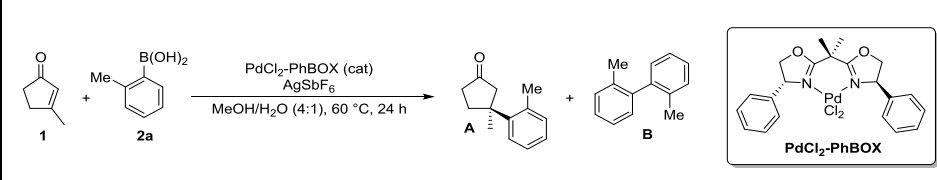
As evident from Scheme 3, the Michael additions to 3-methyl cyclopent-2-enone generally gave satisfying results. As expected, an increase in the steric bulk of the *ortho*-substituent led to diminished yields, but in the case of the relatively small *ortho*-fluoro and *ortho*-chloro arylboronic acids low yields were obtained as well (20% and 12% respectively for **3c** and **3d**). These low yields might be attributed to electronic effects, thus in order to achieve acceptable yields for these substrates the catalyst loading was doubled to 10 mol% leading to 51% and 31% isolated yield for *ortho*-fluoro and *ortho*-chloro phenylboronic acid, respectively.

With these results in hand, we expanded the reaction scope in the Michael acceptor to 3-methyl cyclohex-2-enone. In all cases the isolated yields significantly dropped, though *ortho*-methyl, *ortho*-methoxy, and 2-methoxy-5-methyl phenylboronic acid (see **4a**, **4b** and **4i**) gave acceptable yields (41%, 55% and 63% respectively). In contrast with 3-methyl cyclopent-2-enone, doubling of the catalyst loading did not always result in significantly better yields. In the case of *ortho*-chloro phenylboronic acid (see **4d**) only 8% of the desired product was isolated after two days of reaction, which clearly indicates the limits of this approach.

The conjugate addition of *ortho*-substituted arylboronic acids to 3-methyl cyclohept-2-enone was shortly investigated but did not lead to yields over 10% using 8 mol% of catalyst. This result is surprising to us since in our previously reported system, 3-methyl cyclohept-2-enone was tolerated as a substrate (using phenylboronic acid).<sup>[10]</sup> Since no electronic reasons can be given to describe the failure of the reaction, we attribute this to steric hindrance.

With the Michael addition of *ortho*-substituted arylboronic acids to cyclic  $\beta$ -disubstituted enones accomplished, we had the ambition to develop an asymmetric variant of this transformation using our previously developed catalyst. This reaction is expected to be significantly more challenging since steric interactions are more pronounced in enantioselective catalysis. Initial studies using *o*-tolylboronic acid, employing 15 mol% of catalyst PdCl<sub>2</sub>-PhBOX, and 40 mol% AgSbF<sub>6</sub> at 60 °C, clearly showed this was the case since the impurity profile of the reaction was dominated by homo-coupling of the arylboronic acid. Therefore we set out to optimize the reaction to reduce this unwanted side product (Table 1).





Entry	Strategy	Cat (mol%)	Ag-salt (mol%)	Additive	A:B ratio <sup>a</sup>
1	Previous conditions <sup>[7]</sup>	15	AgSbF <sub>6</sub> (40 mol%)	-	1:5
2	Lewis Acid Activation	15	AgSbF <sub>6</sub> (40 mol%)	<i>i.e.</i> Sc(OTf) <sub>3</sub> , Yb(OTf) <sub>3</sub> , In(OTf) <sub>3</sub> , Ce(OTf) <sub>3</sub> (40 mol%)	1:4
3	Change of stoichiometry	15	AgSbF <sub>6</sub> (40 mol%)	Enone (7 eq)	2.5:1
4	Dichloroethane as solvent <sup>[6]</sup>	15	AgCF <sub>3</sub> CO <sub>2</sub> (40 mol%)	NH <sub>4</sub> PF <sub>6</sub> (40 mol%) H <sub>2</sub> O (8 eq)	20:1
5		8	AgCF <sub>3</sub> CO <sub>2</sub> (20 mol%)	NH <sub>4</sub> PF <sub>6</sub> (40 mol%) H <sub>2</sub> O (8 eq)	18:1
6		4	AgCF <sub>3</sub> CO <sub>2</sub> (10 mol%)	NH <sub>4</sub> PF <sub>6</sub> (40 mol%) H <sub>2</sub> O (8 eq)	12:1
7		4	AgCF <sub>3</sub> CO <sub>2</sub> (10 mol%)	NH <sub>4</sub> PF <sub>6</sub> (40 mol%) H <sub>2</sub> O (8 eq)	3.5:1

Reaction conditions: The arylboronic acid and the palladium catalyst were mixed. A solution of enone in solvent was added. The silver salt was added either as a solid or in an aqueous solution. The reactions were performed at 60 °C. <sup>a</sup> The A:B ratio was determined by GC-MS analysis.

**Table 1.** Optimization of the reaction conditions in the conjugate addition of ortho-tolylboronic acid to  $\beta$ -methyl cyclopentenone.

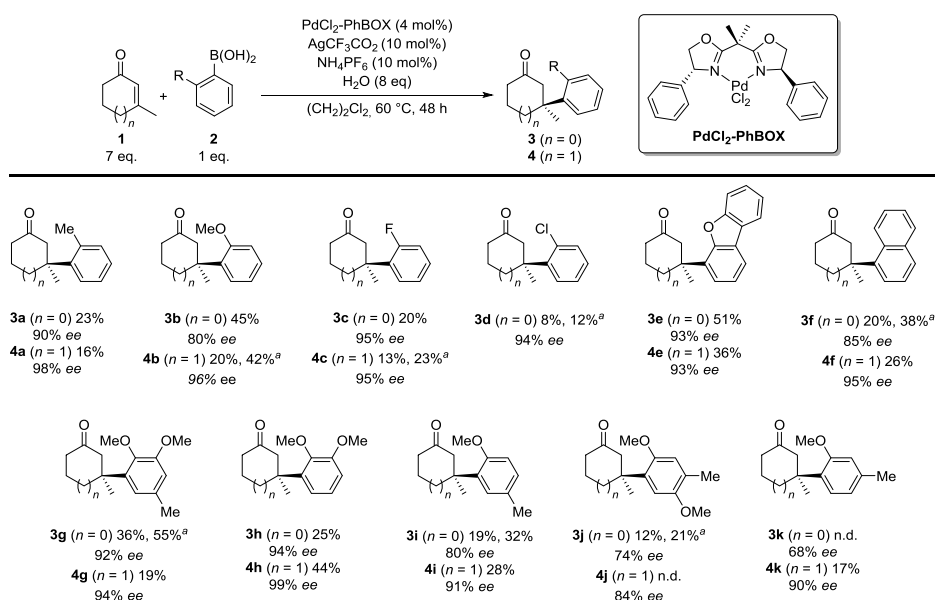
Lewis acid activation of the enone increases its reactivity as a Michael acceptor. The use of 40 mol% of either Mg, Zn, Fe or Cu triflate gave negligible results and therefore the stronger coordinating rare-earth metal triflates Sc(OTf)<sub>3</sub>, Yb(OTf)<sub>3</sub>, In(OTf)<sub>3</sub>, and Ce(OTf)<sub>3</sub> were applied. A slight enhancement of the product versus homo-coupling ratio was observed but still the reaction was greatly in favor of the latter. Homo-coupling of arylboronic acids is generally observed using Pd-catalysis,<sup>[12]</sup> and can be counterbalanced by changing the stoichiometry of the reaction, applying the reaction partner in excess.<sup>[13]</sup> As  $\beta$ -methyl cyclopentenone and  $\beta$ -methyl cyclohexenone are less expensive than most arylboronic acids, this is an attractive approach. Using three equivalents of enone, the product ratio changed to 1.5 : 1 in favor of the Michael adduct. A further enhancement to 2 : 1 was observed using five equivalents of enone and ultimately a 2.5 : 1 ratio was found using seven equivalents.

During this optimization process, Stoltz and Houk reported a mechanistic investigation of the Pd-catalyzed asymmetric Michael addition of arylboronic acids to enones.<sup>[14]</sup> It was shown that the chemical yields previously obtained, could be enlarged by adding

***Pd-catalyzed Asymmetric Conjugate Addition of Ortho-substituted Arylboronic Acids***

$\text{NH}_4\text{PF}_6$  (30 mol%) and water (5 eq) to their system. We adopted these conditions by changing the solvent from MeOH/ $\text{H}_2\text{O}$  to dichloroethane, and the silver salt from  $\text{AgSbF}_6$  to  $\text{AgCF}_3\text{CO}_2$  to obtain a similar system, still using 7 eq of the enone.<sup>[15]</sup> This proved to be highly beneficial for the formation of the Michael adduct since the product ratio dramatically increased to 20:1. With this result in hand, the catalyst loading was lowered to 8 mol% leading to a slight decrease of the product ratio (18:1). Further reduction to 4 mol% of catalyst resulted in a respectable 12:1 ratio in favor of the Michael adduct, however at the cost of longer reaction times. Finally we also attempted to reduce the number of additives ( $\text{AgCF}_3\text{CO}_2$  and  $\text{NH}_4\text{PF}_6$ ) by combining them in the form of  $\text{AgPF}_6$ . Surprisingly, this led to an unaccountable lowering of the product ratio to 3.5 : 1.

With the reaction conditions optimized, the scope of the reaction was studied (Scheme 4). An immediate observation was that very good to excellent enantioselectivities were obtained, albeit that the isolated yields were moderate, and in some cases low. For some reactions (see **4b**, **4c**, **3f**, **3i** and **3j**), due to the initially low isolated yield, the catalyst loading was doubled. This led, as expected, to an approximate doubling of the yield. Interestingly, in some cases (see **3f** vs. **4f**, **3h** vs. **4h**, **3i** vs. **4i** and **3k** vs. **4k**) addition to 3-methyl cyclohex-2-enone gave higher yields than addition to 3-methyl cyclopent-2-enone. These results are in contrast to the conjugate addition reactions with the bipyridine system (Scheme 3). It is also notable that the conjugate additions to 3-methyl cyclohex-2-enone give equal or higher enantiomeric excesses (up to 22% *ee* higher, see **3k** vs. **4k**) than the additions to 3-methyl cyclopent-2-enone.



**Scheme 4.** Asymmetric Pd-catalyzed conjugate addition of arylboronic acids to  $\beta$ -methyl cyclic enones. <sup>a</sup> reactions were performed with double catalyst and Ag-salt loading.

## CHAPTER 5

The general observation that the yields are higher, and *ee*'s are lower, for conjugate additions to cyclopentenone compared to cyclohexenone are speculated to be the consequence of steric hindrance. The chiral environment of the catalyst allows "easy" access of the cyclopentenone (faster reaction, higher yield) but with a decreased facial bias (lower *ee*). On the other hand, cyclohexenone does not enter the chiral environment of the catalyst that easily (slower reaction, more protodeboronation) but when it does, it does so with an increased facial bias.

The moderate yields were found to result from significant protodeboronation of the boronic acids. According to literature, this side reaction can be attributed to multiple factors, especially when taken into account the low reaction rate of the asymmetric Michael addition. Given the conditions of the conjugate addition, protodeboronation<sup>[16a, 12b]</sup> might be associated with: 1) Pd-catalyzed protodeboronation<sup>[16c]</sup> 2) Ag-catalyzed protodeboronation<sup>[16d-h]</sup> 3) heat-induced protodeboronation<sup>[16i-j]</sup> 4) fluoride-mediated protodeboronation (with  $\text{PF}_6^-$  as a potential  $\text{F}^-$  source)<sup>[16k,l]</sup> 5) acid-catalyzed protodeboronation<sup>[16m-o]</sup> and finally 6) water-induced protodeboronation.<sup>[16p]</sup> It is likely that more than one of these factors plays an important role here but we were not able to suppress this unwanted side reaction.<sup>[17]</sup>

That the moderate yields obtained here do not stand out, is apparent from a recent report by the Sigman group, as discussed earlier.<sup>[9]</sup> For their asymmetric Pd-catalyzed remote benzylic quaternary stereocenter formation using arylboronic acids, the yields are typically 50-80%, however when using *o*-tolylboronic acid and dibenzofuran-4-boronic acid the yields dropped significantly to 35% and 25% respectively.

Despite significant protodeboronation, the substrate scope is respectable, although some *ortho*-substituted arylboronic acids and functionalized enones failed to react (Figure 1). It is not surprising that larger *ortho*-substituents such as CHO, NO<sub>2</sub>, CF<sub>3</sub>, *i*Pr and CO<sub>2</sub>Me impeded the reaction. In addition, di-*ortho* substitution was not tolerated. Variation of the five-membered enone in terms of substitution at the  $\alpha$ - or  $\gamma$ -position also led to failure of reaction, as did substituting the  $\alpha'$ -position of 3-methyl cyclohex-2-enone with a geminal dimethyl moiety.

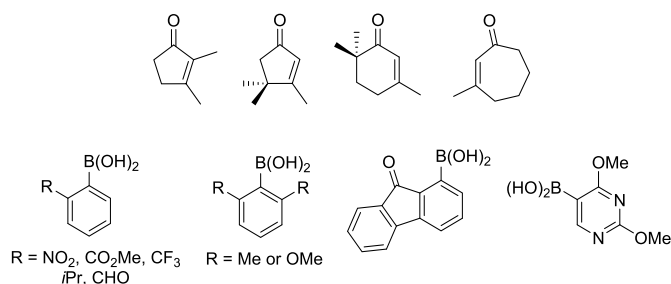


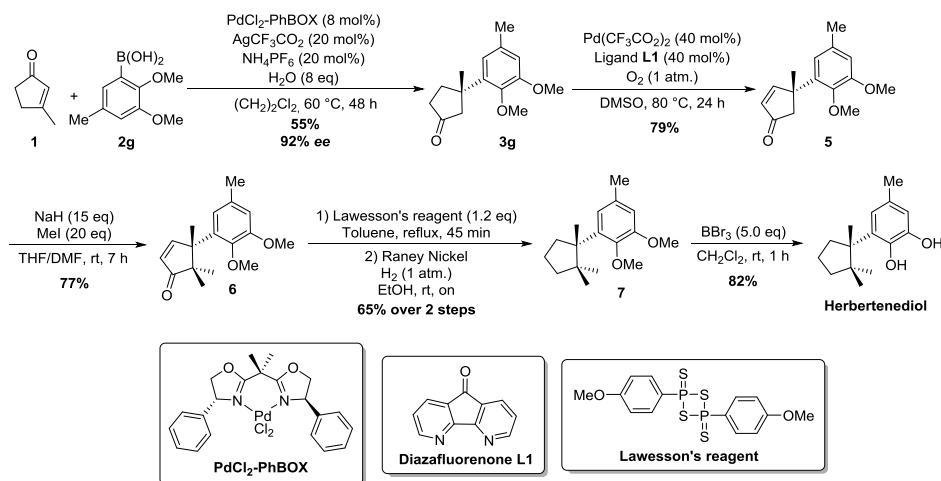
**Figure 1.** Unreactive substrates and boronic acids in the Pd-catalyzed asymmetric Michael addition.

### 5.3 The shortest asymmetric total syntheses of herbertenediol and enokipodin A and B

Being able to construct the sterically very congested motif of an *ortho*-substituted arene connected to a quaternary stereocenter created the opportunity for the asymmetric total synthesis of the biologically active natural products herbertenediol, enokipodin A, and B. Herbertenediol is a sesquiterpene isolated from the liverworts *Herberta adunca*<sup>[18]</sup> and *Radula perrottetii*,<sup>[19]</sup> and has been subjected to biological studies, which showed potent anti-lipid peroxidation activity in rat brain homogenates (100% inhibition at 1  $\mu\text{g/mL}$ ).<sup>[20]</sup>

To date, seven (!) asymmetric syntheses of herbertenediol have been reported,<sup>[21]</sup> with the shortest route reported by Abad and co-workers<sup>[21d]</sup> comprising ten linear steps. Here the quaternary stereocenter was introduced by means of substrate control, as in the approach of Lin<sup>[21e]</sup> and Kita *et al.*<sup>[21f,g]</sup> The Bringmann laboratory employed a kinetic resolution,<sup>[21b]</sup> as did the Monti group,<sup>[21h]</sup> to furnish enantiopure material. Meyers<sup>[21a]</sup> and Fukuyama<sup>[21c]</sup> relied on the use of a chiral auxiliary. We reasoned that direct introduction of the quaternary stereocenter by means of an asymmetric conjugate addition of a suitable substituted phenylboronic acid allowed to shorten the synthesis of herbertenediol considerably.

The synthesis of herbertenediol started with the asymmetric conjugate addition of 2,3-dimethoxy-5-methyl phenylboronic acid **2g** to 3-methyl cyclopentenone employing 8 mol% of PdCl<sub>2</sub>-PhBOX, and afforded the desired Michael adduct **5** in 55% yield and high enantioselectivity (92% *ee*, Scheme 5). In order to selectively install the geminal dimethyl moiety without generating (hard to separate) regioisomers, **3g** was subjected to an oxidative dehydrogenation. Initially, several stoichiometric oxidation procedures (DDQ,<sup>[22]</sup> IBX,<sup>[23]</sup> and iodic acid<sup>[24]</sup>) were applied, which led to low isolated yields (<30%) and over-oxidized products.<sup>[25]</sup> A suitable alternative was found in the Pd(CF<sub>3</sub>CO<sub>2</sub>)<sub>2</sub>/4,5-diazafluorenone **L1** catalyzed oxidation, recently developed by Stahl and co-workers.<sup>[26]</sup> Stahl reported cyclopentenone oxidation with oxygen (7.2 bar, 9% in N<sub>2</sub>) using 5 mol% of catalyst, whereas catalyst decomposition was observed at atmospheric pressure. Also in the current case, oxidation of **3g** at atmospheric pressure led to catalyst decomposition and only 15% conversion (GC-MS) was observed after 12 and 24 h. For practical reasons we decided to increase the catalyst loading to 40 mol%, at atmospheric oxygen pressure, which yielded 79% of enone **5**.



**Scheme 5.** A short asymmetric total synthesis of herbertenediol.

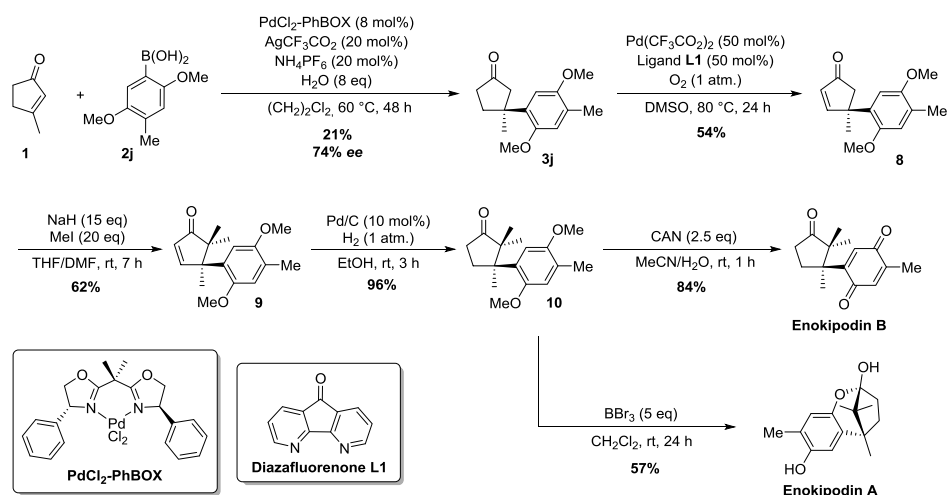
With **5** in hand, a one-pot geminal dimethylation as described by Srikrishna was employed yielding 77% of **6**.<sup>[27]</sup> In order to acquire fully reduced product **7**, several procedures were considered. Deoxygenation by means of a classic Wolff-Kishner reduction was reported to be problematic in related systems and was therefore rejected.<sup>[28]</sup> Deoxygenation employing a Mazingo reduction (thioketalization/Raney nickel desulfurization with the saturated analogue of **6**) also has been reported to be problematic,<sup>[21a]</sup> although it was successfully applied recently in a very similar system.<sup>[27]</sup> To clarify these contradicting literature reports we performed the reaction under similar conditions as reported.<sup>[27]</sup> In our hands the reaction proved to be extremely slow and prone to side product formation, leading to an inseparable mixture of mainly oligomeric products, and only minor amounts of desired product. This observation is in line with a very recent report by Yoshida and co-workers, who also encountered reproducibility issues.<sup>[29]</sup> Alternatively, Meyers and co-workers described a reduction protocol in which **6** was converted into the corresponding thioketone and was subsequently reduced with Raney nickel (Ra/Ni), leading to **7** in 58% yield over the two steps.<sup>[21a]</sup> This strategy proved to be reproducible in our hands, providing us with **7** in 65% yield. An important, previously not reported, observation was that freshly prepared Ra/Ni had to be used for reproducible results. With commercial Ra/Ni, the reaction did not provide the desired product. This is likely due to the high activity of freshly prepared Ra/Ni (in which H<sub>2</sub> is adsorbed on the catalyst) compared to commercial Ra/Ni (no absorbed H<sub>2</sub> for safe shipment). Demethylation using BBr<sub>3</sub> then furnished herbertenediol in 82% yield, in a total of six steps, the shortest asymmetric synthesis to date.<sup>[30]</sup>

In 2000, the sesquiterpenes enokipodin A and B were isolated from the culture broth of the edible mushroom “enokidake” (*Flammulina velutipes*).<sup>[31]</sup> It was found that these

*Pd-catalyzed Asymmetric Conjugate Addition of Ortho-substituted Arylboronic Acids*

oxidized  $\alpha$ -cuparenone-type compounds possess antimicrobial activity against *Cladosporium herbarum* and *Bacillus subtilis*.<sup>[32]</sup> However, it is mainly their sterically congested structure that has attracted the synthetic community to embark on asymmetric syntheses of these molecules.<sup>[33]</sup> Two of the three endeavors produced enokipodin B in a longest linear sequence of eleven steps, and one additional step for the enokipodin A synthesis. Kuwahara's approach was based on the use of a chiral auxiliary<sup>[33c,d]</sup> whereas Yoshida installed the quaternary stereocenter by substrate control.<sup>[33b]</sup> In the most recent, ten step formal, enokipodin B synthesis, Hoveyda directly installed the benzylic quaternary center using an elegant multicomponent Ni-, Zr-, and Cu-catalyzed strategy.<sup>[33a]</sup>

Our synthesis of enokipodin A and B started with the asymmetric Michael addition of boronic acid **2j** to 3-methyl cyclopent-2-enone, yielding **3j** in 21% yield and a good enantioselectivity of 74% *ee* (Scheme 6). Introduction of the  $\alpha,\beta$ -unsaturation was subsequently achieved using the previously described Pd(CF<sub>3</sub>CO<sub>2</sub>)<sub>2</sub>/4,5-diazafluorenone catalyzed oxidation, in 54% yield. Dimethylation followed by hydrogenation of enone **9** gave ketone **10** (60% yield over two steps), a common synthetic intermediate to access the desired natural products. Indeed, enokipodin A and B were both readily obtained in just one step, from **10** by either a cerium ammonium nitrate oxidation, leading to enokipodin B in 84% yield, or a BBr<sub>3</sub> mediated demethylation, providing enokipodin A in 57% yield. Though not the synthesis with the highest enantiomeric excess, we did manage to reduce the longest linear sequence from ten (enokipodin B) and eleven (enokipodin A) to only five steps.



**Scheme 6.** Asymmetric total synthesis of enokipodin A and enokipodin B.

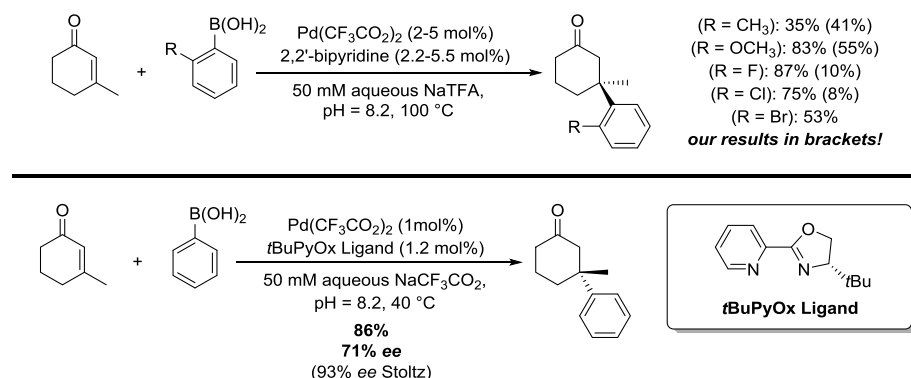
## 5.4 Conclusion

In summary, we successfully incorporated *ortho*-substituted arylboronic acids in both the non-stereoselective as well as the asymmetric Pd-catalyzed Michael addition to  $\beta$ -disubstituted cyclic enones. In the non-stereoselective reaction, good yields are generally obtained with 3-methyl cyclopent-2-enone as the substrate and moderate yields with 3-methyl cyclohex-2-enone. In the asymmetric reaction, very good to excellent enantioselectivities are obtained, although yields stay moderate. Nevertheless, based on this method, the asymmetric total synthesis of the biologically active sesquiterpenes herbertenediol (92% *ee*), enokipodin A and enokipodin B (74% *ee*) was achieved with routes that are considerably shorter than previously reported.

## 5.5 Discussion and outlook

The development of this catalytic methodology originated from the idea to embark on the shortest asymmetric total synthesis of mastigophorene A and B (see chapter 6). The reaction served its purpose in the total synthesis of herbertenediol, the monomeric unit of the mastigophorenes A and B. However, when reflecting on our efforts to achieve an efficient catalytic method, we do need to address the problems associated with the low to moderate isolated yields. As shown in this chapter the original catalytic procedure for conjugate addition to cyclic 3-methyl enones (Scheme 1),<sup>[7]</sup> had to be drastically altered in order to produce the desired products. We did however struggle in gaining control over unwanted protodeboronation of the arylboronic acid. In retrospect, changing the original reaction medium (MeOH/H<sub>2</sub>O 4:1) to dichloroethane also provides the opportunity to re-investigate<sup>[7,10]</sup> the use of potassium aryl trifluoroborates, potassium trihydroxyarylborates or phenyl *N*-methyliminodiacetic acid (MIDA) arylboronates as alternative arylboronic acid sources.

In a recent effort Van Zeeland and Stanley did show some promising results in achieving efficient construction of sterically congested bisbenzylic and *ortho*-substituted benzylic quaternary centers (Scheme 7).<sup>[34]</sup>



**Scheme 7.** Pd-catalyzed conjugate additions in an aqueous NaCF<sub>3</sub>CO<sub>2</sub> medium.

Racemic conjugate additions of five *ortho*-substituted arylboronic acids were performed using aqueous NaCF<sub>3</sub>CO<sub>2</sub>, at pH 8.2, as the reaction medium. The results generally show considerably higher isolated yields compared to ours and it was postulated that the reactivity of the Pd-catalyst is enhanced by the use of the aqueous NaCF<sub>3</sub>CO<sub>2</sub> medium. Additionally the conditions were also shown to be suitable in the asymmetric variant using Stoltz' catalytic system.<sup>[6]</sup> Some chiral induction was lost however, as the enantiomeric excess of 71% was somewhat lower than the 93% originally reported by the Stoltz laboratory.

When re-investigation of our developed methodology is aspired, the conditions reported by Van Zeeland and Stanley might serve as a good starting point. The high reaction temperatures needed for construction of the *ortho*-substituted benzylic quaternary center does raise the question however whether it will be useful in the development of an asymmetric variant. High temperatures are generally avoided in asymmetric catalysis as stereochemical induction by the catalyst might erode, although there are exceptions.<sup>[35]</sup>

## 5.6 Experimental section

### General methods:

All reactions were performed using oven-dried glassware (except the screw cap vials) under an atmosphere of nitrogen (unless otherwise specified) by standard Schlenk techniques, using dry solvents. Reaction temperature refers to the temperature of the oil bath.

Solvents were taken from a MBraun solvent purification system (SPS-800). All other reagents were purchased from Sigma-Aldrich, Acros, TCI Europe, Combi-Blocks, Strem or Fluorochem and used without further purification unless noted otherwise. Silver hexafluoroantimonate (AgSbF<sub>6</sub>), silver hexafluorophosphate (AgPF<sub>6</sub>), and silver trifluoroacetate (AgCF<sub>3</sub>CO<sub>2</sub>) were stored in a nitrogen dry-box in the absence of light. The bisoxazoline ligand used was stored at -20 °C. PdCl<sub>2</sub>-(*R,R*-PhBOX) catalyst was prepared as described and stored in the fridge at 4 °C.

TLC analysis was performed on Merck silica gel 60/Kieselguhr F254, 0.25 mm. Compounds were visualized using either Seebach's stain (a mixture of phosphomolybdic acid (25 g), cerium (IV) sulfate (7.5 g), H<sub>2</sub>O (500 mL) and H<sub>2</sub>SO<sub>4</sub> (25 mL)), a KMnO<sub>4</sub> stain (K<sub>2</sub>CO<sub>3</sub> (40 g), KMnO<sub>4</sub> (6 g), H<sub>2</sub>O (600 mL) and 10% NaOH (5 mL)), an Alizarin stain<sup>[36]</sup> or elemental iodine.

Flash chromatography was performed using SiliCycle silica gel type SiliaFlash P60 (230 – 400 mesh) as obtained from Screening Devices or with automated column chromatography using a Reveleris flash purification system purchased from Grace Davison Discovery Sciences.

<sup>1</sup>H- and <sup>13</sup>C-NMR spectra were recorded on a Varian AMX400 or a Varian 400-MR (400 and 101 MHz, respectively) using CDCl<sub>3</sub> or DMSO-*d*<sub>6</sub> as solvent, unless stated otherwise. Chemical shift values are reported in ppm with the solvent resonance as the internal standard (CDCl<sub>3</sub>: δ 7.26 for <sup>1</sup>H, δ 77.16 for <sup>13</sup>C, DMSO-*d*<sub>6</sub> δ 2.50 for <sup>1</sup>H). Data



## CHAPTER 5

are reported as follows: chemical shifts ( $\delta$ ), multiplicity (s = singlet, d = doublet, dd = double doublet, ddd = double double doublet, td = triple doublet, t = triplet, q = quartet, b = broad, m = multiplet), coupling constants  $J$  (Hz), and integration.

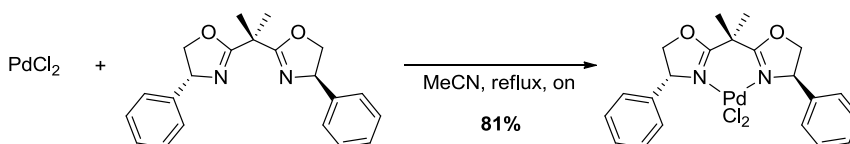
GC-MS measurements were performed with an HP 6890 series gas chromatography system equipped with a HP 5973 mass sensitive detector. GC measurements were made using a Shimadzu GC 2014 gas chromatograph system bearing a AT5 column (Grace Alltech) and FID detection

Enantiomeric excesses were determined by chiral HPLC analysis using a Shimadzu LC-10ADVP HPLC instrument equipped with a Shimadzu SPD-M10AVP diode-array detector. Integration at three different wavelengths (254, 225, 190 nm) was performed and the reported enantiomeric excess is an average of the three integrations. Retention times ( $t_R$ ) are given in min.

High resolution mass spectra (HRMS) were recorded on a Thermo Scientific LTQ Orbitrap XL. Optical rotations were measured on a Schmidt+Haensch polarimeter (Polartronic MH8) with a 10 cm cell (c given in g/mL) at ambient temperature ( $\pm 20$  °C).

### General procedure for the racemic conjugate additions:

To a 4 mL vial with Teflon-coated screw cap was added 2,2'-bipyridine (0.05 mmol, 7.5 mol%) and palladium trifluoroacetate (0.033 mmol, 5 mol%). The solids were dissolved in a pre-mixed MeOH/H<sub>2</sub>O (9:1) solution (2 mL) and the vial was placed in a pre-heated oil bath at 60 °C and stirred for 15 min. The solution was cooled to rt and the  $\alpha,\beta$ -unsaturated ketone (3.33 mmol, 5 eq) and the boronic acid (0.66 mmol, 1 eq), dissolved in a solution of MeOH/H<sub>2</sub>O (9:1, 1 mL) were added. The reaction was stirred at 60 °C for 48 h. The crude mixture was flushed over a short silica plug and the elute was dried over MgSO<sub>4</sub>, filtered and concentrated under reduced pressure. Then the mixture was purified by flash chromatography with pentane : ether as the eluent.



### PdCl<sub>2</sub>-(*R,R*-PhBOX) catalyst:

To an oven-dried Schlenk flask charged with palladium(II) chloride (520 mg, 2.93 mmol) was added a solution of (4*R*,4'*R*)-2,2'-(propane-2,2-diyl)bis(4-phenyl-4,5-dihydrooxazole) (1.00 g, 2.99 mmol, 1.02 eq) in dry MeCN (15 mL). An additional 10 mL of dry MeCN was used to rinse the walls of the flask. The Schlenk flask was equipped with a reflux condenser and the reaction was refluxed for 3.5 h. Over time an orange-red suspension formed which after the reaction was cooled to 0 °C with an ice-bath and filtered through a glass-filter (pore-size 4). The residue was washed twice with pentane and dried under an N<sub>2</sub> atmosphere. PdCl<sub>2</sub>-(*R,R*-BOX) catalyst (1.22 g, 2.38 mmol, 81% yield) was isolated as an orange solid.

### ***Pd-catalyzed Asymmetric Conjugate Addition of Ortho-substituted Arylboronic Acids***

<sup>1</sup>H-NMR (400 MHz, DMSO-D<sub>6</sub>): d = 7.54–7.40 (m, 10H), 5.81 (d, *J* = 8.6 Hz, 2H), 4.96 (t, *J* = 9.1 Hz, 2H), 4.55 (d, *J* = 8.2 Hz, 2 H), 1.96 ppm (s, 6H).

Characterization matched the previously reported data.<sup>[7]</sup>

#### **General Procedure for the enantioselective conjugate additions:**

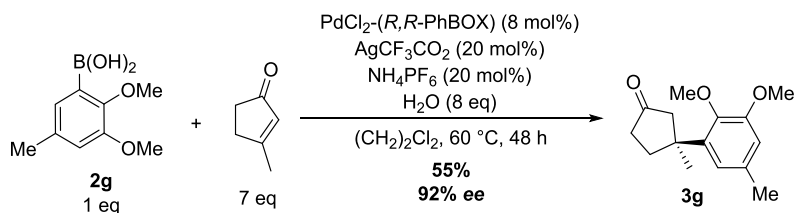
A 4 mL vial with Teflon-coated screw-cap was charged with Pd-Catalyst (0.021 mmol, 4 mol%), the *ortho*-substituted arylboronic acid (0.52 mmol), silver trifluoroacetate (0.052 mmol, 10 mol%), and ammonium hexafluorophosphate (0.052 mmol, 10 mol%). To the solids was added dichloroethane (0.75 mL) and the mixture was stirred at rt for 5 min. *Not all solids dissolved.* To the reaction mixture was subsequently added the β,β-disubstituted enone (3.64 mmol, 7 eq) in dichloroethane (0.75 mL). Demineralized water (4.16 mmol, 8 eq) was added. The vial was sealed and placed in a pre-heated oil bath at 60 °C. Within 30 min a black precipitate (AgCl) was formed. The reaction was allowed to stir for 48 h. The reaction mixture was cooled to rt where after it was filtered through a small silica plug, and flushed with ether (2-3 column volumes). The elute was concentrated under reduced pressure and the resulting oil was purified using flash chromatography employing a mixture of pentane : ether as the eluent.

#### **General procedure for the preparation of Raney nickel:**

An aqueous solution of NaOH (6.4 M, 500 mL) was cooled with an ice/salt bath. To the cooled solution a nickel/aluminum alloy (Ni : Al = 50 : 50, 100 g) was added in small portions over two h. The temperature was never allowed to rise above 15 °C. After addition, the ice/salt bath was removed and the suspension was allowed to warm to rt. The water was decanted and an aqueous solution of NaOH (2.5 M, 200 mL) was added to the residue. Stirring was applied for 15 min where after the suspension was allowed to settle. Decantation of the alkali solution was performed and the residue was washed with water. Washing and decantation was repeated until the washings were pH-neutral. The Raney nickel residue was washed with three portions of EtOH (95%, 600 mL) and three times with absolute EtOH (600 mL). The Raney Nickel was stored under absolute ethanol.

#### ***Important notes for the preparation and use of Raney nickel:***

- *During preparation of the Raney nickel significant quantities of hydrogen gas evolved*
- *The Raney nickel as prepared contains adsorbed hydrogen (sponge catalyst) and is therefore highly flammable!*
- *Raney nickel is pyrophoric when dry!*
- *Storage of the Raney Nickel can lead to pressure build-up in the storage container!*



**(S)-3-(2,3-dimethoxy-5-methylphenyl)-3-methylcyclopentanone (3g):**

An oven-dried Schlenk tube was charged with  $\text{PdCl}_2\text{-(R,R-PhBOX)}$  (83 mg, 0.163 mmol, 8 mol%), (2,3-dimethoxy-5-methylphenyl)boronic acid **2g** (800 mg, 4.08 mmol, 1 eq), silver trifluoroacetate (90 mg, 0.408 mmol, 20 mol%), and ammonium hexafluorophosphate (66.5 mg, 0.408 mmol, 20 mol%). Three vacuum-nitrogen cycles were applied. To the solids was added dichloroethane (4 mL) and the mixture was stirred at rt for 5 min. Not all solids dissolved. To the mixture was added 3-methylcyclopent-2-enone (2.8 mL, 28.5 mmol, 7 eq) in dichloroethane (4 mL). Demineralized water (8 eq) was added. The Schlenk tube was sealed and the reaction was heated to 60 °C in a pre-heated oil bath. Within 30 min the precipitate (Ag-salt) turned black. The reaction was allowed to react for 48 h.

The reaction mixture was cooled to rt where after it was filtered through a small silica plug, and flushed with ether (2-3 column volumes). The elute was concentrated under reduced pressure and the resulting oil was purified using flash column chromatography employing a mixture of pentane : ether (5 : 1) as the eluent. (S)-3-(2,3-dimethoxy-5-methylphenyl)-3-methylcyclopentanone (367 mg, 36% yield, 92% ee) **3g** was isolated as a colorless oil which solidified overnight.

$^1\text{H-NMR}$  (400 MHz,  $\text{CDCl}_3$ )  $\delta$  6.67 (d,  $J = 1.7$ , 1H), 6.60 (d,  $J = 1.3$ , 1H), 3.85 (s, 3H), 3.85 (s, 3H), 2.66 (dd,  $J = 63.9, 10.0$ , 2H), 2.44 – 2.25 (m, 4H), 2.31 (s, 3H), 1.36 (s, 3H).

$^{13}\text{C-NMR}$  (101 MHz,  $\text{CDCl}_3$ )  $\delta$  219.30, 152.77, 145.17, 141.03, 132.79, 118.69, 111.80, 60.26, 55.52, 52.56, 42.77, 36.00, 35.16, 27.01, 21.38.

HRMS (ESI+): Calculated mass  $[\text{M}+\text{H}]^+$   $\text{C}_{15}\text{H}_{21}\text{O}_3 = 249.1485$ ; found: 249.1486.

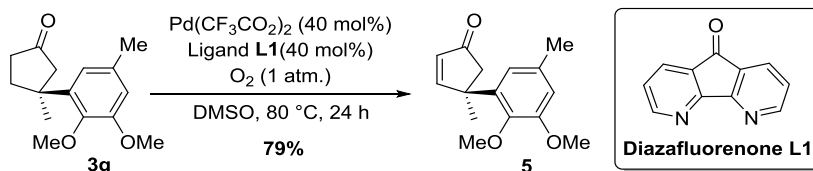
Chiral HPLC analysis on a Chiracel AD-H column, *n*-Heptane : *i*-PrOH = 99 : 1, 40 °C, flow = 0.5 mL/min, UV detection at 190 nm, 225 nm and 254 nm, retention times (min): 15.1 (minor) and 16.0 (major)

$[\alpha]_{\text{D}}^{20} = -47.2$  ( $\text{CHCl}_3$ ,  $c = 0.0041$ ) for a 92% ee sample.

Melting point = 76.2 °C

***Pd-catalyzed Asymmetric Conjugate Addition of Ortho-substituted Arylboronic Acids***

*Note:* The boronic acid required for the Michael addition was prepared according to a literature procedure. See: A. Abad. C. Agullo. A.C Cunat. D. Jimenez. R.H. Perni, *Tetrahedron*, **2001**, *57*, 9727.



**(R)-4-(2,3-dimethoxy-5-methylphenyl)-4-methylcyclopent-2-enone (5):**

This reaction was performed, based on the procedure by Stahl *et al.*<sup>[26]</sup> To an oven-dried Schlenk tube were added palladium trifluoroacetate (82 mg, 0.248 mmol, 40 mol%), and 5H-cyclopenta[1,2-b:5,4-b']dipyridin-5-one **L1** (45.1 mg, 0.248 mmol, 40 mol%). To the mixture was added a solution of (*S*)-3-(2,3-dimethoxy-5-methylphenyl)-3-methylcyclopentanone **3g** (150 mg, 0.604 mmol) in DMSO (2 mL). An oxygen filled balloon (1 atm) was attached to the reaction set up. While vigorously stirring, the Schlenk tube was purged with three vacuum/O<sub>2</sub> cycles. The reaction mixture was allowed to stir at 80 °C for 24 h. GC-MS showed complete conversion of the starting material.

The reaction was cooled to rt and diluted with water. The aqueous layer was extracted five times with CH<sub>2</sub>Cl<sub>2</sub> and the combined organic layers were dried over Na<sub>2</sub>SO<sub>4</sub>, filtered and concentrated under reduced pressure. Flash column chromatography employing pentane : ether (3:2) furnished pure (*R*)-4-(2,3-dimethoxy-5-methylphenyl)-4-methylcyclopent-2-enone (117 mg, 79% yield) **5** as a colorless oil, which solidified overnight.

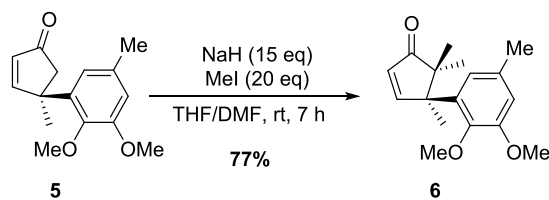
<sup>1</sup>H-NMR (400 MHz, CDCl<sub>3</sub>) δ 7.84 (d, *J* = 5.6, 1H), 6.66 (d, *J* = 1.6, 1H), 6.57 (d, *J* = 1.3, 1H), 6.13 (d, *J* = 5.6, 1H), 3.82 (s, 3H), 3.76 (s, 3H), 2.64 (dd, *J* = 49.8, 18.6, 2H), 2.28 (s, 3H), 1.55 (s, 3H).

<sup>13</sup>C-NMR (101 MHz, CDCl<sub>3</sub>) δ 209.78, 171.37, 152.96, 145.14, 137.98, 132.96, 130.55, 119.17, 112.45, 60.45, 55.71, 51.07, 47.33, 28.26, 21.44.

HRMS (ESI+): Calculated mass [M+H]<sup>+</sup> C<sub>15</sub>H<sub>19</sub>O<sub>3</sub> = 247.13287; found: 247.13301

(ESI+): Calculated mass [M+Na]<sup>+</sup> C<sub>15</sub>H<sub>19</sub>O<sub>3</sub>Na = 269.1148; found: 269.1150.

[α]<sub>D</sub><sup>20</sup> = -31.2 (CHCl<sub>3</sub>, *c* = 0.006) for a 92% *ee* sample.



**(R)-4-(2,3-dimethoxy-5-methylphenyl)-4,5,5-trimethylcyclopent-2-enone (6):**

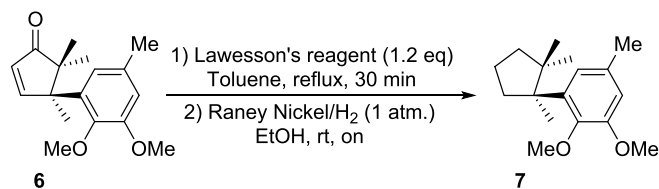
The dimethylation was based on a procedure by Srikrishna *et al.*<sup>[27]</sup> To a suspension of NaH (341 mg, 60% dispersion in oil, 8.53 mmol, washed with pentane, 15 eq) in dry THF (4 mL) was added a solution of (*R*)-4-(2,3-dimethoxy-5-methylphenyl)-4-methylcyclopent-2-enone (140 mg, 0.568 mmol) **5** in dry THF (3 mL) and DMF (0.35 mL). The resulting suspension was stirred for 15 min where after iodomethane (708  $\mu$ l, 11.4 mmol, 20 eq) was added. The reaction was stirred for 7 h after which GC-MS and TLC indicated complete conversion of the starting material. The reaction was carefully quenched with water (5 mL) where after the phases were separated. The aqueous phase was extracted with ether (3x5 mL) and the combined organic layers were treated once with brine. The organic layer was dried over Na<sub>2</sub>SO<sub>4</sub>, filtered and concentrated under reduced pressure. Flash column chromatography employing pentane : ether (4 : 1) afforded (*R*)-4-(2,3-dimethoxy-5-methylphenyl)-4,5,5-trimethylcyclopent-2-enone (120 mg, 77% yield) **6** as a colorless oil. The oil crystallized quickly giving transparent (white appearing!) crystals.

<sup>1</sup>H-NMR (400 MHz, CDCl<sub>3</sub>)  $\delta$  7.93 (d, *J* = 5.6, 1H), 6.66 (d, *J* = 1.7, 1H), 6.49 (s, 1H), 6.07 (d, *J* = 5.8, 1H), 3.85 (s, 3H), 3.81 (s, 3H), 2.30 (s, 3H), 1.48 (s, 3H), 1.25 (s, 3H), 0.66 (s, 3H).

<sup>13</sup>C-NMR (101 MHz, CDCl<sub>3</sub>)  $\delta$  214.55, 171.22, 152.68, 145.27, 135.91, 132.72, 125.63, 120.57, 112.05, 60.24, 55.53, 50.80, 26.00, 22.20, 21.34, 19.62, 13.95.

HRMS (ESI<sup>+</sup>): Calculated mass [M+H]<sup>+</sup> C<sub>17</sub>H<sub>23</sub>O<sub>3</sub><sup>+</sup> = 275.1641; found: 275.1642.

$[\alpha]_D^{20}$  = -58.5 (CHCl<sub>3</sub>, *c* = 0.004) for a 92% *ee* sample.



**(S)-1,2-dimethoxy-5-methyl-3-(1,2,2-trimethylcyclopentyl)benzene (7):**

The procedure was based on a publication by Myers.<sup>[21a]</sup> To a solution of (*R*)-4-(2,3-dimethoxy-5-methylphenyl)-4,5,5-trimethylcyclopent-2-enone (100 mg, 0.364 mmol) **6** in dry toluene (5 mL) was added Lawesson's reagent (177 mg, 0.437 mmol, 1.2 eq). The suspension was heated to reflux for 45 min. The suspension turned into a clear bright pink solution over time. TLC using pentane : ether (4 : 1) indicated complete conversion of the enone into the thioenone.

The reaction mixture was cooled to rt, filtered over a small fluorosil column and flushed with CH<sub>2</sub>Cl<sub>2</sub>. The elute was concentrated under reduced pressure and purified using flash column chromatography (5% EtOAc in hexane) only isolating the pink fractions. The fractions were concentrated to a bright pink oil which was dissolved in EtOH (8 mL). To the solution freshly prepared Raney nickel was added. A hydrogen balloon was fixed to the flask and the reaction mixture was purged with three vacuum/H<sub>2</sub> cycles. The reaction was stirred overnight where after the reaction was filtered over a silica plug and flushed with pentane : ether (1 : 1). Evaporation of the solvent under reduced pressure gave a slight yellow oil. Flash chromatography using 4% ether in pentane afforded (*S*)-1,2-dimethoxy-5-methyl-3-(1,2,2-trimethylcyclopentyl)benzene (62 mg, 0.236 mmol, 65% yield) **7** as a colorless oil. The oil crystallized overnight producing transparent (white appearing!) crystals.

<sup>1</sup>H-NMR (400 MHz, CDCl<sub>3</sub>) δ 6.82 (s, 1H), 6.67 (s, 1H), 3.88 (s, 3H), 3.84 (s, 3H), 2.76 – 2.63 (m, 1H), 2.36 (s, 3H), 1.92 – 1.74 (m, 3H), 1.74 – 1.64 (m, 1H), 1.63 – 1.51 (m, 1H), 1.43 (s, 3H), 1.20 (s, 3H), 0.78 (s, 3H).

<sup>13</sup>C-NMR (101 MHz, CDCl<sub>3</sub>) 153.10, 146.76, 140.17, 131.60, 121.69, 111.11, 60.39, 55.64, 51.62, 45.03, 40.98, 39.02, 26.92, 25.30, 24.25, 21.76, 20.44.

HRMS (ESI<sup>+</sup>): Calculated mass [M+H]<sup>+</sup> C<sub>17</sub>H<sub>27</sub>O<sub>2</sub><sup>+</sup> = 263.2005; found: 263.2007.

[α]<sub>D</sub><sup>20</sup> = -26.1 (CHCl<sub>3</sub>, c = 0.00115) for a 92% *ee* sample.



**(*S*)-5-methyl-3-(1,2,2-trimethylcyclopentyl)benzene-1,2-diol (herbertenediol):**

The procedure was based on a publication by Myers.<sup>[21a]</sup> To a solution of (*S*)-1,2-dimethoxy-5-methyl-3-(1,2,2-trimethylcyclopentyl)benzene (15 mg, 0.057 mmol, 1 eq) **7** in dry CH<sub>2</sub>Cl<sub>2</sub> (1 mL) at 0 °C was added BBr<sub>3</sub> (285 μL, 0.285 mmol, 5 eq, 1 M in CH<sub>2</sub>Cl<sub>2</sub>). The reaction mixture was allowed to warm to rt and was stirred for 1 h. TLC using 5% ether in pentane indicated complete conversion of the starting material. The reaction mixture was added to a 2% aqueous solution of NaHCO<sub>3</sub>. The phases were separated and the aqueous phase was extracted three times with CH<sub>2</sub>Cl<sub>2</sub>. The combined organic phases were washed with brine, dried over MgSO<sub>4</sub>, filtered and concentrated under reduced pressure affording a white solid. Flash column chromatography using pentane : ether (7 : 3) afforded (*S*)-5-methyl-3-(1,2,2-trimethylcyclopentyl)benzene-1,2-diol (11 mg, 0.047 mmol, 82 % yield) **1** as a white solid.

<sup>1</sup>H-NMR (400 MHz, CDCl<sub>3</sub>) δ 6.69 (s, 1H), 6.58 – 6.54 (m, 1H), 5.35 (s, 1H), 4.98 (s, 1H), 2.68 – 2.54 (m, 1H), 2.23 (s, 3H), 1.82 – 1.70 (m, 3H), 1.70 – 1.62 (m, 1H), 1.61 – 1.50 (m, 0H), 1.42 (s, 3H), 1.19 (s, 3H), 0.77 (s, 3H).

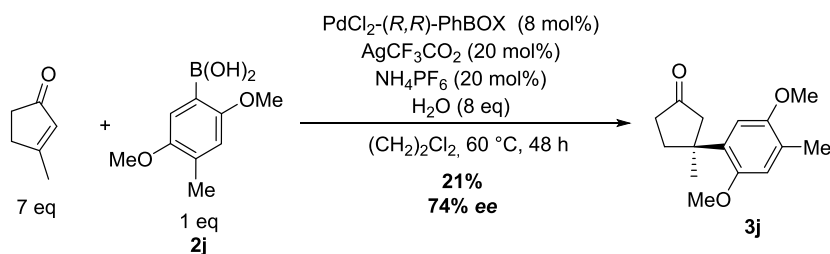
<sup>13</sup>C-NMR (101 MHz, CDCl<sub>3</sub>) δ 143.48, 141.03, 133.63, 128.48, 122.06, 113.58, 51.26, 44.99, 41.08, 39.37, 26.98, 25.56, 22.98, 21.30, 20.41.

HRMS (ESI<sup>+</sup>) Calculated mass [M-H]<sup>+</sup> C<sub>15</sub>H<sub>21</sub>O<sub>2</sub><sup>+</sup> = 233.1536; found: 233.1544.

[α]<sub>D</sub><sup>20</sup> = -52.3 (CHCl<sub>3</sub>, *c* = 0.0047) for a 92% *ee* sample.

The analytical data matches with that of the natural isolate.<sup>[18]</sup>

*Pd-catalyzed Asymmetric Conjugate Addition of Ortho-substituted Arylboronic Acids*



**(S)-3-(2,5-dimethoxy-4-methylphenyl)-3-methylcyclopentanone (**3j**):**

To an oven dried Schlenk tube were added palladium catalyst (42 mg, 0.143 mmol, 8 mol%), (2,5-dimethoxy-4-methylphenyl)boronic acid (350 mg, 1.79 mmol) **2j**, silver trifluoroacetate (44 mg, 0.358 mmol, 20 mol%) and ammonium hexafluorophosphate (32 mg, 0.358 mmol, 20 mol%) and the Schlenk tube was alternated through three vacuum/nitrogen cycles. Dichloroethane (2.5 mL) was added to the solids and the mixture was stirred for 10 min at rt. Not all the solids dissolved. Then, 3-methylcyclopent-2-enone (1.2 g, 12.5 mmol, 7 eq) in dichloroethane (2.5 mL) was added. Demineralized water (260  $\mu$ L, 14.3 mmol, 8 eq) was added and the reaction was stirred at 60 °C. After 48 h, the mixture was cooled to rt, filtered over a silica plug and flushed with ether. The elute was concentrated and purified by flash column chromatography using pentane : ether (4 : 1). (S)-3-(2,5-dimethoxy-4-methylphenyl)-3-methylcyclopentanone **3j** was obtained as a colorless oil (93 mg, 21% yield, 74% ee).

<sup>1</sup>H-NMR (400 MHz, CDCl<sub>3</sub>)  $\delta$  6.71 (s, 2H), 3.80 (s, 3H), 3.78 (s, 3H), 2.63 (dd, *J* = 18.1, 6.5, 2H), 2.44 – 2.26 (m, 4H), 2.21 (s, 3H), 1.38 (s, 3H).

<sup>13</sup>C-NMR (101 MHz, CDCl<sub>3</sub>)  $\delta$  219.63, 151.34, 151.33, 134.04, 125.33, 114.67, 109.75, 56.16, 55.53, 52.35, 42.58, 36.33, 34.94, 26.28, 15.87.

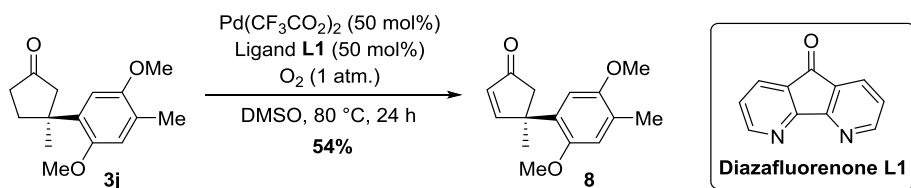
HRMS (ESI<sup>+</sup>): Calculated mass [M+H]<sup>+</sup> C<sub>15</sub>H<sub>21</sub>O<sub>3</sub><sup>+</sup> = 249.1485; found: 249.1474.

$[\alpha]_D^{20}$  = -15.6 (CHCl<sub>3</sub>, *c* = 0.002) for a 74% ee sample.

Chiral HPLC analysis on a Chiracel AD-H column, *n*-Heptane : *i*-PrOH = 97 : 3, 40 °C, flow = 0.5 mL/min, UV detection at 190 nm, 225 nm and 254 nm, retention times (min): 15.0 (minor) and 16.0 (major).

*Note:* The boronic acid required for the Michael addition was prepared according to a literature procedure. See: K. Shishido, Y. Shoji, M. Yoshida. *Org. Lett.* **2009**, *11*, 1441.





**(R)-4-(2,5-dimethoxy-4-methylphenyl)-4-methylcyclopent-2-enone (8):**

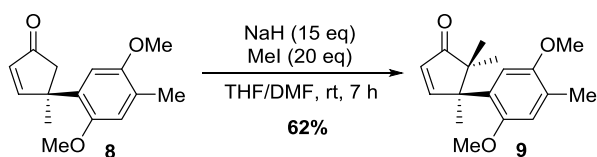
This reaction was performed based on the procedure by Stahl *et al.*<sup>[26]</sup> To an oven-dried Schlenk tube was added palladium trifluoroacetate (150 mg, 0.47 mmol, 50 mol%) and diazafluorenone (85 mg, 0.47 mmol, 50 mol%). Compound **3j** (293 mg, 1.18 mmol) was dissolved in DMSO (4 mL) and added to the mixture. The Schlenk was purged with three vacuum/oxygen cycles, and the reaction was allowed to stir for 24 h at rt. Water (12 mL) was added and the reaction mixture was extracted with DCM (3x30 mL). The combined organic layers were washed with brine (30 mL), dried over  $\text{Na}_2\text{SO}_4$ , filtered and concentrated under reduced pressure. The crude mixture was purified by flash chromatography with pentane : ether (4 : 1) to yield (R)-4-(2,5-dimethoxy-4-methylphenyl)-4-methylcyclopent-2-enone **8** as a colorless oil (157 mg, 54% yield).

$^1\text{H-NMR}$  (400 MHz,  $\text{CDCl}_3$ )  $\delta$  7.80 (d,  $J = 5.7$ , 1H), 6.71 (s, 1H), 6.66 (s, 1H), 6.16 (d,  $J = 5.6$ , 1H), 3.79 (s, 3H), 3.75 (s, 3H), 2.67 (dd,  $J = 83.9, 18.7$ , 2H), 2.21 (s, 3H), 1.57 (s, 3H).

$^{13}\text{C-NMR}$  (101 MHz,  $\text{CDCl}_3$ )  $\delta$  210.02, 170.73, 151.23, 151.17, 131.15, 130.88, 126.02, 114.83, 110.00, 56.21, 55.60, 50.36, 47.13, 27.36, 15.98.

HRMS (ESI+): Calculated mass  $[\text{M}+\text{H}]^+$   $\text{C}_{15}\text{H}_{19}\text{O}_3^+ = 247.13287$ ; found: 247.13284.  
 (ESI+): Calculated mass  $[\text{M}+\text{Na}]^+$   $\text{C}_{15}\text{H}_{18}\text{O}_3\text{Na}^+ = 269.1148$ ; found: 269.1148.

$[\alpha]_{\text{D}}^{20} = -55.2$  ( $\text{CHCl}_3$ ,  $c = 0.006$ ) for a 74% *ee* sample.



**(R)-4-(2,5-dimethoxy-4-methylphenyl)-4,5,5-trimethylcyclopent-2-enone (9):**

The dimethylation was based on a procedure by Srikrishna *et al.*<sup>[27]</sup> NaH (222 mg, 5.55 mmol, 15 eq, 60% suspension in oil) was washed with pentane and suspended in dry THF (3 mL). Compound **8** (92 mg, 0.37 mmol) was added in dry THF (2 mL) and dry DMF (0.23 mL) and stirred for 15 min. MeI (0.46 mL, 7.4 mmol, 20 eq) was added and the reaction was stirred at rt. After 7 h, the reaction was carefully quenched with  $\text{H}_2\text{O}$  (5

*Pd-catalyzed Asymmetric Conjugate Addition of Ortho-substituted Arylboronic Acids*

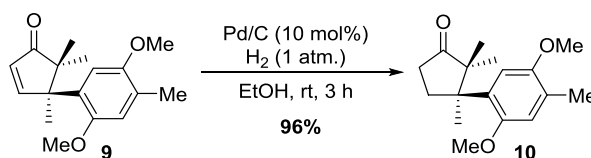
mL) at 0 °C and extracted with ether (3x10 mL). The combined organic layers were washed with brine (10 mL), dried over Na<sub>2</sub>SO<sub>4</sub>, filtered and concentrated under reduced pressure. The crude mixture was purified by flash chromatography with pentane : ether (4 : 1) to yield **9** as a colorless oil (64 mg, 62% yield).

<sup>1</sup>H-NMR (400 MHz, CDCl<sub>3</sub>) δ 7.88 (d, *J* = 5.9, 1H), 6.71 (s, 1H), 6.53 (s, 1H), 6.12 (d, *J* = 5.7, 1H), 3.77 (s, 6H), 2.21 (s, 3H), 1.49 (s, 3H), 1.26 (s, 3H), 0.67 (s, 3H).

<sup>13</sup>C-NMR (101 MHz, CDCl<sub>3</sub>) δ 214.85, 170.68, 151.56, 151.36, 129.60, 126.68, 125.78, 114.59, 111.27, 56.09, 55.30, 54.73, 50.78, 25.65, 24.89, 19.99, 15.97.

HRMS (ESI+): Calculated mass [M+H]<sup>+</sup> C<sub>17</sub>H<sub>23</sub>O<sub>3</sub><sup>+</sup> = 275.1641; found: 275.1641.

(ESI+): Calculated mass [M+Na]<sup>+</sup> C<sub>17</sub>H<sub>22</sub>O<sub>3</sub>Na<sup>+</sup> = 297.1461; found: 297.1461.



**(R)-3-(2,5-dimethoxy-4-methylphenyl)-2,2,3-trimethylcyclopentanone (10)**

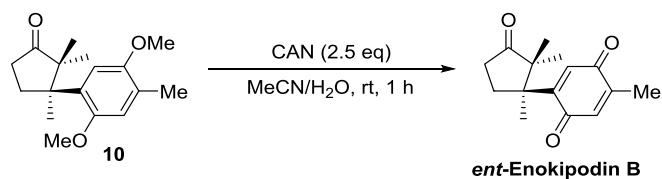
Pd/C (20 mg, 10% activated Pd on charcoal) was added to an oven-dried Schlenk tube. Compound **9** (47 mg, 0.17 mmol) was dissolved in ethanol (1 mL) and added to the tube which was subsequently equipped with a hydrogen balloon and subjected to three vacuum/hydrogen cycles. After stirring for 3.5 h at rt, the mixture was flushed over a silica plug and concentrated under reduced pressure to give **10** as a colorless oil (45 mg, 96% yield).

<sup>1</sup>H-NMR (400 MHz, CDCl<sub>3</sub>) δ 6.85 (s, 1H), 6.68 (s, 1H), 3.80 (s, 3H), 3.71 (s, 3H), 2.49 (ddd, *J* = 20.2, 17.1, 10.2, 3H), 2.21 (s, 3H), 2.10 – 1.98 (m, 1H), 1.38 (s, 3H), 1.23 (s, 3H), 0.70 (s, 3H).

<sup>13</sup>C-NMR (101 MHz, CDCl<sub>3</sub>) δ 222.80, 151.85, 151.23, 132.44, 125.25, 114.29, 111.47, 56.19, 54.76, 52.67, 48.82, 34.42, 32.56, 23.47, 21.74, 21.57, 15.76.

HRMS (ESI+): Calculated mass [M+H]<sup>+</sup> C<sub>17</sub>H<sub>25</sub>O<sub>3</sub><sup>+</sup> = 277.1798; found: 277.1798.

[α]<sub>D</sub><sup>20</sup> = -13.2 (CHCl<sub>3</sub>, *c* = 0.005) for a 75% *ee* sample.



**(S)-2-methyl-5-(1,2,2-trimethyl-3-oxocyclopentyl)cyclohexa-2,5-diene-1,4-dione (enokipodin B)**

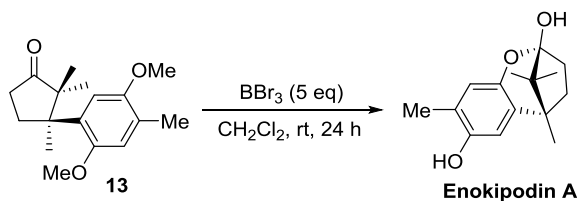
This reaction was performed according to the procedure of Srikrishna *et al.*<sup>[37]</sup> **10** (44 mg, 0.16 mmol) was dissolved in CH<sub>3</sub>CN (3 mL) and water (3 mL) and added to an oven-dried Schlenk tube. CAN (219 mg, 0.4 mmol, 2.5 eq) was added and the reaction was stirred at rt for 1 h. The reaction mixture was extracted with DCM (3x5 mL) and the combined organic layers were washed with brine (10 mL), dried over Na<sub>2</sub>SO<sub>4</sub> and concentrated under reduced pressure. The purification was performed using flash chromatography with pentane : ether (4 : 1) to yield enokipodin B as a yellow solid (33 mg, 84% yield).

<sup>1</sup>H-NMR (400 MHz, CDCl<sub>3</sub>) δ 6.69 (s, 1H), 6.56 (s, 1H), 2.54 – 2.35 (m, 2H), 2.27 (dd, *J* = 21.7, 10.9, 1H), 2.04 (s, 3H), 1.91 – 1.83 (m, 1H), 1.32 (s, 3H), 1.22 (s, 3H), 0.76 (s, 3H).

<sup>13</sup>C-NMR (101 MHz, CDCl<sub>3</sub>) δ 221.00, 188.30, 187.89, 153.58, 144.57, 135.42, 134.25, 52.47, 49.07, 33.88, 31.19, 23.21, 22.27, 20.75, 15.04.

HRMS (ESI+): Calculated mass [M+H]<sup>+</sup> C<sub>15</sub>H<sub>19</sub>O<sub>3</sub><sup>+</sup> = 247.1328; found: 247.1328.

[α]<sub>D</sub><sup>20</sup> = -24.8 (CHCl<sub>3</sub>, *c* = 0.01) for a 74% *ee* sample.



**(2R,5R)-5,8,10,10-tetramethyl-2,3,4,5-tetrahydro-2,5-methanobenzo[b]oxepine-2,7-diol (ent-enokipodin A):**

Compound **10** (50 mg, 0.18 mmol) was dissolved in DCM (10 mL) and cooled to 0 °C. BBr<sub>3</sub> (0.9 mL, 0.9 mmol, 5 eq) was added dropwise. The light brown solution was stirred for 24 h at rt. The reaction was quenched with a saturated aqueous solution of NaHCO<sub>3</sub> (10 mL) and extracted with DCM (3x10 mL). The combined organic layers were washed with brine (10 mL), dried over Na<sub>2</sub>SO<sub>4</sub>, filtered and concentrated. The

Pd-catalyzed Asymmetric Conjugate Addition of Ortho-substituted Arylboronic Acids

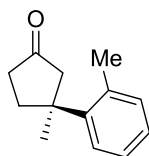
crude mixture was purified by flash chromatography with pentane : ether (3 : 1) to yield pure enokipodin A as transparent (*white appearing!*) crystals (25 mg, 57% yield).

$^1\text{H-NMR}$  (400 MHz,  $\text{CDCl}_3$ )  $\delta$  6.55 (s, 1H), 6.50 (s, 1H), 4.25 (s, 1H), 2.69 (s, 1H), 2.17 (s, 3H), 2.14 – 2.03 (m, 2H), 1.90 (td,  $J = 12.1, 6.5$ , 1H), 1.82 – 1.73 (m, 1H), 1.24 (s, 3H), 1.09 (s, 3H), 0.80 (s, 3H).

$^{13}\text{C-NMR}$  (101 MHz,  $\text{DMSO-}d_6$ )  $\delta$  148.34, 145.05, 130.24, 122.06, 115.91, 110.41, 109.01, 46.73, 42.82, 38.34, 35.20, 18.44, 15.96, 15.79, 15.64.

HRMS (APCI+): Calculated mass  $[\text{M}+\text{H}]^+$   $\text{C}_{15}\text{H}_{21}\text{O}_3^+$  = 249.1485; found: 249.1482.

$[\alpha]_{\text{D}}^{20} = +77.0$  ( $\text{CHCl}_3$ ,  $c = 0.006$ ) for a 74% *ee* sample.



**3-methyl-3-(o-tolyl)cyclopentenone (3a):**

This compound was prepared according to the general procedure and purified with flash chromatography using pentane : ether (4 : 1) as the eluent. Racemic synthesis = 82% yield, enantioselective synthesis 23% yield, 90% *ee*.

$^1\text{H-NMR}$  (400 MHz,  $\text{CDCl}_3$ )  $\delta$  7.25 – 7.12 (m, 4H), 2.67 (dd,  $J = 55.6, 17.5$ , 2H), 2.45 (s, 3H), 2.53 – 2.35 (m, 4H), 1.38 (s, 3H).

$^{13}\text{C-NMR}$  (101 MHz,  $\text{CDCl}_3$ )  $\delta$  218.32, 146.40, 135.37, 132.40, 126.34, 126.07, 125.92, 52.72, 44.31, 35.85, 35.77, 26.40, 22.44.

HRMS (ESI+): Calculated mass  $[\text{M}+\text{Na}]^+$   $\text{C}_{13}\text{H}_{16}\text{ONa}^+$  = 211.1093; found: 211.1084.

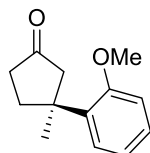
$[\alpha]_{\text{D}}^{20} = -35.9$  ( $\text{CHCl}_3$ ,  $c = 0.01$ ) for a 90% *ee* sample.

Chiral HPLC analysis on a Chiracel OB-H column, *n*-Heptane : *i*-PrOH = 99 : 1, 40 °C, flow = 0.5 mL/min, UV detection at 190 nm, 225 nm and 254 nm, retention times (min): 25.8 (minor) and 28.5 (major).

Chiral HPLC analysis on a Chiracel AS-H column, *n*-Heptane : *i*-PrOH = 99 : 1, 40 °C, flow = 0.5 mL/min, UV detection at 190 nm, 225 nm and 254 nm, retention times (min): 13.0 (minor) and 14.0 (major).

## CHAPTER 5

Chiral HPLC analysis Phenomenex LUX 5 $\mu$  Cellulose-3 column, *n*-Heptane : *i*-PrOH = 99 : 1, 40 °C, flow = 0.5 mL/min, UV detection at 190 nm, 225 nm and 254 nm, retention times (min): 9.5 (minor) and 10.5 (major).



### 3-(2-methoxyphenyl)-3-methylcyclopentanone (3b):

This compound was prepared according to the general procedure and purified employing flash chromatography using pentane : ether (4 : 1) as the eluent. Racemic synthesis = 69% yield, enantioselective synthesis 45% yield, 80% *ee*

$^1\text{H-NMR}$  (400 MHz,  $\text{CDCl}_3$ )  $\delta$  7.26 – 7.10 (m, 2H), 6.95 – 6.82 (m, 2H), 3.79 (s, 3H), 2.59 (dd,  $J = 18.1, 18.1$  2H), 2.41 – 2.23 (m, 4H), 1.36 (s, 3H).

$^{13}\text{C-NMR}$  (101 MHz,  $\text{CDCl}_3$ )  $\delta$  219.93, 157.66, 136.14, 127.72, 126.29, 120.52, 111.39, 54.97, 52.31, 42.66, 36.41, 34.90, 26.21.

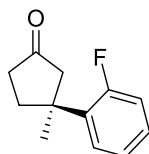
HRMS (ESI+): Calculated mass  $[\text{M}+\text{H}]^+ \text{C}_{13}\text{H}_{17}\text{O}_2^+ = 205.1223$ ; found: 205.1214.

$[\alpha]_{\text{D}}^{20} = -21.0$  ( $\text{CHCl}_3$ ,  $c = 0.01$ ) for a 80% *ee* sample.

Chiral HPLC analysis on a Chiracel AD-H column, *n*-Heptane : *i*-PrOH = 99 : 1, 40 °C, flow = 0.5 mL/min, UV detection at 190 nm, 225 nm and 254 nm, retention times (min): 19.0 (minor) and 20.9 (major).

Chiral HPLC analysis on a Phenomenex LUX 5 $\mu$  Cellulose-3 column, *n*-Heptane : *i*-PrOH = 99 : 1, 40 °C, flow = 0.5 mL/min, UV detection at 190 nm, 225 nm and 254 nm, retention times (min): 9.8 (minor) and 11.5 (major).

Chiral HPLC analysis on a Chiracel OB-H column, *n*-Heptane : *i*-PrOH = 99 : 1, 40 °C, flow = 0.5 mL/min, UV detection at 190 nm, 225 nm and 254 nm, retention times (min): 24.8 (minor) and 29.3 (major).



**3-(2-fluorophenyl)-3-methylcyclopentanone (3c):**

This compound was prepared according to the general procedure and purified with flash chromatography using pentane : ether (4 : 1) as the eluent. Racemic synthesis = 20% yield (51% with double catalyst loading), enantioselective synthesis 20% yield, 95% *ee*.

$^1\text{H-NMR}$  (400 MHz,  $\text{CDCl}_3$ )  $\delta$  7.32 – 7.23 (m, 2H), 7.19 – 7.03 (m, 2H), 2.71 – 2.59 (m, 2H), 2.54 – 2.34 (m, 4H), 1.44 (s, 3H).

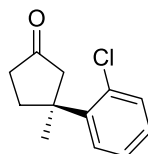
$^{13}\text{C-NMR}$  (101 MHz,  $\text{CDCl}_3$ )  $\delta$  218.50, 218.48, 162.57, 160.11, 134.99, 134.87, 128.45, 128.37, 127.11, 127.05, 124.28, 124.25, 116.62, 116.39, 52.09, 52.06, 42.29, 42.27, 36.26, 36.25, 34.81, 34.78, 26.96, 26.94 (*Spectrum contains the double amount of peaks due to carbon-fluorine coupling*).

HRMS (ESI<sup>+</sup>): Calculated mass  $[\text{M}+\text{H}]^+$   $\text{C}_{12}\text{H}_{14}\text{OF}^+$  = 193.1023; found: 193.1014.

$[\alpha]_{\text{D}}^{20}$  = -23.8 ( $\text{CHCl}_3$ ,  $c$  = 0.01) for a 95% *ee* sample.

Chiral HPLC analysis on a Chiracel AD-H column, *n*-Heptane : *i*-PrOH = 99 : 1, 40 °C, flow = 0.5 mL/min, UV detection at 190 nm, 225 nm and 254 nm, retention times (min): 20.4 (major) and 21.7 (minor).

Chiral HPLC analysis on a Chiracel AS-H column, *n*-Heptane : *i*-PrOH = 99 : 1, 40 °C, flow = 0.5 mL/min, UV detection at 190 nm, 225 nm and 254 nm, retention times (min): 12.1 (major) and 13.2 (minor).



### 3-(2-chlorophenyl)-3-methylcyclopentanone (3d):

This compound was prepared according to the general procedure and purified with flash chromatography using pentane : ether (4 : 1) as the eluent. Racemic synthesis = 12% yield (31% with double catalyst loading), enantioselective synthesis 8% yield (12% with double catalyst loading), 94% *ee*.

$^1\text{H-NMR}$  (400 MHz,  $\text{CDCl}_3$ )  $\delta$  7.38 (dd,  $J = 7.8, 1.5$ , 1H), 7.32 (dd,  $J = 7.8, 1.8$ , 1H), 7.25 (td,  $J = 7.6, 1.6$ , 1H), 7.18 (td,  $J = 7.6, 1.7$ , 1H), 2.78 (dd,  $J = 101.0, 17.9$ , 2H), 2.55 – 2.34 (m, 4H), 1.48 (s, 3H).

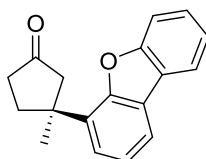
$^{13}\text{C-NMR}$  (101 MHz,  $\text{CDCl}_3$ )  $\delta$  218.51, 144.94, 133.48, 131.83, 128.02, 127.73, 127.12, 52.23, 44.49, 36.28, 35.22, 25.68.

HRMS (ESI+): Calculated mass  $[\text{M}+\text{H}]^+$   $\text{C}_{12}\text{H}_{14}\text{OCl}^+$  = 209.07277; found: 209.07185  
 (ESI+): Calculated mass  $[\text{M}+\text{Na}]^+$   $\text{C}_{12}\text{H}_{13}\text{OCINa}^+$  = 231.0547; found: 231.0537.

$[\alpha]_{\text{D}}^{20} = -22.4$  ( $\text{CHCl}_3$ ,  $c = 0.01$ ) for a 94% *ee* sample.

Chiral HPLC analysis on a Chiracel OD-H column, *n*-Heptane : *i*-PrOH = 99 : 1, 40 °C, flow = 0.5 mL/min, UV detection at 190 nm, 225 nm and 254 nm, retention times (min): 23.9 (minor) and 29.2 (major).

Chiral HPLC analysis on a Phenomenex LUX 5 $\mu$  Cellulose-3 column, *n*-Heptane : *i*-PrOH = 99 : 1, 40 °C, flow = 1.0 mL/min, UV detection at 190 nm, 225 nm and 254 nm, retention times (min): 9.5 (major) and 10.4 (minor).



### 3-(dibenzo[b,d]furan-4-yl)-3-methylcyclopentanone (3e)

This compound was prepared according to the general procedure and purified with flash chromatography using pentane : ether (4 : 1) as the eluent. Racemic synthesis = 69% yield, enantioselective synthesis 51% yield, 93% *ee*.

Pd-catalyzed Asymmetric Conjugate Addition of Ortho-substituted Arylboronic Acids

$^1\text{H-NMR}$  (400 MHz,  $\text{CDCl}_3$ )  $\delta$  7.91 (d,  $J = 7.7$ , 1H), 7.82 (dd,  $J = 6.1, 2.8$ , 1H), 7.56 (d,  $J = 8.2$ , 1H), 7.47 – 7.40 (m, 1H), 7.34 – 7.29 (m, 1H), 7.27 (d,  $J = 3.6$ , 2H), 2.83 (dd,  $J = 49.5, 17.8$ , 2H), 2.60 – 2.30 (m, 4H), 1.56 (s, 3H).

$^{13}\text{C-NMR}$  (101 MHz,  $\text{CDCl}_3$ )  $\delta$  218.76, 155.77, 153.87, 132.25, 127.22, 124.85, 124.06, 123.75, 122.92, 122.80, 120.65, 119.19, 111.70, 51.94, 42.56, 36.48, 34.74, 26.77.

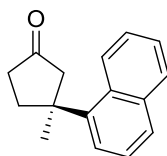
HRMS (ESI+): Calculated mass  $[\text{M}+\text{H}]^+ \text{C}_{18}\text{H}_{17}\text{O}_2^+ = 265.1223$ ; found: 265.1212.

$[\alpha]_{\text{D}}^{20} = -15.8$  ( $\text{CHCl}_3$ ,  $c = 0.01$ ) for a 93% *ee* sample.

Chiral HPLC analysis on a Chiracel AD-H column, *n*-Heptane : *i*-PrOH = 99 : 1, 40 °C, flow = 0.5 mL/min, UV detection at 190 nm, 225 nm and 254 nm, retention times (min): 25.9 (major) and 29.5 (minor).

Chiral HPLC analysis on a Chiracel OD-H column, *n*-Heptane : *i*-PrOH = 99 : 1, 40 °C, flow = 0.5 mL/min, UV detection at 190 nm, 225 nm and 254 nm, retention times (min): 37.0 (major) and 44.3 (minor).

Chiral HPLC analysis on a Phenomenex LUX 5 $\mu$  Cellulose-3 column, *n*-Heptane : *i*-PrOH = 99 : 1, 40 °C, flow = 1.0 mL/min, UV detection at 190 nm, 225 nm and 254 nm, retention times (min): 16.7 (minor) and 23.8 (major).



**3-methyl-3-(naphthalen-1-yl)cyclopentenone (3f):**

This compound was prepared according to the general procedure and purified with flash chromatography using pentane : ether (4 : 1) as the eluent. Racemic synthesis = 73% yield, enantioselective synthesis 20% yield (38% with double catalyst loading), 85% *ee*.

$^1\text{H-NMR}$  (400 MHz,  $\text{CDCl}_3$ )  $\delta$  8.20 (d,  $J = 8.1$ , 1H), 7.93 – 7.86 (m, 1H), 7.82 – 7.72 (m, 1H), 7.54 – 7.45 (m, 2H), 7.45 – 7.39 (m, 2H), 2.89 (dd,  $J = 18.1, 7.6$ , 2H), 2.72 – 2.34 (m, 4H), 1.70 (s, 3H).

$^{13}\text{C-NMR}$  (101 MHz,  $\text{CDCl}_3$ )  $\delta$  218.50, 143.75, 135.07, 131.22, 129.78, 128.11, 125.79, 125.43, 125.30, 125.21, 123.46, 53.90, 44.62, 36.67, 36.38, 27.91.

HRMS (ESI+): Calculated mass  $[\text{M}+\text{H}]^+ \text{C}_{16}\text{H}_{17}\text{O}^+ = 225.1273$ ; found: 225.1264.

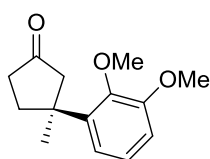


## CHAPTER 5

$[\alpha]_D^{20} = -23.2$  ( $\text{CHCl}_3$ ,  $c = 0.01$ ) for a 85% *ee* sample.

Chiral HPLC analysis on a Chiracel AS-H column, *n*-Heptane : *i*-PrOH = 99 : 1, 40 °C, flow = 1.0 mL/min, UV detection at 190 nm, 225 nm and 254 nm, retention times (min): 24.4 (major) and 27.5 (minor).

Chiral HPLC analysis on a Phenomenex LUX 5 $\mu$  Cellulose-3 column, *n*-Heptane : *i*-PrOH = 99 : 1, 40 °C, flow = 1.0 mL/min, UV detection at 190 nm, 225 nm and 254 nm, retention times for racemate (min): 19.8 and 37.3.



### 3-(2,3-dimethoxyphenyl)-3-methylcyclopentanone (3h):

This compound was prepared according to the general procedure and purified with flash chromatography using pentane : ether (4 : 1) as the eluent. Racemic synthesis = 65% yield, enantioselective synthesis 25% yield, 94% *ee*.

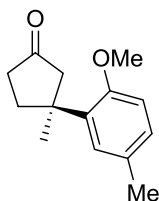
$^1\text{H-NMR}$  (400 MHz,  $\text{CDCl}_3$ )  $\delta$  7.01 (t,  $J = 8.0$ , 1H), 6.84 (dd,  $J = 15.7, 7.7$ , 2H), 3.88 (s, 3H), 3.87 (s, 3H), 2.64 (dd,  $J = 64.4, 17.9$ , 2H), 2.45 – 2.26 (m, 4H), 1.37 (s, 3H).

$^{13}\text{C-NMR}$  (101 MHz,  $\text{CDCl}_3$ )  $\delta$  219.53, 153.22, 147.58, 141.62, 123.44, 118.36, 111.15, 60.41, 55.70, 52.68, 42.96, 36.14, 35.27, 27.11.

HRMS (ESI+): Calculated mass  $[\text{M}+\text{H}]^+ \text{C}_{14}\text{H}_{19}\text{O}_3^+ = 235.1328$ ; found: 235.1327.

$[\alpha]_D^{20} = -30.2$  ( $\text{CHCl}_3$ ,  $c = 0.01$ ) for a 94% *ee* sample.

Chiral HPLC analysis on a Chiracel OD-H column, *n*-Heptane : *i*-PrOH = 99 : 1, 40 °C, flow = 0.5 mL/min, UV detection at 190 nm, 225 nm and 254 nm, retention times (min): 31.3 (minor) and 34.2 (major).



**3-(2-methoxy-5-methylphenyl)-3-methylcyclopentanone (3i):**

This compound was prepared according to the general procedure and purified with flash chromatography using pentane : ether (4 : 1) as the eluent. Racemic synthesis = 78% yield, enantioselective synthesis 19% yield (32% with double catalyst loading), 80% *ee*.

$^1\text{H-NMR}$  (400 MHz,  $\text{CDCl}_3$ )  $\delta$  7.05 – 6.98 (m, 2H), 6.80 (d,  $J = 8.2$ , 1H), 3.80 (s, 3H), 2.62 (dd,  $J = 18.2, 11.5$ , 2H), 2.47 – 2.31 (m, 4H), 2.30 (s, 3H), 1.38 (s, 3H).

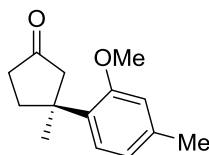
$^{13}\text{C-NMR}$  (101 MHz,  $\text{CDCl}_3$ )  $\delta$  219.92, 155.55, 135.88, 129.46, 127.80, 127.09, 111.37, 55.06, 52.30, 42.53, 36.38, 34.89, 26.23, 20.70.

HRMS (ESI+): Calculated mass  $[\text{M}+\text{H}]^+ \text{C}_{14}\text{H}_{19}\text{O}_2^+ = 219.13796$ ; found: 219.13786.  
(ESI+): Calculated mass  $[\text{M}+\text{Na}]^+ \text{C}_{14}\text{H}_{18}\text{O}_2\text{Na} = 241.1199$ ; found: 241.1197.

$[\alpha]_{\text{D}}^{20} = -132.3$  ( $\text{CHCl}_3$ ,  $c$  0.01) for a 80% *ee* sample.

Chiral HPLC analysis on a Chiracel AD-H column, *n*-Heptane : *i*-PrOH = 99 : 1, 40 °C, flow = 0.5 mL/min, UV detection at 190 nm, 225 nm and 254 nm, retention times (min): 15.2 (minor) and 16.8 (major).

Chiral HPLC analysis on a Chiracel OD-H column, *n*-Heptane : *i*-PrOH = 99 : 1, 40 °C, flow = 0.5 mL/min, UV detection at 190 nm, 225 nm and 254 nm, retention times (min): 15.9 (major) and 23.8 (minor).



**3-(2-methoxy-4-methylphenyl)-3-methylcyclopentanone (3k):**

This compound was prepared according to the general procedure and purified with flash chromatography using pentane : ether (4 : 1) as the eluent. Racemic synthesis = 78% yield, enantioselective synthesis 19% yield (32% with double catalyst loading), 80% *ee*.

## CHAPTER 5

$^1\text{H-NMR}$  (400 MHz,  $\text{CDCl}_3$ )  $\delta$  7.08 (d,  $J = 7.8$ , 1H), 6.74 (d,  $J = 7.8$ , 1H), 6.72 (s, 1H), 3.81 (d,  $J = 4.5$ , 3H), 2.61 (q, 2H), 2.44 – 2.27 (m, 7H), 1.37 (s, 3H).

$^{13}\text{C-NMR}$  (101 MHz,  $\text{CDCl}_3$ )  $\delta$  219.98, 157.51, 137.57, 133.16, 126.10, 120.97, 112.35, 54.89, 52.38, 42.35, 36.40, 34.94, 26.29, 21.22.

HRMS (ESI+): Calculated mass  $[\text{M}+\text{H}]^+ \text{C}_{14}\text{H}_{19}\text{O}_2^+ = 219.13796$ ; found: 219.13799  
(ESI+): Calculated mass  $[\text{M}+\text{Na}]^+ \text{C}_{14}\text{H}_{18}\text{O}_2\text{Na}^+ = 241.11990$ ; found: 241.11995.

$[\alpha]_{\text{D}}^{20} = -29.8$  ( $\text{CHCl}_3$ ,  $c = 0.01$ ) for a 80% *ee* sample.

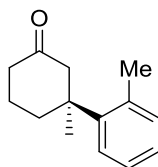
Chiral HPLC analysis on a Phenomenex LUX  $5\mu$  Cellulose-3 column, *n*-Heptane : *i*-PrOH = 99 : 1, 40 °C, flow = 1.0 mL/min, UV detection at 190 nm and 225 nm, retention times (min): 35.0 (major) and 37.4 (minor).

Chiral HPLC analysis on a Chiracel AS-H column, *n*-Heptane : *i*-PrOH = 99 : 1, 40 °C, flow = 0.5 mL/min, UV detection at 190 nm, 225 nm and 254 nm, retention times for racemate (min): 20.7 and 22.6.

Chiral HPLC analysis on Chiracel OB-H column, *n*-Heptane : *i*-PrOH = 99 : 1, 40 °C, flow = 0.5 mL/min, UV detection at 190 nm, 225 nm and 254 nm, retention times for racemate (min): 35.7 and 39.9.

Chiral HPLC analysis on a Chiracel OD-H column, *n*-Heptane : *i*-PrOH = 99 : 1, 40 °C, flow = 0.5 mL/min, UV detection at 190 nm, 225 nm and 254 nm, retention times for racemate (min): 32.6 and 37.5.

*Note:* The boronic acid required for the Michael addition was prepared according to the literature procedures: P. Wucher, V. Goldbach, S. Mecking, *Organometallics* **2013**, *32*, 4516 and J.A. Lowe III, J.P. Whittle, (Pfizer Inc.) US6235747 B1, **2001**.



### **3-methyl-3-(*o*-tolyl)cyclohexanone (4a):**

This compound was prepared according to the general procedure and purified with flash chromatography using pentane : ether (4 : 1) as the eluent. Racemic synthesis = 41% yield, enantioselective synthesis 16% yield, 98% *ee*.

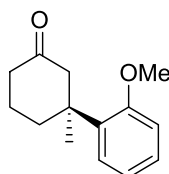
Pd-catalyzed Asymmetric Conjugate Addition of Ortho-substituted Arylboronic Acids

$^1\text{H-NMR}$  (400 MHz,  $\text{CDCl}_3$ )  $\delta$  7.25 – 7.21 (m,  $J = 4.3$ , 1H), 7.17 – 7.10 (m, 3H), 3.00 (d,  $J = 14.2$ , 1H), 2.54 (s, 3H), 2.47 (d,  $J = 14.4$ , 2H), 2.31 (t,  $J = 6.8$ , 2H), 1.99 – 1.82 (m, 2H), 1.67 – 1.57 (m, 1H), 1.42 (s, 3H).

$^{13}\text{C-NMR}$  (101 MHz,  $\text{CDCl}_3$ )  $\delta$  211.86, 144.31, 135.70, 133.49, 127.14, 126.59, 126.24, 55.11, 44.22, 40.84, 36.02, 27.41, 23.43, 21.91.

HRMS (ESI+): Calculated mass  $[\text{M}+\text{H}]^+ \text{C}_{14}\text{H}_{19}\text{O}^+ = 203.1430$ ; found: 203.1430.

Chiral HPLC analysis on a Chiracel OD-H column, *n*-Heptane : *i*-PrOH = 99.5 : 0.5, 40 °C, flow = 0.5 mL/min, UV detection at 190 nm, 225 nm and 254 nm, retention times (min): 23.9 (minor) and 26.9 (major).



**3-(2-methoxyphenyl)-3-methylcyclohexanone (4b):**

This compound was prepared according to the general procedure and purified with flash column chromatography using pentane : ether (4 : 1) as the eluent. Racemic synthesis = 55% yield, enantioselective synthesis 20% yield (42% with double catalyst loading), 96% *ee*.

$^1\text{H-NMR}$  (400 MHz,  $\text{CDCl}_3$ )  $\delta$  7.22 (t,  $J = 7.6$ , 2H), 6.91 (t,  $J = 8.1$ , 2H), 3.84 (s, 3H), 3.00 (d,  $J = 14.1$ , 1H), 2.63 – 2.52 (m, 1H), 2.45 (d,  $J = 14.9$ , 1H), 2.31 (t,  $J = 6.9$ , 2H), 1.93 – 1.77 (m, 2H), 1.71 – 1.61 (m, 1H), 1.40 (s, 3H).

$^{13}\text{C-NMR}$  (101 MHz,  $\text{CDCl}_3$ )  $\delta$  212.36, 157.84, 134.79, 127.78, 127.40, 120.61, 111.80, 54.92, 53.41, 42.83, 40.97, 35.02, 26.37, 22.18.

HRMS (ESI+): Calculated mass  $[\text{M}+\text{H}]^+ \text{C}_{14}\text{H}_{19}\text{O}_2^+ = 219.1379$ ; found: 219.1371.

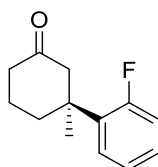
$[\alpha]_{\text{D}}^{20} = +52.5$  ( $\text{CHCl}_3$ ,  $c = 0.01$ ) for a 96% *ee* sample.

Chiral HPLC analysis on a Chiracel AD-H column, *n*-Heptane : *i*-PrOH = 99 : 1, 40 °C, flow = 0.5 mL/min, UV detection at 190 nm, 225 nm and 254 nm, retention times (min): 17.9 (major) and 19.2 (minor).

## CHAPTER 5

Chiral HPLC analysis on a Phenomenex LUX 5 $\mu$  Cellulose-3 column, *n*-Heptane : *i*-PrOH = 99 : 1, 40 °C, flow = 1.0 mL/min, UV detection at 190 nm, 225 nm and 254 nm, retention times (min): 9.3 (major) and 9.9 (minor).

Chiral HPLC analysis on a Chiracel OD-H column, *n*-Heptane : *i*-PrOH = 99 : 1, 40 °C, flow = 0.5 mL/min, UV detection at 190 nm, 225 nm and 254 nm, retention times for racemate (min): 19.4 and 21.1



### 3-(2-fluorophenyl)-3-methylcyclohexanone (4c):

This compound was prepared according to the general procedure and purified with flash chromatography using pentane : ether (4 : 1) as the eluent. Racemic synthesis = 10% yield (with double catalyst loading), enantioselective synthesis 13% yield (23% with double catalyst loading), 95% *ee*.

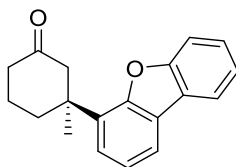
<sup>1</sup>H-NMR (400 MHz, CDCl<sub>3</sub>)  $\delta$  7.25 – 7.18 (m, 2H), 7.10 – 6.98 (m, 2H), 2.94 (d, *J* = 14.7, 1H), 2.50 – 2.41 (m, 2H), 2.33 (t, *J* = 6.7, 2H), 1.97 – 1.86 (m, 2H), 1.68 – 1.58 (m, 1H), 1.41 (s, 3H).

<sup>13</sup>C-NMR (101 MHz, CDCl<sub>3</sub>)  $\delta$  218.55, 218.53, 162.59, 160.13, 135.00, 134.88, 128.47, 128.38, 127.12, 127.07, 124.29, 124.26, 116.64, 116.40, 52.11, 52.08, 42.31, 42.28, 36.28, 36.27, 34.83, 34.80, 26.98, 26.96 (*Spectrum contains double amount of peaks due to the carbon-fluorine coupling*).

HRMS (ESI+): Calculated mass [M+H]<sup>+</sup> C<sub>13</sub>H<sub>16</sub>OF<sup>+</sup> = 207.1179; found: 207.1170.

$[\alpha]_D^{20}$  = +46.1 (CHCl<sub>3</sub>, *c* = 0.01) for a 95% *ee* sample.

Chiral HPLC analysis on a Phenomenex LUX 5 $\mu$  Cellulose-3 column, *n*-Heptane : *i*-PrOH = 99 : 1, 40 °C, flow = 0.5 mL/min, UV detection at 190 nm, 225 nm and 254 nm, retention times (min): 14.0 (minor) and 15.0 (major).



**3-(dibenzo[b,d]furan-4-yl)-3-methylcyclohexanone (4e):**

This compound was prepared according to the general procedure and purified with flash chromatography using pentane : ether (4 : 1) as the eluent. Racemic synthesis = 14% yield (20% with double catalyst loading), enantioselective synthesis 36% yield, 93% *ee*.

<sup>1</sup>H-NMR (400 MHz, CDCl<sub>3</sub>) δ 7.95 (d, *J* = 7.7, 1H), 7.85 (d, *J* = 6.0, 1H), 7.61 (d, *J* = 7.7, 1H), 7.47 (t, *J* = 7.8, 1H), 7.38 – 7.27 (m, 3H), 3.15 (d, *J* = 14.3, 1H), 2.85 – 2.77 (m, 1H), 2.64 (d, *J* = 14.4, 1H), 2.39 (t, *J* = 6.8, 2H), 2.12 – 1.88 (m, 3H), 1.61 (s, 3H).

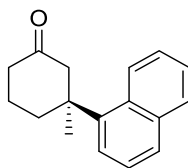
<sup>13</sup>C-NMR (101 MHz, CDCl<sub>3</sub>) δ 211.78, 155.67, 153.77, 131.93, 127.23, 125.10, 124.87, 124.13, 123.08, 122.87, 120.68, 119.38, 111.76, 53.09, 42.75, 41.17, 35.69, 27.06, 22.39.

HRMS (ESI+): Calculated mass [M+H]<sup>+</sup> C<sub>19</sub>H<sub>19</sub>O<sub>2</sub><sup>+</sup> = 279.1379; found: 279.1367

[α]<sub>D</sub><sup>20</sup> = +77.1 (CHCl<sub>3</sub>, *c* = 0.01) for a 93% *ee* sample.

Chiral HPLC analysis on a Chiracel OD-H column, *n*-Heptane : *i*-PrOH = 99 : 1, 40 °C, flow = 0.5 mL/min, UV detection at 190 nm, 225 nm and 254 nm, retention times (min): 25.5 (major) and 27.9 (minor).

Chiral HPLC analysis on a Chiracel AD-H column, *n*-Heptane : *i*-PrOH = 99 : 1, 40 °C, flow = 0.5 mL/min, UV detection at 190 nm, 225 nm and 254 nm, retention times for racemate (min): 18.4 and 45.6.



**3-methyl-3-(naphthalen-1-yl)cyclohexanone (4f):**

This compound was prepared according to the general procedure and purified with flash chromatography using pentane : ether (4 : 1) as the eluent. Racemic synthesis = 20% yield (34% with double catalyst loading), enantioselective synthesis 26% yield, 95% *ee*.

## CHAPTER 5

$^1\text{H-NMR}$  (400 MHz,  $\text{CDCl}_3$ )  $\delta$  8.41 (d,  $J = 8.4$ , 1H), 7.88 (d,  $J = 7.5$ , 1H), 7.74 (dd,  $J = 6.9$ , 2.4, 1H), 7.53 – 7.43 (m, 2H), 7.42 – 7.34 (m, 2H), 3.10 (d,  $J = 13.1$ , 1H), 2.89 – 2.80 (m, 1H), 2.64 (d,  $J = 14.6$ , 1H), 2.36 (t,  $J = 6.8$ , 2H), 2.17 (ddd,  $J = 13.6$ , 9.8, 3.6, 1H), 1.94 – 1.82 (m, 1H), 1.71 (s, 3H), 1.52 – 1.43 (m, 1H).

$^{13}\text{C-NMR}$  (101 MHz,  $\text{CDCl}_3$ )  $\delta$  211.99, 142.28, 135.42, 130.86, 130.05, 128.35, 126.19, 125.31, 125.17, 125.03, 56.15, 44.58, 40.95, 37.23, 28.52, 22.07 (one carbon signal missing due to overlap of two carbon signals).

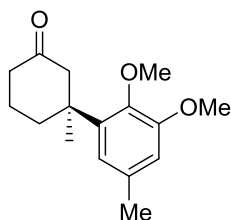
HRMS (ESI+): Calculated mass  $[\text{M}+\text{H}]^+$   $\text{C}_{17}\text{H}_{19}\text{O}^+$  = 239.14304; found: 239.14196  
(ESI+): Calculated mass  $[\text{M}+\text{Na}]^+$   $\text{C}_{17}\text{H}_{18}\text{ONa}^+$  = 261.1249; found: 261.1239.

$[\alpha]_{\text{D}}^{20} = +98.5$  ( $\text{CHCl}_3$ ,  $c = 0.01$ ) for a 95% *ee* sample.

Chiral HPLC analysis on a Phenomenex LUX  $5\mu$  Cellulose-3 column, *n*-Heptane : *i*-PrOH = 99 : 1, 40 °C, flow = 1.0 mL/min, UV detection at 190 nm, 225 nm and 254 nm, retention times (min): 13.1 (minor) and 15.5 (major).

Chiral HPLC analysis on a Chiracel OD-H column, *n*-Heptane : *i*-PrOH = 99 : 1, 40 °C, flow = 0.5 mL/min, UV detection at 190 nm, 225 nm and 254 nm, retention times for racemate (min): 27.2 and 41.1.

Chiral HPLC analysis on a Chiracel AD-H column, *n*-Heptane : *i*-PrOH = 99 : 1, 40 °C, flow = 0.5 mL/min, UV detection at 190 nm, 225 nm and 254 nm, retention times for racemate (min): 18.2 and 26.0.



### 3-(2,3-dimethoxy-5-methylphenyl)-3-methylcyclohexanone (4g):

This compound was prepared according to the general procedure and purified with flash chromatography using pentane : ether (4 : 1) as the eluent. Racemic synthesis = 44% yield, enantioselective synthesis 19% yield, 94% *ee*.

$^1\text{H-NMR}$  (400 MHz,  $\text{CDCl}_3$ )  $\delta$  6.66 (s, 1H), 6.61 (s, 1H), 3.85 (s, 3H), 3.84 (s, 3H), 2.96 (d,  $J = 14.5$ , 1H), 2.54 – 2.44 (m, 1H), 2.40 (d,  $J = 14.3$ , 1H), 2.34 – 2.30 (m, 2H), 2.28 (s, 3H), 1.92 – 1.80 (m, 2H), 1.71 – 1.58 (m, 2H), 1.39 (s, 3H).

Pd-catalyzed Asymmetric Conjugate Addition of Ortho-substituted Arylboronic Acids

$^{13}\text{C}$ -NMR (101 MHz,  $\text{CDCl}_3$ )  $\delta$  212.15, 153.13, 145.69, 139.34, 132.86, 120.05, 112.19, 60.38, 55.76, 54.04, 43.10, 40.99, 36.07, 27.61, 22.22, 21.66.

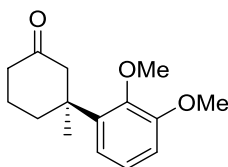
HRMS (ESI+): Calculated mass  $[\text{M}+\text{H}]^+$   $\text{C}_{16}\text{H}_{23}\text{O}_3^+$  = 263.1641; found: 263.1642.  
(ESI+): Calculated mass  $[\text{M}+\text{Na}]^+$   $\text{C}_{16}\text{H}_{22}\text{O}_3\text{Na}^+$  = 285.1461; found: 285.1462.

$[\alpha]_{\text{D}}^{20}$  = +29.7 ( $\text{CHCl}_3$ ,  $c$  = 0.01) for a 94% *ee* sample.

Chiral HPLC analysis on a Chiracel AS-H column, *n*-Heptane : *i*-PrOH = 99 : 1, 40 °C, flow = 0.5 mL/min, UV detection at 190 nm, 225 nm and 254 nm, retention times (min): 18.3 (minor) and 25.5 (major).

Chiral HPLC analysis on a Chiracel AD-H column, *n*-Heptane : *i*-PrOH = 99 : 1, 40 °C, flow = 0.5 mL/min, UV detection at 190 nm, 225 nm and 254 nm, retention times for racemate (min): 24.2 and 25.5.

*Note:* The boronic acid required for the Michael addition was prepared according to a literature procedure. See: A. Abad. C. Agullo. A.C Cunat. D. Jimenez. R.H. Perni, *Tetrahedron*, **2001**, 57, 9727.



**3-(2,3-dimethoxyphenyl)-3-methylcyclohexanone (4h):**

This compound was prepared according to the general procedure and purified with flash chromatography using pentane : ether (4 : 1) as the eluent. Racemic synthesis = 17% yield (28% with double catalyst loading), enantioselective synthesis 44% yield, 99% *ee*.

$^1\text{H}$ -NMR (400 MHz,  $\text{CDCl}_3$ )  $\delta$  6.97 (t,  $J$  = 8.1, 1H), 6.85 (d,  $J$  = 7.1, 1H), 6.82 (d,  $J$  = 8.0, 1H), 3.88 (s, 3H), 3.86 (s, 3H), 2.97 (d,  $J$  = 14.3, 1H), 2.51 (t,  $J$  = 9.5, 1H), 2.42 (d,  $J$  = 14.4, 1H), 2.35 – 2.25 (m, 2H), 1.94 – 1.80 (m, 2H), 1.71 – 1.58 (m, 1H), 1.41 (s, 3H).

$^{13}\text{C}$ -NMR (101 MHz,  $\text{CDCl}_3$ )  $\delta$  212.04, 153.43, 147.98, 139.74, 123.34, 119.56, 111.41, 60.35, 55.75, 54.06, 43.20, 40.94, 36.02, 27.62, 22.19.

HRMS (ESI+): Calculated mass  $[\text{M}+\text{H}]^+$   $\text{C}_{15}\text{H}_{21}\text{O}_3^+$  = 249.1485; found: 249.1484.



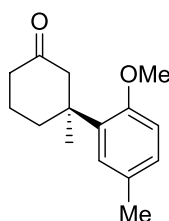
## CHAPTER 5

Chiral HPLC analysis on a Chiracel OD-H column, *n*-Heptane : *i*-PrOH = 99 : 1, 40 °C, flow = 0.5 mL/min, UV detection at 190 nm, 225 nm and 254 nm, retention times (min): 25.1 (minor) and 28.3 (major).

Chiral HPLC analysis on a Phenomenex LUX 5 $\mu$  Cellulose-3 column, *n*-Heptane : *i*-PrOH = 99 : 1, 40 °C, flow = 1.0 mL/min, UV detection at 190 nm, 225 nm and 254 nm, retention times for racemate (min): 12.4 and 14.7.

Chiral HPLC analysis on a Chiracel AD-H column, *n*-Heptane : *i*-PrOH = 99 : 1, 40 °C, flow = 0.5 mL/min, UV detection at 190 nm, 225 nm and 254 nm, retention times for racemate (min): 23.1 and 28.7.

Chiral HPLC analysis on a Chiracel AD-H column, *n*-Heptane : *i*-PrOH = 99.5 : 0.5, 40 °C, flow = 0.5 mL/min, UV detection at 190 nm, 225 nm and 254 nm, retention times for racemate (min): 16.5 and 17.9.



### 3-(2-methoxy-5-methylphenyl)-3-methylcyclohexanone (i):

This compound was prepared according to the general procedure and purified with flash chromatography using pentane : ether (4 : 1) as the eluent. Racemic synthesis = 63% yield, enantioselective synthesis 28% yield, 91% *ee*.

<sup>1</sup>H-NMR (400 MHz, CDCl<sub>3</sub>)  $\delta$  7.00 (s, 2H), 6.79 (d, *J* = 8.9, 1H), 3.80 (s, 3H), 2.99 (d, *J* = 14.2, 1H), 2.63 – 2.50 (m, 1H), 2.44 (d, *J* = 13.6, 1H), 2.31 (t, *J* = 6.8, 2H), 2.27 (s, 3H), 1.93 – 1.77 (m, 2H), 1.74 – 1.62 (m, 1H), 1.39 (s, 3H).

<sup>13</sup>C-NMR (101 MHz, CDCl<sub>3</sub>)  $\delta$  212.53, 155.83, 134.69, 129.68, 128.28, 127.95, 111.90, 55.13, 53.40, 42.73, 41.06, 35.12, 26.39, 22.25, 20.86.

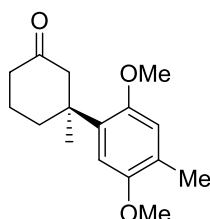
HRMS (ESI<sup>+</sup>): Calculated mass [M+H]<sup>+</sup> C<sub>15</sub>H<sub>21</sub>O<sub>2</sub><sup>+</sup> = 233.1536; found: 233.1377.

$[\alpha]_D^{20}$  = +44.1 (CHCl<sub>3</sub>, *c* = 0.01) for a 91% *ee* sample.

Chiral HPLC analysis on a Chiracel AD-H column, *n*-Heptane : *i*-PrOH = 99 : 1, 40 °C, flow = 0.5 mL/min, UV detection at 190 nm, 225 nm and 254 nm, retention times (min): 13.5 (minor) and 15.4 (major).

Pd-catalyzed Asymmetric Conjugate Addition of Ortho-substituted Arylboronic Acids

Chiral HPLC analysis on a Chiracel OD-H column, *n*-Heptane : *i*-PrOH = 99 : 1, 40 °C, flow = 0.5 mL/min, UV detection at 190 nm, 225 nm and 254 nm, retention times (min): 14.2 (major) and 16.0 (minor).



**3-(2,5-dimethoxy-4-methylphenyl)-3-methylcyclohexanone (j):**

This compound was prepared according to the general procedure and purified with flash chromatography using pentane : ether (4 : 1) as the eluent. Racemic synthesis = 73% yield, enantioselective synthesis <10% yield using double catalyst loading 84% *ee*.

<sup>1</sup>H-NMR (400 MHz, CDCl<sub>3</sub>) δ 6.73 (s, 1H), 6.70 (s, 1H), 3.78 (s, 3H), 3.77 (s, 3H), 2.98 (d, *J* = 14.4, 1H), 2.68 – 2.57 (m, 1H), 2.41 (d, *J* = 14.4, 1H), 2.29 (t, *J* = 7.0, 2H), 2.19 (s, 3H), 1.91 – 1.81 (m, 1H), 1.81 – 1.73 (m, 1H), 1.65 – 1.55 (m, 1H), 1.40 (s, 3H).

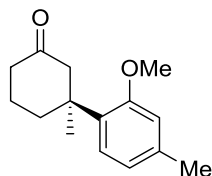
<sup>13</sup>C-NMR (101 MHz, CDCl<sub>3</sub>) δ 212.48, 151.39, 151.32, 132.40, 125.20, 115.22, 111.14, 56.04, 55.63, 53.97, 43.29, 41.05, 35.25, 27.07, 22.34, 15.85.

HRMS (ESI+): Calculated mass [M+H]<sup>+</sup> C<sub>16</sub>H<sub>23</sub>O<sub>2</sub><sup>+</sup> = 263.16417; found: 263.1644.  
(ESI+): Calculated mass [M+Na]<sup>+</sup> C<sub>16</sub>H<sub>22</sub>O<sub>3</sub>Na<sup>+</sup> = 285.1461; found: 285.1463.

[α]<sub>D</sub><sup>20</sup> = +18.7 (CHCl<sub>3</sub>, *c* = 0.003) for a 84% *ee* sample.

Chiral HPLC analysis on a Phenomenex LUX 5μ Cellulose-3 column, *n*-Heptane : *i*-PrOH = 99 : 1, 40 °C, flow = 1.0 mL/min, UV detection at 190 nm, 225 nm and 254 nm, retention times (min): 26.3 (minor) and 26.8 (major).

Chiral HPLC analysis on a Chiracel OD-H column, *n*-Heptane : *i*-PrOH = 99 : 1, 40 °C, flow = 0.5 mL/min, UV detection at 190 nm, 225 nm and 254 nm, retention times for racemate (min): 21.4 and 22.3.



### 3-(2-methoxy-4-methylphenyl)-3-methylcyclohexanone (4k):

This compound was prepared according to the general procedure and purified with flash chromatography using pentane : ether (4 : 1) as the eluent. Racemic synthesis = 76% yield, enantioselective synthesis = 17% yield, 90% *ee*.

$^1\text{H-NMR}$  (400 MHz,  $\text{CDCl}_3$ )  $\delta$  7.08 (d,  $J = 8.4$ , 1H), 6.72 (d,  $J = 6.9$ , 2H), 3.82 (s, 3H), 2.98 (d,  $J = 14.5$ , 1H), 2.62 – 2.50 (m, 1H), 2.43 (d,  $J = 14.3$ , 1H), 2.32 (s, 3H), 2.29 (d,  $J = 7.2$ , 2H), 1.91 – 1.84 (m, 1H), 1.84 – 1.76 (m, 1H), 1.71 – 1.60 (m, 1H), 1.38 (s, 3H).

$^{13}\text{C-NMR}$  (101 MHz,  $\text{CDCl}_3$ )  $\delta$  212.49, 157.71, 137.66, 131.84, 127.27, 121.12, 112.80, 54.90, 53.50, 42.56, 40.99, 35.12, 26.51, 22.21, 21.15.

HRMS (ESI+): Calculated mass  $[\text{M}+\text{H}]^+$   $\text{C}_{15}\text{H}_{21}\text{O}_2^+$  = 233.15361; found: 233.15370.  
 (ESI+): Calculated mass  $[\text{M}+\text{Na}]^+$   $\text{C}_{15}\text{H}_{20}\text{O}_2\text{Na}^+$  = 255.1355; found: 255.1356

$[\alpha]_{\text{D}}^{20} = +33.2$  ( $\text{CHCl}_3$ ,  $c = 0.01$ ) for a 90% *ee* sample.

Chiral HPLC analysis on a Chiracel OD-H column, *n*-Heptane : *i*-PrOH = 99 : 1, 40 °C, flow = 0.5 mL/min, UV detection at 190 nm, 225 nm and 254 nm, retention times (min): 23.5 (major) and 25.2 (minor).

*Note:* The boronic acid required for the Michael addition was prepared according to literature procedures: P. Wucher, V. Goldbach, S. Mecking, *Organometallics*, **2013**, *32*, 4516 and J.A. Lowe III, J.P. Whittle, (Pfizer Inc.) US6235747 B1, **2001**.

## 5.7 References

- [1] *Quaternary Stereocenters: Challenges and Solutions for Organic Synthesis*, eds. J. Christoffers and A. Baro Wiley-VCH, Weinheim, **2005**, For selected reviews on the synthesis of quaternary stereocenters, see: a) I. Denissova, L. Barriault, *Tetrahedron*, **2003**, *59*, 10105. b) C. J. Douglas, L. E. Overman, *Proc. Natl. Acad. Sci. U.S.A.* **2004**, *101*, 5363. c) J. Christoffers, A. Baro, *Adv. Synth. Catal.* **2005**, *347*, 1473. d) B. M. Trost, C. Jiang, *Synthesis*, **2006**, 369. e) J. T. Mohr, B. M. Stoltz, *Chem. Asian J.* **2007**, *2*, 1476. f) P. G. Cozzi, R. Hilgraf, N. Zimmermann, *Eur. J. Org. Chem.* **2007**, *36*, 5969. g) J. P. Das, I. Marek,

- Chem. Commun.* **2011**, 47, 4593. h) Y. Liu, S.-J. Han, W.-B. Liu, B. M. Stoltz. *Acc. Chem. Res.* **2015**, 48, 740.
- [2] C. Hawner, A. Alexakis, *Chem. Commun.* **2010**, 46, 7295. See also: A. Alexakis, N. Krausse, S. Woodward, in *Copper-catalyzed Asymmetric Synthesis*, chapter 2. eds. A. Alexakis, N. Krausse, S. Woodward), Wiley-VHC, Weinheim, **2014**.
- [3] For Selected examples: a) K.P. McGrath, A. H. Hoveyda, *Angew. Chem. Int. Ed.* **2014**, 53, 1910. b) D. Willcox, S. Woodward, A. Alexakis, *Chem. Commun.* **2014**, 50, 1655. c) D. Müller, A. Alexakis, *Chem. Eur. J.* **2013**, 19, 15226. d) D. Müller, A. Alexakis, *Org. Lett.* **2013**, 15, 1594. e) C. Bleschke, M. Tissot, D. Müller, A. Alexakis, *Org. Lett.* **2013**, 15, 2152. f) J. A. Dabrowski, M. T. Villaume, A. H. Hoveyda, *Angew. Chem. Int. Ed.* **2013**, 52, 8156. g) J. A. Dabrowski, F. Haeffner, A. H. Hoveyda, *Angew. Chem. Int. Ed.* **2013**, 52, 7694. h) D. Müller, A. Alexakis, *Chem. Commun.* **2012**, 48, 12037. i) D. Müller, M. Tissot, A. Alexakis, *Org. Lett.* **2011**, 13, 3040. j) M. Tissot, A. Pérez Hernández, D. Müller, M. Mauduit, A. Alexakis, *Org. Lett.* **2011**, 13, 1524. k) T. L. May, J. A. Dabrowski, A. H. Hoveyda, *J. Am. Chem. Soc.* **2011**, 133, 736. l) C. Hawner, D. Müller, L. Gremaud, A. Felouat, S. Woodward, A. Alexakis, *Angew. Chem. Int. Ed.* **2010**, 49, 7769. m) A. Wilsily, E. Fillion, *J. Org. Chem.* **2009**, 74, 8583. n) A. Wilsily, E. Fillion, *Org. Lett.* **2008**, 10, 2801. o) E. Fillion, A. Wilsily, *J. Am. Chem. Soc.* **2006**, 128, 2774.
- [4] a) R. Shintani, W.-L. Duan, T. Hayashi, *J. Am. Chem. Soc.* **2006**, 128, 5628. b) R. Shintani, Y. Tsutsumi, M. Nagaosa, T. Nishimura, T. Hayashi, *J. Am. Chem. Soc.* **2009**, 131, 13588. c) R. Shintani, M. Takeda, T. Nishimura, T. Hayashi, *Angew. Chem. Int. Ed.* **2010**, 49, 3969. d) R. Shintani, T. Hayashi, *Org. Lett.* **2011**, 13, 350.
- [5] For reports on quaternary stereocenter formation using arylboronic acids see a) P. Mauleón, J. C. Carretero, *Chem. Commun.* **2005**, 4961. b) B. T. Hahn, F. Tewes, R. Fröhlich, F. Glorius, *Angew. Chem. Int. Ed.* **2010**, 49, 1143.
- [6] a) K. Kikushima, J. C. Holder, M. Gatti, B. M. Stoltz, *J. Am. Chem. Soc.* **2011**, 133, 6902. b) S. E. Shockley, J. C. Holder, B. M. Stoltz, *Org. Lett.* **2014**, 16, 6362. c) S. E. Shockley, J. C. Holder, B. M. Stoltz, *Org. Process Res. Dev.* **2015**, 19, 974.
- [7] a) A. L. Gottumukkala, K. Matcha, M. Lutz, J. G. de Vries, A. J. Minnaard, *Chem. Eur. J.* **2012**, 18, 6907. b) see: PhD dissertation of Aditya L. N. R. Gottumukkala, *Palladium-catalyzed carbon-carbon bond formation under reductive, oxidative and neutral conditions*, University of Groningen, **2013**.
- [8] As stated by the authors from reference 6 “Substituents at the 2-position of the arylboronic acid were detrimental to the yields and stereoselectivity of the reaction with enone (3-methyl hex-2-enone), although 2-fluorophenylboronic acid underwent the desired reaction to provide a product in 32% yield and

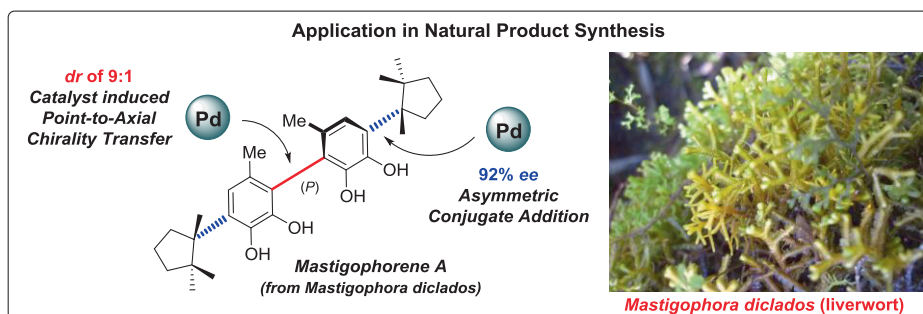
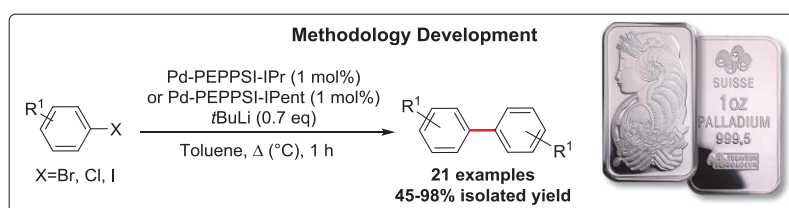
- 77% *ee*". Later work (see ref. 14) showed that the yield could be enhanced to 77% for the same transformation.
- [9] T.-S. Mei, H. H. Pater, M. S. Sigman, M. S. *Nature*, **2014**, 508, 340.
- [10] a) A. L. Gottumukkala, J. Suljagic, K. Matcha, J. G. de Vries, A. J. Minnaard, *ChemSusChem*. **2013**, 6, 1636. b) For a similar transformation see: S. Lin, X. Lu, *Org. Lett.* **2010**, 12, 2536.
- [11] The use of 7 eq of Michael acceptor resulted from the optimization of the conditions for the enantioselective transformation. Though not ideal, the enone is significantly cheaper than the boronic acids and could be easily retrieved in pure form by flash chromatography.
- [12] Undesired Pd-catalyzed homo-coupling as a side product is mentioned in: a) G. A. Molander, B. Biolatto, *J. Org. Chem.* **2003**, 68, 4302. b) A. J. J. Lennox, G. C. Lloyd-Jones, *Isr. J. Chem.* **2010**, 50, 664. c) A. J. J. Lennox, G. C. Lloyd-Jones, *Chem. Soc. Rev.* **2014**, 43, 412.
- [13] Homo-coupling suppression by using an excess of boronic acid is mentioned in: M. S. Wong, X. L. Zhang, *Tet. Lett.* **2001**, 42, 4087.
- [14] J. C. Holder, L. Zou, A. N. Marziale, P. Liu, Y. Lan, M. Gatti, K. Kikushima, K. N. Houk, B. M. Stoltz, *J. Am. Chem. Soc.* **2013**, 135, 14996.
- [15] The silver salt was changed to get the same counter-ion as reported by Stoltz *et al.* (see ref. 6 and 14).
- [16] For general remarks on protodeboronation a) D. G. Hall, In *Boronic Acids: Preparation and Applications in Organic Synthesis, Medicine and Materials – Second Completely Revised Edition*, (Eds.: Hall, D. G.), Wiley-VCH : Weinheim, **2011**. Chapter 1. b) See reference 12b.
- For specific types of protodeboronation reactions see: (1) *Pd-catalyzed protodeboronation*: c) H. G. Kuivila, J. F. Reuwer Jr., J. A. Mangravite, *J. Am. Chem. Soc.* **1964**, 86, 2666. (2) *Ag-catalyzed protodeboronation*: d) A. Michaelis, P. Becker, *Chem. Ber.* **1882**, 15, 180. e) W. Seaman, J. R. Johnson, *J. Am. Chem. Soc.* **1931**, 53, 711. f) J. R. Johnson, M. G. van Campen Jr., O. Grummitt, *J. Am. Chem. Soc.* **1938**, 60, 111. g) H. G. Kuivila, J. F. Reuwer Jr., J. A. Mangravite, *J. Am. Chem. Soc.* **1964**, 86, 2666. h) C. Pourbaix, F. Carreaux, B. Carboni, H. Deleuze, *Chem. Commun.* **2000**, 1275. (3) *Heat induced protodeboronation*: i) M. A. Beckett, R. J. Gilmore, K. Idrees, *J. Organomet. Chem.* **1993**, 455, 47. j) C.-Y. Lee, S.-J. Ahn, C.-H. Cheon, *J. Org. Chem.* **2013**, 78, 12154. (4) *Fluoride mediated protodeboronation*: k) S. Nave, R. P. Sonawane, T. G. Elford, V. K. Aggarwal, *J. Am. Chem. Soc.* **2010**, 132, 17096. l) M. J. Hesse, C. P. Butts, C. L. Willis, V. K. Aggarwal, *Angew. Chem. Int. Ed.* **2012**, 51, 12444. (5) *Acid-catalyzed protodeboronation*: m) H. G. Kuivila, K. V. Nahabedian, *J. Am. Chem. Soc.* **1961**, 83, 2159. n) H. G. Kuivila, K. V. Nahabedian, *J. Am. Chem. Soc.* **1961**, 83, 2164. o) K. V. Nahabedian, H. G. Kuivila, H.G. *J. Am. Chem. Soc.* **1961**, 83, 2167. (6) *Protodeboronation by hydrolysis*: p) A. D. Ainley, F. Challenger, *J. Chem. Soc.* **1930**, 2171.

- [17] For general strategies to mitigate protodeboronation, see reference 12b. For protodeboronation suppression by addition of excess of boronic acid see: a) Y. Takaya, M. Ogasawara, T. Hayashi, *J. Am. Chem. Soc.* **1998**, *120*, 5579. For protodeboronation suppression by temperature lowering see: b) T. Hayashi, M. Takahashi, Y. Takaya, M. Ogasawara, *J. Am. Chem. Soc.* **2002**, *124*, 5052. In our catalytic system an excess of arylboronic acid leads to significant biaryl formation. This product, in some cases, proved to be very difficult to separate from the desired Michael adduct. Lowering the reaction temperature led to significant retardation of the catalytic process.
- [18] A. Matsuo, S. Yuki, M. Nakayama, *J. Chem. Soc. Perkin Trans.* **1986**, 701.
- [19] M. Toyota, T. Kinugawa, Y. Asakawa, *Phytochemistry* **1994**, *37*, 859.
- [20] Y. Fukuyama, Y. Kiriya, M. Kodama, *Tetrahedron Lett.* **1996**, *37*, 1261.
- [21] Asymmetric total syntheses of herbertenediol: a) A. P. Degnan, A. I. Meyers, *J. Am. Chem. Soc.* **1999**, *121*, 2762. (b) G. Bringmann, T. Pabst, P. Henschel, J. Kraus, K. Peters, E.-M. Peters, D. S. Rycroft, J. D. Connolly, *J. Am. Chem. Soc.* **2000**, *122*, 9127. c) Y. Fukuyama, K. Matsumoto, Y. Tono, R. Yokoyama, H. Takahashi, H. Minami, H. Okazaki, Y. Mitsumoto, *Tetrahedron* **2001**, *57*, 7127. d) A. Abad, C. Agulló, A. C. Cuñat, D. Jiménez, R. H. Perni, *Tetrahedron*, **2001**, *57*, 9727. e) A.-M. Zhang, G.-Q. Lin, *Chin. J. Chem.* **2001**, *19*, 1245. f) Y. Kita, J. Futamura, Y. Ohba, Y. Sawama, J. K. Ganesh, H. Fujioka, *J. Org. Chem.* **2003**, *68*, 5917. (g) Y. Kita, J. Futamura, Y. Ohba, Y. Sawama, J. K. Ganesh, H. Fujioka, *Tetrahedron Lett.* **2003**, *44*, 411. h) S. Acherar, G. Audran, F. Fotiadu, H. Monti, *Eur. J. Org. Chem.* **2004**, 5092. For racemic syntheses see: i) Y. Fukuyama, Y. Kiriya, M. Kodama, *Tetrahedron Lett.* **1996**, *37*, 1261. j) P. D. Gupta, A. Pal, A. Roy, D. Mukherjee, *Tetrahedron Lett.* **2000**, *41*, 7563. k) Y. Fukuyama, K. Matsumoto, Y. Tono, R. Yokoyama, H. Takahashi, H. Minami, H. Okazaki, Y. Mitsumoto, *Tetrahedron* **2001**, *57*, 7127. l) A. Srikrishna, M. S. Rao, *Tetrahedron Lett.* **2001**, *42*, 5781. m) A. Srikrishna, M. S. Rao, *Synlett* **2002**, 340. n) A. Srikrishna, G. Satyanarayana *Tetrahedron* **2006**, *62*, 2892.
- [22] H. E. Zimmerman, R. D. Little, *J. Am. Chem. Soc.* **1974**, *96*, 4623.
- [23] K. C. Nicolaou, T. Montagnon, P. S. Baran, Y.-L. Zhong, *J. Am. Chem. Soc.* **2002**, *124*, 2245.
- [24] K. C. Nicolaou, T. Montagnon, P. S. Baran, *Angew. Chem. Int. Ed.* **2002**, *41*, 1386.
- [25] Over-oxidation was observed mainly in the form of benzylic oxidation.
- [26] T. Diao, T. J. Wadzinski, S. S. Stahl, *Chem. Sci.* **2012**, *3*, 887.
- [27] A. Srikrishna, P. C. Ravikumar, *Tetrahedron* **2006**, *62*, 9393.
- [28] a) D. H. R. Barton, D. A. J. Ives, B. R. Thomas, *J. Chem. Soc.* **1955**, 2056. b) D. H. R. Barton, D. A. J. Ives, B. R. Thomas, *J. Chem. Soc.* **1954**, 903.
- [29] M. Yoshida, T. Kasai, T. Mizuguchi, K. Namba, *Synlett* **2014**, *25*, 1160.

- [30] Comparison of the optical rotation of the synthetic material with that of the natural source revealed that the absolute stereochemistry matched that of the natural product. Therefore we conclude that the conjugate addition of the boronic acid **4** to 3-methyl cyclopent-2-enone, using PdCl<sub>2</sub>-(*R,R*-PhBOX), furnishes the Michael adducts with the (*S*)-configuration.
- [31] N. K. Ishikawa, K. Yamaji, S. Tahara, Y. Fukushi, K. Takahashi, K. *Phytochemistry* **2000**, *54*, 777.
- [32] N. K. Ishikawa, Y. Fukushi, K. Yamaji, S. Tahara, K. Takahashi, *J. Nat. Prod.* **2001**, *64*, 932.
- [33] For asymmetric Enokipodin A and B syntheses see: a) K. P. McGrath, A. H. Hoveyda, *Angew. Chem. Int. Ed.* **2014**, *53*, 1910. b) M. Yoshida, Y. Shoji, K. Shishido, *Org. Lett.* **2009**, *11*, 1441. c) M. Saito, S. Kuwahara, *Biosci. Biotechnol. Biochem.* **2005**, *69*, 374. d) S. Kuwahara, M. Saito, *Tetrahedron Lett.* **2004**, *45*, 5047.  
For racemic syntheses see: e) A. Srikrishna, M. S. Rao, *Synlett* **2004**, 374. f) F. Secci, A. Frongia, J. Ollivier, P. P. Piras, *Synthesis* **2007**, 999. g) J. A. Luján-Montelongo, J. G. Avila-Zarraga, *Tetrahedron Lett.* **2010**, *51*, 2232. h) D. Lebœuf, C. M. Wright, A. J. Frontier, *Chem. Eur. J.* **2013**, *19*, 4835.
- [34] R. van Zeeland, L. M. Stanley, *ACS Catal.* **2015**, *5*, 5203.
- [35] J-G. Boiteau, A. J. Minnaard, B. L. Feringa, *J. Org. Chem.* **2003**, *68*, 9481.
- [36] F. Duval, T. A. van Beek, H. Zuilhof, *Synlett*, **2012**, *23*, 1751.
- [37] A. Srikrishna, M. Srinivasa Rao, *Indian J. Chem.* **2010**, *49b*, 1363.

## \*\*\* CHAPTER 6 \*\*\*

### ‡ Pd-Catalyzed, *t*BuLi-mediated dimerization of Aryl Halides and its Application in the Atropselective Total Synthesis of Mastigophorene A ‡



**ABSTRACT:** This chapter describes the investigation into new palladium-catalyzed homo-coupling methodology to construct symmetrical biaryl compounds. With the recent advent of Pd-catalyzed cross-coupling reactions of organolithium reagents, an efficient homo-coupling of in situ generated aryllithium reagents with a Pd-PEPPSI catalyst could be developed. Although the overall scope of Pd-catalyzed cross-coupling reactions with organolithium reagents is quite impressive, the methodology lacks application within the realms of natural product synthesis. Application of the newly developed methodology was found in the shortest atropselective construction of the naturally occurring, chiral biaryl compound, mastigophorene A.

This chapter has been published in part:

J. Buter, D. Heijnen, C. Vila, V. Hornillos, E. Otten, M. Giannerini, A. J. Minnaard, B. L. Feringa, *Angew. Chem. Int. Ed.* **2016**, 55, 3620

The synthetic efforts described in this chapter resulted from collaboration with the Feringa laboratory. Development of the Pd-catalyzed homo-coupling was performed by Dr. C. Vila, Dr. V. Hornillos and Dr. M. Giannerini. The substrate scope was investigated by Dr. C. Vila. Homo-coupling of test substrates for the mastigophorene A synthesis were performed by D. Heijnen.



## 6.1 Introduction

The synthesis of biaryl compounds has been studied for more than a century<sup>[1]</sup> and is an important process in organic chemistry, as the biaryl structure is present in numerous natural products, bioactive compounds, agrochemicals, dyes and ligands. Symmetric biaryls play a crucial role in catalysis as a range of ligands possess this structural motif (Figure 1). Furthermore, natural products with a symmetric biaryl moiety, not necessarily enantiopure, show interesting biological activities.<sup>[2]</sup>

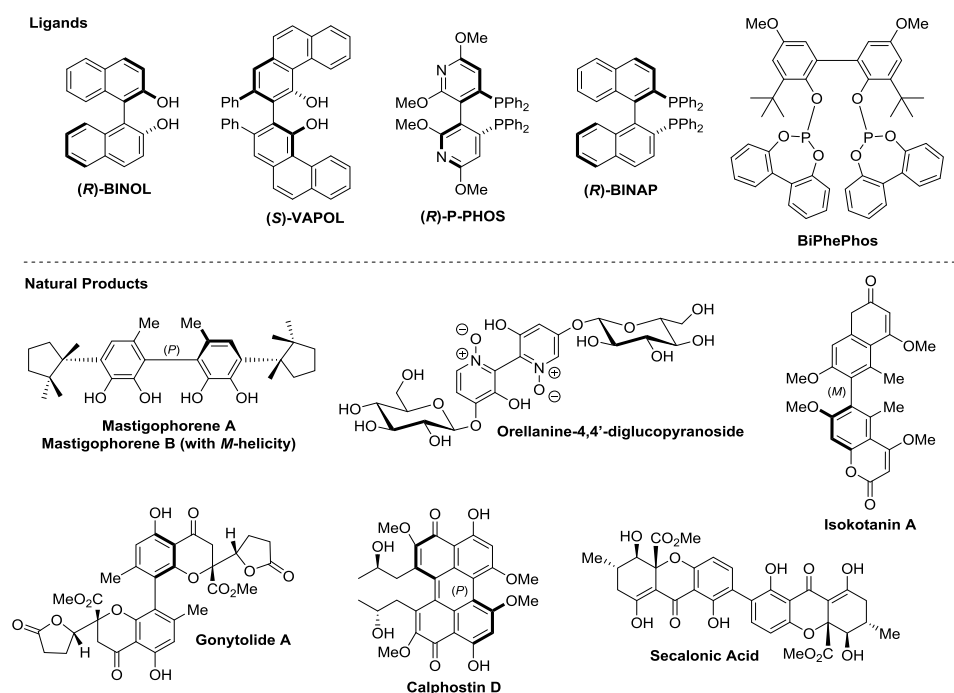


**Figure 1.** Representative ligands and natural products with a symmetric biaryl structure.

In 1901, Ullmann reported the synthesis of biaryls from aryl halides using stoichiometric amounts of copper under harsh reaction conditions.<sup>[3,4]</sup> Over the years, several coupling methodologies have been described using nickel, palladium or iron complexes as the catalyst, with different organic halides and organometallics such as Grignard, zinc, boron or tin reagents.<sup>[5]</sup> These methods, however, are generally not employed in the synthesis of symmetric tetra-*ortho*-substituted biaryls, with the exception of the Suzuki-Miyaura coupling. Despite low catalyst loadings, an excellent scope and mostly good to excellent yields, the Suzuki-Miyaura coupling commonly requires two different, independently synthesized, reagents to be coupled, namely an aryl halide and an aryl boron reagent. This feature makes the synthesis of symmetrical biaryl compounds inherently less efficient, especially when considering natural product synthesis where step-count is an important issue.

Aryllithium reagents are readily prepared via halogen-lithium exchange or direct metalation,<sup>[6]</sup> and might provide a valuable alternative for the synthesis of symmetric biaryls. Moreover, as boron, tin or zinc reagents are frequently prepared from the corresponding lithium reagents,<sup>[7]</sup> the direct use of organolithium reagents could be beneficial as it eliminates additional transformations and purification processes.

Important advances have been made in recent years although homo-coupling of organolithium reagents using Pd-catalysis has received only little attention. Spring and co-workers reported the homo-coupling of aryllithium reagents formed by directed lithiation, that underwent transmetalation with, stoichiometric, copper (I) and subsequent oxidation of the cuprate yielding the corresponding biaryls.<sup>[8]</sup> Yoshida and co-workers reported a FeCl<sub>3</sub>-catalyzed oxidative homo-coupling of aryllithium reagents in a flow system.<sup>[9]</sup> The corresponding biaryls were obtained with good yields in very short reaction times at temperatures of -48 to +24 °C. Recently, Taillefer described methodology for the FeCl<sub>2</sub>-catalyzed oxidative homo-coupling of aryl bromides and iodides in the presence of *s*BuLi (1.6 eq) or *t*BuLi (2 eq), with a wide substrate scope.<sup>[10]</sup> In addition, Lu presented a vanadium tetrachloride (1 mol%) catalyzed oxidative homo-coupling of aryllithium reagents, prepared via lithium-halogen exchange with *n*BuLi, although only three different biaryls were reported and the reaction required 10-12 h to provide the corresponding products.<sup>[11]</sup> Homo-coupling of seven aryllithium compounds catalyzed by a [NiCl<sub>2</sub>dppp]-2,2-bipyridyl complex (0.7 mol%) was demonstrated by Carter and co-workers.<sup>[12]</sup> These reactions were carried out at room temperature and good yields ranging from 72% to 86% were obtained.

Most of these protocols require *in situ* preparation of the organolithium at low temperatures and the use of stoichiometric or super-stoichiometric amounts of a lithium reagent for the lithium-halogen exchange. Moreover, the methodologies reported so-far did not involve the construction of sterically congested tetra-*ortho*-substituted biaryls, except for three examples of Cu-mediated coupling reported by Spring and co-workers.<sup>8</sup> As far as we know, application of this type of coupling methodology in the synthesis of biaryl containing natural products has not been reported.

Recently the Feringa laboratory published a series of papers reporting the palladium-catalyzed cross-coupling of alkyl- and aryllithium reagents with aryl halides/triflates.<sup>[13,14]</sup> Concurrent with our synthetic efforts to synthesize mastigophorenes A and B (Figure 1) the Feringa group was well on its way developing a palladium-catalyzed homo-coupling of aryllithium reagents. We strengthened our efforts by collaborating with the Feringa laboratory which resulted in the development of novel homo-coupling methodology with direct application in natural product synthesis. In this chapter we thus present a highly efficient and selective homo-coupling of aryl halides in the presence of *t*BuLi (0.7 eq), using 1 mol% of a palladium catalyst (PEPPSI-IPr or PEPPSI-IPent) featuring short reaction times (1 h) at rt. In addition, we were eager to apply this methodology in the construction of the naturally occurring symmetric, tetra-*ortho*-substituted, biaryl compounds mastigophorene A or B (Figure 1). The chiral biaryl axis was installed with surprisingly high diastereoselectivity via

## CHAPTER 6

point-to-axial chirality transfer from a remote stereocenter induced by the Pd-PEPPSI-IPent catalyst.

### 6.2 Development of a Pd-catalyzed homo-coupling employing aryllithium reagents

We initially chose 2-bromoanisole as a model substrate (Table 1), in which the halogen-lithium exchange process is facilitated due to coordination and stabilization by the methoxy group at the *ortho* position. The aryllithium reagent was added slowly to the 2-bromoanisole (**1a**) in toluene at room temperature using QPhos<sup>[15]</sup>-Pd<sub>2</sub>dba<sub>3</sub> **C1** (entries 1-3) or Pd-PEPPSI-IPent<sup>[16]</sup> **C2** (entries 4-6). These were the best catalysts selected from a short screening (*see experimental section*).

**1a**  $\xrightarrow[\text{Toluene, rt, 1 h}]{\text{Palladium catalyst (x mol\%), RLi (n eq)}}$  **2a** + **3** + **4**

**C1:** QPhos-Pd<sub>2</sub>dba<sub>3</sub> (4:1)

**C2:** R = *i*Pent, Pd-PEPPSI-IPent

**C3:** R = *i*Pr, Pd-PEPPSI-IPr

Entry	Pd-cat (x mol%)	RLi (n eq)	<b>2a</b> (%) <sup>a</sup> Yield (%) <sup>b</sup>	<b>3</b> (%) <sup>a</sup>	<b>4</b> (%) <sup>a</sup>
1	<b>C1</b> (5%)	<i>n</i> BuLi (1 eq)	62	trace	38
2	<b>C1</b> (5%)	<i>s</i> BuLi (1 eq)	83	10	7
3	<b>C1</b> (5%)	<i>t</i> BuLi (1 eq)	96	trace	4 <sup>c</sup>
4	<b>C2</b> (5%)	<i>n</i> BuLi (1 eq)	64	3	33
5	<b>C2</b> (5%)	<i>s</i> BuLi (1 eq)	94	4	2
6	<b>C2</b> (5%)	<i>t</i> BuLi (1 eq)	full <sup>d</sup>	trace	trace
7	<b>C1</b> (2.5%)	<i>t</i> BuLi (0.7 eq)	89	trace	11 <sup>c</sup>
8	<b>C2</b> (2.5%)	<i>t</i> BuLi (0.7 eq)	full <sup>d</sup> (84)	trace	trace
9	<b>C2</b> (1%)	<i>t</i> BuLi (0.7 eq)	98 (86)	trace	2 <sup>c</sup>
10	<b>C3</b> (1%)	<i>t</i> BuLi (0.7 eq)	full <sup>d</sup> (91)	trace	trace
11	-	<i>t</i> BuLi (1 eq)	-	full	-

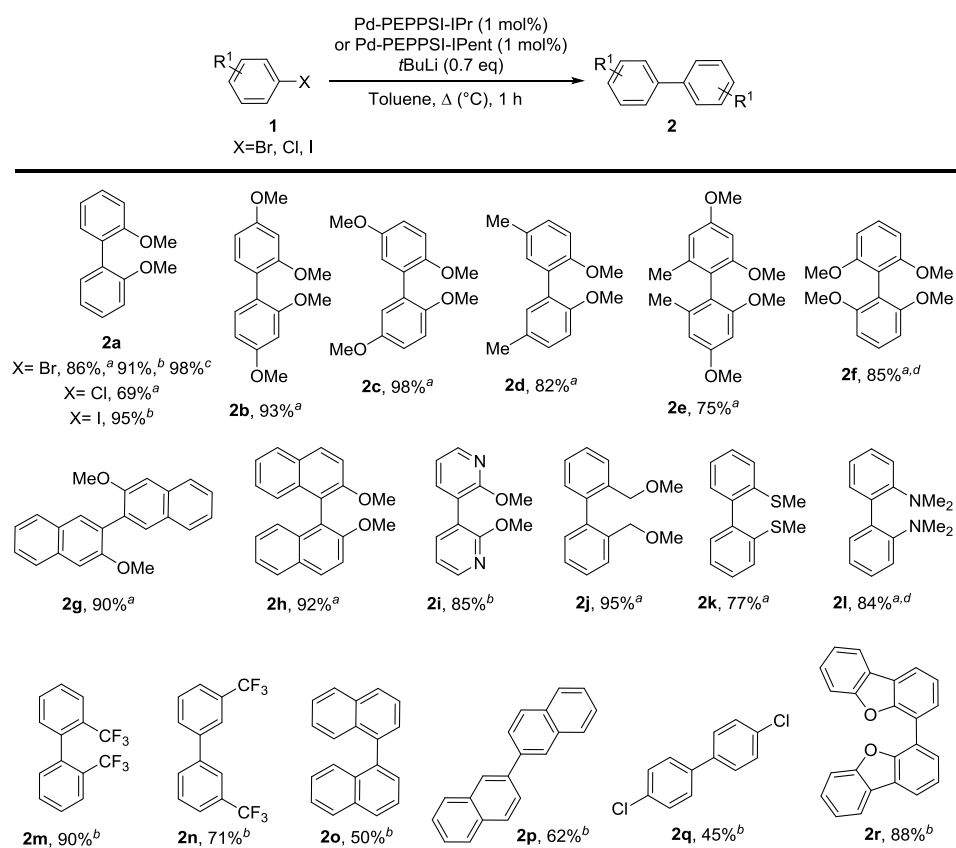
Reaction conditions: **1a** (0.3 mmol) and the palladium catalyst in 2 mL of toluene at 20 °C; RLi (*n* eq) diluted to 1 mL with toluene was added dropwise over 1 h. <sup>a</sup> Conversions were determined by GC-MS analysis. <sup>b</sup> Isolated yield, after column chromatography, in brackets. <sup>c</sup> R = *i*Bu. <sup>d</sup> >99% conversion.

**Table 1.** Palladium-catalyzed dimerization of 2-bromoanisole.

We studied the homo-coupling reaction using the commercially available alkyllithium reagents *n*BuLi (entries 1 and 4), *s*BuLi (entries 2 and 5) and *t*BuLi (entries 3 and 6) to generate the corresponding (2-methoxyphenyl)lithium *in situ*. The highest selectivity for the formation of 2,2'-dimethoxy-1,1'-biphenyl **2a** (entries 3 and 6) was obtained when *t*BuLi was used. Subsequently, we tried to reduce the catalyst loading to 2.5 mol% (entries 7-8) and the amount of *t*BuLi to 0.7 eq. Full conversion to **2a** (84% isolated yield), was observed when Pd-PEPPSI-IPent was used as a catalyst, while QPhos-Pd<sub>2</sub>dba<sub>3</sub> **C1** was less selective and some alkylated anisole was observed. The catalyst loading could be reduced to 1 mol% (entry 9), without erosion in the yield and selectivity. Finally, Pd-PEPPSI-IPr<sup>[17]</sup> **C3**, was also tested, and full conversion to the product **2a** was achieved, with 91% isolated yield (entry 10). Without Pd-catalyst no coupling reaction takes place (entry 11).

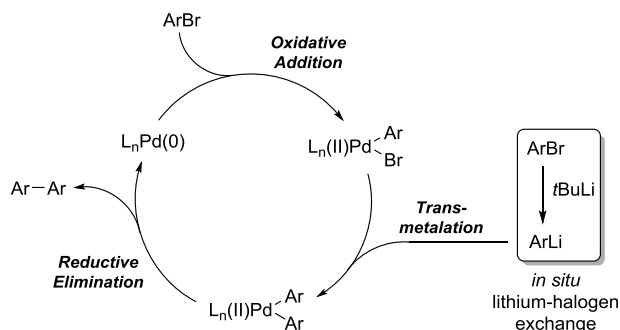
With the optimized conditions in hand (entries 9 and 10), we studied the scope and limitations of our new methodology (Scheme 1). With 2-chloroanisole, full conversion was not achieved and **2a** was obtained in 69% isolated yield using Pd-PEPPSI-IPent, while with 2-iodoanisole **2a** was obtained in 95% yield. These results are explained by a faster lithium-halogen exchange of the bromide or iodide, than that of the chloride and this favors the catalytic homo-coupling and the selective formation of the biaryl. Next, various aromatic bromides with a methoxy group at the *ortho* position were studied. Biaryls **2b**, **2c** and **2d**, with different electron-donating substituents at the aromatic ring, were obtained with excellent yields. Even 2,2',4,4'-tetramethoxy-6,6'-dimethyl-1,1'-biphenyl **2e**, a tetra-*ortho*-substituted biaryl, was successfully synthesized in 75% yield in 1 h at room temperature. When 2-bromo-1,3-dimethoxybenzene was used, the reaction had to be performed at 50 °C, in order to obtain the corresponding tetra-*ortho*-substituted biaryl **2f**, in 85% yield. Although a higher temperature was required, probably due to the steric hindrance of the two coupling partners, selectivity was not affected. 2,2'-Dimethoxy-1,1'-binaphthalene **2g** and 2,2'-dimethoxy-1,1'-binaphthalene **2h** were obtained in 90% and 92% yields, respectively.

Importantly, heterocycles are also efficient coupling partners, as is illustrated by the smooth dimerization of 3-bromo-2-methoxypyridine, and the corresponding bipyridine **2i** was isolated in 85% yield. Other aryl bromides with electron-donating groups at the *ortho* position to the bromide such as thiomethyl or *N,N*-dimethylamino were also tested, providing the corresponding biaryls **2k** and **2l**. Subsequently, we performed the reaction with aryl bromides bearing electron-withdrawing groups such as *ortho*-bromotrifluoromethylbenzene and *meta*-bromotrifluoromethylbenzene, affording the corresponding fluorinated biaryls **2m** and **2n** with good yields. The use of 1-bromonaphthalene, 2-bromonaphthalene and *para*-chlorobromobenzene, led to a lower selectivity and the products (**2o-q**) were obtained with moderate yields. However, 4-bromodibenzofuran reacted efficiently and afforded biaryl **2r** in 88% yield. To demonstrate the synthetic utility of the present methodology, **2a** was prepared on a gram scale (1.12 g, 6 mmol) using 0.5 mol% of Pd-PEPPSI-IPr in 98% yield in 2 h.



**Scheme 1.** Scope of the Pd-catalyzed homo-coupling of aryl halides in the presence of *t*BuLi. <sup>a</sup> 1 mol% Pd-PEPPSI-IPent was used. <sup>b</sup> 1 mol% Pd-PEPPSI-IPr was used. <sup>c</sup> 6 mmol scale reaction using 0.5 mol% of Pd-PEPPSI-IPr in 2 h. <sup>d</sup> The reaction was performed at 50 °C.

The proposed catalytic cycle for the reaction is depicted in scheme 2, and is believed to follow “classic” Pd cross-coupling mechanism. Oxidative addition of the Pd<sup>0</sup>-catalyst into the aryl bromide takes place, generating the Ar-Pd<sup>II</sup>-Br species. This is followed by transmetalation of the aryllithium reagent, formed *in situ* by lithium-halogen exchange, forming Ar-Pd<sup>II</sup>-Ar, which undergoes reductive elimination to afford the desired symmetric biaryl product and regenerating the Pd<sup>0</sup> catalyst.



Scheme 2. Proposed catalytic cycle.

### 6.3 Application in the asymmetric total synthesis of mastigophorene A

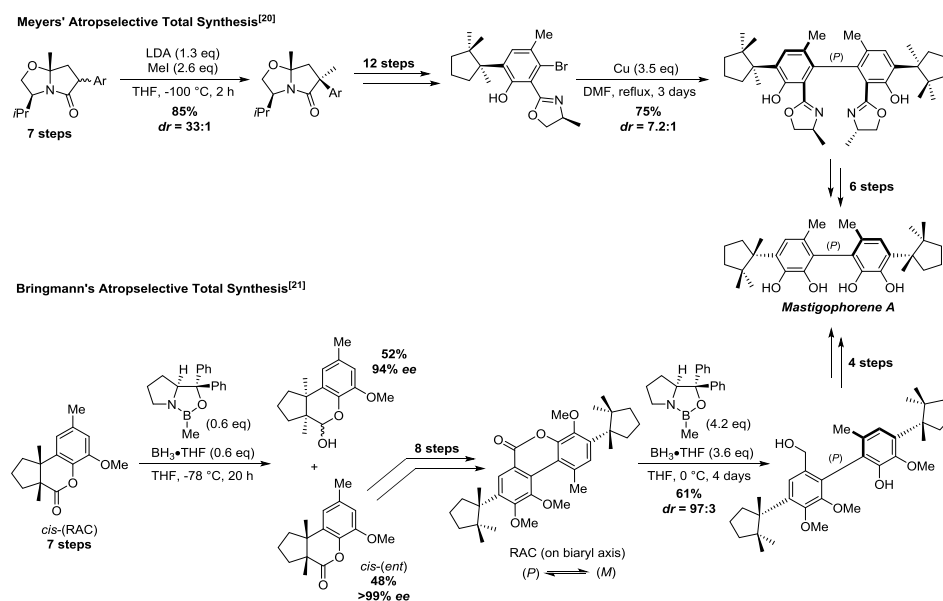
Although the recently developed palladium-catalyzed cross-coupling reactions using organolithium reagents display a broad scope,<sup>[14]</sup> no application has been reported so far within the realms of natural product synthesis. The efficiency of the homo-coupling procedure described here prompted us to explore the method in a total synthesis leading to the dimeric sesquiterpenes mastigophorene A and B (Figure 1).

Isolated from the liverwort *Mastigophora diclados*,<sup>[18a]</sup> mastigophorene A and B showed neurotrophic (nerve growth stimulating) activity,<sup>[18b]</sup> and have therefore been regarded as leads for therapeutic agents for neurodegenerative diseases.<sup>[19]</sup> Additionally, it was found that mastigophorenes A and B exhibit neuroprotective properties at concentrations as low as 0.1-1  $\mu$ M.<sup>[18c]</sup> But foremost it is their molecular architecture, a highly sterically congested benzylic quaternary stereocenter together with a chiral biaryl axis, which sparked our interest.

To date, three total syntheses of mastigophorene A and B have been reported, two of which are atropselective (Scheme 3). Meyers and Degnan installed the biaryl axis atropselectively using a chiral auxiliary-assisted asymmetric Ullmann coupling,<sup>[20]</sup> whereas Bringmann's strategy relied on installation of the chiral biaryl axis using a dynamic kinetic resolution.<sup>[21]</sup>

In the latest endeavor, Fukuyama constructed enantiopure herbertenediol which was subsequently dimerized to the mastigophorenes A and B employing a horseradish peroxidase-catalyzed oxidative coupling, giving a mixture of the atropisomers (64 : 36, 28% combined yield) in favor of mastigophorene B.<sup>[18c]</sup> This ratio matches that obtained from the natural isolate and therefore it is questionable whether the enzyme directly participates in the formation of the bond.<sup>[18a,b]</sup> The Fukuyama synthesis comprises 17 synthetic transformations whereas the Meyers and Bringmann approaches, in large part due to the atropselective nature of their syntheses, consisted of over 20 steps. Evident from the reported syntheses is that stereoselective introduction of the benzylic quaternary stereocenter, and biaryl axis required elaborate synthetic strategies (Scheme 3).

## CHAPTER 6

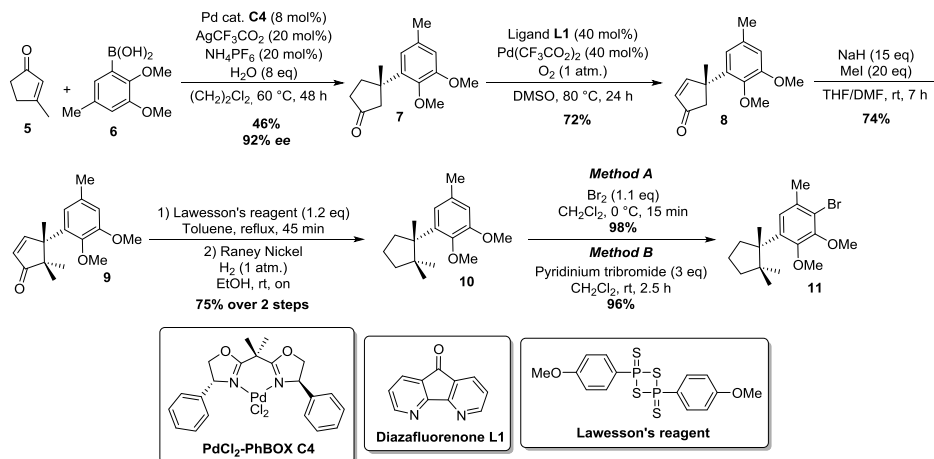


**Scheme 3.** Meyers<sup>[20]</sup> and Bringmann's<sup>[21]</sup> atropselective total syntheses of mastigophorene A.

Recently, we reported an asymmetric Pd-catalyzed conjugate addition of *ortho*-substituted arylboronic acids to cyclic enones, with application in the asymmetric total synthesis of (–)-herbertenediol (the mastigophorene A and B monomer), in just six steps (see Chapter 5).<sup>[22]</sup> This synthetic sequence in combination with the previously developed Pd-catalyzed homo-coupling was envisioned to give straightforward access to enantioenriched mastigophorenes A and B. The hindered biaryl axis in the mastigophorenes presented us with the challenge to construct this stereochemical element in a diastereoselective manner.

Our synthetic approach thus relied on the construction of enantiopure bromodimethoxyherbertenediol **11** (Scheme 4), following our previously reported route to herbertenediol (see Chapter 5).<sup>[22]</sup> This compound was synthesized starting with the Pd-catalyzed asymmetric conjugate addition of *ortho*-substituted arylboronic acid **6** to 3-methylcyclopent-2-enone **5**.<sup>[22]</sup> The benzylic quaternary stereocenter was installed in 46% yield with 92% *ee*. Dehydrogenation of **7**, following a modified procedure reported by the Stahl laboratory,<sup>[23]</sup> provided enone **8** in 72% yield. Geminal dimethylation and subsequent removal of the enone functionality (thioenone formation and RaNi reduction)<sup>[20]</sup> gave rise to dimethoxyherbertenediol **10** in 56% over the three steps. Subsequently, **10** was brominated with either Br<sub>2</sub> or pyridinium tribromide furnishing aryl bromide **11**, setting the stage for the pivotal homo-coupling.

**Pd-Catalyzed, *t*BuLi-mediated dimerization of Aryl Halides**

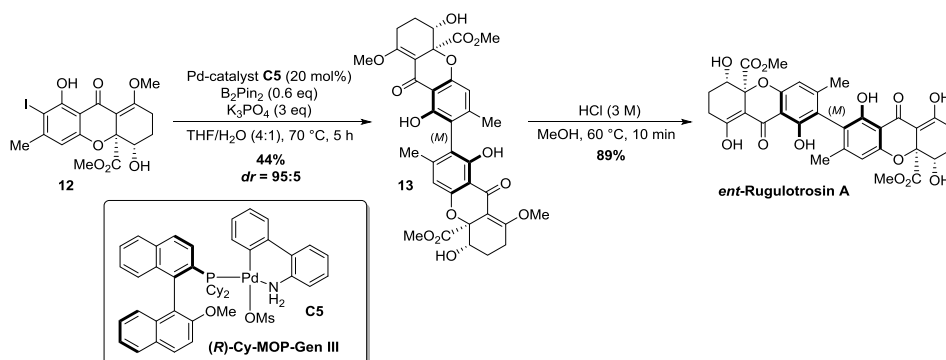


**Scheme 4.** *Asymmetric Synthesis of bromo-dimethoxyherbertenediol 11.*

Initial attempts, employing the optimized conditions of the reported method for homo-coupling (*vide supra* and Table 2), barely afforded the desired dimeric product (~5% isolated yield) since the reaction suffered from significant dehalogenation of **11**, and incomplete conversion. GC-MS analysis however revealed an intriguing feature of the reaction, namely that formation of dimerized product, although in small amounts, was accompanied by a high diastereoselectivity of 9:1. This result indicated that there is a substantial influence of the *para*-substituent on the homo-coupling outcome, suggesting a steric interaction between the catalyst/ligand system and the *para*-benzylic stereocenter, transferring its stereochemical information. This result is of significant importance since catalyst-induced point-to-axial chirality transfer in biaryl containing natural products is rarely reported.

Several accounts of point-to-axial chirality transfer, in which remote chiral centers are used to influence atropselectivity, are known within the literature. These reports however mainly focus on natural products bearing a chiral binaphthyl axis in combination with relatively proximal stereocenters.<sup>[24]</sup> Other reports involve molecules in which the global structure, due to conformational constraints, rather than the stereochemical relationships proximal to the biaryl axis, dictates the atropselectivity.<sup>[25]</sup> Concurrent with our work a case of catalyst-induced point-to-axial chirality transfer in the asymmetric total synthesis of chiral biaryl containing rugulotrosin A was communicated.<sup>[26]</sup> In a systematic study by the Porco Jr. laboratory it was found that depending on the ligand used, the chiral biaryl axis could be introduced in good to excellent diastereomeric ratios using a Suzuki-Miyaura reaction. Dimerization of **12** was most efficiently achieved using chiral Pd-catalyst **C5**, providing protected *ent*-rugulotrosin **13** in 44% yield with a diastereoselectivity of 95 : 5 (Scheme 5).<sup>[26]</sup>





**Scheme 5.** Catalyst-induced point-to-axial chirality transfer in the atropselective total synthesis of *ent-rugulotrosin A*.<sup>[26]</sup>

Motivated by the obtained diastereoselectivity in the homo-coupling of bromide **11**, we were eager to improve the conversion towards the desired dimeric product. In the second attempt (Table 2, entry 2) the reaction was performed at elevated temperature (40 °C) and with 1 eq. of *t*BuLi, albeit with no significant improvement compared to entry 1. We suspected that the *t*-butyl bromide, formed in the lithium-halogen exchange, was prone to elimination and/or oxidative addition of the catalyst (*vide infra*), thereby forming a competing pathway with the catalytic cycle. Switching the lithium source to MeLi (MeBr cannot eliminate) however did not lead to improvement as no conversion was obtained (entry 3). Another way to circumvent the *in situ* formation of *t*-butyl bromide is by pre-formation of the aryllithium species, by reaction of bromide **11** with two equivalents of *t*BuLi. Addition of the pre-formed aryllithium to a solution of **11** and Pd-PEPPSI-IPent catalyst (entry 4), did not provide dimer **14** at all. Heating of the reaction to 40 °C and 70 °C (entry 5 and 6) did show some improvement, forming homo-coupled product **14**, but still no satisfying result was obtained.

Further optimization for homo-coupling of **11** was delayed at this point since all synthetic material was consumed. Because enantiopure bromide **11** was deemed precious and a more rigorous optimization procedure was necessary, we decided to switch to a model system. It was reasoned that the crowded cyclopentyl scaffold in **11**, although apparently remote from the coupling site, impeded successful homo-coupling by slowing down the reaction. This led us to investigate the influence of steric bulk of the *para*-substituent on the Pd-catalyzed homo-coupling. As model substrates, analogues of **11** with a methyl or a *t*-butyl<sup>[27]</sup> substituent were prepared (Scheme 6).

Entry	Cat. (Mol%)	RLi (eq)	Temp. (°C)	14 (%) <sup>a,b</sup>	11 (%) <sup>a</sup>	10 (%) <sup>a</sup>
1	2	<i>t</i> BuLi (0.7)	20	17	55	28
2	5	<i>t</i> BuLi (1.0)	40	25	-	75
3	5	<i>Me</i> Li (0.55)	40	-	>99	-
4	5	ArLi (0.5) <sup>c</sup>	20	-	78	22
5	5	ArLi (0.5) <sup>b,c</sup>	40	27	43	30
6	5	ArLi (0.5) <sup>b,c</sup>	70	21	50	29

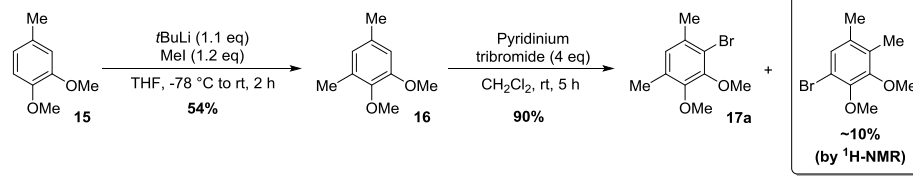
Reaction conditions: **11** (0.2 mmol) and the palladium catalyst in 1.6 mL of toluene at 20 °C; RLi (*n* eq) diluted to 0.6 mL with toluene was added dropwise over 1 h. <sup>a</sup> Relative ratios were determined by GC-MS analysis. <sup>b</sup> *dr* = 9:1 <sup>c</sup> ArLi = lithium-halogen exchange product of **11** was used. Lithium-halogen exchange was performed by addition of *t*BuLi (2 eq) to **11** in -20 °C dry THF.

**Table 2.** Attempts to construct tetramethoxymastigophore **14**.

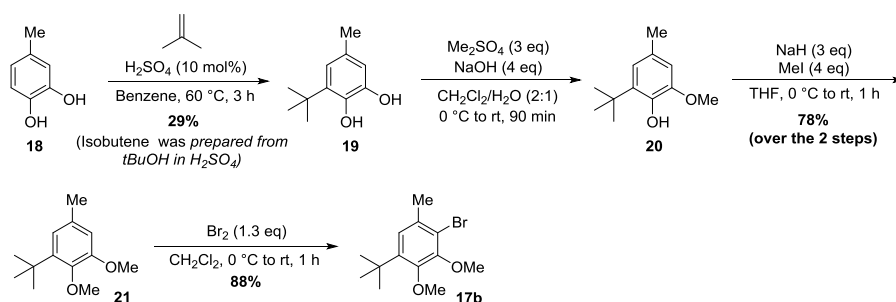
Methyl substituted analogue **17** was obtained starting with a directed *ortho*-lithiation of commercially available **15**. With two lithiation sites present, the bulky *t*BuLi was chosen to achieve at least some selectivity for deprotonation. After careful flash chromatographic separation and GC-MS analysis of all fractions, collecting those fractions exhibiting ~90% purity, desired product **16** was obtained in 54% yield. Bromination with pyridium tribromide smoothly afforded bromide **17** in 90%, with an overall purity of ~90% which was considered sufficient for studying the homo-coupling reaction. The synthesis of *t*-butyl substrate **22** was initiated by Friedel-Crafts alkylation of catechol **18** with isobutene.<sup>[28]</sup> The obtained 29% yield for **19** did not reflect the yield obtained in the literature (72%), as the reaction was carried out under non-ideal conditions. Ideally an atmosphere of isobutene is used, applying a balloon on the reaction vessel, but practical constraints forced us to bubble isobutene (obtained from dehydration of *t*-butanol) through the reaction mixture. *Tert*-butyl catechol **19** was then subjected to NaOH and Me<sub>2</sub>SO<sub>4</sub> to construct **21**, however, due to reasons unknown only mono-methylation occurred to produce phenol **20**. Work-up of the reaction mixture and subjecting the crude to NaH and MeI then furnished the desired dimethylated product **21**, in 78% over the two steps. Bromination with elemental bromine produced bromide **17b** in 88% yield. Although this sequence seems redundant, direct *tert*-butylation of 3,4-dimethoxytoluene **15** provided a regioisomeric product (*see experimental section*)!

## CHAPTER 6

### Para-methyl model substrate **17a**



### Para-tert-butyl model substrate **17b**

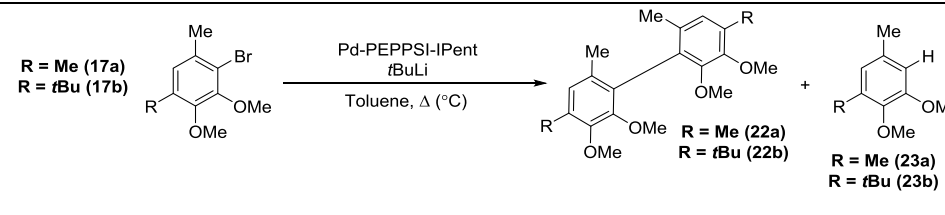


**Scheme 6.** Synthesis of model substrates for the Pd-catalyzed homo-coupling.

With the desired model substrates in hand the dimerization reaction could be studied (Table 3). Homo-coupling of methyl substrate **17a** under slightly modified conditions, using 5 mol% Pd-PEPPSI-IPent and 1.2 eq. *t*BuLi, gave 68% isolated yield of the corresponding biaryl product (Table 3, entry 1). However, upon application of these conditions on *t*-butyl substituted **17b**, a poor selectivity for homo-coupling over debromination was observed, and consequently the isolated yield dropped significantly. Optimization of the reaction conditions, for methyl substrate **17a**, by increasing catalyst loading or temperature did not lead to increased selectivity (entry 2 and 3). We also tried to improve our result from entry 1 by changing the concentration of either the lithiating reagent or the substrate, unfortunately leading to increased amounts of dehalogenation (entry 4 and 5). Failure was also met with a more gradual addition of *t*BuLi by direct contact of the tip of the needle with the reaction surface, providing dehalogenation exclusively, a result that remained unexplained (entry 6).

Also other catalysts (Pd-PEPPSI-IPr, Pd<sub>2</sub>dba<sub>3</sub>/XPHOS,<sup>[29]</sup> and Pd(P*t*Bu<sub>3</sub>)<sub>2</sub>) were investigated to achieve efficient coupling. Despite our efforts using these catalysts, no homo-coupling could be achieved for the methyl substrate **17a**. Notably, the failure of Pd-PEPPSI-IPr to achieve homo-coupling seems surprising, however congruent results were obtained by Organ and co-workers, who showed that formation of sterically hindered tetra-*ortho*-substituted biaryls using arylboron reagents, was facilitated by Pd-PEPPSI-IPent, whereas Pd-PEPPSI-IPr showed poor or no catalytic activity at all.<sup>[16a,c]</sup> It was postulated that the steric topology around the palladium nucleus is crucial, and that reactivity of the catalyst was facilitated by “flexible steric bulk” in the ligand.<sup>[30]</sup>

*Pd-Catalyzed, *t*BuLi-mediated dimerization of Aryl Halides*

					
<b>Entry</b>	<b>Cat (mol%)</b>	<b>SM</b>	<b>23 (%)<sup>a</sup></b>	<b>22 (%)<sup>a</sup> Yield (%)<sup>b</sup></b>	<b>notes</b>
1	2	<b>17a</b>	25	75 (68)	-
2	5	<b>17a</b>	25	75	-
3	5	<b>17a</b>	75	25	40 °C
4	5	<b>17a</b>	25	55	Diluted <i>t</i> BuLi <sup>c</sup>
5	5	<b>17a</b>	80	20	Conc. reaction
6	5	<b>17a</b>	>98	-	Cont. Add.
7	5	<b>17a</b>	15	85 (79)	0 °C
8	5	<b>17a</b>	15	85	Aliq. Add. <sup>d</sup>
9	5	<b>17b</b>	50	50	0 °C
10	5	<b>17b</b>	20	80 (75%)	See entry 7 and 8 <sup>d</sup>

Reaction conditions: **17** (0.3 mmol) and the palladium catalyst in 2 mL of toluene at 20 °C; *t*BuLi (1.2 eq) diluted to 1 mL with toluene was added dropwise over 1 h, unless otherwise noted. <sup>a</sup> Conversions were determined by GC-MS analysis. <sup>b</sup> Isolated yield, after column chromatography, in brackets. <sup>c</sup> incomplete conversion. <sup>d</sup> *t*BuLi added at 2 drops per 5 min interval.

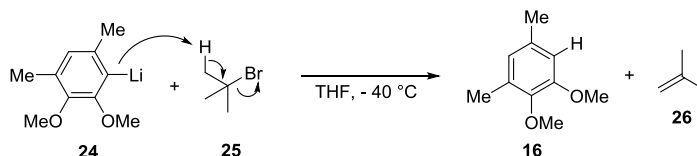
**Table 3.** Optimization of the homo-coupling for sterically congested substrates.

With the above mentioned optimization attempts for methyl substrate **17a** being fruitless, we decided to apply a lower reaction temperature (0 °C) and aliquoted addition (two drops per five minutes) of the *t*BuLi (entry 7 and 8 respectively). Both conditions led to significant improvement of the selectivity, as 85% conversion to the desired product **22a**, compared to 75% in entry 1, was observed. Isolation provided the desired homo-coupled product **23a** in a satisfying 79% yield. Lowering the reaction temperature was also used in the dimerization of **17b**, providing only a modest selectivity for the formation of **22a** (entry 9). When we subjected **17b** to the low temperature combined with the slow addition conditions from entry 8 and 9, we were pleased to see that this reaction smoothly provided the homo-coupled product **22b** in an excellent 75% isolated yield (entry 10).

Throughout the optimization process (Table 2 and 3), dehalogenation of the aryl bromides was the only side product, raising the question where the proton originates from. Upon quenching the reaction mixture with methyl iodide instead of methanol, the corresponding methylated product was detected only in trace amounts. This suggests

CHAPTER 6

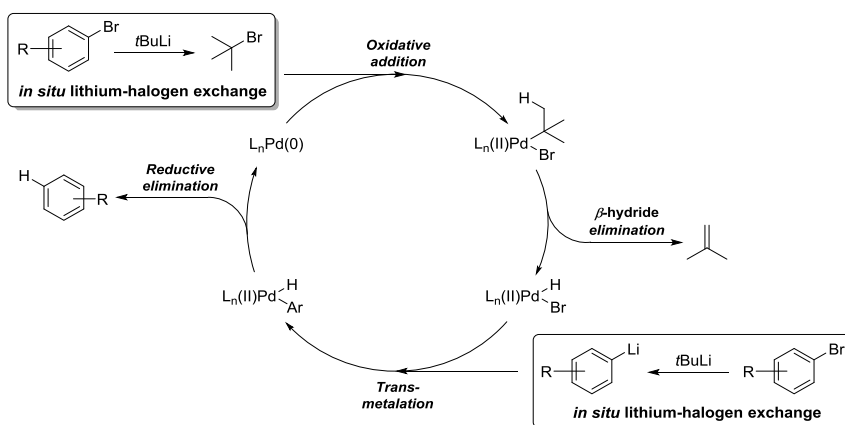
that the majority of protonation occurs during reaction and not upon quenching. One possibility, namely deprotonation of the generated *t*-butyl bromide by the *in situ* formed aryllithium species **24**, was examined. Formation of the latter at  $-40\text{ }^{\circ}\text{C}$  (in the absence of Pd-PEPPSI-IPent), addition of *t*-butyl bromide, and consecutive (immediate!) quenching with methyl iodide showed no methyl incorporation, and full conversion towards the dehalogenated product **16** was observed (Scheme 7).



Scheme 7. Quenching of the *in situ* generated aryllithium species.

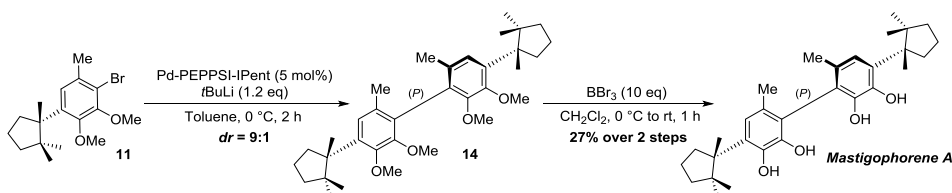
Reasoning that the electron rich aryllithium reagent is indeed rather basic, the deprotonation of *t*-butyl bromide, performed at  $-40\text{ }^{\circ}\text{C}$ , strongly supports the hypothesis that protonation originates from elimination of *t*-butyl bromide. This side reaction is most likely promoted by the slower homo-coupling reaction due to the large substituents present in **11**. Fortunately, the competition between Pd-catalyzed homo-coupling and dehalogenation could be shifted towards homo-coupling by lowering the temperature to  $0\text{ }^{\circ}\text{C}$  and slow addition of *t*BuLi, keeping the concentration of *t*-butyl bromide low (Table 3, entry 10).

The experiment mentioned above does not rule out a mechanism in which the palladium catalyst is involved (Scheme 8). The catalyst can perform an oxidative insertion into *t*-butyl bromide **25**, followed by  $\beta$ -hydride elimination, forming a Br-Pd<sup>II</sup>-H species and isobutene. Transmetalation with ArLi in this species leads to Ar-Pd<sup>II</sup>-H, and subsequent reductive elimination could also lead to debrominated product **16**, and regeneration of the Pd<sup>0</sup> catalyst.



Scheme 8. Proposed Pd-catalyzed dehalogenation via a Pd-hydride species.

Following the optimization, the anticipated homo-coupling of enantiopure mastigophorene building block **11** was performed (Scheme 9). Gratifyingly, applying the optimized conditions we obtained tetramethoxymastigophorene **14**, although inseparable at this stage (*vide infra*) from the debrominated starting material, dimethoxyherbertenediol **10** (Scheme 4). Upon investigation of the homo-coupling product mixture, exhibiting a diastereomeric ratio of 9:1, by <sup>1</sup>H-NMR, an intense resonance at  $\delta$  1.95 (s, 6H) was observed which is characteristic of (*P*)-helicity in mastigophorene analogue **14**.<sup>[20]</sup> This obtained diastereoselectivity approaches the 97 : 3 diastereoselectivity obtained in Bringmann's atropselective total synthesis,<sup>[21]</sup> and matches with the 88 : 12 diastereomeric ratio obtained in atropselective total synthesis by the Meyers laboratory (Scheme 3).<sup>[20]</sup>



**Scheme 9.** End-game of the atropselective mastigophorene A total synthesis.

As previously stated, the observed diastereoselectivity strongly suggests a catalyst-induced point-to-axial chirality transfer, involving a steric interaction between the catalyst and the *para*-benzylic quaternary stereocenter. This hypothesis is substantiated by the fact that an oxidative coupling (no imposed steric hindrance of the added reagent) using di-*tert*-butyl peroxide of the herbertenediol monomethyl ether, provided the mastigophorenes A and B analogues with very low asymmetric induction (*dr* = 40 : 60) in favor of mastigophorene B.<sup>[31]</sup> The same ratio was obtained from the natural isolate, clearly indicating a chiral bias towards (*M*)-helicity exerted by the crowded cyclopentyl moiety alone.<sup>[18a,b]</sup> It is therefore even more noticeable that the point-to-axial chirality transfer in the homo-coupling to (*P*)-**14** overcomes this intrinsic stereochemical bias towards (*M*)-helicity.

Tetramethoxymastigophorene A (**14**) was thus obtained together with the dehalogenated compound dimethoxyherbertenediol **10** which we were not able to separate by flash column chromatography (Scheme 9). We therefore decided to subject the mixture to BBr<sub>3</sub> (90% yield), cleaving the methyl ethers. In this stage the side products from the previous step were separated using flash column chromatography affording pure mastigophorene A in 27% yield over two steps. Unfortunately, and despite our homo-coupling optimization efforts (*vide supra*), we obtained only a modest yield (~30%) accompanied with significant dehalogenation. This result reflects the degree of steric hindrance exerted by the cyclopentyl scaffold on the outcome of the reaction, compared to *tert*-butyl model substrate **17b**.

The synthetic natural product was identified by means of NMR analysis and optical rotation to indeed accord with mastigophorene A (observed rotation =  $-67.9$  ( $c = 0.4$ ,  $\text{CHCl}_3$ ); literature<sup>[18b]</sup> =  $-65.3$  ( $c = 0.4$ ,  $\text{CHCl}_3$ )). Conclusive evidence of the axial configuration was obtained by X-ray crystallography, clearly showing (*P*)-helicity (Figure 2).

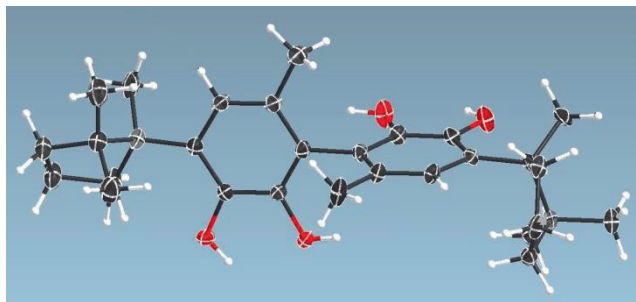


**Figure 2.** X-ray Structure of Mastigophorene A.

## 6.4 Conclusion

In summary, we have developed a new and efficient catalytic system for the synthesis of symmetric biaryls from aryl halides in the presence of *t*BuLi (0.7 eq) using only 1 mol% of palladium catalyst. The reaction takes place at ambient temperatures and generally provides good to excellent yields. A wide scope of symmetric biaryl compounds was shown, even allowing the construction of tetra-*ortho*-substituted symmetric biaryls in high yields. Additionally, we successfully implemented the newly developed methodology in the shortest atropselective total synthesis of mastigophorene A in just eight steps. Although considerable optimization of the reaction conditions was required to effect successful homo-coupling, we did manage to obtain the biaryl linkage with a diastereoselectivity of 9:1 due to catalyst-induced point-to-axial chirality transfer. Compared to the previous stereoselective syntheses (>20 steps) this is a major improvement and a consequence of the straightforward enantioselective installation of the benzylic quaternary stereocenter in 92% *ee* and the highly diastereoselective homo-coupling.

## 6.5 Discussion and future prospects

### 6.5.1 Reflection on the Pd-catalyzed homo-coupling

The current chapter was recently published. In the referee reports, interesting points were raised regarding the stoichiometry and mechanism of the reaction. These points are addressed in this paragraph as they are not substantiated by thorough experimentation, but rather on what is known in the literature.

It is well known that lithium-halogen exchange reactions using *t*BuLi are generally performed with two equivalents of *t*BuLi.<sup>[32]</sup> This is necessary as the lithium-halogen

exchange produces *t*-butyl bromide which in turn undergoes a fast elimination reaction with a second molecule of *t*BuLi. Performing these reaction with less than two equivalents of *t*BuLi therefore results in incomplete lithiation. This was pointed out by one of the referees as in our homo-coupling method we use just 0.7 equivalents of *t*BuLi (which corresponds to 1.4 eq for the Li-Br exchange) and achieve yields up to 98%, indicating complete lithiation. We reason that elimination of *t*-butyl bromide is suppressed by a right combination of solvent, addition time of the *t*BuLi, and a high catalyst turn-over frequency.

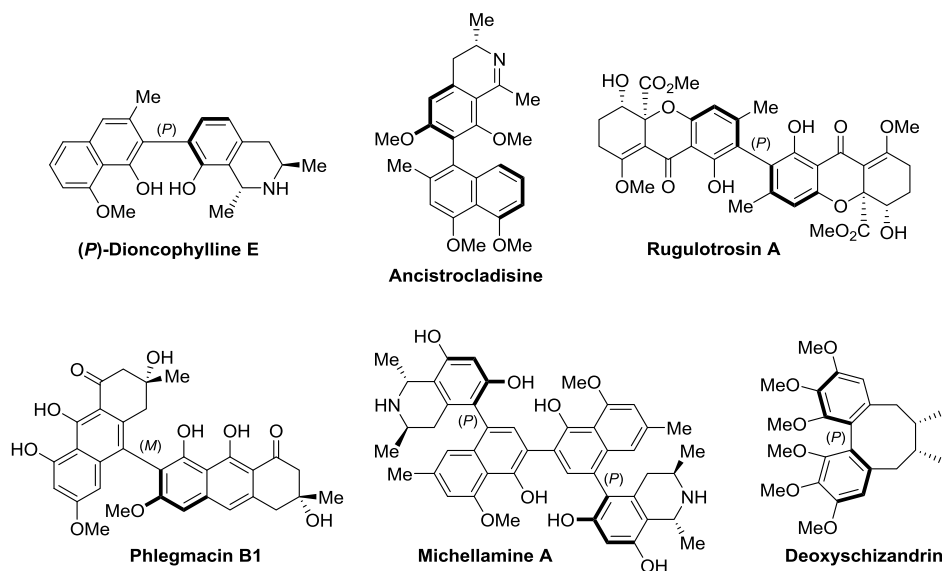
Using toluene as the solvent is postulated to be effective in taming the reactivity of *t*BuLi. The reagent forms tetramers in this solvent that are less reactive than the monomer present in THF,<sup>[33]</sup> the solvent commonly used for lithium-halogen exchange reactions. Support for this argument comes from the observation that in the Pd-catalyzed hetero-coupling of aryllithium reagents with aryl bromides, Et<sub>2</sub>O as the solvent had a detrimental effect on the reaction outcome.<sup>[14i]</sup> This is attributed as well to the lower aggregation state of the, therefore more reactive, *t*BuLi. Also the slow addition of *t*BuLi to the reaction mixture is assumed to be important as it keeps the concentration of the reagent low. These two factors in combination with a high turn-over frequency of the catalyst are thought to suppress the elimination of *t*-butyl bromide.

Another issue addressed in the referee reports was the mechanism of the reaction. The referee considered an ionic mechanism debatable as toluene is a non-polar solvent, and therefore a radical mechanism proposed by the referee. We however refute this argument as radical reactions in toluene are prone to produce significant amounts of side products arising from formation of benzylic radicals. Since no such side products, even not in trace amounts, were observed in GC-MS analysis we do have strong evidence to exclude a radical type mechanism.

The observed diastereoselectivity in the mastigophorene A synthesis provides an additional argument against an ionic mechanism. A ratio of 9:1 in favor of the product with (*P*)-helicity was obtained (Scheme 9). In contrast, the biosynthesis of mastigophorene A and B via radical oxidative coupling of herbertenediol (the mastigophorene monomer), results in a diastereomeric ratio of 6:4 in favor of mastigophorene B, containing (*M*)-helicity.<sup>[18a,b]</sup> This result was confirmed by Bringmann and co-worker who reported a biomimetic synthesis of the mastigophorenes A and B, involving a radical oxidative coupling.<sup>[31]</sup> In case our reaction would predominantly proceed via a radical mechanism, the coupling of the aryl radical species without the aid of a catalyst is expected to give a more “biomimetic”, that is hardly any stereoselectivity, outcome. A more thorough investigation is needed to address this issue, and it is intriguing that recently a stereoselective enzymatic biaryl coupling has been reported as well.<sup>[34]</sup>



### 6.5.2 Other natural product targets for the point-to-axial chirality transfer using the Pd-catalyzed homo-coupling of aryllithium reagents



**Scheme 10.** Natural products as targets for catalyst-induced point-to-axial chirality transfer by Pd-catalyzed biaryl coupling of aryllithium reagents.

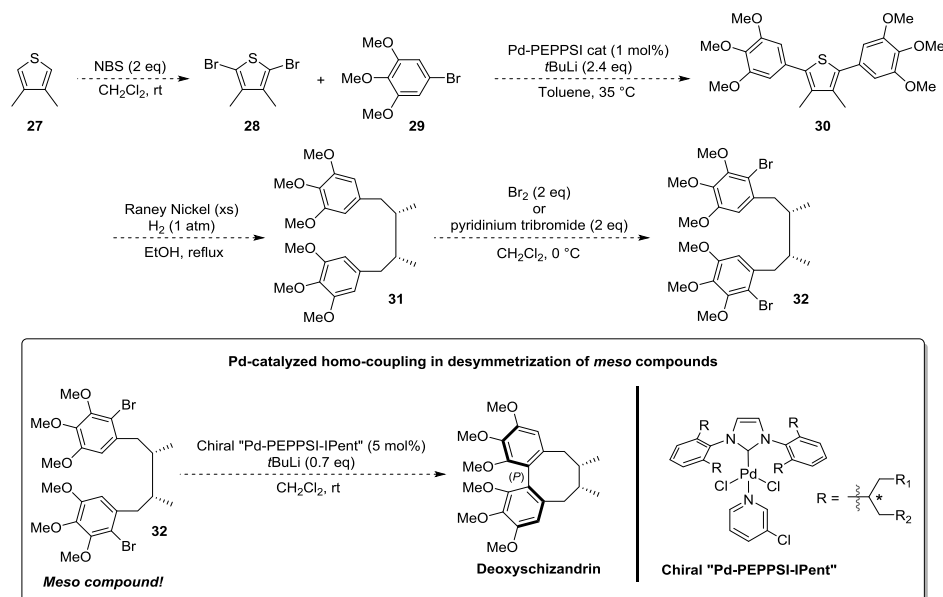
A most intriguing result in the presented total synthesis of mastigophorene A is the catalyst-induced point-to-axial chirality transfer from an apparently remote stereocenter. As previously discussed, reports on this phenomenon are scarce in the literature. Therefore the catalyst-induced point-to-axial chirality transfer can be seen as an opportunity in stereoselective natural product synthesis. In scheme 10 a set of intricate chiral biaryl containing natural products is presented that can potentially be made with the homo-coupling methodology reported in this chapter, and using the recently communicated hetero-biaryl coupling using aryllithium reagents.<sup>[14i]</sup> In order to gain information about the scope and limitations, research should (*authors opinion!*) focus on natural isolates with even more remote point-chiral stereocenters (e.g. ancistrocladisine<sup>[35]</sup> and rugulotrosin A<sup>[36]</sup>) and sterically less demanding point-chiral moieties (e.g. phlegmacin B1<sup>[37]</sup> and dioncophylline E<sup>[38]</sup>).

The synthesis of a chiral biaryl axis, and to a lesser extent a chiral binaphthyl axis, is intrinsically difficult when the used methodology requires high temperatures, especially when the inversion barrier is low.<sup>[1c,d]</sup> We were therefore pleased to find that the homo-coupling in the mastigophorene A synthesis was successfully performed at 0 °C minimizing the risk of inversion (pseudo-racemization). Therefore, although a configurationally stable tetra-*ortho*-substituted biaryl axis was crafted in the current study, the method is suitable as well for more labile chiral tri- or even disubstituted

biaryl axes. The low temperature used in the homo-coupling of aryllithium reagents is therefore advantageous compared to the widely used Suzuki coupling, which in the majority of cases requires heating.<sup>[39]</sup> To substantiate this assertion, the total synthesis of tri-*ortho*-substituted dioncophylline E is envisioned. It is known that the molecule is unstable at room temperature and therefore a low temperature construction of the chiral biaryl axis is essential to obtain stereochemically pure material. To push the boundaries of the methodology even further, one can aim at the total synthesis of the intricate michellamine A.<sup>[40]</sup> This molecule contains three chiral biaryl axes of which the outer two are configurationally stable, and the middle one prone to isomerization! A synthetically pleasing prospect is the potential of a point-to-axial chirality transfer in the construction of the outer biaryl axes, and an axial-to-axial chirality transfer to construct the central bis-substituted biaryl axis.

A final example of a natural product, potentially accessible using the Pd-catalyzed coupling of aryllithium reagents, is deoxyschizandrin.<sup>[41]</sup> This molecule is a member of so-called dibenzocyclooctadiene lignans and this class of natural products exhibits interesting biological activity.<sup>[42]</sup> A proposal for a short asymmetric total synthesis is outlined in scheme 11.

Starting from dimethylthiophene **27**, dibromothiophene **28** is readily obtained.<sup>[43]</sup> Performing the Pd-catalyzed hetero-coupling of aryllithium reagents<sup>[14i]</sup> on bromothiophene **28** and aryl bromide **29** can then lead to biaryl thiophene **30**. From a step-count perspective accessing **30** in one step is preferable, although such reaction has not been reported yet using the lithium cross-coupling chemistry. If troublesome, it is envisioned that **30** should be readily obtained via a two-step sequence. It is known from the literature that thiophene **30** can be completely reduced with Raney nickel, although a mixture of diastereomers was obtained.<sup>[44]</sup> This is however not problematic as bromination of **31** provides bromo compound **32**, of which the diastereomers could be separated by recrystallization.<sup>[45]</sup> This molecule just has to undergo the biaryl coupling reaction to provide deoxyschizandrin. We hypothesize that this coupling can be accomplished using the methodology described within this chapter, together with point-to-axial chirality transfer from the *syn*-1,2-dimethyl group. Since **32** is a *meso*-compound the intriguing possibility arises to desymmetrize **32** by using a chiral version of the Pd-PEPPSI-IPENT catalyst.



**Scheme 11.** A proposed asymmetric total synthesis of deoxyschizandrin.

A final aspect of the catalyst-induced point-to-axial chirality transfer that needs to be addressed is the issue of catalyst-control. Whereas in this chapter the diastereoselectivity was as such unexpected, it is hailed as an important result. Critical assessment however, touches upon the fact that only mastigophorene A was constructed, so what if one requires mastigophorene B? The most obvious is to perform a catalyst/ligand screening, however this is not deemed the most promising approach as only a very limited set of catalysts was shown to perform the coupling of aryllithium reagents in general. In the total synthesis of rugulotrosin A by Porco Jr. and co-workers (Scheme 5), for example, a whole range of different catalyst was screened to accomplish the dimerization.<sup>[26]</sup> Even with both enantiomers of the chiral catalysts, good to excellent diastereoselectivities were reported exclusively in favor of (*M*)-helicity. The answer might therefore not lie in the use of the same methodology to access both atropisomers, which poses a significant limitation of the method. Even the use of similar chemistry with mechanistic resemblance (e.g. switching from a Suzuki to a Negishi coupling) might be a dead end. Therefore the use of a different biaryl coupling methodology, with different mechanistic characteristics should be evaluated as well. The answer is not trivial and only experimentation (in combination with deep thinking) can provide one.

## 6.6 Experimental section

### General methods:

All reactions were carried out under a nitrogen atmosphere using oven dried glassware and using standard Schlenk techniques. Reaction temperature refers to the temperature of the oil bath. The dry solvents were taken from an MBraun solvent purification system (SPS-800). Pd<sub>2</sub>(dba)<sub>3</sub>, SPhos, XPhos, DavePhos, CPhos, Qphos, PCy<sub>3</sub>, Pd-PEPPSI-IPr and Pd-PEPPSI-IPent were purchased from Aldrich, and P(*t*Bu)<sub>3</sub> was obtained from Strem chemicals, and used without further purification. *n*BuLi (1.6 M solution in hexane) was purchased from Acros. *t*BuLi (1.7 M in pentane), *sec*BuLi (1.4 M in cyclohexane), *i*PrLi (0.7 M in pentane) were purchased from Aldrich. All the aromatic halides were commercially available and were purchased from Aldrich, with the exception of 3-bromo-2-methoxypyridine, 2-bromo-3-methoxynaphthalene and 1-bromo-2-methoxynaphthalene (TCI Europe).

TLC analysis was performed on Merck silica gel 60/Kieselguhr F254, 0.25 mm. Compounds were visualized using either Seebach's stain (a mixture of phosphomolybdic acid (25 g), cerium (IV) sulfate (7.5 g), H<sub>2</sub>O (500 mL) and H<sub>2</sub>SO<sub>4</sub> (25 mL)), a KMnO<sub>4</sub> stain (K<sub>2</sub>CO<sub>3</sub> (40 g), KMnO<sub>4</sub> (6 g), water (600 mL) and 10% NaOH (5 mL)), or elemental iodine. Flash chromatography was performed using SiliCycle silica gel type SiliaFlash P60 (230 – 400 mesh) as obtained from Screening Devices or with automated column chromatography using a Reveleris flash purification system purchased from Grace Davison Discovery Sciences. Reveleris pre-fabricated silica cartridges were purchased and used, for automated column chromatography, containing 40 μm silica.

GC-MS measurements were performed with an HP 6890 series gas chromatography system with an HP1 or HP5 column (Agilent Technologies, Palo Alto, CA), equipped with an HP 5973 mass sensitive detector.

High resolution mass spectra (HRMS) were recorded on a Thermo Scientific LTQ Orbitrap XL. (ESI+, ESI- and APCI). <sup>1</sup>H-, <sup>13</sup>C- and <sup>19</sup>F-NMR spectra were recorded on a Varian AMX400 (400, 101 and 376 MHz, respectively) using CDCl<sub>3</sub> as solvent unless stated otherwise. Chemical shift values are reported in ppm with the solvent resonance as the internal standard (CDCl<sub>3</sub>: δ 7.26 for <sup>1</sup>H, δ 77.16 for <sup>13</sup>C). Data are reported as follows: chemical shifts (δ in ppm), multiplicity (s = singlet, d = doublet, dd = double doublet, ddd = double double doublet, td = triple doublet, t = triplet, q = quartet, b = broad, m = multiplet), coupling constants *J* (Hz), and integration.

Enantiomeric excesses were determined by chiral HPLC analysis using a Shimadzu LC-10ADVP HPLC instrument equipped with a Shimadzu SPD-M10AVP diode-array detector. Integration at three different wavelengths (254, 225, 190 nm) was performed and the reported enantiomeric excess is an average of the three integrations.

Optical rotations were measured on a Schmidt+Haensch polarimeter (Polartronic MH8) with a 10 cm cell (c given in g/mL) at ambient temperature (±20 °C).

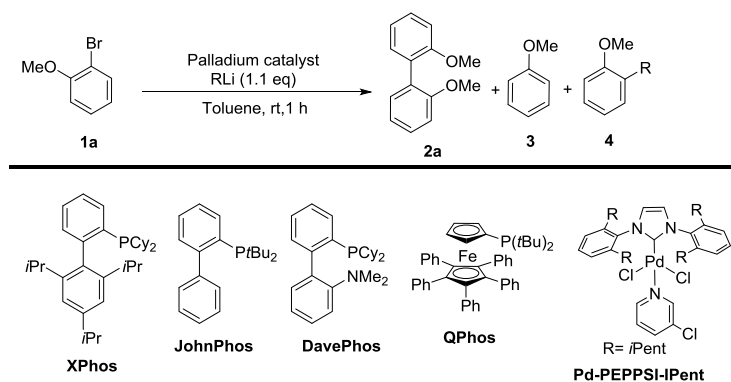
### General procedure for the palladium catalyzed homo-coupling of aryl halides reagents in the presence of *t*BuLi:

In a dry Schlenk flask, Pd-PEPPSI-IPr or Pd-PEPPSI-IPent (1 mol%) and aromatic halide (0.3 mmol) were dissolved in 2 mL of dry toluene and the solution was stirred at room temperature. *t*BuLi (0.7 eq., 0.21 mmol, 0.12 mL of 1.7 M commercial solution) was diluted with toluene to reach the concentration of 0.21 M; this solution was slowly added (flow rate=1 mL/h) by the use of a syringe pump. After the addition was completed, the reaction was quenched with methanol, and the solvent was evaporated under reduced pressure to afford the crude product, which was then purified by column chromatography.

### Gram scale reaction:

In a dry Schlenk flask Pd-PEPPSI-IPr (0.5 mol%, 0.003 mmol, 22.5 mg) and 2-bromoanisole (6 mmol, 1.12 g, 0.75 mL) were dissolved in 30 mL of dry toluene. A solution of *t*BuLi (0.7 eq., 4.2 mmol, 2.5 mL of 1.7 M commercial solution) was slowly added over 2h by the use of a syringe pump. After the addition was completed, the reaction was quenched with methanol, and the solvent was evaporated under reduced pressure to afford the crude mixture. The product **2a** was then purified by column chromatography (SiO<sub>2</sub>, *pentane* : Et<sub>2</sub>O 95:5) affording **2a** as an oily substance (637 mg, 2.97 mmol, 98% yield).

### Optimization homo-coupling of 2-bromoanisole in the presence of organolithium reagent:

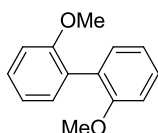


Entry	Pd (x mol%)	Ligand (x mol%)	RLi (1.1 eq)	Conv (%)	2a (%)	3 (%)	4 (%)
1	Pd(PtBu <sub>3</sub> ) <sub>2</sub> (5 mol%)	-	<i>i</i> PrLi	Full	0	100	0
2	Pd <sub>2</sub> dba <sub>3</sub> (2.5 mol%)	XPhos (10 mol%)	<i>i</i> PrLi	Full	32	68	0
3	Pd <sub>2</sub> dba <sub>3</sub>	JohnPhos	<i>i</i> PrLi	Full	9	91	0

*Pd-Catalyzed, tBuLi-mediated dimerization of Aryl Halides*

	(2.5 mol%)	(10 mol%)					
4	Pd <sub>2</sub> dba <sub>3</sub> (2.5 mol%)	DavePhos (10 mol%)	<i>i</i> PrLi	Full	30	70	0
5	Pd <sub>2</sub> dba <sub>3</sub> (2.5 mol%)	QPhos (10 mol%)	<i>i</i> PrLi	Full	100	0	0
6	Pd-PEPPSI-IPent (5 mol%)	-	<i>i</i> PrLi	Full	100	0	0
Conversions were determined with GC-MS analysis							

**Spectral data of compounds 2a-2q:**

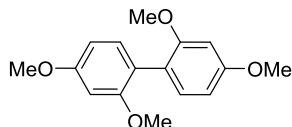


**2,2'-dimethoxy-1,1'-biphenyl (2a):**

White solid obtained after column chromatography (SiO<sub>2</sub>, *pentane* : ether 95:5), 29 mg, 91% yield.

<sup>1</sup>H-NMR (400 MHz, CDCl<sub>3</sub>) δ 7.38-7.33 (m, 2H), 7.28 (dd, *J* = 7.4, 1.5 Hz, 2H), 7.07-6.98 (m, 4H), 3.80 (s, 6H).

<sup>13</sup>C-NMR (101 MHz, CDCl<sub>3</sub>) δ 157.0, 131.5, 128.6, 127.8, 120.3, 111.1, 55.7.



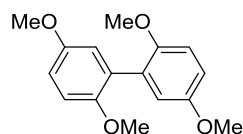
**2,2',4,4'-tetramethoxy-1,1'-biphenyl (2b):**

Yellow solid obtained after column chromatography (SiO<sub>2</sub>, *pentane* : ether 95:5), 38 mg, 93% yield, m.p. = 92-94 °C.

<sup>1</sup>H-NMR (400 MHz, CDCl<sub>3</sub>) δ 7.16 (d, *J* = 8.6 Hz, 2H), 6.58-6.53 (m, 4H), 3.85 (s, 3H), 3.77 (s, 3H).

<sup>13</sup>C-NMR (101 MHz, CDCl<sub>3</sub>) δ 160.0, 158.1, 131.9, 120.1, 104.1, 98.9, 55.7, 55.3.

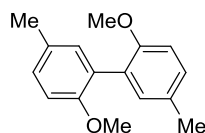
HRMS (ESI<sup>+</sup>): [M+H]<sup>+</sup> calculated for C<sub>16</sub>H<sub>19</sub>O<sub>4</sub><sup>+</sup> = 275.12779; found: 275.12807.

**2,2',5,5'-tetramethoxy-1,1'-biphenyl (2c):**

Yellow solid obtained after column chromatography (SiO<sub>2</sub>, *pentane* : ether 95:5), 40 mg, 98% yield.

<sup>1</sup>H-NMR (400 MHz, CDCl<sub>3</sub>) δ 6.92 (d, *J* = 8.6 Hz, 2H), 6.89-6.84 (m, 4H), 3.79 (s, 6H), 3.74 (s, 6H).

<sup>13</sup>C-NMR (101 MHz, CDCl<sub>3</sub>) δ 153.3, 151.3, 128.6, 117.1, 113.4, 112.4, 56.5, 55.7.

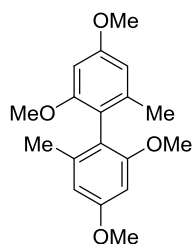
**2,2'-dimethoxy-5,5'-dimethyl-1,1'-biphenyl (2d):**

White solid obtained after column chromatography (SiO<sub>2</sub>, *pentane* : ether 95:5), 30 mg, 82% yield, m.p. = 58-60 °C.

<sup>1</sup>H-NMR (400 MHz, CDCl<sub>3</sub>) 7.13 (dd, *J* = 8.3, 1.8 Hz, 2H), 7.05 (d, *J* = 2.2 Hz, 2H), 6.88 (d, *J* = 8.3 Hz, 0H), 3.76 (s, 6H), 2.33 (s, 6H).

<sup>13</sup>C-NMR (101 MHz, CDCl<sub>3</sub>) δ 155.0, 132.0, 129.5, 128.9, 127.8, 111.1, 55.9, 20.5.

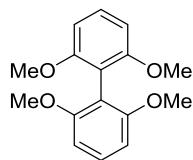
HRMS (ESI+, *m/z*): calculated for C<sub>16</sub>H<sub>18</sub>O<sub>2</sub> [M+H]<sup>+</sup>: 243.13796; found: 243.13824.

**2,2',4,4'-tetramethoxy-6,6'-dimethyl-1,1'-biphenyl (2e):**

White solid obtained after column chromatography (SiO<sub>2</sub>, *pentane* : ether 95:5), 34 mg, 75% yield.

<sup>1</sup>H-NMR (400 MHz, CDCl<sub>3</sub>) 6.45 (d, *J* = 2.1 Hz, 2H), 6.41 (d, *J* = 2.3 Hz, 2H), 3.84 (s, 6H), 3.69 (s, 6H), 1.94 (s, 6H).

$^{13}\text{C-NMR}$  (101 MHz,  $\text{CDCl}_3$ )  $\delta$  159.4, 158.2, 139.2, 118.4, 106.1, 96.2, 55.8, 55.1, 20.0.

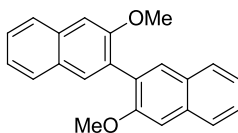


**2,2',6,6'-tetramethoxy-1,1'-biphenyl (2f):**

White solid obtained after column chromatography ( $\text{SiO}_2$ , *pentane* : ether 95:5), 35 mg, 85% yield.

$^1\text{H-NMR}$  (400 MHz,  $\text{CDCl}_3$ )  $\delta$  7.31 (t,  $J = 8.3$  Hz, 2H), 6.67 (d,  $J = 8.3$  Hz, 4H), 3.74 (s, 12H).

$^{13}\text{C-NMR}$  (101 MHz,  $\text{CDCl}_3$ )  $\delta$  158.4, 128.7, 104.5, 56.2.

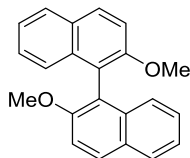


**3,3'-dimethoxy-2,2'-binaphthalene (2g):**

White solid obtained after column chromatography ( $\text{SiO}_2$ , *pentane* : ether 95:5), 42 mg, 90% yield.

$^1\text{H-NMR}$  (400 MHz,  $\text{CDCl}_3$ )  $\delta$  7.82 (d,  $J = 8.7$  Hz, 4H), 7.80 (s, 2H), 7.49 (d,  $J = 7.6$  Hz, 2H), 7.38 (d,  $J = 7.6$  Hz, 2H), 7.26 (s, 2H), 3.90 (s, 6H).

$^{13}\text{C-NMR}$  (101 MHz,  $\text{CDCl}_3$ )  $\delta$  156.3, 134.4, 130.3, 129.9, 128.7, 127.7, 126.5, 126.3, 123.7, 105.4, 55.7.



**2,2'-dimethoxy-1,1'-binaphthalene (2h):**

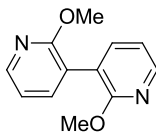
White solid obtained after column chromatography ( $\text{SiO}_2$ , *pentane* : ether 95:5), 43 mg, 92% yield.

$^1\text{H-NMR}$  (400 MHz,  $\text{CDCl}_3$ )  $\delta$  7.98 (d,  $J = 9.0$  Hz, 2H), 7.87 (d,  $J = 8.1$  Hz, 2H), 7.47 (d,  $J = 9.0$  Hz, 2H), 7.34-7.30 (m, 2H), 7.22 (t,  $J = 7.3$  Hz, 2H), 7.12 (d,  $J = 8.5$  Hz, 2H), 3.77 (s, 6H).



## CHAPTER 6

$^{13}\text{C}$ -NMR (101 MHz,  $\text{CDCl}_3$ )  $\delta$  155.0, 134.0, 129.4, 129.2, 127.9, 126.3, 125.2, 123.5, 119.6, 114.2, 56.9.

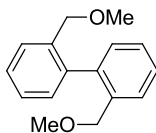


### 2,2'-dimethoxy-3,3'-bipyridine (2i):

White solid obtained after column chromatography ( $\text{SiO}_2$ , *pentane* : ether 95:5), 29 mg, 91% yield.

$^1\text{H}$ -NMR (400 MHz,  $\text{CDCl}_3$ )  $\delta$  8.18 (dd,  $J = 5.0, 1.9$  Hz, 2H), 7.59 (dd,  $J = 7.3, 1.9$  Hz, 2H), 6.95 (dd,  $J = 7.3, 5.0$  Hz, 2H), 3.92 (s, 6H).

$^{13}\text{C}$ -NMR (101 MHz,  $\text{CDCl}_3$ )  $\delta$  161.2, 146.2, 139.6, 119.9, 116.5, 53.5.



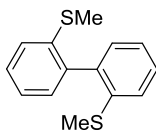
### 2,2'-bis(methoxymethyl)-1,1'-biphenyl (2j):

White solid obtained after column chromatography ( $\text{SiO}_2$ , *pentane* : ether 95:5), 35 mg, 95% yield, m.p. = 71-73 °C.

$^1\text{H}$ -NMR (400 MHz,  $\text{CDCl}_3$ )  $\delta$  7.54 (d,  $J = 7.6$  Hz, 2H), 7.39 (td,  $J = 7.5, 1.4$  Hz, 2H), 7.32 (td,  $J = 7.5, 1.3$  Hz, 2H), 7.16 (dd,  $J = 7.5, 1.1$  Hz, 2H), 4.15 (s, 4H), 3.24 (s, 6H).

$^{13}\text{C}$ -NMR (101 MHz,  $\text{CDCl}_3$ )  $\delta$  139.5, 136.2, 129.6, 128.0, 127.6, 127.1, 72.2, 58.3.

HRMS (ESI+):  $[\text{M}+\text{Na}]^+$  calculated for  $\text{C}_{16}\text{H}_{18}\text{O}_2\text{Na}^+$  = 265.11990; found: 265.12013.

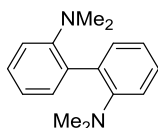


### 2,2'-bis(methylthio)-1,1'-biphenyl (2k):

White solid obtained after column chromatography ( $\text{SiO}_2$ , *pentane* : ether 99:1), 29 mg, 77% yield.

$^1\text{H}$ -NMR (400 MHz,  $\text{CDCl}_3$ )  $\delta$  7.39 (t,  $J = 7.5$  Hz, 2H), 7.31 (d,  $J = 7.9$  Hz, 2H), 7.23 (d,  $J = 7.4$  Hz, 2H), 7.19 (t,  $J = 7.7$  Hz, 2H), 2.39 (s, 6H).

$^{13}\text{C-NMR}$  (101 MHz,  $\text{CDCl}_3$ )  $\delta$  138.8, 138.1, 130.0, 128.5, 125.0, 124.5, 15.7.



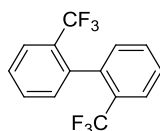
***N2,N2,N2',N2'*-tetramethyl-[1,1'-biphenyl]-2,2'-diamine (2l):**

White solid obtained after column chromatography ( $\text{SiO}_2$ , *pentane* : ether 95:5), 30 mg, 84% yield, m.p. = 69-71 °C.

$^1\text{H-NMR}$  (400 MHz,  $\text{CDCl}_3$ )  $\delta$  7.37 (dd,  $J = 7.6, 1.5$  Hz, 2H), 7.27 (t,  $J = 7.6$  Hz, 2H), 7.08 (d,  $J = 8.1$  Hz, 2H), 6.99 (t,  $J = 7.4$  Hz, 2H), 2.61 (s, 6H).

$^{13}\text{C-NMR}$  (101 MHz,  $\text{CDCl}_3$ )  $\delta$  150.3, 133.3, 131.5, 127.6, 120.9, 118.0, 42.9.

HRMS (ESI+):  $[\text{M}+\text{H}]^+$  calculated for  $\text{C}_{16}\text{H}_{21}\text{N}_2^+$  = 241.16993; found: 241.17014.



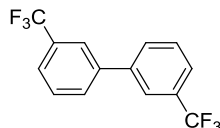
**2,2'-bis(trifluoromethyl)-1,1'-biphenyl (2m):**

Oil obtained after column chromatography ( $\text{SiO}_2$ , *pentane*), 39 mg, 90% yield.

$^1\text{H-NMR}$  (400 MHz,  $\text{CDCl}_3$ ) 7.75 (dd,  $J = 7.6, 1.2$  Hz, 2H), 7.59-7.47 (m, 4H), 7.30 (d,  $J = 7.4$  Hz, 1H).

$^{13}\text{C-NMR}$  (101 MHz,  $\text{CDCl}_3$ )  $\delta$  137.4, 131.5, 130.6, 128.1, 125.9, 123.9 (q,  $J_{\text{C-F}} = 274.0$  Hz).

$^{19}\text{F-NMR}$  (376 MHz,  $\text{CDCl}_3$ )  $\delta$  -58.2.



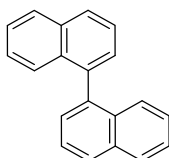
**3,3'-bis(trifluoromethyl)-1,1'-biphenyl (2n):**

Colorless oil obtained after column chromatography ( $\text{SiO}_2$ , *pentane*), 31 mg, 71% yield.

$^1\text{H-NMR}$  (400 MHz,  $\text{CDCl}_3$ )  $\delta$  7.84 (s, 2H), 7.78 (d,  $J = 7.7$  Hz, 2H), 7.67 (d,  $J = 7.8$  Hz, 2H), 7.60 (t,  $J = 7.7$  Hz, 2H).

$^{13}\text{C}$ -NMR (101 MHz,  $\text{CDCl}_3$ )  $\delta$  140.5, 130.5, 129.5, 124.7 (q,  $J = 7.5$  Hz), 124.0 (q,  $J_{\text{C-F}} = 272.3$  Hz), 124.0 (q,  $J_{\text{C-F}} = 3.8$  Hz).

$^{19}\text{F}$ -NMR (376 MHz,  $\text{CDCl}_3$ )  $\delta$  -62.5.

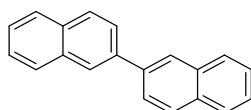


**1,1'-binaphthalene (2o):**

White solid obtained after column chromatography ( $\text{SiO}_2$ , *pentane*), 19 mg, 50% yield.

$^1\text{H}$ -NMR (400 MHz,  $\text{CDCl}_3$ )  $\delta$  7.97 (d,  $J = 8.2$  Hz, 2H), 7.96 (d,  $J = 8.2$  Hz, 2H), 7.61 (t,  $J = 7.5$  Hz, 2H), 7.53-7.46 (m, 4H), 7.41 (d,  $J = 8.4$  Hz, 2H), 7.30 (ddd,  $J = 8.3, 6.8, 1.1$ , 2H).

$^{13}\text{C}$ -NMR (101 MHz,  $\text{CDCl}_3$ )  $\delta$  138.4, 133.5, 132.8, 128.1, 127.9, 127.8, 126.6, 126.0, 125.8, 125.4.

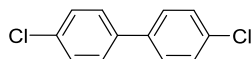


**2,2'-binaphthalene (2p):**

White solid obtained after column chromatography ( $\text{SiO}_2$ , *pentane*), 24 mg, 62% yield.

$^1\text{H}$ -NMR (400 MHz,  $\text{CDCl}_3$ )  $\delta$  8.19 (s, 2H), 7.96 (t,  $J = 9.1$  Hz, 4H), 7.90 (dd,  $J = 8.4, 1.7$  Hz, 2H), 7.57-7.48 (m, 4H).

$^{13}\text{C}$ -NMR (101 MHz,  $\text{CDCl}_3$ )  $\delta$  138.4, 133.7, 132.7, 128.5, 128.2, 127.7, 126.4, 126.1, 126.0, 125.7.

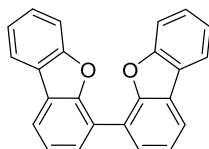


**4,4'-dichloro-1,1'-biphenyl (2q):**

White solid obtained after column chromatography ( $\text{SiO}_2$ , *pentane*), 15 mg, 45% yield.

$^1\text{H}$ -NMR (400 MHz,  $\text{CDCl}_3$ )  $\delta$  7.48 (d,  $J = 8.7$  Hz, 4H), 7.41 (d,  $J = 8.7$  Hz, 4H).

$^{13}\text{C}$ -NMR (101 MHz,  $\text{CDCl}_3$ ) 138.4, 133.7, 129.0, 128.2.

**4,4'-bidibenzo[*b,d*]furan (2r):**

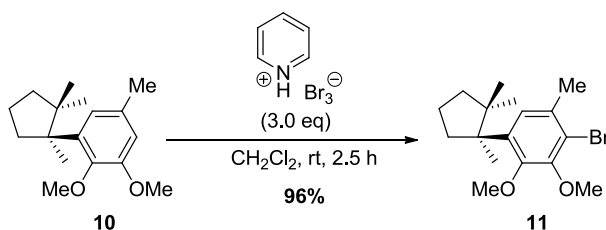
White solid obtained after column chromatography (SiO<sub>2</sub>, *pentane* : ether 98:2), 44 mg, 50% yield.

<sup>1</sup>H-NMR (400 MHz, CDCl<sub>3</sub>) δ 8.08-8.03 (m, 4H), 8.02 (dd, *J* = 7.6, 1.2 Hz, 2H), 7.62-7.53 (m, 4H), 7.51-7.46 (m, 2H), 7.40 (td, *J* = 7.5, 1.0 Hz, 2H)

<sup>13</sup>C-NMR (101 MHz, CDCl<sub>3</sub>) δ 156.2, 153.7, 128.6, 127.2, 124.9, 124.3, 122.9, 122.8, 121.0, 120.7, 120.3, 111.9.

**Experimental section and data for the Mastigophorene total synthesis:**

For the synthesis of dimethoxyherbertenediol **10** (92% *ee*) see chapter 5 and/or J. Buter, R. Moezelaar, A.J. Minnaard, *Org. Biomol. Chem.* **2014**, *12*, 5883 - Supporting Information.

**(*S*)-2-bromo-3,4-dimethoxy-1-methyl-5-(1,2,2-trimethylcyclopentyl)benzene (11) (Method A):**

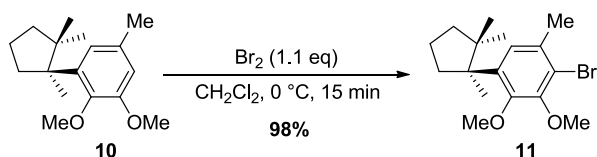
To a solution of (*S*)-1,2-dimethoxy-5-methyl-3-(1,2,2-trimethylcyclopentyl)benzene **10** (230 mg, 0.877 mmol) in dry CH<sub>2</sub>Cl<sub>2</sub> (10 mL) was added pyridinium tribromide (841 mg, 2.63 mmol, 3 eq) in four portions over 1 h (not all solids dissolved!). The reaction was monitored by TLC analysis (2% ether in pentane) and GC-MS analysis which both showed complete conversion after 2.5 h.

To the reaction mixture was added aqueous saturated NaHCO<sub>3</sub> (10 mL). The phases were separated and the organic layer was washed twice with water (2x10 mL). The combined aqueous layers were back-extracted once with CH<sub>2</sub>Cl<sub>2</sub> (10 mL). The combined organic phases were washed with brine, dried over Na<sub>2</sub>SO<sub>4</sub>, filtered and concentrated under reduced pressure. Flash column chromatography using 2% ether in pentane as the eluent afforded pure (*S*)-2-bromo-3,4-dimethoxy-1-methyl-5-(1,2,2-

trimethylcyclopentyl)benzene **11** (287 mg, 0.842 mmol, 96% yield) as a slight yellow oil.

$^1\text{H-NMR}$  (400 MHz,  $\text{CDCl}_3$ )  $\delta$  6.98 (s, 1H), 3.83 (s, 3H), 3.81 (s, 3H), 2.63 – 2.46 (m, 1H), 2.35 (s, 3H), 1.84 – 1.55 (m, 5H), 1.35 (s, 3H), 1.13 (s, 3H), 0.69 (s, 3H).

$^{13}\text{C-NMR}$  (101 MHz,  $\text{CDCl}_3$ )  $\delta$  151.90, 150.86, 139.83, 132.11, 125.74, 117.68, 60.40, 59.88, 51.62, 44.92, 41.07, 39.19, 26.98, 25.37, 24.08, 23.14, 20.52.

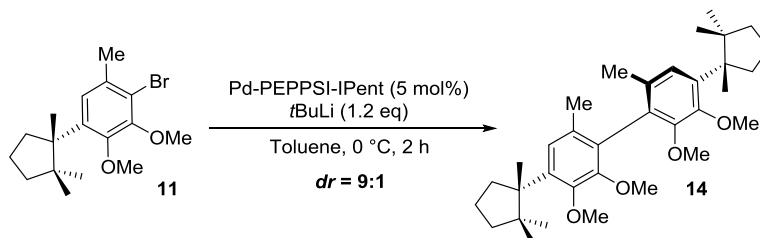


**(S)-2-bromo-3,4-dimethoxy-1-methyl-5-(1,2,2-trimethylcyclopentyl)benzene (11)**  
**(Method B):**

To a cooled ( $0\text{ }^\circ\text{C}$ ) solution of (*S*)-1,2-dimethoxy-5-methyl-3-(1,2,2-trimethylcyclopentyl)benzene **10** (110 mg, 0.42 mmol) in dry  $\text{CH}_2\text{Cl}_2$  (4 mL) was added dibromine (23  $\mu\text{l}$ , 3.90 mmol, 1.1 eq). After addition the reaction mixture was stirred for 15 min. after which GC-MS and TLC analysis indicated complete conversion of the starting material. The reaction mixture was then quenched with an aqueous saturated  $\text{NaHCO}_3$  solution. The phases were separated and the aqueous phase was extracted twice with  $\text{CH}_2\text{Cl}_2$ . The organic phase was dried over  $\text{Na}_2\text{SO}_4$ , filtered, and concentrated under reduced pressure. The residual oil was subjected to flash column chromatography employing pentane as the eluent afforded pure (*S*)-2-bromo-3,4-dimethoxy-1-methyl-5-(1,2,2-trimethylcyclopentyl)benzene **11** (140 mg, 0.410 mmol, 98% yield) as a slight yellow oil.

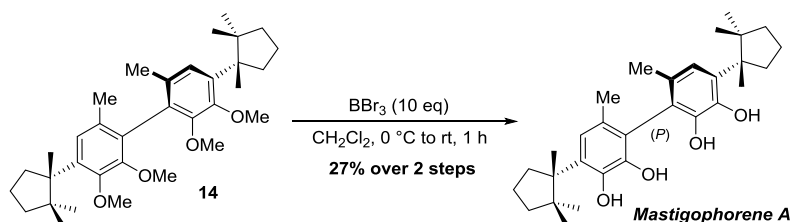
$^1\text{H-NMR}$  (400 MHz,  $\text{CDCl}_3$ )  $\delta$  6.98 (s, 1H), 3.83 (s, 3H), 3.81 (s, 3H), 2.63 – 2.46 (m, 1H), 2.35 (s, 3H), 1.84 – 1.55 (m, 5H), 1.35 (s, 3H), 1.13 (s, 3H), 0.69 (s, 3H).

$^{13}\text{C-NMR}$  (101 MHz,  $\text{CDCl}_3$ )  $\delta$  151.90, 150.86, 139.83, 132.11, 125.74, 117.68, 60.40, 59.88, 51.62, 44.92, 41.07, 39.19, 26.98, 25.37, 24.08, 23.14, 20.52.



**2,2',3,3'-tetramethoxy-6,6'-dimethyl-4,4'-bis((*S*)-1,2,2-trimethylcyclopentyl)-1,1'-biphenyl (tetramethoxymastigophorene A) (14):**

In a dry Schlenk flask, Pd-PEPPSI-IPent (12 mg, 19  $\mu$ mol, 5 mol%) and (*S*)-2-bromo-3,4-dimethoxy-1-methyl-5-(1,2,2-trimethylcyclopentyl)benzene **11** (125 mg, 0.37 mmol) were dissolved in dry toluene (1.5 ml) and the solution was cooled to 0 °C with an ice bath. *t*BuLi (265  $\mu$ L, 1.7 M in hexanes, 0.44 mmol, 1.2 eq) was slowly added (per 2 drops with 5 min intervals, total addition time = 40 min) by the aid of a syringe pump. After the addition was completed the reaction mixture was stirred for one additional hour after which the reaction was quenched with methanol. Celite was added, and the solvent evaporated under reduced pressure. The residue was directly loaded onto a prepared flash column, and eluted using pentane as the eluent, affording a mixture of the two diastereoisomers in a diastereomeric ratio of 9:1 (detected by GC-MS), mixed with dimethoxyherbertenediol **10**. <sup>1</sup>H-NMR analysis showed a major resonance at  $\delta$  1.95 which corresponds to (*P*)-helicity as found in mastigophorene A.



**(*S*)-6,6'-dimethyl-4,4'-bis((*S*)-1,2,2-trimethylcyclopentyl)-[1,1'-biphenyl]-2,2',3,3'-tetraol (Mastigophorene A):**

To a solution of 2,2',3,3'-tetramethoxy-6,6'-dimethyl-4,4'-bis((*S*)-1,2,2-trimethylcyclopentyl)-1,1'-biphenyl **14** (contaminated with dimethoxyherbertenediol **10**) (62 mg, 0.119 mmol) in dry CH<sub>2</sub>Cl<sub>2</sub> cooled to 0 °C was added dropwise BBr<sub>3</sub> (1.2 mL, 1 M in CH<sub>2</sub>Cl<sub>2</sub>, 1.2 mmol, 10 eq). The ice-bath was removed and the reaction mixture was allowed to warm to rt and stirred for 1 h. TLC indicated complete conversion of the starting material after which the reaction mixture was poured onto 5% aqueous NaHCO<sub>3</sub> (4 mL). The phases were separated and the aqueous phase was extracted twice with CH<sub>2</sub>Cl<sub>2</sub>. The combined organic phases were dried over Na<sub>2</sub>SO<sub>4</sub>, filtered and loaded on Celite. This concentrated sample was loaded on a silica cartridge where after automated flash column chromatography was performed employing a pentane : ether (9 : 1 to 8 : 2)

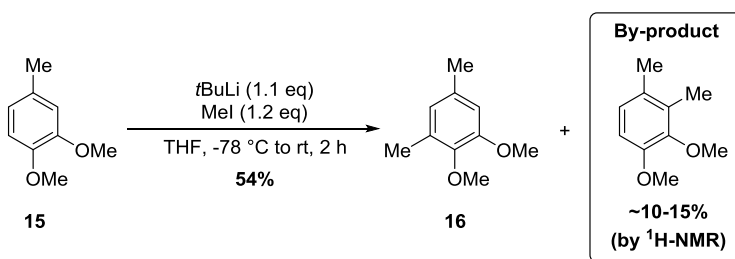
## CHAPTER 6

gradient as the eluent, to give pure mastigophorene A (23 mg, 27% over 2 steps, 0.05 mmol) which crystallized upon standing at rt.

$^1\text{H-NMR}$  (400 MHz,  $\text{CDCl}_3$ )  $\delta$  6.87 (s, 2H), 5.58 (s, 2H), 4.73 (s, 2H), 2.73 – 2.65 (m, 2H), 1.94 (s, 6H), 1.83 – 1.53 (m, 10H), 1.46 (s, 6H), 1.21 (s, 6H), 0.80 (s, 6H).

$^{13}\text{C-NMR}$  (101 MHz,  $\text{CDCl}_3$ )  $\delta$  141.72, 140.65, 134.02, 126.81, 122.88, 117.09, 51.49, 45.13, 41.31, 39.05, 27.35, 25.69, 22.98, 20.59, 19.37.

$[\alpha]_{\text{D}}^{20} = -67.9$  ( $\text{CHCl}_3$ ,  $c = 0.4$ ) for a 92% *ee* sample; literature value:  $[\alpha]_{\text{D}}^{19} = -65.3$  ( $\text{CHCl}_3$ ,  $c = 0.4$ ).<sup>[18b]</sup>



### 1,2-dimethoxy-3,5-dimethylbenzene (**16**):

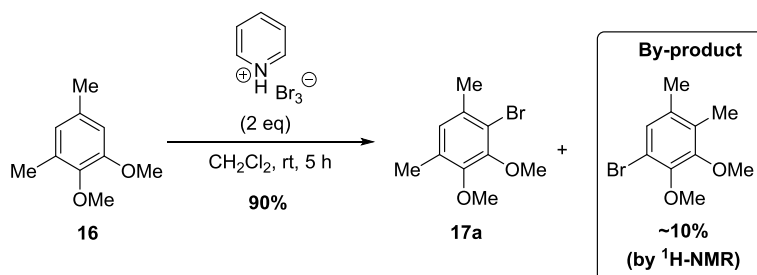
To a solution of 1,2-dimethoxy-4-methylbenzene **15** (5 ml, 34.8 mmol) in dry THF (75 mL), cooled to  $-78\text{ }^\circ\text{C}$ , was added dropwise  $t\text{BuLi}$  (22.5 mL, 1.7 M in hexanes, 1.1 eq) by syringe pump (22.5 mL/h). A bright yellow solution formed upon addition. After addition the reaction mixture was allowed to warm-up to  $0\text{ }^\circ\text{C}$ , whereupon a suspension formed. The reaction mixture was then cooled to  $-78\text{ }^\circ\text{C}$  and iodomethane (2.60 ml, 41.8 mmol, 1.2 eq) was added dropwise. The reaction mixture was allowed to warm-up to rt and was stirred an additional hour at this temperature.

The reaction mixture was quenched using an aqueous saturated  $\text{NH}_4\text{Cl}$  solution (100 mL). After phase separation, the aqueous layer was washed three times with ether. The combined organic layers were dried over  $\text{Na}_2\text{SO}_4$ , filtered, and concentrated under reduced pressure to afford a yellow oil. Flash column chromatography was performed employing pentane : ether = 9 : 1. The individual fractions were analyzed with GC-MS and the fractions of >85% purity (the desired compound elutes first!) were combined affording 1,2-dimethoxy-3,5-dimethylbenzene **16** (3.1 g, 18.7 mmol, 54% yield) with ~85% purity based on  $^1\text{H-NMR}$  analysis.

$^1\text{H-NMR}$  (400 MHz,  $\text{CDCl}_3$ )  $\delta$  6.58 (s, 2H), 3.84 (s, 3H), 3.77 (s, 3H), 2.28 (s, 3H), 2.24 (s, 3H).

$^{13}\text{C-NMR}$  (101 MHz,  $\text{CDCl}_3$ )  $\delta$  152.42, 145.18, 133.39, 131.54, 123.30, 110.92, 60.20, 55.72, 21.29, 15.78.

HRMS (ESI+): Calculated mass  $[M+H]^+$   $C_{10}H_{15}O_2^+$  = 167.1067; found: 167.1066.



**2-bromo-3,4-dimethoxy-1,5-dimethylbenzene (17a):**

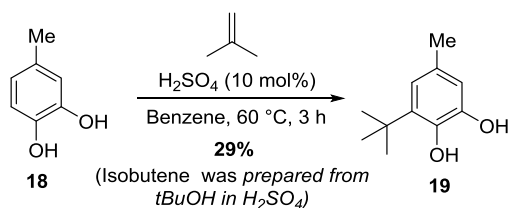
To a solution of 1,2-dimethoxy-3,5-dimethylbenzene **16** (3.0 g, 18 mmol) in dry  $CH_2Cl_2$  (150 mL) was added pyridinium tribromide (11.5, 36.1 mmol, 2 eq) portionwise over 1 h. The wall of the Schlenk flask was rinsed with dry  $CH_2Cl_2$  after each addition. The reaction was followed by TLC analysis (2% ether in pentane) and showed complete conversion after 5 h. To the reaction mixture was added an aqueous saturated  $NaHCO_3$  solution (10 mL). The phases were separated and the organic layer was washed twice with water (2x10 mL). The combined aqueous layers were back-extracted once with  $CH_2Cl_2$  (10 mL). The combined organic phases were washed with brine, dried over  $Na_2SO_4$ , filtered and concentrated under reduced pressure. Flash column chromatography using 2% ether in pentane as the eluent afforded 2-bromo-3,4-dimethoxy-1,5-dimethylbenzene **17a** (4.0 g, 16.3 mmol, 90% yield) as a slight yellow oil with ~90% purity based on  $^1H$ -NMR analysis.

$^1H$ -NMR (400 MHz,  $CDCl_3$ )  $\delta$  6.69 (s, 1H), 3.84 (s, 3H), 3.76 (s, 3H), 2.38 (s, 3H), 2.36 (s, 3H).

$^{13}C$ -NMR (101 MHz,  $CDCl_3$ )  $\delta$  151.55, 145.86, 133.63, 132.39, 118.50, 111.97, 60.66, 55.97, 24.05, 16.79.

HRMS (ESI+ and APCI) analysis could not be performed due to ion-suppression. GC-MS analysis gave the following mass fragmentation: Calculated mass  $[M]^+$   $C_{10}H_{13}O_2^{79}Br^+$  = 244.01; found: 246 ( $M^+$  isotope), 244 ( $M^+$ ), 231 ( $M-CH_3$  isotope) $^+$ , 229 ( $M-CH_3$ ) $^+$ , 216 ( $M-(CH_3)_2$  isotope) $^+$ , 214 ( $M-(CH_3)_2$ ) $^+$ .



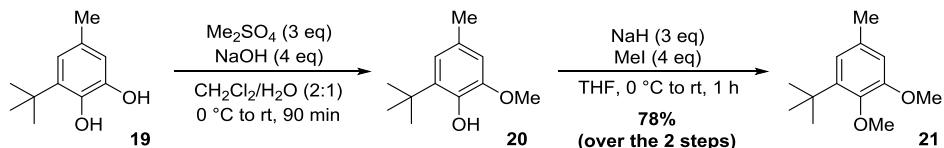


### 3-(*tert*-butyl)-5-methylbenzene-1,2-diol (**19**):

To a suspension of 4-methylbenzene-1,2-diol **18** (2.6 g, 20.94 mmol) in benzene (50 mL) was added sulfuric acid (110  $\mu$ L, 2.1 mmol, 10 mol%). The mixture was cooled with an ice/salt bath (-10 to -5  $^\circ$ C) and isobutene\* was bubbled through the solution for 2 h. The Schlenk vessel was then closed and the reaction was heated to 60 $^\circ$ C and stirred for 3 h. Full conversion was not obtained but it was decided to quench the reaction with a saturated aqueous NaHCO<sub>3</sub> solution where after the phases were separated. The organic layer was washed with water, dried using MgSO<sub>4</sub>, filtered and concentrated under reduced pressure. The isolated oil was purified using flash column chromatography employing pentane : ether (3:2) affording 3-(*tert*-butyl)-5-methylbenzene-1,2-diol **19** as a yellowish oil (1.1 g, 6.10 mmol, 29% yield).

\* The isobutene was generated by slow addition of solid *tert*-butanol to concentrated sulfuric acid. The isobutene formed was led through a cannula (double tipped needle), into the flask containing 4-methylbenzene-1,2-diol and sulfuric acid.

The analytical data was in agreement with those reported in the literature.<sup>[28]</sup>



### 1-(*tert*-butyl)-2,3-dimethoxy-5-methylbenzene (**21**):

To a cooled (0  $^\circ$ C) solution of 3-(*tert*-butyl)-5-methylbenzene-1,2-diol **19** (1.1 g, 6.10 mmol) in CH<sub>2</sub>Cl<sub>2</sub> (8 mL) and water (4 mL) were added sodium hydroxide (976 mg, 24.4 mmol, 4 eq) and dimethyl sulfate (1.73 mL, 18.3 mmol, 3 eq). The reaction mixture was allowed to stir for 90 min after which GC-MS analysis showed complete conversion to the monomethylated compound. No significant change was observed upon subsequent stirring overnight.

The reaction mixture was carefully quenched using conc. aqueous NH<sub>3</sub> and the organic phase was removed by evaporation. The aqueous layer was extracted twice with pentane. The combined organic phases were dried over MgSO<sub>4</sub>, filtered and concentrated under reduced pressure. NMR analysis and GC-MS analysis indicated ~95% monomethylated compound **20** with ~5% of the desired dimethylated product **21**. The crude product was used in the next step.

To a suspension of NaH (732 mg, 60% dispersion in oil, 3 eq) in dry THF (8 mL), cooled to 0 °C, was slowly added a solution of the monomethylated product in dry THF (7 mL). After addition, iodomethane (1.52 ml, 24.4 mmol, 4 eq) was added dropwise after which the reaction mixture was allowed to warm to rt. GC-MS analysis after 1h indicated complete conversion. The reaction mixture was cooled to 0 °C, diluted with ether, and carefully quenched by the dropwise addition of water. After quenching the phases were separated and the aqueous phase was extracted twice with ether. The combined organic phases were washed with brine, dried over MgSO<sub>4</sub>, filtered and concentrated under reduced pressure affording 1-(*tert*-butyl)-2,3-dimethoxy-5-methylbenzene **21** (992 mg, 4.76 mmol, 78% yield over 2 steps).

*Analytical data of the monomethylated compound 20:*

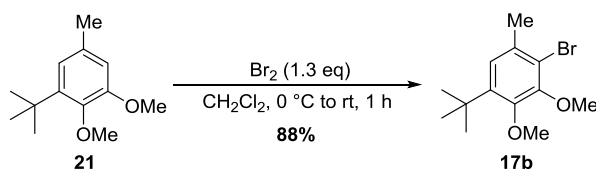
<sup>1</sup>H-NMR (400 MHz, CDCl<sub>3</sub>) δ 6.69 (s, 1H), 6.60 (s, 1H), 5.82 (s, 1H), 3.87 (s, 3H), 2.29 (s, 3H), 1.40 (s, 9H).

<sup>13</sup>C-NMR (101 MHz, CDCl<sub>3</sub>) δ 146.56, 142.02, 135.25, 127.92, 119.45, 109.44, 56.17, 34.68, 29.57, 21.53.

*Analytical data of the bismethylated compound 21:*

<sup>1</sup>H-NMR (400 MHz, CDCl<sub>3</sub>) δ 6.74 (s, 1H), 6.67 (s, 1H), 3.88 (s, 3H), 3.87 (s, 3H), 2.33 (s, 3H), 1.41 (s, 9H).

<sup>13</sup>C-NMR (101 MHz, CDCl<sub>3</sub>) δ 153.08, 146.36, 142.95, 132.39, 119.36, 111.57, 60.47, 55.77, 35.07, 30.72, 21.71.



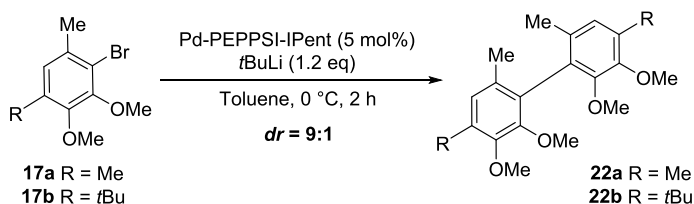
**2-bromo-5-(*tert*-butyl)-3,4-dimethoxy-1-methylbenzene (17b):**

To a cooled (0 °C) solution of 1-(*tert*-butyl)-2,3-dimethoxy-5-methylbenzene **21** (625 mg, 3.00 mmol) in dry CH<sub>2</sub>Cl<sub>2</sub> (10 mL) was added a solution of dibromine (201 μl, 3.90 mmol, 1.05 eq) in dry CH<sub>2</sub>Cl<sub>2</sub> (1.5 mL). After addition the reaction mixture was allowed to warm to rt and stirred for 1h. GC-MS and TLC analysis indicated complete conversion of the starting material. The reaction mixture was then quenched with an aqueous saturated Na<sub>2</sub>S<sub>2</sub>O<sub>3</sub> solution. The phases were separated and the organic phase was washed with brine. The organic phase was dried over Na<sub>2</sub>SO<sub>4</sub>, filtered, and concentrated under reduced pressure. The residual oil was subjected to flash column chromatography employing pentane : ether (99 : 1) as the eluent, affording 2-bromo-5-(*tert*-butyl)-3,4-dimethoxy-1-methylbenzene **17b** (756 mg, 2.63 mmol, 88% yield) as a slightly yellow oil.

## CHAPTER 6

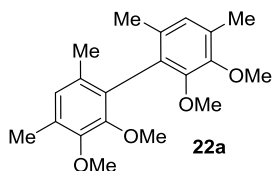
$^1\text{H-NMR}$  (400 MHz,  $\text{CDCl}_3$ )  $\delta$  6.95 (s, 1H), 3.91 (s, 3H), 3.84 (s, 3H), 2.37 (s, 3H), 1.37 (s, 9H).

$^{13}\text{C-NMR}$  (101 MHz,  $\text{CDCl}_3$ )  $\delta$  151.44, 150.76, 142.47, 132.72, 123.50, 118.04, 60.40, 59.97, 35.05, 30.53, 23.07.



### General procedure for the optimized Pd-catalyzed homo-coupling of the sterically hindered substrates 17a and 17b:

In a dry Schlenk flask, Pd-PEPPSI-*i*Pent (5 mol%, 1  $\mu\text{mol}$ ) and the substrate (0.2 mmol) were dissolved in dry toluene (0.7 ml) and the solution was cooled to 0 °C with an ice bath. *t*BuLi (141  $\mu\text{L}$ , 1.7 M in hexanes, 0.24 mmol, 1.2 eq) was slowly added (per 2 drops with 5 min intervals, total addition time = 40 min) by the aid of a syringe pump. After the addition was completed the reaction mixture was stirred for one additional hour after which the reaction was quenched with methanol. Celite was added, and the solvent evaporated under reduced pressure. The residue was directly loaded onto a prepared flash column, and eluted using pentane : ether as the eluent affording the homo-coupling product as an oil.



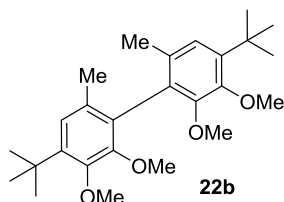
### 2,2',3,3'-tetramethoxy-4,4',6,6'-tetramethyl-1,1'-biphenyl (22a):

Prepared according to the general procedure of the Pd-catalyzed homo-coupling in 79% isolated yield.

$^1\text{H-NMR}$  (400 MHz,  $\text{CDCl}_3$ )  $\delta$  6.58 (s, 2H), 3.84 (s, 6H), 3.77 (s, 6H), 2.28 (s, 6H), 2.23 (s, 6H).

$^{13}\text{C-NMR}$  (101 MHz,  $\text{CDCl}_3$ )  $\delta$  151.16, 145.51, 132.90, 131.55, 130.16, 111.25, 60.41, 55.63, 19.99, 12.86.

HRMS (ESI+): Calculated mass  $[\text{M}+\text{H}]^+$   $\text{C}_{20}\text{H}_{27}\text{O}_4^+$  = 331.1904; found: 331.1902.

**4,4'-di-*tert*-butyl-2,2',3,3'-tetramethoxy-6,6'-dimethyl-1,1'-biphenyl (22b):**

Prepared according to the general procedure of the Pd-catalyzed homo-coupling in 75% isolated yield as a waxy solid.

$^1\text{H-NMR}$  (400 MHz,  $\text{CDCl}_3$ )  $\delta$  6.93 (s, 2H), 3.86 (s, 6H), 3.64 (s, 6H), 1.95 (s, 6H), 1.42 (s, 18H).

$^{13}\text{C-NMR}$  (101 MHz,  $\text{CDCl}_3$ )  $\delta$  151.10, 150.55, 142.05, 130.82, 130.03, 122.83, 59.93, 59.68, 35.04, 30.81, 19.88.

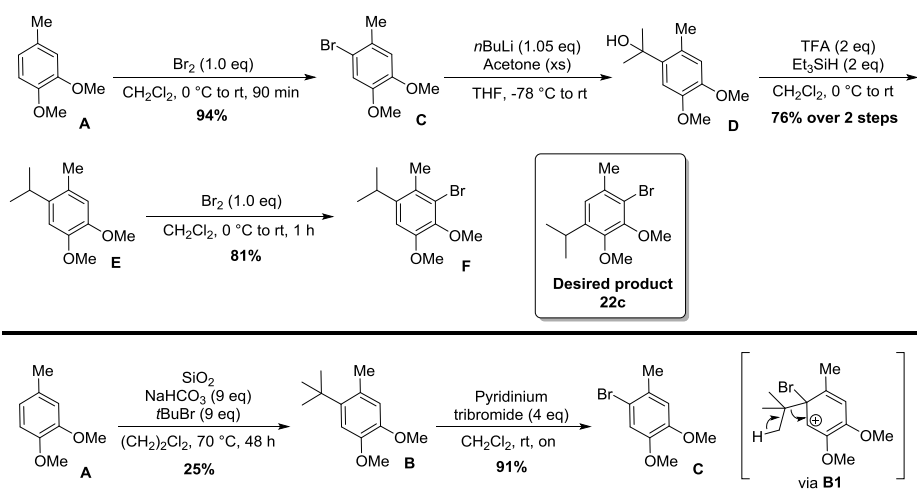
HRMS (ESI<sup>+</sup>): Calculated mass  $[\text{M}+\text{H}]^+$   $\text{C}_{24}\text{H}_{39}\text{O}_4^+$  = 415.2843; found: 415.2839.

**Attempted synthesis of isopropyl analogue 22c:**

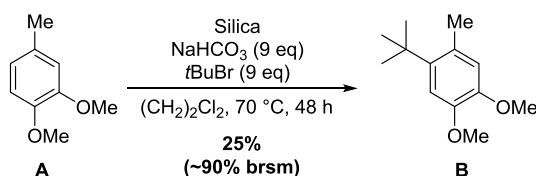
For our investigation of the influence of the *para*-substituent on the outcome of the Pd-catalyzed homo-coupling, we also tried to construct isopropyl test substrate **22c** (Scheme 12, see below). Although initially considered to be **22c**, the product turned out to be **F**. The synthesis started from 3,4-dimethoxytoluene that was brominated with dibromine to provide **C**. Interestingly, **C** was also obtained in a different, peculiar, way. In our preparation of *t*-butyl substrate **22b** we initially tried to *tert*-butylate 3,4-dimethoxytoluene **A**, but this provided us with the undesired regioisomer **B**. Surprisingly we found that bromination of **B** with pyridinium tribromide led to successful bromination, albeit that the *t*-butyl group was removed simultaneously. The product's analytical data were consistent with aryl bromide **C**, which indicated *ipso*-bromination. We therefore must assume that *ipso* intermediate **B1** was formed which eliminates isobutylene from the molecule, as indicated.

At first sight this sequence seems useless, however giving it some thought the reaction might have a useful application. To the best of our knowledge, bromine-*t*-butyl exchange via *ipso*-bromination is extremely rare.<sup>[46]</sup> We postulate that this sequence might be useful if the *t*-butyl functionality could act as a kind of protecting group, in the sense that it acts as a masked bromo substituent. The advantage is that the *t*-butyl moiety is robust and tolerant to a wide variety of reaction conditions (lithiation, palladation!). Although we present here only one example, removal of the *t*-butyl group was high yielding and easy to perform. A bromine atom was installed selectively which allows further functionalization, for instance using lithium cross-coupling chemistry. We are well aware that this reaction probably only applies to special cases, but its scope can be established by performing a systematic study into its potential.

CHAPTER 6



Scheme 12. Attempted synthesis of isopropyl substrate 22c.



**1-(*tert*-butyl)-4,5-dimethoxy-2-methylbenzene (B):**

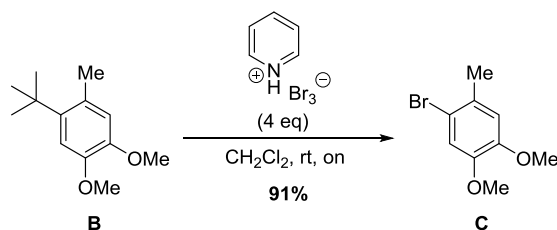
To a mixture of 1,2-dimethoxy-4-methylbenzene **A** (5.2 g, 34 mmol), silica (17 g) and sodium bicarbonate (25.8 g, 308 mmol) in dichloroethane (120 mL) was added 2-bromo-2-methylpropane (34.5 ml, 308 mmol) and the mixture was stirred at 70 °C overnight. The reaction mixture turned blue/purple to green over time. The green color dissipated slowly, and when completely vanished the reaction did not progress any further (based on GC-MS analysis after 48 h). The reaction mixture was filtered, and concentrated under reduced pressure. Flash column chromatography employing pentane : ether (95 : 5) afforded the product, however, due to similar  $R_f$  values of the starting material and the product, the individual column fractions had to be analyzed by GC-MS. All fractions with >95% purity were isolated yielding virtually pure 1-(*tert*-butyl)-4,5-dimethoxy-2-methylbenzene **B** (1.78 g, 8.55 mmol, 25% yield).

$^1\text{H-NMR}$  (400 MHz,  $\text{CDCl}_3$ )  $\delta$  6.93 (s, 1H), 6.64 (s, 1H), 3.87 (s, 3H), 3.85 (s, 3H), 2.48 (s, 3H), 1.40 (s, 9H). $\ddagger$

$^{13}\text{C-NMR}$  (101 MHz,  $\text{CDCl}_3$ )  $\delta$  146.44, 146.10, 140.14, 128.39, 116.11, 110.89, 56.12, 55.78, 35.45, 31.01, 22.64

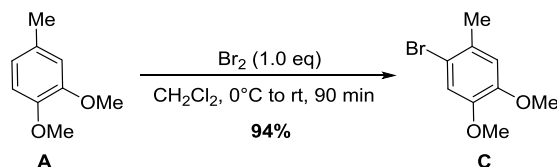
HRMS (ESI $^+$ ): Calculated mass  $[\text{M}+\text{H}]^+ \text{C}_{13}\text{H}_{20}\text{O}_2^+ = 209.1536$ ; found: 209.1536

‡ The obtained  $^1\text{H-NMR}$  spectrum differed slightly from previous reported data; A. P. Morgenstern, C. Schuijt, W. Nauta, *J. Chem. Soc. C.* **1972**, 3706. It is important to note that the  $^1\text{H-NMR}$  spectrum within this report was obtained on a 60 MHz spectrometer at 38 °C.



#### 1-bromo-4,5-dimethoxy-2-methylbenzene (B) (Method A):

To a solution of 1-(*tert*-butyl)-4,5-dimethoxy-2-methylbenzene **B** (1.78 g, 8.55 mmol) in dry  $\text{CH}_2\text{Cl}_2$  (100 mL) was added pyridinium tribromide (10.9 g, 34.2 mmol, 4 eq) portion wise over 1 h. The wall of the Schlenk flask was rinsed with dry  $\text{CH}_2\text{Cl}_2$  after each addition. The reaction was stirred overnight at rt after which GC-MS and TLC analysis indicated complete conversion. The suspension was filtered and to the filtrate was added an aqueous saturated  $\text{NaHCO}_3$  solution. The phases were separated and the organic layer was washed twice with water. The organic phases were washed with brine, dried over  $\text{Na}_2\text{SO}_4$ , filtered and concentrated under reduced pressure. Flash column chromatography using 3% ether in pentane as the eluent afforded pure 1-bromo-2,3-dimethoxy-5-methylbenzene **C** (1.8 g, 7.79 mmol, 91% yield) as a yellow oil.



#### 1-bromo-2,3-dimethoxy-5-methylbenzene (C) (Method B):

To a solution of 1,2-dimethoxy-4-methylbenzene **A** (943  $\mu\text{L}$ , 6.57 mmol) in dry  $\text{CH}_2\text{Cl}_2$  (20 mL), cooled to 0 °C, was added slowly a solution of dibromine (338  $\mu\text{L}$ , 6.57 mmol, 1 eq) in dry  $\text{CH}_2\text{Cl}_2$  (4 mL). The reaction mixture was allowed to warm-up to rt at which it was stirred for 1.5 h. GC-MS analysis indicated selective formation of the desired product. The reaction was quenched with saturated aqueous  $\text{Na}_2\text{S}_2\text{O}_3$ . The phases were separated and the aqueous layer was extracted once using  $\text{CH}_2\text{Cl}_2$ . The combined organic phases were washed with brine, dried over  $\text{Na}_2\text{SO}_4$ , filtered and concentrated under reduced pressure. Flash column chromatography employing 3% ether in pentane afforded pure 1-bromo-2,3-dimethoxy-5-methylbenzene **C** (1.30 g, 5.63 mmol, 94% yield).

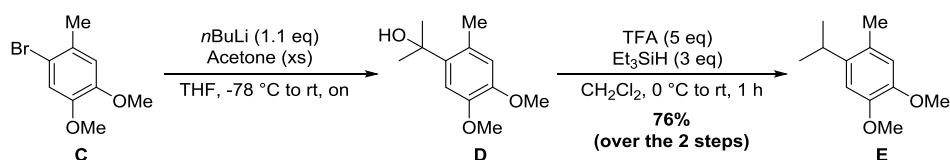
## CHAPTER 6

$^1\text{H-NMR}$  (400 MHz,  $\text{CDCl}_3$ ) 7.00 (s, 1H), 6.73 (s, 1H), 3.85 (s, 3H), 3.83 (s, 3H), 2.33 (s, 3H).

$^{13}\text{C-NMR}$  (101 MHz,  $\text{CDCl}_3$ )  $\delta$  148.12, 147.60, 129.52, 115.25, 114.37, 113.51, 56.10, 55.94, 22.28.

*HRMS (ESI+ and APCI) analysis could not be performed due to ion-suppression. GC-MS analysis gave the following mass fragmentation: Calculated mass  $[\text{M}]^+$   $\text{C}_9\text{H}_{11}\text{O}_2^{79}\text{Br}^+ = 229.99$ ; found: 232 ( $\text{M}^+$  isotope), 230 ( $\text{M}^+$ ), 217 ( $\text{M}-\text{CH}_3$  isotope) $^+$ , 215 ( $\text{M}-\text{CH}_3$ ) $^+$ , 108 ( $\text{M}-(\text{CH}_3)_2\text{Br}$ ) $^+$ .*

*The analytical data are in accordance with the previously reported analytical data. See: J. L. Charlton, K. Koh, G. Plourde, *Can. J. Chem.* **1990**, *68*, 2028.*



### 1-isopropyl-4,5-dimethoxy-2-methylbenzene (E):

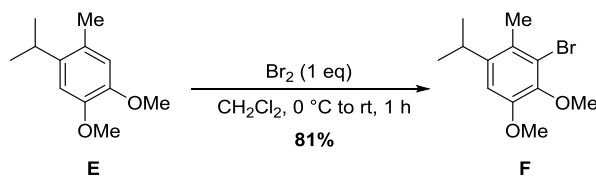
A solution of 1-bromo-4,5-dimethoxy-2-methylbenzene **C** (1.0 g, 4.3 mmol) in dry THF (20 mL) was cooled to  $-78\text{ }^\circ\text{C}$ . To the solution was slowly added *n*BuLi (1.9 mL, 2.5 M in hexanes, 4.7 mmol, 1.1 eq). The mixture was allowed to stir for 30 min. Acetone (2 mL) was added dropwise and the mixture was allowed to reach rt and stirred overnight. The reaction mixture was quenched with MeOH (5 mL) where after the reaction mixture was concentrated under reduced pressure. The crude reaction mixture was used in the next step.

A solution of alcohol **D** (1.0 g, 4.76 mmol) in dry  $\text{CH}_2\text{Cl}_2$  (40 mL) was cooled to  $0\text{ }^\circ\text{C}$ . 2,2,2-trifluoroacetic acid (1.65 mL, 21.6 mmol, 5 eq) and triethylsilane (2.07 mL, 13 mmol, 3 eq) were added and the reaction was stirred at  $0\text{ }^\circ\text{C}$  for 1 h. The reaction was complete after this time and the reaction mixture was allowed to warm to rt. The reaction was concentrated under reduced pressure. Flash column chromatography employing pentane : ether (95 : 5) as the eluent afforded 1-isopropyl-4,5-dimethoxy-2-methylbenzene **E** (643 mg, 3.31 mmol, 76% yield over 2 steps)

$^1\text{H-NMR}$  (400 MHz,  $\text{CDCl}_3$ )  $\delta$  6.79 (s, 1H), 6.67 (s, 1H), 3.88 (s, 3H), 3.10 (p,  $J = 6.9$  Hz, 1H), 2.29 (s, 3H), 1.23 (d,  $J = 6.9$  Hz, 6H).

$^{13}\text{C-NMR}$  (101 MHz,  $\text{CDCl}_3$ )  $\delta$  147.22, 146.49, 138.85, 126.91, 113.72, 108.78, 56.11, 55.89, 29.12, 23.41, 18.73.

HRMS (ESI+): Calculated mass  $[\text{M}+\text{H}]^+ \text{C}_{12}\text{H}_{19}\text{O}_2^+ = 195.1380$ ; found: 195.1380.

**3-bromo-1-isopropyl-4,5-dimethoxy-2-methylbenzene (F):**

To a solution of 1-isopropyl-4,5-dimethoxy-2-methylbenzene **E** (590 mg, 3.04 mmol) in dry CH<sub>2</sub>Cl<sub>2</sub> (10 mL) was added slowly a solution of dibromine (156 μL, 3.04 mmol, 1 eq) in dry CH<sub>2</sub>Cl<sub>2</sub> (6 mL). After addition the reaction was stirred at rt for 60 min after which GC-MS indicated full conversion. The reaction mixture was quenched by the addition of saturated aqueous Na<sub>2</sub>S<sub>2</sub>O<sub>3</sub> (8 mL). The phases were separated and the organic phase was washed with brine, dried over MgSO<sub>4</sub>, filtered and concentrated under reduced pressure. Flash column chromatography using pentane : ether (98 : 2) afforded 3-bromo-1-isopropyl-4,5-dimethoxy-2-methylbenzene **F** (672 mg, 2.46 mmol, 81% yield) as a yellowish oil.

<sup>1</sup>H-NMR (400 MHz, CDCl<sub>3</sub>) δ 6.79 (s, 1H), 3.87 (s, 3H), 3.83 (s, 3H), 3.18 (p, *J* = 6.8 Hz, 1H), 2.38 (s, 3H), 1.22 (d, *J* = 6.9 Hz, 6H).

<sup>13</sup>C-NMR (101 MHz, CDCl<sub>3</sub>) δ 151.32, 144.33, 143.42, 127.59, 121.62, 108.79, 60.32, 56.25, 30.56, 23.37, 18.39.

HRMS (ESI<sup>+</sup>): Calculated mass [M+H]<sup>+</sup> C<sub>12</sub>H<sub>18</sub>O<sub>2</sub><sup>79</sup>Br<sup>+</sup> = 273.0485; found: 273.0487.

**6.7 References**

- [1] a) *Synthesis of Biaryls*; (Ed. I. Cepanec) Elsevier. Amsterdam, **2004**. b) G. Bringmann, R. Walter, R. Weirch, *Angew. Chem. Int. Ed.* **1990**, *29*, 977. c) G. Bringmann, A. J. Price Mortimer, P. A. Keller, M. J. Gresser, J. Garner, M. Breuning, *Angew. Chem. Int. Ed.* **2005**, *44*, 5384. On the topic of stereoselective biaryl couplings see: d) J. Wencel-Delord, A. Panossian, F. R. Leroux, F. Colobert, F. *Chem. Soc. Rev.* **2015**, *44*, 3481.
- [2] a) O. Baudoin, F. Gueritte, *Stud. Nat. Prod. Chem.* **2003**, *29*, 355. b) M. C. Kozłowski, B. J. Morgan, E. C. Linton, *Chem. Soc. Rev.* **2009**, *38*, 3193. c) G. Bringmann, T. Gulder, T. A. M. Gulder, M. Breuning, *Chem. Rev.* **2011**, *111*, 563.
- [3] F. Ullmann J. Bielecki, *Chem. Ber.* **1901**, *34*, 2174.
- [4] J. Hassan, M. Sévignon, C. Gozzi, E. Schulz, M. Lemaire, *Chem. Rev.* **2002**, *102*, 1359.
- [5] a) *Metal-Catalyzed Cross-Coupling Reactions*, Vol. 1, (Eds. A. de Meijere, S. Bräse, M. Oestreich) Wiley-VCH, Weinheim, **2013**. b) *Metal-Catalyzed Cross-Coupling Reactions and more*, 3 volume set, (Eds. A de Meijere, F. Diederich)



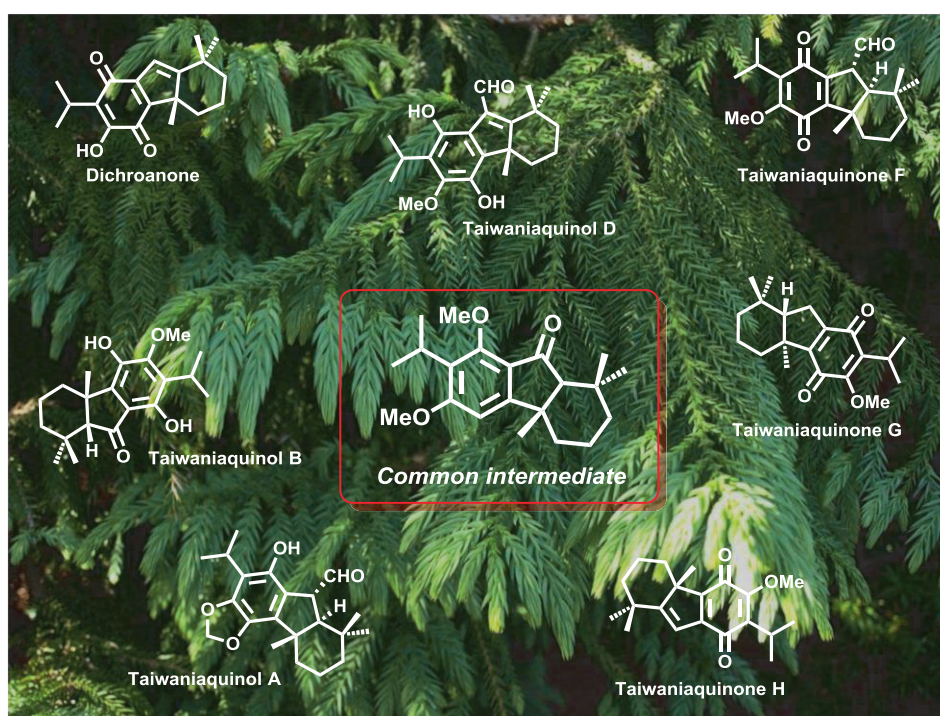
- Wiley-VCH, Weinheim, **2004** (c) *Transition Metals for Organic Synthesis* (Eds. M. Beller, C. Bolm) Wiley-VCH, Weinheim, **2004**. (d) *New Trends in Cross-Coupling: theory and applications*, (Ed. T. Colacot) Royal Society of Chemistry, Cambridge, **2014**
- [6] a) *The Chemistry of Organolithium Compounds* (Eds. Z. Rappoport, I. Marek) WILEY-VCH, Weinheim, **2004**. (b) *Lithium Compounds in Organic Synthesis* (Eds. R. Luisi, V. Capriati) WILEY-VCH: Weinheim, **2014**. (c) V. Snieckus, *Chem. Rev.* **1990**, *90*, 879.
- [7] a) J. Board, J. L. Cosman, T. Rantanen, S. P. Singh, V. Snieckus, *Platinum Metals Rev.* **2013**, *57*, 234. b) E. J. Anctil, V. Snieckus in *Metal Catalyzed Cross-Coupling Reactions*, Vol. 1 (Eds. A. de Meijere, F. Diederich), Wiley-VCH, Weinheim, **2004**, 761.
- [8] D. S. Surry, D. J. Fox, S. J. F. Macdonald, D. R. Spring, *Chem. Commun.* **2005**, 2589.
- [9] a) A. Nagaki, Y. Uesugi, Y. Tomida, J-I. Yoshida, *Beilstein J. Org. Chem.* **2011**, *7*, 1064. For other cross-coupling with organolithium reagents in flow, see: b) A. Nagaki, A. Kenmoku, Y. Moriwaki, A. Hayashi, J-I. Yoshida, *Angew. Chem. Int. Ed.* **2010**, *49*, 7543. c) A. Nagaki, Y. Moriwaki, S. Haraki, A. Kenmoku, N. Takabayashi, A. Hayashi, J-I. Yoshida, *Chem. Asian J.* **2012**, *7*, 1061.
- [10] D. Toummini, F. Ouazzani, M. Taillefer, *Org. Lett.* **2013**, *15*, 4690.
- [11] F. Lu, *Tetrahedron Lett.* **2012**, *53*, 2444.
- [12] S. B. Jhaveri, K. R. Carter, *Chem. Eur. J.* **2008**, *14*, 6845.
- [13] For seminal work: a) S-I. Murahashi, M. Yamamura, K-I. Yanagisawa, N. Mita, K. Kondo, *J. Org. Chem.* **1979**, *44*, 2408. For a highlight, see: b) V. Pace, R. Luisi, *ChemCatChem* **2014**, *6*, 1516. For an application of Murahashi coupling in a polymerisation process, see: c) K. Fuji, S. Tamba, K. Shono, A. Sugie, A. Mori, *J. Am. Chem. Soc.* **2013**, *135*, 12208. For the use of a silicon-based transfer agent, see: d) A. B. Smith III, A. T. Hoye, D. Martinez-Solorio, W-S. Kim, R. Tong, *J. Am. Chem. Soc.* **2012**, *134*, 4533. (e) M. H. Nguyen, A. B. Smith III, *Org. Lett.* **2013**, *15*, 4258. (f) M. H. Nguyen, A. B. Smith III, *Org. Lett.* **2014**, *16*, 2070.
- [14] a) M. Giannerini, M. Fañanás-Mastral, B. L. Feringa, *Nat. Chem.* **2013**, *5*, 667. b) V. Hornillos, M. Giannerini, C. Vila, M. Fañanás-Mastral, B. L. Feringa, *Org. Lett.* **2013**, *15*, 5114. c) M. Giannerini, V. Hornillos, C. Vila, M. Fañanás-Mastral, B. L. Feringa, *Angew. Chem. Int. Ed.* **2013**, *52*, 13329. d) C. Vila, M. Giannerini, V. Hornillos, M. Fañanás-Mastral, B. L. Feringa, *Chem. Sci.* **2014**, *5*, 1361. e) C. Vila, V. Hornillos, M. Giannerini, M. Fañanás-Mastral, B. L. Feringa, *Chem. Eur. J.* **2014**, *20*, 13078. f) V. Hornillos, M. Giannerini, C. Vila, M. Fañanás-Mastral, B. L. Feringa, *Chem. Sci.* **2015**, *6*, 1394. g) L. M. Castelló, V. Hornillos, C. Vila, M. Giannerini, M. Fañanás-Mastral, B. L. Feringa, *Org. Lett.* **2015**, *17*, 62. h) D. Heijnen, V. Hornillos, B. P. Corbet, M. Giannerini, B. L. Feringa, *Org. Lett.* **2015**, *17*, 2662. i) C. Vila, S. Cembellín,

- V. Hornillos, M. Giannerini, M. Fañanás-Mastral, B. L. Feringa, *Chem. Eur. J.* **2015**, *21*, 15520.
- [15] N. Kataoka, Q. Shelby, J. P. Stambuli, J. F. Hartwig, *J. Org. Chem.* **2002**, *67*, 5553.
- [16] a) M. G. Organ, S. Çalimsiz, M. Sayah, K. H. Hoi, A. J. Lough, *Angew. Chem. Int. Ed.* **2009**, *48*, 2383. b) M. Dowlut, D. Mallik, M. G. Organ, *Chem. Eur. J.* **2010**, *15*, 4279 c) S. Çalimsiz, M. Sayah, D. Mallik, M. G. Organ, *Angew. Chem. Int. Ed.* **2010**, *49*, 2014.
- [17] a) C. J. O'Brien, E. A. B. Kantchev, N. Hadei, C. Valente, G. A. Chass, J. C. Nasielski, A. Lough, A. C. Hopkinson, M. G. Organ, *Chem. Eur. J.* **2006**, *12*, 4743. b) M. G. Organ, S. Avola, I. Dubovyk, N. Hadei, E. A. B. Kantchev, C. J. O'Brien, C. Valente, *Chem. Eur. J.* **2006**, *12*, 4749.
- [18] a) Y. Fukuyama, M. Toyota, Y. Asakawa, *J. Chem. Soc., Chem. Commun.* **1988**, 1341. b) Y. Fukuyama, Y. Asakawa, *J. Chem. Soc., Perkin Trans. I* **1991**, 2737. c) Y. Fukuyama, K. Matsumoto, Y. Tono, R. Yokoyama, H. Takahashi, H. Minami, H. Okazaki, Y. Mitsumoto *Tetrahedron*, **2001**, *57*, 7127.
- [19] S. D. Skaper, F. S. Walsh, *Mol. Cell. Neurosci.* **1998**, *12*, 179.
- [20] A. P. Degnan, A. I. Meyers, *J. Am. Chem. Soc.* **1999**, *121*, 2762.
- [21] G. Bringmann, T. Pabst, P. Henschel, J. Kraus, K. Peters, E.-M. Peters, D. S. Rycroft, J. D. Connolly, *J. Am. Chem. Soc.* **2000**, *122*, 9127.
- [22] J. Buter, R. Moezelaar, A. J. Minnaard, *Org. Biomol. Chem.* **2014**, *12*, 5883.
- [23] T. Diao, T. J. Wadzinski, S. S. Stahl, *Chem. Sci.* **2012**, *3*, 887.
- [24] For point-to-axial chirality transfer in binaphthyl systems a) C. A. Broka, *Tetrahedron Lett.* **1991**, *32*, 859. b) R. S. Coleman, E. B. J. Grant, *J. Am. Chem. Soc.* **1994**, *116*, 8795. c) B. H. Lipshutz, L. M. Keith, *Angew. Chem. Int. Ed.* **1999**, *38*, 3530. d) S. Huang, T. B. Peterson, B. Lipshutz, *J. Am. Chem. Soc.* **2010**, *132*, 14021. e) Y. S. Park, C. I. Grove, M. González-López, S. Urgaonkar, J. C. Fettingler, J. T. Shaw, *Angew. Chem. Int. Ed.* **2011**, *50*, 3730.
- [25] a) D. A. Evans, C. J. Dinsmore, P. S. Watson, M. R. Wood, T. I. Richardson, B. W. Trotter, J. L. Katz, *Angew. Chem. Int. Ed.* **1998**, *37*, 2704. b) K. C. Nicolaou, C. N. C. Boddy, *J. Am. Chem. Soc.* **2002**, *124*, 10451. c) M. E. Layton, C. A. Morales, M. D. Shair, *J. Am. Chem. Soc.* **2002**, *124*, 773. d) N. Z. Burns, I. N. Krylova, R. N. Hannoush, P. S. Baran, *J. Am. Chem. Soc.* **2009**, *131*, 9172.
- [26] T. Qin, S. L. Skraba-Joiner, Z. G. Khalil, R. P. Johnson, R. J. Capon, J. A. Porco Jr. *Nat. Chem.* **2015**, *7*, 234.
- [27] G. Bringmann, T. Pabst, S. Busemann, K. Peters, E.-M. Peters, *Tetrahedron*, **1998**, *54*, 1425.
- [28] J. Pospíšil, L. Taimr, *Collect. Czech. Chem. Commun.* **1965**, *30*, 1092.
- [29] X. Huang, K. W. Anderson, D. Zim, L. Jiang, A. Klapars, S. L. Buchwald, *J. Am. Chem. Soc.* **2003**, *125*, 6653.

- [30] The use of the term “flexible steric bulk” was introduced in: G. Altenhoff, R. Goddard, C. W. Lehmann, F. Glorius, *Angew. Chem. Int. Ed.* **2003**, *42*, 3690.
- [31] a) G. Bringmann, T. Pabst, D. S. Rycroft, J. D. Connolly, *Tetrahedron Lett.* **1999**, *40*, 483.
- [32] a) D. Seebach, H. Neumann, *Chem. Ber.* **1974**, *107*, 847. b) E. J. Corey, D. J. Beames, *J. Am. Chem. Soc.* **1972**, *94*, 7210. c) W. F. Bailey, E. R. Punzalan, *J. Org. Chem.* **1990**, *55*, 5404.
- [33] W. Bauer, W. R. Winchester, P. von Ragué Schleyer, *Organometallics* **1987**, *6*, 2371.
- [34] L. S. Mazzaferro, W. Hüttel, A. Fries, M. Müller, *J. Am. Chem. Soc.* **2015**, *137*, 12289.
- [35] For the isolation and structure elucidation of ancistrocladisine see: a) T. R. Govindachari, P. C. Parthasarathy, H. K. Desai, *Indian J. Chem.* **1972**, *10*, 1117. b) T. R. Govindachari, P. C. Parthasarathy, T. G. Rajagopalan, H. K. Desai, K. S. Ramachandran, E. Lee, *J. Chem. Soc. Perkin Trans. 1* **1975**, 2134.
- [36] For the isolation and structure elucidation of rugulotrosin A see: M. Stewart, R. J. Capon, J. M. White, E. Lacey, S. Tennant, J. H. Gill, M. P. Shaddock, *J. Nat. Prod.* **2004**, *67*, 728.
- [37] For the isolation and structure elucidation of phlegmacin B1 see: a) W. Steglich, E. Z. Töpfer-Petersen, *Z. Naturforsch.* **1972**, *27b*, 1286. b) W. Steglich, E. Töpfer-Petersen, I. Pils, *Z. Naturforsch.* **1973**, *28c*, 354. (c) M. Müller, K. Lamottke, W. Steglich, S. Busemann, M. Reichert, G. Bringmann, P. Spiteller, *Eur. J. Org. Chem.* **2004**, 4850.
- [38] For the isolation and structure elucidation of dioncophylline E see: G. Bringmann, K. Messer, K. Wolf, J. Mühlbacher, M. Grüne, R. Brun, A. M. Louis, *Phytochemistry* **2002**, *60*, 389.
- [39] D. Zhang, Q. Wang, *Coord. Chem. Rev.* **2015**, *286*, 1.
- [40] For the isolation and structure elucidation of michellamine see: M. R. Boyd, Y. F. Hallock, J. H. Cardellina II, K. P. Manfredi, J. W. Blunt, J. B. McMahon, R. W. Buckheit, Jr., G. Bringmann, M. Schäffer, G. M. Cragg, D.W. Thomas, J. G. Jato, *J. Med. Chem.* **1994**, *37*, 1740.
- [41] Y. Ikeya, H. Taguchi, I. Yosioka, H. Kobayashi, *Chem. Pharm. Bull.* **1979**, *27*, 2695.
- [42] J. Chang, J. Reiner, J. Xie, *Chem. Rev.* **2005**, *105*, 4581.
- [43] Y. Kiya, J. C. Henderson, G. R. Hutchinson, H. D. Abruña, *J. Mater. Chem.* **2007**, *17*, 4366.
- [44] A. Minato, K. Tamao, K. Suzuki, M. Kumada, *Tetrahedron Lett.* **1980**, *21*, 4017.
- [45] S. Zheng, S. J. Aves, L. Laraia, W. R. J. D. Galloway, K. G. Pike, W. Wu, D. R. Spring, *Chem. Eur. J.* **2012**, *18*, 3193.
- [46] T. Yamato, R. Okabe, Y. Yamada, *J. Chem. Res (S)*, **2003**, 632.

## \*\*\* CHAPTER 7 \*\*\*

### ‡ Towards an Asymmetric Total Synthesis of the Taiwaniaquinoids ‡



**ABSTRACT:** *With the advent of the palladium-catalyzed asymmetric conjugate addition of arylboronic acids to  $\beta$ -substituted cyclic enones, application of the methodology was envisioned within the total synthesis of the taiwaniaquinoid family. Originally isolated from the evergreen coniferous tree, *Taiwania cryptomerioides* Hayata, the taiwaniaquinoids exhibits an unusual [6,5,6]-abeoabietane skeleton. Together with a benzylic quaternary stereocenter the overall molecular architecture of this class of molecules forms a significant synthetic challenge to us. Our approach relied on the asymmetric installation of the quaternary stereocenter on a rarely used substituted cycloheptenone. The synthetic route was continued with an investigation of a domino reaction involving a ring contraction/acylation strategy for direct construction of the [6,5,6]-abeoabietane core structure.*

## 7.1 Introduction

*Taiwania cryptomerioides* Hayata (Cupressaceae) is an evergreen coniferous tree endemic to the central mountains of Taiwan, the south of China and Vietnam. Extensive studies on plant material (leaves, bark, roots and wood) have resulted in the isolation and characterization of a wide range of diterpenes,<sup>[1]</sup> sesquiterpenes,<sup>[2]</sup> lignans<sup>[3]</sup> and biflavones<sup>[4]</sup> and other classes of natural products.<sup>[5]</sup> In 1995, Cheng and co-workers communicated the isolation of five novel diterpenes from the leaves of *T. cryptomerioides*.<sup>[6]</sup> These diterpenes all possessed an unusual [6,5,6]-*abeo*abietane skeleton, which had not been found in nature before. The natural products (Figure 1) were named taiwaniaquinone A, taiwaniaquinone B, and taiwaniaquinone C, as well as taiwaniaquinol A and taiwaniaquinol B. In 1996 the same group reported two more compounds from this class, namely taiwaniaquinone D and taiwaniaquinone E.<sup>[7]</sup> Other natural products containing the [6,5,6]-*abeo*abietane skeleton were found in the roots of *Salvia dichroantha* Stapf (Lamiaceae) by the Yesilada laboratory, who reported the isolation of three novel diterpenes named dichroanal A, dichroanal B, and dichroanone.<sup>[8]</sup> Standishinal, a structurally related compound, was found in *Thuja standishii*, an evergreen tree from the Cupressaceae family.<sup>[9]</sup> The list was extended even further when three more [6,5,6]-*abeo*abietane diterpenes were isolated from the bark of *T. cryptomerioides*.<sup>[10]</sup> These isolates were named taiwaniaquinone F, taiwaniaquinol C, and taiwaniaquinol D. Even with these products added to the taiwaniaquinone family, the search for more continued which led to the isolation of taiwaniaquinone G, taiwaniaquinone H, taiwaniaquinol E, and taiwaniaquinol F, again from bark of *T. cryptomerioides*.<sup>[11]</sup>

Although the taiwaniaquinoid family members are structurally closely related, there are several taiwaniaquinoids isolated which molecular architecture is much more complex. In 1996 the Cheng group isolated five cycloaddition products from taiwaniaquinone A with  $\beta$ -myrcene or *trans*-ozic acid and named them taiwaniadducts A-E.<sup>[7]</sup> Taiwaniadduct A represents the [4+2] cycloaddition product from taiwaniaquinone A and  $\beta$ -myrcene. Taiwaniadducts B and C are regioisomers resulting from the Diels-Alder cycloaddition between taiwaniaquinone A and *trans*-ozic acid, whereas taiwaniadduct D is the result of an ene-reaction of taiwaniadduct B. Lastly, taiwaniadduct E is formed by a [5+2] cycloaddition of taiwaniaquinone A and *trans*-ozic acid. Further studies into this class of cycloadducts from taiwaniaquinoids also led to the isolation of the taiwaniadducts F-I.<sup>[12]</sup> Taiwaniadduct F is the regioisomeric [5+2] adduct of taiwaniadduct E. The latter molecule in an oxidized form, taiwaniadduct G, of which the biosynthetic precursor is taiwaniaquinone C, was also found. Arguably, the most complex taiwaniaquinoid type molecule, although not isolated from the natural source, is taiwaniadduct H. This putative natural product was obtained by bismethylation of taiwaniadduct I, which upon standing for three weeks underwent a [2+2] cycloaddition reaction. Although taiwaniadduct J remains a putative natural product, its occurrence in nature is not unlikely. As a matter of fact, the taiwaniadducts

F-I were isolated from the leaves of *T. cryptomerioides*, and since leaves are harvesters of light, a photochemical cyclization of taiwaniadduct I is not implausible.

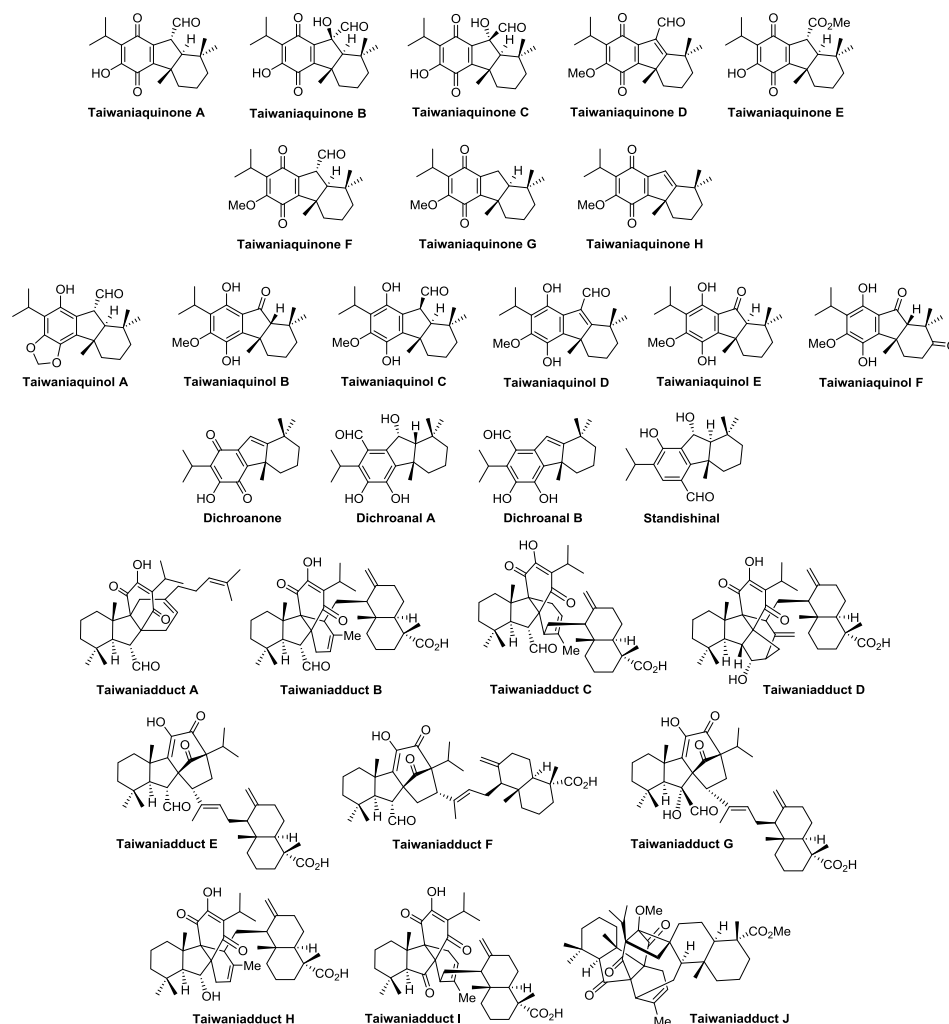


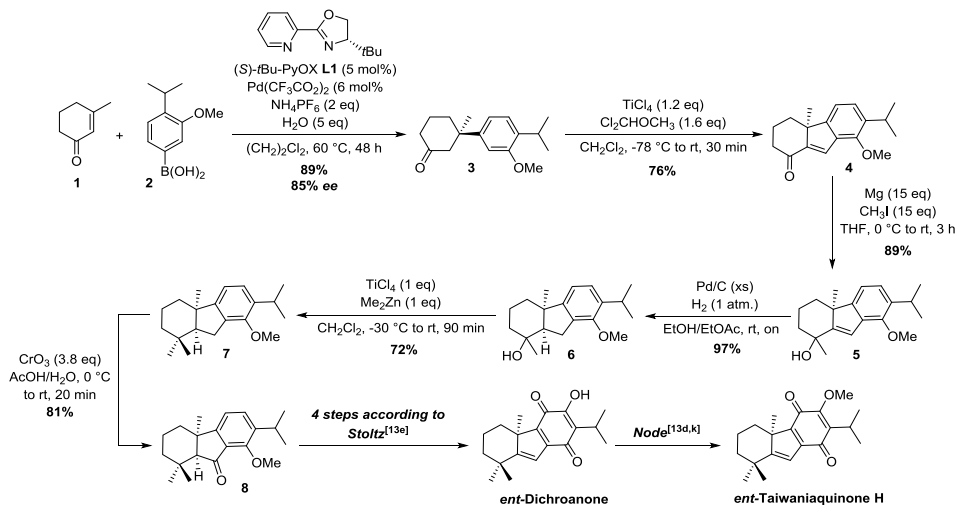
**Figure 1.** The taiwaniaquinoid family members, related compounds and taiwaniadducts A-J.

The taiwaniaquinoids received a lot of attention from the synthetic organic chemistry community and a plethora of racemic and asymmetric total syntheses have been reported.<sup>[13]</sup> As did many research groups, we envisioned the taiwaniaquinoid family a suitable platform to show the utility of in-house developed methodology. Bearing a quaternary stereocenter<sup>[14]</sup> we saw opportunities to use our recently developed Pd-catalyzed asymmetric conjugate addition of arylboronic acids to install this moiety.<sup>[15]</sup> With the recent advances in the palladium-catalyzed asymmetric conjugate addition of

arylboronic acids,<sup>[16]</sup> it is however not surprising that this methodology had already been used in the construction of the taiwaniaquinoids.

## 7.2 Previous total syntheses of the taiwaniaquinoids based on asymmetric conjugate additions

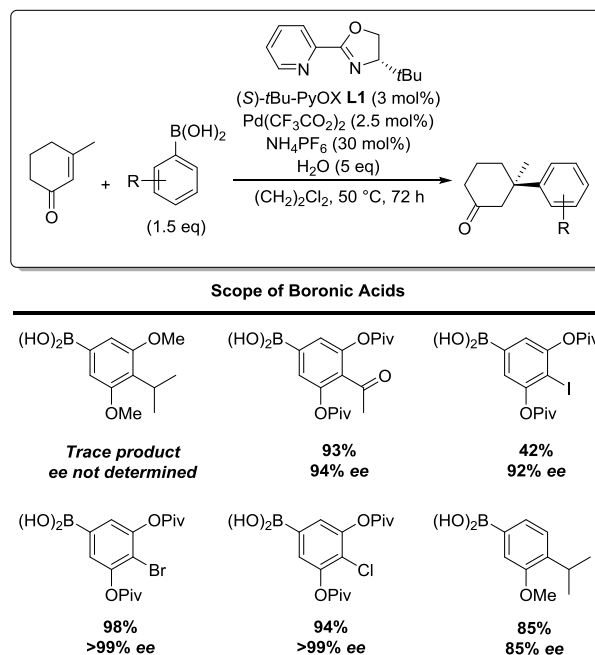
In 2014, the Qin laboratory communicated an asymmetric formal total synthesis of *ent*-dichroanone and consequently *ent*-taiwaniaquinone H (Scheme 1).<sup>[13u]</sup> In their synthesis Qin and co-workers employed the asymmetric Michael addition conditions developed by the Stoltz laboratory.<sup>[16]</sup> Introduction of the benzylic quaternary stereocenter was efficiently achieved in 89% yield, with a very good enantiomeric excess of 85%. The formed Michael adduct **2** lacks an essential carbon which is needed for formation of the B-ring. A Rieche formylation of the aromatic ring in **3** (*para* to the methoxy group), using 1-dichlorodimethyl ether with TiCl<sub>4</sub>, was gratifyingly accompanied by an intramolecular aldol condensation to construct the [6,5,6]-system in 76%. The geminal dimethyl moiety was introduced in a three step sequence starting with a Grignard addition to ketone **4**. Hydrogenation of the double bond afforded subsequently the saturated tertiary alcohol **6**. The second methyl group was introduced using Reetz reagent (Me<sub>2</sub>TiCl<sub>2</sub> generated from TiCl<sub>4</sub>/Me<sub>2</sub>Zn) to furnish **7**. Benzylic oxidation with CrO<sub>3</sub> gave then rise to ketone **8**, a precursor used by the Stoltz lab in their 2006 total synthesis of dichroanone.<sup>[13c]</sup>



**Scheme 1.** Qin's formal asymmetric total synthesis of *ent*-dichroanone and *ent*-taiwaniaquinone H.

Not long after Qin's formal total synthesis, the Stoltz laboratory reported their total synthesis endeavors of the taiwaniaquinoids.<sup>[13i]</sup> In their publication it was reported that the enantiomeric excess of the Michael adduct was depending on the electronic

properties of the *para*-substituent of the arylboronic acid. A small substrate scope (Scheme 2) was investigated and it was found that the highest enantioselectivities were obtained with electron-withdrawing substituents at the *para*-position.



**Scheme 2.** Optimization of the asymmetric conjugate addition for taiwaniaquinoid synthesis.

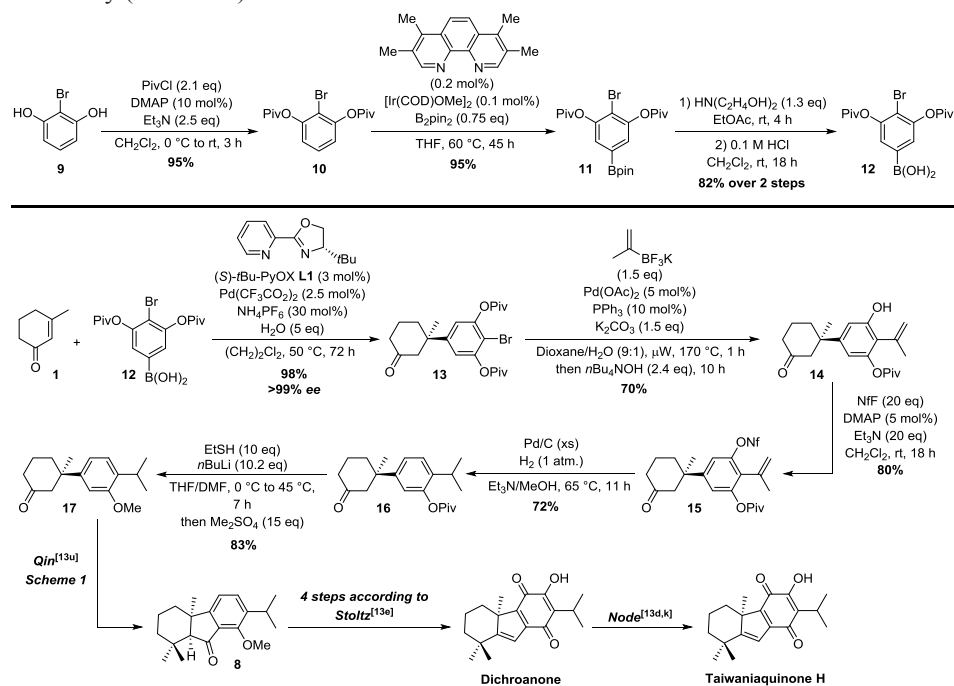
With a substrate scope developed, Stoltz and co-workers decided to use arylboronic acid **12**, with a bromine atom in the *para*-position, in their formal total synthesis as it was shown to give 98% yield with >99% ee in the conjugate addition step (Scheme 3). This was a considerable improvement over the Michael addition reported by the Qin laboratory (*vide supra*), however the substitution pattern in **13** required significant modification to arrive at a suitable precursor for the taiwaniaquinoids.

Installation of the isopropyl functionality proved cumbersome as steric hindrance imposed by the pivaloyl groups impeded reaction of the aryl bromide. The problem was eventually solved by a Molander-Suzuki-Miyaura coupling between potassium isopropenyltrifluoroborate and aryl bromide **13**, under microwave conditions at 170 °C (!). The crude reaction mixture was treated with Bu<sub>4</sub>NOH to furnish isopropenyl phenol **14** in 70% yield. Even with one pivaloyl group removed, formylation under a variety of conditions proved to be fruitless and attention was therefore given to reductive removal of the hydroxy group. Conversion into the nonaflate and subsequent hydrogenation with Pd/C effectively removed the nonaflate and reduced the isopropenyl group to give **16**. Removal of the pivaloyl group followed by methylation furnished **17**, a common



## CHAPTER 7

intermediate to *ent*-dichroanone and *ent*-taiwaniaquinone H as reported by the Qin laboratory (Scheme 1).



**Scheme 3.** A formal total synthesis of dichroanone and taiwaniaquinone H by the Stoltz lab.

The two described syntheses were novel entries to the already rich taiwaniaquinoid total synthesis literature. The report from the Stoltz laboratory is especially interesting as a substrate scope study provided important information with regard to the electronic factors governing enantioselectivity in the asymmetric conjugate addition.<sup>[13t]</sup> As the two syntheses were published concurrent with our own efforts (this chapter) we were pleased to see that the rather obvious asymmetric conjugate addition to 3-methyl cyclohexanone had been undertaken. As illustrated in our synthetic design (*vide infra*) we wanted to conduct a more daunting conjugate addition, introducing the benzylic quaternary stereocenter to a rarely used substituted cycloheptenone.

Thus, in this chapter our effort towards an asymmetric total synthesis of the taiwaniaquinoids is discussed. A thorough investigation of a Pd-catalyzed asymmetric conjugate addition to a rarely used functionalized cycloheptenone was performed. In addition we also studied the steps following the conjugate addition, namely a novel ring contraction/cyclization sequence. Despite our enduring synthetic efforts we did not construct the natural products yet, however, important experimental data has been gathered with respect to the asymmetric conjugate addition and rearrangement/cyclization protocol.

### 7.3 Retrosynthetic, strategic and mechanistic analysis

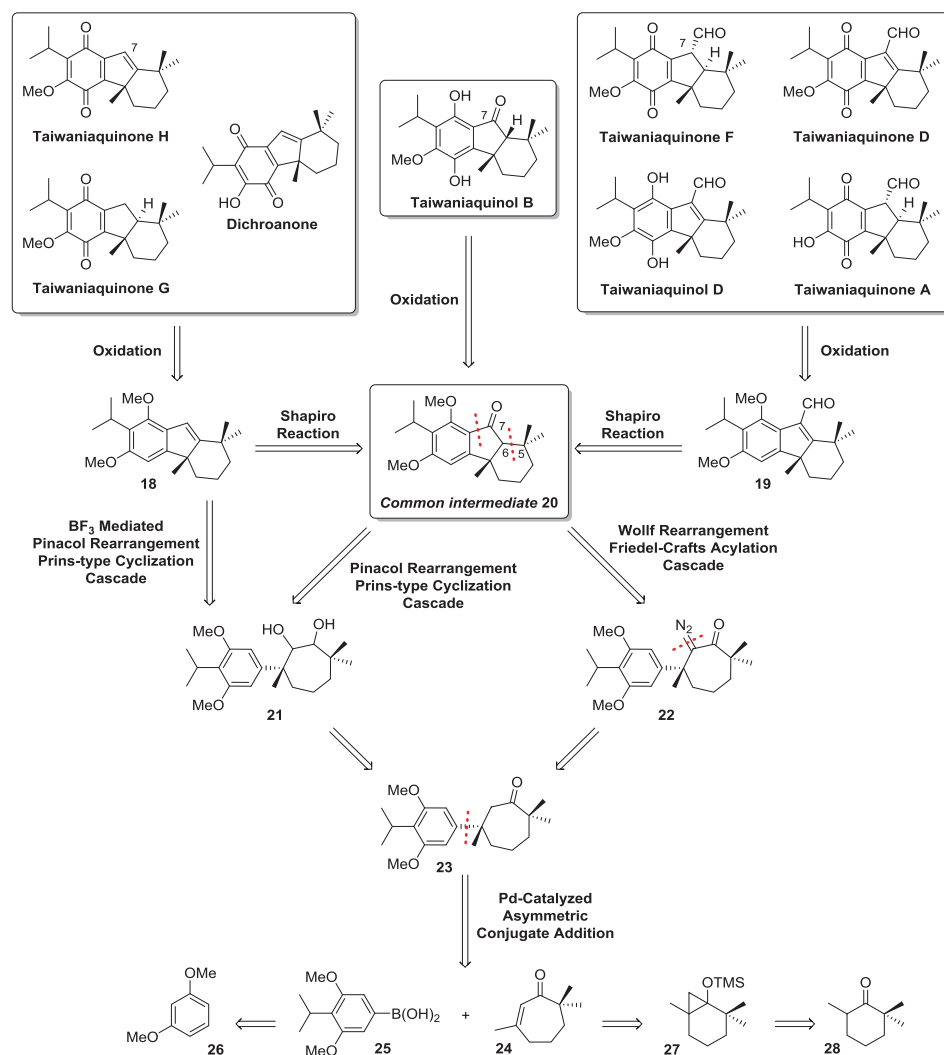
On the outset of our retrosynthetic analysis (Scheme 4) of the taiwaniaquinoid family members we first divided the molecules into three groups; (1) C7 oxidized (taiwaniaquinol B), (2) C7 “reduced” (taiwaniaquinone H and G, and dichroanone), and (3) C7 formylated (taiwaniaquinone A, D, and A, and taiwaniaquinol D). In order to access all the aforementioned taiwaniaquinoids in an efficient manner, divergence was of utmost importance. To address this, we carefully consulted the rich catalogue of taiwaniaquinoid total syntheses.<sup>[13]</sup> From the previous endeavors it was extracted that late stage oxidation was frequently used to construct the taiwaniaquinoids. In search for a suitable reduced form of the natural products we arrived at common intermediate **20**. This molecule is oxidized at C7 in the form of a ketone, which gives straightforward access to taiwaniaquinol B.<sup>[13b]</sup> When, in the forward direction, a Shapiro reaction is performed on ketone **20**, quenching with H<sup>+</sup> or a formylation agent should provide C7 “reduced” molecule **18** and C7 formylated compound **19**, respectively. Both are precursors of their respective natural products.

With the divergence guaranteed, common intermediate **20**, and more specifically the [6,5,6]-abeoabietane skeleton, was examined. In this stage of the synthesis, key disconnections in the carbon framework have to be made, and as the literature shows a diverse arsenal of strategies can be used.<sup>[13]</sup> As our envisioned synthesis was biased by implementation of our in-house developed Pd-catalyzed asymmetric conjugate addition to install the benzylic quaternary stereocenter, we were left with disconnection of the B-C rings (the C7-aryl bond). Combination of this transform with a disconnection of the C5-C6 bond traces back to a functionalized seven-membered ring, either diol **21** or  $\alpha$ -diazo ketone **22**. From a synthetic point of view this means that construction of the [6,5,6]-abeoabietane skeleton involves the ring contraction of the cycloheptanone, followed by an acylation reaction of an intermediary formed species (see scheme 5 for a mechanistic rationale). Such reaction for diol **21** might even lead directly to C7 “reduced” product **18**.

The two retrons, **21** and **22**, are envisioned to be accessible from a common precursor, namely cycloheptenone **23**. In this molecule the retrosynthetic disconnection of the  $\beta$ -benzylic quaternary center is most obvious, providing Michael acceptor **24** and arylboronic acid **25** as suitable precursors. These compounds both have to be synthesized, but are readily traced back to the commercially available starting materials 1,3-dimethoxybenzene **26** and 2,6,6-trimethyl cyclohexanone **28**.

It should be emphasized here, that asymmetric conjugate addition reactions to functionalized cycloheptenones are rare in the literature. However, we intended to walk treacherous paths since science, and the scientist performing the work(!), does not benefit from doing the obvious. Our in-house developed asymmetric Pd-catalyzed conjugate addition to cycloheptenone **24** allows us to assess the utility and potential of the method. In addition, after obtaining Michael adduct **23**, we are faced with the

exciting problem of constructing the [6,5,6]-*abeo*abietane framework via a novel rearrangement/cyclization cascade.

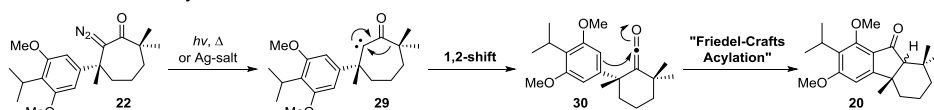


**Scheme 4.** Retrosynthetic analysis of several taiwaniaquinoid family members.

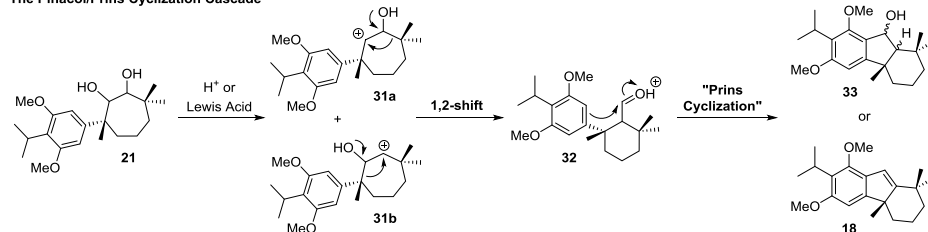
As indicated in the retrosynthetic analysis scheme, the rearrangement of either cycloheptanone **21** or **22** is envisioned to be accompanied by a cyclization event. This particular cascade, simultaneous construction of the A and B ring, is unprecedented within the total synthesis of the taiwaniaquinoids and can therefore be regarded as an intriguing entry to the literature. To achieve the domino reaction, a suitable synthetic strategy had to be designed. Not only do we aim at a facile access to the cascade precursor, but as is inherent to the art of total synthesis, also the right balance between

rigidity and flexibility of the synthetic plan has to be found. This prerequisite is of crucial importance as it allows adaptation to unplanned and unforeseen circumstances which can otherwise lead to dead-ends.<sup>[17]</sup> Extrapolating this philosophy to the cascade reaction, it is desired that multiple rearrangement methodologies can be scrutinized, preferably under a variety of reaction conditions. With this in mind we eventually came up with the three strategies outlined in scheme 5.

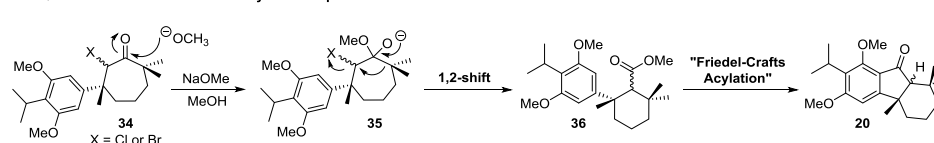
**The Wolff/Friedel-Crafts Acylation Cascade**



**The Pinacol/Prins Cyclization Cascade**



**The Quasi-Favorskii/Friedel-Crafts Acylation Sequence**



**Scheme 5.** A mechanistic rationale for the rearrangement/cyclization sequences.

Our initial idea was to effect the rearrangement/cyclization cascade by constructing  $\alpha$ -diazoketone **22**. Diazoketones can be synthesized in a variety of ways and are well known substrates for the Wolff rearrangement.<sup>[18]</sup> Treatment of an  $\alpha$ -diazoketone with light, heat, a silver salt or other transition metals (though the latter is less common), expels nitrogen from the molecule affording carbene **29**.<sup>[19]</sup> A 1,2-shift, also known as the Wolff rearrangement takes place, contracting the seven-membered ring into a cyclohexane, thereby forming ketene **30**. The ketene, a highly reactive electrophilic intermediate, is then postulated to be trapped in an intramolecular Friedel-Crafts type acylation producing **20**. The trapping of the ketene by the aryl moiety has some literature precedent as in the Fillion total synthesis of some taiwaniaquinoids a ketene intermediate was generated and intramolecularly intercepted by the nucleophilic aryl moiety.<sup>[13b]</sup>

As an alternative to the Wolff rearrangement/Friedel-Crafts acylation cascade we also designed a ring contraction strategy based on a (semi)pinacol rearrangement.<sup>[20,19]</sup> Treatment of diol **21** with a Brønsted or a Lewis acid promotes a dehydration to create

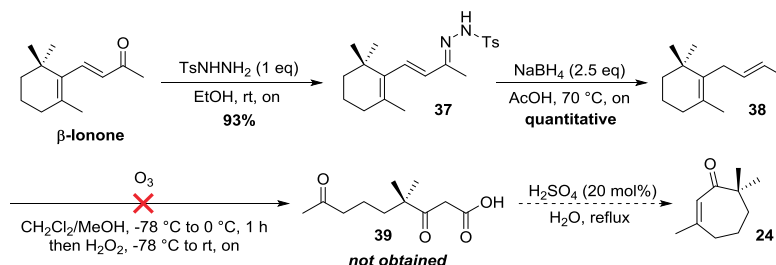
carbocation **31**. Rearrangement of the carbon skeleton to a cyclohexane ring would then provide aldehyde **32**. Due to the presence of an acid in the reaction mixture this aldehyde functionality gets activated, setting it up for a nucleophilic attack of the aromatic ring. Alcohol **33** would be the product from this sequence, but it is very likely that the acidic conditions also give rise to dehydration to give alkene **18**. This however has not been shown in the standishinal total synthesis by Node *et al.* who showed the feasibility of a Prins-type cyclization, with a substrate similar to **32**, without further dehydration taking place.<sup>[13aa]</sup> The cascade might also be used in the form of a semipinacol rearrangement by converting of one of the alcohol functionalities into a good leaving group (*i.e.* OMs), and subsequent Lewis acid or base treatment.

Classical pinacol rearrangements are not frequently used within total synthesis due to problematic regioselective carbocation formation, consequently leading to a mixture of products. An intriguing feature of our synthetic design is that carbocations **31a** and **31b** rearrange to the same product. A drawback of this reaction, however, is that carbocation formation can also give rise to a Wagner-Meerwein rearrangement<sup>[19]</sup> (1,2-methyl shift) instead of a ring contraction.

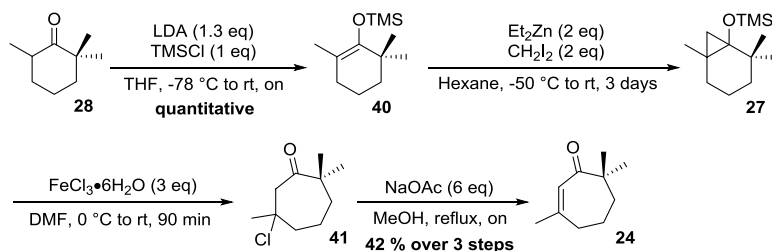
Lastly we also designed a ring contraction via a quasi-Favorskii rearrangement. Nucleophilic attack by methoxide anion on  $\alpha$ -halide ketone **34** produces tetrahedral intermediate **35**. A 1,2-shift expelling a chloride anion from the molecule gives rearranged product **36** bearing a methyl ester function. The reaction stops in this stage but ester activation by a strong acid (*i.e.* polyphosphoric acid = PPA) is proposed to give a Friedel-Crafts acylation to construct the B-ring of the [6,5,6]-*abeo*abietane scaffold.

#### 7.4 Ventures into the asymmetric conjugate addition to cycloheptenone **24**

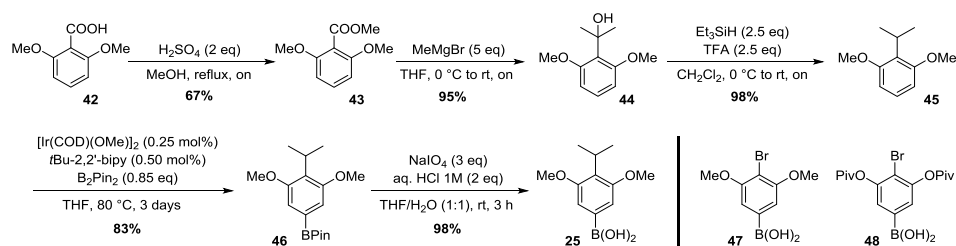
Our initial approach to cycloheptenone **24** started from commercially available, naturally occurring,  $\beta$ -ionone (Scheme 6), as a very early literature report pointed in this direction.<sup>[21]</sup>  $\beta$ -Ionone was reacted with tosylhydrazine to produce hydrazone **37** in 93% yield. Reduction of the tosylhydrozone using NaBH<sub>4</sub> was accompanied by migration of the double bond to furnish alkene **38** in quantitative yield.<sup>[22]</sup> The alkene was subjected to multiple ozonolysis-with-oxidative-work-up attempts,<sup>[23]</sup> however despite extensive efforts we did not obtain carboxylic acid **39** nor it decarboxylated counterpart. The obtained product mixture turned out to be hopelessly complex. We did not investigate it in great detail, but the side products were probably the result of Criegee type rearrangements<sup>[24]</sup> of the intermediate ozonides.

Scheme 6. Attempted synthesis of cycloheptenone **24** from  $\beta$ -ionone.

Our second approach however, based on a report by Chen and co-workers,<sup>[25]</sup> proved to be successful and we obtained cycloheptenone **24** in appreciable amounts (Scheme 7). Starting from 2,6,6-trimethyl cyclohexanone **28**, TMS-enolate **40** was prepared under standard conditions and subjected to a Simmons-Smith cyclopropanation.<sup>[26,19]</sup> The obtained compound **27** was then subjected to a ring-opening reaction with ferric chloride to yield chlorinated cycloheptenone **41**. Chloride elimination using sodium acetate provided the desired cycloheptenone **24**, in 42% yield from TMS-enolate **40**.

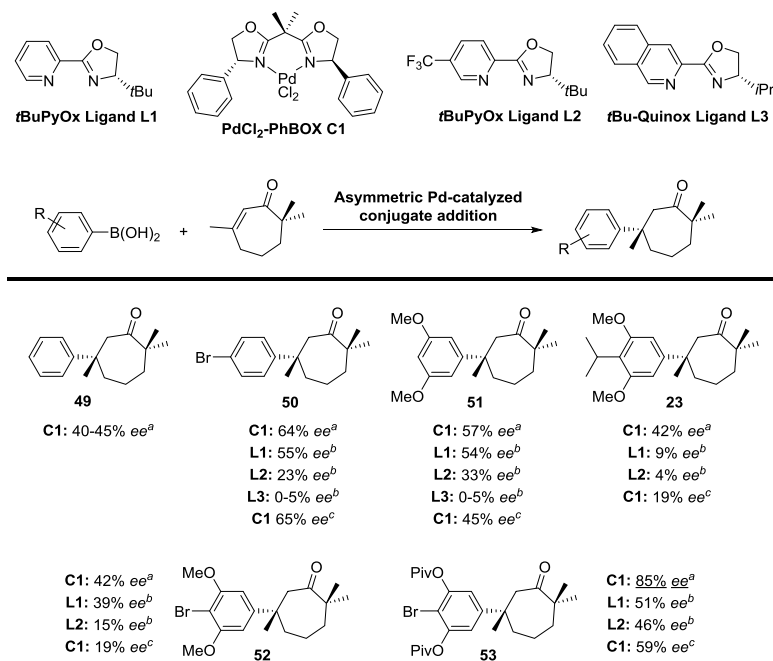
Scheme 7. A successful synthesis of cycloheptenone **24**.

The construction of arylboronic acid **25** was initiated by esterification of benzoic acid **42**. Ester **43** was then subjected to a double Grignard addition to yield benzyl alcohol **44** in 95% yield. Reduction with  $\text{Et}_3\text{SiH}$  and TFA gave isopropyl derivative **45**. An iridium-catalyzed C-H borylation according to Hartwig's procedure,<sup>[27,13n]</sup> provided pinacolboronate **46**. This was smoothly converted into the desired arylboronic acid **25** by  $\text{NaIO}_4$  treatment in acidic THF.<sup>[28]</sup> Using this sequence we also constructed arylboronic acids **47** and **48**.<sup>[13i]</sup>



**Scheme 8.** Synthesis of the arylboronic acid **25**.

With the building blocks in hand, the anticipated Pd-catalyzed asymmetric conjugate addition to cycloheptenone **24** could be investigated (Scheme 9).<sup>[15]</sup> In our screening process we were focused on both stereoselectivity and yield, as conjugate additions to cycloheptenone **24** are non-existent in the literature. Beside our in-house developed asymmetric conjugate addition with PdCl<sub>2</sub>-PhBOX **C1**,<sup>[15]</sup> we also investigated Stoltz conditions<sup>[16]</sup> using *t*BuPyOx ligand **L1**, CF<sub>3</sub>-*t*BuPyOx ligand **L2**, and *t*Bu-Quinox ligand **L3**.

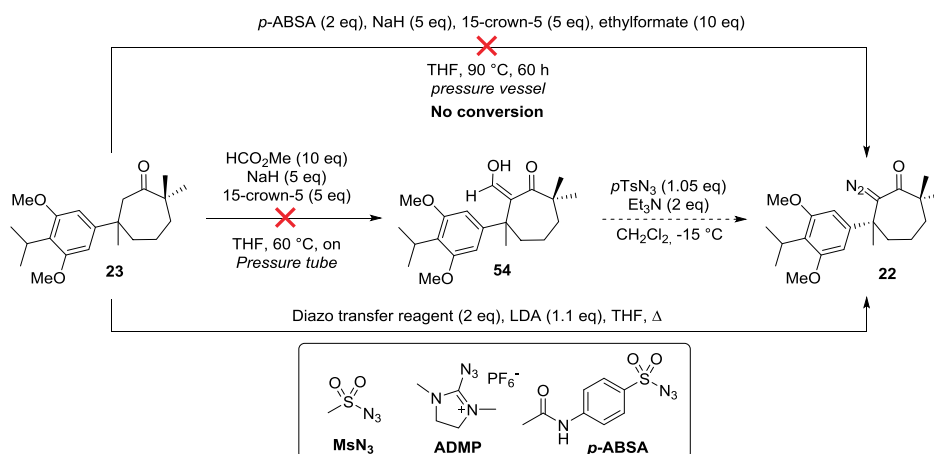


**Scheme 9.** Investigation of the asymmetric conjugate addition to cycloheptenone **24**. <sup>a</sup> enone (1 eq), boronic acid (2 eq), PdCl<sub>2</sub>-PhBOX **C1** (10 mol%), AgSbF<sub>6</sub> (25 mol%), MeOH/H<sub>2</sub>O, 40 °C, overnight. <sup>b</sup> Pd(CF<sub>3</sub>CO<sub>2</sub>)<sub>2</sub> (10 mol%), ligand **L1-L3** (12 mol%), NH<sub>4</sub>PF<sub>6</sub> (0.5 eq), H<sub>2</sub>O (5 eq), enone (1 eq), dichloroethane, 40 °C, overnight. <sup>c</sup> enone (1 eq), boronic acid (2 eq), PdCl<sub>2</sub>-PhBOX **C1** (10 mol%), AgSbF<sub>6</sub> (25 mol%), H<sub>2</sub>O (5 eq), dichloroethane, 40 °C, overnight.

Throughout the screening process we confirmed the observation by Stoltz *et al.*<sup>[13f]</sup> that electron withdrawing arylboronic acids provided the desired products with higher enantioselectivities. We also found that catalyst **C1** gave better results when using MeOH/H<sub>2</sub>O as the reaction medium instead of dichloroethane. Another trend was that catalyst **C1** performed consistently better, in terms of asymmetric induction, than the ligand systems **L1-L3**, of which the Stoltz system<sup>[16]</sup> comprising ligand **L1** performed the best. The use of pivaloyl arylboronic acid **48**<sup>[13f]</sup> in the conjugate addition gave the best enantioselectivity, providing Michael adduct **53** in an appreciable 85% *ee*. The stumble block, however, was that the reaction provided just ~15% of product **53**, as the reaction suffered from protodeboronation of the arylboronic acid. Disappointingly, changing the reaction parameters (stoichiometry, catalyst loading, temperature, addition of oxidants) were all in vain and acceptable isolated yields were not obtained.<sup>[29]</sup> Because of time constraints we decided to shift our attention to the ring contraction/cyclization cascade reaction, of which we were well aware it needed considerable scrutiny.

### 7.5 Investigation into the ring contraction of the cycloheptanone adduct

As we were able to produce significant quantities of racemic Michael adduct **23**, we decided to explore the Wolff rearrangement/Friedel-Crafts acylation cascade. In order to perform this event,  $\alpha$ -diazo ketone **22** had to be constructed (Scheme 10). A classical approach to prepare  $\alpha$ -diazo ketones is by means of a deformylative Regitz diazo transfer.<sup>[19]</sup> Unfortunately, this failed as formylation of **23** proved to be troublesome. Multiple attempts were made but **54** was not detected, even not under pressurized conditions. We postulate that reversibility of the formylation reaction is the problem and therefore we attempted a one-pot formylation/deformylative Regitz diazo transfer. Also this reaction was met with failure and no trace of  $\alpha$ -diazo ketone **22** was observed.

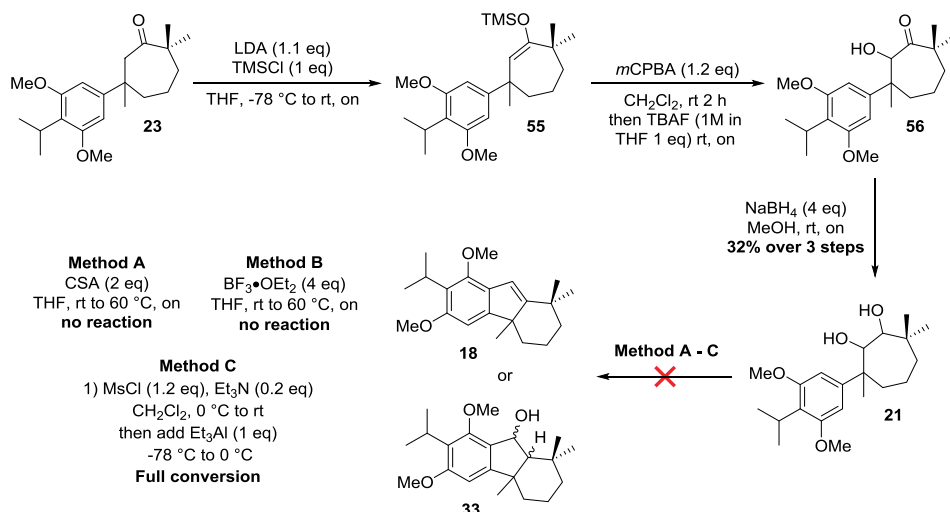


Scheme 10. Synthetic efforts towards the synthesis of  $\alpha$ -diazo ketone **22**.



We also tried to perform the reaction with several diazo transfer reagents without prior formylation.  $\text{MsN}_3$  and ADMP proved to be ineffective, giving no conversion of the starting material. To our delight, traces of  $\alpha$ -diazo ketone **22** were formed with *p*-ABSA but the reaction seemed to grind to a halt in an early stage. Pushing the reaction using more base and *p*-ABSA were fruitless and complete conversion could not be achieved. Additionally we found the reaction to be irreproducible and isolation proved to be problematic, leading us to abandon this approach for the time being.

Concurrent with our efforts to construct  $\alpha$ -diazo ketone **22**, we also investigated the (semi)pinacol rearrangement approach to effect the cascade reaction (Scheme 11). For this, diol **21** had to be constructed which proved to be facile. The formation of TMS-enolate **55** allowed to perform an  $\alpha$ -hydroxylation using a Rubottom oxidation.<sup>[19]</sup> The TMS-enolate was epoxidized with *m*CPBA followed by treatment with TBAF providing  $\alpha$ -hydroxy ketone **56**. The ketone functionality was reduced by the action of  $\text{NaBH}_4$  furnishing diol **21** in 32% over the three steps.



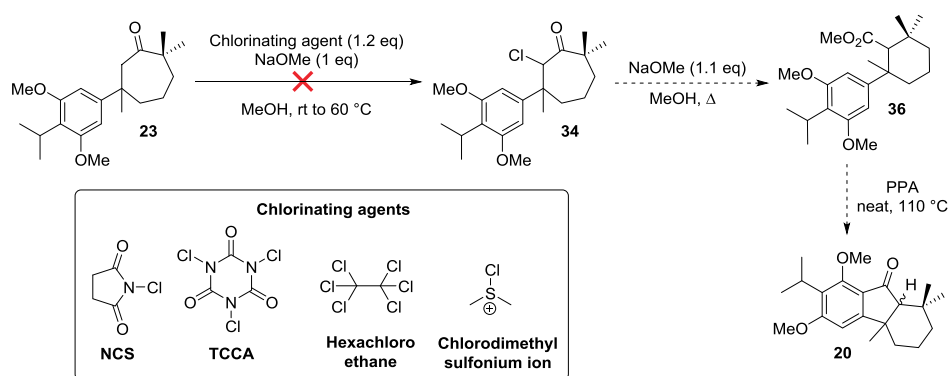
**Scheme 11.** Investigation of the pinacol and semipinacol rearrangement strategy.

At first we tried to initiate a classical pinacol rearrangement by treating diol **21** with camphorsulfonic acid and  $\text{BF}_3 \cdot \text{OEt}_2$  at room temperature. Surprisingly no conversion was observed and diol **21** was re-isolated, a result repeated even when applying elevated temperatures. The impediment of the reaction was unclear and the only obvious candidate is steric hindrance as the hydroxy groups are flanked by sterically congested quaternary carbons. This is contradicted by the fact that mesylation could be achieved, but treatment of the mesylate with  $\text{Et}_3\text{Al}$  provided a complex reaction mixture in which the desired ring contraction product was not detected. A mixture of undesired Wagner-Meerwein shifted isomers was obtained instead.

Yet another way to induce ring contraction is by means of a quasi-Favorskii rearrangement.<sup>[19]</sup> A quasi-Favorskii ring contraction is a modification of the classical

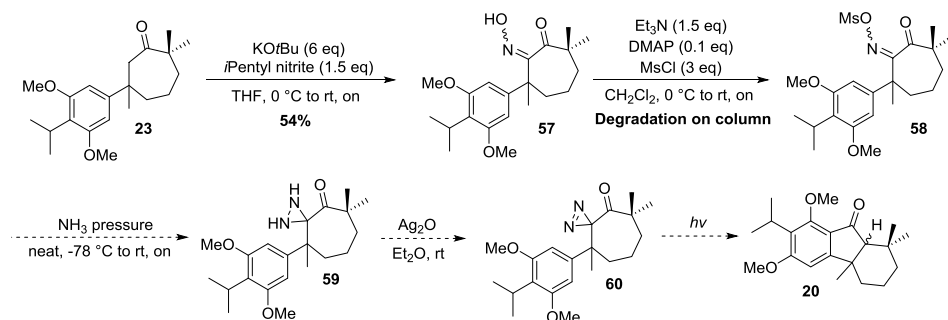
Favorskii reaction in which an  $\alpha$ -halo ketone is deprotonated at the  $\alpha'$ -position, leading to contraction of the ring via an intermediary cyclopropanone. Since our compound does not contain  $\alpha'$ -hydrogens, the ring contraction is induced by direct nucleophilic attack on the carbonyl group as outlined in scheme 5.

The  $\alpha$ -chlorination of ketone **23** was performed under a variety of condition using several chlorinating reagents like *N*-chlorosuccinimide (NCS), trichloroisocyanuric acid (TCCA), hexachloroethane and *in situ* generated chlorodimethyl sulfonium ion (Scheme 12). The base used in the reaction was NaOMe as this reagent can serve both as base and nucleophile to do the deprotonation and nucleophilic attack respectively. Again our efforts proved to be fruitless as no significant conversion was achieved. Again, this disappointing outcome is attributed to severe steric hindrance by the benzylic quaternary center.



**Scheme 12.** Quasi-Favorskii rearrangement strategy toward ketone **20**.

Our final pursuit to perform the ring contraction led us back to our initial attempts to effect a domino reaction via a Wolff rearrangement. Although  $\alpha$ -diazo ketone formation was troublesome, we did come up with an alternative approach, in some way at the cost of the step count of the synthesis. The idea is to synthesize diazirine **60** (Scheme 13) which upon irradiation produces carbene **29** (Scheme 5). The carbene would then undergo Wolff-rearrangement followed by Friedel-Crafts acylation to form [6,5,6]-abeoabietane **20**.



**Scheme 13.** A diazirine-mediated entry to the Wolff rearrangement/Friedel-Crafts cascade.

Due to time constraints we were unable to perform the four step synthesis of diazirine **60** but we did manage to obtain oxime **57** by reaction of ketone **23** with *iso*-pentyl nitrite under basic conditions. The mesylation was performed and did show conversion, although TLC analysis indicated the presence of side products. Flash column chromatography was performed to isolate mesylated oxime **58** but decomposition on the column created an even more complex product mixture. Although the side products were not identified, it is not unlikely that these arise from Beckmann rearrangements/fragmentation type reactions. Up to now this is the status quo.

## 7.6 Conclusions

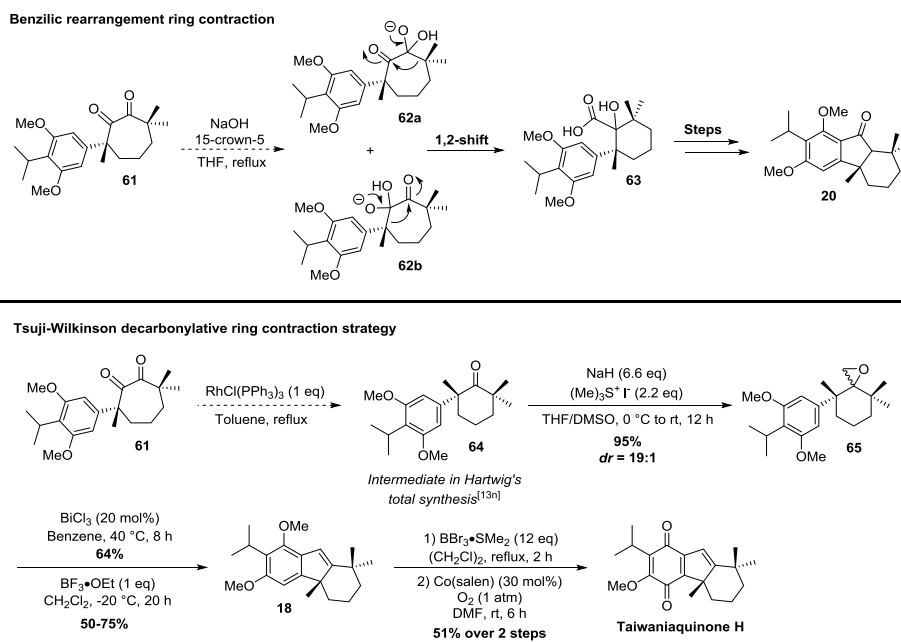
In summary, we have not completed the total synthesis of the taiwaniaquinoid family members, yet! Throughout our synthetic quest we obtained valuable information regarding our synthetic design. The palladium-catalyzed asymmetric conjugate addition of arylboronic acids to cycloheptenone **24** proved to be more challenging than expected although we did manage to construct Michael adduct **53** in 85% *ee*. The isolated yield, however, remained poor and further investigation is needed to solve this problem. It would not violate the strategy (though it would damage our pride) to study this reaction with rhodium catalysis instead of palladium catalysis. Although literature support is as thin as with palladium, it seems that protodeboronation is less of a problem with rhodium catalysts.

Unfortunately we also struggled to perform our anticipated ring contraction as in most cases synthesis of the starting material was troublesome. Despite the many setbacks we are optimistic that we will be able to perform the desired ring contraction. The ring contraction via the diazirine (Scheme 12) deserves further attention as it has the potential to directly form tricyclic ketone **20** according to our initial hypothesis (Scheme 5).

## 7.7 Future prospects and discussion

As discussed, in most cases we did not manage to obtain the substrates necessary for the domino reaction. And when successful, the subsequent domino reaction failed. Therefore, two new routes to effect the ring contraction are presented in scheme 14. We propose one strategy based on a benzylic rearrangement and one on a Tsuji-Wilkinson decarbonylation. Interestingly, both proposed routes start from a common precursor and can therefore be investigated in parallel.

In order to perform the benzylic rearrangement,  $\alpha$ -diketone **61** has to be constructed, planned by oxidation of diol **21** (the substrate in the pinacol rearrangement strategy, *vide supra*). Treatment of the diketone with the hydroxide ion likely leads to nucleophilic attack on either carbonyl functionality. This initiates the benzylic rearrangement which for both intermediates **62a** and **62b** leads to the same product, namely  $\alpha$ -hydroxy acid **63**. Several steps are required to construct subsequently tricyclic ketone **20**, and in particular the removal of the tertiary alcohol makes this route synthetically more laborious and challenging.



Scheme 14. Proposed ring contraction reactions.

An alternative and more attractive route is subjecting  $\alpha$ -diketone **61** to stoichiometric amounts of Wilkinson's catalyst leading to a Tsuji-Wilkinson decarbonylation.<sup>[30]</sup> The extrusion of either carbonyl from the molecule, in the form of CO, results in a ring contraction to furnish ketone **64**. The formed ketone is a substrate which cannot undergo further reaction, thereby stopping in this stage. Interestingly, **64** has been used in the

asymmetric total synthesis of taiwaniaquinone H and taiwaniaquinol B by the Hartwig laboratory, as depicted.<sup>[13n]</sup>

## 7.8 Experimental section

### General remarks:

All reactions were performed using oven-dried glassware under an atmosphere of nitrogen (unless otherwise specified) by standard Schlenk techniques, using dry solvents. Reaction temperature refers to the temperature of the oil bath/cooling bath. Solvents were taken from an MBraun solvent purification system (SPS-800). All other reagents were purchased from Sigma-Aldrich, Acros, TCI Europe or Fluorochem and used without further purification unless noted otherwise.

TLC analysis was performed on Merck silica gel 60/Kieselguhr F254, 0.25 mm. Compounds were visualized using either Seebach's stain (a mixture of phosphomolybdic acid (25 g), cerium (IV) sulfate (7.5 g), H<sub>2</sub>O (500 mL) and H<sub>2</sub>SO<sub>4</sub> (25 mL)), a KMnO<sub>4</sub> stain (K<sub>2</sub>CO<sub>3</sub> (40 g), KMnO<sub>4</sub> (6 g), H<sub>2</sub>O (600 mL) and 10% NaOH (5 mL)), or elemental iodine.

Flash chromatography was performed using SiliCycle silica gel type SiliaFlash P60 (230 – 400 mesh) as obtained from Screening Devices or with automated column chromatography using a Reveleris flash purification system purchased from Grace Davison Discovery Sciences.

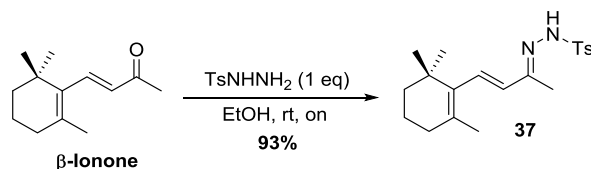
<sup>1</sup>H- and <sup>13</sup>C-NMR spectra were recorded on a Varian AMX400 or a Varian 400-MR (400 and 100.59 MHz, respectively) using CDCl<sub>3</sub> or DMSO-*d*<sub>6</sub> as solvent, unless stated otherwise. Chemical shift values are reported in ppm with the solvent resonance as the internal standard (CDCl<sub>3</sub>: δ 7.26 for <sup>1</sup>H, δ 77.16 for <sup>13</sup>C, MeOH-*d*<sub>4</sub> δ 3.31 for <sup>1</sup>H, δ 49.0 for <sup>13</sup>C). Data are reported as follows: chemical shifts (δ), multiplicity (s = singlet, d = doublet, dd = double doublet, ddd = double double doublet, ddp = double double pentet, td = triple doublet, t = triplet, q = quartet, b = broad, m = multiplet), coupling constants *J* (Hz), and integration.

GC-MS measurements were performed with an HP 6890 series gas chromatography system equipped with a HP 5973 mass sensitive detector. GC measurements were made using a Shimadzu GC 2014 gas chromatograph system bearing an AT5 column (Grace Alltech) and FID detection

Enantiomeric excesses were determined by chiral HPLC analysis using a Shimadzu LC-10ADVP HPLC instrument equipped with a Shimadzu SPD-M10AVP diode-array detector. Integration at three different wavelengths (254, 225, 190 nm) was performed and the reported enantiomeric excess is an average of the three integrations. Retention times are given in min.

High resolution mass spectra (HRMS) were recorded on a Thermo Scientific LTQ Orbitrap XL. Optical rotations were measured on a Schmidt+Haensch polarimeter (Polartronic MH8) with a 10 cm cell (c given in g/mL) at ambient temperature (±23 °C). Melting points were recorded on a Stuart SMP 11 apparatus.

## Experimental procedures and data:

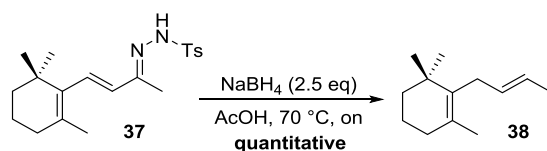
 **$\beta$ -Ionone tosylhydrazone (37):**

$\beta$ -Ionone (67.4 mL, 331.2 mmol) was dissolved in EtOH (125 mL). *p*-Toluenesulfonylhydrazide (61.68 g, 331.2 mmol, 1 eq) was added portion-wise. The solution solidified within 15 min. EtOH (1 L) was added to allow stirring and the solution was stirred overnight. The suspension was filtered and the obtained white solid was dried in a vacuum oven at 80 °C. This yielded  $\beta$ -ionone tosylhydrazone **37** as a white solid (110.5 g, 306.5 mmol, 93% yield).

<sup>1</sup>H-NMR (400 MHz, CDCl<sub>3</sub>)  $\delta$  7.87 (d, *J* = 8.4 Hz, 2H), 7.31 (d, *J* = 8.0 Hz, 2H), 6.50 (d, *J* = 16.6 Hz, 1H), 6.12 (d, *J* = 16.6 Hz, 1H), 2.42 (s, 3H), 2.01 (t, *J* = 6.4 Hz, 2H), 1.92 (s, 3H), 1.66 (d, *J* = 1.0 Hz, 3H), 1.64 – 1.56 (m, 2H), 1.48 – 1.42 (m, 2H), 0.99 (s, 6H).

HRMS (APCI+): Calculated mass [M+H]<sup>+</sup> C<sub>20</sub>H<sub>29</sub>N<sub>2</sub>O<sub>2</sub>S<sup>+</sup> = 361.1950; found: 361.1942.

The analytical data are in agreement with: a) R. O. Hutchins, M. Kacher, L. Rua, *J. Org. Chem.* **1975**, *40*, 923. b) V. P. Miller, D-Y. Yang, T. M. Weigel, O. Han, H-W. Liu, *J. Org. Chem.* **1989**, *54*, 4175.

**(*E*)-2-(but-2-en-1-yl)-1,3,3-trimethylcyclohex-1-ene (38):**

NaBH<sub>4</sub> (10 g, 378 mmol, 2.5 eq) was slowly added to acetic acid (0.5 L) while cooling in an ice bath to maintain the temperature below 40 °C. Subsequently,  $\beta$ -ionone tosylhydrazone **37** (55.5 g, 151 mmol, 1 eq) was added and the suspension was heated to 70 °C. At an oil bath temperature of 62 °C a clear solution was obtained. The solution was stirred for 3 h after which GC-MS showed complete conversion of the starting material. The solution was cooled to rt, subsequently poured over crushed ice, and slowly basified with 8 M NaOH<sub>aq</sub>. The NaOAc was removed by filtration and the product was extracted with pentane. The organic layer was dried over MgSO<sub>4</sub>, filtered and subsequently evaporated. The crude product (**38**) was purified by flash column

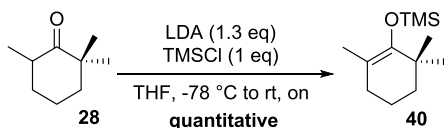
## CHAPTER 7

chromatography (pentane) and was obtained as a mixture of *E:Z* isomers in quantitative yield as a colourless oil.

$^1\text{H-NMR}$  (400 MHz,  $\text{CDCl}_3$ )  $\delta$  5.39 – 5.33 (m, 2H), 2.71 (s, 2H), 1.96 – 1.90 (m, 3H), 1.64 (dp,  $J = 3.2, 1.7$  Hz, 4H), 1.60 – 1.52 (m, 3H), 1.42 (ddd,  $J = 7.6, 4.0, 2.0$  Hz, 2H), 0.97 (s, 3H), 0.97 (s, 3H).

$^{13}\text{C-NMR}$  (101 MHz,  $\text{CDCl}_3$ )  $\delta$  135.48, 130.85, 128.16, 124.50, 40.05, 35.13, 33.05, 31.72, 28.63, 19.95, 19.79, 18.01.

The analytical data are in agreement with: R. O. Hutchins, M. Kacher, L. Rua, *J. Org. Chem.* **1975**, *40*, 923.



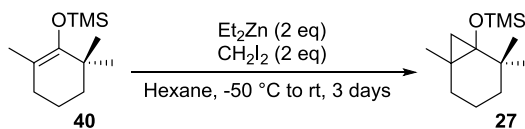
### Trimethyl((2,6,6-trimethylcyclohex-1-en-1-yl)oxy)silane (40):

A dried Schlenk flask purged with nitrogen was charged with dry THF (25 mL) and cooled to  $-78$  °C. Diisopropylamine (3.7 mL, 20 mmol, 1.1 eq) was added, followed by slow addition of *n*BuLi (1.6 M in hexane, 15 mL, 24 mmol, 1.3 eq) over five minutes. The resulting solution was stirred for an additional 20 min at  $-78$  °C. 2,2,6-trimethylcyclohexanone **28** (3.09 g, 18.5 mmol) was dissolved in dry THF (25 mL) and slowly added to the LDA solution at  $-78$  °C. The reaction mixture was stirred for another 30 min at  $-78$  °C and then for 30 min at  $0$  °C by the aid of an ice bath. Trimethylsilyl chloride (2.35 mL, 18.5 mmol, 1 eq) was added slowly, the ice bath was removed and the resulting mixture was stirred at rt. After 19 h, the reaction was quenched with sat. aq.  $\text{NaHCO}_3$  (50 mL) and extracted with pentane (3x 50 mL). The combined organic layer was washed with water (100 mL) and brine (100 mL), dried over  $\text{MgSO}_4$  and concentrated under reduced pressure to afford product **40** as yellow liquid (4.5 g) which was used without further purification.

$^1\text{H-NMR}$  (400 MHz,  $\text{CDCl}_3$ )  $\delta$  1.96 (t,  $J = 6.1$  Hz, 2H), 1.54 (s, 5H), 1.52 – 1.46 (m, 2H), 1.02 (s, 6H), 0.21 (s, 9H).

$^{13}\text{C-NMR}$  (101 MHz,  $\text{CDCl}_3$ )  $\delta$  150.05, 110.38, 40.08, 35.21, 31.68, 27.57, 19.64, 17.84, 1.13.

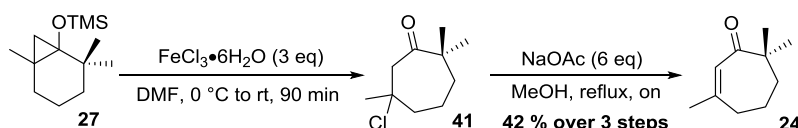
The analytical data are in agreement with: T. Poisson, V. Dalla, F. Marsais, G. Dupas, S. Oudeyer, V. Levacher, *Angew. Chem. Int. Ed.* **2007**, *46*, 7090.

**Trimethyl((2,2,6-trimethylbicyclo[4.1.0]heptan-1-yl)oxy)silane (27):**

A dried Schlenk flask purged with nitrogen was charged with hexane (40 mL) and cooled to  $-60\text{ }^{\circ}\text{C}$ . Neat diethylzinc (3.0 mL, 36.4 mmol, 2 eq) was added slowly followed by addition of TMS enolate **40** (4.1 g, 18.2 mmol) in hexane (5 mL). Methylene iodide (6 mL, 74 mmol, 4 eq) was then added to the mixture at  $-50\text{ }^{\circ}\text{C}$  over 4 h via a syringe pump and the mixture was stirred overnight at  $-50\text{ }^{\circ}\text{C}$ . The mixture was warmed to rt over the course of 4 h. After stirring for 19 h at rt, pyridine (15 mL, 185 mmol, 10 eq) was carefully added at  $0\text{ }^{\circ}\text{C}$ . Then water (150 mL) was added and the mixture was extracted with pentane (2x100 mL) and Et<sub>2</sub>O (100 mL). The combined organic phases were washed with sat. aq. CuSO<sub>4</sub> (200 mL), water (200 mL) and brine (200 mL), dried over MgSO<sub>4</sub> and concentrated. The crude was analyzed by NMR (42% conversion) and the crude was subjected to another cyclopropanation with diethylzinc (1.77 mL, 21.5 mmol) addition at  $-50\text{ }^{\circ}\text{C}$ , and methylene iodide (3.5 mL, 43 mmol) addition at  $-40\text{ }^{\circ}\text{C}$ . After CH<sub>2</sub>I<sub>2</sub> addition the reaction mixture was allowed to warm to  $10\text{ }^{\circ}\text{C}$  and stirred for 3 d. Further work-up was performed as described and crude cyclopropane **27** (8.1 g yellow liquid) was used without further purification.

<sup>1</sup>H-NMR (400 MHz, CDCl<sub>3</sub>)  $\delta$  1.77 – 1.65 (m, 2H), 1.60 – 1.50 (m, 2H), 1.20 – 1.15 (m, 2H), 1.13 (s, 3H), 1.06 (s, 3H), 0.99 (s, 3H), 0.50 (d,  $J = 5.2\text{ Hz}$ , 1H), 0.36 (d,  $J = 5.6\text{ Hz}$ , 1H), 0.14 (s, 9H).

<sup>13</sup>C-NMR (101 MHz, CDCl<sub>3</sub>)  $\delta$  69.04, 37.35, 33.99, 32.22, 28.58, 25.04, 23.64, 22.25, 21.56, 17.76, 2.10.

**3,7,7-trimethylcyclohept-2-en-1-one (24):**

A round bottom flask was charged with crude cyclopropane **27** (3.5 g, 15.5 mmol) in DMF (80 mL). The solution was cooled to  $0\text{ }^{\circ}\text{C}$  and FeCl<sub>3</sub>·6H<sub>2</sub>O (12.7 g, 47 mmol, 3 eq) was added portionwise. After complete addition, the ice bath was removed and the reaction mixture was stirred at rt for 18 h. The solution was then poured into an ice-cold aqueous 1 M HCl solution (150 mL). The aqueous layer was extracted with diethyl ether (3x50 mL) and the combined organic extracts were washed with an aqueous 1 M HCl solution (100 mL), water (100 mL) and brine (100 mL), dried over MgSO<sub>4</sub> and concentrated. The resulting crude chloride **41** was dissolved in MeOH (80 mL) and



## CHAPTER 7

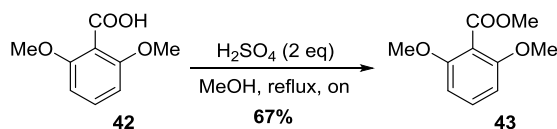
sodium acetate (7.7 g, 93 mmol, 6 eq) was added. The mixture was then refluxed for 22 h. The solvent was evaporated and the residue was taken up in diethyl ether (80 mL) and subsequently washed with an aqueous saturated NaHCO<sub>3</sub> solution (2x 20 mL) and brine (50 mL). The organic phase was dried over MgSO<sub>4</sub> and concentrated. The product was purified by column chromatography (pentane : Et<sub>2</sub>O = 98/2) and product **24** was obtained as pale yellow liquid (1.19 g, 7.80 mmol, 42% yield over 3 steps from **28**).

<sup>1</sup>H-NMR (400 MHz, CDCl<sub>3</sub>) δ 5.82 – 5.76 (m, 1H), 2.27 (t, *J* = 5.9 Hz, 2H), 1.83 (d, *J* = 3.9 Hz, 3H), 1.75 – 1.65 (m, 2H), 1.65 – 1.60 (m, 2H), 1.12 (s, 6H)

<sup>13</sup>C-NMR (101 MHz, CDCl<sub>3</sub>) δ 209.39, 152.15, 127.36, 48.86, 38.04, 38.01, 27.24, 26.69 (2x CH<sub>3</sub>), 22.33.

HRMS (ESI<sup>+</sup>): [M+H]<sup>+</sup> calculated mass C<sub>10</sub>H<sub>17</sub>O<sup>+</sup> = 153.1274, found: 153.1270.

The analytical data are in agreement with: A. Krief, J. L. Laboureur, *J. Chem. Soc., Chem. Commun.* **1986**, 702.



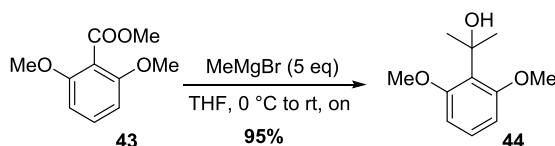
### Methyl 2,6-dimethoxybenzoate (**43**):

2,6-Dimethoxybenzoic acid **42** (7.23 g, 39.7 mmol, 1 eq) was dissolved in methanol (200 mL) and cooled to 0 °C. Concentrated H<sub>2</sub>SO<sub>4</sub> (0.88 mL, 15.9 mmol, 0.4 eq) was added and the resulting mixture was stirred at rt overnight (in the course of the reaction an additional 1.1 eq of conc. H<sub>2</sub>SO<sub>4</sub> was added). The mixture was concentrated under reduced pressure to approximately 50 mL, added to an ice-cold saturated aqueous NaHCO<sub>3</sub> solution (200 mL) and extracted with EtOAc (3x 100 mL). The combined organic extracts were washed with water (200 mL) and brine (200 mL), dried over MgSO<sub>4</sub> and concentrated under reduced pressure to give ester **43** as off-white crystals (5.22 g, 26.6 mmol, 67% yield).

<sup>1</sup>H-NMR (400 MHz, CDCl<sub>3</sub>) δ 7.32 – 7.21 (m, 1H), 6.61 – 6.49 (m, 2H), 3.92 – 3.86 (m, 3H), 3.83 – 3.75 (m, 6H).

<sup>13</sup>C-NMR (101 MHz, CDCl<sub>3</sub>) δ 157.92, 127.68, 124.47, 106.10, 74.20, 56.21, 31.13.

The analytical data are in agreement with: F. Moghaddam, F. Matloubi, M. Mahdi, *Tet. Lett.* **2010**, 51, 540.

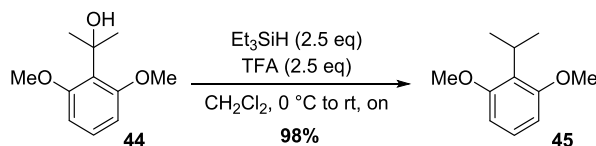
**2-(2,6-Dimethoxyphenyl)propan-2-ol (44):**

A dried Schlenk flask purged with nitrogen was charged with MeMgBr (3 M in THF, 22 mL, 66 mmol, 5 eq) and cooled to 0 °C. Methyl 2,6-dimethoxybenzoate **43** (2.57 g, 13.1 mmol, 1 eq) was dissolved in dry THF (10 mL) and added to the Grignard solution over 10 min. The mixture was allowed to warm to rt and stirred for 17 h. The reaction mixture was then cooled to 0 °C and quenched with saturated aqueous NH<sub>4</sub>Cl (50 mL) and extracted with Et<sub>2</sub>O (3x 75 mL). The combined organic phases were washed with brine (100 mL), dried over MgSO<sub>4</sub> and concentrated under reduced pressure to give alcohol **44** as colorless liquid (2.45 g, 12.5 mmol, 95% yield).

<sup>1</sup>H-NMR (400 MHz, CDCl<sub>3</sub>) δ 7.15 (t, *J* = 8.3 Hz, 1H), 6.61 (d, *J* = 8.4 Hz, 2H), 5.74 (s, 1H), 3.84 (s, 6H), 1.65 (s, 6H).

<sup>13</sup>C-NMR (101 MHz, CDCl<sub>3</sub>) δ 157.92, 127.68, 124.47, 106.10, 74.20, 56.21, 31.13.

The analytical data are in agreement with: Liao, L. M. Stanley, J. F. Hartwig, *J. Am. Chem. Soc.* **2011**, *133*, 2088.

**2-Isopropyl-1,3-dimethoxybenzene (45):**

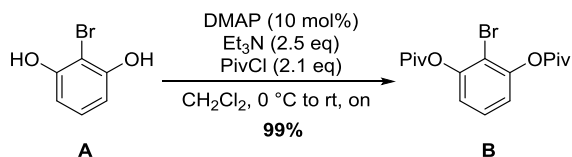
A dried Schlenk flask purged with nitrogen was charged with 2-(2,6-dimethoxyphenyl)propan-2-ol **44** (2.43 g, 12.4 mmol, 1 eq). CH<sub>2</sub>Cl<sub>2</sub> (12 mL) and triethylsilane (5 mL, 31 mmol, 2.5 eq) were then added. The resulting solution was cooled to 0 °C. TFA (2.4 mL, 31 mmol, 2.5 eq) was added dropwise to the cooled solution over 10 min. After complete addition, the reaction mixture was stirred for an additional 30 min at 0 °C and then for 18 h at rt. The solvent was evaporated and the crude product was purified by column chromatography (pentane : Et<sub>2</sub>O = 95/5). Product **45** was obtained in 98% yield as a colorless liquid containing 27 wt.% 1,1,1,3,3,3-hexaethyldisiloxane (3 g, 12 mmol).

<sup>1</sup>H-NMR (400 MHz, CDCl<sub>3</sub>) δ 7.11 (t, *J* = 8.3 Hz, 1H), 6.55 (d, *J* = 8.3 Hz, 2H), 3.81 (s, 6H), 3.62 (p, *J* = 7.1 Hz, 1H), 1.30 (d, *J* = 7.1 Hz, 6H)

<sup>13</sup>C-NMR (101 MHz, CDCl<sub>3</sub>) δ 158.77, 126.62, 124.62, 104.70, 55.87, 24.21, 20.82

## CHAPTER 7

The analytical data are in agreement with: Liao, L. M. Stanley, J. F. Hartwig, *J. Am. Chem. Soc.* **2011**, *133*, 2088.



### 2-Bromo-1,3-phenylene bis(2,2-dimethylpropanoate) (B):

A dried Schlenk flask purged with nitrogen was charged with 2-bromobenzene-1,3-diol **A** (5.00 g, 26.5 mmol, 1 eq) and DMAP (323 mg, 2.65 mmol, 0.1 eq) and dissolved in CH<sub>2</sub>Cl<sub>2</sub> (180 mL). Then, Et<sub>3</sub>N (9.22 mL, 66.1 mmol, 2.5 eq) was added and the resulting solution was cooled to 0 °C using an ice bath. Pivaloyl chloride (6.83 mL, 55.5 mmol, 2.1 eq) was added neat to the ice cold reaction mixture slowly over 2 h using a syringe pump. The mixture was allowed to warm to rt and stirred for another 14 h after complete addition. The reaction was quenched by the addition of a saturated aqueous NH<sub>4</sub>Cl solution (150 mL) and extracted with CH<sub>2</sub>Cl<sub>2</sub> (2x50 mL). The combined organic phases were then washed thoroughly with a saturated aqueous CuSO<sub>4</sub> solution, H<sub>2</sub>O and brine. The organic layers was dried over MgSO<sub>4</sub> and concentrated under reduced pressure to afford pivaloyl ester **B** as an off-white solid (9.41 g, 99% yield).

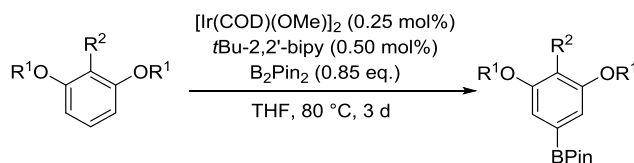
<sup>1</sup>H-NMR (400 MHz, CDCl<sub>3</sub>) δ 7.32 (t, *J* = 8.2 Hz, 1H), 7.00 (d, *J* = 8.2 Hz, 2H), 1.40 (s, 18H).

<sup>13</sup>C-NMR (101 MHz, CDCl<sub>3</sub>) δ 175.77, 149.75, 128.02, 120.83, 111.35, 39.42, 27.28.

HRMS (ESI+): [M+H]<sup>+</sup> calculated for C<sub>16</sub>H<sub>22</sub>BrO<sub>4</sub><sup>+</sup> = 357.0696; found 357.0696.

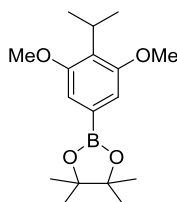
The analytical data are in agreement with: S. E. Shockley, J. C. Holder, B. M. Stoltz, *Org. Lett.* **2014**, *16*, 6362.

### General procedure for the iridium-catalyzed aromatic C-H borylation:



A pressure tube was purged with nitrogen and charged with [Ir(COD)(OMe)]<sub>2</sub> (0.26 mol%), 6,6'-di-tert-butyl-2,2'-bipyridine (0.54 mol%) and bis(pinacolato)diboron (0.85 eq). Dry THF (1.2 mL/mmol) was added and the solids were dissolved at rt. The C-H borylation substrate (1 eq) was added, the pressure vessel was tightly closed and the resulting mixture was stirred at 80 °C for 3 d. The reaction mixture was cooled to rt and

the solvents were evaporated. Water was added and the mixture was extracted three times with Et<sub>2</sub>O. The combined organic layer was washed with water (2x) and brine, dried over MgSO<sub>4</sub> and concentrated under reduced pressure. The crude product was purified as indicated below.



**2-(4-Isopropyl-3,5-dimethoxyphenyl)-4,4,5,5-tetramethyl-1,3,2-dioxaborolane (46):**

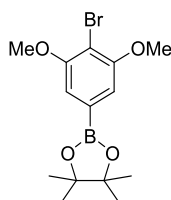
Purified by flash chromatography (pentane : Et<sub>2</sub>O = 9:1). White crystalline solid. (3.15 g, 83%, contains 5 mol% 1,3-dimethoxy-2-isopropyl benzene).

<sup>1</sup>H-NMR (400 MHz, CDCl<sub>3</sub>) δ 6.99 (s, 2H), 3.85 (s, 6H), 3.63 (hept, *J* = 7.1 Hz, 1H), 1.34 (s, 12H), 1.28 (d, *J* = 7.0 Hz, 6H).

<sup>13</sup>C-NMR (101 MHz, CDCl<sub>3</sub>) δ 158.32, 128.24, 120.3, 110.58, 83.84, 55.99, 24.97, 24.43, 20.63.

HRMS (ESI+): [M+H]<sup>+</sup> calculated for C<sub>17</sub>H<sub>28</sub>BO<sub>4</sub><sup>+</sup> = 307.2075; found 307.2074.

The analytical data are in agreement with: Liao, L. M. Stanley, J. F. Hartwig, *J. Am. Chem. Soc.* **2011**, *133*, 2088.



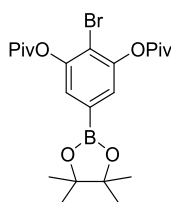
**2-(4-Bromo-3,5-dimethoxyphenyl)-4,4,5,5-tetramethyl-1,3,2-dioxaborolane (C):**

Purified by flash chromatography (pentane : Et<sub>2</sub>O = 9:1). White crystals (3.71 g, 96% yield).

<sup>1</sup>H-NMR (400 MHz, CDCl<sub>3</sub>) δ 6.98 (s, 2H), 3.94 (s, 6H), 1.35 (s, 12H).

<sup>13</sup>C-NMR (101 MHz, CDCl<sub>3</sub>) δ 156.68, 129.16, 110.31, 104.74, 84.15, 56.55, 24.87.

HRMS (ESI+): [M+H]<sup>+</sup> calculated for C<sub>14</sub>H<sub>21</sub>BBro<sub>4</sub><sup>+</sup> = 343.0711; found 343.0709.



**2-Bromo-5-(4,4,5,5-tetramethyl-1,3,2-dioxaborolan-2-yl)-1,3-phenylene bis(2,2-dimethylpropanoate) (D):**

Purified by flash chromatography (pentane : Et<sub>2</sub>O = 95:5). Off-white crystals (3.74 g, 75% yield).

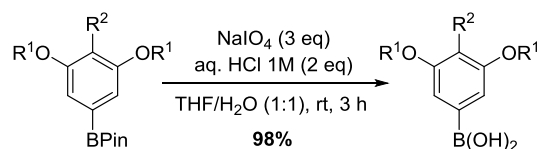
<sup>1</sup>H-NMR (400 MHz, CDCl<sub>3</sub>) δ 7.38 (s, 2H), 1.39 (s, 18H), 1.32 (s, 12H).

<sup>13</sup>C-NMR (101 MHz, CDCl<sub>3</sub>) δ 175.84, 149.40, 129.8, 126.62, 114.96, 84.54, 39.43, 27.34, 24.96.

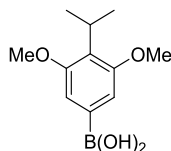
HRMS (ESI+): [M+H<sup>+</sup>] calculated for C<sub>22</sub>H<sub>33</sub>BBro<sub>6</sub><sup>+</sup> = 483.1548; found 483.1542.

The analytical data are in agreement with: S. E. Shockley, J. C. Holder, B. M. Stoltz, *Org. Lett.* **2014**, *16*, 6362.

**General procedure for the synthesis of boronic acids from the corresponding boronic acid pinacol esters:**



A flask was charged with pinacol boronate (1 eq) and THF/H<sub>2</sub>O = 1/1 (4 mL/mmol). NaIO<sub>4</sub> (3 eq) was added in one portion at rt and the reaction mixture was stirred for 15 min. Then an aqueous 1 M HCl solution (2 eq) was added and the solution was stirred at rt. Upon completion of the reaction (monitored by TLC) the solution was concentrated under reduced pressure to approximately half its volume. The resulting suspension was extracted 3 times with EtOAc. The combined organic layer was washed three times with an aqueous 1 M Na<sub>2</sub>S<sub>2</sub>O<sub>3</sub> solution, then with water and brine. The organic phase was dried over MgSO<sub>4</sub> and concentrated to give the product. No further purification was required.



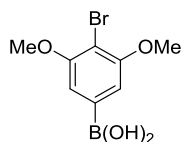
**(4-Isopropyl-3,5-dimethoxyphenyl)boronic acid (25):**

White solid (790 mg, 98% yield).

$^1\text{H-NMR}$  (400 MHz, acetone- $d_6$ )  $\delta$  7.14 (s, 2H), 7.11 (s, 2H), 3.81 (s, 6H), 3.63 (septet,  $J = 7.1$  Hz, 1H), 1.25 (d,  $J = 7.1$  Hz, 6H).

$^{13}\text{C-NMR}$  (101 MHz, acetone- $d_6$ )  $\delta$  158.85, 126.81, 110.91, 55.99, 24.97, 24.43, 20.63.

HRMS (ESI+):  $[\text{M}+\text{H}]^+$  calculated for  $\text{C}_{11}\text{H}_{18}\text{BO}_4^+$  = 223.1136; found 223.1129.



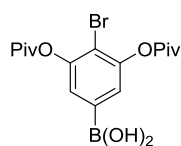
**(4-Bromo-3,5-dimethoxyphenyl)boronic acid (47):**

White solid (237 mg, 98% yield).

$^1\text{H-NMR}$  (400 MHz, DMSO- $d_6$ )  $\delta$  7.10 (s, 2H), 3.81 (s, 6H).

$^{13}\text{C-NMR}$  (101 MHz, DMSO- $d_6$ )  $\delta$  156.32, 130.6, 110.41, 102.55, 56.58.

HRMS (ESI+):  $[\text{M}+\text{H}]^+$  calculated for  $\text{C}_8\text{H}_9\text{BrBO}_4^+$  = 260.9928; found 260.9752.



**(4-Bromo-3,5-bis(pivaloyloxy)phenyl)boronic acid (48):**

Off-white solid (1.74 g, 99% yield)

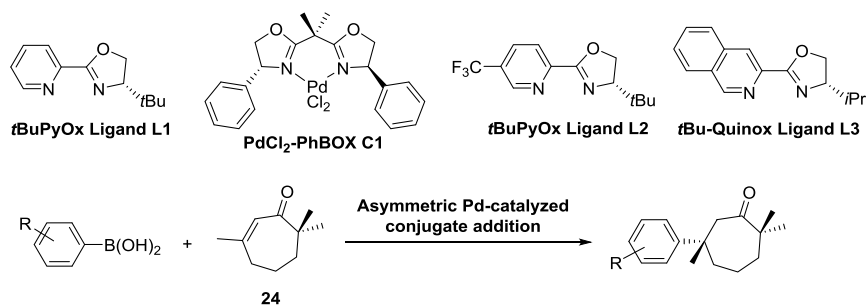
$^1\text{H-NMR}$  (400 MHz, acetone- $d_6$ )  $\delta$  7.53 (s, 2H), 7.50 (s, 2H), 1.40 (s, 18H).

$^{13}\text{C-NMR}$  (101 MHz, acetone- $d_6$ )  $\delta$  176.08, 150.22, 135.8, 127.02, 112.6, 39.86, 27.44.

HRMS (ESI+):  $[\text{M}+\text{H}]^+$  calculated for  $\text{C}_{16}\text{H}_{23}\text{BrBO}_6^+$  = 401.0766; found 401.0723.

## CHAPTER 7

The analytical data are in agreement with: S. E. Shockley, J. C. Holder, B. M. Stoltz, *Org. Lett.* **2014**, *16*, 6362.



### General procedure for the racemic conjugate addition of arylboronic acids to cycloheptenone **24**:

Pd(CF<sub>3</sub>CO<sub>2</sub>)<sub>2</sub> (22 mg, 0.07 mmol, 0.1 eq) and 2,2'-bipyridine (15 mg, 0.1 mmol, 0.15 eq) were suspended in 1 mL of MeOH/H<sub>2</sub>O = 9/1. The mixture was stirred for 20 min at 60 °C and then allowed to cool to rt followed by addition of 3,7,7-trimethylcyclohept-2-en-1-one (100 mg, 0.66 mmol, 1 eq) in 0.5 mL MeOH/ H<sub>2</sub>O = 9/1 and (4-isopropyl-3,5-dimethoxyphenyl)boronic acid (177 mg, 0.79 mmol, 1.2 eq) as solid. The walls of the flask were rinsed with another 0.5 mL MeOH/ H<sub>2</sub>O = 9/1. The resulting mixture was stirred at room temperature for 3 d. The solvents were evaporated and the crude product was filtered over a short silica plug (Et<sub>2</sub>O) and concentrated under reduced pressure. The product was purified by column chromatography.

### General procedure for the Pd(CF<sub>3</sub>CO<sub>2</sub>)<sub>2</sub>/pyridyl-oxazoline/NH<sub>4</sub>PF<sub>6</sub> catalysts:

Pd(CF<sub>3</sub>CO<sub>2</sub>)<sub>2</sub> (10.9 mg, 0.033 mmol, 10 mol%), the ligand **L1-L3** (10.7 mg, 12 mol%) and NH<sub>4</sub>PF<sub>6</sub> (26.8 mg, 0.164 mmol, 0.5 eq) were dissolved in dichloroethane (0.2 mL). 30 μL H<sub>2</sub>O was added and the mixture was stirred at rt for 15 min. Enone **24** (50 mg, 0.33 mmol, 1 eq) was added dissolved in dichloroethane (0.9 mL). The appropriate boronic acid (0.66 mmol, 2 eq) was added as a solid and the mixture was stirred at 40 °C overnight.

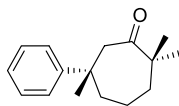
### General procedure for the PdCl<sub>2</sub>/PhBOX/AgSbF<sub>6</sub> catalyst:

Enone **24** (50 mg, 0.33 mmol, 1 eq), the appropriate boronic acid (0.66 mmol, 2 eq), and catalyst **C1** (16.8 mg, 0.033 mmol, 10 mol%) were dissolved in *MeOH* (1.3 mL). AgSbF<sub>6</sub> (28 mg, 0.082 mmol, 25 mol%) was added as a solution in H<sub>2</sub>O (1.3 mL). The mixture was stirred at 40 °C overnight.

or

Enone **24** (50 mg, 0.33 mmol, 1 eq), the appropriate boronic acid (0.66 mmol, 2 eq), catalyst **C1** (16.8 mg, 0.033 mmol, 10 mol%) and AgSbF<sub>6</sub> (28 mg, 0.08 mmol, 25

mol%) were added in a vial. Dichloroethane (1.1 ml) and H<sub>2</sub>O (30 µl, 5 eq) were added. The mixture was stirred at 40 °C overnight.



**C1:** 40-45% ee

**2,2,6-trimethyl-6-phenylcycloheptan-1-one (49):**

The crude product was purified by flash column chromatography eluting with 2% Et<sub>2</sub>O in pentane gradually increasing to 5% Et<sub>2</sub>O in pentane. The product was isolated as a colourless oil (109 mg, 0.47 mmol, 69% yield, 40-45% ee).

<sup>1</sup>H-NMR (400 MHz, CDCl<sub>3</sub>) δ 7.39 (d, *J* = 8.2 Hz, 2H), 7.32 (d, *J* = 7.9 Hz, 2H), 7.20 (t, *J* = 7.2 Hz, 1H), 3.29 (d, *J* = 11.1 Hz, 1H), 2.51 (d, *J* = 11.1 Hz, 1H), 2.11 – 2.01 (m, 1H), 1.82 – 1.68 (m, 4H), 1.65 – 1.51 (m, 1H), 1.26 (s, 3H), 1.13 (d, *J* = 1.2 Hz, 3H), 1.02 (d, *J* = 1.2 Hz, 3H).

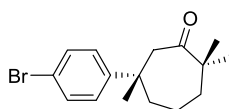
<sup>13</sup>C-NMR (101 MHz, CDCl<sub>3</sub>) δ 216.77, 149.60, 128.43, 126.10, 125.50, 51.63, 47.69, 43.56, 39.97, 39.66, 27.95, 27.63, 24.59, 21.25.

HRMS (ESI<sup>+</sup>): calculated mass [M+H]<sup>+</sup> C<sub>16</sub>H<sub>23</sub>O<sup>+</sup> = 231.1743; found: 231.1739.

Chiral HPLC analysis on a Chiracel OB-H column, *n*-Heptane : *i*-PrOH = 99 : 1, 40 °C, flow = 0.5 mL/min, UV detection at 190 nm, 225 nm and 254 nm, retention times for racemate (min): 12.0 (minor) and 13.9 (major).

Chiral HPLC analysis on a Chiracel OD-H column, *n*-Heptane : *i*-PrOH = 99 : 1, 40 °C, flow = 0.5 mL/min, UV detection at 190 nm, 225 nm and 254 nm, retention times (min): 12.9 (minor) and 14.6 (major).

Chiral HPLC analysis on a Chiracel AS-H column, *n*-Heptane : *i*-PrOH = 99 : 1, 40 °C, flow = 0.5 mL/min, UV detection at 190 nm, 225 nm and 254 nm, retention times (min): 10.8 (minor) and 12.6 (major).



**C1:** 64% ee  
**L1:** 55% ee  
**L2:** 23% ee  
**L3:** 0-5% ee  
**C1:** 65% ee

**2,2,6-trimethyl-6-(4-bromophenyl)-cycloheptan-1-one (50):**

The crude product was purified by flash column chromatography eluting with 10% Et<sub>2</sub>O in pentane. The product was isolated as a colourless oil (71 mg, 0.23 mmol, 35% yield).



## CHAPTER 7

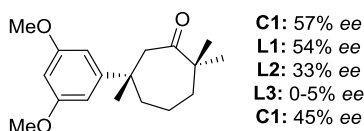
$^1\text{H-NMR}$  (400 MHz,  $\text{CDCl}_3$ )  $\delta$  7.42 (s, 2H), 7.25 (d,  $J = 7.1$  Hz, 2H), 3.20 (d,  $J = 11.2$  Hz, 1H), 2.50 (d,  $J = 11.2$  Hz, 1H), 2.03 (t,  $J = 11.5$  Hz, 1H), 1.80 – 1.64 (m, 4H), 1.64 – 1.50 (m, 1H), 1.22 (s, 3H), 1.11 (s, 3H), 1.00 (s, 3H).

$^{13}\text{C-NMR}$  (101 MHz,  $\text{CDCl}_3$ )  $\delta$  216.16, 148.34, 131.34, 127.43, 119.86, 51.31, 47.57, 43.32, 39.81, 39.47, 27.89, 27.53, 24.77, 21.10.

HRMS (ESI+): calculated mass  $[\text{M}+\text{Na}]^+ \text{C}_{16}\text{H}_{22}\text{BrO}_3^+ = 309.0849$ ; found: 309.0844.

Chiral HPLC analysis on a Chiracel OB-H column, *n*-Heptane : *i*-PrOH = 99 : 1, 40 °C, flow = 0.5 mL/min, UV detection at 190 nm, 225 nm and 254 nm, retention times for racemate (min): 15.3 (minor) and 16.7 (major).

Chiral HPLC analysis on a Chiracel AS-H column, *n*-Heptane : *i*-PrOH = 99 : 1, 40 °C, flow = 0.5 mL/min, UV detection at 190 nm, 225 nm and 254 nm, retention times (min): 14.3 (minor) and 16.1 (major).



### 2,2,6-trimethyl-6-(3,5-dimethoxyphenyl)-cycloheptan-1-one (51):

The crude product was purified by flash column chromatography eluting with 3%  $\text{Et}_2\text{O}$  in pentane gradually increasing to 20%  $\text{Et}_2\text{O}$  in pentane. The product was isolated as a colourless oil (776 mg, 0.48 mmol, 80% yield).

$^1\text{H-NMR}$  (400 MHz,  $\text{CDCl}_3$ )  $\delta$  6.52 (d,  $J = 2.2$  Hz, 2H), 6.32 – 6.27 (m, 1H), 3.77 (s, 6H), 3.22 (d,  $J = 11.3$  Hz, 1H), 2.47 (d,  $J = 11.2$  Hz, 1H), 2.06 – 1.94 (m, 1H), 1.76 – 1.64 (m, 4H), 1.61 – 1.46 (m, 1H), 1.21 (s, 3H), 1.09 (s, 3H), 1.00 (s, 3H).

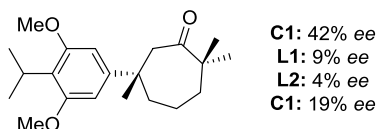
$^{13}\text{C-NMR}$  (101 MHz,  $\text{CDCl}_3$ )  $\delta$  216.49, 160.67, 152.16, 104.25, 97.25, 55.27, 51.46, 47.50, 43.26, 40.10, 39.43, 27.77, 27.59, 24.51, 21.10.

HRMS (ESI+): calculated mass  $[\text{M}+\text{H}]^+ \text{C}_{18}\text{H}_{27}\text{O}_3^+ = 291.1955$ ; found: 291.1953.

Chiral HPLC analysis on a Chiracel OB-H column, *n*-Heptane : *i*-PrOH = 99 : 1, 40 °C, flow = 0.5 mL/min, UV detection at 190 nm, 225 nm and 254 nm, retention times for racemate (min): 24.2 (minor) and 29.5 (major).

Chiral HPLC analysis on a Chiracel OD-H column, *n*-Heptane : *i*-PrOH = 99 : 1, 40 °C, flow = 0.5 mL/min, UV detection at 190 nm, 225 nm and 254 nm, retention times (min): 25.8 (minor) and 33.9 (major).

Chiral HPLC analysis on a Chiracel AS-H column, *n*-Heptane : *i*-PrOH = 99 : 1, 40 °C, flow = 0.5 mL/min, UV detection at 190 nm, 225 nm and 254 nm, retention times (min): 23.5 (minor) and 28.7 (major).



**6-(4-Isopropyl-3,5-dimethoxyphenyl)-2,2,6-trimethylcycloheptan-1-one (23):**

Purification by flash column chromatography (pentane : Et<sub>2</sub>O = 97:3) provided 6-(4-isopropyl-3,5-dimethoxyphenyl)-2,2,6-trimethylcycloheptan-1-one **23** as colorless oil (165 mg, 75% yield).

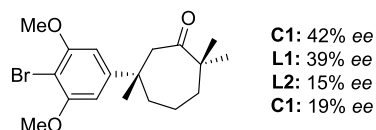
<sup>1</sup>H-NMR (400 MHz, CDCl<sub>3</sub>) δ 6.55 (s, 2H), 3.80 (s, 6H), 3.52 (td, *J* = 14.6, 14.2, 7.8 Hz, 1H), 3.23 (d, *J* = 11.3 Hz, 1H), 2.52 (d, *J* = 11.3 Hz, 1H), 2.04 (t, *J* = 11.5 Hz, 1H), 1.80–1.71 (m, 4H), 1.64 – 1.56 (m, 1H), 1.24 (d, *J* = 4.2 Hz, 6H), 1.13 (s, 3H), 1.03 (s, 3H).

<sup>13</sup>C-NMR (101 MHz, CDCl<sub>3</sub>) δ 216.99, 158.41, 148.54, 122.51, 102.55, 56.08, 51.90, 47.64, 43.48, 40.18, 39.61, 27.94, 27.55, 24.70, 24.10, 21.21, 20.95.

HRMS (ESI+): [M+H]<sup>+</sup> calculated for C<sub>21</sub>H<sub>33</sub>O<sub>3</sub><sup>+</sup> = 333.2424; found 333.2423.

Chiral HPLC analysis on a Chiracel LUX5u Cellulose column, *n*-Heptane : *i*-PrOH = 99.5 : 0.5, 40 °C, flow = 0.5 mL/min, UV detection at 190 nm, 225 nm and 254 nm, retention times (min): 9.9 (minor) and 11.9 (major).

Chiral HPLC analysis on a Chiracel OD-H column, *n*-Heptane : *i*-PrOH = 99 : 1, 40 °C, flow = 0.5 mL/min, UV detection at 190 nm, 225 nm and 254 nm, retention times (min): 10.0 (minor) and 12.2 (major).



**6-(4-Bromo-3,5-dimethoxyphenyl)-2,2,6-trimethylcycloheptan-1-one (52):**

The crude product was purified by column chromatography (pentane : Et<sub>2</sub>O = 9/1) and obtained as white solid (55 mg, 25% yield).

<sup>1</sup>H-NMR (400 MHz, CDCl<sub>3</sub>) δ 6.59 (s, 2H), 3.88 (s, 6H), 3.17 (d, *J* = 11.4 Hz, 1H), 2.57 (d, *J* = 11.5 Hz, 1H), 2.14 (s, 3H), 2.11 – 2.01 (m, 1H), 1.74 (h, *J* = 7.6 Hz, 4H), 1.64 – 1.56 (m, 1H), 1.10 (s, 3H), 0.98 (s, 3H).

## CHAPTER 7

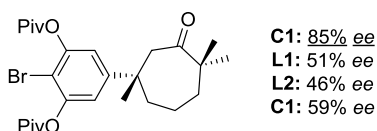
$^{13}\text{C}$ -NMR (101 MHz,  $\text{CDCl}_3$ )  $\delta$  216.59, 156.87, 150.32, 102.84, 98.71, 56.59, 51.90, 47.59, 43.34, 40.60, 39.45, 28.58, 27.37, 25.31, 21.16.

HRMS (ESI+):  $[\text{M}+\text{H}]^+$  calculated for  $\text{C}_{18}\text{H}_{25}\text{BrO}_3^+ = 369.1060$ ; found 369.1054.

Chiral HPLC analysis on a Chiracel OB-H column, *n*-Heptane : *i*-PrOH = 98 : 2, 40 °C, flow = 0.5 mL/min, UV detection at 190 nm, 225 nm and 254 nm, retention times (min): 29.0 (minor) and 32.3 (major).

Chiral HPLC analysis on a Chiracel OD-H column, *n*-Heptane : *i*-PrOH = 98 : 2, 40 °C, flow = 0.5 mL/min, UV detection at 190 nm, 225 nm and 254 nm, retention times (min): 29.0 (minor) and 32.6 (major).

Chiral HPLC analysis on a Chiracel AD-H column, *n*-Heptane : *i*-PrOH = 98 : 2, 40 °C, flow = 0.5 mL/min, UV detection at 190 nm, 225 nm and 254 nm, retention times (min): 28.7 (minor) and 32.0 (major).



### 2-Bromo-5-(1,4,4-trimethyl-3-oxocycloheptyl)-1,3-phenylenebis(2,2-dimethylpropanoate) (53):

The crude product was purified by column chromatography (pentane :  $\text{Et}_2\text{O}$  = 9/1) and obtained as white solid (8% yield).

$^1\text{H}$ -NMR (400 MHz,  $\text{CDCl}_3$ )  $\delta$  1.96 (t,  $J$  = 6.1 Hz, 2H), 1.54 (s, 5H), 1.52 – 1.46 (m, 2H), 1.02 (s, 6H), 0.21 (s, 9H).

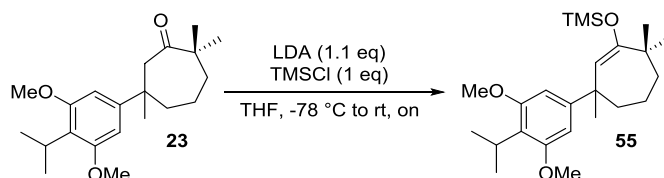
$^{13}\text{C}$ -NMR (101 MHz,  $\text{CDCl}_3$ )  $\delta$  150.05, 110.38, 40.08, 35.21, 31.68, 27.57, 19.64, 17.84, 1.13.

HRMS (ESI+): calculated for  $[\text{M}+\text{H}]^+ \text{C}_{26}\text{H}_{38}\text{BrO}_5^+ = 509.1897$ ; found 509.1887.

Chiral HPLC analysis on a Chiracel OB-H column, *n*-Heptane : *i*-PrOH = 98 : 2, 40 °C, flow = 0.5 mL/min, UV detection at 190 nm, 225 nm and 254 nm, retention times for racemate (min): 10.8 (minor) and 11.9 (major).

Chiral HPLC analysis on a Chiracel OD-H column, *n*-Heptane : *i*-PrOH = 98 : 2, 40 °C, flow = 0.5 mL/min, UV detection at 190 nm, 225 nm and 254 nm, retention times (min): 10.9 (minor) and 12.1 (major).

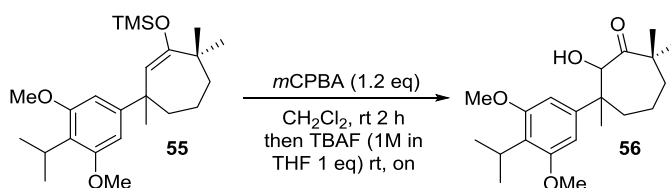
Chiral HPLC analysis on a Chiralcel AD-H column, *n*-Heptane : *i*-PrOH = 98 : 2, 40 °C, flow = 0.5 mL/min, UV detection at 190 nm, 225 nm and 254 nm, retention times (min): 10.9 (minor) and 12.0 (major).



**((3-(4-isopropyl-3,5-dimethoxyphenyl)-3,7,7-trimethylcyclohept-1-en-1-yl)oxy)trimethylsilane (55):**

A dried Schlenk flask purged with nitrogen was charged with dry THF (1.5 mL) and diisopropylamine (84  $\mu$ L, 0.6 mmol, 1.3 eq) and cooled to -78 °C. *n*BuLi 1.6 M in hexane (0.34 mL, 0.55 mmol, 1.2 eq) was added and the solution was stirred for an additional 15 min. 6-(4-Isopropyl-3,5-dimethoxyphenyl)-2,2,6-trimethylcycloheptan-1-one **23** (166 mg, 0.46 mmol, 1 eq) in dry THF (1 mL) was added dropwise at -78 °C. The reaction mixture was stirred for 30 min at -78 °C and for 15 min at 0 °C. Trimethylsilyl chloride (63  $\mu$ L, 0.5 mmol, 1 eq) was added and the reaction mixture was stirred for 18 h at rt. A saturated aqueous NaHCO<sub>3</sub> solution (15 mL) was added, the aqueous phase was extracted with Et<sub>2</sub>O (3x10 mL) and the combined organic phases were washed with brine (30 mL), dried over MgSO<sub>4</sub> and concentrated under reduced pressure. TMS-enol ether **55** was obtained as colorless thick oil (181 mg) and used without further purification.

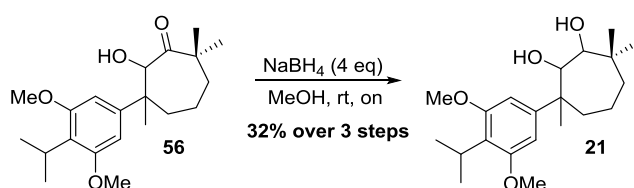
Crude <sup>1</sup>H-NMR (400 MHz, CDCl<sub>3</sub>)  $\delta$  6.58 (s, 2H), 4.87 (s, 1H), 3.78 (s, 6H), 3.63 – 3.50 (m, 1H), 2.15 – 2.06 (m, 1H), 1.98 – 1.90 (m, 1H), 1.84 – 1.73 (m, 2H), 1.61 – 1.54 (m, 2H), 1.29 (d, *J* = 7.5 Hz, 6H), 1.14 (s, 3H), 1.10 (s, 3H), 1.02 (s, 3H), 0.27 (s, 9H).



**7-hydroxy-6-(4-isopropyl-3,5-dimethoxyphenyl)-2,2,6-trimethylcycloheptan-1-one (56):**

A dried Schlenk flask purged with nitrogen was charged with *m*CPBA (77 mg, 0.46 mmol, 1 eq) and dissolved in dry CH<sub>2</sub>Cl<sub>2</sub> (2 mL). The solution was cooled to 0 °C. Crude **55** was dissolved in dry CH<sub>2</sub>Cl<sub>2</sub> (2 mL) in a separate flask and added to the cooled *m*CPBA solution. The flask was rinsed with an additional 0.5 mL dry CH<sub>2</sub>Cl<sub>2</sub>. After complete addition the icebath was removed and the mixture was stirred at rt for 2

h. Water (10 mL) was added and extracted with Et<sub>2</sub>O (3x10 mL). The combined organic extracts were washed with an aqueous 1 M NaOH solution (2x25 mL) and brine (25 mL), dried over MgSO<sub>4</sub> and concentrated under reduced pressure. The crude epoxide/ $\alpha$ -hydroxy ketone mixture (171 mg) was then dissolved in THF (4 mL) and TBAF (1 M in THF, 0.37 mL, 0.37 mmol, 0.8 eq) was added at rt. The mixture was stirred for 17 h. The solvent was evaporated, water (10 mL) was added and the aqueous phase was extracted with Et<sub>2</sub>O (3x10 mL). The combined organic layer was washed with water (25 mL) and brine (25 mL), dried over MgSO<sub>4</sub> and concentrated under reduced pressure to give the crude  $\alpha$ -hydroxy ketone **56** as an orange oil (170 mg), which was used without further purification.



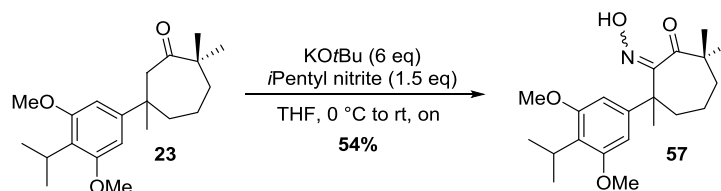
**3-(4-isopropyl-3,5-dimethoxyphenyl)-3,7,7-trimethylcycloheptane-1,2-diol (21):**

The crude  $\alpha$ -hydroxy ketone **56** was dissolved in methanol (4 mL) and NaBH<sub>4</sub> (56 mg, 1.5 mmol, excess) was added as a solid in four portions and the resulting solution was stirred for 19 h at rt. Water (10 mL) was added and the aqueous layer was extracted with EtOAc (3x10 mL). The combined organic extracts were washed with water (30 mL) and brine (30 mL), dried over MgSO<sub>4</sub> and concentrated under reduced pressure to give the crude diol **51** which was purified by column chromatography (pentane : Et<sub>2</sub>O = 8/2). The product was obtained as a white solid (54 mg, 0.146 mmol, 32% over 3 steps). The product obtained was a mixture of diastereoisomers.

<sup>1</sup>H-NMR (400 MHz, CDCl<sub>3</sub>)  $\delta$  6.59 (s, 2H), 4.26 (s, 1H), 3.79 (s, 6H), 3.53 – 3.44 (m, 2H), 2.18 – 2.08 (m, 1H), 1.91 – 1.82 (m, 1H), 1.77 – 1.57 (m, 4H), 1.36 (s, 3H), 1.27 (d,  $J = 7.2$  Hz, 6H), 1.07 (s, 3H), 0.95 (s, 3H).

<sup>13</sup>C-NMR (101 MHz, CDCl<sub>3</sub>)  $\delta$  158.57, 147.14, 122.52, 102.97, 80.79, 80.60, 56.05, 45.58, 37.36, 35.22, 30.45, 28.34, 27.92, 26.76, 24.10, 20.69.

IR (film):  $\nu$  3479, 2954, 2871, 2320, 1608, 1574, 1468, 1411, 1361, 1250, 1141, 1123, 1056, 835 cm<sup>-1</sup>.



**7-(hydroxyimino)-6-(4-isopropyl-3,5-dimethoxyphenyl)-2,2,6-trimethylcycloheptan-1-one (57):**

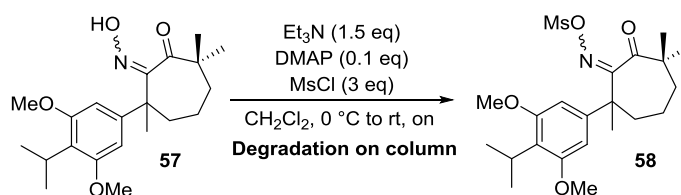
A dried Schlenk flask purged with nitrogen was charged with KO $t$ Bu (1 M in THF, 6 mL, 6 mmol, 6 eq). The solution was cooled to 0 °C. In a separate flask, ketone **23** (333 mg, 1 mmol, 1 eq) and amyl nitrite (0.2 mL, 1.5 mmol, 1.5 eq) were dissolved in dry THF (10 mL) and added to the cooled KO $t$ Bu solution dropwise over 10 min. The resulting mixture was stirred for another 10 min at 0 °C and then for 21 h at rt. The reaction was quenched by addition of a saturated aqueous NH $_4$ Cl solution (25 mL). The aqueous phase was extracted with Et $_2$ O (3x 20 mL) and the combined organic extracts were washed with water (40 mL) and brine (40 mL), dried over MgSO $_4$  and concentrated under reduced pressure. The product was purified by flash chromatography (pentane : Et $_2$ O = 8/2) and oxime **57** was obtained as an off-white solid (197 mg, 0.54 mmol, 54% yield).

$^1$ H-NMR (400 MHz, CDCl $_3$ )  $\delta$  8.28 (br s, 1H), 6.58 (s, 2H), 3.79 (s, 6H), 3.51 (hept,  $J$  = 6.9 Hz, 1H), 1.93 – 1.76 (m, 5H), 1.60 (s, 3H), 1.58 – 1.52 (m, 1H), 1.27 – 1.21 (m, 9H), 1.14 (s, 3H).

$^{13}$ C-NMR (101 MHz, CDCl $_3$ )  $\delta$  211.30, 166.35, 158.35, 145.35, 122.75, 103.24, 77.48, 76.84, 55.96, 45.98, 45.05, 39.21, 37.37, 25.95, 25.48, 24.06, 23.06, 20.84, 20.39.

IR (film):  $\nu$  3317, 2924, 2854, 1704, 1606, 1576, 1456, 1415, 1377, 1249, 1138, 1111, 1055, 947, 735 cm $^{-1}$ .

HRMS (ESI $^+$ ): calculated for [M+H] $^+$  C $_{21}$ H $_{32}$ NO $_4$  $^+$  = 362.2326; found 362.2323.



**6-(4-isopropyl-3,5-dimethoxyphenyl)-2,2,6-trimethyl-7-(((methylsulfonyl)oxy)imino)cycloheptan-1-one (58):**

Oxime **57** (144.6 mg, 0.4 mmol), triethylamine (84  $\mu$ L, 0.6 mmol, 1.5 eq), DMAP (5 mg, 0.04 mmol, 10 mol%) and mesyl chloride (93  $\mu$ L, 1.2 mmol, 3 eq) were dissolved

in dry CH<sub>2</sub>Cl<sub>2</sub> (4 mL) under argon and stirred at rt overnight. The resulting mixture was washed with water and an aqueous 0.25 M HCl solution. The combined aqueous washings were extracted with CH<sub>2</sub>Cl<sub>2</sub> where after the organic extracts were combined and washed with an aqueous saturated NaHCO<sub>3</sub> solution. The organic phase was dried over MgSO<sub>4</sub>, filtered and concentrated under reduced pressure to afford crude *O*-mesyl oxime **58**. Flash column chromatography on SiO<sub>2</sub> gave product decomposition.

## 7.9 References

- [1] S.Y Wang, J. H. Wu, L. F. Shyur, Y. H. Kuo, S. T. Chang, S. T. *Holzforschung* **2002**, *56*, 487. b) C. F. Chyu, H. C. Lin, Y. H. Kuo, *Chem. Pharm. Bull. (Tokyo)* **2005**, *53*, 11. c) C. I. Chang, M-H. Tseng, Y. H. Kuo, *Chem. Pharm. Bull. (Tokyo)* **2005**, *53*, 286.
- [2] a) Y-S. Cheng, Y. H. Kuo, Y. T. Lin, *Chem. Commun.* **1967**, 565. b) Y. T. Lin, Y-S. Cheng, Y. H. Kuo, *Tetrahedron Lett.* **1968**, *9*, 3881. c) Y. H. Kuo, Y-S. Cheng, Y. T. Lin, *Tetrahedron Lett.* **1969**, *10*, 2375. d) Y. H. Kuo, C. F. Chyu, H. Lin, *Chem. Pharm. Bull. (Tokyo)*. **2003**, *51*, 986. e) C. F. Chyu, M. R. Ke, Y. S. Chang, S. C. Chien, Y. H. Kuo, *Helv. Chim. Acta* **2007**, *90*, 1514.
- [3] C. F. Chyu, Y. H. Kuo, *Helv. Chim. Acta* **2007**, *90*, 738.
- [4] M Kamil, M. Ilyas, W. Rahman, N. Hasaka, M. Okigawa, N. Kawano, *J. Chem. Soc. Perkin Trans.1* **1981**, 553.
- [5] a) Y. H. Kuo, C. I. Chang, C. K. Lee, *Chem. Pharm. Bull. (Tokyo)* **2000**, *48*, 597. b) Y. H. Kuo, S. Chien, S. Huang, *Chem. Pharm. Bull. (Tokyo)* **2002**, *50*, 544. c) Y. H. Kuo, C. I. Chang, *J. Nat. Prod.* **2000**, *63*, 650. d) Y. H. Kuo, S. C. Chien, C. C. Kuo, *Planta Med.* **2002**, *68*, 1020.
- [6] W- H. Lin, J-M. Fang, Y-S. Cheng, *Phytochemistry* **1995**, *40*, 871.
- [7] W- H. Lin, J-M. Fang, Y-S. Cheng, *Phytochemistry* **1996**, *42*, 1657.
- [8] K. Kawazoe, M. Yamamoto, Y. Takaiishi, G. Honda, T. Fujita, E. Sezik, E. Yesilada, *Phytochemistry* **1998**, *50*, 493.
- [9] H. Ohtsu, M. Iwamoto, H. Ohishi, S. Matsunaga, R. Tanaka, *Tetrahedron Lett.* **1999**, *40*, 6419.
- [10] C. I. Chang, S. C. Chien, S. M. Lee, Y. H. Kuo, *Chem. Pharm. Bull. (Tokyo)*. **2003**, *51*, 1420.
- [11] C. I. Chang, J. Y. Chang, C. C. Kuo, W. Y. Pan, Y. H. Kuo, *Planta Med.* **2005**, *71*.
- [12] W-H. Lin, J-M. Fang, Y-S. Cheng, *Phytochemistry* **1997**, *46*, 169.
- [13] a) M. Banerjee, R. Mukhopadhyay, B. Achari, A. K. Banerjee, *Org. Lett.* **2003**, *5*, 3931 b) E. Fillion, D. Fishlock, *J. Am. Chem. Soc.* **2005**, *127*, 13144. c) M. Banerjee, R. Mukhopadhyay, B. Achari, A. K. Banerjee, *J. Org. Chem.* **2006**, *71*, 2787. d) L. Planas, M. Mogi, H. Takita, T. Kajimoto, M. Node, *J. Org. Chem.* **2006**, *71*, 2896. e) R. M. McFadden, B. M. Stoltz, *J. Am. Chem. Soc.* **2006**, *128*, 7738. f) S. L. Li, P. Chiu, *Tetrahedron Lett.* **2008**, *49*, 1741. g) S. Tang, Y. Xu, J. He, Y. He, J. Zheng, X. Pan, X. She, *Org. Lett.* **2008**, *10*, 1855.

- h) G. Majetich, J. M. Shimkus, *Tetrahedron Lett.* **2009**, *50*, 3311. i) E. Alvarez-Manzaneda, R. Chahboun, E. Cabrera, E. Alvarez, R. Alvarez-Manzaneda, R. Meneses, H. Es-Samti, A. Fernandez, *J. Org. Chem.* **2009**, *74*, 3384. j) E. Alvarez-Manzaneda, R. Chahboun, E. Cabrera, E. Alvarez, A. Haidour, J. M. Ramos, R. Alvarez-Manzaneda, Y. Charrah, H. Es-Samti, *Org. Biomol. Chem.* **2009**, *7*, 5146. k) M. Node, M. Ozeki, L. Planas, M. Nakano, H. Takita, D. Mori, S. Tamatani, T. Kajimoto, *J. Org. Chem.* **2010**, *75*, 190. l) C. K. Jana, R. Scopelliti, K. Gademann, *Synthesis* **2010**, 2223. m) C. K. Jana, R. Scopelliti, K. Gademann, *Chem. Eur. J.* **2010**, *16*, 7692. n) X. Liao, L. M. Stanley, J. F. Hartwig, *J. Am. Chem. Soc.* **2011**, *133*, 2088. o) E. Alvarez-Manzaneda, R. Chahboun, E. Cabrera, E. Alvarez, A. Haidour, J. M. Ramos, R. Alvarez-Manzaneda, M. Hmamouchi, H. Es-Samti, *Chem. Commun.* **2009**, 592. p) E. Alvarez-Manzaneda, R. Chahboun, E. Alvarez, R. Tapia, R. Alvarez-Manzaneda, *Chem. Commun.* **2010**, *46*, 9244. q) R. Tapia, J. J. Guardia, E. Alvarez, A. Haidour, J. M. Ramos, R. Alvarez-Manzaneda, R. Chahboun, E. Alvarez-Manzaneda, *J. Org. Chem.* **2012**, *77*, 573. r) J. Deng, R. Li, Y. Luo, J. Li, S. Zhou, Y. Li, J. Hu, A. Li, *Org. Lett.* **2013**, *15*, 2022. s) C. Thommen, C. K. Jana, M. Neuburger, K. Gademann, *Org. Lett.* **2013**, *15*, 1390. t) S. E. Shockley, J. C. Holder, B. M. Stoltz, *Org. Lett.* **2014**, *16*, 6362. u) L-Q. Li, M-M. Li, D. Chen, H-M Liu, H. Geng, J. Lin, H-B. Qin, *Tetrahedron Lett.* **2014**, *55*, 5960. v) S. Cai, Z. Xiao, Y. Shi, S. Gao, *Chem. Eur. J.* **2014**, *20*, 8677. w) J. Wang, J. Wang, C. Li, Y. Meng, J. Wu, C. Song, J. Chang, *J. Org. Chem.* **2014**, *79*, 6454. x) X. Yan, X. Hu, *J. Org. Chem.* **2014**, *79*, 4743. y) J. Deng, S. Zhou, W. Zhang, J. Li, R. Li, A. Li, *J. Am. Chem. Soc.* **2014**, *136*, 8185. z) B. N. Kakde, P. Kumari, A. Bisai, *J. Org. Chem.* **2015**, *80*, 9889. aa) T. Katoh, T. Akagi, C. Noguchi, T. Kajimoto, M. Node, R. Tanaka, M. Nishizawa (née Iwamoto), H. Ohtsu, N. Suzuki, K. Saito, *Bioorganic Med. Chem.* **2007**, *15*, 2736. bb) G. Liang, Y. Xu, I. B. Seiple, D. Trauner, *J. Am. Chem. Soc.* **2006**, *128*, 11022. cc) For an extensive review on the taiwaniaquinoids see: G. Majetich, J. M. Shimkus, *J. Nat. Prod.* **2010**, *73*, 284.
- [14] *Quaternary Stereocenters: Challenges and Solutions for Organic Synthesis*, (Eds. J. Christoffers and A. Baro), Wiley-VCH, Weinheim, **2005**, For selected reviews on the synthesis of quaternary stereocenters, see: a) I. Denissova, L. Barriault, *Tetrahedron*, **2003**, *59*, 10105. b) C. J. Douglas, L. E. Overman, *Proc. Natl. Acad. Sci. U.S.A.* **2004**, *101*, 5363. c) J. Christoffers, A. Baro, *Adv. Synth. Catal.* **2005**, *347*, 1473. d) B. M. Trost, C. Jiang, *Synthesis*, **2006**, 369. e) J. T. Mohr, B. M. Stoltz, *Chem. Asian J.* **2007**, *2*, 1476. f) P. G. Cozzi, R. Hilgraf, N. Zimmermann, *Eur. J. Org. Chem.* **2007**, *36*, 5969. g) J. P. Das, I. Marek, *Chem. Commun.* **2011**, *47*, 4593. h) Y. Liu, S-J. Han, W-B. Liu, B. M. Stoltz, *Acc. Chem. Res.* **2015**, *48*, 740.
- [15] a) A. L. Gottumukkala, K. Matcha, M. Lutz, J. G. de Vries, A. J. Minnaard, *Chem. Eur. J.* **2012**, *18*, 6907. b) A. L. Gottumukkala, J. Suljagic, K. Matcha,



- J. G. de Vries, A. J. Minnaard, *ChemSusChem*. **2013**, *6*, 1636. c) For a similar transformation see: S. Lin, X. Lu, *Org. Lett.* **2010**, *12*, 2536. d) J. Buter, R. Moezelaar, A. J. Minnaard, *Org. Biomol. Chem.* **2014**, *12*, 5883. e) see also chapter 5 of this dissertation.
- [16] a) K. Kikushima, J. C. Holder, M. Gatti, B. M. Stoltz, *J. Am. Chem. Soc.* **2011**, *133*, 6902. b) J. C. Holder, L. Zou, A. N. Marziale, P. Liu, Y. Lan, M. Gatti, K. Kikushima, K. N. Houk, B. M. Stoltz, *J. Am. Chem. Soc.* **2013**, *135*, 14996. c) S. E. Shockley, J. C. Holder B. M. Stoltz, *Org. Process Res. Dev.* **2015**, *19*, 974. d) See also references 13t and 13u.
- [17] a) M. A. Sierra, M. C. de la Torre, *Dead ends and detours: Direct ways to successful total synthesis*, Wiley-VHC, Weinheim, **2004**. b) M. A. Sierra, M. C. de la Torre, F. P. Cossío, *More dead ends and detours: En route to successful total synthesis*, Wiley-VHC, Weinheim, **2013**.
- [18] For a review on the Wolff rearrangement see: W. Kirmse, *Eur. J. Org. Chem.* **2002**, 2193.
- [19] L. Kürti, B. Czakó, *Strategic Applications of Named Reactions in Organic Synthesis: Background and Detailed Mechanisms*, Elsevier Academic Press, **2005**.
- [20] For a review on the semi-pinacol rearrangements in natural product synthesis see: Z-L. Song, C-A. Fan, Y-Q. Tu, *Chem. Rev.* **2011**, *111*, 7523.
- [21] R. Fischer, G. Lardellim O. Jeger, *Helv. Chimica Acta* **1951**, *34*, 1577.
- [22] a) R. O. Hutchins, M. Kacher, L. Rua, *J. Org. Chem.* **1975**, *40*, 923. b) V. P. Miller, D-Y. Yang, T. M. Weigel, O. Han, H-W. Liu, *J. Org. Chem.* **1989**, *54*, 4175.
- [23] For the ozonolysis attempts of **38** see the master thesis of Casper de Boer, *Taiwaniaquinoid total synthesis*, University of Groningen, **2015**.
- [24] Z. Zhang, *Comprehensive organic name reactions and reagents; Criegee rearrangement*, eBook - DOI: 10.1002/9780470638859.conrr170.
- [25] H. M. Cheng, W. Tian, P. a. Peixoto, B. Dhudshia, D. Y. K. Chen, *Angew. Chemie - Int. Ed.* **2011**, *50*, 4165.
- [26] M-N. Roy, V. N. H. Lindsay, A. B. Charette in *Stereoselective synthesis: Reactions of carbon-carbon double bonds (Science of Synthesis)*, Ed. J. G. de Vries, Thieme, Stuttgart, **2011**, 1. 731.
- [27] J. M. Murphy, X. Liao, J. F. Hartwig, *J. Am. Chem. Soc.* **2007**, *129*, 15434.
- [28] J. M. Murphy, C. C. Tzschucke, J. F. Hartwig, *Org. Lett.* **2007**, *9*, 757.
- [29] For all our conjugate addition efforts on cycloheptenone **24** see the master thesis of Mira Holzheimer, *Taiwaniaquinoid total synthesis – continued efforts*, University of Groningen, **2016**.
- [30] K. Kaneda, H. Azuma, M. Wayaku, S. Teranishi, *Chem. Lett.* **1974**, 215.

## ***English Summary***

*On the total synthesis of terpenes containing quaternary stereocenters;  
Stereoselective synthesis of the taiwaniaquinoids, mastigophorene A, and  
tuberculosinyl adenosine*

The total synthesis of naturally occurring compounds is a field of research with a long-standing tradition and importance. As a matter of fact, the first synthesis of a natural product, that of urea by Friedrich Wöhler in 1828, spawned the field of organic chemistry. Over the past 200 years an enormous amount of natural products have been synthesized and these had a decisive impact on fields like biochemistry, medicine and biology. Examples of how natural product synthesis benefits daily life are: *the industrial production of vitamins and amino acids, the use of volatile compounds in perfumes and fragrances, and natural products that serve as leads or are actual medicines.*

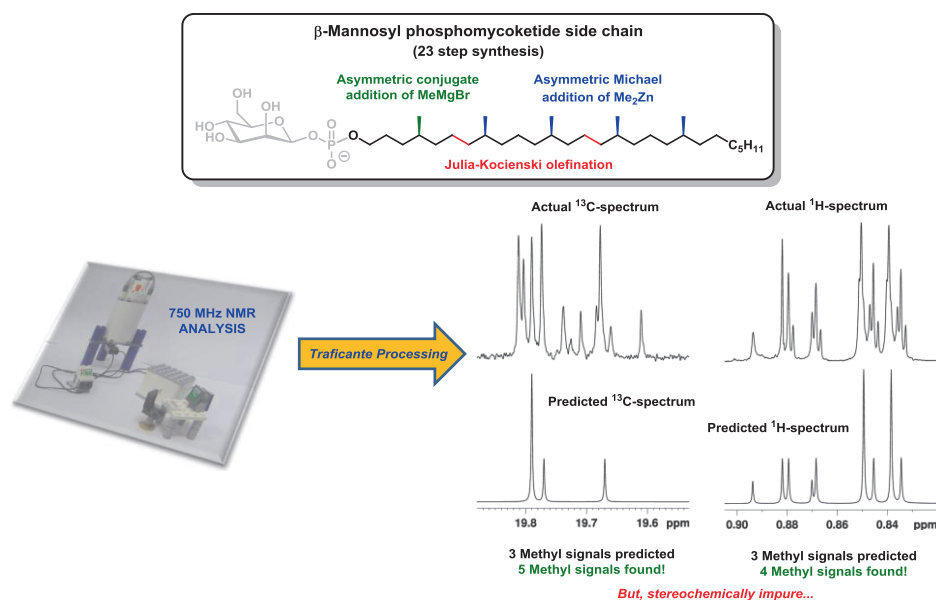
From an academic perspective the practice of organic chemistry is largely driven by curiosity, the development of novel methodology, and the discovery of new reactivity to construct molecules. Natural product synthesis in particular serves as an ideal platform to scrutinize new synthesis methodology by testing it in a complex setting (*complex chemical structures*). The synthesis of a complex natural product elicits the development of new methodology as synthesis in such a complex setting often requires modification of reaction conditions.

In this dissertation the reader will find a detailed description of my work in the field of natural product synthesis. The research focused on the stereoselective synthesis of naturally occurring compounds exhibiting a quaternary stereocenter, a chemical motive generally difficult to construct. In this thesis one will find the development of novel methodology and applications of new chemical reactions within the confines of natural product synthesis. Additionally, our synthetic efforts assisted in the structure elucidation of a novel terpene nucleoside from *Mycobacterium tuberculosis*, confirming its biosynthesis, and producing quantities of material for further biochemical and immunological studies. We also used a natural product, mycoketide, to develop an NMR-based approach to establish the stereochemistry of oligoisoprenoids.

Chapter 2 describes the asymmetric synthesis of this  $\beta$ -mannosyl phosphomycoketide side chain and subsequent NMR analysis thereof (Scheme 1). Exhibiting an all-*syn* 1,5-methyl ramification with five repeating stereogenic methine groups, the determination of the relative stereochemistry and isomeric purity by means of NMR analysis is particularly challenging.

In 2013, Curran and co-workers synthesized all possible (relative) stereoisomers of shorter analogues of the mycoketide side chain containing three repeating methyl branches. It was found that the  $^1\text{H}$ - and  $^{13}\text{C}$ -NMR spectra (750 MHz) were very similar but not identical. Assignment of the specific resonances, for the determination of the isomeric purity, proved to be impossible however as the signals were in too close proximity. Processing of the acquired data with the Traficante algorithm (resolution

enhancement) separated the overlapping signals which, in combination with computational simulation of the spectra, allowed the assignment of the resonances and therefore assessment of the diastereomeric ratio.



**Scheme 1.** Synthesis and NMR analysis of all-(S) mycoketide.

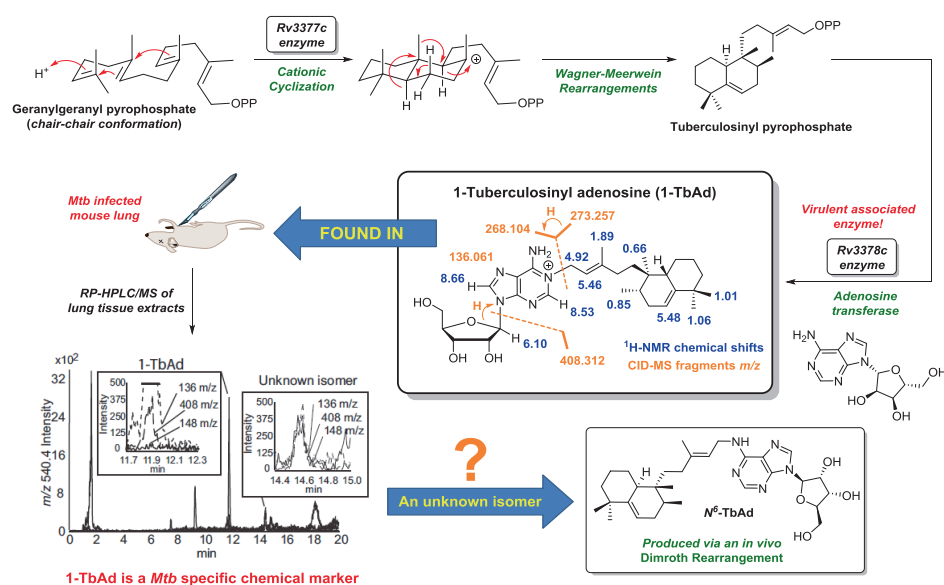
Based on the obtained empirical data the Curran laboratory was able to produce a set of predicted spectra for higher oligoisoprenoids like the phosphomycoketide side chain. To test the validity of this model, actual material was necessary. This material was provided to the Curran laboratory in the form of all-*syn* mycoketide, and a smaller four methyl groups containing analogue.

NMR analysis of the synthetic material showed that somewhere in the synthesis erosion of enantiopurity had taken place, leading to ~70% isomeric purity of the product. However, the obtained <sup>13</sup>C-NMR spectrum, after Traficante processing, showed five separate resonances for the five methyl groups, whereas the predicted spectra were unable to distinguish the three central methyl groups. This result was surprising as the chemical environment of the three central methyl groups is very similar. In the <sup>1</sup>H-NMR spectrum of mycoketide, four of the methyl groups were visible. The research allowed therefore expansion of the model for the prediction of the relative stereochemistry and/or stereopurity assessment of saturated oligoisoprenoids, a common motive in natural products.

The third chapter of this dissertation is the result of a collaboration of several research groups, coordinated by the Moody laboratory at Harvard Medical School. In 2012, Moody and co-workers isolated an unknown, but abundant, natural product from the pathogen *Mycobacterium tuberculosis*. As *Mycobacterium tuberculosis* is responsible

for over 1.5 million deaths annually, the identification of novel molecules is important as this provides insight in the, survival and virulence mechanism of the bacterium. Additionally, pathogen-specific compounds might find application as chemical markers for diagnostic tests for the tuberculosis disease.

Investigation into the molecular architecture of the unknown isolate using mass spectrometry and NMR analysis, led to its assignment as 1-tuberculosinyl adenosine (1-TbAd) (Scheme 2). A total synthesis of the racemate confirmed its structure, and also provided material for initial investigations. As a part of the chemical synthesis, its putative biosynthetic precursor tuberculosinyl pyrophosphate was also produced. With this material the biosynthesis of 1-TbAd was shown to involve the virulence associated enzyme Rv3378c, indicating that this molecule might be important for inducing virulence of *Mycobacterium tuberculosis*.



**Scheme 2.** The discovery and biosynthesis of 1-tuberculosinyl adenosine, and its development into a chemical marker for tuberculosis.

Further analysis showed that 1-TbAd is not only a highly abundant, but also a *Mycobacterium tuberculosis*-specific molecule. This led to the hypothesis that 1-TbAd can act as a specific chemical marker and be used to diagnose tuberculosis. Its potential as a chemical marker was shown by reversed phase HPLC-MS analysis of whole lung homogenates of six tuberculosis infected BLB/C mice. In all samples 1-TbAd was readily detected.

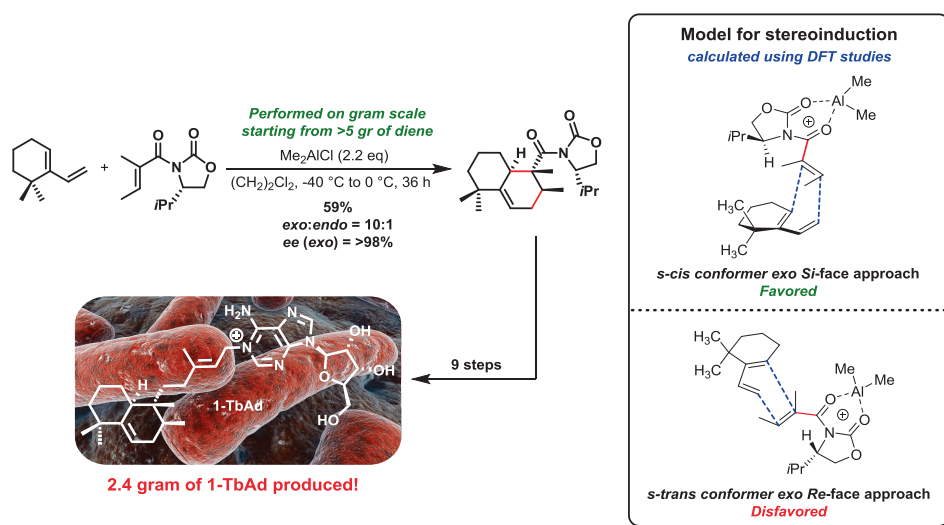
From the chemical marker studies, an isomer of 1-TbAd was detected as well. Again, mass spectrometry and NMR spectroscopy were used to elucidate the structure which was found to correspond to 1-TbAd's pseudo-isomer *N*<sup>6</sup>-TbAd. A chemical synthesis

reinforced this conclusion and also showed the conversion of 1-TbAd into  $N^6$ -TbAd to proceed via a Dimroth rearrangement.

The identification of these novel *Mycobacterium tuberculosis*-specific molecules, in particular that of 1-TbAd, is of significant importance. This molecule has shown to be usable as a chemical marker and is produced by the virulence associated enzyme Rv3378c. Although the role this molecule plays in the virulence/survival of *Mycobacterium tuberculosis* in macrophages remains unknown, we believe an important step has been made to unravel this complex mechanism.

With the discovery of 1-TbAd there is a demand for enantiopure reference material. Unfortunately, the isolation of 1-TbAd from its natural source is laborious and provides only very small quantities. This problem has been solved by the stereoselective synthesis of the natural product as shown in chapter 4 (Scheme 3).

Our venture into the 1-TbAd total synthesis started with a chiral pool strategy. Naturally occurring sclareolide was chosen as a starting material but the 1-TbAd synthesis ground to a halt as our envisioned route failed. A detour was also investigated but unfortunately to no avail.

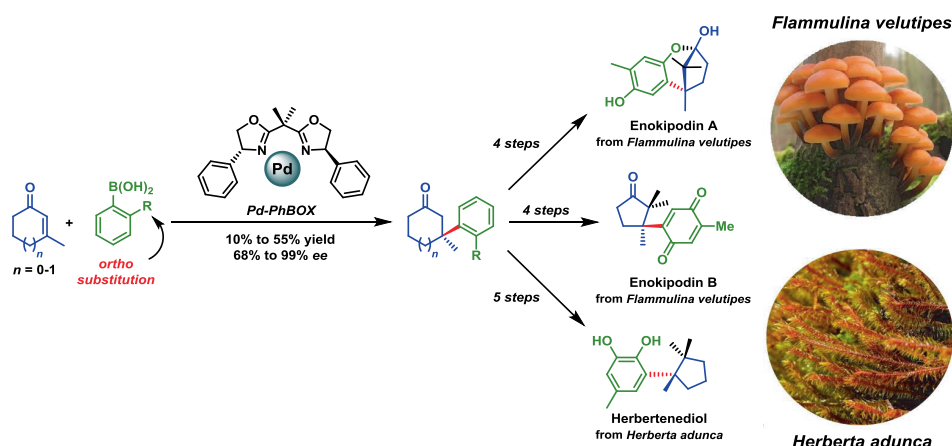


**Scheme 3.** A highly stereoselective synthesis of the halimane skeleton in the gram-scale total synthesis of 1-TbAd

The second strategy chosen to construct the halimane core-structure of 1-TbAd involved a Diels-Alder reaction. A plethora of catalyzed Diels-Alder cycloadditions, ranging from DNA catalysis, organocatalysis to transition metal catalysis, were performed but the Diels-Alder adduct could not be produced at all or with moderate diastereo- and enantioselectivities.

After this investigation we turned our attention to the use of chiral auxiliaries as part of the dienophile. The use of the Evans chiral oxazolidinone proved to be fruitful as the Diels-Alder adduct was produced with high diastereoselectivity (*exo* : *endo* = ~10:1) and excellent enantioselectivity (>98% *ee*) for the desired *exo* diastereomer. Completing the synthesis of enantiopure 1-TbAd took an additional nine steps and produced ~2.5 gram of natural product, sufficient for biological studies. Besides the first asymmetric total synthesis of 1-TbAd, congeners of the natural product (2'-deoxy 1-TbAd, (*Z*)-1-TbAd, and <sup>13</sup>C<sub>ribose</sub>-labelled 1-TbAd) and *N*<sup>6</sup>-TbAd were also constructed. The chapter ends with an investigation into the mechanistic course of the Diels-Alder reaction. A model to explain the stereoselectivity was proposed and validated by *in silico* studies. It was found that the *s-cis* conformer of the dienophile dictates the reaction which proceeds following the Curtin-Hammett principle.

After the synthesis of *Mycobacterium tuberculosis* isolates, the focus was shifted to palladium-catalyzed asymmetric conjugate additions in the construction of several terpene-based natural products. Chapter 5 describes the development of methodology to construct sterically congested benzylic quaternary stereocenters bearing *ortho*-substituents (Scheme 4).

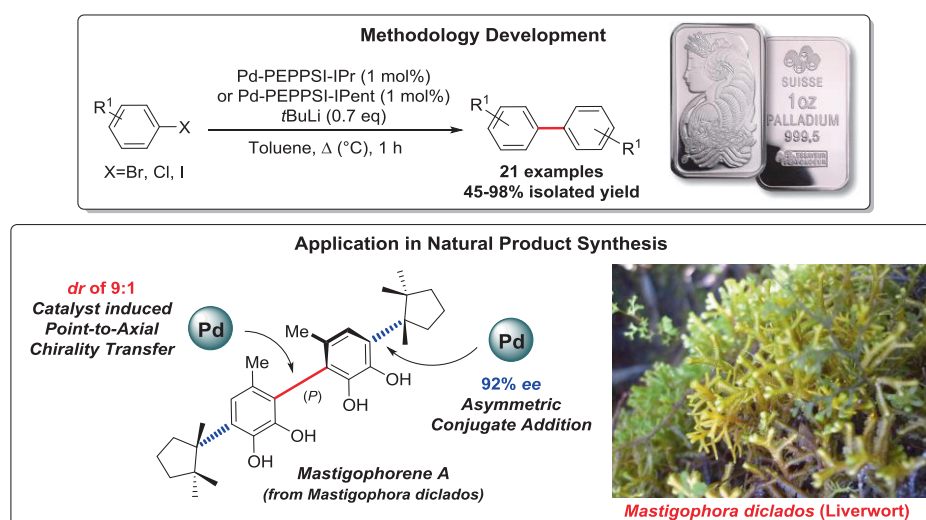


**Scheme 4.** Development of the Pd-catalyzed asymmetric conjugate addition of *ortho*-substituted arylboronic acids to 3-methyl substituted cyclic enones, and its application in natural product synthesis.

Although recent advances in the palladium-catalyzed Michael addition of arylboronic acids to  $\beta$ -substituted enones have been made, reactions with *ortho*-substituted arylboronic acids were shown to be problematic. Optimization of previous in-house developed methodology was performed resulting in the successful addition of *ortho*-substituted arylboronic acids with generally good enantioselectivities. Unfortunately the isolated yields were moderate at best which was attributed to significant protodeboronation of the arylboronic acid. Despite this feature the reaction was shown

to be applicable in the shortest asymmetric total synthesis of herbertenediol and enokipodin A and B.

The short asymmetric total synthesis of herbertenediol set the stage for a concise stereoselective synthesis of its dehydromer mastigophorene A, as presented in chapter 6. The biaryl axis of mastigophorene A and B is chiral and is a challenging functionality to install stereoselectively (Scheme 5).



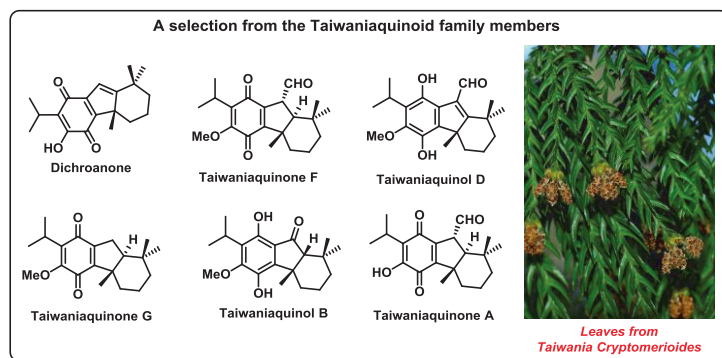
**Scheme 5.** Development of the Pd-catalyzed homo-coupling of aryllithium reagents and its application in the shortest atropselective synthesis of mastigophorene A.

Over the past three years, the Feringa laboratory made significant advances in the palladium-catalyzed cross-coupling of organolithium reagents. Concurrent with our work on herbertenediol, the Feringa group developed methodology for the hetero- and homo-coupling of aryllithium reagents with aryl halides. Combining our efforts led to the shortest asymmetric total synthesis of mastigophorene A in only eight steps. Surprisingly, the chiral biaryl axis was installed with high diastereoselectivity, induced by the seemingly remote benzylic quaternary stereocenter on the *para*-position via so-called catalyst induced point-to-axial chirality transfer.

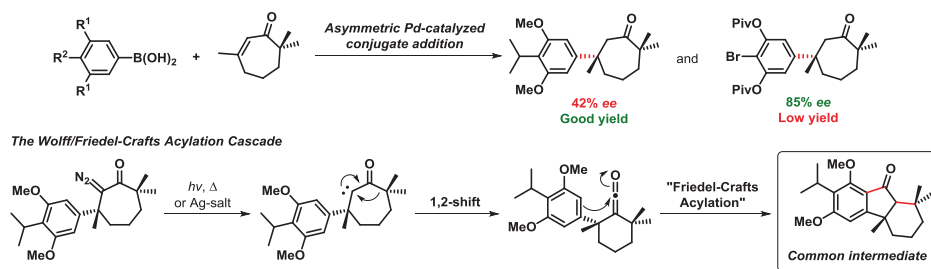
The combination of the described asymmetric conjugate addition and the in this chapter presented homo-coupling of aryllithium reagents, were responsible for the considerable improvement over the 20+ steps needed in previous atropselective total syntheses of mastigophorene A.

In the final chapter of this dissertation, chapter 7, an investigation into the total synthesis of the taiwaniaquinoid family is presented. Bearing an unusual [6,5,6]-*abeoabietane* skeleton, together with a benzylic quaternary stereocenter, this class of molecules opposes a significant synthetic challenge.

Our synthetic route was based on the recently developed Pd-catalyzed asymmetric conjugate additions of arylboronic acids to cyclic enones. A novel feature of this plan was the addition to a rarely used substituted cycloheptenone. The construction of the [6,5,6]-*abeoabietane* core structure was envisioned to be feasible by means of a ring contraction/acylation type domino reaction (Scheme 6).



Synthetic plan towards a common intermediate for the taiwaniaquinoids



**Scheme 6.** Overview of the general synthetic plan explored towards an asymmetric total synthesis of several taiwaniaquinoid family members.

A considerable number of reactions was performed to achieve the asymmetric synthesis of the [6,5,6]-*abeoabietane* skeleton. However, the conjugate addition proved to be very challenging although eventually we managed to achieve an enantioselectivity of 85% *ee*. The isolated yield for the Michael adduct proved to be low and therefore the route was continued with racemic material. Several ring contraction strategies were investigated however to no avail.

Although the synthesis of the [6,5,6]-*abeoabietane* core was not achieved, the synthetic plan should not be considered a dead end. Several other ideas for ring contraction strategies are presented in chapter 7 and work will continue to complete the total synthesis of the taiwaniaquinoids.





## *Nederlandse Samenvatting*

*Over de totaalsynthese van terpenen met quaternaire stereocentra;  
Stereoselectieve synthese van de taiwaniaquinoiden, mastigophoreen A en  
tuberculosinyl adenosine*

De totaalsynthese van natuurstoffen is een belangrijk onderzoeksveld met een lange traditie. De eerste synthese van een natuurstof, ureum, door Friedrich Wöhler in 1828, stond aan de wieg van een nieuw onderzoeksveld binnen de scheikunde, namelijk organische chemie. De laatste twee decennia is een ontzettend groot scala aan natuurstoffen gesynthetiseerd die een grote invloed hebben gehad op andere onderzoeksvelden zoals biochemie, medicijnontwikkeling, en algemene biologie. Dat de organische synthese van natuurstoffen voordelen biedt voor de samenleving blijkt bijvoorbeeld uit: *de industriële productie van vitaminen en aminozuren, het gebruik van vluchtige natuurstoffen in parfums, en het feit dat natuurstoffen medicinale eigenschappen hebben of als leidraad fungeren in de medicijnontwikkeling.*

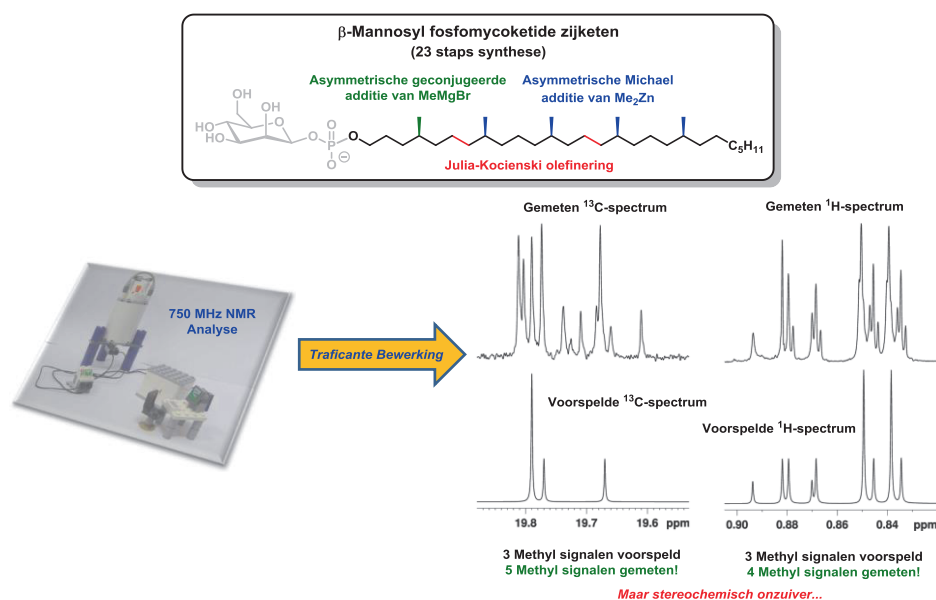
Vanuit een academisch perspectief wordt het beoefenen van organische chemie grotendeels gedreven door nieuwsgierigheid, de ontwikkeling van nieuwe methodologie, en de ontdekking van nieuwe reactiviteit. Natuurstofsynthese in het bijzonder vormt een ideaal platform waarin nieuwe synthese methodologie kan worden getest in *complexe chemische structuren*. Tevens kan de synthese van een complex natuurproduct bijdragen aan de ontwikkeling van nieuwe methodologie aangezien synthese in een complexe setting vaak modificatie van de methodologie vereist.

In dit proefschrift vindt de lezer een gedetailleerde beschrijving van mijn werk in het veld van de natuurstofsynthese. Het onderzoek is toegespitst op de stereoselectieve synthese van natuurstoffen die quaternaire koolstofatomen bevat, een motief dat over het algemeen moeilijk te construeren is. In deze dissertatie vindt men onder andere de ontwikkeling van nieuwe methodologie en de toepassing van nieuwe chemische reacties in de synthese van verscheidende complexe natuurstoffen. Daarnaast hebben onze synthetische inspanningen ook bijgedragen aan de structuuropheldering van twee nieuwe terpeennucleosides geïsoleerd uit *Mycobacterium tuberculosis*. De biosynthese van deze moleculen is ook ontrafeld met behulp van een gesynthetiseerd biosynthetisch intermediair. Tevens zijn significante hoeveelheden aan natuurstof geproduceerd die verder worden gebruikt in biochemische en immunologische studies. Ook is een natuurstof, mycoketide genaamd, gebruikt in de ontwikkeling van een NMR-gebaseerde techniek voor de opheldering van de relatieve stereochemie in oligoisoprenoïden.

Hoofdstuk 2 beschrijft de asymmetrische synthese van de  $\beta$ -mannosyl fosfomycoketide zijketen en de NMR-analyse ervan (Schema 1). De opheldering van de relatieve stereochemie en de bepaling van de isomere zuiverheid van dit soort verbindingen is uitdagend aangezien de stereocentra in het molecuul (een methylvertakking op iedere

vijfde positie met vijf iteraties) te ver van elkaar vandaan zitten om interactie te hebben en dus geanalyseerd te worden met standaard NMR-technieken.

In 2013 communiceerde de Curran-groep de synthese van alle mogelijke (relatieve) stereoisomeren van mycoketide analoga met drie repeterende methylgroepen. NMR analyse liet zien dat  $^1\text{H}$ - en  $^{13}\text{C}$ -NMR spectra (750 MHz) van de isomeren vergelijkbaar waren, maar niet identiek. De toekenning van de signalen met betrekking tot de methylgroepen, voor de bepaling van de isomere zuiverheid, bleek onmogelijk vanwege de overlap van de specifieke signalen. Door het toepassen van een resolutieverhogende techniek (Traficante processing) konden de overlappende signalen dusdanig van elkaar gescheiden worden dat onderscheid kon worden gemaakt. In combinatie met voorspelde spectra van alle relatieve stereoisomeren konden de individuele signalen toegekend worden en daarmee ook de stereochemische zuiverheid (diastereomere ratio).



**Schema 1.** Synthese en NMR analyse van “all-(S) mycoketide”.

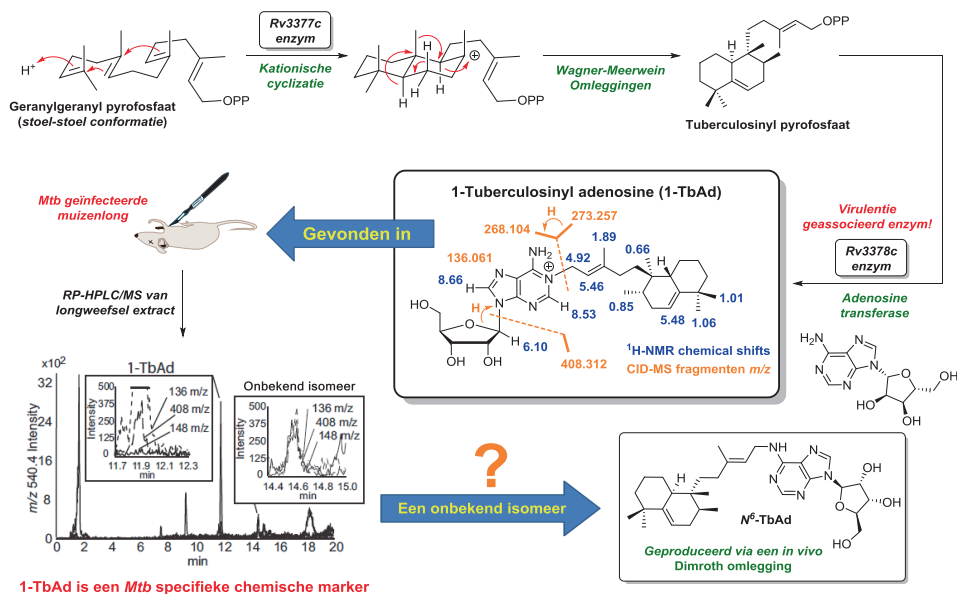
Gebaseerd op de empirische data van de mycoketide analoga heeft het Curran laboratorium een set aan voorspellingen kunnen doen voor homologe oligoisoprenoids, zoals de  $\beta$ -mannosyl fosfomycoketide zijketen. Om dit model enigszins te kunnen valideren is synthetisch materiaal nodig. Dit materiaal is geleverd aan de Curran groep in de vorm van all-*syn* mycoketide en een kleiner, vier methylgroep bevattend, analoog. NMR analyse van de mycoketide zijketen liet zien dat ergens in de synthese erosie van enantiozuiverheid had plaatsgevonden, resulterend in een isomere zuiverheid van  $\sim 70\%$ . Desondanks bevatte het Traficante bewerkte  $^{13}\text{C}$ -spectrum vijf afzonderlijke signalen voor de vijf methylgroepen terwijl de gesimuleerde slecht drie signalen voorspelde. De drie middelste methyl groepen konden in de voorspelling niet worden onderscheiden en

werden daardoor als één signaal voorspeld. Het resultaat is dus opmerkelijk aangezien alle vijf methylgroepen aparte signalen gaven, en dat terwijl de chemische omgeving van vooral de drie middelste methylgroepen nagenoeg hetzelfde is. In het  $^1\text{H}$ -spectrum van mycoketide konden, na Traficante bewerking, vier van de vijf methylgroepen worden onderscheiden. Dit onderzoek heeft door de behaalde resultaten kunnen bijdragen aan de uitbreiding van het voorspelmodel voor de bepaling van de relatieve stereochemie en/of stereozuiverheid van verzadigde oligoisoprenoïden, een veelvoorkomend motief in natuurstoffen.

Het derde hoofdstuk van dit proefschrift is het resultaat van een samenwerking tussen meerdere onderzoekslaboratoria die werd geleid door het Moody laboratorium (Harvard Medical School). In 2012 isoleerde de Moody-groep voor het eerst een onbekende, maar veelvoorkomende, natuurstof uit het pathogeen *Mycobacterium tuberculosis*. Aangezien *Mycobacterium tuberculosis* verantwoordelijk is voor meer dan 1.5 miljoen doden per jaar, is de identificatie van nieuwe, door de bacterie geproduceerde, moleculen erg belangrijk. Deze stoffen kunnen namelijk inzicht geven in het deels onbekende virulentie- en overlevingsmechanisme van de bacterie. Bovendien vormt de isolatie van pathogeen-specifieke stoffen de mogelijkheid tot toepassing als chemische markers voor een diagnostische test voor tuberculosis.

Onderzoek naar de moleculaire architectuur van de onbekende stof met behulp van massaspectrometrie en NMR analyse suggereerde 1-tuberculosinyl adenosine (1-TbAd) als de geïsoleerde stof (Schema 2). Een totaalsynthese van racemisch 1-TbAd bevestigde de structuur en verschaft materiaal voor initieel onderzoek naar 1-TbAd. Als onderdeel van de synthese werd ook de vermeende biosynthetische precursor, tuberculosinylpyrofosfaat, gemaakt. Met dit synthetische materiaal is de biosynthese, waarbij het virulentiegeassocieerde enzym Rv3378c betrokken is, van 1-TbAd bewezen. Doordat de productie van 1-TbAd alleen maar tot stand kan komen in de aanwezigheid van het enzym Rv3378c, is het waarschijnlijk dat 1-TbAd een belangrijke rol speelt in het veroorzaken van virulentie van de *Mycobacterium tuberculosis* bacterie.

Verdere analyse liet zien dat 1-TbAd niet alleen veelvoorkomend is, maar ook specifiek voor *Mycobacterium tuberculosis*. Dit leidde tot de hypothese dat 1-TbAd kan fungeren als een specifieke chemische marker, en dus kan worden gebruikt voor een diagnostische test voor tuberculosis. Dat dit mogelijk is werd aangetoond met behulp van een reversed phase HPLC-MS analyse van biologisch materiaal. De longen van zes muizen, besmet met de tuberculosis bacterie, werden na 21 dagen incubatietijd verwijderd en geëxtraheerd om door tuberculose uitgescheiden stoffen te kunnen isoleren. De longhomogenaatextracten werden daarna geanalyseerd en 1-TbAd werd in alle zes gevallen 1-TbAd gedetecteerd.



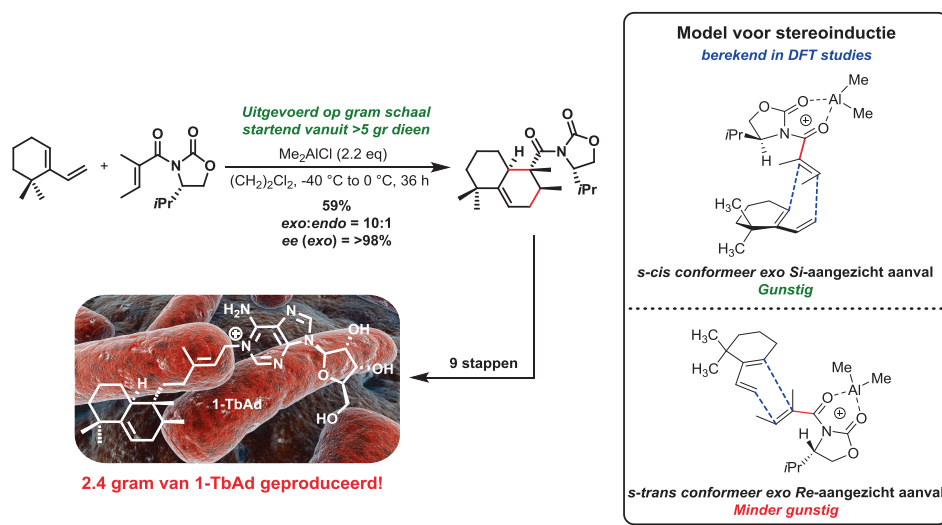
**Schema 2.** De ontdekking en biosynthese van 1-tuberculosinyl adenosine, en de ontwikkeling van een chemische marker voor tuberculose.

Naast de detectie van 1-TbAd in muizenlongen werd ook een isomeer van 1-TbAd gedetecteerd met een langere retentietijd in RP-HPLC analyse. Ook hiervan kon de structuur worden vastgesteld met behulp van massaspectrometrie en NMR. De structuur kwam overeen met het pseudo-isomeer van 1-TbAd;  $N^6$ -TbAd. Chemische synthese van dit molecuul, door middel van een Dimroth-omlegging van 1-TbAd, bevestigde de structuur.

De identificatie van deze twee nieuwe *Mycobacterium tuberculosis*-specifieke moleculen, met 1-TbAd in het bijzonder, is van significant belang. Het is aangetoond dat 1-TbAd kan fungeren als chemical marker en dat het geproduceerd wordt door het virulentie geassocieerde enzym Rv3378c. Ondanks het feit dat de rol van 1-TbAd in virulentie en overleving van de tuberculosis bacterie *in vivo* nog onbekend is, is een belangrijke stap gezet om dit complexe mechanisme te ontrafelen.

Na de ontdekking van 1-TbAd kwam er vraag naar enantiopuur referentiemateriaal. Het organisme zelf is in theorie een goede bron maar in het geval van *Mycobacterium tuberculosis* is de isolatie moeizaam en levert ook nog eens kleine hoeveelheden op. Dit probleem kan worden omzeild door een stereoselectieve synthese van 1-TbAd zoals gedemonstreerd in hoofdstuk 4 (Schema 3).

De ontwikkeling van de stereoselectieve 1-TbAd totaalsynthese startte met een “*chiral pool*” benadering. Natuurlijk voorkomend sclareolide leek op basis van bestaande literatuur een interessante kandidaat, maar helaas bleek de initiële syntheseroute een doodlopende weg. Ook een modificatie van de originele benadering bleek onsuccesvol.



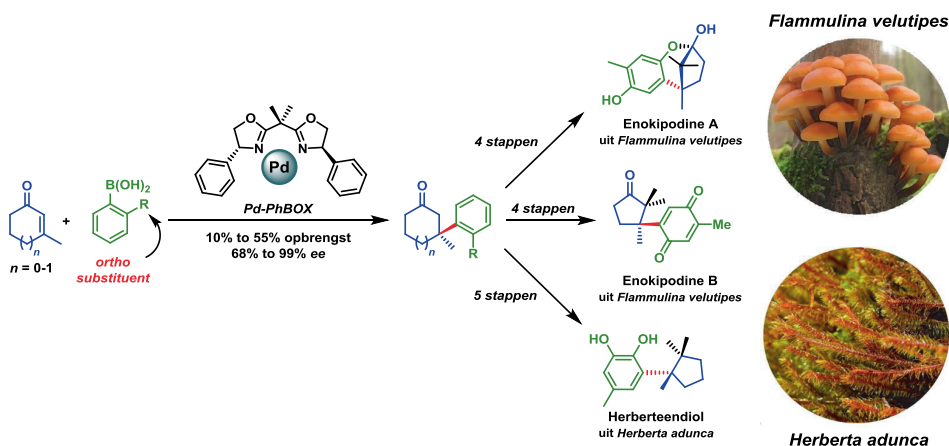
**Schema 3.** Een stereoselectieve synthese van de halimaan hoofdstructuur in 1-TbAd.

De tweede strategie die werd onderzocht was gebaseerd op de Diels-Alder reactie. Een groot aantal Diels-Alder cycloaddities, van DNA-katalyse, organokatalyse tot overgangsmetaalkatalyse, werden uitgevoerd maar produceerden geen Diels-Alder adduct of produceerden dit met ongewenst lage selectiviteit.

Na dit onderzoek werd gefocust op Diels-Alder reacties met een chirale hulpgroep bevestigd aan het dienofiel. Het Evans chirale oxazolidinon bleek het meest succesvol aangezien het Diels-Alder adduct werd gevormd met een hoge diastereoselectiviteit (*exo* : *endo* = ~10:1) en zeer hoge enantioselectiviteit (>98% *ee*) voor het *exo* diastereomeer. De synthese van enantiopuur 1-TbAd werd hierna voltooid na negen additionele stappen. In totaal is ~2.5 gram aan natuurstof geproduceerd, meer dan genoeg voor biologisch en biochemisch vervolgonderzoek. Naast de synthese van 1-TbAd zijn ook de soortgenoten (2'-desoxy 1-TbAd, (*Z*)-1-TbAd en  $^{13}\text{C}_{\text{ribose}}$ -gelabelled 1-TbAd) en  $\text{N}^6$ -TbAd geproduceerd.

Het hoofdstuk eindigt met een onderzoek naar de basis van de opmerkelijke stereoselectiviteit van de Diels-Alder reactie. Een model dat de stereoselectiviteit verklaart wordt voorgesteld en gevalideerd door *in silico* studies. Een interessant gegeven is dat de reactie stapsgewijs en volgens het Curtin-Hammet principe verloopt.

Na synthese van *Mycobacterium tuberculosis* geproduceerde stoffen ging de aandacht uit naar palladium-gekatalyseerde asymmetrische geconjugeerde addities voor de constructie van enkele terpeen-gebaseerde natuurstoffen. Hoofdstuk vijf beschrijft de ontwikkeling van methodologie voor de synthese van sterische gehinderde benzylicke quaternaire stereocentra met een *ortho*-substituut (Schema 4).

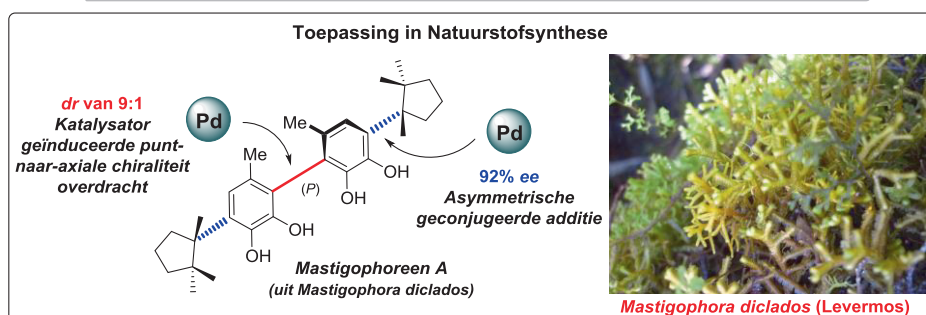
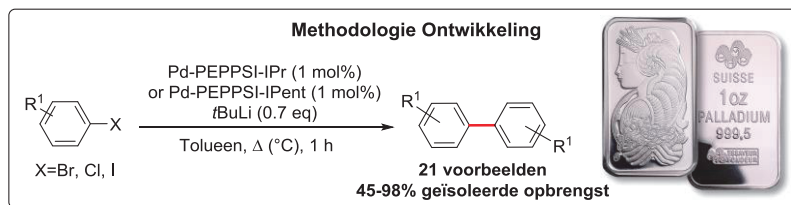


**Schema 4.** Ontwikkeling van een Pd-gekatalyseerde asymmetrische geconjugeerde additie van *ortho*-gesubstitueerde arylboorzuren aan 3-methylcyclopentenon, en de toepassing ervan in natuurstofsynthese.

Ondanks de recente ontwikkeling in de palladium-gekatalyseerde Michael-additie van arylboorzuren aan  $\beta$ -gesubstitueerde enonen, bleken de reacties met *ortho*-gesubstitueerde arylboorzuren problematisch. Optimalisatie van door de Minnaard groep ontwikkelde methodologie was succesvol aangezien nu *ortho*-gesubstitueerde arylboorzuren gekoppeld konden worden met goede tot zeer goede enantioselectiviteit. Helaas bleek de geïsoleerde opbrengst van de stoffen matig tot voldoende als gevolg van protodeborylering van het arylboorzuur. Niettemin bleek de ontwikkelde reactie bruikbaar in zeer korte asymmetrische totaalsynthesen van herberteendiol en enokipodine A en B.

De kortste asymmetrische totaalsynthese van herberteendiol gaf aanleiding tot de ontwikkeling van een beknopte stereoselectieve synthese van mastigophoreen A (het dehydrodimeer van herberteendiol), zoals beschreven in hoofdstuk 6 (Schema 5). Het was met name de uitdaging van de stereoselectieve constructie van de chirale biaryl as in mastigophoreen A en B die de aanleiding was tot het onderzoek.

In de laatste drie jaar heeft het Feringa laboratorium significante bijdragen geleverd aan de palladium-gekatalyseerde koppelingsreacties, door gebruik te maken van organolithiumreagentia. Ten tijde van ons werk aan herberteendiol werd in het Feringa laboratorium onderzoek verricht naar de ontwikkeling van palladium-gekatalyseerde hetero- en homo-koppelingen van aryllithiumreagentia met arylhalides. De combinatie van beide onderzoeken leidde uiteindelijk tot de kortste asymmetrische totaalsynthese van mastigophoreen A, in slechts acht stappen. Een interessante vondst was dat de chirale biaryl as met de nieuwe methodologie geïnstalleerd kan worden met een hoge diastereoselectiviteit door middel van chirale inductie. De chirale inductie was onverwacht maar vindt waarschijnlijk plaats door een katalysator-geïnduceerde punt-naar-axiale chiraliteitsoverdracht.



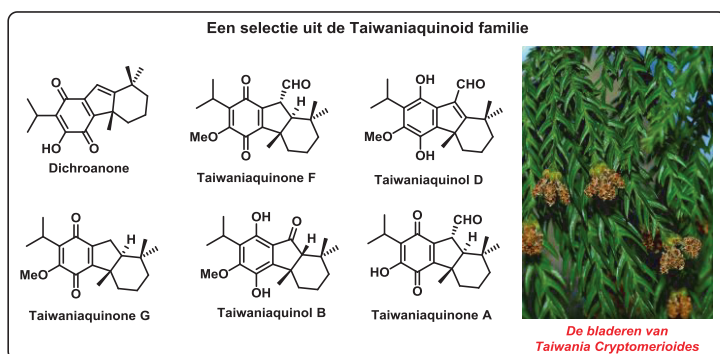
**Schema 5.** Ontwikkeling van de Pd-gekatalyseerde homo-koppeling van aryllithiumreagentia en de toepassing ervan in de kortste stereoselectieve synthese van mastigophoreen A.

De combinatie van de beschreven asymmetrische geconjugeerde additie en, in dit hoofdstuk beschreven, homo-koppeling van aryllithiumreagentia, hebben geleid tot een aanzienlijke inkorting van voorgaande stereoselectieve syntheses waar meer dan 20 stappen voor nodig waren.

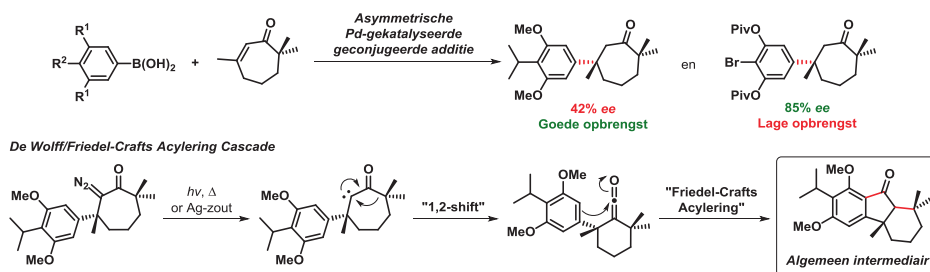
In het laatste hoofdstuk van deze dissertatie, hoofdstuk 7, wordt het onderzoek naar een stereoselectieve synthese van taiwaniaquinoiden gepresenteerd. De taiwaniaquinoid familie bevat het ongewone [6,5,6]-abeoabietaanskelet en een benzylicus quaternair stereocentrum. Deze structurele eigenschappen maken de taiwaniaquinoiden een uitdagend doelwit voor de synthetisch organisch chemicus.

Het syntheseplan werd ontwikkeld met de Pd-gekatalyseerde asymmetrische geconjugeerde additie van arylboorzuren aan cyclische enonen als stereocentrum introducerende stap. Een nieuw aspect van deze synthese is de implementatie van de Michael additie aan een gesubstitueerd cycloheptenon. Voor constructie van de taiwaniaquinoïde [6,5,6]-abeoabietaan basisstructuur werd een dominoreactie verondersteld die verloopt via een ringcontractie/acylering sequentie (Schema 6).





Synthetisch plan voor de synthese van een algemeen intermediair



**Schema 6.** Een overzicht van het algemene synthese plan voor de stereoselectieve constructie van verscheidende taiwaniaquinoid familieleden.

Een intensief onderzoek, met een grote hoeveelheid aan reacties, werd uitgevoerd om het [6,5,6]-abeoabietaan skelet te maken. Helaas bleek de geconjugeerde additie problematischer dan verwacht. Uiteindelijk is de geconjugeerde additie uitgevoerd met een goede enantioselectiviteit van 85%, maar de opbrengst bleek erg laag. De racemische reactie daarentegen bleek voldoende materiaal op te leveren voor de geanticipeerde ringcontractie/acylering strategie. Voor de ringcontractie stap zijn de Wolff, pinacol en quasi-Favorskii omleggingen uitgetoetst, maar die bleken helaas niet productief.

Ondanks het niet behalen van de doelstelling is het synthetische plan nog niet van de baan. Er zijn nog enkele ringcontractiemethodes die aandacht verdienen en die zijn ter afsluiting besproken in hoofdstuk 7.

## *Acknowledgements/Dankwoord*

So, that's it....After six and a half years of working in the Minnaard laboratory, of which four years of doctoral research, I'm done. It goes without saying that the work presented in this dissertation could have not come about without the help of a plethora of people within and outside of the Stratingh institute. Over the past six and a half years so many people have been helpful to me, and therefore it might be that I forgot to thank certain individuals. Please understand this is not a personal insult but a short coming of my memory. I'm truly grateful for all the help and suggestions I received! Not surprisingly I want to start my last words of this thesis by thanking my promotor, Prof. Minnaard.

Best Adri, het is nu zo een zeven jaar geleden dat wij elkaar voor het eerst spraken. Ik moest een masteronderzoek gaan uitvoeren en in mijn gesprek met u vroeg u mij wat ik graag zou willen doen. Ik vertelde dat ik "die-hard synthetic organic chemistry" wilde uitvoeren. Met een brede lach op uw gezicht antwoorde u mij; "dan ben je bij mij aan het juiste adres", en dit was geen gelogen woord. Tijdens het uitvoeren van masteronderzoek bood u mij een promotieplaats in natuurstofsynthese aan. Ondanks enige twijfel in het begin heb ik toch uw aanbod aangenomen, en dit is tot op heden het beste besluit dat ik ooit genomen heb.

Tijdens mijn promotieonderzoek heeft u mij een vrijheid gegeven die ik niet had durven wensen. Daarnaast stond u altijd voor mij klaar om mijn ideeën te bediscussiëren. Uw enthousiasme, kennis, en met name uw geloof in mijn kunnen heeft mij ontzettend geholpen om mijzelf te ontwikkelen niet allen als onderzoeker, maar ook als persoon. Het klinkt wellicht wat overdreven, maar ik zie u daadwerkelijk als mijn chemische vader en ik blijf uw mijn hele leven dankbaar dat ik onder uw supervisie mijn promotieonderzoek heb mogen uitvoeren. Ik zal altijd loyaal aan u blijven en u kunt altijd een beroep op mij doen in de toekomst. Dank U wel!

I Also would like to thank the reading committee, consisting of Prof. van Maarseveen (University of Amsterdam), Prof. Maulide (University of Vienna), and Prof. de Vries (Leibniz institute for catalysis/University of Groningen), for their fast assessment of my doctoral thesis and useful corrections and comments.

This thesis could have not come about without the fruitful collaborations with several research groups since a large part of the work in this dissertation was performed in collaboration. For this I would like to thank Prof. Dennis P. Curran and Prof. K. A. Damodaran (Pittsburgh University – Chapter 2), Prof. Barry B. Snider (Brandeis University – early stages of the TbAd synthesis) and Prof. Ben. L. Feringa and the lithium cross-coupling team (Chapter 6).

In particular I want to thank Prof. Branch D. Moody (Harvard medical school) for the collaboration on the tuberculosinyl adenosines (Chapter 3 and 4). Our collaboration started late 2011, is still ongoing, and resulted in several publications. Although it took

over two years to finalize the synthesis of 1-TbAd you have always remained supportive and patient, my thanks for that! I also want to thank you for the opportunity to participate in the “Gates teleconferences” and meeting in Toulouse, even though I was not a formal member working on the Gates foundation project. All in all, it was a great pleasure to work with you and I’m excited and honored that you accepted me in your group as a post-doctoral researcher. Also your (former) group member(s); Dr. Tan-Yun Cheng, Dr. Emily Layre, and Dr. David Young, are kindly acknowledged for the great collaboration.

Natuurlijk moet ik ok de technische staf bedanken voor al hun hulp tijdens mijn onderzoek. Zonder de hulp van de hierna genoemde mensen was mijn onderzoek zonder enige twijfel stukken minder soepel verlopen. Theodora Tiemersma-Wegman, Monique Smith, Pieter van der Meulen, Oetze Staal, Johan Kuiper, Joop Luider, Anton Nolle, Hans van der Velde. Bedankt! Ook wil ik hierbij het gehele magazijn bedanken voor hun hulp!

I also want to thank all the people who I’ve met and got the pleasure to work with within the Stratingh institute. One can imagine that over six and a half years of working for the institute, the list of people is enormous. Therefore I don’t want to mention individual names because for sure I will miss some. Instead I want to thank all of you collectively for the great time I had as a (PhD) student at the University of Groningen.

Over the past years I was also fortunate enough to guide a whole bunch of students. I’m sincerely grateful to you all for choosing the projects I put forward. Guiding you during your research was a valuable experience for me which I will take with me during my further career. Although most of the work performed by you did not make its way into this thesis, I’m happy with all the hard work you put in the projects. Thank you, Dorus Heijnen, Patrick Wilmink, Jerre Edens, Renée Moezelaar (2x), Ruben Andringa, Guillaume Le Calvez, Casper de Boer, Christian Bohmer, Alwin Hartman, Mira Holzheimer, Elise Jonkheim en Ashmir Plantijn.

Als laatste wil ik graag mijn ouders bedanken. Lieve pa en ma, Het is moeilijk onder woorden te brengen hoe cruciaal jullie bijdrage aan dit proefschrift is geweest. Laat het voorop staan dat zonder jullie steun en toeverlaat ik nooit dit proefschrift had kunnen schrijven. Jullie steun tijdens mijn educatieve loopbaan en die tijdens mij promotieonderzoek zijn van onschatbare waarde geweest. Ook al zal het niet altijd duidelijk zijn geweest wat ik precies deed, ik kon altijd mijn spreekwoordelijke ei bij jullie kwijt betreffende mijn onderzoek. De adviezen die ik heb gekregen, met name van jou pa, zal ik nooit vergeten, en hebben mij ontzettend geholpen met werk gerelateerde zaken niet direct van invloed op mijn onderzoek. Dank jullie wel!



